



The
University
Of
Sheffield.

**Insights into the opportunistic fungal pathogen *Cryptococcus* and
neutrophilic inflammation using zebrafish models**

Aleksandra Bojarczuk

A thesis submitted for the degree of Doctor of Philosophy

The University of Sheffield
Department of Infection, Immunity & Cardiovascular disease

Submission Date: January 2020

Abstract

The innate immunity provides the first line of defence against infection and inflammation. Zebrafish are a proven model for understanding the *in vivo* biology of infection and immunity. Here I describe how I have developed and used zebrafish models to understand three different aspects of infection and immunity: 1) The development and use of a zebrafish model of the human fungal infection *Cryptococcus neoformans* 2) Understanding the virulence of the hypervirulent *Cryptococcus gattii* and 3) The mechanisms of action of the immunosuppressive drug mycophenolate mofetil (MMF).

I have established an innate *in vivo* model for macrophage response to *Cryptococcus* by injecting cryptococci into zebrafish embryos. I have developed a high-content imaging method in a zebrafish model of cryptococcosis. This approach enabled me the discovery that while macrophages are critical for control of *C. neoformans*, a failure of macrophage response is not the limiting defect in fatal infections. I found that phagocytosis is inhibited early in infection and that increases in cryptococcal number are driven by intracellular proliferation. Moreover, macrophages favourably phagocytose cryptococci with smaller polysaccharide capsules and that capsule size is greatly increased over twenty-four hours of infection, a change that is sufficient to severely limit further phagocytosis.

I then used the zebrafish model of cryptococcosis to determine the virulence of *C. gattii*. I have identified a mutant in the hyper virulent strain R265 that is attenuated *in vivo*. The attenuation of the mutant, R265 GFP14 was further confirmed in a mouse model of infection. I analysed the interaction of macrophages and R265 GFP cryptococci in zebrafish and found that the transgenic R265 GFP was rapidly cleared. Whole genome sequences revealed that R265 GFP14 has 32 kb deletion in chromosome 1, resulting in the loss of six genes. R265 wild-type and R265 GFP14 were characterised for carbon sources utilisation.

Finally, following up on colleagues' use of my zebrafish model of cryptococcosis, I investigated the action of MMF on neutrophilic inflammation. I showed that MMF

treatment resulted in neutrophil cell death by apoptosis *in vivo*, thereby reducing neutrophilic inflammation.

Thus in this thesis, I demonstrate how I combined the study of infection and immunity to better understand diseases that cause the biggest disease burden in humans. I pioneered novel approaches to studying cryptococcosis using an experimental zebrafish model, which demonstrated for the first time how the early interactions with macrophages determined the outcome of infection. I subsequently used my model to study the virulence of an emerging pathogen, Vancouver strain R265 of *C. gattii*, identifying a genome region that may be important for virulence. Finally, from my cryptococcosis model a new mechanism for the immunosuppressant mycophenolate mofetil was identified in macrophages. Using my expertise in neutrophilic inflammation I was able to show that there was a second mechanism in neutrophils and this may explain the usefulness of this drug in treating chronic inflammation.

Acknowledgements

I would like to acknowledge everyone who has helped me to reach this goal. Firstly, I would like to thank Prof Zofia Filipkowska, my master's supervisor in Poland, who inspired me and introduced me to the world of microbiology. My master's degree enabled me to realise that microbiology has a great impact on our lives and it is important in many different professions.

I wish to thank Prof Stephen Renshaw for employing me in his lab. This was my first appointment at The University of Sheffield, which introduced me to the fascinating field of inflammation and neutrophils.

I particularly thank Dr Simon Johnston, who appointed me to have a central role in infection research on the interaction between macrophages and the fatal fungal pathogen *Cryptococcus*. Simon gave me an opportunity to start postgraduate study and became my PhD supervisor.

I would also like to express my appreciation to my friend Dr Agnieszka Urbanek for her advice in many aspects of my PhD including scientific ideas and technique. Many thanks to Dr Paweł Łusyganicz and Dr Tomasz Prajsnar for scientific advice and guidance during the writing process. I am thankful to my friends Roy Shekle, Laura Gordon and Sarah Keen for checking my grammar!

I would like to thank my family, to whom I dedicate this dissertation. Special thanks go to my husband Peter who had to undertake my domestic duties and look after our daughters for most of the time. Peter, thank you for your patience and understanding! I also thank my girls, Hanna and Milla for not stopping loving me, even when I did not have time for them. I also thank my parents, Urszula and Mieczysław for their support and for looking after my daughters when Peter could not.

Finally, I am ever grateful to The University of Sheffield for enabling me to conduct the PhD programme via staff candidate.

TABLE OF CONTENTS

Abstract	2
Acknowledgements	4
Abbreviations	10
List of tables	15
List of figures	15
Chapter 1: Introduction	19
1.1 Significance of the research proposed	19
1.2 <i>Cryptococcus</i> spp.	21
1.2.1 <i>Cryptococcus</i> biology	25
1.2.2 Cryptococcal disease	30
1.1.2.1 <i>C. neoformans</i> and <i>C. gattii</i> infections in HIV/AIDS, otherwise compromised and immunocompetent individuals	31
1.1.2.2 HIV naïve patients	33
1.2.3 Virulence of <i>Cryptococcus</i>	38
1.2.4 Experimental models of cryptococcosis	61
1.3 The innate immunity	65
1.3.1 Neutrophils	68
1.3.1.1 Neutrophils in infection and inflammation	68
1.3.1.2 Neutrophil recruitment	69
1.3.1.3 Neutrophil diapedesis and chemotaxis	70
1.3.1.4 Neutrophils phagocytosis, degranulation, respiratory burst, swarms and extracellular traps	71
1.3.1.5 Neutrophil response to infection/inflammation	74
1.3.1.6 Neutrophil longevity and death	75
1.3.1.7 Inflammatory disease	78
1.3.2 Macrophages	78
1.2.2.1 Origin of macrophages	78
1.2.2.2 Macrophage recruitment in infection/inflammation	79
1.2.2.3 Macrophage activation and polarisation	83
1.2.2.4 Macrophages diapedesis and chemotaxis	84
1.2.2.5 Macrophages phagocytosis and phagosome maturation	84
1.2.2.6 Macrophage longevity and death	86
1.2.2.7 Other cells	88
1.4 The adaptive immune system	88

1.5 The innate immune response to <i>Cryptococcus</i>	90
1.6 Inflammation and disease.....	93
1.6.1 Inflammation and infection.....	96
1.6.1.1 The course of inflammatory response to infection	96
1.6.1.1.1 Recognition of infection.....	97
1.6.1.1.2 Recruitment of inflammatory cells to site of infection ..	100
1.6.1.1.2.1 Mediators of inflammation	100
1.6.1.1.3 Control of infection and elimination of pathogens.....	103
1.6.1.1.4 Termination of inflammation.....	105
1.6.1.2 Sterile inflammation.....	106
1.7 Thesis aims.....	114
Chapter 2: Materials and Methods	118
2.1 Ethics statement.....	118
2.2 Fish husbandry	118
2.2.1 Zebrafish lines used in the study.....	119
2.3 Cryptococcal strains cultivation	122
2.3.1 <i>Cryptococcus</i> strains used in this study.....	122
2.4 Preparation of <i>C. gattii</i> culture for phenotypic microarrays	126
2.5 Phenotypic microarrays.....	128
2.6 Cryptococcal culture and counting.....	129
2.7 <i>In vitro</i> growth of <i>C. gattii</i> strains in rich and minimal media	130
2.8 General zebrafish techniques.....	131
2.8.1 Tail fin injury.....	131
2.8.2 Time course counting.....	133
2.8.3 Compound treatment of zebrafish larvae.....	133
2.8.3.1 MMF	134
2.8.3.2 SP600125	135
2.8.3.3 AZA	136
2.8.3.4 Z-VAD.....	137
2.8.4 Inflammation assays.....	137
2.8.4.1 Recruitment.....	137
2.8.4.2 Resolution	138
2.8.4.3 Total number of neutrophils.....	138
2.8.4.5 Apoptosis	139

2.8.4.6 Reverse migration	142
2.8.5 Infection assay	145
2.8.5.1 Preparation of <i>C. neoformans</i> / <i>C. gattii</i> culture prior to injection	145
2.8.5.2 Needles for microinjections	146
2.8.5.3 Zebrafish microinjections	146
2.9 Preparation of <i>C. gattii</i> culture for mice infections	149
2.10 Zebrafish survival assay	150
2.11 Disposal of zebrafish and microbiological waste	150
2.12 Statistical analysis.....	150
Chapter 3: <i>Cryptococcus neoformans</i> intracellular proliferation and capsule size determines early macrophage control of infection	153
3.1 Introduction	153
3.1.1 The importance of <i>C. neoformans</i> , interactions with macrophages and the polysaccharide capsule	153
3.1.2 The need for the development of a new integrated model of cryptococcosis	157
3.1.3 The development of a new integrated model of cryptococcosis and commentary on resulting publication (Bojarczuk <i>et al.</i> , 2016) ...	159
3.2 The publication <i>Cryptococcus neoformans</i> intracellular proliferation and capsule size determines early macrophage control of infection (Bojarczuk <i>et al.</i> , 2016)	161
3.2.1 Supplementary data	177
3.3 Discussion	188
Chapter 4: Characterisation of a virulence and growth defect in <i>Cryptococcus gattii</i> strain R265 with a genomic defect following GFP transformation	194
4.1 Introduction	194
4.1.1 Comparison of <i>C. neoformans</i> and <i>C. gattii</i> geographical distribution	194
4.1.2 Comparison of <i>C. neoformans</i> and <i>C. gattii</i> infection	195
4.1.3 <i>C. gattii</i> R265 and hypothesis.....	197
4.2 Results	199
4.2.1 <i>Cryptococcus gattii</i> R265 infection results in decreased host survival than <i>C. neoformans</i> strain KN99 in a zebrafish model.....	199
4.2.2 R265 GFP14 is avirulent in C57BL/6 mice	201

4.2.3 R265 GFP14 has lost six genes deleted during generation of the GFP-tagged derivative of R265	203
4.2.4 <i>In silico</i> analysis of function of six genes deleted during generation of the GFP-tagged derivative of R265.....	205
4.2.5 <i>C. gattii</i> R265 GFP14 does not grow in the zebrafish	210
4.2.6 R265 GFP14 shows a growth deficit in the minimal medium....	217
4.2.7 <i>C. gattii</i> R265 GFP14 exhibits different use of carbon sources	220
4.2.8 Conclusions	238
4.3 Discussion	239
4.3.1 Temperature and thermotolerance	241
4.3.2 GFP insertion	242
4.3.2.1 GFP insertion effect on the course of infection.....	242
4.3.2.2 GFP insertion site	244
4.3.3 Virulence.....	245
4.3.3.1 Virulence of R265 wt and KN99 wt in a zebrafish model of infection	245
4.3.3.2 Avirulence of R265 GFP14 in a mouse model of infection .	246
4.3.3.3 <i>C. gattii</i> R265 GFP14 does not grow in the zebrafish	246
4.3.4 Analysis of phenotypes produced by R265 wt and R265 GFP14	249
4.3.5 The mechanism of R265 GFP14 attenuation <i>in vivo</i>	263
4.3.6 Future work	269
4.3.7.1 Genetic work in R265 wt and animal survival assay	269
4.3.7.2 Genes function.....	270
4.3.7.3 Future work in respect to metabolic profiling of R265 wt and R265 GFP14.....	272
4.3.7.4 Linking data to assess why deleted genes are important for R265 wt virulence	274
4.3.7 Major experiments to bring Chapter 4 towards publication.....	275
Chapter: 5 Mycophenolate mofetil increases inflammation resolution in zebrafish via neutrophil apoptosis.....	281
5.1 Introduction	281
5.1.1 Mechanism of MMF on lymphocytes and other effects on other cells.....	281
5.1.2 MMF effects on glycosylation and adhesion.....	284
5.1.3 Side effects of MMF described in clinical studies	288

5.1.4 MMF in autoimmunity.....	288
5.1.5 MMF's pharmacokinetics	289
5.1.6 Azathioprine (AZA)	292
5.1.7 MMF versus AZA	295
5.1.8 Conclusions, hypothesis and the research model.....	297
5.2 Results	298
5.2.1 Neutrophilic inflammation is reduced with MMF treatment.....	298
5.2.2 AZA does not replicate the effect of MMF treatment on neutrophilic inflammation.....	305
5.2.3 Reverse migration is not the mechanism by which MMF accelerates inflammation resolution <i>in vivo</i>	308
5.2.4 MMF induces neutrophil apoptosis in the tail injury model	311
5.3 Discussion	316
5.3.1 The dose of MMF used in the study	316
5.3.2 Neutrophilic inflammation is reduced with MMF treatment.....	317
5.3.3 AZA does not replicate the effect of MMF treatment on neutrophilic inflammation.....	321
5.3.4 MMF induces neutrophil apoptosis in the tail injury model	322
5.3.5. Summary and future.....	328
Chapter 6: Overall discussion and future work.....	333
6.1 The zebrafish model of <i>C. neoformans</i> infection	333
6.2 Assessment of <i>Cryptococcus gattii</i> virulence in zebrafish and mice	344
6.3 Mycophenolate mofetil (MMF) increases inflammation resolution in zebrafish via neutrophil apoptosis.....	350
6.4 Thesis summary	351
Appendix 1	353
Appendix 2	395
Bibliography.....	403

Abbreviations

6MP	6-mercaptopurine
6TA	6-thioinosic acid
6TGN	6-thioguanine nucleotides
6TU	6-thiouric acid
AcMPAG	acyl glucuronide
AIDS	Acquired Immunodeficiency Syndrome
AMP	adenosine monophosphate
Anno Domini	AD
AnxA1	Annexin A1
AO	aldehyde oxidase
APC	antigen presenting cell
ATP	adenosine triphosphate
AZA	azathioprine
BAC	bacterial artificial chromosome
BAL	bronchoalveolar lavage
Bcl-2	B-cell lymphoma 2
BLAST	basic local alignment search tool
BMDM	bone marrow-derived macrophages
C1q R	first subcomponent of the C1 complex of the classical pathway of complement activation
C5a	complement component C5a
CCL	C-C chemokine ligand CCR
CEO	chief executive officer
CCL	chemokine (C-C motif) ligand
CCR	C-C chemokine receptor
cGMP	cyclic guanosine monophosphate
CLR	C-type lectin receptors
CNS	central nervous system
CR3	complement receptor 3
CR4	complement receptor 4
CrAg	cryptococcal antigen
CSF	cerebrospinal fluid

CXCL	chemokine (C-X-C motif) ligand
DAMP	damage-associated molecular pattern
DC	dendritic cell
dGTP	deoxyguanosine triphosphate
DNA	deoxyribonucleic acid
EC	endothelial cell
ER	endoplasmic reticulum
FcR	Fc receptor
FcR γ	Fc receptor γ -chain
FPR1	formyl peptide receptor 1
GAL4	galactose responsive transcription factor
G-CSF	granulocyte-colony stimulating factor
GM-CSF	granulocyte macrophage-colony stimulating factor
GMP	guanosine monophosphate
GRO	growth-regulated oncogene
GRO/KC	keratinocyte chemoattractant of human growth-regulated oncogene
GTP	guanosine diphosphate
HIV	Human Immunodeficiency Virus
HMGB1	high-mobility group box 1 protein
hpc	hour(s) post photoconversion
hpi	hour(s) post infection
HPRT	hypoxanthine guanine phosphoribosyltransferase
hpt	hour(s) post treatment
HSP	heat shock protein
HUVEC	human umbilical vein endothelial cell
I/R	ischemia/reperfusion
iC3b	complement component iC3b
ICAM-1	intercellular adhesion molecule 1
IFN γ	interferon gamma
IFR	interferon-regulatory factors
Ig	immunoglobulin
IL	interleukin
IL-RA	interleukin-1 receptor antagonist
IMP	inosine monophosphate

IMPDH	inosine-5'-monophosphate dehydrogenase
IMPDH	monophosphate dehydrogenase
JAK	Janus kinase
KC	keratinocyte chemoattractant
KEGG	Kyoto Encyclopedia of Genes and Genomes
LC3	Microtubule-Associated Protein 1 Light Chain 3, LIR
LFA	lateral flow immunochromatographic assay
LFA-1	Lymphocyte function-associated antigen 1
LPS	lipopolysaccharide
LTB4	leukotriene B4
MCMV	murine cytomegalovirus
MCP-1	monocyte chemotactic protein 1
MCP-1	chemokine-monocyte chemoattractant 1
MCP-2	chemokine-monocyte chemoattractant 2
MCP-3	monocyte chemotactic protein 3
MDL-1	myeloid DAP12-associating lectin-1
MeMP	methylmercaptapurine
MeTIMP	methyl thioinosine monophosphate
Mincle	macrophage-inducible C-type lectin
MIP-1	macrophage inflammatory protein 1
MIP-2	macrophage inflammatory protein 2
MMF	mycophenolate mofetil
MPA	mycophenolic acid
MPAG	7-O-mycophenolic acid glucuronide
MPO	myeloperoxidase
MPs	mannoproteins
NAD	nicotinamide adenine dinucleotide
NAD ⁺	the oxidised form of NAD
NADH	the reduced form of NAD
NADP	nicotinamide adenine dinucleotide phosphate
NADP ⁺	the oxidised form of NADP
NADPH	the reduced form of NADP
NCBI	Information from National Centre for Biotchnology Information
NET	neutrophil extracellular trap

NF- κ B	nuclear factor kappa-light-chain-enhancer of activated B cells
NK	natural killer cell
NLR	nucleotide-binding oligomerisation domain–like (Nod-like) receptor
NLRP3	NOD-, LRR- and pyrin domain-containing 3
PAMP	pathogen-associated molecular pattern
PECAM-1	platelet/endothelial-cell adhesion molecule 1
PG	prostaglandin
PI3K	phosphatidylinositol 3-kinase
Plb	phospholipase
PM1	phenotypic microarray 1
PMN	polymorphonuclear leukocyte
PRPP	amidophosphoribosyltransferase
PRR	pattern recognition receptor
PS	phosphatidylserine
RAGE	receptor for advanced glycation end products
RBC	red blood cell
RLR	RIG-like receptors
RNA	ribonucleic acid
ROS	reactive oxygen species
rpm	revolutions per minute
RT	room temperature
SAGE	serial analysis of gene expression
SD	standard deviation
SOT	solid organ transplant
STAT	signal transducer and activator of transcription
TCA	tricarboxylic acid cycle
TGDP	6-thioguanine diphosphate
TGF β 1	transforming growth factor β 1
TGMP	6-thioguanine monophosphate
TGN	thioguanine nucleotides
TGTP	6-thioguanine triphosphate
TIMP	thioinosine monophosphate
TLR	Toll-like receptor

TNF α	tumour necrosis factor alpha
TPMT	thiopurine S-methyltransferase
TSP	thrombospondin
UAS	upstream activation sequence
VCAM-1	vascular cell adhesion molecule 1
VIO	Vancouver Island Outbreak
WT	wild-type
XO	xanthine oxidase
YPD	yeast extract peptone dextrose
YPDA	yeast extract peptone dextrose agar

List of tables

Table 1.1 Current and proposed species within the <i>C. neoformans/C. gattii</i> species complex.....	23
Table 1.2 Legend to figure 1.3.....	59
Table 1.3 Mouse and human blood monocyte subsets.....	82
Table 1.4 Inflammatory mediators.....	102
Table 1.5 Phagocytic receptors (examples).....	104
Table 1.6 Examples of intracellular and extracellular triggers of sterile inflammation.....	108
Table 2.1 Zebrafish lines used in the study.....	121
Table 2.2 Cryptococcal strains used in the study.....	124
Table 2.3 Compound treatments in MMF study.....	134
Table 4.1 List of genes deleted in R265 GFP14.....	209
Table 4.24 The summary of core experiments to bring Chapter 4 towards manuscript publication.....	280

List of figures

Figure 1.1 Infection route.....	27
Figure 1.2 Phases of the <i>C. neoformans</i> life cycle.....	29
Figure 1.3 Principle virulence factors of <i>Cryptococcus</i> species.....	58
Figure 2.1 Haemocytometer grid.....	130
Figure 2.2 Tail transection of 2 dpf zebrafish larva.....	132
Figure 2.3 Zebrafish model of neutrophil apoptosis at the tail fin injury site.....	141
Figure 2.4 Zebrafish model of neutrophil reverse migration.....	144
Figure 2.5 Schematic diagram of larva showing the site of microinjection with <i>C. neoformans/C. gattii</i>	148
Figure 3.1 Schematic interaction of <i>Cryptococcus</i> with macrophages.....	156
Figure 4.1 Survival of <i>nacre</i> zebrafish larvae at 3 dpi is increased with <i>C. neoformans</i> KN99 wt as compared to <i>C. gattii</i> R265 wt injected.....	200
Figure 4.2 Survival of <i>nacre</i> zebrafish larvae at 3 dpi is increased with <i>C. gattii</i> R265 GFP14 strain as compared to <i>C. gattii</i> R265 wt.....	200

Figure 4.3 Survival of <i>nacre</i> zebrafish larvae at 3 dpi injected with <i>C. neoformans</i> KN99 wt or KN99 GFP strains is identical.....	200
Figure 4.4 Survival of C57BL/6 mice infected with R265 GFP14 is 100%.....	202
Figure 4.5 Diagrammatic representation of genome sequencing differences between <i>C. gattii</i> strains R265 wt and R265 GFP14.....	204
Figure 4.6 R265 GFP14 does not grow in any of the analysed infected zebrafish.....	211
Figure 4.7 The number of extracellular cryptococci is lower than the number of intracellular cryptococci at 48 and 72 hpi.....	211
Figure 4.8 The number of intracellular cryptococci does not change throughout the course of infection.....	213
Figure 4.9 The number of extracellular cryptococci declines over the time of infection.....	213
Figure 4.10 The percentage proportion of intracellular R265 GFP14 cryptococci is the greatest at 72 hpi.....	215
Figure 4.11 The number of infected macrophages does not change over the course of infection.....	215
Figure 4.12 Phagocytic index (PI) is relatively constant throughout the course of infection.....	216
Figure 4.13 The R265 GFP14 strain had a deficit in growth in the minimal media in comparison to R265 wt.....	219
Figure 4.14 Representative images of the redox dye D colour changes.....	222
Figure 4.15 Representative images of kinetic traces.....	223
Figure 4.16 The end-point metabolic profile at 36 hours for all of metabolites.....	226
Figure 4.17 NADH production kinetics in R265 wt and R265 GFP14 with D-xylose.....	227
Figure 4.18 NADH production kinetics in R265 wt and R265 GFP14 with D-mannose.....	227
Figure 4.19 NADH production kinetics in R265 wt and R265 GFP14 with tricarballic acid.....	228
Figure 4.20 NADH production kinetics in R265 wt and R265 GFP14 with L-lyxose.....	228
Figure 4.21 NADH production kinetics in R265 wt and R265 GFP14 with D, L-malic acid.....	229

Figure 4.22 NADH production kinetics in R265 wt and R265 GFP14 with bromosuccinic acid.....	229
Figure 4.23 NADH production kinetics in R265 wt and R265 GFP14 with L-asparagine.....	230
Figure 4.24 NADH production kinetics in R265 wt and R265 GFP14 with sucrose.....	230
Figure 4.25 NADH production kinetics in R265 wt and R265 GFP14 with L-lactic acid.....	231
Figure 4.26 NADH production kinetics in R265 wt and R265 GFP14 with citric acid.....	231
Figure 4.27 NADH production kinetics in R265 wt and R265 GFP14 with fumaric acid.....	232
Figure 4.28 NADH production kinetics in R265 wt and R265 GFP14 with acetic acid.....	232
Figure 4.29 NADH production kinetics in R265 wt and R265 GFP14 with pyruvic acid.....	233
Figure 4.30 NADH production kinetics in R265 wt and R265 GFP14 with m-tartaric acid.....	233
Figure 4.31 NADH production kinetics in R265 wt and R265 GFP14 with Tween 40.....	234
Figure 4.32 NADH production kinetics in R265 wt and R265 GFP14 with Tween 80.....	234
Figure 4.33 NADH production kinetics in R265 wt and R265 GFP14 with α -ketoglutaric acid.....	235
Figure 4.34 NADH production kinetics in R265 wt and R265 GFP14 with glucuronamide.....	235
Figure 4.35 NADH production kinetics in R265 wt and R265 GFP14 with methyl pyruvate.....	236
Figure 4.36 NADH production kinetics in R265 wt and R265 GFP14 with L-serine.....	236
Figure 4.37 NADH production kinetics in R265 wt and R265 GFP14 with D-fructose.....	237
Figure 4.38 Diagrammatic representation of proposed model of R265 GFP14 infection progression in zebrafish larvae.....	249
Figure 5.1 Purine biosynthesis pathways including the de novo pathway and salvage pathway, showing the central position of inosine monophosphate (IMP) and point of action for MPA.....	287

Figure 5.2 Pharmacokinetics of MMF after oral administration.....	291
Figure 5.3 AZA metabolic pathway.....	294
Figure 5.4 Biochemical pathways of AZA and MMF.....	296
Figure 5.5 MMF accelerates resolution of neutrophilic inflammation <i>in vivo</i> ...	300
Figure 5.6 MMF results in a more than 2-fold reduction in the proportion of neutrophils at the wound site between 6-24 hpi.....	302
Figure 5.7 Representative images of larvae treated with DMSO and MMF after 6 and 24 hours of incubation.....	303
Figure 5.8 MMF has no effect on the total number of neutrophils.....	304
Figure 5.9 AZA does not accelerate the resolution of neutrophilic inflammation.....	306
Figure 5.10 AZA has no effect on the total number of neutrophils.....	307
Figure 5.11 Representative images of <i>mpx:Kaede</i> larvae DMSO and MMF treated larvae at 0 and 8 hours post photoconversion.....	309
Figure 5.12 MMF does not promote reverse migration <i>in vivo</i>	310
Figure 5.13 Representative images of <i>mpx:GFP</i> zebrafish fixed and stained 12 hpi for colocalisation of neutrophil (FITC-TSA) and apoptotic (TUNEL) markers.....	312
Figure 5.14 MMF increases neutrophil apoptosis at the site of inflammation.....	313
Figure 5.15 MMF reduces the number of neutrophils at the site of injury at 12 hpi.....	313
Figure 5.16 The effect of MMF is reversed with Z-VAD at both 6 and 24 hpi	315
Figure 6.1 A simplified diagram of cellular respiration.....	348

Chapter 1: Introduction

1.1 Significance of the research proposed

Infectious and inflammatory diseases are the biggest burdens onto human health, with little prospect this will change in the coming decades. Infection and immunity are drivers of a huge number of diseases from cancer to heart disease to neurodegeneration. We still do not know much details of how the immunity works or how diseases develop. By studying infection and immunity we intend to develop new strategies to prevent, fight and defeat infection, and to prevent and target immune and inflammatory disorders. Here, in this chapter I will introduce the background underlying my thesis aims and results.

Firstly, I aim to understand fundamental mechanisms through which *C. neoformans* and *C. gattii* infections develop. Currently, novel infectious diseases are emerging and old infectious diseases are spreading. Infectious diseases may be unpredictable with the potential for global outbreaks (McArthur, 2019). Lately, the increasing incidence of *C. neoformans* infection as a concomitant disease of AIDS patients, the outbreak of a hyper virulent *C. gattii* strain in Vancouver Island and cryptococcosis associated high mortality urged the medical mycology community to study these organisms (reviewed by (Idnurm and Lin, 2015)). The study of *Cryptococcus* has been made possible due to its well-defined virulence factors, along with advanced technical improvements. In the Introduction chapter I review the recent advances in our understanding of *C. neoformans* and *C. gattii*, including *Cryptococcus* biology, virulence factors and key signalling pathways regulating virulence, along with the interaction between these pathogens and the host immune system. I think for anyone else who wants to read my thesis a general understanding of the immunity as well as immune response to *Cryptococcus* is important.

In order to determine how infections cause disease in humans, a complex biological system is often required. Such a model enables studying the myriad of host-pathogen interactions associated with infections. While conventional mammalian models have the advantage of relatively close similarity to humans,

they have limits. Thus, I review advantages and disadvantages of animal models. This is an important research area as at the time I started my work in the Johnston lab, there was no model, which would enable tracking macrophages (that are the dominant phagocytic cells interacting with *Cryptococcus*) and cryptococci in the entire body of a host and so host-pathogen interactions in real-time. I therefore pay attention to zebrafish as a model host for invasive fungal infections, with a great emphasis that this animal has a potential to be used as an experimental model of cryptococcal infection. Thus, one way to overcome the problem of the lack of zebrafish model of *Cryptococcus* infection is just to establish such a system. Therefore, the first part of the project asks whether zebrafish can serve as a model. This system could also be used to answer a question regarding the difference between *C. neoformans* and *C. gattii* infections. The literature is not evident in terms of how *C. gattii* causes a disease and what the difference between them two species in this aspect is. The second part of the project asks whether *C. gattii* assessment in the zebrafish model of cryptococcosis will reveal the cause of its virulence

Various pathogenic factors, such as infection or tissue damage, can induce inflammation. In this sense, infection is linked with inflammation and vice versa. These cells specified and maintained to resolve inflammation, destroy pathogens and return to homeostasis, communicate together and regulate each other. A growing number of inflammatory conditions have been described, wherein the initiating trigger does not involve infection. In addition, more clinicians are now turning to immunosuppressants to treat inflammatory diseases. I aim to understand immune responses to inflammation under immunosuppressive regime.

As my research is focussed on understanding the mechanisms of normal, physiological and pathological immune responses and due to the fact that infection and inflammation signalling pathways very often overlap, it is sensible to review inflammation and disease as well as the course of inflammation/infection. Not only macrophages are reviewed in this thesis, but also neutrophils since they have aroused a lot of interest in the inflammatory process. Neutrophilic inflammation is crucial for the maintenance of health and life. Failure to resolve the response in a timely manner might cause detrimental damage to

healthy tissue because of the release of toxic granule contents of persisting neutrophils (Haslett, 1992). Such neutrophils cause chronic inflammation. This in turn is linked with infections and autoimmune conditions. These cases require immunosuppression (reviewed by (Kanterman *et al.*, 2012)). Despite the clinical problem of unresolved neutrophilic inflammation, few effective therapies are available, none of which directly target the neutrophil. One of the widely used treatments in immune-mediated diseases is mycophenolate mofetil (MMF). Despite its long clinical success in inflammatory diseases, no previous study has investigated MMF mechanism of action in terms of inflammation. The third part of the project aims to reveal such a mechanism.

The thesis is written in an alternative format with the following chapters: Introduction section (Chapter 1), Materials and Methods section (Chapter 2) and three Result chapters (Chapter 3-5), of which Chapter 3 is a published article whereas Chapter 4 is written in a conventional way and Chapter 5 is based on a preprint version of the manuscript in revision. A general discussion (Chapter 6) is given at the end to summarise all the work.

1.2 *Cryptococcus* spp.

Cryptococcus is an environmental, saprophytic yeast that causes opportunistic infection and has become medically important over the last half century due to the AIDS pandemic, becoming one of the leading causes of death in AIDS, and causing rare severe infections within immunocompetent individuals. The pathogenic *Cryptococcus* species complex consists of two sibling basidiomycetous yeast taxa, *Cryptococcus neoformans* and *Cryptococcus gattii* (reviewed by (Kwon-Chung and Varma, 2006; Ngamskulrungraj, Gilgado, *et al.*, 2009; Hagen *et al.*, 2015; Kwon-Chung *et al.*, 2017)). However, the debate regarding the lineages and nomenclature of *C. neoformans/C. gattii* species complex is still ongoing.

The sister pathogenic species are closely related but distinguishable. Major differences exist in basidiospore morphology (reviewed by (Kwon-Chung *et al.*, 2014; You and Xu, 2018)) and their environmental niche (reviewed by (Lin and

Heitman, 2006)), and morphologic characteristics *in vivo*, e.g. *C. neoformans* var. *gattii* undergoes reversible phenotype switching during murine infections, whereas this process is irreversible in *C. neoformans* var. *neoformans* and *C. neoformans* var. *grubii* (Jain *et al.*, 2006).

Two varieties: *C. neoformans* var. *grubii* (serotype A) (Franzot *et al.*, 1999) and *C. neoformans* var. *neoformans* (serotype D) (Kwon-Chung, 1975), as well as AD hybrid strains (Lucas *et al.*, 2010) were assigned to *C. neoformans* with serotype A causing most of cryptococcal disease (reviewed by (Mitchell and Perfect, 1995, Steenbergen and Casadevall, 2000)). *C. gattii* consisted of 2 serotypes: B and C ((Wilson *et al.*, 1968), reviewed by (Mitchell and Perfect, 1995)). There have also been several molecular types: *C. neoformans* var. *grubii* represented by VNI and VNII corresponding to AFLP1 and AFLP1A, respectively; *C. neoformans* var. *neoformans* was represented by VNIV and AFLP2; serotype AD was assigned to VNIII and AFLP3. *C. gattii* serotypes have been classified as: VGI- VGIV corresponding to AFLP4, AFLP6, AFLP5, and AFLP7, respectively (Meyer *et al.*, 2009). Recently, it has been accepted to separate *C. neoformans* var. *grubii* from *C. neoformans* var. *neoformans*, and to introduce five species within *C. gattii* upon biological and genetic differences between species (Table1) (Hagen *et al.*, 2015; Kwon-Chung *et al.*, 2017).

In this thesis, when I mention *C. neoformans* and *C. gattii*, I am denoting the *C. neoformans* species complex (*C. neoformans*, *C. deneoformans*) and *C. gattii* species complex (*C. gattii*, *C. bacillisporus*, *C. deuterogattii*, *C. tetragattii* and *C. decagattii*), respectively.

Table 1.1 Current and proposed species within the *C. neoformans*/*C. gattii* species complex

current species name	MLST Clade/ AFLP-genotype	PCR- fingerprinting/RFLP- genotype	sero- type	proposed species name
<i>Cryptococcus neoformans</i> var. <i>grubii</i>	Clade F, AFLP1	VNI	A	<i>Cryptococcus neoformans</i>
	Clade G, AFLP1A/VNB	VNII	A	
	Clade H, AFLP1B	VNII	A	
<i>Cryptococcus neoformans</i> var. <i>neoformans</i>	Clade I, AFLP2	VNIV	D	<i>Cryptococcus deneoformans</i>
<i>Cryptococcus neoformans</i> intervariety hybrid	AFLP3	VNIII	AD	<i>Cryptococcus neoformans</i> x <i>Cryptococcus deneoformans</i> hybrid
<i>Cryptococcus gattii</i>	Clade D, AFLP4	VGI	B	<i>Cryptococcus gattii</i>
	Clade C, AFLP5	VGIII	C	<i>Cryptococcus bacillisporus</i>
	Clade A, AFLP6	VGII	B	<i>Cryptococcus deuterogattii</i>
	Clade E, AFLP7	VGIV	C	<i>Cryptococcus tetragattii</i>
	Clade B, AFLP10	VGIV/VGIIIc	B	<i>Cryptococcus decagattii</i>

Table 1.1 (continued)

<i>Cryptococcus neoformans</i> var. <i>neoformans</i> x <i>Cryptococcus gattii</i> AFLP4/VGI hybrid	AFLP8	-	BD	<i>Cryptococcus deneoformans</i> x <i>Cryptococcus gattii</i> hybrid
<i>Cryptococcus neoformans</i> var. <i>grubii</i> x <i>Cryptococcus gattii</i> AFLP4/VGI hybrid	AFLP9	-	AB	<i>Cryptococcus neoformans</i> x <i>Cryptococcus gattii</i> hybrid
<i>Cryptococcus neoformans</i> var. <i>grubii</i> x <i>Cryptococcus gattii</i> AFLP6/VGII hybrid	AFLP11	-	AB	<i>Cryptococcus neoformans</i> x <i>Cryptococcus deuterogattii</i> hybrid

Adapted from (Hagen *et al.*, 2015).

1.2.1 *Cryptococcus* biology

The route of infection and infectious propagules

Cryptococcus is predominantly found in the environment as a budding yeast, the form most commonly associated with clinical infection (reviewed by (Hull and Heitman, 2002; Kwon-Chung *et al.*, 2014)). Infections are developed from the environment, supposedly by inhalation of airborne desiccated yeast or spores, which are believed to be infectious propagules ((Velagapudi *et al.*, 2009; Walsh *et al.*, 2019); reviewed by (Levitz, 1991; Kwon-Chung *et al.*, 2014)). The environmental sources include bird guano and certain trees (Mitchell *et al.*, 2011). Infectious propagules are inhaled into the lungs, which become the primary site of infection (Figure 1.1). Spores are produced by mating (Kwon-Chung, 1975, 1976b) or monokaryotic fruiting (Erke, 1976; Wickes *et al.*, 1996). The yeast form is also infectious as shown in the wide range of mice or zebrafish studies. It is widely accepted that the small size of the cell is perfect to enter the lungs (reviewed by (Hull and Heitman, 2002)). For instance, the typical median size of intracellular cryptococcal cells (H99 GFP) cultured *in vitro* in YPD is from 3 to 8 μm at 25°C (Johnston *et al.*, 2016). The literature emphasises that the size of the infectious propagule can restrict the pulmonary entry and that particles larger than 5 μm are subjected to the mucociliary action of the human lung epithelium (Hatch, 1961; Knowles and Boucher, 2002). However, mice inhalation model is a forced inhalation system, which is probably quite different to how a human might breathe in a yeast cell. In a laboratory setting *Cryptococcus* can grow as a yeast and reproduce by budding. The yeast is the form that is isolated from human infection (Bovers *et al.*, 2008, Senghor *et al.*, 2018). Budding mode provides the fastest reproduction method and gives rise to two independent cells in mitosis (reviewed by (Lin, 2009)). *Cryptococcus* is also able to produce pseudohyphae and this distinguished type has sporadically been observed in patients infected by both *C. neoformans* serotypes A and D, and *C. gattii* (Lee *et al.*, 2012). Interestingly, Neilson and colleagues showed that after co-incubation of yeast from *C. neoformans* with *Acanthamoeba polyphaga*, the fungus cells are phagocytosed and killed, leaving only pseudohyphae. It was speculated that

perhaps pseudohyphal forms of the fungus always exist and the amoeba aids their survival by absorbing the yeast cells without absorbing the pseudohyphae, or, alternatively the amoeba stimulates the morphological switch. It could also be that pseudohyphae formation provides an anti-phagocytic strategy, if the pseudohyphae are too large to be engulfed, or an escaping strategy to exit the host cell after phagocytosis (Neilson et al., 1978). Pseudohyphae grow in an elongated chain with mother and daughter cell attachments (reviewed by (Hull and Heitman, 2002, Trevijano-Contador *et al.*, 2016).

Nonetheless, sexual reproduction is a route by which infectious basidiospores are produced and this is reviewed below.

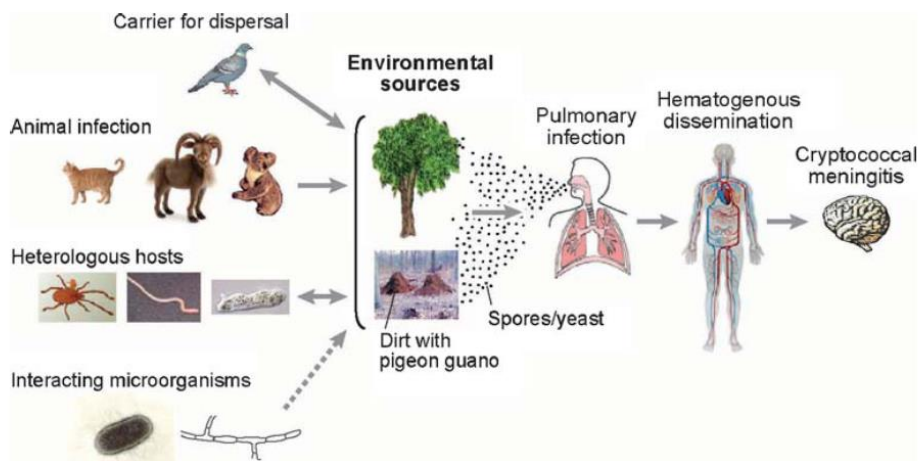


Figure 1.1 Infection route. Birds, certain trees, many animals as well as insects, worms and amoebae have been found to harbour *Cryptococcus*. Infectious propagules are inhaled into the lungs, which become the primary site of infection. Cryptococcal dissemination may lead to meningitis or meningoencephalitis. Taken from (Lin and Heitman, 2006).

Cryptococcus sexual reproduction and life cycle

Sexual reproduction of *C. neoformans* var. *neoformans*, serotype D, and *C. neoformans* var. *gattii*, serotypes B and C, was discovered in mid-1970 (Kwon-Chung, 1975, 1976a, 1976b). A haploid *Cryptococcus* cell possesses one mating type locus, this being compared to a sex chromosome in more advanced organisms. The fungal MAT locus encodes either **a** or α allele that is responsible for the cell gender. Sexual reproduction is maintained by mating (Sun *et al.*, 2019). Bisexual mating involves partners of opposite mating types **a** and α whereas unisexual involves the same mating types, namely α and α (reviewed by (Wang and Lin, 2011)). To be exact, there are 3 pathways of sexual reproduction: mating between **a** and α , diploid filamentation upon the opposite mating type fuse and haploid fruiting in the α cell type (Figure 1.2). In mating, two opposite mating haploids fuse and maintained at 25°C, grow as dikaryon filaments, with clamp cells tied to the filaments. In response to an unknown signal, the dikaryon makes a specialised basidium, in which nuclear fusion and meiosis occur. This is followed by mitosis and production of haploid **a** and α basidiospores by budding on four characteristic chains on the basidium. In diploid filamentation, two haploids fuse when are maintained at 37°C. In the moment of fusion, haploid cells and their nuclei fuse to make a yeast form diploid cell that grows as a diploid yeast. As a result of the decreased temperature, brought to 25°C, this diploid changes into monokaryotic filaments with unfused clamp cells. A basidium is made, meiosis followed by mitosis produces **a** and α basidiospores by budding on the basidium.

In both cases, as for mating and diploid filamentation, 50% **a** and 50% α is obtained. The next mechanism of sexual breeding is haploid fruiting. Haploid cells under nutrient deprived conditions make monokaryotic filaments with unfused clamp cells, basidia and fruit haploid α spores. In this strategy, diploid monokaryotic results from haplo α cells endoduplication or cell and nuclear fusion. Clamp cells remain unfused, basidium and haplo basidiospores are formed. Basidiospores are proficient to germinate and grow as haploid cells. Alternatively, they inaugurate one of the three fates all over again (reviewed by (Hull and Heitman, 2002, Idnurm *et al.*, 2005)).

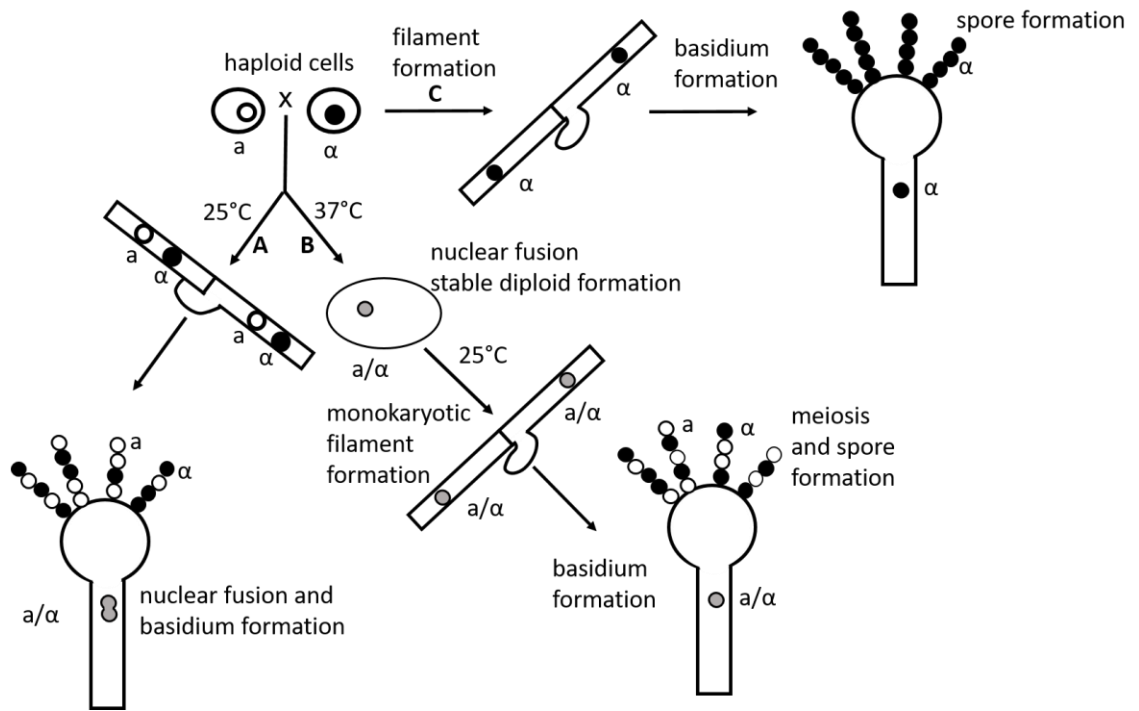


Figure 1.2 Phases of the *C. neoformans* life cycle. (A) mating, (B) diploid filamentation and (C) haploid fruiting. Adapted from (Hull and Heitman, 2002).

Cryptococcus distribution

C. neoformans has a global distribution and has been isolated from a variety of sources with particularly high concentrations in avian excreta and soil (Ellis and Pfeiffer, 1990; Levitz, 1991; Cafarchia *et al.*, 2006; Mitchell *et al.*, 2011). In contrast, *C. gattii* is not as widespread and it is mainly localised to the tropical and subtropical zones and associated trees, in particular with *Eucalyptus* (Kwon-Chung and Bennett, 1984; Sorrell, 2001; Ellis and Pfeiffer, 1990). However, *C. gattii* has also been isolated in temperate regions of Europe, e.g. *C. bacillisporus* and *C. tetragattii* (Hagen *et al.*, 2015). Moreover, it was the tropical fungus *C. deuterogattii* that caused the fatal fungal outbreak on Vancouver Island spreading to the Canadian mainland and into the USA (Stephen *et al.*, 2002; Hoang *et al.*, 2004; MacDougall *et al.*, 2007). This highlights continual evolution of this pathogen into a new environment.

While *Cryptococcus* is not an obligate human pathogen, it possesses sophisticated mechanisms enabling it to adapt to human hosts (reviewed by (Kronstad *et al.*, 2011)); understanding these mechanisms will enable more specific targeting of this opportunistic and increasingly significant pathogen.

1.2.2 Cryptococcal disease

Cryptococcosis, also known as cryptococcal disease, refers to infection caused by fungi from the genus *Cryptococcus*, mostly by the species *C. neoformans* and *C. gattii*. The interaction between *Cryptococcus* and the host leads to a broad range of outcomes, from asymptomatic to systemic infections (reviewed by (Lin and Heitman, 2006; Taylor-Smith and May, 2016)).

C. neoformans (serotype A) is thought to be responsible for approximately 95% of cryptococcal infections and the remaining 4% to 5% of infections are assigned to *C. neoformans* (serotype D) or *C. gattii* (serotypes B/C) (reviewed by (Maziarz and Perfect, 2016)).

Most people exposed to the fungus never get sick from it. Disseminated cryptococcosis is rare in hosts with intact immunity. This means that host defence mechanisms are highly effective at combating cryptococcal disease (Casadevall

et al., 2018). In fact, individuals who never reported cryptococcal infection have antibodies to *C. neoformans* (Chen *et al.*, 1999). However, when the immune system is affected, cryptococci will proliferate and disseminate. This is the case of the immunocompromised such as HIV/AIDS patients. Dissemination might reach the brain by crossing the blood barrier to cause meningoencephalitis and central nervous system (CNS) infection without treatment is lethal. In contrast to *C. neoformans*, which predominantly affects the immunocompromised, *C. gattii* predominantly attacks the immunocompetent in North America (MacDougall *et al.*, 2007). However, a subsequent report indicated that some of the patients were immunosuppressed (Galanis and MacDougall, 2010).

1.1.2.1 *C. neoformans* and *C. gattii* infections in HIV/AIDS, otherwise compromised and immunocompetent individuals

C. neoformans infection principally affects AIDS patients worldwide, especially in sub-Saharan Africa (Park *et al.*, 2009). It was estimated that globally, the annual number of cryptococcal meningitis was 223 100 cases among HIV/AIDS patients with fatalities estimated at 181 100 (Rajasingham *et al.*, 2017). There is also clinical evidence of infections in other immunocompromised cases related to, e.g. lymphoma or being under immunosuppressive regimen due to lupus erythematosus (Korfel *et al.*, 1998; Kiertiburanakul *et al.*, 2006). The majority of infections in the immunocompromised are caused by serotypes A and D of *C. neoformans*, whereas *C. gattii* serotypes B and C account for a smaller proportion of cryptococcosis that often affects the immunocompetent (Jarvis and Harrison, 2008).

If *C. neoformans* infection is not controlled, it can result in life threatening meningitis and/or meningoencephalitis, again in both compromised (Luma *et al.*, 2013) and competent individuals (Malhotra *et al.*, 2017). The literature often reports that HIV-associated cryptococcosis frequently presents with meningitis rather than a respiratory disease. This does not mean that there is no pulmonary involvement. Pulmonary features of cryptococcosis are involved in patients with AIDS (Meyohas *et al.*, 1995; Woodring *et al.*, 1996). It is just that the CNS involvement indicates the advanced stage of HIV infection ((Tenforde *et al.*,

2017). As mentioned, globally, in 2014, 223 100 cases of cryptococcal meningitis were estimated resulting in 181 100 deaths. Globally, cryptococcal meningitis was estimated to be responsible for 15% of AIDS-related deaths. Thus, cryptococcosis is associated with AIDS-related mortality (Rajasingham *et al.*, 2017). Cumulative data enrolled in the two largest prospective trials on AIDS patients described the most common symptoms of HIV-associated *C. neoformans* meningitis: fever, meningismus, visual disturbance and cough (Saag *et al.*, 1992; van der Horst *et al.*, 1997). What is worrying is the fact that while annually 278 000 people are estimated to have cryptococcal antigenaemia, 73% of cryptococcal meningitis cases occur in sub-Saharan Africa (Rajasingham *et al.*, 2017). This means that Africa suffers the greatest burden of this disease (Rajasingham *et al.*, 2017) and remains a huge challenge particularly in resource limited settings.

In contrast to *C. neoformans*, *C. gattii* infections mainly present with pulmonary disease and mostly the immunocompetent are affected (reviewed by (Chen *et al.*, 2014); (Speed and Dunt, 1995; Dewar and Kelly, 2008) but may also cause respiratory disease among HIV-infected persons (Bruner *et al.*, 2018). In addition, cases of *C. gattii* meningoencephalitis in HIV-infected patients have been reported rarely in areas with high HIV prevalence, such as Botswana and sub-Saharan Africa (Steele *et al.*, 2010) and in the USA (Bruner *et al.*, 2018).

To note, the general trend is that *C. neoformans* causes CNS infection, whereas *C. gattii* causes pulmonary diseases. Similarly, mice infected with *C. neoformans* succumb due to CNS involvement, while BALB/c and C57BL/6 mice (two strains used to exclude difference in pathogenesis between the two species) infected with *C. gattii*- due to pulmonary infection (Ngamskulrungrroj, Chang, Sionov, *et al.*, 2012).

The trend is also that *C. neoformans* affects the immunocompromised and *C. gattii*- the immunocompetent. However, there are counter examples, e.g. *C. neoformans* genotypes infecting HIV negative patients (Chau *et al.*, 2010) or *C. gattii* infection of HIV-infected individuals (Steele *et al.*, 2010; Springer *et al.*, 2014). Apart from the CNS or pulmonary involvement, *Cryptococcus* can affect other less frequent body sites such as skin (Jarašūnienė *et al.*, 2020), prostate (S. I. Shah *et al.*, 2017), eyes (Yamada *et al.*, 2019) and bone/joints (reviewed by

(Maziarz and Perfect, 2016)). *C. neoformans* primary cutaneous infection is rare and it is usually associated with skin injury and direct inoculation of the yeast. However, this type of infection can occur in normal host immune state and immunocompromised (Christianson *et al.*, 2003). The skin usually presents with papules, nodules, ulcers or draining sinuses (Neuville *et al.*, 2003). Bone involvement is usually associated with osseous lesions (Vender *et al.*, 1988), swollen soft tissue and pain in the affected area (Wood and Miedzinski, 1996). Prostatic cryptococcosis presents with severe urinary retention (M. R. Chang *et al.*, 2007) and eye disease-with cystic growth (Chapman-Smith, 1977).

1.1.2.2 HIV naïve patients

The most common manifestation of the disease in HIV-negative patients is pulmonary cryptococcosis (Kiertiburanakul *et al.*, 2006). It is hard to estimate the proportion of cryptococcosis in HIV naïve patients given there will be a number of people living with AIDS not in care and undiagnosed or misdiagnosed, especially in low-income countries (Oladele *et al.*, 2017; Rajasingham *et al.*, 2017).

Solid organ transplant patients

Cryptococcosis is one of the most commonly reported invasive fungal infections in solid organ transplants (SOTs) (Rubin *et al.*, 1981; Pappas *et al.*, 2010; Taimur, 2018). Cryptococcosis usually occurs after 16 to 21 months post-transplantation. Most cases of cryptococcosis in SOTs develop after acquiring a new primary fungal infection or upon a quiescent infection reactivation that has been dormant due to the course of immunosuppressants during the post-transplant period (Pappas *et al.*, 2010). The overall incidence of cryptococcosis globally in 1988 was estimated as 2.8% with an overall death rate of 42% (Husain *et al.*, 2001). Approximately 33% of the SOT patients have cryptococcosis confined to the lungs (Singh *et al.*, 2007). However, the disease might spread to the CNS. It is estimated that 39-55% of SOT recipients have CNS involvement (Husain *et al.*, 2001; Singh *et al.*, 2007). The patients suffer from headaches, meningismus, and disturbed vision (Wu *et al.*, 2002; Henao-Martínez and Beckham, 2015).

Interestingly, cryptococcal meningitis is less common in SOT recipients when compared to HIV patients (Davis *et al.*, 2009). SOT requires immunosuppression. The immunosuppression following organ transplant is a major risk for developing cryptococcal disease (Baddley and Forrest, 2013). The immune suppression is to minimise the chance of the organ being rejected. The primary immunosuppressants in SOTs are calcineurin inhibitors such as cyclosporine or tacrolimus. SOT recipients treated with calcineurin inhibitors develop cryptococcosis. Interestingly, calcineurin inhibitors treatment is likely to result in cryptococcosis limited to the lungs but not to a disseminated disease (Singh *et al.*, 2007). Antibodies against T cells are also used in immunosuppression in SOT (Mahmud *et al.*, 2010; Jasiak and Park, 2016). However, increasing use of these antibodies may lead to more frequent occurrence of cryptococcosis in SOT (Silveira *et al.*, 2007). This is because these antibodies are used as immunosuppressants (Wofsy, 1990; Focosi *et al.*, 2011). There are also cases of donor-derived cryptococcosis (Baddley *et al.*, 2011; Camargo *et al.*, 2017). The literature is not evident which serotype of *C. neoformans* causes most infections in SOT patients. With regard to *C. gattii*, although the infections are prevalent in the immunocompetent, the species can also affect SOT patients. For example, the Oregon subtype VGIIc is responsible for 70% mortality in SOTs in that region between 2004 and 2011 (Forrest *et al.*, 2015). Mortality rates in SOT recipients with cryptococcosis have typically ranged from 33% to 42% and may go up to 49% when CNS is involved (Husain *et al.*, 2001).

HIV-negative and non-transplant patients

Cryptococcus can also affect individuals with other predisposing factors, such as liver cirrhosis (Lin *et al.*, 2015), cancers (Kontoyiannis *et al.*, 2001), steroids (Wilson *et al.*, 1970; Nidhi *et al.*, 2017), diabetes mellitus (Li *et al.*, 2017), systemic lupus erythematosus (Matsumura *et al.*, 2011; Fang *et al.*, 2016) or combinations of other immunocompromised groups. It is important to note that medical conditions underlying diseases are indeed predisposing factors likely due to identifiable immunodeficiency. However, there are reports of cryptococcal infections in apparently healthy individuals. It is plausible to think that expanded immunological tests may reveal previously unknown risks in otherwise healthy

cryptococcosis patients (Kwon-Chung *et al.*, 2014). For instance, recently anti-granulocyte macrophage-colony stimulating factor (GM-CSF) autoantibodies were detected in the plasma of otherwise immunocompetent patients and the strains from these patients were reported as *C. gattii* and *C. neoformans* (Saijo *et al.*, 2014). Anti-GM-CSF autoantibodies were also detected in HIV-uninfected otherwise healthy patients with cryptococcal meningitis and it was suggested that this antibody might predispose patients to cryptococcosis (Rosen *et al.*, 2013). Since GM-CSF is important in alveolar macrophages differentiation and function (Shibata *et al.*, 2001), autoantibodies will inhibit GM-CSF signalling and thus predispose patients to cryptococcosis, wherein GM-CSF is critical for control of cryptococcal lung infection in mice (Chen *et al.*, 2007, 2016). Thus, immunological tests seem useful to perform to diagnose risks associated with the development of cryptococcosis.

Cryptococcosis can be also environment-acquired, e.g. an immunocompetent patient with newly diagnosed metastatic cancer develops the disease after occupational exposure to avian excreta (Malhotra *et al.*, 2017). There is also a report that *C. neoformans* was isolated from bagpipes. Whether or not the patient was infected from the bagpipes or bagpipes were secondarily infected-will always remain a mystery (Cobcroft *et al.*, 1978). The plausible answer would be that it was the patient who infected the bagpipes with his sputum.

Diagnostics

There are several diagnostic methods available to detect *Cryptococcus*. The standard is cerebrospinal fluid (CSF) culture. CSF analysis is invaluable because diseases either develop within its bounding membranes (such as meningitis) or parameningeal structures of the brain (e.g. brain abscess) (Jurado and Walker, 1990). Unfortunately the procedure is long (up to two weeks) (Rajasingham *et al.*, 2019) and can produce false negatives (reviewed by (Rhein and Boulware, 2012)). The India ink microscopy enables easy visualisation of the capsule and is the primary diagnostic tool because it is relatively cheap. Although the India ink was recommended as a routine workup on cryptococcosis where its efficacy was described at 84% (Coovadia *et al.*, 2015), the work of (Boulware *et al.*, 2014)

showed that the sensitivity of the India ink is highly dependent on the fungal burden, i.e. the sensitivity decreases with lower burden. The sensitivity of the India ink was calculated at 86% when the fungal burden was high. This means that 1 in 7 diagnoses can be missed. In the case of lower burden (CSF value <1000/ml of CSF), the sensitivity was only 42% (Boulware *et al.*, 2014). The standard is also the detection of cryptococcal antigen (CrAg) in serum or in CSF (Rajasingham *et al.*, 2019). This can be achieved by CrAg including latex agglutination or lateral flow immunochromatographic assay (LFA). CrAg testing by either latex agglutination or LFA was more sensitive than CSF culture, although there were false negative results for LFA (Boulware *et al.*, 2014). Latex agglutination has a sensitivity and specificity of >99% in serum and CSF (Jaye *et al.*, 1998; Kambugu *et al.*, 2008). However it is expensive, laborious and the work of (Boulware *et al.*, 2014) demonstrated that LFA is more sensitive to lower antigen levels compared to the latex method. LFA seems a faster and easier technique as it is a dipstick. Anticryptococcal antibodies on the test strip bind CrAg present in the drop of serum/ plasma/CSF sample, which results in a visible line (Rajasingham *et al.*, 2012). LFA shows the best performance (99.3% sensitivity and 99.1% specificity in CSF). LFA is recognised as “point-of-care” testing for cryptococcosis prior pre-emptive administration of antifungals in resource-limited settings with a high incidence of HIV and cryptococcal diseases (Perfect and Bicanic, 2015; Mamuye *et al.*, 2016).

Treatment

The choice of treatment for cryptococcal disease depends on both the affected organs and the host's immune status. There are guidelines for cryptococcosis in patients: 1) without HIV infection (pulmonary and non-CNS disease; CNS disease), and 2) AIDS-related cryptococcosis (cryptococcal meningitis, cryptococcal pneumonia) (Saag *et al.*, 2000). In HIV-negative, it is crucial to perform lumbar puncture (LP) to rule out the possibility of CNS infection. LP procedure is performed with a hollow needle inserted into the fluid around the lower part of the spinal cord to collect CSF (Saag *et al.*, 2000). In the first case, the goal is prevention of dissemination into the CNS. This is achieved by antifungal therapy with fluconazole, itraconazole or amphotericin B.

In case of significant bone/skin infection, surgery is recommended. The immunocompromised with non-CNS pulmonary and extrapulmonary disease should be treated as patients with CNS disease (Dromer, Mathoulin, Dupont, Brugiere, *et al.*, 1996).

In case of CNS involvement in non-HIV patients, the ultimate objective is the CSF sterilisation and achieved by amphotericin B and flucytosine treatment in the immunocompetent for two weeks (Bennett *et al.*, 1979; Dismukes *et al.*, 1987; Yao *et al.*, 2005). This is the induction phase aimed for the rapid sterilisation of CFS. The immunosuppressed should follow the induction, consolidation and maintenance described for treating cryptococcal meningitis in HIV disease. As for non-HIV patients the consolidation phase introduced designed to kill any remaining cryptococcal cells relies on fluconazole for eight-ten weeks (van der Horst *et al.*, 1997; Beardsley *et al.*, 2019). The maintenance therapy to minimise the risk of the relapse includes fluconazole for a year (Perfect *et al.*, 2010).

In AIDS-related cryptococcal pneumonia, the treatment commonly involves fluconazole (Saag *et al.*, 2000; Krysan, 2015).

In case of AIDS- associated meningeal cryptococcosis, the recommendations are amphotericin B combined with flucytosine (Larsen *et al.*, 1990; van der Horst *et al.*, 1997; Warkentien and Crum-Cianflone, 2010) or amphotericin B when flucytosine cannot be given (Saag *et al.*, 1992, Tenforde *et al.*, 2018). This is the induction phase. After the two week period of successful induction therapy, consolidation therapy. This is achieved with fluconazole administered for 8 weeks (van der Horst *et al.*, 1997). If fluconazole cannot be given, itraconazole is acceptable (Denning *et al.*, 1989). Next, the maintenance therapy is introduced. This is achieved with fluconazole for 6-12 months (Perfect *et al.*, 2010).

In HIV patients with cryptococcal meningitis and CD4-positive T cell counts below 100 cells/ μ l, antiretroviral therapy (ART) is recommended following the completion of the antifungal induction treatment, preferably when CSF has been sterilised (Perfect and Bicanic, 2015). ART decreased the incidence of cryptococcosis among AIDS patients during the 1990s in the USA but the fact that these patients continue to develop cryptococcosis might result from limited access to health care (Mirza *et al.*, 2003). Since cryptococcal meningitis is the

most common HIV-associated disease in sub-Saharan Africa and this region continues to have the greatest burden of the disease globally (Rajasingham *et al.*, 2017) it raises a concern whether those patients have access to ART.

Complications of cryptococcosis

Raised intracranial pressure is a common complication of cryptococcal meningitis. It is dangerous and linked to visual abnormalities and hearing loss (Graybill *et al.*, 2000; Temfack *et al.*, 2019). In both HIV-negative and HIV-positive patients with cryptococcal meningitis, elevated intracranial pressure is one of the cryptococcal indices. Elevated intracranial pressure is defined as opening pressure 200 mm H₂O, measured as an opening pressure at lumbar puncture with the patient in a lateral decubitus position (Doherty and Forbes, 2014). The ultimate objective of the induction treatment is CSF drainage and a radiographic imaging of the brain (Denning *et al.*, 1991). The next complication is cryptococcal immune reconstitution inflammatory syndrome (C-IRIS). The treatment of cryptococcal meningitis and ART commencement might trigger a paradoxical immune response, wherein deterioration of cryptococcal disease that is thought to be caused by recovery of *Cryptococcus*-specific immune responses (reviewed by (Haddow *et al.*, 2011)). This was reported in 30% of HIV patients with *C. neoformans* (Shelburne *et al.*, 2005). The problem is C-IRIS might be caused by too early or too late introduced ART (Perfect and Bicanic, 2015). The management of C-IRIS includes prednisone or dexamethasone tapered over a 2-6 week period as well as LP (Abassi *et al.*, 2015).

1.2.3 Virulence of *Cryptococcus*

A common term in the description of pathogens is a virulence factor. In its simplest definition, it describes the relative infectiousness or a microorganism's ability to overcome the natural host defences. Nevertheless, virulence is an expression of the interaction of the pathogen with its host (reviewed by (Swearengen, 2018)). Thus, in studying fungal virulence, the use of experimental models, such as *in vitro* or *in vivo* systems, is amenable. A successful model of disease will mimic the host-pathogen interactions, which make up the intrinsic

factors of the model. Such model aids understanding of how a disease develops and enables testing potential treatment approaches. The reported experimental models of cryptococcosis are described in section 1.2.4 Experimental models of cryptococcosis. The study of virulence traits among *Cryptococcus* represents a growing focus in the field with the aim of revealing new biological principles or to better understand and treat cryptococcosis. Apart from the use of *in vitro* or animal systems, several tools are available to study cryptococcal virulence. Whole genome sequencing of representatives of both sibling species resulted in hundreds of reference assemblies (reviewed by (Cuomo *et al.*, 2018)), enabling comparative genome studies and microarray studies. This allows to explore virulence genes and understand the molecular basis of virulence mechanisms during cryptococcosis (Kraus *et al.*, 2004; Fan *et al.*, 2005). Fungal genomics opens up a range of experimental opportunities. For instance dynamic genome changes were revealed between *C. gattii* and *C. neoformans* with a hypothesis that those contributed to speciation and virulence (D'Souza *et al.*, 2011). Serial analysis of gene expression (SAGE) to compare the *C. neoformans* transcriptomes at different time-points of mice lung infection with expression patterns from *in vitro* culture or from CSF in a rabbit model of experimental meningitis, revealed that pulmonary infections led to elevated expression of genes related the production and utilisation of acetyl-CoA (Hu *et al.*, 2008). Gene expression microarray analysis comparing highly virulent *C. gattii* R265 and less virulent R272 strains from Vancouver Island revealed virulence candidate genes, e.g. capsule-associated gene, *cas3* or linked to cell wall assembly: glucan 1,3 β -glucosidase and chitin synthase 7 (*chs7*) (Ngamskulrungrroj *et al.*, 2011). Another way to investigate virulence is to study gene loss and characterisation of e.g. phenotypes related to virulence. This can be achieved *in vitro* or *in vivo*. Gene loss also enables virulence candidate genes discovery. A recent work from Nielsen lab found novel genes associated with virulence in mice, e.g. sugar transporter *itr4*, antiphagocytic *app1*, one hypothetical protein-encoding gene (CNAG_02176), as well as genes encoding two additional hypothetical proteins that have orthologues only in *C. neoformans* var. *grubii* (CNAG_04922 and CNAG_06332) and one hypothetical protein with broad taxonomic distribution (CNAG_06968) (Gerstein *et al.*, 2019).

Collectively, these studies outline a critical role for cryptococcal virulence. As part of their defence mechanism many pathogenic species express a wide array of virulence factors adding to their effectiveness, or pathogenesis, enabling them to replicate and disseminate within a host. This brings up an opportunity to discuss the origin of cryptococcal virulence as at first glance *Cryptococcus* seems to be an evolved human pathogen. The vast majority of publications completely ignore the origin of cryptococcal virulence. Moreover, most publications make an impression that *Cryptococcus* is an evolved human pathogen. This is not true. *Cryptococcus* is not a primary pathogen of humans. It is an environmentally occurring pathogen. It does not live with people, humans do not get infected with it unless they are immunocompromised or inhale it with contaminated air. Moreover, *Cryptococcus* is mainly found in soil and trees, so humans probably represent inadvertent hosts rather than a primary niche (Ma, 2009). Simultaneously, the literature demonstrates that *Cryptococcus* is more than just an opportunistic pathogen because it is equipped to evade, subvert and manipulate the host immunity system, while maintaining intracellular growth (Springer *et al.*, 2012). However, from the point of view of virulence origin, it is thought that *Cryptococcus* virulence originated due to accidental pathogenesis (Casadevall and Pirofski, 2007). This concept posits that *Cryptococcus* virulence has arisen independently of a host, by chance alone, to generate microbes that possess attributes necessary for virulence in some hosts (Casadevall and Pirofski, 2007).

Studies of the determinants for pathogenicity have implications for our understanding of host-pathogen interactions. *Cryptococcus* displays several virulence factors, equipping the pathogen for successful invasion of the host, causing fungal pneumonia and meningitis. The following subsections will expand on these virulence factors.

Thermotolerance

Fungi grow between 20°C and 40°C. *C. neoformans* grows at 37°C and its growth rate is highly suppressed between 39°C and 40°C. In contrast, *C. gattii* is not as robust at 37°C (Fernandes *et al.*, 2016), with reported cell death at 40°C within

24 hours ((Hagen *et al.*, 2015), reviewed by (Mitchell and Perfect, 1995)).

However, despite growing slowly or failing to grow at 37°C *in vitro* (Mitchell and Perfect, 1995; Bemis *et al.*, 2000), cryptococci are thermotolerant and growing at mammalian temperature is essential for their virulence (Martinez *et al.*, 2001; Perfect, 2006). The ability to survive at elevated temperature is therefore crucial and this is regulated by calcineurin (Odom *et al.*, 1997; Chen *et al.*, 2013), a Ca²⁺/calmodulin-activated serine/threonine-specific phosphatase (Liu *et al.*, 1991). A good indication of this is the fact, that *C. neoformans* can survive in the avian gastrointestinal tract (about 40°C) (Swinne-Desgain, 1976; Soltani *et al.*, 2013) and proficiently escape avian macrophages via vomocytosis or cell enlargement (Johnston *et al.*, 2016).

Virulence-associated enzymes

It appears that although opportunistic, the fungus seems to be highly adapted to the host environment. Some of the earliest work looking at host-pathogen interactions employed macrophages cultures (Diamond and Bennett, 1973). Cryptococci do not necessarily leave the phagosome as they can survive acidic status of phagolysosome as well as alkaline induced phagocyte killing (Levitz *et al.*, 1997, 1999; Ost *et al.*, 2015)). Killing by reactive oxygen or nitrogen species production has yielded conflicting findings. For instance, hydrogen peroxide (Diamond *et al.*, 1972; Chaturvedi *et al.*, 1996, Upadhyia *et al.*, 2013), hypochlorous acid or hydroxide kill the fungus efficiently (Chaturvedi *et al.*, 1996, Brown *et al.*, 2009). Contrarily, resistance to reactive oxidative and nitrosative species is maintained through the production of a variety of enzymes that break down the oxygen and nitrogen compounds. Superoxide dismutase (SOD) (Figure 1.3) converts superoxide radicals into hydrogen peroxide and molecular oxygen (Fridovich, 1995). *C. neoformans sod1* mutant strains were more prone to be influenced by reactive oxygen species *in vitro* and less virulent in the mouse inhalational model (Cox *et al.*, 2003). Flavohemoglobin denitrosylase (Figure 1.3) has been reported to detoxify nitric oxide and flavohemoglobin *FHB1* gene knock-out showed reduced virulence in murine macrophages (De Jesús-Berríos *et al.*, 2003). Another virulence enzyme is thiol peroxidase (Figure 1.3) encoded by 3 genes: *TSA1* and *TSA2*, *TSA4*, and Missal showed that *tsa1* mutants were

sensitive to hydrogen peroxide and nitrogen oxide in inhalation and tail vein mice models, which resulted in attenuated virulence (Missall *et al.*, 2004). Mice receiving urease restored strains were characterised by high cryptococcal loads in the brains (Olszewski *et al.*, 2004) and alternative oxidase (Figure 1.3) *aox1* mutant strain was strikingly less virulent than both the wild-type and the reconstitute strain in the murine inhalational model and its growth was attenuated in alveolar macrophages (Akhter *et al.*, 2003).

There is some evidence *Cryptococcus* boosts essential nutrients via membrane disruption by phospholipase secretion (reviewed by (Djordjevic, 2010; DeLeon-Rodriguez and Casadevall, 2016)) (Figure 1.3) and therefore hydrolyses phospholipids. Phospholipases contribute to encountering the host, injury and lysis (Ghannoum, 2000). Evans and colleagues (2015) showed *PLB1* knock-out strain of *C. neoformans* had a thorough defect in intracellular growth within host macrophages ascribable to a 50% decrease in proliferation and a 2-fold escalation in cryptococcal killing within the phagosome (Evans *et al.*, 2015). Interestingly, the Plb1 protein of *C. gattii* is larger in mass with a preference for saturated lipid substrates, e.g. dipalmitoyl phosphatidylcholine (Latouche *et al.*, 2002). Since *C. gattii* often causes large lung lesions and dipalmitoyl phosphatidylcholine is abundant in the surfactant lining with the small air spaces of the mammal lung (Gupta *et al.*, 1994; Holm *et al.*, 1996; Bernhard *et al.*, 2001), this may explain why *C. gattii* usually targets the lungs.

Although not previously concerned as proteolytic, *Cryptococcus* can hydrolyse peptide bonds via secretion of proteases (Figure 1.3). Proteolysis of human plasma proteins *in vitro* by *C. neoformans* (Muller and Sethi, 1972) and the synthesis of proteases *in vitro* by a clinical isolate of the *C. neoformans* have been reported (Brueske, 1986).

Cryptococcus also synthesises trehalose (Ngamskulrungrroj, Himmelreich, *et al.*, 2009; Botts *et al.*, 2014) (Figure 1.3) that has been reported to protect proteins and stabilise a biological membrane under heat and cold, starvation, desiccation, osmotic or oxidative stress, exposure to toxicants, and hypoxia in yeasts (reviewed by (Yancey and Siebenaller, 1999; Brown *et al.*, 2007)). *C. neoformans*

genes mediating the trehalose pathways are required for growth *in vitro* at 37°C (Petzold *et al.*, 2006), which might appear to be the reason for causing diseases in humans. The trehalose mutant is avirulent in rabbits and mice (Petzold *et al.*, 2006). The trehalose pathway is also evident in virulence of the highly virulent Vancouver Island *C. gattii* strain, R265 (Ngamskulrunroj, Himmelreich, *et al.*, 2009). The authors showed that deletion of three genes putatively involved in trehalose biosynthesis resulted in the yeast cell death *in vitro*.

A harsh host environment is not only represented by low levels of CO₂, but O₂ is deprived, too. *Cryptococcus* grows very well under atmospheric oxygen conditions and has to overcome hypoxic conditions. Two independent studies conducted by Chang (Y. C. Chang *et al.*, 2007) and Chun (Chun *et al.*, 2007), revealed similar conclusions about the role of *SRE1* (a homologue of the mammalian sterol regulatory element-binding protein (SREBP) and *SCP1* (the SREBP cleavage-activating protein (SCAP)) in response to low levels of oxygen. Chang identified the homologs of *Sre1* and *Scp1*, mutated the genes and analysed phenotypes whereas Chun screened a number of deletion mutants with disrupted growth under low oxygen revealing four genes involved: *SCP1*, *SRE1*, *STP1* and *TOC2*. In both investigations, although using different serotypes of *C. neoformans*, deletions of either *SRE1* or *SCP1* resulted in impaired growth of *C. neoformans* under low oxygen conditions (<3%).

Melanin

One of the defining characteristics of *C. neoformans* is its ability to synthesise melanin (Figure 1.3), a brown to black, hydrophobic, high mass, cell wall associated pigment produced by laccase (Figure 1.3) (Wang *et al.*, 1995, Lee *et al.*, 2019) contributing to the virulence (reviewed by (Butler and Day, 1998; Jacobson, 2000; Zaragoza, 2019)). Rhodes and colleagues showed melanin mutants of *C. neoformans* were less virulent in mice (Rhodes *et al.*, 1982). Amongst many mechanisms by which the pigment adds to pathogenesis, the most important one is scavenging activities against ROS and nitrogen-derived radicals (Jacobson and Tinnell, 1993; Wang and Casadevall, 1994). The fungus possesses two laccase genes, *LAC1* and *LAC2* (Williamson, 1994; Williamson *et*

al., 1998), of which only the first enzyme, Lac1 primarily contributes to melanin synthesis. The corresponding gene however is disunited amongst *C. neoformans* and *C. gattii* (Sugita *et al.*, 2001; Tanaka *et al.*, 2005). Melanisation within *C. gattii* is promoted by *SOD1* as shown in Narasipura's work (Narasipura *et al.*, 2003). It appears that some antibodies can access melanin during infection in a mouse model (Nosanchuk *et al.*, 1998), which is encouraging from a medical point of view, given the pigment is hidden in the cell wall, not in the capsule constituting the first barrier marking off the host. Nevertheless, the first line of defence against ROS weapons provides the yeast capsule and its protective role corresponds to its size (Zaragoza *et al.*, 2008).

Mannitol

C. neoformans synthesises D-mannitol *in vitro* (Onishi and Suzuki, 1968; Wong *et al.*, 1990) and CSF D-mannitol concentrations correspond with severity of infection during experimental meningitis *in vivo* in rabbits (Wong *et al.*, 1990). Under certain assumptions, this was construed as the reason for the raised intracranial pressure in cryptococcal meningitis seen in patients and it is thought to be responsible for the high mortality of this group (Loyse, Wainwright, *et al.*, 2013).

Nevertheless, the best studied virulence factor is the yeast capsule, absent in other fungal pathogens (reviewed by (Zaragoza *et al.*, 2008)).

The polysaccharide capsule

The unique morphological component of *C. neoformans* and *C. gattii* when stained with India ink is a polysaccharide capsule. This technique serves as the main approach to visualise the pathogen both clinically in patients' samples in order to diagnose cryptococcosis, and in experimental settings to detect changes in the size of the capsule. The capsule has been studied for many decades highlighting its importance in driving virulence (Goren and Warren, 1968; Wang *et al.*, 2018; Casadevall *et al.*, 2019). The most studied work on the fungal capsule has been performed using *C. neoformans* as this is its main virulence factor. This arises from McClelland's work where the capsule was the only

significant variable in a regression analysis to estimate the relative contributions of virulence factors (McClelland, et al., 2006). Given its importance in promoting cryptococcal infection potentially leading to a fatal disease, a great effort has been put into capsule research to understand its impact on human health.

The composition of the capsule started to be extensively researched in the eighties and is now well described. Classically the capsule is described as composed of two polysaccharides: glucuronoxylomannan (GXM) (Figure 1.3), comprising 90-95% of its mass and galactoxylomannan (GalXM) (Figure 1.3) accounting for 5-8%, together with mannoproteins (MPs) (Figure 1.3) contributing in less than 1%. The GXM is made of a chain of mannose residues with substitutions of glucuronic acid and xylose. The GalXM consists of a chain of galactose residues with substitutions of xylose and mannose (Frases et al., 2009; McFadden, et al., 2006; Bhattacharjee et al., 1979a; Bose et al., 2003; Walenkamp et al., 1999; Cherniak and Jones, 1988; Cherniak and Sundstrom, 1994). The distinctive difference between *C. neoformans* and *C. gattii* are differences in the structure of GXMs (Cherniak et al., 1992; Young and Kozel, 1993; Otteson et al., 1994).

The capsule composition is worldwide accepted with MPs being a subject of conflict. MPs are considered as the minor components, however, their role in capsule architecture remains unknown (reviewed by (Zaragoza et al., 2009)). Nonetheless, the knowledge regarding MPs has to be improved. A recent publication has shown MPs are efficiently uptaken and presented by dendritic cells to T cells (Mansour et al., 2006).

Some articles explored the localisation of MPs in the capsule and did not find they were integrated with GXM or GalXM, but rather constituted in the inner cell wall (Vartivarian et al., 1989). Reiss and colleagues (Reiss et al., 1984) found MPs and GalXM in sera of cryptococcosis patients. Walenkamp et al. investigated the role of whole cryptococci, GXM, GalXM, and MPs on leukocytes *in vitro* and found increased levels of tumour necrosis factor alpha (TNF α) after 3 hours incubation with all of the tested treatments on monocytes sourcing this protein of healthy patients (Walenkamp et al., 1999). The findings were also reproduced by Delfino (Delfino et al., 1996). This suggests MPs might serve as protective agents against

Cryptococcus. Pitzurra and colleagues demonstrated MPs induced interleukin-12 (IL-12), a cytokine that is involved in protective signalling against the pathogen (Pitzurra *et al.*, 2000). The interaction of GalXM and MPs with polymorphonuclear leukocytes was also investigated by Dong and Murphy showing *in vitro* that *C. neoformans* GXM, but not GalXM or MPs appear in culture filtrates in significant quantities, induces leukocyte chemotaxis (Dong and Murphy, 1993). Leukocytes locomotion was also tested in a murine model using a cryptococcal antigen and sponge implantation where it was observed that culture filtrates antigens of *C. neoformans* var. *gattii* (serotype B and C) isolates inhibited chemotactic responses of polymorphonuclear leukocytes as compared to *C. neoformans* var. *neoformans* (Dong and Murphy, 1995). The finding could suggest *C. gattii* manipulates phagocytic cells to escape killing.

Specht *et al.* suggested MPs were potent immunogenic compounds triggering mammalian T-cell responses. It is not clear though which of the Th lineages they evoke (Levitz and Specht, 2006). Despite MPs promoting protective responses (Vecchiarelli, 2000), research to develop a vaccine using a recombinant mannoprotein showed very little protection (Specht *et al.*, 2017). GXM and MPs have contrasting roles in the regulation of the immune system. Not only GXM provides a negative signal for T cell proliferation, but it is proposed that actively shed GXM, having a large molecular mass and being viscous in a solution (McFadden *et al.* 2006), contributes to elevated intracranial pressure, a crucial contributor to patient morbidity, due to its weight (Bicanic *et al.*, 2009). Raised pressure is established by mechanical obstruction of cerebrospinal fluid. Clinical studies have supported this hypothesis but there are currently no experimental models that allow the mechanistic study. The disruption of the blood brain barrier (BBB) and choroid plexus (CP) has been proposed as a mechanism for the raised intracranial pressure ((Loyse, Thangaraj, *et al.*, 2013), reviewed by (Profaci *et al.*, 2020)). The BBB and CP (where CSF is produced) are potential entry points of cryptococci into the CNS.

The first study examining *ex vivo* capsular phenotype in cryptococcal meningitis and its correlation with host clinical and immune parameters revealed that strains with larger cells and capsules were associated with increased opening pressure

measured by lumbar puncture to look for evidence of conditions affecting the brain (E. J. Robertson *et al.*, 2014). When disseminated into the brain, the fungus can cause meningoencephalitis with symptoms that include headache, fever, vision issues and personality changes (reviewed by (Brizendine and Pappas, 2010)).

Elevated GXM concentrations can be found in serum and cerebrospinal fluid of patients with cryptococcal disease (McFadden *et al.*, 2006) and GXM serves as a cryptococcal antigen in cryptococcosis detection (Monari *et al.*, 2006). GXM inhibits T lymphocytes proliferation by reducing phagocytosis (Syme *et al.*, 1999) and induces apoptosis of lymphocytes from rats *in vitro* (Chiapello *et al.*, 2003). This phenomenon was further confirmed by the same authors *in vivo* (Chiapello *et al.*, 2004). Lately, it was found that T cell apoptosis is induced *in vitro* by binding Fas ligand expressed by GXM loaded macrophages (Monari *et al.*, 2005). GXM modulates inflammatory cytokine response, which varies among neutrophils and macrophages and the phagocytes responses will be discussed further in section 1.5 The innate immune response to *Cryptococcus*.

The capsule pertains in and of itself to a physical barrier between the fungal cell and the host immune system. McGaw and Kozel demonstrated that IgG binds encapsulated cryptococci but this is found on the surface of a cell wall thereby masking the IgG in a manner such that Fc-mediated phagocytosis is disrupted (McGaw and Kozel, 1979). Kozel and Pfrommer showed that encapsulated cryptococci activate complement through the alternative pathway, which results in deposition of iC3b on the capsular surface, implying this is the ligand that interacts with phagocytic cells C3 receptors during phagocytosis (Kozel and Pfrommer, 1986). Interestingly, the *C. neoformans* capsule is highly dynamic as it is able to change its structure and size in response to various stimuli. The composition varies tremendously in multiple biological contexts, even between strains. Cherniak and colleagues analysed 106 isolates, identifying 6 structure motifs in GXM and 8 chemotypes, suggesting each strain has a distinctive capsule (Cherniak, Valafar, *et al.*, 1998). Capsule structures in both lab strains and clinical isolates of the same strain can change over time (Garcia-Hermoso and Janbon, 2004; Franzot *et al.*, 1998). Capsules grown *in vitro* usually have an average thickness of 2.8 μm and in tissue homogenates around 20 μm (Rivera,

et al., 1998) and sizes vary between strains (Neilson et al., 1977, Fernandes et al., 2016).

Cryptococcus utilises complex signalling networks systems to sense its environments and control development of virulence (reviewed by (Kozubowski et al., 2008)). In the case of the capsule, these involve, e.g. cAMP (Alspaugh et al., 2002), cAMP-MAPK (Bahn et al., 2005), calcium–calmodulin–calcineurin pathway, *cap60* expression (Lian et al., 2005) or Ras1 pathway (Zaragoza et al., 2003). Therefore, modulation of capsule size is possible by testing a range of factors influencing these pathways, i.e. HCO₃, iron or serum. As for HCO₃, the biosynthesis of cryptococcal capsule is dependent on adenylyl cyclase activity (Alspaugh et al., 2002). The dissolved bicarbonate directly stimulates adenylyl cyclase to induce cAMP synthesis (Klengel et al., 2005). *C. neoformans* senses CO₂, which diffuses across the plasma membrane and in the form of HCO₃ directly stimulates adenylyl cyclase encoded by *CAC1* gene (Alspaugh et al., 2002) to induce cAMP synthesis (Klengel et al., 2005). Next, iron distress results in an elevated transcript level for *CAP60* gene that is required for capsule synthesis while iron-replete conditions elevate components of the calcium–calmodulin–calcineurin pathway (Lian et al., 2005). Then, cAMP and Ras1 pathway are both necessary for serum-induced capsule enlargement pointing to the role of *CAC1*, *PKA1* and *RAS1* (Zaragoza et al., 2003). Most experiments in the field have been carried out with 10% heat-inactivated fetal calf serum as a potent inducing factor for capsule growth. This is the percentage and serum type that was used in the publication of (Zaragoza et al., 2003). Given early evidence for complement opsonisation of *C. neoformans* in phagocytosis assays with heat-inactivated serum (Diamond et al., 1972), the inactivation is to inactivate complement proteins and to avoid confounding effects, e.g. in immune response studies using immune cell cultures.

Capsule size also changes in response to temperature. One major issue in earlier (Zaragoza et al., 2003) research concerned serum induced capsule growth at 24, 30, and 37°C. Importantly, the volume of the capsule was significantly larger at 37°C and showed a discrepancy between the absolute volumes and the relative amount of capsule compared to the cell size. This discrepancy attributed to the size of the cell body being smaller at lower temperatures. Thus, the temperature

does not impact the proportion of capsule produced by the cell, but it affects the cell body size (Zaragoza *et al.*, 2003).

In contrast, addition of sodium chloride produces a reduction in capsule size (Dykstra *et al.*, 1977). The salt induces physico-chemical contraction of capsular gel (Jacobson *et al.*, 1989). The signalling downstream of sodium for capsule restriction is not understood. However, the most likely, a high osmotic pressure causes a loss of a significant part of the water content of the capsule, which in turn, results in an increased packed cell volume and thereby a decreased capsule size (Zaragoza *et al.*, 2009). Nonetheless, the high-osmolarity glycerol (HOG) pathway is also involved in the response to osmotic shock (reviewed by (Kozubowski *et al.*, 2008)).

In a laboratory set up, the size of the capsule appears to be rather small (Littman, 1958). The author studied the effects of various nutrients on *C. neoformans* encapsulation and successfully demonstrated the dependence of the capsule size on constituents such as amino acids, vitamins, and carbon sources. However, he was not able to verify which component of the capsule was responsible for this phenomenon. Granger *et al.* discovered that encapsulation highly increases *in vitro* within *C. neoformans* H99 strains isolated from cerebrospinal fluid when exposed to high concentration of CO₂/HCO₃ and became resistant to phagocytic engulfment after serum addition used as opsonin (Granger *et al.* , 1985). However, the study did not indicate the phenomenon was due to the serum only. In contrast, some studies showed inhibitory effects of serum on cryptococci growth (Reiss and Szilagyi, 1967). CO₂ availability and its role in capsular enlargement was also tested by Vartivarian and colleagues, reflecting upon physiological conditions confronting the host environment (Vartivarian *et al.*, 1993). The study was linked to iron level where the group found *in vitro* iron deprivation increased the effect of CO₂ on capsule thickness. Finally, Zaragoza and colleagues proved the capsule enlargement in physiological media was due to the presence of serum, however this was not due to the iron limitation (Zaragoza *et al.*, 2003). This was the first study to indicate that the serum alone is a potent inducing factor, i.e. in the absence of CO₂ and after incubation in phosphate buffered saline (PBS). H99 strains were used to investigate the effects

of both serum and CO₂. Capsule size was dependent on the type of a media used and the media determined whether the strain was efficiently responsive to serum or CO₂. Sera from a number of animals showed the ability to promote capsule growth. The increase in capsule size observed *in vitro* suggests a mechanism for the capsular enlargement observed during animal infection (Zaragoza et al, 2003).

A number of authors have recognised that the capsule size increases dramatically during mammalian infection (Cruickshank et al., 1973; Love et al, 1985, Mukaremera *et al.*, 2019). The increase in the capsule volume for *C. neoformans* has also been confirmed *in vivo* in the zebrafish embryo (Bojarczuk *et al.*, 2016). Cruickshank et al. reported an unusual isolate reaching up to 40 µm in the lungs of an African patient, despite the same isolate having a normal appearance on Sabouraud dextrose agar plates (Cruickshank *et al.*, 1973). Another compartment that stimulates capsule enlargement is the brain (Love et al. 1985).

Conversely, a dramatic reduction in capsule size is increased by high osmotic pressure, high salt (NaCl) concentration or the binding of a large quantity of antibody to the capsule (Dykstra *et al.*, 1977; Zaragoza and Casadevall, 2006). Modulation of the capsule *in vitro* with NaCl prior to infection of zebrafish was not sufficient to inflate macrophages uptake or survival of fish as compared to acapsular mutant *cap59* (Bojarczuk *et al.*, 2016). Interestingly, strains with severely compromised capsule formation are not virulent in murine models. Fromtling (1982) obtained acapsular strains by mutagen treatment of *C. neoformans* in order to construe the genes involved in capsule synthesis. Both antibody labelling and India ink stain along with immunochemical analysis showed the dearth of exterior negative charge in acapsular mutants, which is apparent in wild type strains. Genetic analysis revealed chromosomal genes important for capsule synthesis (Fromtling *et al.*, 1982). The analysis was further explored by Chang and colleagues (Chang and Kwon-Chung, 1994, 1998, 1999; Chang *et al.*, 1996). The first gene discovered to play a role in capsule production was *CAP59*, the removal of which resulted in the absence of the capsule. Their aim was to establish the function of the gene, using the deletion mutant and missense mutation, the result of which was a phenotype with disrupted transport

of GXM. Secretion of hydrolysing enzymes was normal in *cap59* mutant leading to the hypothesis that the gene was involved in the export of GXM from the cytoplasm (García-Rivera *et al.*, 2004). Moreover, virulence can be restored by complementation of the acapsular phenotype (Chang and Kwon-Chung, 1994). Authors also identified three other genes linked with the capsule synthesis: *CAP64*, *CAP60* and *CAP10* along with their locations in the genome (Chang *et al.*, 1996; Chang and Kwon-Chung, 1998, 1999). Deletion of these genes confirmed the lack of virulence in a murine model (Chang and Kwon-Chung, 1994, 1998, 1999; Chang *et al.*, 1996).

Acapsular strains cannot replicate in phagocytic cells *in vitro* (Feldmesser *et al.*, 2000), which is also conserved in the zebrafish model of cryptococcosis using *cap59* mutant (Bojarczuk *et al.*, 2016). Thus, the capsule and its components are recognised to be an important virulence factor.

Glycosphingolipid glucosylceramide

Glycosphingolipid glucosylceramide (GlcCer) is a wall component of *C. neoformans* (Rodrigues *et al.*, 2000). GlcCer is another adaptation to the host environment, thus considered as a virulence regulator. Knock-out of the *C. neoformans* glucosylceramide synthase (Figure 1.3) in a immunocompetent mouse model delivered two phenotypes: a) avirulent in nasal infection, unable to disseminate into the brain and contained in the lungs and b) virulent resulting in a fatal infection, when mice were injected intravenously (Rittershaus *et al.*, 2006). GlcCer was required for fungal growth in alveolar spaces and in the bloodstream (neutral/alkaline pH), but not in the host intracellular (acidic) environment, such as in the phagolysosome of lung macrophages. Indeed, a GlcCer mutant did not grow *in vitro* at a neutral/alkaline pH, yet it had no growth defect at an acidic pH (Rittershaus *et al.*, 2006). Even if the mutant was introduced intranasally, cryptococcal growth in the alveoli was arrested. When the mutant grew intracellularly, mice produced a lung granuloma, which efficiently contained the mutant. This resulted in longer host survival as compared with mice challenged with the mutant intravenously. A possible explanation of this is behind the pH and CO₂ concentration. The blood's pH is approximately 7.4 and the CO₂ is

approximately 5%. Therefore, the mutant growth in the blood was arrested until cryptococci were either internalised by phagocytic cells or left the bloodstream to infect the organs, in which they formed abscesses. In both the intracellular environment and in abscesses, the pH is acidic, and the mutant can grow. For instance, in the brain of mice challenged intravenously, the mutant was contained within abscesses. The author hypothesised that once the acidic abscess is formed, the mutant resumes its growth, and this will lead to meningoencephalitis (Rittershaus *et al.*, 2006).

Reflecting upon the study, other authors explored further and used T- and NK-cell-immunodeficient mice that do not produce granulomas (Kechichian *et al.*, 2007). In those, the *gcs1* (GlcCer synthase) mutant introduced intranasally efficiently proliferated in the acidic alveolar macrophages of the lungs and was able to disseminate into the brain (Kechichian *et al.*, 2007). The possible explanation of the proliferation in the lungs is that the cryptococci glycosphingolipid might be adapted to CO₂ concentrations in the host tissues. Usually it reaches 5%. Since GlcCer is required for experimental murine infections that are initiated by inhalation, but not by injection (Rittershaus *et al.*, 2006), it is speculated that *gcs1* mutant prefers the acidic lysosome of alveolar macrophages over extracellular niche (Mitchell, 2006). This also highlights targeting GlcCer could be beneficial in the immunocompromised.

Interestingly, glucosylceramide and sterols accumulate in extracellular vesicles produced by cryptococci. It has been shown *in vitro* in J774 cells and *in vivo* in mice that these vesicles are secreted across the cell wall. They also contain GXM. These findings provide a novel mechanism for the release of the major virulence factor of *C. neoformans* (Rodrigues *et al.*, 2007). The research group also identified seventy-six protein components of *C. neoformans* extracellular vesicle, of which was oxidative stress related. Vesicles were also characterised by laccase and urease activity (Rodrigues, Nakayasu, *et al.*, 2008). The vesicles are successfully established as “virulence bags” (Figure 1.3) (Rodrigues, Nakayasu, *et al.*, 2008; Rodrigues, Nimrichter, *et al.*, 2008) and transported through the cell wall (reviewed by (Rodrigues, Nimrichter, *et al.*, 2008)).

Metal homeostasis

Upon the host entrance, beside oxygen and nutrient paucity, cryptococci experience low metal ion concentrations that are required for virulence enzymes such as urease (Figure 1.3), laccase or superoxide dismutase. A question could be raised: do low metal ion levels influence *Cryptococcus* virulence? Results demonstrate that this is true and that again, *Cryptococcus* possesses its exit strategies, e.g. *C. neoformans* expresses ferroxidases, which enable the reductive iron uptake system to promote the utilisation of transferrin, an important iron source (Jung *et al.*, 2009).

Copper is involved in iron acquisition, oxygen transport, and cellular metabolism. It is also required in melanin synthesis through iron homeostasis or membrane trafficking likely to be leading to laccase loading in the cell wall (Silva *et al.*, 2011). With limited copper, cryptococci activate the transcription of the copper transport genes. As for zinc, *C. neoformans* var. *grubii* and *C. gattii* express *ZAP1* gene encoding the transcription factor Zap1p regulating Zrt1p and Zrt2p zinc transporters homologs (Silva *et al.*, 2011). It has been demonstrated in *C. gattii* that disruption of the *ZAP1* gene diminishes the virulence of the pathogen (de Oliveira Schneider *et al.*, 2012).

Mating types

Clinical and environmental strains represent one of two mating type alleles: MATa or MAT α (Kwon-Chung, 1976b). It has been put forward that a mating type plays a role in the pathogenesis. This is supported by the fact the vast majority of clinical cases are of MAT α (Kwon-Chung and Bennett, 1978). MAT α strains elicit more virulence than congenic MATa strains in mice infected with *Cryptococcus neoformans* var. *neoformans* (Kwon-Chung *et al.*, 1992), and isolates from the Vancouver Island cryptococcosis outbreak in 1999 also representing the MAT α mating type (Fraser *et al.*, 2005).

C. neoformans has never been reported to undergo sexual reproduction in nature (reviewed by (Fu *et al.*, 2015)). However, *C. neoformans* can readily mate bisexually under laboratory conditions. This includes media containing pigeon

guano (Nielsen *et al.*, 2007) and live plants (Xue *et al.*, 2007). Interestingly, *C. gattii* opposite mating does not occur on pigeon guano medium (Nielsen *et al.*, 2007) but it does on plant medium (Xue *et al.*, 2007). This suggests that guano is not a realised ecological niche for *C. gattii* and might correlate with the fact that *C. neoformans* is often isolated from pigeon guano whereas *C. gattii* is not. Instead, *C. gattii* is readily isolated from plants (Nielsen *et al.*, 2007). On the other hand, the fact that under laboratory conditions *C. neoformans* mates on plant medium, might suggest that this species can complete its sexual cycle in nature. It is suggested that plant derived materials can overcome the inhibition of mating by light (Xue *et al.*, 2007), which was recognised as an inhibiting factor in mating (Idnurm and Heitman, 2005).

However, most clinical and environmental isolates of *C. neoformans* and *C. gattii* are of the α mating type, which indicates uncommon opportunity for opposite-sex mating (reviewed by (Phadke *et al.*, 2014)). It is not clear why the populations are largely unisexual if sexual reproduction is a significant component of species survival (Nielsen *et al.*, 2007). On the other hand, it is likely that unisexual reproduction might happen on purpose. Most clinical cases are of A serotype having MAT α mating-type allele (Litvintseva and Mitchell, 2009). Unisexual mating between two closely related α isolates of *C. gattii* is thought to give rise to a hypervirulent alpha type, the causative agent of an outbreak in the Pacific Northwest of the United States and Canada (Fraser *et al.*, 2005; Byrnes, 2011). Within A serotype congenic **a** and α are comparable in terms of virulence in cryptococcal murine meningitis using a rabbit virulence model (Nielsen *et al.*, 2003). As for serotype D, in mice MAT α is more virulent than MAT**a** (Kwon-Chung *et al.*, 1992; Chang *et al.*, 2000). Within serotype B, *C. gattii* MAT α strains are suggested to be more virulent than MAT**a** strains based on the prevalence of MAT α in human infection in a global collection of 163 *C. gattii* strains (Ngamskulrunroj *et al.*, 2008). Within serotype C, it is hard to access which of the mating type is more virulent as the literature is not evident in such comparisons. However, the 176 strains of serotype C isolated from HIV patients in South Africa were MAT α (Litvintseva *et al.*, 2005). Indeed, serotype C seems to be linked with AIDS (Karstaedt *et al.*, 2002; Fraser *et al.*, 2005).

Biofilm

One of the stress resistance mechanisms evolved by the fungus is biofilm formation. These are masses of microorganisms formed on surfaces and held together by an extracellular matrix (Blankenship and Mitchell, 2006). *Cryptococcus* forms biofilms by the release of capsular polysaccharide to the solid surface to create an exopolysaccharide matrix. It has been demonstrated *in vitro* some antibodies can inhibit production of biofilms by encapsulated cryptococci (Martinez and Casadevall, 2005).

Titan and microcells

C. neoformans can greatly modulate its own cell size during infection by forming titan cells that can be up to 100 microns in diameter, in contrast to typical size cells of 5-7 microns (Zaragoza and Nielsen, 2013). The earlier study of (Zaragoza *et al.*, 2010) indicated the capsule was tough, highly cross-linked and resilient to the cryptococcal cell in a murine model of cryptococcosis. Giant cells are defiant to oxidative and nitrosative stress (Okagaki *et al.*, 2011), still too big to be phagocytosed and killed in the lungs (Okagaki and Nielsen, 2012). This emphasises gigantism becoming a new facet in cryptococcal pathogenesis.

In addition to the large cells, *Cryptococcus* can also produce very small cells, called microcells. Alanio and colleagues identified a subpopulation both *in vitro* in J774 macrophage and *in vivo* in OF1 or BALB/c mice, less prone to grow under standard conditions. Perhaps this reflects upon dormancy (Alanio, *et al.*, 2015).

Phenotypic switching

Another attribute of the fungus that has been extensively explored is phenotype switching (Jain and Fries, 2008; Guerrero, *et al.* Fries, 2006). Phenotypic switching occurs in both *C. neoformans* and *C. gattii*. *C. neoformans* var. *gattii* undergoes reversible phenotype switching during murine infections, whereas this process is irreversible in *C. neoformans* var. *neoformans* and *C. neoformans* var. *grubii* (Jain *et al.*, 2006). With *C. neoformans*, the switching occurs *in vivo* following serial passages through mice and leads to an increase in virulence

calling changes to the capsule and/or the cell wall (Fries, et al., 2001). Colonies might appear as smooth, mucoid, wrinkled, serrated or as pseudohyphal (reviewed by (Gupta and Fries, 2010)).

Vomocytosis

Vomocytosis was first reported in 2006 by two independent groups showing the ability of *C. neoformans* to exit phagocytes non-lytically, with the survival of both cells (Alvarez and Casadevall, 2006; Ma *et al.*, 2006). It occurs through fusion of the phagosome and plasma membrane, which could possibly be due to the pathogen modulating the intracellular signals (Johnston and May, 2010), with the plasma membrane, releasing the cryptococcal cell (Ma *et al.*, 2006). The process of *C. neoformans* and *C. gattii* expulsion has been seen in macrophages cell lines (Alvarez and Casadevall, 2006; Ma *et al.*, 2006; Alvarez *et al.*, 2008), primary murine macrophages (Alvarez and Casadevall, 2006), primary birds macrophages (Johnston et al., 2016) and primary human macrophages (Alvarez and Casadevall, 2006; Alvarez, et al., 2009). It is also conserved in zebrafish (Bojarczuk *et al.*, 2016; Gilbert *et al.*, 2017). The non-lytic escape of the pathogen from immune cells is thought to aid in the dissemination and therefore to have a great impact on the progression of disease. However, this implication does not apply to birds that despite being vectors of the disease, do not succumb to cryptococcosis (Littman and Borok, 1968; Johnston et al., 2016). The questions that then naturally arise are: does vomocytosis protect host macrophages from parasitism or is it fundamental to the dissemination of *C. neoformans* in cryptococcal meningitis (Bojarczuk *et al.*, 2016) or *C. gattii* infections?

It is evident now cryptococci are adept intracellular pathogens, with complex pathways, that enable them to proliferate within and eventually exit from host phagocytes. However, while virulence of *C. neoformans* has been discussed by a great number of authors in literature, additional studies to understand more completely the key tenets of *C. gattii* are required. Why *C. gattii*, which is found mostly in association with trees and how it causes diseases in healthy humans- are still unsolved questions. Could more have been known about *C. neoformans* and *C. gattii* virulence determinants, if an *in vivo* model of cryptococcal disease

was developed, that would allow for detailed cellular analysis and concentrate on the innate immunity, which is the first line of defence against any invasion of the human body? Having the animal model, research on cryptococcosis can massively expand and my work can definitively add novel data that represents an addition to virulence knowledge of those cryptococcal species.

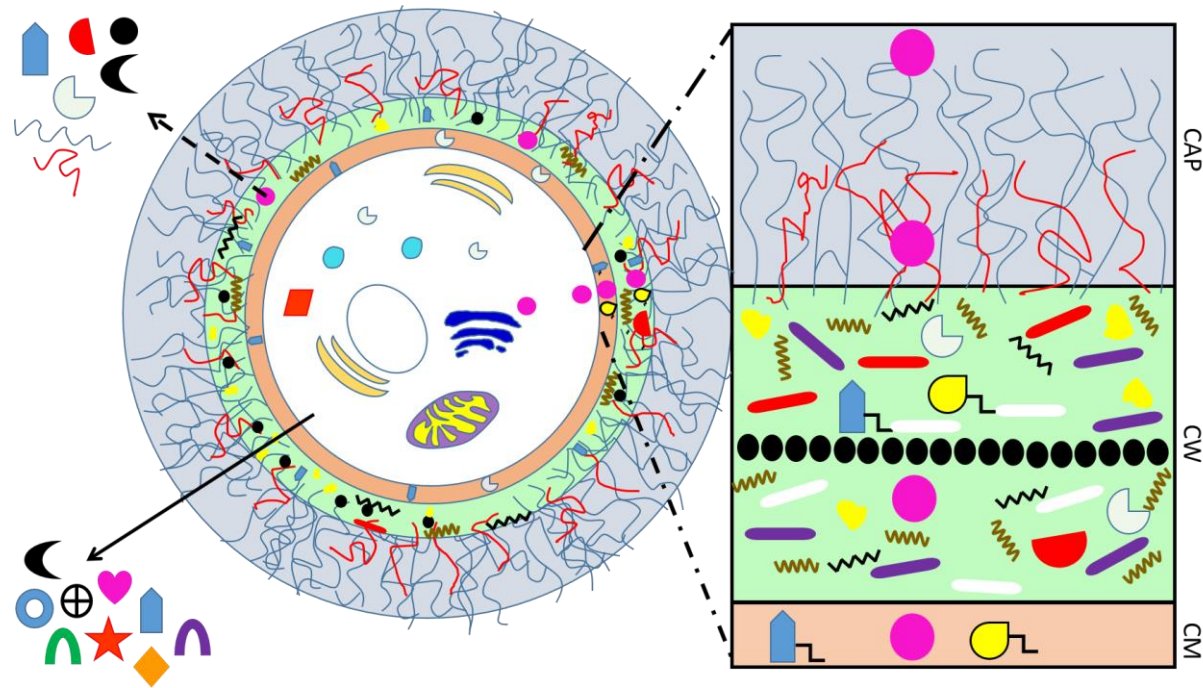


Figure 1.3 Principle virulence factors of *Cryptococcus* species. Dashed dotted line represents enlarged area of the cell membrane (CM), the cell wall (CW) and the capsule (CAP). CM area in beige, CW area in light green, CAP in blue-grey. Dashed arrow represents the content of a virulence bag. Solid arrow represents soluble excreted enzymes. Adapted from (Gilbert *et al.*, 2011; Almeida and Wolf, 2015). Figure legend in Table 1.2.

Table 1.2 Legend to figure 1.3













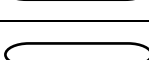









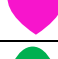






symbol	description
	nucleus
	endoplasmic reticulum
	mitochondrion
	Golgi apparatus
	vacuole
	phospholipase B1
	virulence bag
	chitin deacetylase 2 (Cda2); mannoprotein type
	glycosylphosphatidylinositol (GPI) anchor
	chitin
	chitosan
	mannoprotein
	α -glucan
	β (1,6)-glucan
	β (1,3)-glucan
	GXM
	GalXM
	laccase
	glucosylceramide synthase (Gcs1)
	melanin
	urease
	DNase
	flavinhemoglobin denitrosylase (FHB1)
	alternative oxidase (Aox1)
	thiol peroxidase (Tsa1)

Table 1.2 (continued)

	glutathione peroxidase (Glr1)
	protease
	superoxide dismutase (Sod)
	trehalose

1.2.4 Experimental models of cryptococcosis

There have been many different experimental models of cryptococcosis. In case of *Cryptococcus*, primary cells such as macrophages (Bolaños and Mitchell, 1989; Levitz and DiBenedetto, 1989), neutrophils (Kozel *et al.*, 1984; Dong and Murphy, 1997), endothelial (Ibrahim *et al.*, 1995; Coenjaerts *et al.*, 2006), epithelial (Guillot, Carroll, Badawy, *et al.*, 2008), dendritic (Bauman *et al.*, 2000; Vecchiarelli *et al.*, 2003), NK cells (Ma *et al.*, 2004) or lymphocytes (Zheng *et al.*, 2007; Cheng *et al.*, 2009) have been widely studied. So have been their lines, e. g. macrophages (Ma *et al.*, 2006; Qin *et al.*, 2011), neutrophils (Qureshi *et al.*, 2011), endothelial (Chang *et al.*, 2004; Vu *et al.*, 2009), epithelial (Merkel and Cunningham, 1992), dendritic (Lupo *et al.*, 2008), NK cells (Ma *et al.*, 2004) or lymphocytes (Pericolini *et al.*, 2009). However, *in vivo* models seem more convincing than *in vitro* because they are a complex living system, encompassing the process, pathway, or function under study while being part of a larger “living test tube.” The complexity of the host-pathogen interaction cannot be mimicked by *in vitro* studies. Data obtained from an animal aid us in demonstrating events or interactions that are not possible to collect by other reliable alternative way (reviewed by (Capilla *et al.*, 2007)). *In vivo* models complement *in vitro* studies and can stand alone. Moreover, laboratory animal research models may be modified using genetic technologies that enable testing of specific pathways. There is a significant number of *in vivo* experimental models of cryptococcosis, which can be grouped into invertebrate and vertebrate. Advantages of invertebrates are fewer ethical restrictions, low costs, a well-developed innate immunity, widely available molecular tools and the possibility of enabling high-throughput infection and drug screening assays (Mylonakis *et al.*, 2007). However, no single model can answer all questions and in this aspect it should be noted that invertebrates do not possess the adaptive immune system. The basic underlying mechanisms of immune response can therefore be studied relying on the innate system, which is the most ancient form of pathogen (reviewed by (Sabiiti *et al.*, 2012)). Many invertebrates have been studied in the cryptococcal field, e.g. *Galleria mellonella* (a larvae of the greater wax moth) (Mylonakis *et al.*, 2005), *Caenorhabditis elegans* (a non-parasitic transparent

nematode) (Mylonakis *et al.*, 2002), *Dictyostelium discoideum* (a soil-living social amoeba) (Steenbergen *et al.*, 2001), *Acanthamoeba castellanii* (Fuchs and Mylonakis, 2006) and *Drosophila melanogaster* (a fruit fly) (Thompson *et al.*, 2014). However, these models suffer some disadvantages. For instance, some invertebrates are less susceptible to infection as compared to mice (*G. mellonella* (Bouklas *et al.*, 2015), represent restriction to a specific organ (infection in *C. elegans* restricted to intestine; reviewed by (Sabiiti *et al.*, 2012)), there is no consistency with a natural route of infection (neither the fruit fly nor the moth do not do not represent the natural route of infection unless an opening in cuticle is made) or inability to study phagocytosis (*C. elegans* lack professional phagocytes).

For this reason, any, including cryptococcal research very often uses vertebrates, namely mammals that are biologically very similar to humans in evolutionary terms. These include mice (Wozniak *et al.*, 2011; Ngamskulrungrroj, Chang, Sionov, *et al.*, 2012), rats (Goldman *et al.*, 2000; Wright *et al.*, 2002) and rabbits (Steen *et al.*, 2003; Lee *et al.*, 2010). Rats are used as a model of latency and rabbits of meningitis (reviewed by (Gerstein and Nielsen, 2017)). However, mice are most commonly used. They are a popular choice because they are well established and characterised. The mouse and human genome share approximately 30,000 homologous genes and the proportion of genes without homology between them is less than 1% (reviewed by (Capilla *et al.*, 2007)). This means that parallels and gaps can be identified readily, allowing for the design of robust experimental approaches. However, a controversial publication on the recapitulation of human conditions also exists. A recent study that compared human and mouse immune responses, reported poor correlation between the two organisms (Seok *et al.*, 2013). Yet, whether mice accurately recapitulate the differences in human disease and whether the mouse model identifies subtle variations in virulence factors that impact the outcome of human disease remains unexplored (Mukaremera *et al.*, 2019).

Mice are sensitive to minor changes in food, bedding and light exposure. This might impact experimental results (Reardon, 2016). However, a few mice cryptococcal models exist, e.g. inhalation (Mukaremera *et al.*, 2019),

intraperitoneal (Lim *et al.*, 1980), intravenous (Ngamskulrungraj, Chang, Sionov, *et al.*, 2012; Neal *et al.*, 2017) or intracranial (Thompson *et al.*, 2012), which opens up a range of experimental opportunities. The downside of the mouse model is that pulmonary infection will disseminate to the CNS and yet human infection is rarely synchronous. There are also differences in cryptococcal disease presentations. For instance, R265, VGIIa type strain of *C. gattii* from the Vancouver Island outbreak typically presents with pulmonary disease in humans (Galanis *et al.*, 2009; Harris *et al.*, 2011) whereas *C. neoformans* manifests in meningitis in both compromised (Luma *et al.*, 2013) and competent individuals (Malhotra *et al.*, 2017). Currently, it is difficult to establish an organ specific infection model. Most recently this shortfall has been partly addressed by (Neal *et al.*, 2017) that established a model of meningoencephalitis. Another limitation is susceptibility. For instance, CBA/J mice are more susceptible to intratracheal *C. neoformans* infection than BALB/c mice (Zaragoza *et al.*, 2007). The next issue is reduced imaging potential. Mice do not allow real-time visualisation of the dynamic interaction between innate immune cells and the pathogen. Therefore, they are used for specific experimental time-points. In addition, similarly to rats and rabbits, a variety of genetic backgrounds and genetic tools are available. Of note, a guinea pig model also exists (Kirkpatrick *et al.*, 2007), where oral doses of antifungals sufficient to control fungal infections are similar to the doses in humans (Odds *et al.*, 2000). However, the zebrafish emerges as an attractive model system for a number of human diseases. Zebrafish are ideally suited to be a model for infection and immunity to *Cryptococcus* due to embryos being transparent and hence the potential for *in vivo* subcellular resolution imaging in the entire body of a living vertebrate, which allows interpretation of the whole organismal immune response. In addition, zebrafish are easily bred and when infected-make large-scale studies possible. They give power to complex correlations between host and pathogen at a scale that is not possible in other vertebrates. Zebrafish are proven models of human disease (Lieschke and Currie, 2007), infection biology (Tobin *et al.*, 2010; Volkman *et al.*, 2010; Adams *et al.*, 2011) and of immune cell (Renshaw *et al.*, 2006). They are also proven in high throughput drug discovery (Bowman and Zon, 2010; MacRae and Peterson, 2015). Unlike other non-mammalian models (e.g. *C. elegans*, *D. melanogaster*,

G. mellonella), the zebrafish immune system is highly similar to humans (Lieschke and Trede, 2009) and more than 80% of human genes related to diseases are present in zebrafish (Howe *et al.*, 2013). The study of the innate immune response to *C. neoformans* is not confounded by adaptive immunity because innate and adaptive immune systems develop at different rates. Thus, few ethical restraints apply to zebrafish research at the stage <5.2 days post fertilisation, after which they become protected animals. Zebrafish are also genetically tractable (Lieschke and Currie, 2007). Genome analysis shows that zebrafish share many orthologous genes, and even conserved synteny, with mammals. Zebrafish are vertebrates and thus evolutionarily closer to humans than are, e.g. the fruit fly and the nematode, and they are easier to work with and to study than mice (Van Der Sar *et al.*, 2004). Paralogues divergence is mostly limited to differences in the timing and tissue specificity of expression. This highlights that extra care should be taken in constructing knockout mutations and designing antisense oligonucleotides (Van Der Sar *et al.*, 2004). Another drawback is that although pathogen sensing occurs through PRRs as in vertebrates and zebrafish have a set of 20 putative orthologs of mammalian TLRs, only half of these are orthologs of human TLR family members (Jault *et al.*, 2004). This means the immune response might be slightly different than in humans. In addition, zebrafish lack lungs, which means that this infection route cannot be achieved. The next pitfall applies to inbreeding. Zebrafish do not tolerate it well and rapidly lose fertility (Monson and Sadler, 2010). Nevertheless, zebrafish have become an important animal model to study host-pathogen interactions *in vivo*. Mammalian models do not allow real-time visualisation of the dynamic interaction between innate immune cells and yeasts at distinct sites within the host. They do not permit good visual access to events of pathogenesis at the cellular level, either (Feldmesser *et al.*, 2000; Tenor *et al.*, 2015; Rosowski *et al.*, 2018). This is important when the aim is to investigate early events following dissemination of *Cryptococcus* in a transparent host (Bojarczuk *et al.*, 2016). Therefore, the zebrafish model is ideal. Of note, it is not intentional to replace other vertebrate models such as mice with zebrafish. Instead, zebrafish can reveal fundamental concepts of microbial pathogenesis and host defence

and therefore can help to develop innovative therapies to combat human infection (reviewed by (Gomes and Mostowy, 2020)).

1.3 The innate immunity

The innate immune system constitutes the first line of defence against invading microbial pathogens and is a key for the resolution of inflammation. The innate immune response is non-specific as anything identified as non-self becomes a target. The system comprises: 1) a physical barrier to infection, e.g. epithelial surfaces and tight-junctions between them (reviewed by (Guttman and Finlay, 2009)), mucus and cilia in the lung (reviewed by (Bustamante-Marin and Ostrowski, 2018)) 2) anti-microbial molecules, such as lysozyme (reviewed by (Callewaert and Michiels, 2010)) or defensins (reviewed by (Lisowski et al., 2013)) and 3) innate immune cells.

The innate immunity can be recognised as two branches, the afferent arm for sensing, and the efferent side for combating, with each having cellular and humoral components. The afferent humoral elements include, e.g. lipopolysaccharide binding protein (LBP), that binds to bacterial lipopolysaccharide (LPS), collectins, soluble pattern-recognition molecules, whereas efferent humoral involve, e.g. cytokines, small secreted proteins released by various cells, acting in an autocrine, paracrine or endocrine manner, modulating immune cell behaviour. Other examples of the humoral effector arm include antimicrobial lysozyme, lactoferrin and the complement system. The complement is a series of serum proteins critical for defence from microbial invasion and clearance of immune complexes and injured cells, activated by 3 pathways: classical (antigen/antibody-mediated), lectin or alternative (microbial surface-mediated) (reviewed by (Noris and Remuzzi, 2013)). The afferent cellular can be represented by pattern recognition receptors (PRRs) and the efferent cellular by cell adhesion proteins expressed on the cell surface involved in binding with other cells or with the extracellular matrix (ECM) in the process of cell migration. Other examples of the effector cellular arm include reactive oxygen species, critical components of the antimicrobial repertoire of macrophages and

neutrophils, such as hydrogen peroxide or nitric oxide ((Garaude *et al.*, 2016) and (reviewed by (Beutler, 2004; Nguyen *et al.*, 2017))).

The cellular innate system in vertebrates largely relies on cells of myeloid origins, including polymorphonuclear phagocytes (basophils, eosinophils and neutrophils), and mononuclear (macrophages and dendritic cells (DCs) (reviewed by (Romo *et al.*, 2016))). The reliance on those cells is important in cases where physical barriers are crossed and pathogens gain entry into the host tissues. The innate immune cells recognise the presence of foreign pathogens via pattern recognition. PRRs expressed on the plasma membrane of these cells detect conserved microbial components known as pathogen-associated molecular patterns (PAMPs) or damage-associated molecular patterns (DAMPs). The PRRs family includes Toll-like receptors (TLRs), nucleotide-binding oligomerisation domain (NOD)-like receptors (NLRs), RIG-I-like receptors (RLRs), C-type lectin receptors (CLRs) and AIM2 (absent in melanoma 2)-like receptors ((reviewed by (Chen and Nuñez, 2010; Takeuchi and Akira, 2010))). DAMPs are endogenous (intracellular and extracellular) molecules released following tissue injury, stress or cell death. The PRRs, PAMPs and DAMPs are reviewed in Recognition of infection. DAMPS are described in more detail in section 1.6.1.2 Sterile inflammation.

Activated innate immune cells at the site of infection or injury initiate immune pathways that degrade pathogens via signalling cascades, which results in cytokine release, immune cell chemotaxis, inflammation and phagocytosis (reviewed by (Newton and Dixit, 2012))). Phagocytosis can be initiated via two routes: via contact with particles that have been decorated (opsonised) with complement/antibody allowing the phagocyte to recognise the particle indirectly via Fc receptors (FcRs) and complement receptors (CRs) (reviewed by ((Henneke and Golenbock, 2004))) or direct binding via pattern recognition receptors (reviewed by (Ofek *et al.*, 1995))).

Innate immune system links to the adaptive immune system, which is the targeted response and refers to the long lasting antigen-specific immunity against previously encountered non-self particles. There is a cross talk between the systems. For example, B cells of the adaptive system produce antibodies and

antigen/antibody complexes initiate the classical pathway of complement activation. DCs of the innate system present an antigen to T and B cells of the adaptive and T cells can also regulate DCs (Ruedl *et al.*, 1999; Manickasingham and e Sousa, 2000; Mailliard *et al.*, 2002; Muraille *et al.*, 2002). Epithelium, initially considered as a physical barrier acting as the first line of defence against invading organisms, also express PRRs (Kauffman, 2006; Kato *et al.*, 2007), chemokines (Manzer *et al.*, 2006), cytokines (Jung *et al.*, 1995) and defensins (McCray and Bentley, 1977). Moreover, epithelial cells can trigger and modify the activation and differentiation of DCs, B cells, and T cells (reviewed by (Schleimer *et al.*, 2007)). However, e.g. DCs secrete pro-inflammatory cytokines, which upregulate the expression of class I major histocompatibility complex (MHC-I) on airway epithelial cells to enhance the antiviral responses (Ank and Paludan, 2009). In regards to B cells, it is recognised, they produce cytokines (pro- and anti-inflammatory). The production of pro-inflammatory cytokines by B lymphocytes (Harris *et al.*, 2000), specifically interferon gamma (IFN γ) and TNF α have direct injurious effects on both endothelial and epithelial cells, thereby contributing to both allograft rejection and inflammatory renal disease (Haas *et al.*, 1997; Ishii *et al.*, 2011).

The adaptive immune system requires professional antigen presenting cells (APCs). They phagocytose and degrade pathogens, and present pathogen antigens on MHC-II molecules for recognition by CD4⁺ T cells. This promotes a further immune response, including the further release of cytokines resulting in recruitment of more immune cells (reviewed by (Iwasaki and Medzhitov, 2010)). Non-professional APCs, such as eosinophils, basophils, neutrophils and mast cells, express MHC class I molecules. Only in certain settings they can upregulate MHC class II molecules (reviewed by (Kambayashi and Laufer, 2014)). Antigens displayed by MHC I are recognised by cytotoxic CD8⁺ T cells that kill cells that contain pathogens (reviewed by (Chaplin, 2010)). What links the two systems are also natural killer cells (NK cells). They are cytotoxic lymphocytes of T and B lymphoid progenitor, important in cytokine production (reviewed by (Geiger and Sun, 2016)). NK cells respond rapidly against pathogens and do not possess antigen-specific receptors (only T and B cells do), which classifies them to be the cells of the innate immunity. However, the action of NK cells is similar to that of

effector and memory CD8⁺ T by mediating cytotoxicity upon encounter of its cognate ligand on a target cell. Moreover, NK cells possess a specific receptor for the murine cytomegalovirus (MCMV). Those characteristics categorise NK cells also to the adaptive immune cells (reviewed (Sun and Lanier, 2010)).

1.3.1 Neutrophils

1.3.1.1 Neutrophils in infection and inflammation

Neutrophils are the most abundant (40% to 70%) granulocytes in most mammals. They are of myeloid origin and possess one nucleus typically divided into 2–5 lobes.

Neutrophils provide a first line of defence against numerous infectious pathogens, such as bacteria, fungi, and protozoa. Neutrophils are involved in infection and inflammation. Infection means the invasion of an organism by disease-causing agents, e.g. pathogens. Inflammation is a general term for the local accumulation of fluid, plasma proteins and white blood cells that is initiated by physical injury, local immune response or infection. Neutrophils are the first cells that come out of the blood to deal with infection, i.e. they migrate to infected or injured sites to kill pathogens and remove cellular debris. At the site of infection or inflammation, they will recognise and phagocytose pathogens with the goal of killing microbes via different cytotoxic mechanisms (reviewed (Rosales *et al.*, 2016)). From this point of view, neutrophils are beneficial during infection as neutropenic patients are susceptible to infections (reviewed by (Wang, 2018)). The vast majority of the literature describes neutrophils as being involved mostly in inflammation. However, this results from the fact that researchers interested in inflammation very often concentrate on neutrophils. What cannot go unnoticed is that neutrophils evolved to leave the blood to prevent infection. Thus, their primordial role is to prevent infection. Their role in inflammation evolved from the role of infection because every infection is associated with inflammation and the fact that neutrophils have to be controlled. Otherwise, neutrophils can be damaging and implicated in tissue damage, e.g. upon the spillage of their cytotoxic content when they do not die by apoptosis (Haslett, 1999; Miles *et al.*, 2009). Tissue damage

caused by neutrophils is seen in chronic inflammation (reviewed by (Medzhitov, 2010)). Other example represents a situation, when neutrophils detect TNF α but do not encounter a microorganism after migrating to tissues, they release their granules into the extracellular space to create a harsh environment for nearby pathogens (Nathan, 2006). In this sense, the tissue damage aids microbes containment but is also harmful to the host.

1.3.1.2 Neutrophil recruitment

Neutrophils are produced in the bone marrow from haematopoietic stem cells. This process is regulated by the cytokine granulocyte-colony stimulating factor (G-CSF) driving the maturation and functional activation of neutrophils (reviewed by (Berliner, 2008)). The bone marrow pool serves as a reserve, available for release. In addition, intravascular (marginated) neutrophil pools within the capillary beds of the spleen, liver and lung exist (reviewed by (Summers et al., 2010)). Mature neutrophils are continually released into the circulation. The neutrophils exit the bone marrow at a rate of 10^{11} cells per day (reviewed by (Furze and Rankin, 2008)). In response to inflammation or infection, neutrophils are mobilised to exit the bone marrow. The stimuli to leave the bone marrow are pro-inflammatory chemoattractant factors such as leukotriene B₄ (LTB₄), complement factor C5a, IL-8 (reviewed by (Furze and Rankin, 2008)). Resting neutrophils from the circulation can be primed by bacterial products and cytokines or chemokines, e.g. TNF α , GM-CSF, IL-8 and IFN γ (reviewed by (Hallett and Lloyds, 1995)). Thus, the neutrophils become primed to be recruited to the sites of injury, inflammation or infection. The priming is a two-step process. In the first one, the key players are TNF α , IL-1 β , and pathogen associated molecular patterns (PAMPs) such as endotoxins. In the second, IL-8, LTB₄ and GM-CSF, are important (reviewed by (Summers *et al.*, 2010)). A proper priming ensures augmented respiratory burst activity, degranulation and longevity (reviewed by (Vogt *et al.*, 2018)). Activated and primed neutrophils will roll, adhere and transmigrate to the site of inflammation/infection (reviewed by (Muller, 2013; Liew and Kubes, 2019)). The pathways involved in neutrophils recruitment are well studied and involve, e.g. Phosphoinositide 3-Kinase (PI3K) and Mitogen

Activated Protein Kinase (MAPK) signalling (Curnock *et al.*, 2002; Heit *et al.*, 2002).

1.3.1.3 Neutrophil diapedesis and chemotaxis

TNF α , IL-1 β , and IL-17 that are produced during inflammation/infection, initiate the process of neutrophil recruitment to the site of infection/inflammation. These cytokines generate expression of P-selectin, E-selectin and members of the integrin superfamily on the luminal surface (reviewed by (Borregaard, 2010)). E- and P-selectins are expressed by inflamed endothelial cells whereas L-selectin is expressed by most leukocytes. P-selectin is also expressed by activated platelets (reviewed by (Ley *et al.*, 2007; Filippi, 2016)). E- and P-selectins bind P-selectin ligand 1 (PSGL-1) and L-selectin, which are expressed constitutively on neutrophil microvilli (reviewed by (Borregaard, 2010)). E-selectin also binds to glycosylated CD44 and E-selectin ligand 1 (reviewed by (Ley *et al.*, 2007)). Selectins bind ligands on the surface of neutrophils to facilitate the rolling process. After rolling, firm adhesion occurs. This is via integrins. Neutrophils express high levels of the lymphocyte function-associated antigen (LFA-1) or macrophage antigen-1 (Mac-1) (reviewed by (Ley *et al.*, 2007)). Chemokines and cytokines activate leukocyte integrins binding to immunoglobulin superfamily members, such as ICAM-1 (Campbell *et al.*, 1996; Wooten *et al.*, 2008). This is termed 'inside-out' signalling (anchoring leukocytes to the extracellular matrix (ECM)), which alters the conformation of β 2 integrins such as LFA-1 or Mac-1. The next step is 'outside-in' signalling. This is described as extracellular stimuli induce intracellular changes, i.e. ligation of a cell-surface receptor activates signalling pathways inside the cell. The signalling initiates transmigration (reviewed by (Zarbock and Ley, 2008)). Inside-out and outside-in signalling can occur concurrently (reviewed by (Legate *et al.*, 2009)) or a switch from a paracellular to a transcellular route can take place (reviewed by (Petri *et al.*, 2008)).

Once firm adhesion is established, neutrophils will travel transcellularly, across one epithelial cell, at non-junctional locations, through the endothelial cell, or paracellularly, between two tightly apposed endothelial cells (reviewed by (Petri

et al., 2008)). The main players in either type of migration are LFA-1 and Mac-1 adhesion molecules on neutrophils and their ligands ICAM-1 and ICAM-2 (reviewed by (Borregaard, 2010)). Mac-1 points to paracellular migration (Phillipson *et al.*, 2009; Woodfin *et al.*, 2009) whereas ICAM-1 to transcellular migration (Yang *et al.*, 2005), although other signalling molecules are also acknowledged. For example, in paracellular migration, endothelial cell-selective adhesion molecule (ESAM), ICAM-2 and CD99, platelet/endothelial-cell adhesion molecule 1 (PECAM1) and possibly endothelial-cell junctional molecules, such as junctional adhesion molecule A (JAM-A), are involved. In transcellular, ICAM-1 ligation translocates ICAM-1 to actin- and caveolae-rich regions. ICAM-1 containing caveolae link together forming vesiculo-vacuolar organelles (VVOs) that form an intracellular channel through which a leukocyte can migrate (reviewed by (Ley *et al.*, 2007)).

Next, in response to chemical signals, such as C5a, LTB₄, IL-8 and chemokines (e.g. CXCL4) neutrophils perform a directional migration along a chemical gradient (chemotaxis) (reviewed by (Cichetti *et al.*, 2002; Petri and Sanz, 2018)). The chemoattractant hierarchy is as follows: lipid mediators, such as LTB₄ appear to initiate neutrophil recruitment cascades. Then, the attracted leukocytes produce cytokines, which in turn, induce the local release of chemokines, thus amplifying neutrophil recruitment. This is termed lipid–cytokine–chemokine cascade (Sadik and Luster, 2012).

1.3.1.4 Neutrophils phagocytosis, degranulation, respiratory burst, swarms and extracellular traps

Neutrophils internalise both opsonised and non-opsonised particles. The principal opsonic receptors of neutrophils are Fc receptors and a sub- group of β 2 integrins, bind to immunoglobulin or complement-coated particles, respectively. The main Fc receptors of human resting neutrophils are Fc γ RIIA (CD32) and Fc γ RIIIb (CD16) (reviewed by (Lee *et al.*, 2003; Rosales, 2017; Wang and Jönsson, 2019)) (Table 1.5 in section 1.6.1.1.3 Control of infection and elimination of pathogens). Non-opsonic receptors include pattern recognition receptors (PRRs) (Table 1.5). The binding of a receptor with ligands on the

phagocytic target is crucial to the initiation of phagocytosis (Herant *et al.*, 2006). During phagocytosis an increase of intracellular free calcium is detected immediately after initiation of phagocytosis in neutrophils (Sawyer *et al.*, 1985). More specifically, in Fc γ -receptor (Fc γ R) induced phagocytosis an increase of intracellular calcium occurs (Young *et al.*, 1984). The role of calcium in Fc γ R-mediated phagocytosis remains controversial. Fc γ R mediated phagocytosis in neutrophils was reported calcium dependent (Kobayashi *et al.*, 1995) or independent (Della *et al.*, 1990). However, for complement CR3-mediated phagocytosis in neutrophils, calcium plays no role (Lew *et al.*, 1985; Della *et al.*, 1990). Internalisation of a pathogen requires actin polymerisation (Aderem and Underhill, 1999; Engqvist-Goldstein and Drubin, 2003) and later on actin depolarisation to complete phagosome closure. This is regulated by calcium, which also is required for fusion of antimicrobial neutrophilic granules with phagosomes (Bengtsson *et al.*, 1991) and at least in part, for respiratory burst (Kim-Park *et al.*, 1997). A few types of cytotoxic granules exist: primary (azurophilic), secondary (specific) and tertiary (gelatinase). Azurophilic granules are secreted first in myelopoiesis at the promyelocyte stage and are myeloperoxidase (MPO) positive. They also contain various proteolytic enzymes, such as defensins, lysosomal hydrolases, and neutral serine proteinases, such as elastase, proteinase 3 (Pr3), and cathepsin G, which are antimicrobial (reviewed by (Falloon and Gallin, 1986; Van Der Veen *et al.*, 2009; Yin and Heit, 2018)). The secondary and tertiary granules formed later during neutrophil maturation, contain overlapping sets of proteins, but are peroxidase negative (Faurischou and Borregaard, 2003; Van Der Veen *et al.*, 2009). Neutrophils release granules content by degranulation, or exocytosis, of membrane-bound secretory granules (reviewed by (Lacy, 2006)). The primed granules exocytosis is hierarchical. First secondary and tertiary granules are discharged and then primary (Van Der Veen *et al.*, 2009; Vogt *et al.*, 2018). This is because of the order of the synthesis, wherein the secondary and tertiary are produced last. It is critical that neutrophil granules do not spill their cytotoxic content into surrounding tissue. Therefore a control mechanism exists, wherein the granules do not spill out until receptors in the plasma membrane or phagosome membrane signal to the cytoplasm to activate their movement to the cell membrane for secretion of their contents by

degranulation (reviewed by (Lacy, 2006; Mollinedo, 2019; Lodge *et al.*, 2020)). Particular importance attaches to the azurophil's myeloperoxidase. This enzyme reacts with hydrogen peroxide (H_2O_2), formed by the NADPH oxidase and with chloride anion to produce hypochlorous acid (Harrison and Schultz, 1976). This forms a strong antimicrobial system (reviewed by (Klebanoff, 2005; Lazarevic-Pasti *et al.*, 2015; Ndrepepa, 2019)). This is linked to a respiratory burst, which is the rapid release of reactive oxygen species (ROS). During phagocytosis, the oxygen species are of paramount importance because they contribute to the destruction and killing of engulfed pathogens. Not only is hypochlorous acid produced. For instance, the superoxide anion O_2^- and H_2O_2 , the products of NADPH oxidase (reviewed by (Roos *et al.*, 1988; Babior, 2004)) give rise to several additional ROS. Both H_2O_2 and O_2^- are potent oxidising and antimicrobial agents. The cytotoxic effects of O_2^- and H_2O_2 are achieved due to reactions with other antimicrobial systems to generate more ROS, e.g. hydroxyl radical ($\text{OH}\cdot$), singlet oxygen ($^1\text{O}_2$). For instance, superoxide reacts with either hypochlorous acid (HOCl) or nitric oxide ($\text{NO}\cdot$) to form the hydroxyl radical ($\text{OH}\cdot$). As mentioned, hypochlorous acid (HOCl) is formed by the action of myeloperoxidase (MPO). The nitric oxide ($\text{NO}\cdot$) is produced by the action of nitric oxide synthase (NOS). Singlet oxygen can be formed by the non-enzymatic dismutation of O_2^- and in a reaction between hydrogen peroxide and hypochlorite (OCl^-). Singlet oxygen has recently been shown to react with H_2O in an antibody-catalysed reaction to form hydrogen peroxide and ozone (O_3) (reviewed by (Robinson *et al.*, 2004; Onyango, 2016)). Apart from oxygen species, the process of phagocytosis is facilitated by reactive nitrogen species (RNS). The above-mentioned nitric oxide ($\text{NO}\cdot$) is in fact considered as RNS by means of nitric oxide synthase (NOS). Apart from the reaction with superoxide (O_2^-) to form hydroxyl radical ($\text{OH}\cdot$) (Ramos *et al.*, 1992), it can also produce peroxynitrite (ONOO^-) from superoxide (O_2^-) (Carreras *et al.*, 1994). Peroxynitrite is another type of RNS that oxidises tissue non-protein and protein sulfhydryl groups making it a cytotoxic agent (Radil *et al.*, 1991). Recently, it has been shown that peroxynitrite mediates the failure of neutrophil migration (Torres-Duñas *et al.*, 2007). This means that the respiratory burst and RNS products are not only able to destroy pathogens but may also have detrimental effects for the host. Moreover, ROS/RNS are

generated as by-products of cellular metabolism. Fortunately, the housekeeping production of reactive species is generally neutralised by constitutive antioxidant defences (reviewed by (Paiva and Bozza, 2014)) e.g. superoxide dismutase (SOD) converts O_2^- to H_2O_2 .

Neutrophils can also produce swarms in response to an inflammatory stimulus or infection. This has recently been explored *in vivo* in the zebrafish embryo by inducing sterile inflammation via tail injury or infecting the zebrafish with *S. aureus* by otic vesicle injection (Isles *et al.*, 2019). The 'pioneer neutrophil' is thought to release additional chemoattractants to recruit more neutrophils (Ng *et al.*, 2011; Lämmermann *et al.*, 2013). The swarming has also been observed *in vitro* in response to *C. neoformans* (Sun and Shi, 2016).

Neutrophils perform also another distinct antimicrobial activity termed neutrophil extracellular traps (NETs). This is described as extruding a meshwork of chromatin fibres furnished with granule-derived antimicrobial peptides and enzymes such as neutrophil elastase, cathepsin G, and MPO. The stimuli for NETs production are IL-8 and lipopolysaccharides (LPS) (Brinkmann *et al.*, 2004). At the same time, defects in the signalling cascades that cause NET formation (such as deficiencies in generating ROS in chronic granulomatous disease or neutrophil serine proteases in Papillon–Lefèvre syndrome) are linked to pathologies characterised by chronic autoimmunity and inflammation, both of sterile and infectious origin (reviewed by (Boeltz *et al.*, 2019)).

1.3.1.5 Neutrophil response to infection/inflammation

Various pathogenic factors, such as infection or tissue injury, can induce inflammation by causing tissue damage. A response to inflammation in the absence of microbial organisms is termed the sterile inflammatory response. It is well known that the immune system recognises foreign particles via pattern recognition. In case of microbial infection, Toll-like receptors (TLRs) expressed on the plasma membrane of phagocytic cells such as neutrophils, detect conserved microbial components known as pathogen-associated molecular patterns (PAMPs). In the sterile inflammation so without pathogen involvement,

damage-associated molecular patterns (DAMPs) are detected by TLRs (reviewed by (Chen and Nuñez, 2010)). Pathways that have evolved to respond to infection are also used to respond to non-microbial triggers (sterile inflammation), although some distinct pathways exist, e.g. receptor for advanced glycation end products (RAGE) is distinct to the sterile inflammation (reviewed by (Shen *et al.*, 2013)). Generally, both infectious and non-infectious stimuli and cell damage activate inflammatory signalling pathways, most commonly the nuclear factor kappa-light-chain-enhancer of activated B cells (NF-κB), mitogen-activated protein kinase (MAPK) and Janus kinase/signal transducers and activators of transcription (JAK/STAT) pathways (reviewed by (Chen *et al.*, 2018)).

1.3.1.6 Neutrophil longevity and death

Circulating neutrophils have a short half-life of approximately 8 hours (Dancey *et al.*, 1976) while activated neutrophils that have migrated into tissue have a half-life of up to four days (Edwards *et al.*, 2004). That means that under inflammatory conditions, their longevity significantly increases, which ensures the presence of primed neutrophils at the site of inflammation (reviewed by (Summers *et al.*, 2010)). The longevity results from exposure to pro-inflammatory mediators such as GM-CSF, IL-1β, TNFα and IFNγ, which interfere with apoptotic pathways (Colotta *et al.*, 1992). The extended lifespan of inflammatory neutrophils at the site of inflammation is also supported by their continuous recruitment and inhibition of the normal spontaneous neutrophil apoptosis. This is to allow neutrophils to perform their function effectively.

Of note, more recently, literature has emerged that offers a contradictory finding about circulating life span. *In vivo* ²H₂O labelling of human neutrophils suggested a mean lifespan of 5.4 days (Pillay *et al.*, 2010).

However, it should be emphasised there is a reason why neutrophils are considered as suicidal killers and concomitantly key effectors of immunity (Selders *et al.*, 2017). The half-life in the circulation is short because they constitutively undergo apoptosis. As mentioned, under steady-state conditions about 10¹¹ neutrophils turn over per day in a healthy human adult (reviewed by (Cartwright *et al.*, 1964; Summers *et al.*, 2010)). Therefore, spontaneous

(constitutive) neutrophil apoptosis is crucial for the maintenance of immune system homeostasis. This occurs in the absence of cytokines or other pro-inflammatory mediators prior to their removal by macrophages through the process of efferocytosis (Savill *et al.*, 1989). If neutrophils are not removed, they accumulate. This disadvantage would be further exacerbated by neutrophilia. The accumulation of neutrophils and their toxic cargo in the tissues is linked to e.g. shortness of breath and hypoxia as well as neurologic deficits. This might be due to increased blood viscosity and obstructed blood flow (reviewed by (Summers *et al.*, 2010)).

Activated neutrophils do not undergo apoptosis. This means they do not undergo apoptosis just yet because if they are activated they are performing their function e.g. at a site of injury or infection.

Once that is done, inflammation is resolved. Inflammatory neutrophils undergo apoptosis and then are cleared by tissue macrophages (Savill and Haslett, 1995). This is how affected or damaged cells during disease conditions are eliminated and promotion of the resolution of inflammatory responses occurs (Bratton and Henson, 2011). If neutrophils are not removed, i.e. the inflammatory response fails to resolve, host tissue injury occurs resulting in chronic inflammatory diseases.

Apoptosis (type 1-programmed cell death) is the most common type of death. However, others exist: necrosis or suicidal NETosis (reviewed by (Iba *et al.*, 2013)). All of these death types have a significant implication in health and disease. For instance, necrosis is disadvantageous because it is crucial to keep the neutrophil cell membrane integrity, which is assured by apoptosis (Savill and Haslett, 1995). If apoptotic neutrophils are not effectively removed from inflamed sites, they may undergo secondary necrosis, losing their membrane integrity and spilling out their destructive contents (Majno and Joris, 1995) again initiating inflammatory signalling (Ward *et al.*, 1999). If apoptosis is delayed, neutrophils persist and this may cause host tissue injury. Uncontrolled degranulation and release of ROS into the ECM medium contribute to tissue damage. Normally the uncontrolled activity of elastase, Pr3, and cathepsin G is counterbalanced by endogenous serine protease inhibitors (reviewed by (Korkaz *et al.*, 2010)). The release of ROS can inactivate these inhibitors, allowing these proteases to

damage the ECM (reviewed by (Weiss, 1989)). Thus, it is understandable that delayed apoptosis delays the resolution of inflammation (Loynes *et al.*, 2010). Apoptosis includes DNA fragmentation (Matute-Bello *et al.*, 1997). Apoptotic neutrophils expose phosphatidylserine (PS) (Frasch *et al.*, 2004), which functions as an eat-me signal to macrophages (Fadok, De Cathelineau, *et al.*, 2001). In NETosis, PS is not exposed (Fuchs *et al.*, 2007). The exposure of PS in necrotic cells is debatable (see section 1.6.1.1.4 Termination of inflammation). In contrast to apoptosis and necrosis, the cell membrane breaks (Fuchs *et al.*, 2007). Apoptotic and necrotic cells are removed by macrophages. However, necrotic to a lesser extent (Brouckaert *et al.*, 2004). NETosis suicidal neutrophils are also removed by macrophages, representing an anti-inflammatory mechanism (Farrera and Fadeel, 2013).

Of note, accelerated neutrophil death leads to neutropenia and delayed neutrophil death results in neutrophilia. The balance between neutrophil life-and-death is an important determinant of the degree of tissue injury, infection and inflammation.

An intriguing phenomenon of resolving the inflammatory response is represented by reverse migration. This is described as a migration phenotype away from inflamed sites back to the circulation, promoting neutrophils clearance at the wound (Tharp, 2005; Buckley *et al.*, 2006; Mathias *et al.*, 2006). Perhaps in this manner neutrophils are preserved when they are no longer needed to fight infection. However, a question might be raised whether re-entering circulation could disseminate inflammation into other organs, eventually leading to damage (reviewed by (Kolaczkowska and Kubes, 2013)). The contribution of reverse migration to resolution of inflammation remains to be elucidated (reviewed by (De Oliveira *et al.*, 2016)).

Inflammation (including the sterile one) and infection encompassing the time-course, control and termination of these processes are described in section 1.6 Inflammation and disease.

1.3.1.7 Inflammatory disease

As described above neutrophils are a major cause of inflammation driving a number of significant diseases. The diseases result from a failed inflammatory response and persistent neutrophilic inflammation. Associated risks are a significant host tissue damage and chronic inflammation. The latter is usually accompanied by tissue destruction. In this aspect, neutrophils contribute to the pathogenesis of many inflammatory diseases. The examples of pathological and chronic diseases are: asthma, chronic obstructive pulmonary disease (COPD), cystic fibrosis (CF), bronchiectasis (reviewed by (Gernez *et al.*, 2010)) or idiopathic pulmonary fibrosis (IPF) (Kinder *et al.*, 2008).

1.3.2 Macrophages

Macrophages functions are phagocytosis, antigen presentation and immunomodulation through cytokine production (reviewed by (Dale *et al.*, 2008)).

1.2.2.1 Origin of macrophages

In the past few years, the understanding of macrophage origin has been drastically changed.

Macrophages, similar to neutrophils, are myeloid immune cells. This means that they also originate in the bone marrow. The common myeloid progenitor is the precursor of macrophages and neutrophils. However, in the blood the haematopoietic stem cells give rise to e.g. neutrophils and monocytes. Only when there is tissue damage or infection, the monocytes will leave the circulation and differentiate into macrophages (J. Yang *et al.*, 2014). Blood monocytes can also give rise to monocyte-derived dendritic cells under inflammatory conditions (reviewed by (Ginhoux and Jung, 2014; Qu *et al.*, 2014)). It was long thought all macrophages originated from a continuum of monocytic differentiation. However, tissue-resident macrophage populations exist within specific organs/tissue. Adult tissue resident macrophages derive from embryonic progenitors that seed developing tissues before birth (reviewed by (Ginhoux and Jung, 2014)). This means that many resident tissue macrophages are set up very early in fetal

tissues and persist into adulthood independently of blood monocyte input in the steady state (Ginhoux *et al.*, 2010; Jakubzick *et al.*, 2013). Tissue macrophages can undergo self-renewal, e.g. arterial ones (Ensan *et al.*, 2016) from embryonic precursors seeded at birth rather than constant recruitment from blood (reviewed by (Ginhoux and Jung, 2014)). Tissue macrophages are derived from three different developmental programs in humans. The first wave (primitive) begins in the yolk sac. Here, amongst others, macrophage progenitors arise and afterwards give rise to pre-macrophages and then yolk sac or primitive macrophages at the origin of microglia. Primitive macrophages infiltrate all tissues and generate microglia in the brain. The primitive wave is without monocytic intermediates. The second wave (transient) also occurs in the yolk sac and gives rise to erythro-myeloid progenitors. These give rise to the first fetal monocytes. Erythro-myeloid progenitors derived fetal monocytes seed most embryonic tissues apart from the brain. These fetal monocytes differentiate into most adult resident macrophage populations. The last wave (definitive) starts in the aorta-gonads-mesonephros in the yolk sac and generates first haematopoietic stem cells. During this wave, haematopoietic stem cells-derived monocytes also emerge from the fetal liver. These monocytes contribute to the long-lived macrophage pool established at birth whereas the adult haematopoiesis starts in the bone marrow. To summarise, most tissue-resident macrophages are long-lived cells derived from a transient haematopoietic wave of erythromyeloid progenitors emerging in the yolk sac (reviewed by (Yoder, 2014; Hoeffel and Ginhoux, 2018)). This means that a definition of macrophages should reflect on two types: 1) resident macrophages- fetally derived resident white blood cells that live and proliferate within tissues and 2) monocyte derived macrophage- definitive derived monocyte that differentiates into a macrophage following extravasation.

1.2.2.2 Macrophage recruitment in infection/inflammation

After maturation monocytes are discharged by the bone marrow into the bloodstream (reviewed by (Teh *et al.*, 2019)). The recent mice data suggest that chemokines, namely MCP-3 and MCP-1 activate C-C chemokine receptor type 2 (CCR2) and this mobilises monocytes to exit the bone marrow (Tsou *et al.*, 2007). Upon infection or tissue injury, monocytes are rapidly recruited to the affected

tissue. Thus, they egress the circulation and in tissues, depending on the received signal from the environment, differentiate into either tissue macrophages or dendritic cells. Granulocyte-macrophage colony stimulating factor (GM-CSF) together with IL-4 differentiates monocytes into dendritic cells. Macrophage colony-stimulating factor (M-CSF) induces them to become a macrophage (Chapuis *et al.*, 1997). Interestingly, GM-CSF results in M1-like inflammatory phenotype of macrophages whereas M-CSF (also known as CSF-1) stimulation results in a homeostatic or anti-inflammatory M2-like macrophage phenotype (Verreck *et al.*, 2004).

The literature classifies blood monocytes as: classical, intermediate and non-classical. Human and mice monocytes types are listed in Table 1.3. The literature is not consistent in terms of nomenclature and classification of human and mice monocytes. Some publications describe three subsets (classical, intermediate and non-classical) in both species (Ziegler-Heitbrock *et al.*, 2010) and some three in humans but two in mice (classical and non-classical) (Shi and Pamer, 2011). Some classify mice monocytes upon the level of expression of an inflammatory monocyte marker Ly6C rising three subsets with high, middle and low (Sunderkötter *et al.*, 2004; J. Yang *et al.*, 2014) and others differentiate between high and low (Serbina *et al.*, 2008; Ziegler-Heitbrock *et al.*, 2010; Shi and Pamer, 2011). The exit from the bone marrow requires expression of the chemokine receptor CCR2 (Shi and Pamer, 2011). Classical monocytes are Ly6C⁺⁺ in mice, which correspond to CD14⁺CD16⁻ monocytes in humans. Non-classical are Ly6C⁺ monocytes in mice, which correspond to CD14^lCD16⁺ in humans. Intermediate are represented by CD14⁺⁺CD16 in humans (Wolf *et al.*, 2019). Human classical monocytes constitute about 80–95% of circulating monocytes, intermediate about 2–8% and non-classical about 2–11% (reviewed by (Sampath *et al.*, 2018)). The classical Ly6C⁺⁺ in mice are described as pro-inflammatory (Geissmann *et al.*, 2003). However, recently a subset of mice monocytes lacking expression of Ly6C was found to patrol blood vessels as these monocytes crawled on the luminal side of the endothelium, in steady-state condition, within most blood vessels in the dermis and within branches of the mesenteric vein and the mesenteric artery (Auffray *et al.*, 2007).

There is some discrepancy between human non-classical and intermediate monocytes characteristics. A publication of (Cros *et al.*, 2010) described the intermediate as primarily responsible for pro-inflammatory cytokine production and non-classical as patrolling. In the work of (Mukherjee *et al.*, 2015) the non-classical were the dominant producers of pro-inflammatory cytokines. Moreover, the intermediate were also phagocytic and inflammatory.

Human *in vivo* deuterium labelling depicted that classical monocytes circulate in the blood for a day, intermediate for 4 days and non-classical for 7 days (Patel *et al.*, 2017). Most classical monocytes leave the circulation or die, whereas the remaining cells transition into intermediate monocytes. Intermediate monocytes all transition to non-classical monocytes. Non-classical monocytes either leave the circulation or die. The half-lives possibly correlate to functional attributes of the monocytes subgroups (Patel *et al.*, 2017).

Classical murine monocytes exit the bone marrow and extravasate into peripheral inflamed tissues, in response to *Listeria monocytogenes* infection, thus are described as antimicrobial (Serbina and Pamer, 2006). The extravasation for non-classical is rare in the absence of an inflammatory stimulus. However, they show extravasation upon *Listeria* infection and thus they could be described as not only patrolling, but also antimicrobial (Auffray *et al.*, 2007).

Table 1.3 Mouse and human blood monocyte subsets

species	subsets	markers	chemokines receptors	functions
human	classical	CD14 ⁺⁺ CD16 ⁻	CCR2 ⁺⁺ CX3CR1 ⁺	phagocytosis (Mukherjee <i>et al.</i> , 2015)
	intermediate	CD14 ⁺⁺ CD16 ⁺	CX3CR1 ⁺⁺ CCR2 ⁺	phagocytosis and pro-inflammatory (Mukherjee <i>et al.</i> , 2015)
	non-classical	CD14 ⁺ CD16 ⁺⁺	CX3CR1 ⁺⁺ CCR2 ⁺	pro-inflammatory (Wong <i>et al.</i> , 2011; Mukherjee <i>et al.</i> , 2015) patrolling (Cros <i>et al.</i> , 2010)
mice	classical	Ly6C ⁺⁺	CCR2 ⁺⁺ CX3CR1 ⁺	pro-inflammatory (Geissmann <i>et al.</i> , 2003) antimicrobial (Serbina and Pamer, 2006)
	non-classical	Ly6C ⁻ /Ly6C ⁺	CX3CR1 ⁺⁺ CCR2 ⁺	patrolling (Auffray <i>et al.</i> , 2007)

Human monocytes divided into three subsets based on the cell surface expression of the cell surface expression of CD14 and CD16. Mice monocytes divided into two subsets based on the cell surface expression of Ly6C. The + denotes an expression level that is low, whereas ++ denotes high, - is undetectable. CCR2, CC-chemokine receptor 2; CX3CR1, CX3C-chemokine receptor 1. Adapted from (Shi and Pamer, 2011; J. Yang *et al.*, 2014).

1.2.2.3 Macrophage activation and polarisation

Macrophages can undergo polarisation, which results in a specific macrophage phenotype. Polarisation enables macrophages to gain specific functional programs in response to the signals from their environment. This is linked to the roles they play in immunity (reviewed by (Wynn *et al.*, 2013)). The stimuli for polarisation can be cytokines, microbial ligands or cell damage ligands. Depending on the type of the stimulus that macrophages are exposed to, they can be subjected to classical (Th1) or alternative (Th2) activation. For instance Th1 cytokine IFN γ (Nathan *et al.*, 1983) or LPS (Pabst and Johnston, 1980) polarise macrophages to M1 phenotype. LPS can also lead to the switch from M2 to M1 cell phenotype (Zheng *et al.*, 2013). M1 phenotype displays pro-inflammatory and antimicrobial properties whereas M2 promotes tissue repair and healing (reviewed by (Italiani and Boraschi, 2014; Ley, 2017)). Biomarkers to identify M1 macrophages include IL-12, nitric oxide synthase (iNOS), chemokine (C-X-C motif) ligand CXCL9, CXCL10. As for M2 there will be, e.g. IL-27R α , CCL17, Insulin-like growth factor (IGF-1) or CXCL11 (reviewed by (Mosser and Edwards, 2008)).

As mentioned, polarisation enables the performance of different programs. For example, activation of murine macrophages with IFN γ *in vitro* and *in vivo* enhances hydrogen peroxide release (Murray *et al.*, 1985), which is a known agent used for pathogen degradation. The treatment of zebrafish embryos that lack the adaptive system with IFN γ results in *C. neoformans* improved clearance explained by enhanced macrophage infiltration to the site of infection and linked to pro-inflammatory IL-1 β expression (Kamuyango, 2017). LPS treated macrophage THP-1 cells produce cytokines such IL-6, IL-8 and TNF α (Liu *et al.*, 2018). Pro-inflammatory cytokine production is a hallmark of acute inflammation. However, macrophages stimulated by Th2 cytokines adopt an alternative phenotype characterised by a high capacity for endocytic clearance. For example, IL-4 reduces pro-inflammatory TNF α production and enhances mannosylated ligands clearance (Stein *et al.*, 1992). IL-4 also enhances the turnover of anti-inflammatory IL-6 mRNA in LPS-stimulated monocytes (Fenton *et al.*, 1992). Anti-inflammatory cytokines are a hallmark of the resolution phase

of inflammation. Thus, macrophage activation and polarisation is important in tissue homeostasis, disease pathogenesis, resolved and unresolved inflammation (Murray *et al.*, 2014). There has to be a balance between M1 and M2 polarisation to ensure homeostasis. In terms of disease, M1 macrophages can be implicated in sustaining inflammation, thus to be detrimental to health. LPS activated macrophages release nitric oxide (Hibbs *et al.*, 1988) and this molecule is highly antimicrobial but its overproduction, by the logic, can lead to tissue damage. This complicates inflammation resolution (Pfeilschifter *et al.*, 1996). This means that when the M1/M2 balance is not assured, chronic inflammation and diseases might ensue. For instance a disequilibrium is linked to correlates with development of inflammatory bowel disease (Lissner *et al.*, 2015).

1.2.2.4 Macrophages diapedesis and chemotaxis

The migration is dictated by the inflammatory environment (Serbina *et al.*, 2011). The important question is how macrophages arrive at the site of infection/inflammation. Considering that macrophages are derived from monocytes and monocytes in the blood do the same as neutrophils, the monocyte migration will apply (see section 1.3.1.3 Neutrophil diapedesis and chemotaxis). Simultaneously, a population of resident macrophages might already be at the site of infection/infection.

1.2.2.5 Macrophages phagocytosis and phagosome maturation

Macrophages internalise both opsonised and non-opsonised particles. The opsonic receptors of macrophages are Fc receptor family, which bind antibodies (on macrophages IgG, IgM or IgA), or the complement family. Non-opsonic phagocytic receptors are pattern recognition receptors (PRRs), e.g. Dectin-1 or mannose receptor. The examples of these receptors are displayed in Table 1.4.

Fc receptor- induced phagocytosis results in the production of pro-inflammatory molecules such as reactive oxygen intermediates and arachidonic acid metabolites, whereas complement-induced phagocytosis does not lead to the

secretion of either of these molecules (Wright and Silverstein, 1983; Aderem *et al.*, 1985).

Macrophage phagosomes follow the endocytic pathway, with processes transforming it into a phagolysosome (Vieira *et al.*, 2002). As mentioned, neutrophil phagocytosis represents an event of the phagosome integrating with neutrophil granules. As described, in neutrophils, during phagocytosis, increases of intracellular ionised calcium are observed and these are essential for phagosome-granule (lysosome) fusion. In contrast, for macrophages, the literature suggests the calcium dependence phagosomal maturation might be less rigorous than in neutrophils (reviewed by (Nunes and Demaurex, 2010)).

While in macrophages ROS are produced only during FcγR mediated phagocytosis (Wright and Silverstein, 1983; Aderem *et al.*, 1985), in neutrophils, ROS are produced in both FcγR and CR3-mediated phagocytosis (Follin and Dahlgren, 1992). During phagocytosis by macrophages, calcium was not required for the oxidative burst, and although macrophages did require a basal amount of calcium to generate RNS, rises in calcium were not necessary for generation of nitric oxide (NO) (Myers and Swanson, 2002). Perhaps macrophages are successful killers because nitric oxide synthase (iNOS) does not require calcium rises (reviewed by (Mitchell and Feron, 1997)).

The respiratory burst is performed, as in the case of neutrophils, the main products of NADPH oxidase are the superoxide anion O_2^- and H_2O_2 (reviewed by (Roos *et al.*, 1988)). Therefore, the ROS formed will be the same as for neutrophils. The exception will pertain to MPO-deficient macrophages. Recognised sources for MPO are primarily neutrophils and monocytes. Monocytes contain about one third of MPO found in neutrophils (Bos *et al.*, 1978). During monocyte differentiation to tissue macrophages, MPO expression is generally lost (reviewed by (Klebanoff, 2005)). However, some macrophages contain MPO, e.g. Kupffer cells (Brown *et al.*, 2001), which are specialised resident macrophages. Therefore, for these cells the production of hypochlorous acid will be anticipated. As mentioned, hydrogen peroxide reacts with a combination of chloride and MPO from azurophilic granules, to form hypochlorous acid (reviewed by (Klebanoff, 2005)).

The killing of macrophages is also facilitated by reactive nitrogen species (RNS). These are derived from nitric oxide produced via the enzymatic activity of inducible nitric oxide synthase (iNOS) (reviewed by (Fang, 2004)). iNOS expression is related to classically activated macrophages, i.e. after induction by IFN γ or LPS (Ding *et al.*, 1988). Elevated iNOS expression is observed in inflamed human tissue macrophages (Moilanen *et al.*, 1997) and infiltrating monocyte-derived macrophages (Kashem *et al.*, 1996). The product of iNOS, nitric oxide (NO \cdot), as reviewed is cytotoxic (Hibbs *et al.*, 1988). It also gives rise to many downstream toxic metabolites that together constitute the M1 killing machinery (reviewed by (Ley, 2017)). For instance NO \cdot reacts with superoxide to form peroxynitrite. At acidic pH, peroxynitrite is protonated and forms peroxynitrous acid, which decomposes to form a strong oxidant with the properties of hydroxyl radical (OH \cdot) (Beckman *et al.*, 1990). Macrophages also synthesise nitrite and nitrate (Iyengar *et al.*, 1987). Nitrate is relatively harmless unless reduced to nitrite (reviewed by (Drew and Leewenburgh, 2002)). Nitrite is bactericidal in combination with MPO and hydrogen peroxide (Klebanoff, 1993). Of note, reactive oxygen intermediates seem to be important in some signalling pathways, e.g. NF- κ B (reviewed by (Iles and Forman, 2002)).

1.2.2.6 Macrophage longevity and death

Pioneer work from van Furth demonstrated, using radiolabelled cells *in vivo*, that 57% of the monocytes in the peripheral blood circulated for 48 hours and only a small fraction (14%) were found at 7 days (van Furth and Cohn, 1968).

The lifespan of macrophages is not clearly defined. Some tissue macrophages can survive by self-renewal (Ensan *et al.*, 2016) and long-lived tissue-resident macrophages of embryonic origin can develop (Ginhoux *et al.*, 2015; Gordon and Plüddemann, 2017). Some macrophages are not self-renewed. Intestinal macrophages have a half-life of 4–6 weeks and are not self-renewed, relying on a constant replenishment by the bone marrow-derived monocytes (Bain *et al.*, 2014). Heart macrophages are not capable of self-maintenance either and have an estimated half-life of 8-12 weeks (Epelman *et al.*, 2014; Molawi *et al.*, 2014). To conclude, the longevity varies with macrophage species. However, there is no

data on macrophages exact longevity. The literature mostly talks about compulsory neutrophils clearance. In fact, macrophages perform efferocytosis. This was shown in zebrafish (Loynes *et al.*, 2010), mouse (Cox *et al.*, 1995) or humans (Grigg *et al.*, 1991). Clearance of macrophages in the resolution of inflammation is not clear. The fate of macrophages that engulfed apoptotic neutrophils is unclear. It seems they should withstand the harsh environment of infection/inflammation to enable the clearance of apoptotic or necrotic corpses. They are resistant to, e.g. Fas-induced apoptosis. Macrophages express Fas and FasL (Kiener *et al.*, 1997). These ligands can induce apoptotic cell death in cells that express them but macrophages do not undergo spontaneous apoptosis upon stimulation by an agonistic anti-Fas antibody (Kiener *et al.*, 1997). It is suggested that the expression of Fas-associated death domain-like interleukin 1 β -converting enzyme (FLICE)-inhibitory protein (Flip) in macrophages spares macrophages from death by Fas-mediated apoptosis (Perlman *et al.*, 1999). However, they do undergo apoptosis *in vivo* without the interference of the adaptive when challenged with immunosuppressant, mycophenolate mofetil (MMF). The pathway remains unknown (Gibson *et al.*, 2018). *In vitro*, TNF α , an apoptotic stimulus (Rath and Aggarwal, 1999), induces macrophage apoptosis when NF- κ B is suppressed (Liu *et al.*, 2004). Thus, apoptosis could be one of the fates of macrophages. Other death types are described as, e.g. pyroptosis, necroptosis or and parthanatos (reviewed by (Liu and Sun, 2019; Robinson *et al.*, 2019)). Pyroptosis is a form of programmed cell death, which is highly pro-inflammatory due to a rapid rupture of the plasma-membrane releasing its contents (Fink and Cookson, 2006) (Bergsbaken *et al.*, 2009). Necroptosis is a programmed cell death regulated by receptor-interacting protein kinase 1 (RIPK1) and receptor-interacting protein kinase 3 (RIPK3) (Vandenabeele *et al.*, 2010). As in the case of any cell when the immunity is dysregulated and overwhelmed, it seems also possible that macrophages can die by necrosis. The general concept of macrophages being cleared by emigration from the previously inflamed site to lymph nodes (Bellingan *et al.*, 1996) has recently been refuted. The newest mice data showed a local death of macrophages (Gautier *et al.*, 2013). Retention of macrophages has to be reduced because macrophages can also contribute to the development of chronic diseases. In fact, high

macrophage/monocyte count is a hallmark of several autoimmune diseases, e.g. rheumatoid arthritis (Janossy *et al.*, 1981), Crohn's disease (Demetter *et al.*, 2005). The issue is that in chronic wounds, pro-inflammatory macrophages do not change their phenotype into anti-inflammatory and they remain in the tissue. This is thought to be associated with the impairment in tissue repair (reviewed by (Zhao *et al.*, 2016)). Nonetheless, regardless of their function, no previous research has investigated the life span of all types of macrophages.

1.2.2.7 Other cells

Other cells making up the cellular component are DCs and natural killer (NK) cells. Dendritic cells arise from the bone marrow and are present in the peripheral tissues such as the epithelial layer of the skin, gut, parenchyma and organs interstitial. They are bone marrow derived from the same lineage of cells as monocytes and act as powerful antigen presenters to CD4+ and CD8+ T cells (reviewed by (León *et al.*, 2005; Merad *et al.*, 2009)), thereby providing a link between innate and adaptive immunity. Natural killer cells generate rapid responses to viruses and tumors. They are cytotoxic lymphocytes of T and B lymphoid progenitor, important in cytokine production (reviewed by (Geiger and Sun, 2016)). Originally, they were defined as effector lymphocytes of innate immunity. Nowadays they are also described as mounting a form of antigen-specific immunologic memory. This view moves them to be adaptive immune cells (reviewed by (Vivier *et al.*, 2016)).

1.4 The adaptive immune system

The adaptive immune system provides a long lasting immune response against previously encountered pathogens. The adaptive immune response is induced upon activation of specialised antigen-presenting cells, namely dendritic and B cells (Lemke, 2018). DCs are activated directly by pathogen-associated molecular pattern recognition and indirectly via inflammatory mediators produced by other cells that recognise conserved pathogen molecules (reviewed by (Reis e Sousa, 2004; Gallo and Gallucci, 2013)). An immature DC uptakes and processes an antigen. This changes the status of immature into mature dendritic

cell. Mature DC will present the antigen and activate T cells (reviewed by (Banchereau and Steinman, 1998)).

Cells of the adaptive immune system include the effectors of cellular immune responses, the T lymphocytes and the B-lymphocytes. They are named after their tissues of maturation, the thymus gland and bone, respectively. Adaptive immunity represents a tightly regulated interplay between antigen-presenting cells and T and B cells (reviewed by (Bonilla and Oettgen, 2010; Gaudino and Kumar, 2019)).

Lymphocytes

T cells can be categorised into two main groups CD4⁺ and CD8⁺ for the different glycoproteins present on their cell surface and interact with other cells through the T cell receptor (TCR). The TCRs recognise antigens only if coupled with MHC molecules. Cytotoxic T cells have CD8⁺ co-receptor on their cell surface. Helper express CD4⁺. CD4⁺ cells have two distinct phenotypes Th1 and Th2. The cytokines they produce are known as Th1-type and Th2-type cytokines. Th1-type cytokines are considered as pro-inflammatory while Th2 anti-inflammatory (reviewed by (Kaiko *et al.*, 2008)).

B cells drive humoral immunity by producing antibodies. There are many B cell types, thus can be categorised by the cytokine milieu that they secrete (reviewed by (Mauri and Bosma, 2012)). After encountering the antigen, it can either become a memory cell to be activated again or a plasma cell to secrete antibodies (reviewed by (Liu and Banchereau, 1997; Cyster and Allen, 2019)).

Antibodies

Antibodies are produced by plasma cells arising from B cells under the supervision of T cells and other cells, such as dendritic cells (Bonilla and Oettgen, 2010). As a class, they are known as immunoglobulins (Igs). Their different suffixes of the antibody isotypes indicate the different types of heavy chains the antibody contains, i.e. α , γ , δ , ϵ and μ . Accordingly, antibodies isotopes are described as: IgA, IgG, IgD, IgE, and IgM. Fab, more specifically the Fv region

antibody region, binds the antigen. Fc is the antibody tail region responsible for generation of an appropriate immune response for a given antigen by binding to a specific class of Fc receptors. These receptors are important in the engagement of phagocytes with opsonised microbes (reviewed by (Koenderman, 2019)). Fc receptors are found on various cell types. Internalisation and killing of organisms is more efficient if the particle is first opsonised with specific antibody or complement. Antibodies recognise the structure of antigen epitopes, and such antigens do not need to be processed (reviewed by (Parkin and Cohen, 2001)).

The elegance and complexity of the adaptive immune system are largely due to lymphocytes working closely together with innate immune cells. For instance, CD4+ Th1 cells activate DCs (Mailliard *et al.*, 2002) and these will present the antigen to T cells. Thus, antigen presentation bridges the innate and adaptive immune responses.

1.5 The innate immune response to *Cryptococcus*

A detailed introduction to the immune response to cryptococcal infection is in Chapter 3.

The complement

C. neoformans strongly activates the complement via the alternative pathway (Diamond *et al.*, 1974; Laxalt and Kozel, 1979). Recently it has been shown that both *C. gattii* and *C. neoformans* activate complement inhibited serum. This suggests they can activate the alternative pathway. However, complement activation was seen with factor B (required for the alternative pathway activation) deficient serum suggesting activation can also occur in the absence of a functional alternative pathway. Moreover, the complement is not activated in the absence of mannose-binding lectin (MBL) proteins. Activation of the alternative pathway by *C. neoformans* requires both MBL-A and MBL-C types. In contrast, *C. gattii* requires either MBL-A or MBL-C. This suggests the complement might be activated by the pathogen via a few pathways. The most surprising finding is that the alternative pathway requires the presence of C4 fragment shown by C3 decreased deposition in the absence of C4 (Mershon-Shier *et al.*, 2011).

The dependency on the alternative pathway for effective cryptococcal phagocytosis and innate protection is demonstrated by increased mortality in C3 but not C4 complement deficient guinea pigs (Diamond *et al.*, 1973) and mice (Shapiro *et al.*, 2002). The classical pathway does not seem to play a role in complement activation because there is no difference in complement activation using C1q-deficient serum as compared to the wild-type serum (Mershon-Shier *et al.*, 2011). In addition, the polysaccharide capsule inhibits the classical pathway activation (Kozel *et al.*, 1991).

Macrophages

Alveolar macrophages are the first line of defence against pulmonary pathogens (Green and Kass, 1964; Goldstein *et al.*, 1974). Primary infection with *Cryptococcus* is through the pulmonary route and thus macrophages are the dominant phagocytic cells that interact with the fungus.

The function of macrophages is complex, from cryptococcal killing to contributing to disease development (reviewed by (Voelz and May, 2010; Taylor-Smith and May, 2016)). If cryptococci are not killed they can proliferate intracellularly, e.g. *in vitro* in human macrophages (Diamond and Bennett, 1973; Garelnabi *et al.*, 2018) and human fetal microglia (Lee *et al.*, 1995). They also cause lysis of host cells. There are three types of proteins linked to the host cell lysis, i.e. proteases, phospholipases, and pore-forming proteins (reviewed by (Flieger *et al.*, 2018)). To date, no pore-forming proteins have been identified in the fungus genome. Thus, proteases and phospholipases seem potential candidate molecules that may be involved in the permeabilisation of *C. neoformans*-containing phagosomes. Lateral transfer is reported in macrophage lines and primary macrophages (Alvarez and Casadevall, 2007; Ma *et al.*, 2007). The mechanism of lateral transfer remains unclear, although it is actin-dependent (Ma *et al.*, 2007). Finally, cryptococci can be expelled. This is reported in macrophage lines (Alvarez and Casadevall, 2006; Ma *et al.*, 2006; Johnston and May, 2010), primary murine macrophages (Alvarez and Casadevall, 2006). The non-lytic extrusion might impinge the host, e.g. *Cryptococcus* can temporarily reside in macrophages and use them as Trojan horses to later cross the blood brain

barrier, or can maintain the dormant state to be activated upon immunocompromised conditions (reviewed by (Johnston and May, 2013)). Vomocytosis, the non-lytic expulsion, is believed to be dependent on polymerised actin flashes on fungal phagosome through WASP-Arp2/3 pathway (Johnston and May, 2010). A schematic interaction between macrophages and *Cryptococcus* is depicted in Figure 3.1 in section 3.1.1 The importance of *C. neoformans*, interactions with macrophages and the polysaccharide capsule.

Neutrophils

In contrast to discrepancies between the fungicidal activities of different types of macrophages and the fate of internalised yeast, there is more agreement about neutrophils. They efficiently kill *in vitro* via oxidative burst (Tacker *et al.*, 1972; Chaturvedi *et al.*, 1996, Ueno *et al.*, 2019). *In vivo* neutrophils are very potent (Wozniak *et al.*, 2006; Tenor *et al.*, 2015; Davis *et al.*, 2016; Zhang *et al.*, 2016), yet they manage only a partial clearance of cryptococci (Perfect *et al.*, 1980; Gadebusch and Johnson, 1996). Killing is mediated by antimicrobial granules, reactive oxygen species and myeloperoxidase catalysing production of hypochlorous acid, an extremely potent microbicidal agent. However, it has to be highlighted that there is no clinical association between neutrophils and *Cryptococcus*. There are no neutrophils in the lungs in health. Neutrophils are recruited into the lungs during the early phase of cryptococcal infection (Feldmesser *et al.*, 2000). This means that neutrophils recruitment occurs in disease. In this light, macrophages are more important in cryptococcal disease because a population of alveolar macrophages already occupies the lungs, the portal of entry for *Cryptococcus*.

Natural killer and dendritic cells

NK cells also effectively kill *C. neoformans in vitro* (Ma *et al.*, 2004; Wiseman *et al.*, 2007), but *Cryptococcus* suppresses this by inhibiting cytokine secretion (reviewed by (Schmidt *et al.*, 2013)). *In vitro* data shows DCs are more potent than macrophages (Syme *et al.*, 2002): they efficiently phagocytose

Cryptococcus in vitro (Kelly *et al.*, 2005) and this is also seen *in vivo* in a murine model of infection (Wozniak *et al.*, 2006).

Phagocytosis

Uptake of cryptococci has been shown in murine macrophages (Kozel and Follette, 1981), human neutrophils (Dong and Murphy, 1997; Rocha *et al.*, 2015), *in vivo* in zebrafish neutrophils (Tenor *et al.*, 2015) and macrophages (Bojarczuk *et al.*, 2016) as well as in human DCs *in vitro* (Syme *et al.*, 2002) and in mouse DCs (Wozniak *et al.*, 2006).

Autophagy

The host self-degradation pathway of autophagy has been implicated to support intracellular survival and dissemination of *C. neoformans*. Autophagy genes such as *ATG2a*, *ATG5* and *ATG9a*, were shown to be required for growth through RNA interference (RNAi) in RAW 264.7 macrophages (Qin *et al.*, 2011). A similar RNAi approach resulting in *Atg5* loss, led to decreased macrophage fungistatic ability. This suggests that autophagy is important in host defence (Nicola *et al.*, 2012). Interestingly, J774 macrophages infected with *C. gattii* outbreak strains were poorly decorated with LC3 phagosome marker, suggesting no clear role for autophagy in cryptococcal mitochondrial tabularisation, that is thought to be protective from cell death (Voelz *et al.*, 2014) and from autophagic degradation (Gomes *et al.*, 2011).

1.6 Inflammation and disease

Inflammation was originally described as heat, redness, swelling and pain by Cornelius Celsus in the 1st century AD. Inflammation is a general term describing a multistep process triggered by the innate immune cells in response to sterile tissue damage, infection or a combination of both (reviewed by (Barton, 2008; Newton and Dixit, 2012)). The main role of inflammation is to obviate infection or repair damage and thus restore homeostasis (reviewed by (Barton, 2008; Feehan and Gilroy, 2019)). The response is elicited by recognition of an inflammatory stimulus by immune cell receptors via molecular pattern recognition, which leads

to inflammatory signalling cascade and the production of pro-inflammatory mediators. Termination of the inflammatory response and transition to the homeostatic state requires the switch to anti-inflammatory signalling and is termed as the resolution of inflammation (reviewed by (Medzhitov, 2010)).

Neutrophils are the first inflammatory cells to arrive at the site of tissue perturbation (reviewed by (Haslett, 1992; Butterfield *et al.*, 2006)) and are followed by monocytes, which differentiate into tissue macrophages or DCs, depending on the precise signals they receive locally. However, a rapid response requires guarding cells already present in the tissues, provided by residential mast cells and macrophages (reviewed by (Benoist and Mathis, 2002)). The latter are considered to be most prominent and act as sentinels in the early sensing of infection (reviewed by (Barton, 2008)), alongside DCs (reviewed by (Mellman and Steinman, 2001; Webster *et al.*, 2016)). Mature macrophages are important in promoting resolution of inflammation, elimination of apoptotic cells and tissue repair following injury (reviewed by (Koh and DiPietro, 2011)). Neutrophils, in contrast, are important for the host defence but are also implicated in disease pathogenesis. Neutrophils therefore are believed to occupy a pivotal position in the initiation, amplification and resolution processes of inflammation (reviewed by (Haslett, 1992; Mortaz *et al.*, 2018)). They also form extracellular traps (NETs) with extruded DNA strands anchoring bactericidal proteins (Brinkmann *et al.*, 2004). Generally, microbial killing is facilitated by antimicrobial granules of many types, including peroxidase-positive (reviewed by (Faurischou and Borregaard, 2003)), degranulation, respiratory burst and cytokine production (reviewed by (Borregaard, 2010)). During the acute inflammation phase, which occurs over minutes or hours, the influx of neutrophils is rapid. This is followed promptly by an inflow of monocytes maturing into inflammatory macrophages. These sustain the inflammatory response and alter the tissue-resident macrophages role (reviewed by (Serhan and Savill, 2005)).

Inflammation must resolve to allow tissue repair and a return to normal homeostasis; this occurs through a shift in the overarching response to anti-inflammatory signals (reviewed by (Barton, 2008)). The change in the inflammatory pattern is a result of numerous steps, such as removal of the

initiating stimuli, catabolism of pro-inflammatory mediators and inhibition of further neutrophil recruitment and their clearance. Transformation from tissue damage signals to tissue repair occurs as complement and phagocytes kill microbes (reviewed by (Nathan, 2002)). Successful inflammation resolution is facilitated by the constitutive apoptosis of neutrophils and their uptake by macrophages (Savill *et al.*, 1989; Sun *et al.*, 2015). Additionally, macrophages can also induce neutrophil death via a direct cell-cell contact mechanism (Meszaros *et al.*, 2000). Removal of neutrophils can also occur via their reverse migration from inflamed tissue (Tharp, 2005; Buckley *et al.*, 2006; Mathias *et al.*, 2006).

Induction of neutrophil apoptosis and their removal by macrophages is of dual importance. Firstly, it promotes macrophage reprogramming from pro- to anti-inflammatory phenotype (Fadok *et al.*, 1998). Secondly, it preserves neutrophil cell membrane integrity (Savill and Haslett, 1995). If the membrane of apoptotic cells is disrupted very early in their life-span, this leads to secondary necrosis, leading to spillage of the contents of necrotic cells into the adjacent environment, again initiating inflammatory signalling (reviewed by (Ward *et al.*, 1999; Gaipf *et al.*, 2004; Grabiec and Hussell, 2016)). Macrophages engulf apoptotic cells before they lyse, which blocks the release of cytotoxic contents (Fadok, Bratton, Guthrie, *et al.*, 2001). Without this, the elimination of dying cells is perturbed and might evoke autoimmunity (reviewed by (Gaipf *et al.*, 2003)). For example, in systemic lupus erythematosus disorder, impaired apoptotic cell clearance leads to secondary necrosis and inflammation (reviewed by (Shao and Cohen, 2011)).

It is critical that inflammation resolution is well-timed as persisting neutrophils can cause irreversible tissue damage via release of their cytotoxic granules (reviewed by (Haslett, 1992; Schett and Neurath, 2018)). If inflammation continues unchecked, the inflammatory process can lead to the saturation of tissue by lymphocytes and leukocytes which then subsequently form granulomas (reviewed by (K. K. Shah *et al.*, 2017)). Dysregulation of granulocyte apoptosis and clearance leads to persisting inflammation and excessive tissue injury (Haslett, 1997). For instance, disruption of constitutive apoptotic pathways prevents successful resolution and delays neutrophil apoptosis in acute pancreatitis (O'Neill *et al.*, 2000). Normal, controlled inflammation and apoptosis

are essential for the maintenance of health and life and these processes occur all the time, e.g. in skin injuries (Suárez-Peñaranda *et al.*, 2002). In contrast, unresolved inflammation can cause serious host tissue injury resulting in chronic inflammatory diseases, such as chronic obstructive pulmonary disease or autoimmunity, e.g. systemic lupus erythematosus (reviewed by (Nathan and Ding, 2010; Kaplan, 2013)). This potentially leaves the host vulnerable to chronic infections. Therefore, chronic inflammation is linked with infections and autoimmune conditions. These cases, as well as organ transplants, require immunosuppression (reviewed by (Kanterman *et al.*, 2012)). Despite the clinical problem of unresolved neutrophilic inflammation, few effective therapies are available, none of which directly target the neutrophil. One of the widely used treatments in transplantations and immune-mediated diseases, such as immune-related pulmonary fibrotic conditions- is mycophenolate mofetil (MMF). However, data on its mechanism of action in the context of inflammation during immunosuppression and the drug's immunosuppressive impact on the innate immune system are scarce.

Inflammation can be classified as either acute or chronic. The former starts rapidly and becomes severe in a short space of time. Examples include acute bronchitis, acute appendicitis, sinusitis, a physical injury. The latter is characterised by persistence of signs and symptoms, e.g. asthma, chronic sinusitis, rheumatoid arthritis. There are also diseases resulting from an aberrant immune response and termed autoimmune diseases. Neutrophil- related include, i.e. lupus erythematosus, small vessel vasculitis and rheumatoid arthritis (reviewed by (Kaplan, 2013)). Significantly elevated neutrophil numbers are the hallmark of neutrophilic inflammatory disease and their protracted presence and activation can escalate the immune response (Haslett, 1997).

1.6.1 Inflammation and infection

1.6.1.1 The course of inflammatory response to infection

Infection, injury and tissue damage cannot heal without an inflammatory response. Every infection is associated with inflammation and these cells specified and maintained to resolve inflammation, destroy pathogens and return

to homeostasis communicate together and regulate each other. Most injuries are associated with accompanying infection because wounds include the disruption of a physical barrier, such as cuts that microbes will use to bypass the skin. However, in certain cases injury and cell death are found in a sterile setting (reviewed by (Barton, 2008)). The inflammatory response to infection or injury proceeds in four phases: recognition of infection/injury, recruitment of inflammatory cells, control of infection and elimination of the pathogen and termination of inflammation.

1.6.1.1.1 Recognition of infection

The inflammatory response can be initiated by either endogenous or exogenous stimuli. The most well described inflammatory response is that induced by microbial infection (reviewed by (Medzhitov, 2008)). In vertebrates, the innate system recognition occurs via pattern recognition receptors (PRRs), expressed on the plasma membrane of cells, e.g. neutrophils, macrophages and DCs (reviewed by (Medzhitov, 2001; Troutman *et al.*, 2012)). The best characterised PRRs are the Toll-like receptors (TLRs), which detect structurally conserved microbial molecules known as pathogen-associated molecular patterns (PAMPs), e. g. lipopolysaccharides (LPS), flagellin or double- or single-stranded RNA (reviewed by (Medzhitov, 2007)). Upon binding of a pathogen ligand, TLRs trigger a cascade of signalling pathways. This includes the elicitation of pro-inflammatory and anti-inflammatory cytokines (reviewed by (Ozato *et al.*, 2002)). PAMPs are derived from microorganisms. In contrast, damage-associated molecular patterns (DAMPs) are cell-derived. PAMPs initiate and maintain the infectious pathogen-induced inflammatory response, whereas DAMPs initiate and perpetuate a non-infectious inflammatory response, which is discussed in section 1.6.1.2 Sterile inflammation. Five classes of PRRs have been characterised: transmembrane cell surface or endosomal Toll-like receptors (TLRs), cytoplasmic NOD-like receptors (NLRs) and inflammasome, intracellular RIG-I (retinoic acid-inducible gene-I)-like receptors (RLRs), transmembrane C-type lectin receptors (CLRs), and AIM2 (interferon-inducible protein also known as absent in melanoma 2)-like receptors (reviewed by (Chen and Nuñez, 2010)). PRRs can perform as phagocytic transmembrane non-opsonic receptors (e.g. Dectin-1, mannose

receptors) (reviewed by (Johnston and May, 2013)) or proteins implicated in opsonisation and complement activation (e.g., mannose-binding lectin) (reviewed by (Medzhitov, 2001; Barton, 2008)).

TLRs stimulate tissue-resident macrophages to secrete pro-inflammatory cytokines, including TNF α , IL-1 β and IL-6. TNF α and IL-1 β in turn mobilise the local endothelium to dilate blood vessels enabling the recruitment of serum proteins and leukocytes to the site of infection response (reviewed by (Rosenwasser, 1998; Sprague and Khalil, 2010; Duque and Descoteaux, 2014)). TLRs can also directly drive antimicrobial functions by inducing macrophages to upregulate inducible nitric oxide synthase (iNOS) ((Wager *et al.*, 2014); reviewed by (Medzhitov, 2007)). Activation of mouse macrophages by bacterial lipoproteins triggers a nitric oxide mediated killing of *Mycobacterium tuberculosis* (Thoma-Uszynski, 2001). Binding of TLRs and PAMPs results in a pro-inflammatory cascade activating signalling molecules, e.g. nuclear factor- κ B (NF- κ B) and interferon-regulatory factors (IRFs), which in turn drive expression of pro-inflammatory genes including TNF α and IL-1 (reviewed by (Barton, 2008; Mogensen, 2009)). TLRs-PAMP binding drives activation of neutrophils and macrophages, intensifying phagocytosis and the oxidative burst.

The TLR-PAMP binding induces a pro-inflammatory signalling cascade. Transcription factors are activated, e.g. nuclear factor- κ B (NF- κ B), which induces the pro-inflammatory cytokines expression, such as TNF α , IL-6 and IL-12 (reviewed by (Takeda and Akira, 2005; Ospelt and Gay, 2010)). Interferon-regulatory factors (IRFs) also activate TNF α as well as inflammatory IL-12, IL-18. Cytokine secretion is a 'go' signal and results in recruitment of leukocytes from the blood (reviewed by (Muller, 2002; Nathan, 2002)). Examples of other pro-inflammatory cytokines include: chemokine-monocyte chemoattractant 1 (MCP-1) and IFN γ (Rossi *et al.*, 2006). Cytokines including TNF α and IL-1 enhance the expression of a collection of adhesion molecules on vascular endothelial cells, in particular E-, P- and L-selectins. Selectins are involved in trafficking of both the innate cells immune system and T lymphocytes and platelets (reviewed by (Ley, 2003)). Selectins bind ligands on the surface of neutrophils which aids to the

rolling process, and induces 'inside-out' signalling that alters integrin conformation on the neutrophil surface (reviewed by (Muller, 2003; Zarbock and Ley, 2008)).

In addition to membrane-targeted TLRs, inflammatory responses can initiate via activation of cytosolic PRRs, which include nucleotide-binding oligomerisation domain-like (Nod-like) receptors (NLRs) (reviewed by (Strober *et al.*, 2006; Barton, 2008)). NLRs are pivotal in the innate immunity by recognising PAMPs and DAMPs (Y. K. Kim *et al.*, 2016). Nod1 and Nod2 function similarly to that of TLRs, activating NF- κ B, and enhancing expression of pro-inflammatory genes (reviewed by (Strober *et al.*, 2006; Barton, 2008)). Other NLRs detect non-microbial signals triggering activation of cytosolic complexes-inflammasomes involved in activation of inflammatory caspases (reviewed by (Martinon *et al.*, 2009)).

RLRs are also a group of cytosolic PRRs that belong to the RNA helicases family. They specifically recognise RNA species derived from viruses and execute anti-viral signalling via type I interferon (IFN) induction (reviewed by (Yoneyama and Fujita, 2008)).

Another group of cytosolic sensors are AIM2-like receptors. These sense cytoplasmic viral DNA and activate inflammasomes, resulting in IL-1 β and IL-18 maturation (reviewed by (Sparrer and Gack, 2016)).

An example of PRRs is Dectin-1. It is a non-opsonic receptor belonging to CLRs and recognising β -glucans. B-glucan is an important cell wall component in fungi. However, Dectin-1 seems to have little role in the macrophage interaction with cryptococci and not likely to be crucial for the protective host response to *C. neoformans* (Nakamura *et al.*, 2007). Contrary to this, it has been reviewed that Dectin-1 contributes to the production of IL-23, needed for Th17-cell function and protection against fungi (reviewed by (Medzhitov, 2007)).

Innate immune recognition of PAMPs instruct adaptive immune responses. The recognition via pattern recognition receptors on antigen-presenting cells, leads to the activation of adaptive immune responses (reviewed by (Iwasaki and Medzhitov, 2015)).

1.6.1.1.2 Recruitment of inflammatory cells to site of infection

Neutrophils are the first inflammatory cells to arrive at the site of tissue perturbation (reviewed by (Haslett, 1992; Peiseler and Kubes, 2019)). This occurs via the process termed diapedesis. It involves adhesion to the endothelial wall using selectins, integrins and adhesion molecules. Rolling arrest introduces transmigration through the endothelium of the blood vessel, and chemotaxis to sites of inflammation (reviewed by (Wright *et al.*, 2010)). The neutrophil adhesion cascade is highly complex and involves the following stages: the capture and rolling of neutrophils on activated endothelial cells (ECs), slow rolling, firm adhesion to ECs through, luminal crawling along the endothelium until they reach their site of transendothelial cell migration (reviewed by (Voisin and Nourshargh, 2013)). Apart from tissue-resident macrophages already present at the inflamed site (reviewed by (Davies *et al.*, 2013)), another population of macrophages will accumulate within the affected tissue site, governed by Th1 inflammatory response (reviewed by (Helming, 2011)).

1.6.1.1.2.1 Mediators of inflammation

There are many mediators coordinating the course of inflammation (Table 1.4) having various effects on the local environment, either promoting the inflammatory phase of inflammation or triggering pro-resolution events.

Lipid mediators (e.g. prostaglandins, lipoxins, resolvins, protectins) reduce inflammation, increase resolution and tissue repair. They also enhance leukocytes recruitment. Cytokines: TNF α , IL-1, IL-6 activate leukocytes and endothelium as well as induce acute-phase systemic response. Chemokines (i.e. IL-8, MCP-1) affect leukocyte extravasation and chemotaxis (reviewed by (Medzhitov, 2007, 2008; Serhan and Levy, 2018)).

Both neutrophils and macrophages secrete lipid mediators of inflammation: prostaglandins, leukotrienes and platelet-activator factor (PAF). These are rapidly produced to degrade pathogen membrane phospholipids (Janeway *et al.*, 2012b). PAF, IL-8 and CXC chemokines are attractants for neutrophils migration. Lipoxins A₄ and B₄ increase the recruitment of monocytes to inflammatory sites.

Here they mature into macrophages and are crucial in wound healing (Maddox and Serhan, 1996).

Table 1.4 Inflammatory mediators

mediator class	pro-inflammatory	anti-inflammatory
amines	histamines, bradykinin	adrenaline, nor-adrenaline
lipid mediators	PGE ₂ , PGI ₂ , LTB ₄ , LTC ₄	PGJ ₂ , PGA _{1/2} , lipoxins
complement	C3a, C5a	C1q
cyclic nucleotides	cGMP	cAMP
adhesion molecules	E-selectin, P-selectin, ICAM-1, VCAM-1	α _v β ₃ integrin, TSP, PS
cytokines	TNFα, IL-1β, IL-6	TGFβ ₁ , IL-10
chemokines	IL-8 (CXCL8), GRO/KC, MIP1α (CCL3), MCP1 (CCL2)	-

Taken from (Lawrence *et al.*, 2002).

cAMP- cyclic adenosine monophosphate; cGMP- cyclic guanosine monophosphate; ICAM-1- intercellular adhesion molecule 1; IL- interleukin; LT- leukotriene; MCP1- monocyte chemotactic protein 1; MIP1α-macrophage inflammatory protein 1α; PG- prostaglandin; PS-phosphatidylserine; TGFβ₁- transforming growth factor β₁; TNFα tumor necrosis factor α; TSP- thrombospondin; VCAM-1- vascular cell adhesion molecule 1; C1q- first subcomponent of the C1 complex of the classical pathway of complement activation receptor, GRO/KC- keratinocyte chemoattractant of human growth-regulated oncogene; CXCL- chemokine (C-X-C motif) ligand, CCL- chemokine (C-C motif) ligand

1.6.1.1.3 Control of infection and elimination of pathogens

Inflammation resolution is a highly controlled process. Transmigrating cells reorganise their cytoskeleton and change their structural polarisation (reviewed by (Springer, 1994; Garrood *et al.*, 2006)) to permit endocytosis of foreign molecules into phagosomes (reviewed by (Dale *et al.*, 2008)). Neutrophils secrete the antimicrobial components contained in their granules upon cell activation via exocytosis (reviewed by (Lacy, 2006)). These and other secretory vesicles enable destruction of pathogens either extracellularly or following degranulation into the phagolysosome after phagocytosis, with these events primed by TNF α (reviewed by (Lesavre and Halbwachs-Mecarelli, 2000)). Phagocytosis also begins, mediated by a broad array of phagocytic receptors. Examples of human phagocytic receptors are presented in Table 1.5.

Phagocytosis activates a respiratory burst, where NADPH oxidase catalyses the production of reactive oxygen species (reviewed by (Roos *et al.*, 1988)). Superoxide anion O $_2^-$ and hydrogen peroxide H $_2$ O $_2$ are formed to produce yet more reactive oxygen species (ROS) that are highly toxic and able to induce apoptosis in other immune cells (reviewed by (Dahlgren and Karlsson, 1999)). Neutrophils produce myeloperoxidase (MPO) (Agner, 1958) and the MPO secreted into the phagosome during the degranulation (reviewed by (Klebanoff, 2005)), forms hypochlorous acid, a potent oxidant in killing (reviewed by (Kettle and Winterbourn, 1997)). Interestingly, in macrophages Fc receptor-, but not complement receptor-mediated, phagocytosis elicits reactive oxygen intermediates (reviewed by (Aderem and Underhill, 1999)).

Another mechanism of pathogens killing is via low pH. For instance, pH below 2.5 efficiently kills *Escherichia coli* 690, *E. coli* K-12 and *Helicobacter pylori* (Zhu *et al.*, 2006). However, cryptococci can survive acidic status of phagolysosome (Levitz *et al.*, 1999). Proteases also facilitate pathogens elimination. Neutrophil elastase lacking mice are susceptible to *Klebsiella pneumoniae* and *E.coli* (Belaouaj *et al.*, 1998) and macrophage cathepsin L executes non-oxidative killing of phagocytosed *Staphylococcus aureus* (Müller *et al.*, 2014).

Table 1.5 Phagocytic receptors (examples)

	phagocytosis		
	opsonic		non-opsonic
cell type	Fc receptors	complement receptors	PRRs
neutrophils	FcγRIIA/CD32, FcγRIIIB/CD16	CR1(CD35), CR3(CD11b/CD18 integrin)	Dectin-1(C-type lectin), Mincle (C-type lectin), MDL-1(C-type lectin), TLR1, TLR2, TLR3, TLR4, TLR5, TLR7,TLR8, TLR9
macrophages	FcγRI/CD64 FcγRIIA/CD32a FcγRIII/CD16	CR1(CD35), CR3(CD11b/CD18 integrin), CR4(CD11c/CD18)	Dectin-1 (C-type lectin) DEC 205 (C-type lectin) mannose receptor (C-type lectin)

Adapted from (Aderem and Underhill, 1999; Lesavre and Halbwachs-Mecarelli, 2000; Taylor *et al.*, 2005; Futosi *et al.*, 2013; Sándor *et al.*, 2016).

1.6.1.1.4 Termination of inflammation

Termination of inflammation determines restoration of tissue integrity and return to homeostatic state. The inflammatory stimulus must be removed, pro-inflammatory mediators catabolised, further recruitment of inflammatory leukocytes arrested, and their numbers returned to basal tissue levels (reviewed by (Serhan, 2007)). Previous studies have emphasised that the active, complex process of resolution of inflammation initiated in the first few hours after an inflammatory insult, constitutes an integral component of the program of inflammation. Under normal conditions the inflammation resolution is composed of two stages: pro- and anti- inflammatory, therefore a number of authors have recognised the beginning of inflammation programs the end of inflammation (reviewed by (Serhan and Savill, 2005; Headland and Norling, 2015)). It becomes apparent, there has to be a switch from pro- to anti-inflammatory signalling. One of the mechanisms facilitating the anti-inflammatory signalling is granulocyte production of lipoxins, resolvins and protectins that triggers the inhibition of neutrophil recruitment and decrease in vascular permeability, and promotes healing. This occurs post entering tissues, to initiate the termination of inflammation (reviewed by (Serhan and Savill, 2005)).

The mechanism of inflammation resolution also involves clearance of neutrophils by macrophages (Savill *et al.*, 1989). Uptake of apoptotic neutrophils by macrophages reprograms macrophage phenotype from a pro- to an anti-inflammatory, thus to a resolving phenotype, which facilitates the restoration of tissue homeostasis (reviewed by (Ortega-Gómez *et al.*, 2013)). In addition, macrophages can also induce neutrophil death via a direct cell-cell contact mechanism contact that requires the constitutive presentation on macrophages effectors of β_3 integrin subunits, CD36, and membrane-bound TNF α (shown *in vitro* using PMNs and macrophages purified from a wound in rats (Meszaros *et al.*, 2000)). In contrast, macrophage can exert pro-inflammatory properties. This includes responses to necrotic cells, e.g. necrotic cells from uncleared apoptotic cells (reviewed by (Gregory and Devitt, 2004)). Some authors have demonstrated that incubation of macrophages with physically lysed neutrophils, led to the production of macrophage-inflammatory protein 2 (MIP-2), IL-8, TNF α , and IL-10

(Fadok, Bratton, Guthrie, *et al.*, 2001). The effect was due to the cleavage of phosphatidylserine receptor (PSR) on the surface of the macrophages by a protease released upon the lysis of neutrophils, which could be a physiological effect since normally proteases are stored in neutrophil granules and released after neutrophil exposure to inflammatory stimuli. Phosphatidylserine (PS) exposure is critical for the uptake of apoptotic cells (reviewed by (Fadok, Bratton and Henson, 2001)). PS expressed on the apoptotic cell is recognised by macrophages through PSR (Fadok *et al.*, 2000) and believed to be expressed on apoptotic cells due to loss of plasma membrane asymmetry (reviewed by (Henson *et al.*, 2001)) in apoptotic cells. However a recent study by (Krysko *et al.*, 2004) showed PS exposure in late necrotic JB6 cells (caspase -8 deficient, *BCL-2* overexpressing subline derived from the Jurkat E human T-cell lymphoma cell line). Furthermore, the Brouckaert group concluded that necrotic L929 cells become PS positive and were taken up by Mf4/4 macrophages, which did not elicit pro-inflammatory cytokine signalling. However, the extent of the uptake was lesser as compared to apoptotic neutrophils (Brouckaert *et al.*, 2004). Nevertheless, the uptake of apoptotic/necrotic cells is crucial for the successful inflammation resolution.

1.6.1.2 Sterile inflammation

Sterile inflammation occurs in the absence of any microorganisms. It can be triggered by, e.g. endoplasmic reticulum (ER) stress, hypoxic stress, nutrient stress, ischemia reperfusion injury (I/R), trauma including crush injury, crystal-induced inflammation, cellular necrosis and toxin exposure (reviewed by (Rubartelli *et al.*, 2013; Shen *et al.*, 2013)). Examples of triggers of sterile inflammation are presented in Table 1.6.

Similar to that caused by microbes, sterile inflammation can be either resolved or lead to disease. A number of factors are suggested to be important in distinct types of sterile inflammation. These include redox responses, the occurrence of DAMPs and immune stimulatory heat shock proteins (HPs), and vascular remodelling (reviewed by (Rubartelli *et al.*, 2013)). For instance, in I/R which induces tissue injury from the initial hypoxia as well as from the restoration of

blood flow and oxygen, ROS production is enhanced (e.g. in isolated perfused rat lung model (Fisher *et al.*, 1991) and necrosis is also induced (e.g. in a rat gracilis muscle model (Wang *et al.*, 2008)).

The innate immune pathways sensing infection have been involved in sterile inflammation. Sterile inflammatory responses engage receptors that are also known to respond to pathogens. This means that PRRs recognise DAMPs. However, a distinct signalling also exists (reviewed by (Shen *et al.*, 2013; Gong *et al.*, 2020)) and this will be reviewed in this section.

Table 1.6 Examples of intracellular and extracellular triggers of sterile inflammation

DAMP trigger	type of DAMP	sensor+signalling pathway	associated diseases
nuclear proteins *HMGB1	intracellular	*TLR2/4 *RAGE *CD24	*acute kidney injury *acute hepatic injury *acute allograft rejection
mitochondrial components *formylated peptides *DNA *ATP	intracellular	*FPR1 *TLR9 *ATP in combination with NLRP3	*crush injury/trauma *acute hepatic injury *acute kidney injury (ATP+ NLRP3)
monosodium uric acid crystals	intracellular	*IL-1 receptor+MyD88	*gout *acute lung injury induced by bleomycin
hyaluronan	extracellular	*TLR2/4 *CD44 *NLRP3	*acute lung injury induced by bleomycin
cholesterol	extracellular	*NLRP3	*atherosclerosis
particles: silica, asbestos	extracellular	*NLRP3	*lung fibrosis

Broad division of intracellular and extracellular triggers of sterile inflammation. HMGB1-high-mobility group box 1; RAGE-receptor for advanced glycation end products; NLRP3-NOD-, LRR- and pyrin domain-containing 3; MyD88- innate immune signal transduction adaptor molecule; FPR1-formyl peptide receptor 1. Adapted from (Shen *et al.*, 2013).

As described earlier, the detection, containment and restoration to homeostatic tissue state requires foreign molecule recognition by TLRs, which activate an array of signalling pathways. In sterile inflammation, DAMPs (also termed alarmins) play important intracellular roles. In contrast to PAMPs associated with microbes and viruses, DAMPs are endogenous danger signals derived from self and released upon tissue damage or stress, resulting in the activation of an immune response (reviewed by (Fleshner *et al.*, 2017)). DAMPs are regarded as endogenous danger signals due to the induction of potent inflammatory responses by activating the innate immune system during non-infectious inflammation (reviewed by (Chen and Nuñez, 2010; Vénéreau *et al.*, 2015)). Two classes of DAMPs are described, intracellular and extracellular (reviewed by (Chen and Nuñez, 2010; Schaefer, 2014; Patel, 2018)). Intracellular include, e.g. Necrosis-associated the chromatin-associated high-mobility group box 1 (HMGB1) proteins, heat shock proteins (HSPs,) and purine metabolites, e.g. ATP, uric acid. Intracellular DAMPs can also be released into extracellular matrix upon tissue stress and injury or cell death (reviewed by (Chen and Nuñez, 2010; Schaefer, 2014)). Extracellular DAMPs include heparan sulphate and biglycan, hyaluronan. These extracellular matrix fragments are generated through the degradation of the matrix through proteases in response to necrosis or to trigger tissue repair (reviewed by (Chen and Nuñez, 2010; Frevert *et al.*, 2018)).

The most well characterised DAMP is HMGB1. This nuclear protein, bound loosely to chromatin, is present in most cells (reviewed by (Müller *et al.*, 2004)) and enhances DNA bending (reviewed (Agresti and Bianchi, 2003)). When programmed cell death occurs, chromatin is rearranged such that HGMB1 binds irreversibly; in case of unprogrammed cell death the HMGB1 is released from necrotic cells (Scaffidi *et al.*, 2002). Interestingly, FLIP (Fluorescence Loss in Photobleaching) analysis of HeLa cells undergoing mitosis, comprising bleaching of cytoplasmic HMGB1–GFP leads to a rapid and parallel loss of fluorescence from condensed chromosomes and from the cytoplasm. This shows how motile the protein is between the nucleus and cytosol states (Scaffidi *et al.*, 2002). Outside the cell, HMGB1 can bind to the pro-inflammatory receptor RAGE and is internalised via endocytosis. This triggers pyroptosis (another form of programmed cell death) *in vitro* in mice BMDMs and *in vivo* in endotoxemia mice.

HMGB1 is increased in murine renal I/R models (Rabadi *et al.*, 2012) and linked to hepatic I/R (Kamo *et al.*, 2013).

Examples of other alarmins include HSPs, uric acid, defensins, and annexins (reviewed by (Bianchi, 2007)). Uric acid for instance, is the main alarmin released by injured cells (Shi *et al.*, 2003). Precipitation of this chemical within cells as monosodium urate (MSU) crystals activates nucleotide-binding oligomerisation domain-like (NOD)-, leucine-rich repeat (LRR)- and pyrin domain-containing 3 (NLRP3) inflammasome, a cytosolic multi-protein signalling platform known to activate inflammatory responses. For instance, *in vitro* studies have shown, that monocytes/macrophages express NLRP3 under inflammatory stimulus, e.g. murine bone marrow-derived macrophages (BMDM) stimulated with LPS (Sutterwala *et al.*, 2006) or silica (Franchi *et al.*, 2009).

The hallmarks of inflammasome activation are the production of the pro-IL-1 β , its processing to activate caspase-1-activating complex and IL-1 β and IL-18 release ((Martinson *et al.*, 2006; Franchi *et al.*, 2009), reviewed by (Jo *et al.*, 2016)). For instance, a recent study by Martinon *et al.* confirmed the features of inflammasome in THP1 monocytic cell line. The addition of MSU crystals elevated IL-1 β and IL-18, and the caspase-1 dependency of the pro-IL-1 β cleavage was shown by the addition of the caspase-1 inhibitor, zYVAD, which abolished the IL-1 β activation. Interestingly, in an *in vivo* model of crystal-induced peritonitis mice deficient in caspase-1 or IL-1R, a natural inhibitor of IL-1 signalling, exhibited peritoneal reduced neutrophil recruitment, indicating a pivotal role of the inflammasome (Martinson *et al.*, 2006).

It is also clear that mutations of NLRP can activate inflammasome inappropriately, resulting in auto-inflammatory diseases, e.g. familial cold autoinflammatory syndrome (reviewed by (Chen and Nuñez, 2010; Shaw *et al.*, 2011)).

DAMPs, similar to PAMPs, are detected by PRRs. For example, knock-out mice studies revealed that TLR2 and TLR4, together with MyD88, the adaptor protein, which is required for TLR signalling, are necessary for the detection of hyaluronan (Jiang *et al.*, 2005). Interestingly, hyaluronan initiates an inflammatory response through TLR2 and TLR4 by the induction of MIP-2 and promotes recovery from

acute lung injury by the activation of NF- κ B in a TLR-dependent manner (Jiang *et al.*, 2005).

Another receptor of key importance is the DAMP-specific receptor for advanced glycation end products (RAGE) (reviewed by (Chen and Nuñez, 2010; Gong *et al.*, 2020)). As mentioned, innate immune cells respond to the triggers of sterile inflammation through a variety of pathways, some of which are shared with pathways that respond to microorganism. However, some pathways are distinct to sterile inflammation. An example of such signalling is RAGE because RAGE is DAMP-specific receptor. This means that not all sterile inflammatory responses engage receptors that are also known to respond to pathogens (reviewed by (Shen *et al.*, 2013)). RAGE is expressed on a wide-range of cells including neutrophils, DCs, monocytes/macrophages, lymphocytes, cardiomyocytes, and neurons (Brett *et al.*, 1993; Schmidt *et al.*, 1993), and responds to a number of ligands, e.g., advanced glycated end products, DNA, RNA, HMGB1 (reviewed by (Shen *et al.*, 2013; Sorci *et al.*, 2013)). Binding to ligands induces inflammatory cascades including, NF- κ B, Janus kinase (JAK)–signal transducer and activator of transcription (STAT) and MAPK signalling pathways. This results in induction of pro-inflammatory cytokines such as TNF α ((Hofmann *et al.*, 1999; Huang *et al.*, 2001; Shang *et al.*, 2010), reviewed by (Dukic-Stefanovic *et al.*, 2001)).

As with non-sterile inflammation, the resolution of sterile inflammation requires both the inhibition of inflammatory cell recruitment and prompt removal of apoptotic and necrotic cells that remain at the site of injury. Previous studies using PMNs have demonstrated apoptotic neutrophils secrete an anti-inflammatory regulator annexin A1 (ANXA1) and that treatment of monocytes with the ANXA1-containing supernatants of apoptotic granulocytes led to significantly decreased release of pro-inflammatory cytokines, such as TNF α , when the monocytes were endotoxin-challenged (Pupjalis *et al.*, 2011). This treatment hampers monocyte interactions with activated endothelium. In zymosan (glycan derived from yeast cell walls) peritonitis mouse models, *Anxa1* deficient animals display increased PMNs recruitment, as measured by flow cytometry. Intravital microscopy confirmed the neutrophil trafficking of the leukocyte-endothelium interaction process (Chatterjee *et al.*, 2005). Interestingly, PMNs influx was observed in parallel with augmented disappearance of macrophages, in line with previous

study describing early defects in phagocytosis of mice *Anxa1* null macrophages (Yona *et al.*, 2004). *In vitro*, *Anxa1* deficient PMNs were more susceptible to activation shown by CD11b (integrin) expression when PAF was added (Chatterjee *et al.*, 2005). In the light of existing reports, it is conceivable that this mediator triggers neutrophil apoptosis, regulates monocyte recruitment, and promotes apoptotic cell disposal by macrophages. It also induces macrophage reprogramming towards a resolving phenotype (reviewed by (Sugimoto, Vago, *et al.*, 2016)).

As for necrosis, necrotic cells are sensed by the NLRP3 inflammasome. Sterile inflammation triggers a robust accumulation of neutrophils to the site of tissue injury. However, in the absence of NLRP3 inflammasome neutrophil recruitment in the peritoneal cavity was reduced in mice injected with pressure-disrupted B16 cells (a murine melanoma cell line) to induce necrosis. Furthermore, LPS-primed macrophages were stimulated with necrotic pressure-disrupted B16 cells, characterised by increased pro-inflammatory IL-1 β release. This cytokine recruits neutrophils to sites of injury but also causes a number of auto-inflammatory syndromes. Thus, this could be a potential therapeutic target. Moreover, in NLRP3-deficient mouse macrophages exposed to B16 cells grown under hypoxic conditions and macrophages exposed to complement-lysed splenocytes failed to secrete IL-1 β . This suggests that NLRP3, apart from sensing cellular injury induced by pressure disruption can also sense cellular hypoxia or complement-mediated damage (Iyer *et al.*, 2009).

CLRs can also sense non-homeostatic death without microorganism involvement. One of such receptors is Mincle. Mincle is shown to induce pro-inflammatory responses after sensing SAP130 released from dead cells. The nuclear protein SAP130 is a Mincle ligand (Yamasaki *et al.*, 2008).

To summarise, tissue injury in the absence of infection is detected via TLRs and other innate receptors. Although a distinct pathway exists (e.g. RAGE), it remains unclear whether tissue injury and microbial infection represent distinct stresses to the host. The issue is that these processes converge on the same receptors. However, it might be that the same receptor can induce distinct signal

transduction and gene expression when activated by an endogenous or a microbial stimulus (reviewed by (Barton, 2008)). This view is supported by the findings of (Li *et al.*, 2001). It was found that necrotic cells can also induce a TLR2-dependent transcriptional response that is distinct from the response induced by microbial TLR2 ligands. In necrotic cells, TLR2 mediates NF- κ B activation and expression of inflammatory genes such as KC and MIP-2 (Li *et al.*, 2001).

As described, sterile inflammation notifies the host to the presence of a noxious stimulus and activates the innate immunity. However, there are no foreign antigens derived from microbes. Thus, activation of adaptive responses is not the point. This is open to debate whether sterile inflammation enhances the induction of adaptive immunity as compared to inflammation induced by a microorganism (reviewed by (Shen *et al.*, 2013)). The question of inflammation but not sterile inflammation linking to the adaptive immunity as well as the differential signalling by microbial versus endogenous TLR ligands was also reviewed by (Iwasaki and Medzhitov, 2010). The differential signalling by exogenous (microbial) versus endogenous TLR ligands is suggested to be induced through the engagement of different co-receptors. Accordingly, microbial ligands lead to the induction of genes leading to inflammation, tissue repair and the initiation of adaptive immunity. Endogenous ligands are responsible for the induction of TLR signalling for activation of inflammation and tissue repair and do not trigger adaptive immunity (reviewed by (Iwasaki and Medzhitov, 2010)).

Finally, sterile inflammation can be seen as a mechanism of a disease. In this aspect this type of inflammation can contribute to disease progression. For instance, the NLRP3 inflammasome has a critical role in the development of insulin resistance (Zhou *et al.*, 2010; Vandanmagsar *et al.*, 2011) and insulin resistance increases the risk of developing type 2 diabetes. Sterile inflammation is a hallmark of the pathology of many liver diseases, e.g. alcoholic and non-alcoholic steatohepatitis wherein the trigger is hepatocyte death (reviewed by (Kubes and Mehal, 2012)). The importance of sterile inflammation in pathologies illustrates that this type of inflammation can be a mechanism of disease.

When sterile inflammation is not resolved, it has dramatic consequences. An example of this concerns sterile neuroinflammation. Even though it is intended to have a protective role, an excessive inflammatory response can result in further tissue damage (reviewed by (Banjara and Ghosh, 2017)). S100 protein is released at sites of inflammation (Foell *et al.*, 2006) and S100B in Alzheimer's disease, the S100B level is highest in the most severely affected regions of the brain, being associated with plaques (Eldik and Griffin, 1994).

Sterile inflammation is linked to autoimmunity. For instance, systemic lupus erythematosus, is associated with increased circulating levels of double stranded DNA; Muckle–Wells syndrome is caused by missense mutations in the nucleotide-binding oligomerisation domain (NOD)-like receptor family member NLRP3 (reviewed by (Chen and Nuñez, 2010)), NLRP3 inflammasome is upregulated in rheumatoid arthritis (Mathews *et al.*, 2014).

To conclude, further research should be done to investigate the initiation and resolution of sterile inflammation as this could lead to novel therapeutics.

1.7 Thesis aims

When in 2012 I was appointed to the Johnston lab as a research assistant, my role was to complete a research programme with the goal of understanding how cryptococcal infection causes a disease in humans. At the time there was no model, which would enable tracking macrophages (that are the dominant phagocytic cells interacting with *Cryptococcus*) and cryptococci in the entire body of a host. Therefore, there was a pressing demand to extend the range of existing models to study immunity to cryptococcal infection. Zebrafish seemed an attractive tool considering these animals have been used successfully to study fungal pathogens (Brothers *et al.*, 2013; Herbst *et al.*, 2015).

Therefore, I started with the question of developing a zebrafish model of cryptococcosis. I also wanted to address the question of macrophages behaviour during the early phases of infection. More work was added and with the help of colleagues, this resulted in a publication (Bojarczuk *et al.*, 2016), which is demonstrated in Chapter 3.

Chapter 4 concerns *C. gattii* and was linked to the general question I asked when appointed to the Johnston lab- how *Cryptococcus* causes a disease? I focused on R265, which is a clinical hyper virulent *C. gattii* VIO isolate and the mechanism underlying its pathogenicity, growth requirements and mechanism of infection remained unknown. Thus, the question was how *C. gattii* R265 strain has acquired a hyper virulent phenotype that causes disease in immunocompetent individuals.

In science, some discoveries are goal-orientated but some discoveries come about from curiosity and secondary experiments. My colleagues and I showed that MMF reduced macrophages numbers during cryptococcal infection. The reduced numbers in macrophages resulted from cell death (Gibson *et al.*, 2018). One critical innate immune response is triggering neutrophilic inflammation, which subsequent resolution of is essential for the return to homeostasis. Despite the frequent use of MMF in autoimmune and inflammatory conditions, little was known about MMF's direct effects on neutrophils. Therefore, I wanted to ask whether the induction of neutrophil cell death can occur under MMF treatment upon the observation of the macrophage cell death (Gibson *et al.*, 2018).

Thus, I have addressed the following three core hypotheses in this thesis:

- 1) Zebrafish can be used as an experimental model of cryptococcosis to understand the role of macrophages in cryptococcosis.
- 2) *C. gattii* growth assessment in the zebrafish model of cryptococcosis will reveal the cause of its virulence.
- 3) Immunosuppression therapy with the common immunosuppressant mycophenolate mofetil (MMF) has an effect on neutrophils.

In regards to 1), the lack of the *in vivo* model of cryptococcosis was the gap in knowledge at the time the aim of my work was formulated. I aimed to develop a new infection model of the opportunistic fungal pathogen *C. neoformans* in zebrafish. Zebrafish are ideal to be a model of cryptococcal infection due to the potential for *in vivo* subcellular resolution imaging in the entire body of a living

vertebrate. Cell biology data can be interpreted in the context of the whole disease and organism.

The objectives were to investigate the host-pathogen interaction on the (sub)cellular level through imaging of infection using fluorescently labelled pathogen and immune cells, enabling detailed analysis of cell biology data in the context of the whole disease and organism. The study of host and pathogen factors was to determine disease progression and outcome *in vivo*. The focus was on macrophages in particular as they have undoubted significance in anti-cryptococcal immunity.

In regards to 2), the aim was an assessment of R265 virulence *in vivo* in the zebrafish model developed in 1) and an identification of the reasons as to why the strain is virulent. The objectives were to employ R265 GFP14 to facilitate the pathogen visualisation in zebrafish. Both R265 wt and R265 GFP14 show normal growth in macrophages *in vitro* (Voelz *et al.*, 2010). Again, the focus was on macrophages to study host-pathogen interactions *in vivo* in zebrafish. To answer the hypothesis that R265 assessment *in vivo* and *in vitro* will reveal the cause of its virulence, a mouse model of infection as well as metabolic screen were employed.

In regards to 3), the aim of this project was to understand neutrophil responses influenced by MMF with the hypothesis MMF has a direct effect on neutrophil function.

MMF is an immunosuppressive agent used not only in solid organ transplantations, but also in the treatment of autoimmune and inflammatory conditions. A great deal of research on MMF has been conducted on lymphocytes, monocytes, and macrophages. MMF significantly reduces the number of macrophages due to macrophage cell death in the absence of lymphoid cells (Gibson *et al.*, 2018). MMF's direct effects on neutrophils are less clear. No significant progress has been made in this area in spite of frequent MMF use in inflammatory, including neutrophilic conditions. Considering that MMF is given for inflammatory conditions and affects macrophages (Gibson *et al.*, 2018),

the question has arisen if MMF might directly influence neutrophils independent of lymphoid factors. Many questions remain regarding not only the mechanism of MMF by which neutrophils are regulated in inflammatory diseases, where MMF effect is very likely to be founded on innate-adaptive relationship of interdependence. Moreover, what is unknown is the direct effect of MMF on neutrophils in the absence of adaptive immunity. The objectives were to use existing models of inflammation initiation and resolution in zebrafish. I address the question of specific effects of MMF on neutrophils using an *in vivo* zebrafish model of neutrophilic inflammation to understand the mechanism of the immunosuppressive drug, MMF on the innate immune system cell, neutrophil.

Chapter 2: Materials and Methods

2.1 Ethics statement

These studies have been subjected to guidelines set out in UK law in the Animals (Scientific Procedures) Act 1986, under relevant project licenses (infection 40/3574 and P1A4A7A5E; and inflammation 70/8178). Ethical approval was granted by the University of Sheffield Local Ethical Review Panel.

2.2 Fish husbandry

Zebrafish were maintained according to standard protocols (Nüsslein-Volhard and Dahm, 2002) and local animal welfare regulations. Adult fish were maintained on 14-10 hour light cycle at 28°C in UK Home Office approved facilities in the Bateson Centre aquaria at the University of Sheffield. Adults were bred by either marbling or pairing. Marbling technique is with the use of receptacle containing marbles placed into a fish tank overnight. Pairing technique involves placing one female and one male into a small mating tank with a plastic grid at the bottom to enable the embryos to fall into a separate space below and dividing the fish over night with a plastic divider. In all cases, embryos were collected the following morning by pouring the pairing or marble tank water through a plastic tea strainer. Embryos were collected into petri dishes (Scientific Laboratory Supplies Ltd (SLS), UK, Cat. No. PET3004) filled with aquarium water.

After collection, embryos were sorted with a pasteur pipette (Starlab Ltd, UK, Cat. No E1414-0300) in petri plates filled with 1X E3 solution diluted in distilled water and 0.00005% methylene blue was added (E3 10X stock 5 mM NaCl, 0.17 mM KCl, 0.33 mM CaCl₂, 0.33 mM MgSO₄ and 0.5% methylene blue (Sigma Aldrich, UK, Cat. No. 50484) were provided by the aquarium). Healthy and representing the same developmental age embryos were then moved into a new petri dish with 1X E3 and incubated at 28°C. The fish density was 60 embryos per plate. E3 medium consists of the salts required to maintain the pH for optimal embryo development. Methylene blue is an anti-fungal agent, which disrupts classical respiration by transferring electrons from the ubiquinone pool directly to oxygen

(Schirmer *et al.*, 2011). In experiments with *Cryptococcus* methylene blue was not added after zebrafish injections.

Embryos at 2 days post fertilisation (dpf) were dechorionated using two pairs of Dumont No. 5 forceps (SLS, UK, Cat. No. F6521-1EA). Dechoronation occurred in a petri dish filled with 1X E3 containing 0.00005% methylene blue. Using one pair of forceps to hold the chorion, a tear was made in the chorion with the other pair of forceps, releasing the embryo. Dechorionated animals were transferred in a pasteur pipette into another petri plate with 1X E3 and methylene blue.

Embryos were immobilised/anaesthetised by immersion in 0.0168% 3-amino benzoic acid ethyl ester, referred to as tricaine (Henry Schein Animal Health, UK, Cat. No. TJMS222) in 1X E3 for injuring, infection or imaging purposes.

In all experiments, zebrafish were below 5.2 dpf and thus were not protected animals under the Animals (Scientific Procedures) Act 1986.

2.2.1 Zebrafish lines used in the study

The wild-type and transgenic zebrafish lines used in this work are listed in Table 2.1. Zebrafish AB and *nacre* (Lister *et al.*, 1999) were used as wild-types. The transgenic zebrafish lines, *Tg(fms:Gal4.VP16)ⁱ¹⁸⁶*; *Tg(UAS:nfsB.mCherry)ⁱ¹⁴⁹* (Gray *et al.*, 2011), *Tg(mpeg1:mCherryCAAX)^{sh378}* (Bojarczuk *et al.*, 2016), *Tg(mpx:GFP)ⁱ¹¹⁴* referred to as *mpx:GFP* (Renshaw *et al.*, 2006) and *Tg(mpx:Gal4)ⁱ²²²(UAS:Kaede)^{s1999t}* referred to as *mpx:Kaede* (A. L. Robertson *et al.*, 2014), were used in this project.

Tg(fms:Gal4.VP16)ⁱ¹⁸⁶; *Tg(UAS:nfsB.mCherry)ⁱ¹⁴⁹* (Gray *et al.*, 2011), is a compound transgenic line generated by in-crossing *Tg(fms:Gal4.VP16)ⁱ¹⁸⁶* and *Tg(UAS-E1b:nfsB.mCherry)ⁱ¹⁴⁹*. The *Tg(fms:Gal4.VP16)ⁱ¹⁸⁶* was made by using bacterial artificial chromosome (BAC) recombineering. In this line, the *fms* promoter drives the expression of the hybrid transcription factor Gal4-VP16. *Tg(UAS-E1b:nfsB.mCherry)ⁱ¹⁴⁹* line expresses a fusion protein of nitroreductase and mCherry under the UAS promoter. Thus, the resulting compound transgenic line termed *Tg(fms:Gal4.VP16)ⁱ¹⁸⁶*; *Tg(UAS:nfsB.mCherry)ⁱ¹⁴⁹* works using the

GAL4-UAS system, wherein the *fms* promoter drives Gal4 expression, which, in turn, drives expression of the nitroreductase. mCherry fusion protein under the control of UAS. The line labels macrophages where the *fms* promoter is active. The line is in AB background.

Tg(mpeg1:mCherryCAAX)^{sh378} (Bojarczuk *et al.*, 2016) was generated using the Gateway Tol2Kit system (Kwan *et al.*, 2007) by recombining *mpeg1*, mCherryCAAX and a 3'polyA with the gateway destination vector. In this line a membrane targeted mCherry is under the control of the macrophage-specific *mpeg1* promoter (Ellett *et al.*, 2011). The line is in *nacre* background.

In *mpx:GFP* neutrophils are labelled with GFP. Expression of the myeloperoxidase (*mpx*, also called *mpo*) gene is confined to neutrophils (Lieschke *et al.*, 2001). The line was made using BAC recombination. A BAC (zC91B8) containing promoter sequence to the *mpo* gene was modified to contain green fluorescent protein (GFP) sequence. The modified BAC prep was microinjected into one cell stage AB wild-type zebrafish embryos to create the transgenic line (Renshaw *et al.*, 2006).

Mpx:Kaede was made by crossing *Tg(mpx:Gal4.VP16)ⁱ²²²* and *Tg(UAS:Kaede)^{s1999t}* (A. L. Robertson *et al.*, 2014).

The *Tg(mpx:Gal4.VP16)ⁱ²²²* was made using BAC recombineering, replacing GFP with GAL4. The *Tg(UAS:Kaede)^{s1999t}* was imported from the Institute of Molecular and Cell Biology fish facility (Singapore) and originally made by (Davison *et al.*, 2007). The *mpx:Kaede* line is defined as *Tg(mpx:Gal4)ⁱ²²² (UAS:Kaede)^{s1999t}*. This line recapitulates *mpx:GFP* and expresses Kaede, a photoactivatable fluorescent protein, in neutrophils when crossed to UAS:Kaede. *Mpx:Kaede* is in AB background.

Table 2.1 Zebrafish lines used in the study

Zebrafish line	Zebrafish line Description	Reference
<i>nacre</i>	wild-type with loss of pigment cells	(Lister <i>et al.</i> , 1999)
AB	wild-type	The AB line is derived from two lines, A and B, purchased by Streisinger at different times from a pet shop in Albany, Oregon in 1970s.
<i>Tg(fms:Gal4.VP16)^{j186};</i> <i>Tg(UAS:nfsB.mCherry)^{j149}</i>	<i>fms</i> promoter drives GAL4 expression, which, in turn, drives expression of the nitroreductase.mCherry fusion protein under the control of UAS; nfsB.mCherry labelled macrophages	(Gray <i>et al.</i> , 2011)
<i>Tg(mpeg1:mCherryCAAX)^{sh378}</i>	mCherry labelled macrophages under the control of <i>mpeg1</i> promoter	(Bojarczuk <i>et al.</i> , 2016)
<i>Tg(mpx:GFP)^{j114}</i>	referred to as <i>mpx:GFP</i> ; neutrophils labelled with GFP under <i>mpx</i> promoter	(Renshaw <i>et al.</i> , 2006)
<i>Tg(mpx:Gal4)^{j222} (UAS:Kaede)^{s1999t}</i>	referred to as <i>mpx:Kaede</i> ; GFP labelled neutrophils that express Kaede after photoconversion	(A. L. Robertson <i>et al.</i> , 2014)

2.3 Cryptococcal strains cultivation

C. neoformans or *C. gattii* stocks were kept in -80°C freezer (Wolf Laboratories Ltd., UK, Cat. No. U9400-0001) in Microbank™ vials (Fisher Scientific Ltd., UK, Cat. No. 15937902), commonly used in laboratories (Hagen *et al.*, 2015). The Microbank™ incorporate beads and a cryopreservative solution to ensure longer survival of the cultures and higher quantitative recoveries. One bead from a frozen stock was streaked in the laminar flow cabinet with a 2-200 µl filtered tip (SLS, UK, Cat. No. E0030077784) on a petri plate containing yeast extract peptone dextrose agar (YPDA) plate (50g/l YPD broth + agar 2g/l – both from Sigma-Aldrich, Cat. No. Y1375 and 05039, respectively and made up in distilled water) and grown at 28°C for two days. Then the cultures were re-streaked with an inoculation loop (Fisher Scientific Ltd, UK, Cat. No. 11715229) onto fresh YPDA plates in the laminar flow cabinet and cultured for another two days at 28°C. These were the working stocks, kept in the 4°C for the maximum period of 4 weeks (if not contaminated).

2.3.1 Cryptococcus strains used in this study

Cryptococcus strains used in this study are listed in Table 2.2.

C. neoformans H99, KN99 and *C. gattii* R265 were used as wild-types, hereafter referred to as H99 wt, KN99 wt and R265 wt, respectively. H99 wt is serotype A mating type α and it is *C. neoformans* var. *grubii* strain. KN99 wt is a congenic strain in the H99 genetic background and obtained from the Heitman lab (Nielsen *et al.*, 2003). H99 wt and its GFP-expressing derivative H99 GFP were obtained from the May lab (Voelz *et al.*, 2010). H99 GFP is a biolistically transformed H99 wt (Voelz *et al.*, 2010).

C. neoformans cap59 has severely compromised capsule formation (Chang and Kwon-Chung, 1994). *Cap59* mutant was generated by disrupting *CAP59* gene in H99 by biolistic bombardment (Nelson *et al.*, 2001). *Cap59* was obtained from the May lab.

KN99 GFP is a biolistically transformed KN99 wt generated in the May lab (Gibson *et al.*, 2018).

C. gattii R265 wt and R265 GFP14 were obtained from the May lab. R265 GFP14 is a biolistically transformed R265 wt (Voelz *et al.*, 2010).

Table 2.2 Cryptococcal strains used in the study

cryptococcal strain	description		origin and notes
	sero-type, molecular type	additional information	
<i>C. neoformans</i> H99	A, VN1b	clinical isolate, USA, mating type α	(Voelz <i>et al.</i> , 2010)
<i>C. neoformans</i> H99 GFP		GFP-expressing derivative of H99	(Voelz <i>et al.</i> , 2010)
<i>C. neoformans cap59</i>		the polysaccharide capsule production mutant	(Nelson <i>et al.</i> , 2001)
<i>C. neoformans</i> KN99	H99 A background, VN1b	wild-type strain, mating type α	(Nielsen <i>et al.</i> , 2003)
<i>C. neoformans</i> KN99 GFP		GFP-expressing derivative of KN99	(Gibson <i>et al.</i> , 2018)

Table 2.2 (continued)

<i>C. gattii</i> R265	B, VGIIa	wild-type strain, a clinical isolate from Vancouver Island outbreak, Canada	(Kidd <i>et al.</i> , 2004), sequence reads used in Chapter 4 obtained from https://www.ncbi.nlm.nih.gov/sra/SRX213991
<i>C. gattii</i> R265 GFP14		GFP-expressing derivative of R265	(Voelz <i>et al.</i> , 2010), sequence reads used in Chapter 4 obtained from https://www.ncbi.nlm.nih.gov/sra/SRX213992
<i>C. gattii</i> WM276	B, VGI	wild-type strain, an environmental isolate from Australia	the genome used in Chapter 4 was obtained from https://www.ncbi.nlm.nih.gov/genome/45142?genome_assembly_id=277046 and genome assembly from https://www.ncbi.nlm.nih.gov/assembly/GCF_000185945.1

Serotype and additional information are presented if available.

2.4 Preparation of *C. gattii* culture for phenotypic microarrays

The protocol was optimised based on (Zhou *et al.*, 2003; Nielsen *et al.*, 2005). *C. gattii* strains (R265 wild-type (wt) and R265 GFP14) were cultivated as in section 2.3 Cryptococcal strains cultivation.

A day before the infection experiment, petri plates with R265 wt and R265 GFP14 were taken from the 4°C. In the hood, a few colonies were scooped up from across the plate taken with the inoculation loop. The sample was introduced to 2 ml of yeast peptone dextrose (YDP) broth medium (50g in 1 litre of distilled water) added to a 14 ml culture tube (Fisher Scientific Ltd, UK, Cat. No. 11681460) and placed in a rotator, to prevent fungal cells clumping, at 28°C and 20 rotations per minute (rpm) overnight (for 16-18 hours). The minimum of seven samples of each strain was set up for overnight rotation. This was due to 30 ml capacity of turbidimeter tubes (Technopath Distribution Ltd., UK, Cat. No. 72101) used later in the protocol.

The overnight 2 ml liquid culture was mixed by pipetting up and down. 1 ml of this culture was then pelleted at 6,000 rpm, room temperature (RT) for 1 minute in a 1.5 ml microcentrifuge tube (University of Sheffield, UK, Cat. No. 100326Z). Supernatant was removed and cells were washed with 1 ml of 1X phosphate buffered saline ((PBS); ThermoFisher Scientific Ltd, UK, Cat. No. BR0014). To obtain 1X PBS a single tablet was dissolved in 100 ml of distilled water, and autoclaved to sterilise before use. After the wash the cells were resuspend in 12X YNB (Generon, UK, Cat. No. S507-100g) supplemented with histidine (HIS), leucine (LEU) and uracil (URA) (all Sigma-Aldrich, UK, Cat. No. H0750000, L8000-25G and UO750-25G, respectively). The contents of microcentrifuge tubes with fungal cells, 12X YNB and amino acids were transferred into relevant R265 wt and R265 GFP14 turbidimeter tubes. The blank was the supplemented 12X YNB without the cells. The cells were adjusted to 18% transmittance using turbidimeter tubes and a turbidimeter (Biolog, USA, Cat. No. 3587). The fungal cells were then transferred into two separate 1.5 ml microcentrifuge tubes.

The 12X YNB was made according to manufacturer's instructions. 10X YNB is achieved by dissolving 6.7 g in 100 ml distilled water. Thus, 12X YNB was made by adding 8.04 g into 100 ml distilled water. Next, 12X concentrated amino acids (24 mg HIS, 120 mg LEU, and 24 mg URA) were added, i.e. the final concentration of amino acid in the well after addition of IFY-0 was 20 µg/ml HIS and URA, 100 µg/ml LEU. After supplementing YNB medium with amino acids, which are supplements for corresponding auxotrophic markers commonly present in *Saccharomyces* laboratory (personal communication with Biolog, which supplies Technoplast Distribution Ltd. in the UK), the pH of the medium was adjusted to 5.4 and sterilised with 0.22 µm filters (Sigma-Aldrich, UK, Cat. No. SLMPL25SS) in the hood, in agreement with the manufacturer's instructions. Of note, the YNB preparation includes glucose or dextrose addition. Sugar was not added in my protocol as cryptococci will use those substrates instead of what is in the plate.

Next, 10 ml of PM additive was prepared. This comprised 1.2X IFY-0 base (Technopath Distribution Ltd., UK, Cat. 72231) supplemented with 5 mg/ml (NH₄)₂SO₄, (VWR International Ltd, UK, Cat. No. 444445Q), 0.85 mg/ml KH₂PO₄, 0.15 mg/ml K₂HPO₄ and 0.5 mg/ml MgSO₄ (Sigma-Aldrich, UK, Cat. No. P5655, 60353, M2643 respectively), all at 12X. PM additive was then 0.22 µm filter-sterilised in the hood.

The fungal cells along with the PM additive were then carried to Sheffield Institute for Translational Neuroscience (SITraN). With the help of Dr Scott Allen, Senior Non-Clinical Fellow, the experiment was set up as follows: one hour before cells arrived to SITraN, two PM1 plates (Technopath Distribution Ltd., UK, Cat. No 12111) along with a 1.2X IFY-0 base solution were taken out from the 4°C cold room to warm up. In the laminar hood, two centrifuge 15 ml universals (Sigma-Aldrich, UK, Cat. No. CLS430055-500EA) were used: one for R265 wt and one for R265 GFP14. Into each tube, 9.84 ml of IFY-0 base, 1 ml of PM additive, 0.16 ml of dye D (Technopath Distribution Ltd., UK, Cat. No. 74224) and 1 ml of fungal cells in the supplemented 12X YNB and. The dye is light sensitive; therefore, the

light was off in the hood. Next, 100 µl of this master mix was added to R265 wt/ R265 GFP14 PM1 plates.

The plates were sealed with sterile seal-plate film (Sigma-Aldrich, UK, Cat. No. Z369667-100EA) to stop gas transfer and incubated in an OmniLog Phenotype Microarray system at 30°C. The dye colour change was measured every 15 min for 36 hours.

Unfortunately, little that can be said about reagents used in the phenotypic assay because Biolog considers most of the information proprietary (personal communication with Biolog Technical Support). The exact concentrations of chemicals are not important, as long as the concentrations are in a typical range that cells prefer. For example, typical ranges for carbon sources would be 2 to 20 mM (Biolog's policy on disclosing PM MicroPlate Chemistry).

2.5 Phenotypic microarrays

PM1 are only-carbon utilisation plates, which are carbohydrate plates used for metabolic tests for bacteria and fungi. This is a system where fungal cells are metabolically profiled using a 96 well plate assay where every single well is coated with a different energy substrate. Essentially the cells are added to the plate in supplemented media without any carbohydrates as the cells will use those substrates instead of what is in the plate. Therefore, although dextrose is recommended by the supplier to be added to YNB, it was not added on top of amino acids. The plates were incubated at 30°C for 36 hours in an OmniLog machine. The dye D is a redox dye, which picks up electrons from NADH⁺ produced by the cells metabolising the energy substrate in the well. When reduced the dye turns purple and the colour change can be kinetically monitored in the OmniLog machine. The system has a charge-coupled device (CCD) camera taking pictures every 15 minutes and converts the differences in the colour change into CCD Camera Units and then into kinetic data. The metabolic profile of the cells at 144 different points in the cellular metabolic pathway is generated and shows any differences between the cell strains.

2.6 Cryptococcal culture and counting

A day before any experiment including cryptococcal culture, a petri plate with the strain of interest was taken from the 4°C. In the laminar flow cabinet, a few colonies were scooped up from across the plate taken with the inoculation loop. This assures heterogeneity of the sample. The sample was introduced to 2 ml of yeast peptone dextrose (YDP) broth medium (50g/l) added to a 14 ml culture tube (Fisher Scientific Ltd, UK, Cat. No. 11681460) and placed in a rotator, to prevent the cells from clumping. This was at 28°C, 20 rotations per minute (rpm) and overnight (for 16-18 hours).

The overnight 2 ml liquid culture was mixed by pipetting up and down in the laminar flow cabinet. 1 ml of this culture was then pelleted at 6,000 rpm, room temperature (RT) for 1 minute in a 1.5 ml microcentrifuge tube (University of Sheffield, UK, Cat. No. 100326Z) using Genfuge 24D centrifuge (Progen Scientific Ltd, UK, Cat. No. C-2400). While the sample was centrifuging, 95 µl of PBS in the laminar flow hood was added to another microcentrifuge tube. The collected pellet was re-suspended in 1 ml of PBS. 5 µl of re-suspended culture was then added to the previously dispensed 95 µl of PBS (making 1:20 dilution) and mixed by pipetting up and down prior to counting. This was also done in the hood. The sample was then centrifuged and only the pellet was kept. The number of *C. neoformans*/*C. gattii* cells from the 1:20 diluted sample were counted using the Neubauer haemocytometer (Camlab, UK, Cat. No. 1127884).

The haemocytometer was assembled by placing the coverslip carefully on the top of the middle section of the chamber slide. To count each culture, 10 µl of the diluted culture was taken and carefully pipetted between the coverslip and the counting chamber. The cells were counted in the most central 25 squares using a 10X objective lens (Figure 2.1) Each red square of the haemocytometer represents the total volume of $0.1 \text{ mm}^3 = 10^{-4} \text{ cm}^3$ (1 mm² area x 0.1 mm depth). Since 1 cm³ corresponds to the volume of 1 ml, the subsequent cell concentration per ml (and the total number of cells) was calculated as: number of cells per ml = average cell count in the most central 25 squares x dilution (20) x 10⁴ (to correct for 1ml), i.e. 200 cells x 20 x 10⁴ = 4 x 10⁷ cfu/ml.

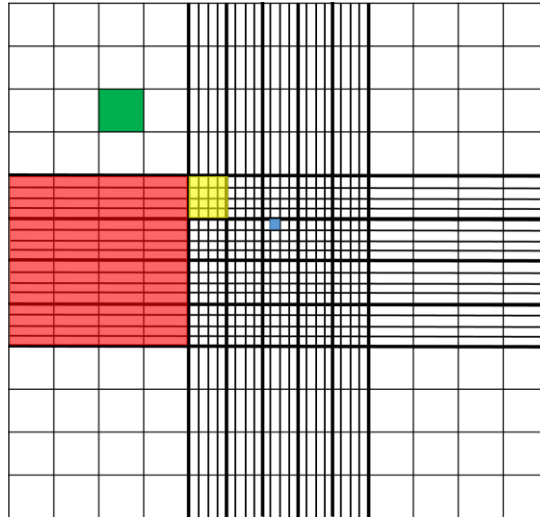


Figure 2.1 Haemocytometer grid. Red square area= 1 mm², to convert into volume: 1 mm² x 0.1 mm (depth)=0.1 mm³=0.1 µl=100 nl; green square area=0.25 mm x 0.25 mm=0.0625 mm², to convert into volume: 0.0625 mm² x 0.1 mm (depth)=0.00625 mm³=0.00625 µl=6.25 nl; yellow square area=1 mm²/25=0.04 mm², to convert into volume: 0.04 mm² x 0.1 mm (depth)= 0.004 mm³=0.004 µl= 4 nl; blue square area=1/25/16=0.0025 mm², to convert into volume: 0.0025 mm² x 0.1 mm (depth)=0.00025 mm³=0.00025 µl=0.25 nl

The correction of 10⁴ results from the following proportions: if there are, e.g. 200 cells in 0.1 mm³ (red square in Figure 2.1) being equal to 200 cells in 0.1 µl, then the number of cells in 1 ml is calculated as:

$$\begin{array}{l} 200 \text{ cells}-0.1\text{mm}^3 \text{ (1 red square)} \\ X \text{ cells}-1 \text{ ml} \end{array}$$

$$\text{this equals to } \frac{200 \text{ cells}-0.1 \mu\text{l (1 red square)}}{X \text{ cells}-1000 \mu\text{l}}$$

$$X \text{ cells} = (1000 \mu\text{l} \times 200 \text{ cells}) / 0.1 \mu\text{l} = 200 \times 10^4$$

2.7 *In vitro* growth of *C. gattii* strains in rich and minimal media

On day 0 two cultures of R265 wt and two of R265 GFP14 were set up overnight as described in section 2.6 Cryptococcal culture and counting. Each sample was in 2 ml of YPD. On day 1, the two R265 wt samples were mixed with each other and the two R265 GFP14 were mixed up with each other. This was to obtain more

volume. Out of these samples, three samples of 1 ml in YPD for each strain were prepared. This was without knowing their concentrations. Then 50 µl of each sample was introduced to 1950 µl of either YPD or the minimal medium. These six samples were incubated overnight at 28°C, 20 rpm. On day 2, the samples were counted in 1ml of PBS on a haemocytometer as described in section 2.6 Cryptococcal culture and counting. However, no difference was observed. Therefore, the cells were re-introduced to either YPD or minimal media and grown for one more day, i.e. incubated overnight at 28°C, 20 rpm. On day 3 final counts were taken.

2.8 General zebrafish techniques

2.8.1 Tail fin injury

Zebrafish larvae were anaesthetised by immersion in 0.0168% of tricaine in a petri dish in 1X E3. A surgical scalpel blade (Fisher Scientific, Cat. No.11738373) was used to fully transect the caudal fin in order to initiate inflammatory response. The injury was always performed at the distal-most point of the pigment gap at 2 dpf (Figure 2.2). After tail transection, fish were transferred into another E3 plate to allow recovery and incubated at 28°C.

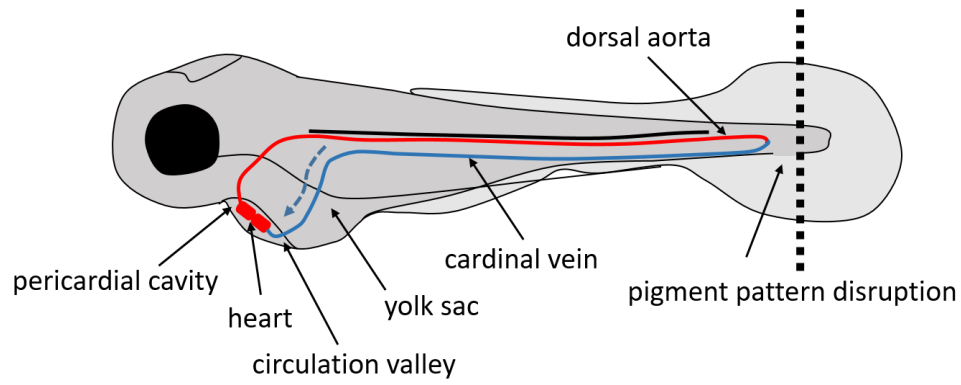


Figure 2.2 Tail transection of 2 dpf zebrafish larva. The tail fin was transected at the point indicated by the dotted black line. The blue dashed line with an arrowhead denotes the direction of blood flow into the circulation valley. Adapted from (Huang et al., 2015).

2.8.2 Time course counting

Following tail transection, larvae were anaesthetised in 0.0168% tricaine and viewed under a fluorescent stereo microscope both in bright field and GFP channels (Nikon SMZ1000). GFP brightness was of 100% on the Nikon C-HGFI Intensilight Precentered Fiber Illuminator whereas bright field lighting was adjusted with the control knob without the illuminator. In each individual fish, the number of neutrophils at the site of injury was counted by eye. The count involved only neutrophils posterior to the circulatory loop.

In all experiments, larvae were immersed in a solution of the test compound diluted in 1X E3 embryo media. In experiments including 1 time-point, larvae were transferred into separate petri dishes with 1X E3 and anaesthetised in 0.0168% tricaine (1 fish per dish). After counting the number of neutrophils persisting at the site of injury, fish were culled.

In experiments including 2 time-points, the number of neutrophils was assessed as described above. Following the count, fish were transferred into fresh 1X E3 medium to allow recovery. Thereafter larvae were added to new wells to achieve the desired concentration of test compounds. Only after the final count, fish were culled.

2.8.3 Compound treatment of zebrafish larvae

96-well plates (SLS, UK, Cat. No. 324001) were set up for experiments involving chemical treatment of larvae. Compounds tested were made up in dimethyl sulfoxide (Sigma Aldrich, UK, Cat. No. D8418). Compound administration was by immersion of the larvae in a solution of the test compound diluted in 1X E3 embryo media. The total well volume was 200 μ l.

Mycophenolate mofetil (MMF) was dissolved in dimethyl sulfoxide (DMSO) to a concentration of 10 mM and then diluted to 1 mM in DMSO. 1 mM aliquots were used to make 1 μ M in 1X E3 medium stored in -20°C. The final working concentration of MMF was 0.5 μ M in 1X E3.

SP600125 was dissolved in DMSO to 30 mM and stored in -20°C. This was then diluted in 1X E3 to a working concentration of 30 µM.

Azathioprine (AZA) was dissolved in DMSO at 37°C into 83 mM aliquots, which were stored at -20°C. These were diluted in 1X E3 to a working concentration of 200 µM.

Z-VAD was dissolved in DMSO to 20 mM and stored at -20°C. The working concentration was 100 µM in 1X E3.

The concentration of DMSO used in vehicle controls was always equal to the highest concentration of DMSO used to dilute compounds in an experiment (Table 2.3). For instance, if MMF and SP600125 were used, the concentration of DMSO used as a control would be equivalent to SP600125 (0.1%).

Table 2.3 Compound treatments in MMF study

Treatment	Final DMSO concentration	Supplier	Product code
0.5 µM MMF	0.05% DMSO	Sigma-Aldrich, UK	SML0284
30 µM SP600125	0.1% DMSO	Cambridge Bioscience, UK	SM41
200 µM AZA	0.2% DMSO	Sigma-Aldrich, UK	A4638
100 µM Z-VAD	0.5% DMSO	Santa Cruz Biotechnology, UK	sc-311561A
100 µM Z-VAD with 0.5µM MMF	0.55% DMSO	as above	as above

2.8.3.1 MMF

Suggested therapeutic range of MMF in liver transplant recipients falls between 1.0–3.5 µg/ml (through serum or plasma levels, equivalent of 3.125 µM -10.9 µM, respectively) (Tredger *et al.*, 2004). In the body of liver transplant patients it ranges from 1.5 µM (0.5 µg/ml) up to 22 µM (7.3 µg/ml) (Dasgupta *et al.*, 2013).

However, in zebrafish MMF produces some toxic effects. The concentration of 0.9 μM /l significantly reduces blood vessel formation and above 1.5 μM /l prevents any extended development of intersegmental blood vessels (Wu *et al.*, 2006). Due to inability to introduce therapeutic doses resulting in the inhibition of angiogenesis, a safe concentration of 0.5 μM has been established in the Johnston lab (Gibson *et al.*, 2018).

2.8.3.2 SP600125

SP600125 is an inhibitor of c-Jun N-terminal kinase that has been suggested to promote TNF α mediated neutrophil apoptosis (Avdi *et al.*, 2001; Hallett *et al.*, 2008). The compound demonstrated a great ability to drive inflammation resolution in zebrafish by significantly reducing the number of neutrophils at 12 hpi as compared to DMSO and GSK650394 (personal communication; A. Robertson). GSK650394 is an inhibitor of serum- and glucocorticoid-regulated kinase-1 (SGK-1) and drives inflammation resolution (Burgon and Renshaw, 2013) but SP600125 is even more potent. Its effect was demonstrated in a zebrafish compound screen for accelerators of inflammation resolution (A. L. Robertson *et al.*, 2014). To minimise the chance of picking up false positives or inhibitors of recruitment, larvae with mounted inflammatory response at 4 hpi were chosen and treated with library compounds. These were tested alongside untreated controls, DMSO vehicle and either 10 μM GSK650394 or 30 μM SP600125 as a positive controls (A. L. Robertson *et al.*, 2014). This was followed by manual scoring at 12 hpi, when inflammation resolution is only partially complete in controls (Renshaw *et al.*, 2006). The manual scoring was between 0 and 3, based on the number of larvae within the well that appeared to have a reduced number of neutrophils at the site of injury at 12 hpi (A. L. Robertson *et al.*, 2014). The mean score of 1.5 was used as the threshold for positive hit selection. In some instances GSK650394 treatment produced a precipitate, thus SP600125, at the concentration of 30 μM was considered to represent a better and more stable control (personal communication; A. Robertson). The secondary screen of 95 hits selected in the initial one- run with SP600125 as a positive control.

Based on those results, SP600125 was used in resolution assays in my zebrafish experimental work. However, it should be noted, the compound has also been reported to affect granulocyte chemotaxis (Zhang *et al.*, 2008) and in zebrafish to block neutrophil recruitment to damaged neuromasts in the lateral line (d'Alençon *et al.*, 2010). Moreover, SP600125 attenuates JUN N-terminal kinase (JNK) mediated recruitment of neutrophils and monocytes to the lungs in a mouse model of LPS-induced lung injury (Arndt *et al.*, 2005; Young and Arndt, 2009). SP600125 inhibits macrophage migration to the wound in the tail injury zebrafish model and this is partially via the inhibition of matrix metalloproteinase 1 (MMP13), which is a down-stream target of the JNK-AP-1 transduction pathway, important in remodelling of the extracellular matrix to assist chemotaxis (Zhang *et al.*, 2008). The line used in the study was transgenic *Tg(zlyz:EGFP)* labelling neutrophils, recruitment of which was suppressed by SP600125. Based on this information, I selected SP600125 to be a positive control in neutrophil recruitment assays.

2.8.3.3 AZA

AZA is composed of 6MP in 55% by molecular weight and 88% of AZA is converted to 6MP (Bradford and Shih, 2011). Metabolism of AZA, as described in section 5.1.6 Azathioprine (AZA), involves three competitive pathways through: 1) hypoxanthine phosphoribosyltransferase (HPRT) activity to convert 6-mercaptopurine (6MP) into 6-thioinosic acid (6TA) followed by inosine-5'-monophosphate dehydrogenase (IMPDH) activity to convert 6TA into 6-thioguanine monophosphate (TGMP), further forming 6-thioguanine nucleotides (6TGNs), of which 6-thioguanine triphosphate (TGTP)-is the main compounds associated with immunosuppression (Lennard *et al.*, 1989); 2) TPMT activity in 6MP conversion into methylmercaptopurines (MeMPNs) associated with hepatic toxicity (Lennard *et al.*, 1989); 3) xanthine oxidase (XO) activity in transformation of 6MP into inactive 6TU (Chan *et al.*, 1990). An assay to detect the major AZA and 6MP toxic metabolites, namely 6TGNs was established using red blood cells (RBCs) (Lavi and Holcenberg, 1985). The level of the toxic metabolites in RBCs influences the dose of AZA. Another approach when establishing the dose is to

check levels of TPMT as patients' genetic polymorphism in TPMT enzyme influences their responsiveness to therapy (Cuffari, 2006). The recommended dose for AZA is 2-2.5 mg/kg per day (Bradford and Shih, 2011).

AZA has been used in zebrafish in two separate studies. Firstly, to investigate drug-induced seizures with no positive result seen at the concentration of 200 and 600 μM in water (Koseki *et al.*, 2014). Secondly, to study the effects on macrophages during cryptococcal infection. The concentration used was 200 μM in 0.16 mM NaOH (Gibson *et al.*, 2018). In this present work, AZA was at the same concentration but dissolved in DMSO.

2.8.3.4 Z-VAD

Z-VAD is a dipeptide pan-caspase inhibitor. It has been shown to have good cell-permeation properties through the plasma membrane to reach caspases (Reed, 2002), where it binds irreversibly to the active site catalytic cysteine of caspases (Mittl *et al.*, 1997). Caspases are related to cysteine proteases mediating cell-suicide proteolytic reactions (Thornberry and Lazebnik, 1998), therefore critical in the intracellular signalling that triggers apoptosis (Jaeschke *et al.*, 2000). Several lines of evidence indicated genetic or pharmacological inhibition of caspases can avert the cell death caused by endogenous and exogenous apoptosis stimuli (Yaoita *et al.*, 1998; Braun *et al.*, 1999; Mocanu *et al.*, 2000). Z-VAD was tested in zebrafish inflammation assays at 100 μM (Loynes *et al.*, 2010). Thus, this dose was used in my work.

2.8.4 Inflammation assays

2.8.4.1 Recruitment

To test neutrophil recruitment to tissue injury larvae were injured at 2 dpf by tail fin transection (Figure 2.2) to initiate an inflammatory response involving recruitment of neutrophils to the site of injury (Renshaw *et al.*, 2006). The number of fluorescent neutrophils was counted by eye at 6 hpi at the wound site under a stereo microscope (Nikon SMZ1000 with Nikon C-HGFI Intensilight Precentered Fiber Illuminator) to detect changes in neutrophil numbers that could indicate

recruitment inhibiting effects of MMF. Neutrophils counted were posterior to the circulatory loop. Zebrafish were anaesthetised by immersion in 0.0168% tricaine in 1X E3 prior to the count.

2.8.4.2 Resolution

To assess MMF activity in accelerating resolution of inflammation, larvae were injured at 2 dpf (Figure 2.2). The number of fluorescent neutrophils recruited to the inflammation site was assessed in the region posterior to the circulatory loop. Neutrophil number was counted manually by eye under a fluorescent stereo microscope (Leica MZ10F, GFP plus filter) at 6 hpi and 24 hpi (2 and 20 hours after addition of MMF, respectively). After 6 hpi count larvae were recovered in fresh 1X E3 and returned to a new well plate. Zebrafish were anaesthetised by immersion in 0.0168% tricaine in 1X E3 prior the counts.

2.8.4.3 Total number of neutrophils

To evaluate the total number of neutrophils, uninjured fish were incubated with compounds for 24 hours and imaged at 6 and 24 hours. Prior to each time- point, fish were anaesthetised by immersion in 1X E3 with 0.0168% tricaine and mounted in agar channels for imaging. Channels were made by adding 200 μ l of 1% agar (Sigma Aldrich, UK, Cat. No. 05039) in 1X E3 containing 0.168% tricaine into glass-bottomed, 96-well plates (SLS, UK, Cat. No. 324001). Channels were cut in cooled agar using GelX4 tips (Alpha Laboratories Ltd, UK, Cat. No. EL2650). Each zebrafish was imaged as two or three contiguous fields of view depending on the age of fish (at 2 dpf fish are shorter and do not require three fields of view; however sometimes 3 dpf did not need three fields either) that were assigned from bright-field images. 81 z sections, 5 μ m apart, were captured in GFP channel and a reference bright-field image was taken. Zebrafish were imaged on a Nikon Ti-E microscope with a CFI Plan Apochromat λ 10X, N.A.0.45 objective lens and using Intensilight fluorescent illumination with ET/sputtered series fluorescent filters 49002 (Chroma, Bellow Falls, VT, USA). Images were captured with a Neo sCMOS camera (Andor, Belfast, UK) and NIS Elements 391 software (Nikon,

Richmond, UK). Nikon Ti-E was fitted with a climate controlled incubation chamber (28 °C; Okolabs, Pozzuoli, Italy).

After 6 hpi imaging, larvae were recovered in fresh 1X E3 and returned to a new numbered 96-well plate to be then imaged at 24 hpi. Image analysis of total neutrophil number was performed using a manual cell counter (VWR International Ltd, UK, Cat. No. 720-0162).

2.8.4.5 Apoptosis

To assess the rate of apoptotic neutrophils *in vivo*, *mpx*:GFP larvae were injured and selected as described in the resolution assay. At 12 hpi larvae were fixed overnight in 4% paraformaldehyde ((PFA); Fisher Scientific Ltd, UK, Cat. No. 11406582) at 4°C. The next day Tyramide Signal Amplification (TSA) staining was performed using TSA plus kit (Fluorescence Systems, Perkin Elmer Inc., Waltham, USA, Cat. No. NEL741001KT). This tags neutrophils *mpx* to allow their visualisation under GFP filter. Before staining, larvae were washed in phosphate buffer saline ((PBS); Oxoid, UK, BR0014G) followed by a brief wash in amplification diluent from TSA kit. Larvae were then incubated at 28°C for 10 min in the dark in a 1:50 dilution of FITC TSA in amplification diluent. This step enabled fluorescence detection because the tyramide amplification reagent is directly labelled with a fluorophore. After the incubation, larvae were washed 3x5 minutes in PBS and checked for successful stain before continuing with fixing at room temperature (RT) for 20 minutes in 4% PFA. To stain for an apoptotic DNA fragmentation- TUNEL (Rhodamine Apoptag Red In Situ) kit was performed (Millipore Ltd, UK, Cat. No S7165) (Figure 2.3). The assay utilises terminal deoxynucleotidyl transferase enzyme (TdT) to catalyse attachment of deoxyuridine triphosphate (dUTP) nucleotides contained in the reaction buffer to the broken DNA, specifically to its free 3'-OH termini. The nucleotides in the reaction buffer are linked with dioxygenin and are further detected by anti-dioxygenin-rhodamine. The new DNA ends generated upon DNA cleavage and detection by enzymatically labeling the free 3'-OH termini with modified nucleotides are typically localised in morphologically identifiable nuclei and apoptotic bodies. The kit does not stain normal or proliferative nuclei

characterised by insignificant numbers of DNA 3'-OH ends. ApopTag Kit detects single and double-stranded breaks associated with apoptosis. For ApopTag Red *in situ* apoptosis detection staining larvae were washed for 3 times 5 min each in PBS, then left at room temperature in 10 µg/ml proteinase K for 90 min, washed 2x5 minutes in PBT (PBS plus 0.1% Tween 20 (Sigma Aldrich, UK, Cat. No. P139)) and fixed for 20 minutes in 4% PFA at RT. This was followed by another 2x5 minutes PBT washes and adding 1:2 of -20°C cold acetone:ethanol (acetone Sigma Aldrich, UK, Cat. No.650501; ethanol Fisher Scientific Ltd, UK, Cat. No. 10428671) for 7 minutes at -20°C. After further 3x5 minutes PBT washes, larvae were incubated in 50 µl equilibration buffer for 1 hr at RT, which was then replaced with 16 µl TdT enzyme and 30 µl reaction buffer for 90 minutes at 37°C. Next, 200 µl Stop Buffer for 3 hours at 37°C was added. This was followed by 3x5 minutes PBT washes, adding 62 µl anti-dig-rhodamine and 68 µl blocking solution, and overnight gently shaking at 4°C. The following day larvae were washed 4 x 30 minutes in PBT, fixed for 30 minutes in 4% PFA at RT, again washed 4 x 5 minutes in PBT and finally stored at -20°C in 80% glycerol (VWR International Ltd, UK, Cat. No. 356350) until imaging. For this purpose, the tail was removed using a surgical blade while fish were placed in a petri dish in 80% glycerol. Then the tails were mounted with 75% glycerol on 76x26 mm glass microscope slides (Thermo Scientific Menzel, UK, Cat. No. 12404070) with a 22x22 mm # 0 (0.08-0.12mm) cover glass (Fisher Scientific Ltd, UK, Cat. No. 015717582) and imaged by confocal microscopy. Confocal images were captured using a Ultraview Nipkow spinning disk confocal (Perkin Elmer) on an Olympus IX81 inverted microscope with 1000x1000 Hamamatsu 9100-50 front illuminated EMCCD camera, with UPLSAPO 20x NA 0.75 objective lens, using Volocity 6.3 (Perkin Elmer, UK). GFP was visualised by excitation at 488 nm and TxRed at 561 nm using GFP emission filter, 527(55), and a 455(80)/615(70)TxRed filter. At least 15 sections 5.57 µm apart, were captured in each channel. Image processing was manual by counting the number of apoptotic dual-positive neutrophils for green and red fluorescence. Rates of apoptosis were assessed by the percentage of TSA-positive neutrophils labelled via TUNEL.

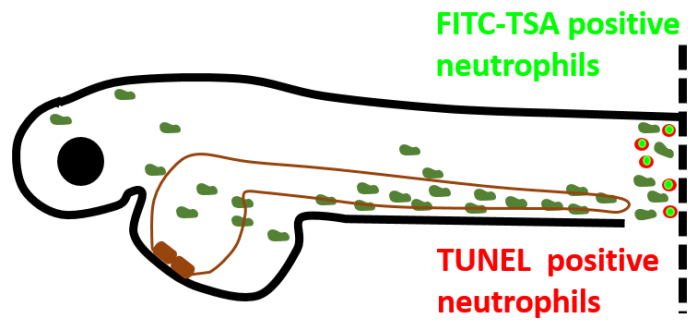


Figure 2.3 Zebrafish model of neutrophil apoptosis at the tail fin injury site. The fin was transected at the point indicated by the dashed black line. The brown line indicates the main circulatory system. Green represents neutrophils. Red indicates TUNEL positive neutrophils. Bright green depicts FITC-TSA positive neutrophils.

2.8.4.6 Reverse migration

In reverse migration assay, tail transection (Figure 2.4) was performed on *Tg(mpx:Gal4)ⁱ²²²(UAS:Kaede)^{s1999t}* line (referred in this thesis to as *mpx:Kaede*) (A. L. Robertson *et al.*, 2014). The line recapitulates expression of *mpx:GFP* line and expresses Kaede specifically in neutrophils. Kaede acts as a green chromophore that is converted to red under UV or violet light (Ando *et al.*, 2002). At 2 dpf, Kaede-positive larvae were selected and the inflammatory response was initiated as in the resolution assay at 2 dpf and at 4 hpi larvae with comparable numbers of recruited neutrophils were immediately treated with MMF or DMSO. At 5 hpi larvae were mounted in 0.8% low melting point agarose (Sigma-Aldrich, UK, Cat. No. A9414) containing the required concentration of MMF or DMSO covered in 1X E3 also containing the required concentrations of test and control compounds in a Lab-Tek^RII four well chamber slide (Fisher Scientific Ltd, UK, Cat. No. 10717931). This was followed by photoconversion at the peak of inflammation (6 hpi) in the region posterior to the circulatory loop. For the conversion, 10X UPLSAPO NA 0.4 objective and an UltraVIEW PhotoKinesis device on an Ultraview Nipkow spinning disk confocal microscope (PerkinElmer Life and Analytical Sciences) was used. Kaede-marked neutrophils were photo-converted from green to red using 120 pulses of the 405 nm laser at 40% laser power (Elks *et al.*, 2011; Dixon *et al.*, 2012). The UltraVIEW PhotoKinesis apparatus was calibrated using fluorescent ink (Stabilo BossTM Berks, UK) as a photo-bleachable substance, marked on a glass microscopic slide. To ensure only the neutrophils in the region posterior were photo-converted, a region of interest was drawn. To ensure Kaede neutrophils were photo-converted, the cells were checked for the loss of green at 488 nm and appearance of red fluorescence at 561 nm (GFP and TxRed diode lasers, respectively). However, the green fluorescence was not always lost completely. Due to technical issues, larvae were time-lapsed on three different microscopes. In the first experiment larvae were imaged on Ultraview Nipkow spinning disk confocal (Perkin Elmer) on an Olympus IX81 inverted microscope with 1000x1000 Hamamatsu 9100-50 front illuminated EMCCD camera, fitted with 10X UPLSAPO NA 0.4 objective lens; controlled through the software Volocity 6.3 (Perkin Elmer, UK). GFP and TxRed

filters (527(55) and 455(80)/615(70), respectively) were used with excitation at 488 nm and 561 nm, respectively. In the second experiment- Nikon Eclipse TE2000-U inverted compound fluorescence microscope fitted with a 10X, 0.30 NA Plan Flour objective and a 1394 ORCA-ERA camera (Hamamatsu Photonics, Hamamatsu City, Japan) with NIS Elements 391 (Nikon, Richmond, UK). 89201 ET GFP/mCherry filters were used. The last set of imaging was performed using a Nikon Ti-E with a CFI Plan Apochromat λ 10X, N.A.0.45 objective lens, a custom built 500 μ m Piezo Z-stage (Mad City Labs, Madison, WI, USA) and using Intensilight fluorescent illumination with ET/sputtered series fluorescent filters: GFP 49002 and mcherry 49008 (Chroma, Bellow Falls, VT, USA). Images were captured with Neo sCMOS, 2560 \times 2160 Format, 16.6 mm \times 14.0 mm Sensor Size, 6.5 μ m pixel size camera (Andor, Belfast, UK) and NIS-Elements (Nikon, Richmond, UK). In all cases, 8 hours time-lapses were recorded with acquisition at 2-minute intervals.

For consistency, robustness and fairness of data, vehicle control and the compound of interest treated fish were photo-converted alternately and time-lapsed in the same order.

Reverse migration was assessed by counting the number of neutrophils that migrated away from the site of injury every 30 minutes over the period 8 hours in the posterior and anterior region to the circulatory loop. The region of interest was at the anterior of the tail and this data set was extracted to plot the number of photo-converted neutrophils leaving the area of transection (Figure 2.4). The length of the anterior region of the tail considered for measurement was on average of 700 μ m.

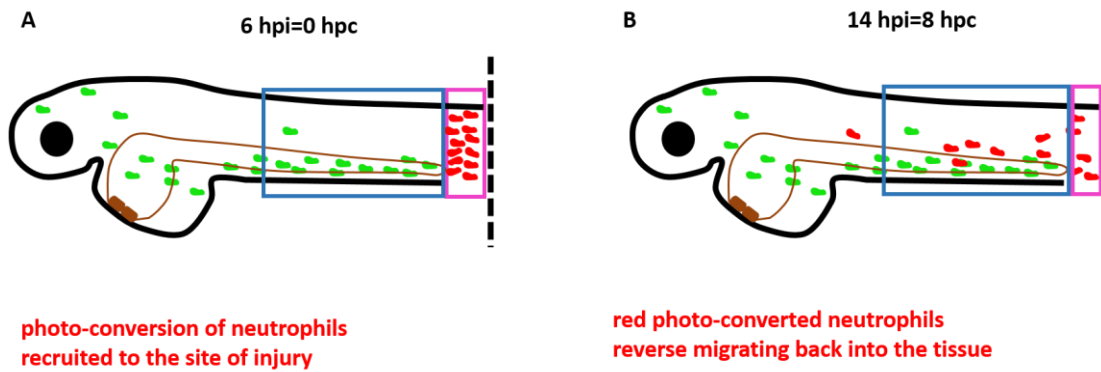


Figure 2.4 Zebrafish model of neutrophil reverse migration. The tail fin was transected at the point indicated by the dashed black line. The brown line indicates the main circulatory system. Green represents not photo-converted neutrophils. Red indicates photo-converted neutrophils. Pink box indicates the posterior region of the tail in which neutrophils were photo-converted. Blue box indicates the anterior region of the tail where reverse migration was assessed. **(A)** Recruited neutrophils photo-converted at 6 hpi (equal to 0 hours post conversion (hpc)). **(B)** Red photo-converted neutrophils reverse migrating back into the tissue at 14 hpi (8 hpc).

2.8.5 Infection assay

2.8.5.1 Preparation of *C. neoformans*/*C. gattii* culture prior to injection

A day before infection, a petri plate with the strain of interest was taken from the 4°C. The culture preparation and counting was as described in Cryptococcal culture and counting. If, e.g. 200 cells were counted then in 1 ml there are 200 cells $\times 20 \times 10^4 = 4 \times 10^7$ cfu/ml.

After calculating the number of cryptococci cells per 1 ml PBS, the pelleted sample was then re-suspended in the correct amount of sterile 10% (vol/vol) Polyvinylpyrrolidinone (PVP), 0.5% Phenol Red (SLS, UK, Cat. No. P0290) in PBS. PVP is a polymer that increases the viscosity of the injection fluid and prevents microbes clustering in the injection needle (Carvalho *et al.*, 2011; Spaink *et al.*, 2013). Phenol Red is a dye used to visualise the infections. The following formula was used to calculate the volume of PVP-Phenol Red:

$C_1V_1=C_2V_2$, where C_1V_1 is concentration/amount (start) and volume (start) and C_2V_2 is concentration/amount (final) and volume (final of 10% PVP, 0.5% Phenol Red in PBS).

This example was to give a 1000 cfu (colony forming unit) injected in the volume of 1 nl into zebrafish based on a suspension containing 4×10^7 cfu/ml:

$$4 \times 10^7 \text{ cfu/ml} \times 1 \text{ ml} = 1000 \text{ cfu/nl} \times V_2$$

$$V_2 = \frac{4 \times 10^7 / \text{ml} \times 1 \text{ ml}}{1000 \text{ cfu/nl}} = \frac{4 \times 10^7}{1000 / \text{nl}} = \frac{4 \times 10^7}{\frac{1000}{0.000001} \text{ ml}} = \frac{4 \times 10^7}{1 \times 10^9 \text{ ml}} = 4 \times 10^{-2} \text{ ml} = 0.04 \text{ ml} = 40 \mu\text{l}$$

This volume then (40 ul) of 10% PVP, 0.5% Phenol Red in PBS was then added in the hood to the pellet and pipetted up and down to achieve a well mixed injecting solution. Serial dilutions of 1000 cfu/nl, to make 500 cfu/nl, 100 cfu/nl and 10 cfu/nl were made, if required.

2.8.5.2 Needles for microinjections

Needles were acquired by stretching borosilicate glass capillaries (Wolf Laboratories Ltd., UK, Cat. No. TW100-4) using P-1000 Next Generation Micropipette Puller micropipette puller located in the Fly Facility (The University of Sheffield, Bateson Centre, Firth Court) pulled into 51-gauge needles. Before injections, a needle was back loaded with an appropriate *Cryptococcus* suspension (see Preparation of *C. neoformans*/prior to injection section) using a microloading pipette and microloading tip ((Fisher Scientific Ltd, UK, Cat. No. 5242956003), then assembled into a holder of a PicoPump (PV 820P) microinjector. The injector had the following settings: pressure 40 pound per square inch (PSI), vent, timed mode, the duration of the solenoid open time of 100 ms. The needle tip was brought into the plane of view of the microscope with the focus on the thinnest region of the tip to be broken using forceps to obtain the correct bevel shape.

The injection volume of 1 nl was then determined using a graticule, on which one drop of mineral oil (Sigma-Aldrich, UK, Cat. No. 330760-1L) was placed. When injected into the oil, a bead of cryptococcal suspension was adjusted through manipulation of the Pneumatic PicoPump. The bead with a diameter of nine bars equalled to 0.5 nl. Therefore, the foot pedal of the PicoPump was depressed twice.

2.8.5.3 Zebrafish microinjections

Microinjections occurred at 24 hpf. On the injection day, zebrafish embryos were first de-chorionated with Dumont forceps (Sigma-Aldrich, UK, Cat. No. F6521-1EA) in a petri plate containing 1X E3 medium with 0.00005% methylene blue. Then de-chorionated embryos were transferred in a disposable 2 ml graduated pasteur pipette (SLS, UK, Cat. No. PIP4208) into another petri plate with 1X E3 medium, 0.00005% methylene blue and 0.0168% tricaine. The embryos were then pipetted out with a glass pipette (SLS, UK, Cat. No. PIP4101) onto a microscopy slide (Thermo Scientific Menzel, UK, Cat. No. 12404070) covered

with 3.5% E3 (no methylene blue) based methylcellulose (Sigma-Aldrich, UK, Cat. No. M0512). Preparation of 3.5 % methylcellulose included mixing, partial freeze and defrost several times in order to facilitate methylcellulose solubilisation. The solution was aliquoted into 20 ml syringes (VWR International Ltd, UK, Cat. No. 613-2046P) and stored at -20°C until shortly before use when it was stored at 28.5°C.

Excess liquid (1X E3 containing tricaine) from the microscopy slide with embryos lined up on methylcellulose was removed to prevent the embryos sliding and methylcellulose being diluted.

Once dispensed the size of cryptococcal solution was calibrated, the larvae were ready to be injected with 1 nl of the required fungus dose, into the yolk sac circulation valley providing a systematic intravenous infection (Figure 2.5).

The mounted microscopy slide was placed under the needle and larvae were injected in one smooth stroke by piercing the yolk sac. This is an area situated close to the heart. To prevent triggering any inflammatory response, the needle broke through the yolk sac circulation valley only once. After injection, the needle was swiftly removed from the larvae. After completing one slide worth of larvae the fish were gently rinsed off with 1X E3 medium without methylene blue, to a clean petri plate filled with 1X E3, no methylene blue. After injections, the fish were looked at under stereo fluorescent Leica MZ10F microscope (bright field and GFP filter) to check the quality of injections. Any fish damaged or accidentally injected elsewhere were excluded from the experiment and culled.

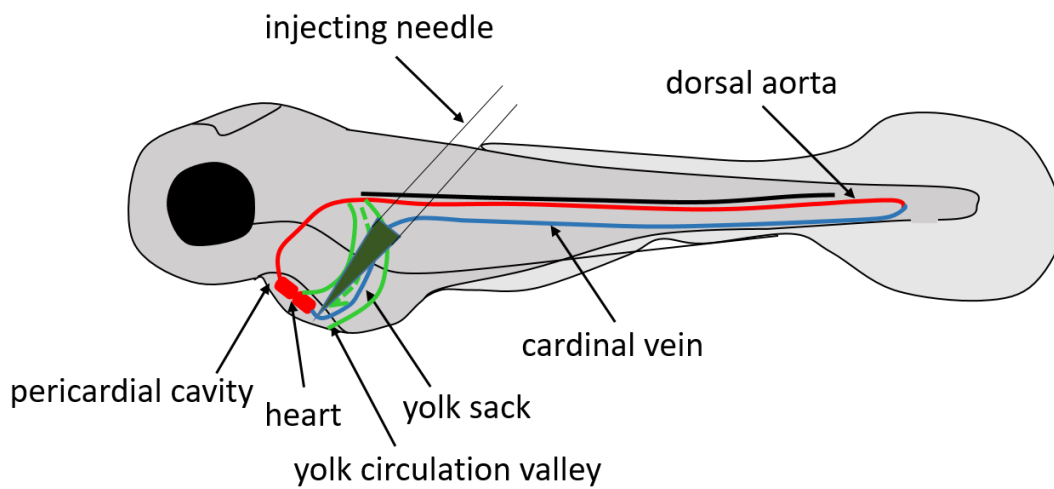


Figure 2.5 Schematic diagram of larva showing the site of microinjection with *C. neoformans*/*C. gattii*. The region injected is between two bright green continuous lines. The bright green dashed line with an arrowhead denotes the direction of blood flow into the circulation valley. Adapted from (Huang et al., 2015).

2.7.5.4 High content imaging method

Infected zebrafish were anaesthetised by immersion in 0.0168 % tricaine in 1X E3 and mounted in agar channels for imaging. Channels were made by adding 200 µl of 1% agar (Sigma Aldrich, UK, Cat. No. 05039) in 1X E3 containing 0.0168 % tricaine into glass-bottomed, 96-well plates (Porvair Sciences, UK, Cat. No 215006). Channels were cut in cooled agar using GelX4 tips. Mounted embryos were imaged on a Nikon Ti-E with a CFI Plan Apochromat λ 10X, N.A.0.45 objective lens, a custom built 500 µm Piezo Z-stage (Mad City Labs, Madison, WI, USA) and using Intensilight fluorescent illumination with ET/sputtered series fluorescent filters 49002 and 49008 (Chroma, Bellow Falls, VT, USA). Images were captured with Neo sCMOS, 2560 × 2160 Format, 16.6 mm x 14.0 mm Sensor Size, 6.5 µm pixel size camera (Andor, Belfast, UK) and NIS-Elements (Nikon, Richmond, UK) using the following settings: 1. GFP, filter 49002, 10 ms exposure, gain 4 2. mCherry, filter 49008, 10 ms exposure, gain 4. Each zebrafish was imaged as three contiguous fields of view that were assigned from bright-field images. 80 z sections, 5 µm apart, were captured in each channel and each position in that order. Each biological repeat contained 40 infected zebrafish, with 3 multi-channel z stacks per fish. The microscope was enclosed in a humidified, 28°C, environmental chamber (Okolabs, Pozzuoli, Italy). After imaging larvae were recovered in fresh E3 and returned to a new numbered 96-well plate (Bojarczuk *et al.*, 2016).

2.9 Preparation of *C. gattii* culture for mice infections

C. gattii strains (R265 wild-type (wt) and R265 GFP14) were cultivated as in the Cryptococcal strains cultivation section. Culturing and counting was the same as described in Preparation of the *C. neoformans*/ culture prior to injection. The dose used, 5×10^4 in 50 µl PBS was chosen upon previous experiments with an intra tracheal dose (surgical) of 1×10^4 in 50 µl PBS (Guillot, Carroll, Homer, *et al.*, 2008) and an intranasal dose of 5×10^4 in 25 µl PBS (Wiesner *et al.*, 2015). The volume of 50 µl seemed to be better as its larger size is more affected by gravity; this potentially allowed more of the dose to be moved down into the lungs. Therefore,

1x10⁶ cfu/ml was made up in PBS and 50 µl of this suspension was used for mice infections. The strains were placed on ice and carried to the Biological Services Unit (BSU).

2.10 Zebrafish survival assay

Zebrafish embryos that had undergone cryptococcal injection were subjected to survival analysis. Zebrafish larvae were checked every 24 hours for their survival or mortality. This was assessed by presence or absence of heartbeat. All zebrafish larvae used in experiments were under 5.2 days post fertilisation (dpf). Statistical analysis was performed as described in the Statistical analysis.

2.11 Disposal of zebrafish and microbiological waste

Zebrafish that had undergone either injection or drug treatment were disposed of just before reaching 5.2 dpf. These are classed as non-procedure and were disposed through bleaching (SLS, UK, Cat. No. CLE0300). The initial concentration of the bleach starts off at 100% but gets diluted as more fish and E3/aquarium water is added. The bleaching is preceded by anaesthesia in 0.0168% tricaine. In the case of *Cryptococcus* challenged zebrafish, 1% virkon (Sigma Aldrich, UK, Cat. No. Z692158) made up in distilled water was applied to plates. These were sealed and disposed through infectious waste.

Microbiological agar plates were sealed as soon as possible after use and disposed through infectious waste. Individual small volume cultures (<10 ml) were inactivated with 1% virkon

2.12 Statistical analysis

Statistical analysis was performed as described in the results and figure legends. Graphing and statistical analysis was performed in GraphPad Software Prism (version 7.04; La Jolla, California USA).

“N” refers to the number of animals per group.

All data sets were investigated for normal or not normal distribution. This was achieved by analysing frequency distribution (histograms) and investigating whether the mean was equal to the mean, which is true in normally distributed data (Peacock and Peacock, 2011). If the data is not normally distributed then nonparametric methods should be used. This was the case for the majority of data in this thesis. There was one case of data transformation to obtain normal distribution. This was done by using the log transformation.

T-tests: Mann-Whitney t-tests were used to test data arising from separate individuals (unpaired data) when data are not normally distributed. Mann-Whitney is a nonparametric test, which does not depend on the assumption that values were sampled from normal distributions. The test was to compare whether there is a difference in the dependent variable (“effect “of the “cause” independent variable) for two independent groups. The test compares if the distribution of the dependent variable is the same for the two groups and therefore from the same population. Mann-Whitney test ranks all of the data and then compares the sum of the ranks for each group to determine whether the groups are the same or not (Peacock and Peacock, 2011)

Survival analysis: The Log-Rank Mantel-Cox test was used to compare the trend of survival between different populations. This test compares the whole curve for each group. The null hypothesis is that there is no tendency for survival time to be shorter in one group than the other (Peacock and Peacock, 2011).

Linear regression: Line of best fit for data points. R^2 is a measure of goodness-of-fit of linear regression. The value (between 0 and 1) represents the percentage of points which line on the line, i.e. 1 represents 100% of all points lying exactly on the line with no scatter (Peacock and Peacock, 2011).

In reverse migration assay, a line of best fit was used to compare the difference in slopes. To test whether the slopes were significantly different, Prism calculated a P value between the slopes. However, the lines generated for both treatments

prior the site of injury were removed for the figure clearness. Only the P value was kept.

Analysis of variance: One-way ANOVA (and nonparametric) was used to determine the difference of mean ranks between two or more groups, when the data were not normally distributed. Kruskal-Wallis test was used for unpaired data at different time-points. Friedman test was used for paired repeated measures. Following nonparametric ANOVA, Prism calculated Dunn's post-test. An ordinary One-way ANOVA cannot have been used as the assumptions for it are normal distribution and equal standard deviation in each group (Peacock and Peacock, 2011).

Two-way analysis of variance, namely repeated measures (RM) two-way ANOVA for paired subjects was used to determine the difference of means between two groups, with one variable. Sidak's post-test was added to this to compare each mean to the other mean at time-points tested. Two-way ANOVA assumes that replicates are sampled from normal distributions. The data were not normally distributed. However, the two-way ANOVA was performed because the assumption of normal distribution is not too important with large samples. The sample size was large in phenotypic array experiments. RM two way-ANOVA was also used on the logarithm transformed data.

Chapter 3: *Cryptococcus neoformans* intracellular proliferation and capsule size determines early macrophage control of infection

3.1 Introduction

3.1.1 The importance of *C. neoformans*, interactions with macrophages and the polysaccharide capsule

C. neoformans was first described as a human pathogen in 1894 after isolation from a sarcoma-like lesion in the infected female's tibia (Busse, 1894). The fungus is recognised as a serious, worldwide public health concern. It is a major pathogen of the immunocompromised, especially AIDS patients. *C. neoformans* is the causative agent of cryptococcosis, a disease that primarily affects HIV immunosuppressed individuals and manifests in meningoencephalitis in these patients (reviewed by (Zaragoza, 2019)). The most recent estimate of global disease burden includes over 200 000 cases of cryptococcal meningitis resulting in over 180 000 deaths. Cryptococcal meningitis causes 15% of AIDS-related deaths globally. 73% of meningitis cases occur in sub-Saharan Africa (Rajasingham *et al.*, 2017). In healthy individuals, *C. neoformans* infection is usually self-resolving.

In most cases, the infection begins in the lungs, where the first cells encountered by cryptococci are alveolar macrophages or dendritic cells (reviewed by (May *et al.*, 2016)). The population of macrophages that live within the lung alveolar airspaces is predominant cell type within the alveolus (reviewed by (Fels and Cohn, 1986)). In bronchoalveolar lavage (BAL) fluid of HIV patients the numbers of alveolar macrophages is significantly lower as compared to non-HIV individuals (Mwale *et al.*, 2017). Thus, they are at risk of developing cryptococcosis. *C. neoformans* is also associated with other immunocompromised groups such as solid transplant patients. These patients also have reduced alveolar macrophages count (Bray *et al.*, 1992).

Macrophages respond to changes in their cytokine microenvironment. Briefly, they undergo polarisation to either M1 or M2 activation phenotype following

exposure to a specific stimulus ((Davis *et al.*, 2013), reviewed by (Wager and Wormley, 2014)). *C. neoformans* is more efficiently killed by M1 than M2 polarised macrophages. M2 (alternatively activated) macrophages cannot contain *C. neoformans* replication (Osterholzer, Surana, *et al.*, 2009; Zhang *et al.*, 2009) while M1 (classically activated) macrophages have antifungal activity (Wormley *et al.*, 2007; Hardison *et al.*, 2010; Kamuyango, 2017).

In recent years, researchers have demonstrated that in experimental mice pulmonary infection *C. neoformans* elicits Th2 response and activation of alternative macrophages (Huffnagle *et al.*, 1998; Osterholzer, Surana, *et al.*, 2009; Hardison *et al.*, 2010). Actually, both types of cytokines, Th1 and Th2 are produced in the lungs during infection but the Th1 predominance is required for the clearance (Hoag *et al.*, 1995, 1997; Wormley *et al.*, 2007). Th2-type immune responses are associated with exacerbation of disease whereas Th1-type immune responses with resistance to cryptococcosis (reviewed by (Mukaremera and Nielsen, 2017)). Cytokine expression in *C. neoformans*-infected lungs changes from Th2 towards Th1 profile over several weeks during infection (Arora *et al.*, 2011). As described, Th1 is required for the clearance as the protection against *Cryptococcus* is associated with M1 or classically activated macrophages. In CNS the clearance is possible due to Th1 cytokines and chemokines (Huffnagle and McNeil, 1999; Buchanan and Doyle, 2000).

Macrophage-*Cryptococcus* interactions have gained great importance among the scientific community because they are the dominant phagocytic cell that interacts with the pathogen. As described in section 1.2.3 Virulence of *Cryptococcus*, the fungus can grow within the host macrophages (intracellular proliferation) or use them for efficient dissemination (escape via non-lytic vomocytosis, cell lysis). Moreover, *Cryptococcus* can be laterally transferred from one macrophage to another. An interesting facet is a latent phase. It is thought that the majority of cryptococcosis cases result from reactivation from latency in instances where severe immune system defect had occurred long before the diagnosis (Garcia-Hermoso *et al.*, 1999). The Trojan horse model, e.g. from the lungs into the

bloodstream and across the blood brain barrier gives an idea how *Cryptococcus* can stay latent (Chrétien *et al.*, 2002; Charlier *et al.*, 2009).

This complex interaction between *Cryptococcus* and macrophages is illustrated in Figure 3.1.

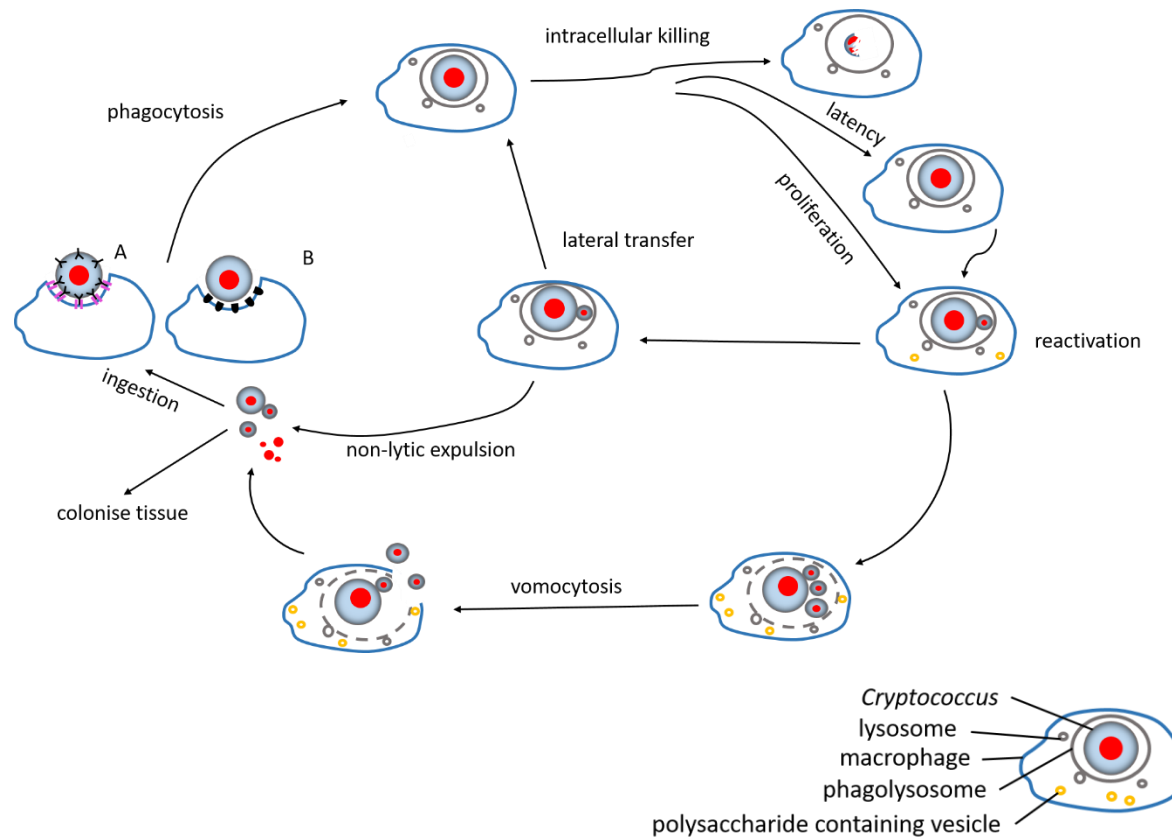


Figure 3.1 Schematic interaction of *Cryptococcus* with macrophages. A opsonic, B non-opsonic phagocytosis. Adapted from (Ma, 2009).

C. neoformans is associated with soil and pigeon excreta (Hagen *et al.*, 2015). Since virulence is usually maintained as a result of selection, the origin of the virulence is difficult to interpret (reviewed by (Steenbergen and Casadevall, 2003)). Whatever the evolutionary path for *C. neoformans* virulence is, it is doubtful that the virulence involved a selection through a vertebrate host (Johnston and May, 2013). It is likely that cryptococcal virulence originated due to environmental selective pressure (Casadevall *et al.*, 2003).

C. neoformans virulence factors include a polysaccharide capsule. The capsule was widely described in section 1.2.3 Virulence of *Cryptococcus*. Briefly, it provides a physical barrier and confers biochemical and immunological properties. It is characterised by a dynamic plasticity that enables adaptation to the host environment for prolonged survival (Cordero *et al.*, 2011). During mammalian infection, the capsule increases in size (Feldmesser *et al.*, 2001).

3.1.2 The need for the development of a new integrated model of cryptococcosis

Innate immunity and especially macrophages are significantly involved in the response to cryptococcosis (reviewed by (Campuzano and Wormley, 2018)). The interaction between *Cryptococcus* and the host immune system is highly complex. The interaction between *Cryptococcus* and macrophages is an established model system for investigation of cryptococcal virulence. Human cases of cryptococcosis caused by acapsular strains are not common (Farmer and Komorowski, 1973). At the time of my appointment to the Johnston lab, previous estimates showed *C. neoformans* caused meningoencephalitis, primarily in the immunocompromised resulting in approximately one million cases and 600 000 deaths annually (Park *et al.*, 2009). At the time the aim of my work was formulated, the existing clinical, *in vitro* cell biology data on host-pathogen interaction as well as *in vivo* data did not permit the simultaneous study of host and pathogen factors that determine disease progression and outcome *in vivo*. As stated in the thesis aims, at the time, there was no model, which would enable to track macrophages and cryptococci in the entire body of a living vertebrate. Therefore, there was a need to extend the range of existing models to study immunity to cryptococcal infection. Zebrafish appeared to be ideally suited to

become the model of cryptococcosis. This was due to for a few key reasons: zebrafish being a vertebrate, embryos transparency, similarity of immune system to mammals, a high genetic homology and high fecundity, genetic manipulation and imaging potential (reviewed by (Goldsmith and Jobin, 2012; Renshaw and Trede, 2012)). It was noted that other animal species could serve as a model, too. However, only the zebrafish has the potential for *in vivo* subcellular resolution imaging in the entire body of a living vertebrate, allowing the interpretation of cell biology data in the context of the whole disease and organism. In addition, zebrafish are easily bred and infected making large-scale studies possible that will give power to complex correlations of host and pathogen disease determinants (reviewed by (Van Der Sar *et al.*, 2004)) at a scale not possible in other vertebrates. In addition zebrafish are proven models of human disease (reviewed by (Dooley and Zon, 2000; Lieschke and Currie, 2007)), immune cell (Renshaw *et al.*, 2006; Colucci-Guyon *et al.*, 2011), infection biology (Tobin *et al.*, 2010; Volkman *et al.*, 2010; Adams *et al.*, 2011) and are also used in drug discovery (reviewed by (MacRae and Peterson, 2015)).

At the time the hypothesis that this organism can serve as an experimental model of cryptococcosis was evidenced by the fact that these animals have been used successfully to study fungal pathogens (Brothers *et al.*, 2013; Herbst *et al.*, 2015). Unquestionable advantages of the zebrafish are low costs of their maintenance, high fecundity and short generation time of only three months, thus zebrafish are more preferable than mice. As mentioned, zebrafish immunity is similar to that of humans. They possess both adaptive (humoral and cellular) and innate components, the latter including macrophages, neutrophils, TLRs, complement factors and cytokines and their signalling molecules (reviewed by (Lieschke and Currie, 2007; Goldsmith and Jobin, 2012)). However, it is important to note the limitations of the zebrafish immunity model. Due to most zebrafish licences allowing the studies until day 5 post fertilisation, the adaptive immunity is missing from infection models. Thus, translating findings from zebrafish research to humans might be difficult, although studying the innate immunity provides a good basis to understand human innate immunity. Another factor could be the fact that zebrafish are maintained at 28°C, not 37°C. 28°C is not the human body

temperature pathogens have evolved to infect at. This should be taken into consideration when interpreting data. On the other hand, *C. neoformans* seems to infect such a wide range of animal species with different thermoregulation (Malik et al., 2011) and therefore, it is likely that pathogenesis does not depend on the host body temperature.

3.1.3 The development of a new integrated model of cryptococcosis and commentary on resulting publication (Bojarczuk et al., 2016)

A model of the early events following dissemination of *C. neoformans* was essential to improve our fundamental understanding of the behaviour of phagocytes during infection. Thus, I started with the question of developing a zebrafish model of cryptococcosis. At the time the aim of my work was formulated our understanding of cryptococcosis used to be based on either *in vitro* analysis of interactions between cryptococci and isolated mammalian cells or *in vivo* studies in murine or leporine hosts. Despite the wealth of *in vitro* or *in vivo* studies on *C. neoformans*, there was no direct *in vivo* data on disease progression. The limitations of the past studies included 1) the difficulties in interpreting studies using isolated macrophages in the context of the progression of infection, and 2) the use of high resolution imaging in understanding immune cell behaviour during animal infection. Consequently, an animal *in vivo* model was required to unravel how the infection causes diseases in humans. A larval zebrafish model of *C. neoformans* infection with microinjections into the yolk sac circulation valley at 48 hpf was proposed (Bojarczuk et al., 2016).

One might argue that the zebrafish infection model had existed before my (Bojarczuk et al., 2016) publication. This is true. There are publications of (Tenor et al., 2015; Davis et al., 2016), which employ the zebrafish model of *C. neoformans* infection. In (Tenor et al., 2015) microinjections were done into caudal vein at 48 hpf, whereas the work of (Davis et al., 2016) utilised intravenous and hindbrain inoculations at 28 hpf. However, I started my work in 2012 and published in 2016, whereas the other groups published earlier. Still, at time of the manuscript preparation there was an *in vivo* model including macrophages interactions but it only partially addressed my question of macrophages role and

behaviour during the course of infection (Tenor *et al.*, 2015). The publication of (Tenor *et al.*, 2015) was cited in mine (Bojarczuk *et al.*, 2016). The work of (Davis *et al.*, 2016) was not mentioned in mine because the final version of the manuscript had been completed.

As described, following uptake, internalised *Cryptococcus* can be destroyed or is able to survive and replicate. It can be transferred between macrophages laterally or exit non-lytically via vomocytosis. I wanted to investigate if these interactions were conserved in the zebrafish. The recapitulation of these events was essential to prove the zebrafish meets the criteria to become a model of infection. I successfully reported these interactions in the zebrafish embryo (cryptococcal internalisation by macrophages, lateral transfer and cryptococcal cell death, all unpublished) before setting the experiments in (Bojarczuk *et al.*, 2016).

As mentioned, the capsule grows during mammalian infection. The work on capsule in the zebrafish model (Bojarczuk *et al.*, 2016) was possible upon evidencing the capsule growth during zebrafish infection (the initial data unpublished).

This chapter is based on a publication published in a multidisciplinary journal Scientific Reports (Bojarczuk *et al.*, 2016). Here, I presented the zebrafish model of *C. neoformans* infection and studied macrophage-cryptococcal cell interactions.

My work in the publication reports: 1) a method for the live quantification of macrophage behaviour in response to *C. neoformans* infection, thus the establishment of a high-content imaging method in a zebrafish model of cryptococcosis that permits the detailed analysis of macrophage interactions with *C. neoformans* during infection; 2) the majority of cryptococci are intracellular after twenty-four hours post infection; 3) intracellular proliferation drives increased numbers of cryptococci at twenty-four hours post infection and this is linked with vomocytosis. The work of others in the publication demonstrates that: 1) macrophages are essential for the early control of cryptococcal fungemia; 2) cryptococci that are phagocytosed within two hours have small polysaccharide capsules that are absent from the fungal cell population twenty-four hours post

infection; 3) enlargement of capsules of initial fungal burden limits phagocytosis and restricts macrophage control of cryptococci. The following figures in the publication are mine: Supplementary Data S1, Supplementary Fig. S1, Supplementary Fig. S2, Supplementary Fig. S2, Supplementary Movie S1, Fig. 1 a-g, Fig. 2 a, Fig. 3 a-f, Fig. 4 a-f, Fig. 5 a-b.

From the results, it is clear that macrophages are critical for control of *C. neoformans* and a failure of macrophage response is not the limiting defect in fatal infections.

The present study confirmed the findings about phagocytosis prevention very early in infection and that increasing numbers of cryptococci are driven by intracellular proliferation. Macrophages preferentially phagocytose cryptococci with smaller polysaccharide capsules and the capsule size increases dramatically over twenty-four hours of infection, a change that is sufficient to limit further phagocytosis. The results found clearly support the hypothesis that differences in cryptococcal capsule size are sufficient to define the limitation of phagocytosis (Bojarczuk *et al.*, 2016).

3.2 The publication *Cryptococcus neoformans* intracellular proliferation and capsule size determines early macrophage control of infection (Bojarczuk *et al.*, 2016)

SCIENTIFIC REPORTS

OPEN

Cryptococcus neoformans Intracellular Proliferation and Capsule Size Determines Early Macrophage Control of Infection

Received: 29 October 2015
Accepted: 26 January 2016
Published: 18 February 2016

Aleksandra Bojarczuk^{1,2,*}, Katie A. Miller^{1,2,*}, Richard Hotham^{1,2}, Amy Lewis^{1,2},
Nikolay V. Ogryzko^{1,2}, Alfred A. Kamuyango^{1,2}, Helen Frost^{3,4}, Rory H. Gibson^{1,2},
Eleanor Stillman⁴, Robin C. May^{3,5}, Stephen A. Renshaw^{1,2} & Simon A. Johnston^{1,2}

Cryptococcus neoformans is a significant fungal pathogen of immunocompromised patients. Many questions remain regarding the function of macrophages in normal clearance of cryptococcal infection and the defects present in uncontrolled cryptococcosis. Two current limitations are: 1) The difficulties in interpreting studies using isolated macrophages in the context of the progression of infection, and 2) The use of high resolution imaging in understanding immune cell behavior during animal infection. Here we describe a high-content imaging method in a zebrafish model of cryptococcosis that permits the detailed analysis of macrophage interactions with *C. neoformans* during infection. Using this approach we demonstrate that, while macrophages are critical for control of *C. neoformans*, a failure of macrophage response is not the limiting defect in fatal infections. We find phagocytosis is restrained very early in infection and that increases in cryptococcal number are driven by intracellular proliferation. We show that macrophages preferentially phagocytose cryptococci with smaller polysaccharide capsules and that capsule size is greatly increased over twenty-four hours of infection, a change that is sufficient to severely limit further phagocytosis. Thus, high-content imaging of cryptococcal infection *in vivo* demonstrates how very early interactions between macrophages and cryptococci are critical in the outcome of cryptococcosis.

Cryptococcus neoformans is a fungal pathogen of humans that causes life-threatening cryptococcal meningitis in immunocompromised patients, in particular those with advanced AIDS¹. Cryptococcal meningitis is also found associated with a large variety of other immune deficient states, including in patients on immunosuppressive therapies^{2,3}, those with hematological malignancy and other more oblique disorders⁴. However, there are a number of unifying features in susceptibility to cryptococcal disease, notably a failure in a pro-inflammatory immune response to primary infection⁴⁻⁶.

Primary infection with *C. neoformans* is thought to occur through the lungs where, in the immunocompetent, the first immune cells to encounter cryptococci will most likely be alveolar macrophages. Macrophages alone seem unable to clear infection and an adaptive immune response leading to a self-resolving granuloma is required⁷. This is supported by *in vitro* data demonstrating that *C. neoformans* appears to be able to efficiently parasitise macrophages. *Cryptococcus* survives and proliferates within the phagosome⁸, can escape non-lytically^{9,10} and may use macrophages as a "Trojan horse"¹¹. However, it is not known how host-pathogen interactions at a cellular level determine the outcome of cryptococcosis.

Our understanding of cryptococcosis has been based on a combination of clinical studies, *in vitro* analysis of interactions between cryptococci and isolated mammalian cells, and *in vivo* studies in rodent or leporine hosts.

¹Department of Infection, Immunity and Cardiovascular Disease, Medical School, University of Sheffield, Sheffield, UK. ²Bateson Centre, University of Sheffield, Sheffield, UK. ³Institute of Microbiology and Infection and School of Biosciences, University of Birmingham, Birmingham, UK. ⁴School of Mathematics and Statistics, University of Sheffield, Sheffield, UK. ⁵NIHR Surgical Reconstruction and Microbiology Research Centre, University Hospitals of Birmingham NHS Foundation Trust, Queen Elizabeth Hospital, Birmingham, UK. *These authors contributed equally to this work. †Present Address: Faculty of Life Sciences, University of Manchester, Manchester, United Kingdom. Correspondence and requests for materials should be addressed to S.A.J. (email: s.a.johnston@sheffield.ac.uk)

In vitro studies offer the advantage of a highly malleable and observable experimental system, but without direct *in vivo* data on disease progression. In contrast, mammalian models provide the opportunity to study progression of infection *in vivo*, but only permit detailed cellular analysis at specific end points.

Most recently this shortfall has been partly addressed using a zebrafish model of cryptococcal disease¹². The zebrafish is ideally suited for this approach due to a combination of vertebrate immunity, ease of imaging and genetic tractability. Zebrafish have, therefore, been used to model a wide range of human pathogens^{13–16}. Using a similar infection model we have developed a high content imaging methodology that permits a full analysis of cryptococcal and macrophage cell interactions during infection. Using this approach we demonstrate that macrophages are essential for control, but are unable to clear, cryptococcal infection. The ability of macrophages to control infection relies on early phagocytosis, which, in turn, is limited by cryptococcal capsule. Finally, we show that enlargement of cryptococcal capsule is sufficient alone to overcome macrophage phagocytosis *in vivo*, leading to uncontrolled fungal growth and death.

Results

A method for the live quantification of macrophage behaviour in response to *Cryptococcus neoformans* infection. The quantification of macrophage and cryptococcal interactions *in vivo* required sub-cellular resolution imaging throughout the host, while being able to follow the same infections across an extended time period. To achieve this aim we developed repeated high-content live fluorescent imaging, with aligned mounting methods, to image 120 individual blood stream infections of 2 days post fertilisation zebrafish larvae from 3 biological repeats (each biological repeat was performed as an independent group of 40 infected fish; see Supplementary Fig. S1; see Materials and Methods for details of imaging and infection model). Our imaging method was sufficiently resolved in x, y and z to identify both macrophage and cryptococcal cells, their relative location (Fig. 1a; see Supplementary Fig. S2), and whether cryptococci were intracellular (Fig. 1b,d,f; see Supplementary Fig. S2) or extracellular (Fig. 1c,e,g; see Supplementary Fig. S2), throughout the zebrafish. This approach allowed us to track individual fungal cells, providing direct counts for the initial fungal burden that were indistinguishable from parallel cfu counts (see Supplementary Fig. S1). From these data we directly quantified the number of infected macrophages, the number of intracellular cryptococci and total number of cryptococci, at 2 and 24 hours post infection (hpi). Thus, we were able to calculate the number of extracellular cryptococci, the proportion of intracellular cryptococci, the number of cryptococci per macrophage or phagocytic index (PI), and changes in total, intracellular, and extracellular cryptococcal cell numbers between 2 and 24 hours of infection (see Supplementary Data S1). Importantly, since this quantification was carried out in anaesthetized and fully recoverable animals, we were able to place these data in the wider context of subsequent progression of infection on an animal-by-animal basis, to investigate the relationship between macrophage responses and disease.

Macrophages are essential for the early control of cryptococcal fungemia. As we were able to analyse macrophage responses non-invasively we could also identify time of death in the same experiment. We stratified our infections into three groups according to their initial fungal burden and found a dose response in survival over 72 hpi but saw little difference before this time point (Fig. 2a). In order to provide finer detail on the progression of infection, we used an intermediate dose range (10^1 – 10^2 cryptococci per infection) and measured the changes in fungal burden over 72 hpi by fluorescence microscopy (Fig. 2b–f). We observed that there were a range of infection outcomes, within this narrow dose range, which we could identify as having low, median and high fungal burdens at 72 hpi (Fig. 2b–d, respectively). We quantified this difference by measuring the fungal burden and found that stratification of 72 hpi infection areas at 10^1 – 10^2 , 10^2 – 10^4 and $>10^4$ square pixels distinguished the same groups (Fig. 2e). Using the 72 hpi divisions we stratified the other time points and found that these groups were present at 24 hpi (Fig. 2f). All three groups showed a significant increase in fungal burden relative to the initial infection but with very large differences in magnitude. The low, median and high groups showed a difference of 2- 10- and 1000-fold increases between 0 and 72 hpi respectively. Having identified differences in the progression of infection in our model we wanted to understand how macrophages contributed to such variability and we used clodronate-containing liposomes to deplete this cell type specifically¹⁷.

Clodronate treatment 24 hours prior to infection (at 24 hpf) resulted in a rapid depletion in macrophage numbers, which was stable 72 hours after treatment, with neutrophil numbers unaffected (Fig. 2g). Depletion of macrophages using clodronate resulted in a large decrease in survival over 72 hours of infection (Fig. 2h). We measured the fungal burden area and, while PBS-containing liposome treatment showed very similar infection dynamics to our previous analysis (Fig. 2i), macrophage depletion resulted in uncontrolled infection (Fig. 2j). Large differences were already present at 24 hpi and this difference continued to increase at 48 hpi and 72 hpi (difference in mean fungal burden 3.9×10^2 , 1.3×10^3 and 2.1×10^4 pixels² respectively; Fig. 2i–k). As depletion of macrophages using clodronate prior to infection resulted in uncontrolled infection we next examined the influence of macrophage depletion later, when control of infection was observed. To establish controlled infection we used a lower initial fungal burden ($<5 \times 10^1$) where we observed restricted cryptococcal growth over 72 hpi (Fig. 2l) and we depleted macrophages at 24 hpi. We measured the resulting fungal burden and found that following macrophage depletion there was large increase in fungal burden at 48 and 72 hpi (48 hpi 2.3-fold increase, $P = 0.0026$; 72 hpi, 5.6-fold increase, $P = 0.0014$; Mann-Whitney test; Fig. 2l). Having established the essential requirement for macrophages in the control of cryptococcal fungemia early in infection, we returned to the question of how the result of the interaction of macrophages with cryptococci influenced the outcome of the infection.

The majority of cryptococci are intracellular after twenty-four hours post infection. We hypothesized that the decreased survival observed at high initial fungal burden in wildtype zebrafish (Fig. 2a) was due to macrophages being overwhelmed, as we had demonstrated for intermediate and low fungal burden via macrophage depletion (Fig. 2j–l). From this hypothesis we predicted that we would see an increase in

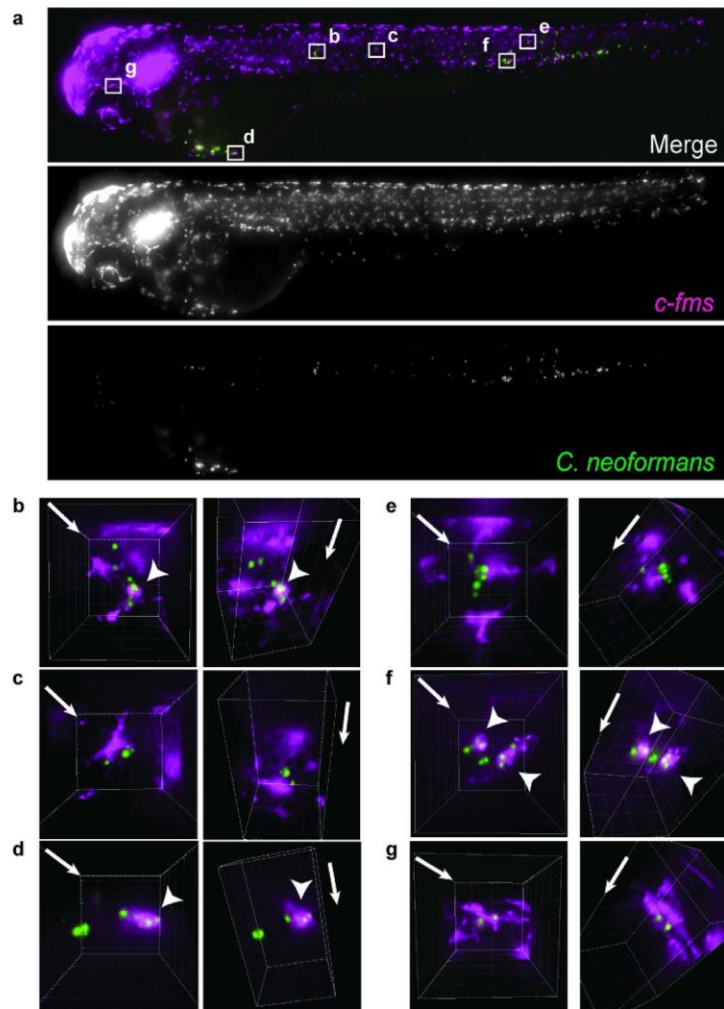


Figure 1. Quantification of macrophage behavior in response to *Cryptococcus* during infection. (a) Maximum intensity z-projection of example image data from high content imaging (see Supplementary Fig. S1) of *Tg(fms:Gal4.VP16)i186; Tg(UAS:nfsB.mCherry)i149* zebrafish, with mCherry labeled macrophages (magenta), infected with 148 cells of *C. neoformans* strain H99GFP (green), at 2 hours post infection. (b–d) Areas boxed in (a) enlarged and reconstructed in three-dimensions. Arrowheads indicate intracellular cryptococci. Image pairs represent different views of same volume with arrows indicating z-axis direction. Image grid is 20 μ m. Images are representative of a total of 120 infections from $n = 3$ repeats (40 infections per independent repeat group).

macrophage responses (i.e. increases in both the number of macrophages containing cryptococci and the number of cryptococci that were intracellular) with increasing inocula up to a threshold where numbers would plateau, corresponding to limited macrophage capacity and control of fungal burden. To test this prediction, we determined the relationship between inoculum and the number of infected macrophages, intracellular cryptococci and the phagocytic index, from our macrophage dataset (Fig 3a–f; see Supplementary Data S1). Analysis of all three measures identified a significant positive linear relationship to inoculum at 2 hpi (linear regression, all P-values < 0.0001; see Fig. 3a–c for individual R^2 -values) but without plateauing at higher inocula. Interestingly, the same relationship was still present at 24 hpi (linear regression, all P-values < 0.0001; see Fig. 3d,e for individual

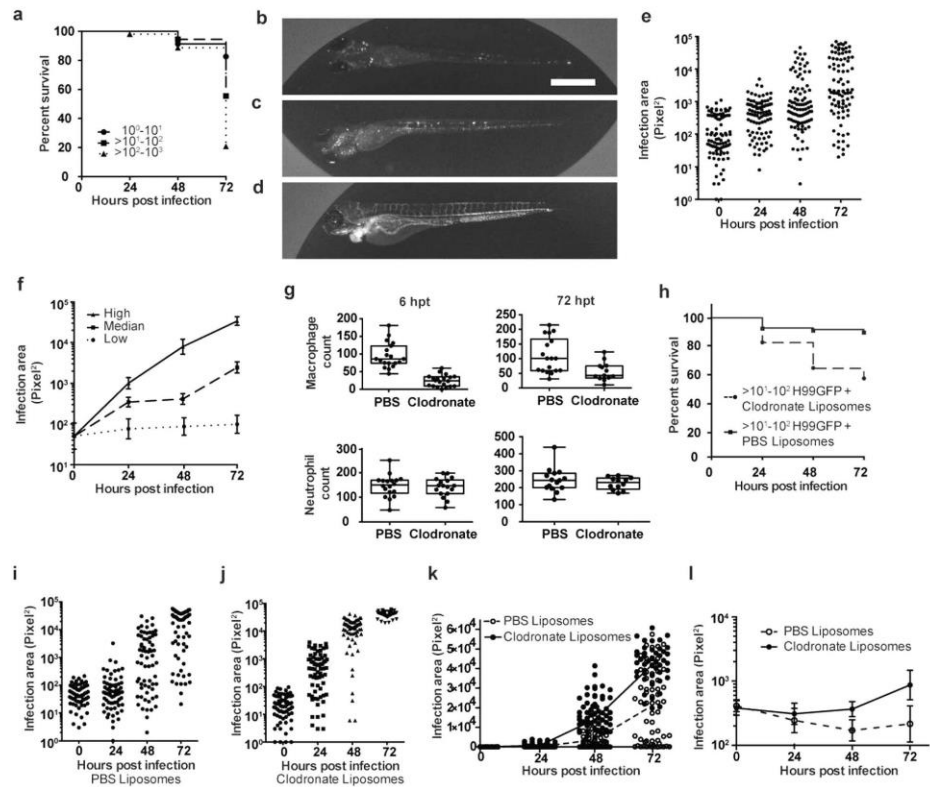


Figure 2. Macrophages are essential for control of cryptococcal fungemia. (a) Stratification of survival over 72 hpi from macrophage response data set. Survival is dependent on dose with a large change in survival between 10^1 and 10^3 . 120 infections from $n = 3$ (each group contains: $10^0-10^1 = 23$, $>10^1-10^2 = 36$, $>10^2-10^3 = 53$). (b–f) Representative images and quantitation of fungal burden from infections with inocula between $>10^1-10^2$ of *Nacre*-strain zebrafish (100 infections from $n = 4$). (b–d) Fluorescence images of low (b), median (c) and high (d), H99GFP infection of zebrafish at 72 hpi with inocula between $>10^1-10^2$. Scale bar is 500 μm . (e) Quantification of fungal burden using area of fluorescent pixels from *C. neoformans* strain H99GFP. Each point is a separate infection with inocula between $>10^1-10^2$, with the same 100 infections over 72 hours. (f) Stratification of (e) using $2\log_{10}$ boundaries at 72 hpi. Geometric mean with 95% confidence intervals. (g) Zebrafish 24 hpf were injected with clodronate or PBS containing liposomes and the numbers of macrophages or neutrophils counted using *Tg(mpeg1:mCherryCAAX)sh378* and *Tg(mpx:GFP)i114* respectively at 6 and 72 hours post treatment. 15 treatments from $n = 3$. (h) Survival of *Nacre*-strain zebrafish infected with inocula between $>10^1-10^2$ of *C. neoformans* strain H99GFP at 48 hpf, following liposome treatment at 24 hpf. $P < 0.0001$, Log-rank (Mantel-Cox), hazard ratio = 4.5 (logrank; 95% confidence interval 3.2,7.7), 140 and 178 infections from clodronate and PBS groups respectively from $n = 3$. (i–k) Quantification of fungal burden using area of fluorescent pixels from *Nacre*-strain zebrafish infected with inocula between $>10^1-10^2$ of *C. neoformans* strain H99GFP at 48 hpf following treatment with liposomes at 24 hpf. Each point the same 75 infections over 72 hours from $n = 3$. (i) PBS (j) Clodronate (k) Linear comparison of individual infection and mean fungal burden values with PBS (open circles and dotted line respectively) or clodronate (filled circles and solid line respectively) treatment. Values are the same as presented (i) and (j). (l) Quantification of fungal burden using area of fluorescent pixels from *Tg(mpeg1:mCherryCAAX)sh378* strain zebrafish infected with $<5 \times 10^1$ of *C. neoformans* strain H99GFP at 48 hpf followed by injection with liposomes at 24 hpi (72 hpi). Points are geometric mean with 95% confidence intervals. The same 25 infections over 72 hours.

R^2 -values). Thus, while essential for control, the capacity of macrophages to respond to increased numbers of cryptococci, over the range tested, did not appear to be limiting. This was despite the large differences between 2 and 24 hpi in absolute numbers of these values. Examining the total number of cryptococci there was only a small increase between 2 and 24 hours of infection regardless of the initial fungal burden (median increase 0.89;

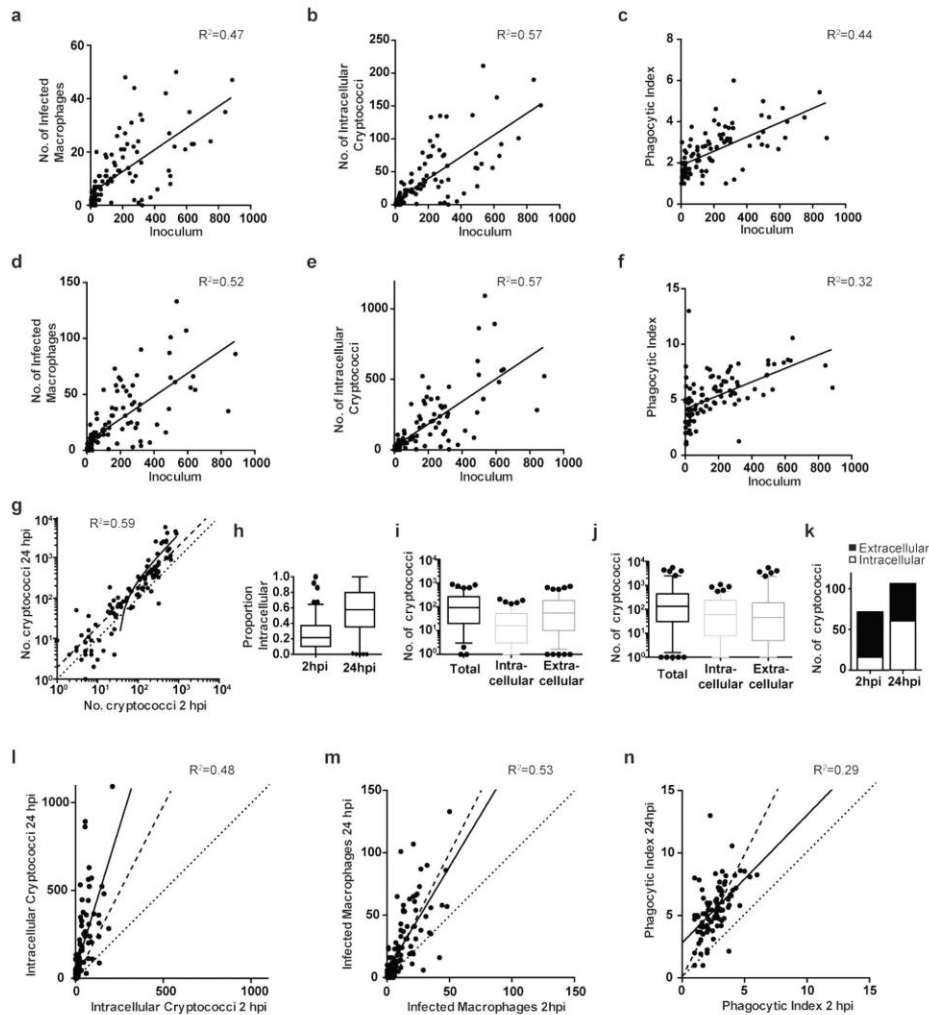


Figure 3. The majority of cryptococci are intracellular at 24 hpi. (a–f) Strong positive correlation between inoculum and (a,d) number of infected macrophages, (b,e) number of intracellular cryptococci and, (c,f) phagocytic index at (a–c) 2 hpi and (d–f) 24 hpi. (g). Less than an average two-fold increase in the total number of cryptococci between 2 and 24 hours. (g). Dotted line represents 1 to 1, whereas dashed line represents 2 to 1, relationship. Each point is a separate infection. Solid lines are linear regression, all linear regression P-values < 0.0001. R-squared values are given for each correlation. (h–k) Shift to majority of cryptococci being intracellular after 24 hpi. (h) The proportion of cryptococci intracellular at 2 and 24 hpi for each infection. Box plot whiskers are 5 and 95 percentiles with outliers plotted. Medians are 0.22 and 0.58 respectively, $P < 0.0001$ (Mann-Whitney). (i,j) Total, intracellular and extracellular cryptococci numbers at 2 hpi (i) and 24 hpi (j) for each infection. Box plots with whiskers at 5 and 95 percentiles with outliers plotted. (k) Median intracellular and extracellular cryptococci numbers at 2 hpi and 24 hpi calculated from data presented in (I,j). For further descriptive statistics and significance comparisons see Table S1. (l–n) Greater increase in number of intracellular cryptococci than the number of infected macrophages between 2 and 24 hpi. Dotted line represents 1 to 1, whereas dashed line represents 2 to 1, relationship. Each point is a separate infection. Solid lines are linear regression, all linear regression P-values < 0.0001. R-squared values are given for each correlation. All data are of 120 infections of *Tg(fms:Gal4.VP16)i186*; *Tg(UAS:nfsB.Cherry)i149* zebrafish with *C. neoformans* strain H99GFP.

see Supplementary Table S1; Fig. 3g). However, the intracellular and extracellular populations of cryptococci changed dramatically between 2 and 24 hpi, with a large shift to the majority of cryptococci being intracellular at 24 hpi (Fig. 3h). Analysis of the distribution of the intracellular and extracellular numbers from each infection demonstrated that this shift was due to a larger increase in intracellular numbers over static or slightly declining extracellular numbers (Fig. 3h–k; see Supplementary Table S1). In addition, there was a much smaller increase in the numbers of infected macrophages than in the number of intracellular cryptococci, resulting in an increased phagocytic index (Fig. 3l–n). As *C. neoformans* is able to proliferate within macrophages⁸ there are two potential explanations for this observation. Either macrophages that already contain cryptococci are more likely to phagocytose further cryptococci (e.g. due to enhanced levels of activation), or this shift is driven by intracellular proliferation of cryptococci already within macrophages (with subsequent phagocytosis later in infection having only a limited contribution to intracellular burden).

Intracellular proliferation drives increased numbers of cryptococci at twenty-four hours post infection. To test our predictions we required high temporal resolution as well as spatial resolution such that we could accurately track individual macrophages over time. We used three-dimensional fluorescence time-lapse, taking images every 2 minutes over 12 hours, to identify the exploitation of macrophages by cryptococci. The first important aspect of macrophage parasitism *in vitro* that we examined was vomocytosis, the non-lytic expulsion of cryptococci from macrophages^{9,10}. The occurrence of vomocytosis has been inferred indirectly *in vivo* but never directly observed¹⁸. We found that the mechanics of non-lytic expulsion were conserved *in vivo* with a characteristic exocytic, concave membrane during expulsion¹⁹ (arrowhead Fig. 4a; see Supplementary Movie S1). In addition, we were able to measure the incidence of vomocytosis and found that 5–15% of macrophages expelled cryptococci over 12 hours (Range from $n = 9$, at least 20 infected macrophages per infection, mean 12%; over 12 hours) and this is consistent with values from mammalian studies^{18,20}. Similarly, intracellular proliferation could be observed clearly, quantified by the timing of each new visible daughter cell, and occurred regularly over the 12 hours of observation (Fig. 4b,c). In contrast, phagocytosis was much less frequent, with relatively few events in each infection imaged compared to intracellular proliferation (Fig. 4d,e). We therefore concluded that the shift in intracellular numbers of cryptococci was due to intracellular proliferation and not phagocytosis, and we sought to identify the cryptococcal or macrophage phenotype that was limiting phagocytosis after the first hours of infection.

Cryptococci that are phagocytosed within two hours have small polysaccharide capsules that are absent from the fungal cell population twenty-four hours post infection. Unlike the numbers of infected macrophages and intracellular cryptococci, the proportion of cryptococci that were intracellular at 2 hpi was only very weakly related to the inoculum (linear regression $P = 0.0499$, $R^2 = 0.035$; Fig. 5a) i.e. over the range of inocula observed, the proportion of cryptococci phagocytosed was stable (median proportion phagocytosed 0.25; 95% CI (0.21, 0.29)). This suggested that there was a consistent subset of the cryptococcal population that was not phagocytosed.

In order to understand how modulating phagocytosis influenced the outcome of infection we attempted to reduce the phagocytosis of cryptococci by blocking likely uptake pathways. Soluble mannan and glucan have been shown to block the uptake of fungal pathogens by macrophages²¹. However, we found that co-injection of these molecules was insufficient to alter uptake of cryptococci by macrophages in our model (see Supplementary Fig. S3). The polysaccharide capsule of *C. neoformans* is its defining clinical microbiological feature and has been reported to have a broad range of immunosuppressive activities including preventing phagocytosis^{22–24}. To define the role of capsule in the pathogenesis of cryptococcosis in our model we used the *cap59* mutant that has severely compromised capsule formation²⁵. Infection with the *cap59* mutant resulted in zero mortality over 72 hours of infection despite using a dose that caused greater than 50% mortality in the parental H99 strain (Fig. 5b). In addition, analysis of the uptake of the *cap59* mutant by macrophages demonstrated that almost all cryptococci were intracellular (Median proportion intracellular 0.93; Fig. 5c). Therefore, we hypothesized that differences in cryptococcal capsule size were sufficient to define the limitation of phagocytosis, both in the primary phase following infection (Fig. 5a) and later in a secondary phase (>2 hpi) where phagocytosis was largely curtailed (Fig. 4f).

We predicted that 2 hpi macrophages would contain cryptococci with smaller capsules than extracellular cryptococci. To measure the size of the cryptococcal capsule *in vivo* accurately, we combined immunofluorescence labeling of the capsule and staining of the cell wall immediately prior to infection. Live measurement of capsule sizes 2 hpi demonstrated that intracellular cryptococci had capsules only about half the radius of extracellular cryptococci capsules (extracellular mean = 0.49 μm , median = 0.43 μm ; intracellular mean = 0.26 μm , median = 0.24 μm ; $P < 0.0001$, Mann-Whitney; Fig. 5d–f; see Supplementary Fig. S4). Furthermore, the relative frequency of the different intracellular and extracellular capsule sizes was sufficient to closely model the distribution of phagocytosis values we had quantified from our previous infections (Fig. 5g).

We next investigated the capsule at 24 hpi, the time point after which we had proposed that capsule was limiting phagocytosis. As changes in capsule could not be observed live in the same way as early in infection we immuno-labeled fixed tissue and found that by 24 hpi cryptococcal capsule was enlarged, with shed capsular material clearly present in surrounding tissue (Fig. 5h). We quantified capsular size *ex vivo* and found that there was a large, and highly consistent, difference in capsule size (Fig. 5i,j; see Supplementary Fig. S4). This large and rapid shift in capsule size potentially explained the limitation of phagocytosis later in infection, given the relative ability of macrophages to phagocytose cryptococci with different capsule sizes and as there was almost no overlap between the capsule size of the initial fungal burden and the fungal cell population at 24 hpi.

Enlargement of capsules of initial fungal burden limits phagocytosis and restricts macrophage control of cryptococci. We tested how the modulation of capsule size influenced the outcome of infection

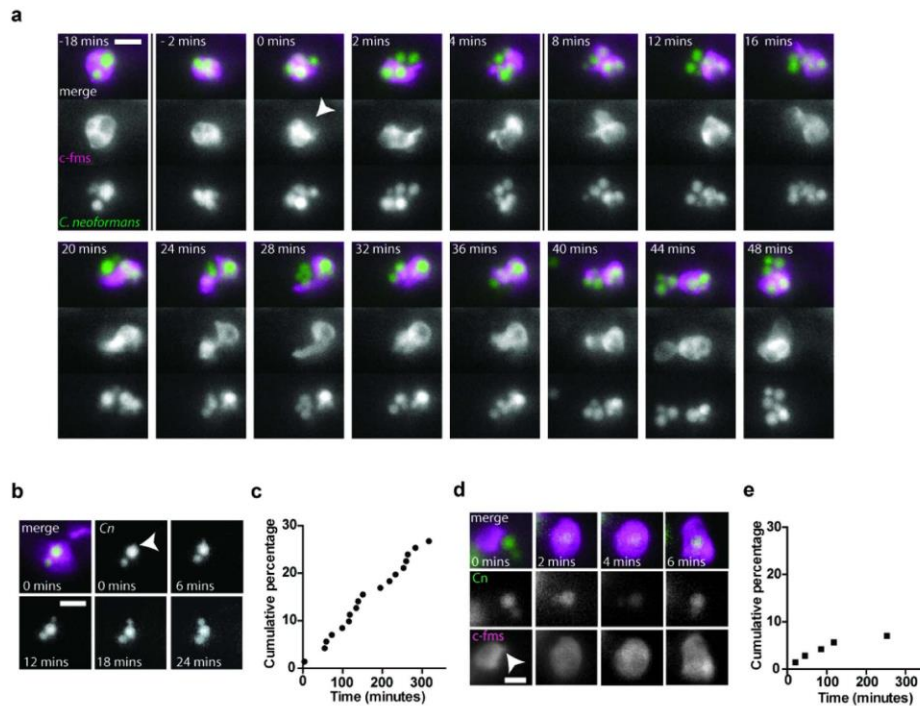


Figure 4. Increase in intracellular numbers of cryptococci is driven by proliferation not phagocytosis.

(a,b,d) Fluorescent time lapse imaging of parasitism of macrophages. *Tg(fms:Gal4.VP16)i186; Tg(UAS:nfsB.mCherry)i149* zebrafish, with mCherry labeled macrophages (c-fms; magenta), infected with *C. neoformans* strain H99GFP (green). Zebrafish were imaged for 12 hours from 2 hpi. Images were captured every 2 minutes. (a) Vomocytosis. Selected frames are presented before and after vomocytic event (0 mins). Arrowhead indicates the formation of concave macrophage membrane with vomocytosis. Vomocytosed cryptococci leave the imaged volume post 48 minutes (see Supplementary Movie S1). Scale bar 10 μ m. (b) Intracellular proliferation. Selected frames are presented from when bud is first visible (arrowhead). (c) Quantification of intracellular proliferation from time lapse imaging. Each occurrence of intracellular budding yeast was counted over 12 hours. Data presented is a cumulative percentage of yeast that budded over the time of observation. (d) Phagocytosis. Selected frames are presented from formation of phagocytic cup (arrowhead). (e) Quantification of phagocytosis from time lapse imaging. Each occurrence of phagocytosis was counted over 12 hours. Data presented is a cumulative percentage of yeast that were phagocytosed over the time of observation. Quantitation of intracellular proliferation and phagocytosis are from 22 infected macrophages and are representative of $n = 5$.

by using *in vitro* culture methods that modified capsule size prior to infection. *In vitro* culture with NaCl was sufficient to significantly reduce capsule size²⁶ (Fig. 6a) but the reduction in capsule was not sufficient to increase uptake by macrophages or survival of infection in contrast to the capsule mutant *cap59* (Fig. 6b,c). The increase in capsule size observed *in vivo* can be induced *in vitro* using mammalian serum, increased ambient CO₂ concentration, limited iron availability increased pH and temperature^{27–29}. We tested combinations of temperature, mammalian growth media (MGM), mammalian serum and nutrient starvation for induction of cryptococcal capsule similar to those that we had observed *in vivo* in zebrafish. A combination of MGM, serum and 37 °C gave a capsule size much larger than growth in rich media and a distribution very similar to that seen at 24 hpi (median = 1.87 μ m vs. 1.81 μ m MGM and 24 hpi respectively, $P = 0.24$, Mann-Whitney; Fig. 6a).

Using induced capsule cultures we were able to probe the effect on macrophage phagocytosis of enlarged capsules at the initiation of infection. When zebrafish were infected with capsule-enlarged *C. neoformans* there were significantly fewer intracellular cryptococci (Fig. 6b,c). Quantification of intracellular cryptococci by live fluorescence imaging showed that there was an approximately two-fold reduction in the proportion of intracellular cryptococci (Fig. 6d). This reduction in intracellular cryptococci had a dramatic impact on survival with almost 80% mortality and an 8.2 hazard ratio in comparison to non-induced cultures (logrank, 95% confidence interval 6.5, 20.0; Fig. 6e) and on fungal burden (difference at 72 hpi 2.8×10^4 , $P = < 0.0001$, Mann-Whitney). We

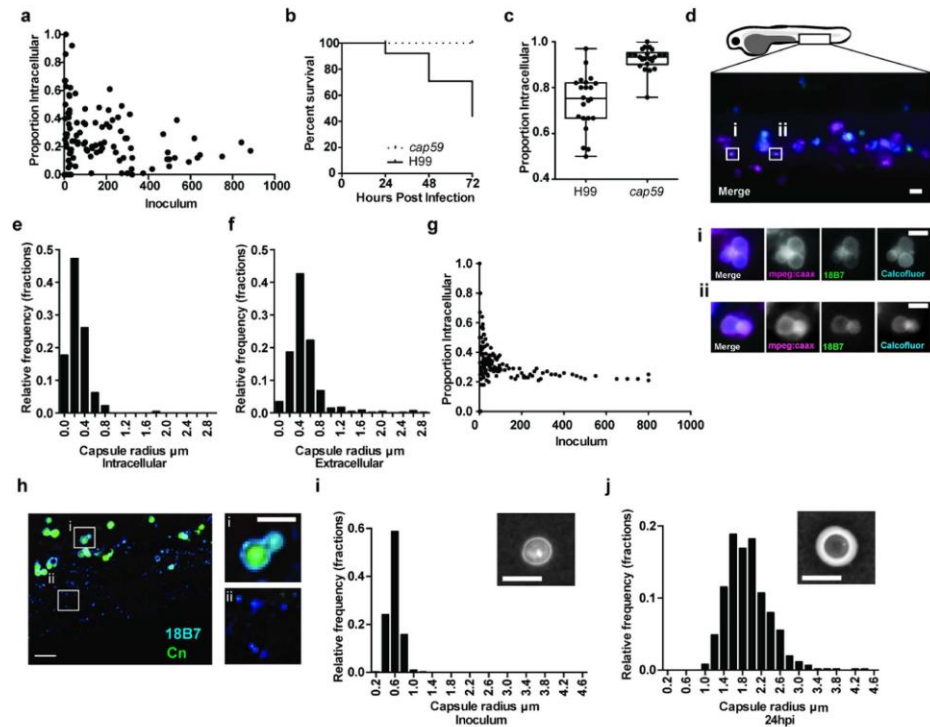


Figure 5. Polysaccharide capsule is smaller on intracellular cryptococci and is greatly enlarged after infection. (a) Association between inoculum and proportion of intracellular cryptococci. Each point is a separate infection. P-value 0.0499. 120 infections of *Tg(fms:Gal4,VP16)i186*; *Tg(UAS:nfsB,mCherry)i149* zebrafish with *C. neoformans* strain H99GFP. (b) Survival of AB strain zebrafish infected with $>10^2$ – 10^3 *C. neoformans* strain H99 or mutant *cap59*. P < 0.0001, logrank (Mantel-Cox), hazard ratio = 10.1 (logrank; 95% confidence interval 5.6, 18.4). 89 and 81 infections from H99 and *cap59* groups respectively, from n = 8. (c) Proportion of intracellular cryptococci 4 hours post infection of *Tg(mpeg1:mCherryCAAX)sh378* with $>10^1$ – 10^2 *C. neoformans* strain H99 or mutant *cap59* labelled with Calcofluor white. Quantitation of 22 infected fish from n = 3 experiments. (d–f) *In vivo* measurement of intracellular and extracellular polysaccharide capsule radius. 1025 cryptococci were measured from 50 infections from n = 5 repeats. (d) Maximum intensity projection from three dimensional fluorescence imaging of *Tg(mpeg1:mCherryCAAX)sh378* (magenta), that labels macrophage membranes, infected with inocula between $>10^1$ – 10^2 of *C. neoformans* strain H99 labeled for polysaccharide capsule (green) and cell wall (cyan). Boxed areas are enlarged in i and ii, and are single z-sections. Scale bar is 20 μ m in left image and 5 μ m in i and ii. (e,f) Intracellular cryptococci have smaller polysaccharide capsules. Relative frequency histograms of capsule radius for intracellular (e) and extracellular (f) cryptococci. (g) Output of probability model using relative numbers within macrophages from (e,f) to calculate proportion of intracellular cryptococci at different inocula given random input (h) Cryptococcal capsule is enlarged and shed at 24 hpi. Fixed tissue of AB strain zebrafish infected with $>10^2$ – 10^3 *C. neoformans* strain H99GFP (green) at 24 hpi labeled with antibody to capsular polysaccharide (cyan). Scale bar 10 μ m. Boxed areas are enlarged in i and ii. Scale bar 5 μ m. (i,j) Cryptococcal capsule size greatly enlarged 24 hpi. Relative frequency histograms of capsule radius for inoculum (i) and 24 hpi (j) cryptococci isolated from AB strain zebrafish infected with $>10^2$ – 10^3 of *C. neoformans* strain H99. Inset panels are example India ink stained samples. Scale bar 5 μ m. 615 cryptococci were measured in 12 infections from n = 3.

therefore concluded that increased capsule size at 24 hpi was sufficient to prevent macrophage control of cryptococcal infection and led to uncontrolled fungal growth and death.

Discussion

Here we have presented analysis of macrophage and cryptococcal cell interactions that enables analysis at a cellular level *in vivo*, non-invasively and over the course of infection. High quality imaging is the mainstay of the zebrafish model and our imaging methodology allows whole organismal imaging of interactions of the

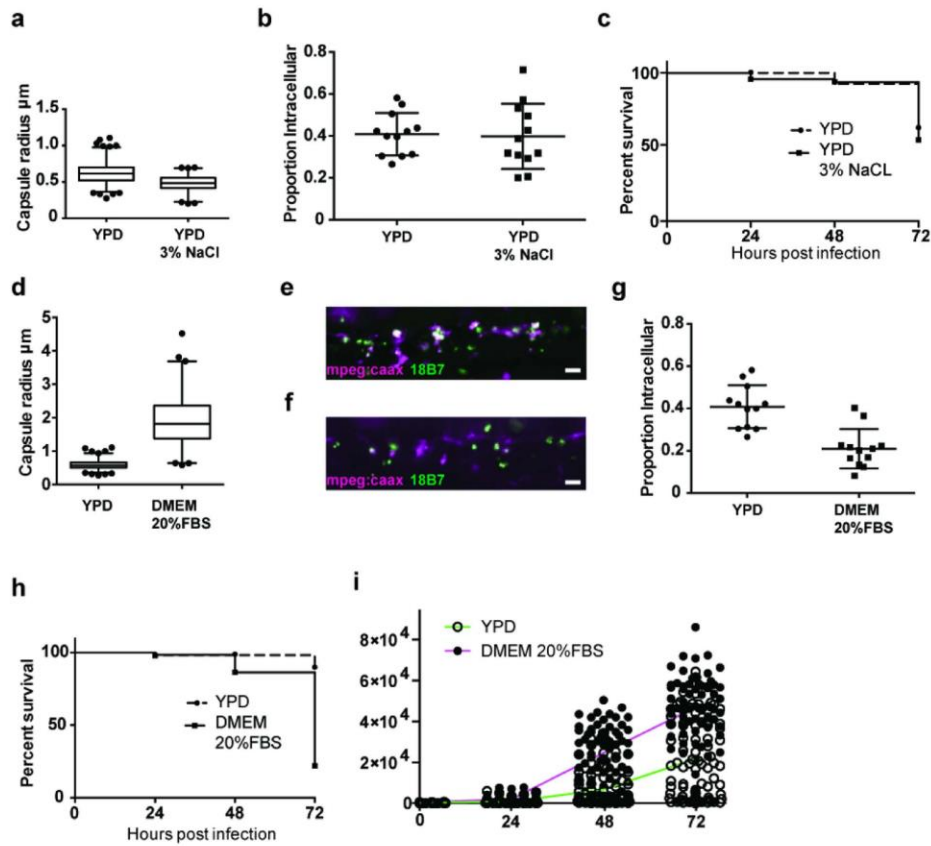


Figure 6. *In vitro* recapitulation of large polysaccharide capsule prevents macrophage phagocytosis *in vivo*. (a) Reduction of cryptococcal capsule *in vitro*. $P < 0.001$, Mann-Whitney; Medians YPD = $0.62 \mu\text{m}$, YPD 3%NaCl = $0.48 \mu\text{m}$. 632 (YPD) and 345 (YPD 3% NaCl) infections, India ink staining from $n = 3$. (b) Proportion of intracellular cryptococci 2 hpi of *Tg(mpeg1:mCherryCAAX)sh378* with $> 10^1$ – 10^2 *C. neoformans* strain H99GFP grown in YPD or YPD 3% NaCl. Each point represents a separate infection from $n = 4$ plotted with median and standard deviation. (c) Survival of AB-strain zebrafish infected with $> 10^1$ – 10^3 of *C. neoformans* strain H99GFP grown in YPD or YPD 3% NaCl ($P = 0.38$, logrank (Mantel-Cox)). 55 (YPD) and 66 (YPD 3% NaCl) infections, from $n = 3$. (d) Induction of cryptococcal capsule *in vitro*. $P < 0.001$, Mann-Whitney, Medians YPD = $0.58 \mu\text{m}$, DMEM 20% FBS = $1.81 \mu\text{m}$. 513 (YPD) and 255 (DMEM 20% FBS) India ink staining from $n = 3$. (e,f) Example maximum intensity projection from three-dimensional fluorescence imaging of *Tg(fms:Gal4.VP16)i186;Tg(UAS:nfsB.mCherry)i149* (magenta) infected with $> 10^1$ – 10^2 of *C. neoformans* strain H99GFP (green) 2 hpi. Intracellular yeast appear white due co-localisation of both colours (e) YPD inoculum. (f) DMEM 20% FBS inoculum. (g) Proportion of intracellular cryptococci 2 hpi of *Tg(mpeg1:mCherryCAAX)sh378* with $> 10^1$ – 10^2 *C. neoformans* strain H99GFP grown in YPD or DMEM 20% FBS. Each point represents a separate infection from $n = 4$ with median and standard deviation. (h) Survival of AB-strain zebrafish infected with $> 10^1$ – 10^2 of *C. neoformans* strain H99GFP grown in YPD or DMEM 20% FBS. $P < 0.0001$, logrank (Mantel-Cox). hazard ratio = 8.2 (logrank; 95% confidence interval 6.5, 20.0). 57 and 59 infections from YPD and DMEM 20% FBS groups respectively, from $n = 3$. (i) Linear comparison of quantification of fungal burden using area of fluorescent pixels from *Nacre*-strain zebrafish infected with between $> 10^1$ – 10^2 of *C. neoformans* strain H99GFP grown in YPD or DMEM 20% FBS. Individual infection and mean fungal burden values with H99GFP grown in YPD (open circles and green line respectively) or H99GFP grown in DMEM 20% FBS (filled circles and magenta line respectively) treatment. Each point is a separate infection; the same 100 (YPD) or 97 (DMEM 20% FBS) infections followed over 72 hours from $n = 3$. Box plots are whiskers at 5 and 95 percentiles with outliers plotted.

host immune system and pathogen cells, non-invasively throughout a vertebrate host. Single plane illumination microscopy (SPIM) and related technologies^{30,31} offer similar benefits, and have the potential for even higher spatial resolution, but our approach has the advantage of being able to image tens to hundreds of infections, in parallel, over a relatively short time period. This means that large datasets can be generated and subjected to robust statistical analysis. A major limiting step to be overcome is that image analysis of such datasets remains largely a manual task. This is due to the complex nature of the detection and segmentation of immune and pathogen cells, and the amount of computation required, as even a single infected zebrafish, at a single time point amounts to over a billion voxels.

A potential limitation to the zebrafish model for studying human infection is that the zebrafish are maintained at 28 °C as opposed to 37 °C. Nevertheless, zebrafish have been used successfully to study a wide range of human bacterial and fungal pathogens^{13–16,32}. Host temperature has a clear role in pathogenicity of fungal pathogens and is one reason why *Cryptococcus neoformans* is a significant pathogen of humans when other cryptococcal species are not³³. However, given that *C. neoformans* appears able to infect such a wide range of animal species, with very different thermoregulation, it is likely that pathogenesis is not dependent of host body temperature³⁴. The trehalose pathway of *C. neoformans* has been shown to be a requirement for growth at 37 °C and the trehalose pathway mutant $\Delta tps1$ is avirulent in mice³⁵. However, the $\Delta tps1$ mutant was also avirulent in zebrafish at 28 °C and the nematode *Caenorhabditis elegans* at 25 °C^{12,35}. Similarly, here we have demonstrated that changes in cryptococcal capsule during infection of zebrafish agree with mammalian studies and are therefore not dependent on body temperature alone.

We sought to understand the behavior of phagocytes during unresolved infection, when the immune system must clear growing yeast cells, by injection of cryptococci into the circulation. This does not model the likely route of human infection of a very low inoculum into the alveolar space but our route of infection directly relates to our aim of studying the early events following dissemination of *C. neoformans*. We note that other models of infection are possible with the zebrafish, whereby pathogens are, for example, introduced to single restricted tissue sites or, most intriguingly, to the swim bladder, an enclosed air/liquid interface of epithelial/mesothelium tissue^{36–38}.

We have demonstrated that, while macrophage phagocytosis of cryptococci contributes to control of infection, in the absence of adaptive immunity, the developing immune system of zebrafish larvae alone (that can be considered a model of vertebrate innate immunity) cannot clear cryptococcal infection. Our model permitted unparalleled detail in the progression of cryptococcal infection and we able to observe distinct outcomes of infection, within narrow ranges of initial fungal burden, that appeared stochastic. The progression of cryptococcal infection was very sensitive to differences in dose and, even within small ranges, this may be sufficient to explain largely the differences in infection progression. However, there were numerous examples of initial fungal burden being independent of severity (see Supplementary Data S1). Therefore a stochastic model (where effect is independent of initial fungal burden but the probability of an effect is not) best fits our current understanding of the progression of cryptococcal infection and is likely also to be applicable to other aspects e.g. the dissemination to the central nervous system.

Nevertheless, macrophages are essential for control, as their depletion had a catastrophic effect on any restriction of fungal burden, even when neutrophil numbers were unaffected. This was also recently demonstrated in zebrafish using a transient knockdown of the Spi-1 transcription factor¹². In addition, depletion of macrophages once infections were controlled still led to increased fungal burden, suggesting they continue to play a critical role even after the initial onset of disease. Previous studies that have depleted macrophages in a mouse lung model of cryptococcosis have shown differing results. Intratracheal or intranasal administration of clodronate liposomes resulted in decreased or unaltered lung fungal burden in three different mouse strains³⁹. However, this approach may not deplete macrophages and dendritic cells in surrounding tissues that may be able to compensate for local loss⁴⁰. In contrast, the depletion of CD11c-expressing macrophages and dendritic cells using a diphtheria toxin-sensitive transgenic caused no observable difference in lung fungal burden 4 days post infection (dpi) but resulted in considerable mortality at 5 dpi⁴⁰. Our results provide an explanation for this finding, by demonstrating that there can be very rapid changes in fungal burden following the loss of macrophage control. Interestingly, macrophage depletion late in infection has been demonstrated to be protective in dissemination of *C. neoformans* and provides evidence for the role of the parasitism of macrophages in dissemination during cryptococcosis¹¹.

Our approach also provides validation for multiple aspects of macrophage parasitism by *C. neoformans* that have previously been characterized *in vitro*. Vomocytosis was originally identified in mammalian macrophages and has been demonstrated in environmental amoeboid hosts^{9,41}. However, this study represents the first time vomocytosis has been directly observed and quantified *in vivo*. The impact of vomocytosis during progression of cryptococcosis is unknown; does vomocytosis protect host macrophages from parasitism or is it fundamental to the dissemination of *C. neoformans* in cryptococcal meningitis? A previous study was able to infer the occurrence of vomocytosis *in vivo* but required the isolation of macrophages from the lung following infection¹⁸. Since this is not a limitation for our zebrafish model, there is now the potential to be able to identify when and how vomocytosis contributes to the pathogenesis of cryptococcal infection.

Similarly, intracellular proliferation is a significant *in vitro* phenomenon but how it contributes to the progression of infection is not known. In the related pathogen *C. gattii*, intracellular proliferation closely correlates with virulence in mice and humans but this has not been observed for *C. neoformans*^{42–44}. We have shown that not only can intracellular proliferation be directly observed *in vivo*¹² but that intracellular proliferation is the principal factor driving the shift in the proportion of cryptococci that were intracellular at twenty-four hours post infection. Thus, the previously described, apparently, higher proportion of phagocytosis observed at 13 hpi is likely due to intracellular proliferation not phagocytosis¹². Interestingly, a similar result was observed in *C. neoformans* infection of mouse lungs between 2 and 8 hours but using a high fungal inoculum, perhaps explaining the much earlier peak in intracellular cryptococci compared to our study⁴⁵. High intracellular growth will be protective to the host

early in infection as there will be limited tissue damage from extracellular growth. Early limitation of damage to host tissue by intracellular growth may also contribute to pathogenesis as this will reduce pro-inflammatory immune signaling permitting cryptococcal infection to become established.

However, whilst intracellular proliferation proceeds rapidly *in vivo*, there is little change in extracellular yeast numbers early in infection, reflecting the need for extracellular yeast to adapt to the host environment prior to the rapid growth seen later in infection. Gene expression analyses during lung infection have demonstrated a similar 'rest' period for extracellular yeast during adaptation^{44,46}. Intriguingly, this does not appear to be the case for intracellular yeast in macrophages, as they are able to proliferate almost immediately. The more rapid changes in intracellular yeast gene expression profile may perhaps be part of a host adaptation to dormancy⁴⁴.

The infectious propagule of human cryptococcosis is most likely a basidiospore or yeast cell desiccated to the extent that it is small enough to reach the deep structures of the lung⁴⁷. In either case the capsule will be very thin or absent, unlikely to inhibit phagocytosis, and thus capsule thickness will likely not be a factor for initial infection in the lungs. Using live imaging of double capsule and cell wall labeled cryptococci *in vivo* we have shown that, even for small capsules following growth in rich media, cryptococcal capsule thickness is a determinant of phagocytosis *in vivo*. The ability of capsular polysaccharide size to interfere with phagocytosis is one of the earliest reported findings in cryptococcal pathogenesis²² but the mechanism by which capsule inhibits phagocytosis, especially opsonic uptake, remains to be proven⁴⁸. Where *C. neoformans* is not controlled and cleared, both intracellular and extracellular cryptococci will rapidly develop enlarged capsules^{45,49}. Our data shows that polysaccharide capsule enlargement occurs rapidly after infection, with larger capsules seen as early as two hours post infection. Cryptococcal capsule enlargement has been described in a zebrafish at 5 dpi¹², however, we find that similarly enlarged capsules are present by 1 dpi. The enlargement of capsule we see during the first 24 hpi infection and infection with *C. neoformans* with capsules similarly enlarged *in vitro*, is sufficient to restrict phagocytosis severely. Thus, the restriction of phagocytosis for any given dose will increase the number of extracellular cryptococci and increase the likelihood of uncontrolled infection. Similar experiments have not been proven to be feasible in the mouse lung infection model due to the inability of large encapsulated yeast to enter deep into the lung²⁶. Infection with an acapsular mutant of *Cryptococcus* results in similar fungal burden to a wildtype cryptococcal strain¹² and we found that an acapsular mutant was avirulent and almost completely limited to residing intracellularly. *In vitro* restriction of capsule did not significantly alter the outcome of any of these measures, presumably as the reduction in capsule size was not sufficient to increase phagocytosis and once in the host capsular polysaccharide was induced as with the normally cultured strain. We therefore presume that damage to host tissues is associated with extracellular growth as the acapsular is avirulent despite considerable intracellular growth and the enhanced mortality in our infections with cryptococci with *in vitro* induced polysaccharide capsules.

Cryptococci have evolved both to evade phagocytosis and survive within phagocytes⁵⁰. Here we have demonstrated a mechanism by which this combination of behaviors, which have presumably evolved to avoid predation in the environment⁵⁰, are particularly destructive in the progression of human cryptococcal infection. The number of fungal organisms in the initial inoculum of human infection is likely to be very low. Therefore, in healthy individuals, with competent adaptive immune responses, it is very likely that all cryptococci will be intracellular and will be killed following the pro-inflammatory activation of macrophages. However, in the absence of such responses the combination of survival within macrophages and the inhibition of phagocytosis by cryptococcal capsule will lead to the uncontrolled progression of infection.

Materials and Methods

Ethics statement. Animal work was carried out according to guidelines and legislation set out in UK law in the Animals (Scientific Procedures) Act 1986, under Project License PPL 40/3574. Ethical approval was granted by the University of Sheffield Local Ethical Review Panel.

Fish husbandry. We used the *Nacre*⁵¹ and *AB* strains as our wild type strains, as indicated in the figure legends. Two macrophage (*Tg(fms:Gal4.VP16):i186*; *Tg(UAS:nfsB.mCherry):i149*⁵² and *Tg(mpeg1:mCherryCAAX)sh378*) and one neutrophil (*Tg(mpx:GFP):i114*⁵³) fluorescent transgenic zebrafish lines were used. Zebrafish strains were maintained according to standard protocols⁵⁴. Adult fish were maintained on a 14:10-hour light/dark cycle at 28 °C in UK Home Office approved facilities in the Bateson Centre aquaria at the University of Sheffield.

Transgenic line generation. We generated a transgenic zebrafish with fluorescently labeled macrophage membranes using the CAAX motif to cause the prenylation of mCherry. The *mpeg1:mCherryCAAX* expression vector was generated using the Tol2 Kit Gateway system⁵⁵ by recombining pME-mCherryCAAX with pDest-Tol2pAG2, p3E-PolyA and the *mpeg1* promoter entry clone⁵⁶. The resulting expression vector was used to generate *Tg(mpeg1:mCherryCAAX)sh378* as described previously⁵⁴.

***C. neoformans* culture.** The *C. neoformans* variety *grubii* strain H99, its GFP-expressing derivative H99GFP and the polysaccharide capsule production mutant *cap59* were used in this study⁵⁷. 2 ml YPD (reagents are from Sigma-Aldrich, Poole, UK unless otherwise stated) cultures were inoculated from YPD agar plates and grown for 18 hours at 28 °C, rotating horizontally at 20 rpm. Cells were pelleted at 3300 g, washed twice with PBS (Oxoid, Basingstoke, UK) and resuspended in 2 ml PBS. In addition, as the *cap59* mutant tended to form cell clumps, the washed *cap59* cells were incubated at room temperature for thirty minutes and only the top 50 µl, that contains only single or doublet cells, used for infections (other strains used in parallel to the *cap59* mutant were treated identically). Washed cells were counted with a hemocytometer and used as described below.

***C. neoformans* capsule induction or restriction.** Cultures of H99 GFP were washed and resuspended in PBS as described above. For capsule induction 0.5 ml of washed cells for each culture was centrifuged and suspended in 2 ml of Dulbecco's Modified Eagle's Medium (DMEM; D5546) with 20% heat inactivated foetal bovine

serum (FBS; F9665) to act as the inducing agent. For capsule restriction 0.5 ml of washed cells for each culture was centrifuged and suspended in 2 ml of YPD with 3% w/v NaCl to act as the restricting agent. Control cultures were also prepared using YPD, and DMEM alone. Cultures were grown for a further 24 hours either rotating at 28 °C or in an orbital shaker at 250 rpm at 37 °C. Cultures were then washed three times in PBS to remove residue of the different growth media. Induction or restriction of capsule of all cultures was assessed using India ink staining described below.

Zebrafish model of *C. neoformans* infection. The volume of counted, washed cryptococci was calculated to give the required inoculum in 1 nl, and this volume was pelleted at 3300 g. Pellets were resuspended in autoclaved 10% Polyvinylpyrrolidone (PVP), 0.5% Phenol Red in PBS (PVP is a polymer that increases the viscosity of the injection fluid and prevents settling of microbes in the injection needle⁵⁸). For co-injection of mannan and laminarin these were added at 100 µg/ml. Embryos were anaesthetised at 2 days post fertilization (dpf) by immersion in 0.168 mg/mL tricaine in E3, transferred onto a microscope slide and covered with 3% methyl cellulose in E3 for injection. Two 0.5 nl boluses were injected into the yolk sac circulation valley. Zebrafish were transferred to fresh E3 to recover from anaesthetic. Any zebrafish that had visible damage from the injection or where the injections were not visually confirmed by the presence of Phenol Red were removed. Zebrafish were maintained at 28 °C.

High content imaging method. Infected zebrafish were anaesthetized by immersion in 0.168 mg/mL tricaine E3 and mounted in agar channels for imaging. Channels were made by adding 200 µl of 1% agar (Cat. No. 05039) in E3 containing 0.168 mg/mL tricaine into glass-bottomed, 96-well plates (Porvair sciences, Wrexham, UK). Channels were cut in cooled agar using GelX4 tips (Geneflow, Staffordshire, UK). Mounted embryos were imaged on a Nikon Ti-E with a CFI Plan Achromat λ 10X, N.A.0.45 objective lens, a custom built 500 µm Piezo Z-stage (Mad City Labs, Madison, WI, USA) and using Intensilight fluorescent illumination with ET/sputtered series fluorescent filters 49002 and 49008 (Chroma, Bellow Falls, VT, USA). Images were captured with Neo sCMOS, 2560 × 2160 Format, 16.6 mm x 14.0 mm Sensor Size, 6.5 µm pixel size camera (Andor, Belfast, UK) and NIS-Elements (Nikon, Richmond, UK) using the following settings: 1. GFP filter 49002, 10 ms exposure, gain 4 2. mCherry filter 49008, 10 ms exposure, gain 4. Each zebrafish was imaged as three contiguous fields of view that were assigned from bright-field images. 80 z sections, 5 µm apart, were captured in each channel and each position in that order. Each biological repeat contained 40 infected zebrafish, with 3 multi-channel z stacks per fish. The microscope was enclosed in a humidified, 28 °C, environmental chamber (Okolabs, Pozzuoli, Italy). After imaging larvae were recovered in fresh E3 and returned to a new numbered 96-well plate.

Processing of high content imaging. High content images were not processed for analysis except adjustment of look-up-tables to temporarily increase local contrast. For presentation in Fig. 1a images were projected in the z-plane using the maximum intensity pixel method. Three-dimensional reconstructions in Fig. 1 and Fig. S2 were performed using Imaris (Bitplane, Zurich, Switzerland).

Macrophage response data set. Eight of the 120 infections were censored at 2 hpi and removed from the analysis, seven due to having an initial fungal burden of zero and one due to the larvae being damaged by the transfer to the imaging plate. A further 2 infections were censored at 24 hpi due to an inability to make the counts due to the quality of the imaging files. Any censored or missing values are indicated by 'NA' in the data tables and were not included in any relevant analysis. The following calculations were performed to obtain values for derived counts: number of extracellular cryptococci = total number of Cryptococci – number of intracellular cryptococci; proportion of intracellular cryptococci = number of intracellular Cryptococci/total number of cryptococci; phagocytic index = number of intracellular Cryptococci/number of infected macrophages; change in cryptococcal numbers between 2 and 24 hpi = (number of cryptococci at 24 hpi – number of cryptococci at 2 hpi)/number of cryptococci at 2 hpi.

Imaging and colony forming units (CFU) counts. Imaging and CFU counts were compared from the same infections. Zebrafish 2 hpi infection were imaged as described above, followed by manual dissociation of individual larvae with microcentrifuge pestles in 200 µl dH₂O (this will lyse host cells while leaving fungal cells intact⁶²). Dissociates were plated on YPD agar and incubated at 28 °C for 48 hours before counting.

Measurement of fungal burden area. Zebrafish were imaged in 96-well plates using Nikon Ti-E with a CFI Plan Achromat UW 2X N.A. 0.06 objective lens, using Intensilight fluorescent illumination with ET/sputtered series fluorescent filters 49002 (Chroma, Bellow Falls, VT, USA). Images were captured with Neo sCMOS, (Andor, Belfast, UK) and NIS-Elements (Nikon, Richmond, UK). Images were exported as tif files and further analysis performed in ImageJ (Schneider *et al.*, 2012). Images were individually cropped to remove the side of the 96-well or any bright debris or noise within the well. Pixels above the intensity corresponding to *C. neoformans* strain H99GFP were selected using a threshold. The same threshold was used for all images. Thresholded images were converted to binary images and the number of pixels counted using the 'analyse pixel' function.

Macrophage depletion using clodronate liposomes. Clodronate or PBS liposomes (Clodronateliposomes, Amsterdam, The Netherlands) were diluted 1:1 in 10% Polyvinylpyrrolidone (PVP), 0.5% Phenol Red in PBS. 1 nl was injected into embryos 1 dpf or 3 dpf (after removal from the chorion) as described above. Specific depletion was confirmed using macrophage (*Tg(mpeg1:mCherryCAAX)sh378*) and neutrophil (*Tg(mpx:GFP)i114*) transgenic zebrafish.

Time lapse imaging. Time lapse imaging was performed as described for high content imaging with the following adjustments: Zebrafish larvae were mounted in 0.8% low melting point agarose (Cat No. A9414) in E3 containing 0.168 mg/mL tricaine. Images were captured with CFI Plan Achromat λ 20X, N.A.0.75 objective lens, 10 z-sections 2.5 μ m apart, with Perfect Focus system, every 2 minutes for 12 hours.

Survival. Survival was assessed by presence or absence of heart-beat. Statistical analysis was performed as described in the text and figure legends.

Live measurement of *C. neoformans* capsule size. *C. neoformans* at 1×10^7 /ml were labeled with monoclonal antibody 18B7 (a gift from Arturo Casadevall) as described previously^{19,59}. 18B7 labeled cryptococci were then labeled with 2.5 μ g/ml FITC secondary antibody and 15 μ g/ml fungal cell wall stain Calcofluor white (Cat No. 18909) for 45 mins at 28 °C, rotating horizontally at 20 rpm (the *cap59* mutant and H99GFP were similarly labeled with Calcofluor white for imaging of cryptococcal uptake in Fig. 5c). Labeled cryptococci were re-counted and injections were performed as above. Imaging was performed as for time lapse except at a single time point 2 hpi and using, in addition, a 31000v2 fluorescent filter for Calcofluor white staining (Chroma, Bellow Falls, VT, USA). NIS Elements (Nikon, Richmond, UK) was used to measure capsule radius by subtracting cell wall diameter from capsule diameter and halving.

Antibody staining. Zebrafish larvae were fixed at room temperature in 4% formaldehyde for 30 minutes rocking, washed three times in PBS with 0.1% Triton-X and incubated rocking for 10 mins. Washing was repeated twice more. Fixed larvae were incubated in 5 μ g/ml 18B7 primary antibody in 500 μ l 0.1% Triton-X solution rocking at 4 °C for 16 hours. Following primary antibody staining, larvae were washed as above. They were then incubated with 5 μ g/ml CF350 secondary antibody (Cat No. SAB4600222) in 500 μ l 0.1% Triton-X rocking at room temperature for 2 hours, washed as above and mounted on microscope slides with 7 μ l Mowiol solution¹⁹ under 13 mm coverslips.

Probability model for prediction of proportion of intracellular cryptococci. We wrote a Microsoft Excel (2011 v14.5.3) spreadsheet containing a probability model that calculated whether an individual cryptococci was phagocytosed or not based on its capsule size. The relative proportions of capsule sizes presented in Fig. 5c,d were used to calculate the probability of phagocytosis given such a capsule size. Thus, using a random number input, probability of phagocytosis (β) was calculated from $\beta = \text{IF}(A < 0.12, 0.71, \text{IF}(A < 0.45, 0.55, \text{IF}(A < 0.786, 0.22, \text{IF}(A < 0.94, 0.11, 0.13))))$ where A is a random number between 0 and 1. Successful phagocytosis (ϕ ; i.e. cryptococcal cell was intracellular) was then scored by: $\phi = \text{IF}(A < \beta, 1, 0)$. ϕ was calculated for each cryptococcal cell in an infection and summed to give the proportion of cryptococci intracellular. The model was run repeatedly over the range of initial fungal burdens observed and plotted (Fig. 5e) as measured data (Fig. 5a).

India ink assay for cryptococcal capsule size. For staining of *C. neoformans* cultures, equal volumes (2 μ l) of cell suspension and India ink (Winsor and Newton, London, UK) were mixed on a microscope slide and mounted under a 13 mm coverslip. For staining of cryptococci following infection, zebrafish larvae were dissociated with microcentrifuge tube pestles in 20 μ l PBS, pelleted at 16300 g for 5 mins, resuspended in 3 μ l PBS, 3 μ l of India ink added and mounted as above. India ink samples were imaged on Leica HC upright microscope with phase contrast PL APO 100 \times 1.4NA objective lens and images captured with ProgRes C14 camera and software. ImageJ was used to measure capsule radius by subtracting cell body diameter from total diameter.

Statistical analysis. Statistical analysis was performed as described in the results and figure legends. We used Graph Pad Prism 6 (v6.0b) for statistical tests and plots.

References

- Park, B. J. *et al.* Estimation of the current global burden of cryptococcal meningitis among persons living with HIV/AIDS. *AIDS* **23**, 525–30 (2009).
- Neofytos, D. *et al.* Epidemiology and outcome of invasive fungal infections in solid organ transplant recipients. *Transpl. Infect. Dis.* **12**, 220–9 (2010).
- Kozic, H., Riggs, K., Ringpfeil, F. & Lee, J. B. Disseminated *Cryptococcus neoformans* after treatment with infliximab for rheumatoid arthritis. *J. Am. Acad. Dermatol.* **58**, S95–6 (2008).
- Panackal, A. A. *et al.* Paradoxical Immune Responses in Non-HIV Cryptococcal Meningitis. *PLoS Pathog.* **11**, e1004884 (2015).
- Jarvis, J. N. *et al.* Cerebrospinal fluid cytokine profiles predict risk of early mortality and immune reconstitution inflammatory syndrome in HIV-associated cryptococcal meningitis. *PLoS Pathog.* **11**, e1004754 (2015).
- Gibson, J. F. & Johnston, S. A. Immunity to *Cryptococcus neoformans* and *C. gattii* during cryptococcosis. *Fungal Genet. Biol.* **78**, 76–86 (2015).
- Shibuya, K. *et al.* Granuloma and cryptococcosis. *J. Infect. Chemother.* **11**, 115–22 (2005).
- Tucker, S. C. & Casadevall, A. Replication of *Cryptococcus neoformans* in macrophages is accompanied by phagosomal permeabilization and accumulation of vesicles containing polysaccharide in the cytoplasm. *Proc. Natl. Acad. Sci. USA* **99**, 3165–70 (2002).
- Ma, H., Croudace, J. E., Lammas, D. a & May, R. C. Expulsion of live pathogenic yeast by macrophages. *Curr. Biol.* **16**, 2156–60 (2006).
- Alvarez, M. & Casadevall, A. Phagosome extrusion and host-cell survival after *Cryptococcus neoformans* phagocytosis by macrophages. *Curr. Biol.* **16**, 2161–5 (2006).
- Charlier, C. *et al.* Evidence of a role for monocytes in dissemination and brain invasion by *Cryptococcus neoformans*. *Infect. Immun.* **77**, 120–7 (2009).
- Tenor, J. L., Oehlers, S. H., Yang, J. L., Tobin, D. M. & Perfect, J. R. Live Imaging of Host-Parasite Interactions in a Zebrafish Infection Model Reveals Cryptococcal Determinants of Virulence and Central Nervous System Invasion. *MBio* **6**, e01425–15 (2015).
- Brothers, K. M. *et al.* NADPH oxidase-driven phagocyte recruitment controls *Candida albicans* filamentous growth and prevents mortality. *PLoS Pathog.* **9**, e1003634 (2013).

14. Mostowy, S. *et al.* The zebrafish as a new model for the *in vivo* study of *Shigella flexneri* interaction with phagocytes and bacterial autophagy. *PLoS Pathog.* **9**, e1003588 (2013).
15. Prajsnar, T. K. *et al.* A privileged intraphagocyte niche is responsible for disseminated infection of *Staphylococcus aureus* in a zebrafish model. *Cell. Microbiol.* **14**, 1600–19 (2012).
16. Tobin, D. M. *et al.* The *Ita4h* locus modulates susceptibility to mycobacterial infection in zebrafish and humans. *Cell* **140**, 717–30 (2010).
17. Bernut, A. *et al.* Mycobacterium abscessus cording prevents phagocytosis and promotes abscess formation. *Proc. Natl. Acad. Sci. USA* **111**, E943–52 (2014).
18. Nicola, A. M., Robertson, E. J., Albuquerque, P., Derengowski, L. da S. & Casadevall, A. Nonlytic exocytosis of *Cryptococcus neoformans* from macrophages occurs *in vivo* and is influenced by phagosomal pH. *MBio* **2**, e00167–11 (2011).
19. Johnston, S. A. & May, R. C. The human fungal pathogen *Cryptococcus neoformans* escapes macrophages by a phagosome emptying mechanism that is inhibited by Arp2/3 complex-mediated actin polymerisation. *PLoS Pathog.* **6**, e1001041 (2010).
20. Voelz, K., Lammas, D. a & May, R. C. Cytokine signaling regulates the outcome of intracellular macrophage parasitism by *Cryptococcus neoformans*. *Infect. Immun.* **77**, 3450–7 (2009).
21. Heinsbroek, S. E. M. *et al.* Stage-specific sampling by pattern recognition receptors during *Candida albicans* phagocytosis. *PLoS Pathog.* **4**, e1000218 (2008).
22. Mitchell, T. G. & Friedman, L. *In vitro* phagocytosis and intracellular fate of variously encapsulated strains of *Cryptococcus neoformans*. *Infect. Immun.* **5**, 491–8 (1972).
23. McClelland, E. E., Bernhardt, P. & Casadevall, A. Estimating the relative contributions of virulence factors for pathogenic microbes. *Infect. Immun.* **74**, 1500–4 (2006).
24. Robertson, E. J. *et al.* *Cryptococcus neoformans* *ex vivo* capsule size is associated with intracranial pressure and host immune response in HIV-associated cryptococcal meningitis. *J. Infect. Dis.* **209**, 74–82 (2014).
25. Chang, Y. C. & Kwon-Chung, K. J. Complementation of a capsule-deficient mutation of *Cryptococcus neoformans* restores its virulence. *Mol. Cell. Biol.* **14**, 4912–9 (1994).
26. Dykstra, M. A., Friedman, L. & Murphy, J. W. Capsule size of *Cryptococcus neoformans*: control and relationship to virulence. *Infect. Immun.* **16**, 129–35 (1977).
27. Granger, D. L., Perfect, J. R. & Durack, D. T. Macrophage-mediated fungistasis *in vitro*: requirements for intracellular and extracellular cytotoxicity. *J. Immunol.* **136**, 672–80 (1986).
28. Vartivarian, S. E. *et al.* Regulation of cryptococcal capsular polysaccharide by iron. *J. Infect. Dis.* **167**, 186–90 (1993).
29. Zaragoza, O., Taborda, C. P. & Casadevall, A. The efficacy of complement-mediated phagocytosis of *Cryptococcus neoformans* is dependent on the location of C3 in the polysaccharide capsule and involves both direct and indirect C3-mediated interactions. *Eur. J. Immunol.* **33**, 1957–67 (2003).
30. Huisken, J., Swoger, J., Del Bene, F., Wittbrodt, J. & Stelzer, E. H. K. Optical sectioning deep inside live embryos by selective plane illumination microscopy. *Science* **305**, 1007–9 (2004).
31. Voie, A. H., Burns, D. H. & Spelman, F. A. Orthogonal-plane fluorescence optical sectioning: three-dimensional imaging of macroscopic biological specimens. *J. Microsc.* **170**, 229–36 (1993).
32. Herbst, S. *et al.* Phagocytosis-dependent activation of a TLR9-BTK-calcineurin-NFAT pathway co-ordinates innate immunity to *Aspergillus fumigatus*. *EMBO Mol. Med.* **7**, 240–58 (2015).
33. Perfect, J. R. *Cryptococcus neoformans*: the yeast that likes it hot. *FEMS Yeast Res.* **6**, 463–8 (2006).
34. Malik, R. *et al.* *Veterinary Insights into Cryptococcosis Caused by Cryptococcus neoformans and Cryptococcus gattii*. (ASM Press, 2011).
35. Petzold, E. W. *et al.* Characterization and regulation of the trehalose synthesis pathway and its importance in the pathogenicity of *Cryptococcus neoformans*. *Infect. Immun.* **74**, 5877–87 (2006).
36. Gratacap, R. L., Rawls, J. F. & Wheeler, R. T. Mucosal candidiasis elicits NF- κ B activation, proinflammatory gene expression and localized neutrophilia in zebrafish. *Dis. Model. Mech.* **6**, 1260–70 (2013).
37. Winata, C. L. *et al.* Development of zebrafish swimbladder: The requirement of Hedgehog signaling in specification and organization of the three tissue layers. *Dev. Biol.* **331**, 222–36 (2009).
38. Hosseini, R. *et al.* Correlative light and electron microscopy imaging of autophagy in a zebrafish infection model. *Autophagy* **10**, 1844–57 (2014).
39. Shao, X. *et al.* An innate immune system cell is a major determinant of species-related susceptibility differences to fungal pneumonia. *J. Immunol.* **175**, 3244–51 (2005).
40. Osterholzer, J. J. *et al.* Role of dendritic cells and alveolar macrophages in regulating early host defense against pulmonary infection with *Cryptococcus neoformans*. *Infect. Immun.* **77**, 3749–58 (2009).
41. Chrisman, C. J., Alvarez, M. & Casadevall, A. Phagocytosis of *Cryptococcus neoformans* by, and nonlytic exocytosis from, *Acanthamoeba castellanii*. *Appl. Environ. Microbiol.* **76**, 6056–62 (2010).
42. Ma, H. *et al.* The fatal fungal outbreak on Vancouver Island is characterized by enhanced intracellular parasitism driven by mitochondrial regulation. *Proc. Natl. Acad. Sci. USA* **106**, 12980–5 (2009).
43. Voelz, K. *et al.* 'Division of labour' in response to host oxidative burst drives a fatal *Cryptococcus gattii* outbreak. *Nat. Commun.* **5**, 5194 (2014).
44. Alano, A., Vernel-Pauillac, F., Sturny-Leclère, A. & Dromer, F. *Cryptococcus neoformans* host adaptation: toward biological evidence of dormancy. *MBio* **6**, e02580–14 (2015).
45. Feldmesser, M., Kress, Y., Novikoff, P. & Casadevall, A. *Cryptococcus neoformans* is a facultative intracellular pathogen in murine pulmonary infection. *Infect. Immun.* **68**, 4225–37 (2000).
46. Hu, G., Cheng, P.-Y., Sham, A., Perfect, J. R. & Kronstad, J. W. Metabolic adaptation in *Cryptococcus neoformans* during early murine pulmonary infection. *Mol. Microbiol.* **69**, 1456–75 (2008).
47. Velagapudi, R., Hsueh, Y.-P., Geunes-Boyer, S., Wright, J. R. & Heitman, J. Spores as infectious propagules of *Cryptococcus neoformans*. *Infect. Immun.* **77**, 4345–55 (2009).
48. Johnston, S. A. & May, R. C. *Cryptococcus* interactions with macrophages: evasion and manipulation of the phagosome by a fungal pathogen. *Cell. Microbiol.* **15**, 403–11 (2013).
49. Rivera, J., Feldmesser, M., Cammer, M. & Casadevall, A. Organ-dependent variation of capsule thickness in *Cryptococcus neoformans* during experimental murine infection. *Infect. Immun.* **66**, 5027–30 (1998).
50. Casadevall, A. Amoeba provide insight into the origin of virulence in pathogenic fungi. *Adv. Exp. Med. Biol.* **710**, 1–10 (2012).
51. Lister, J. A., Robertson, C. P., Lepage, T., Johnson, S. L. & Raible, D. W. *nacre* encodes a zebrafish microphthalmia-related protein that regulates neural-crest-derived pigment cell fate. *Development* **126**, 3757–67 (1999).
52. Gray, C. *et al.* Simultaneous intravital imaging of macrophage and neutrophil behaviour during inflammation using a novel transgenic zebrafish. *Thromb. Haemost.* **105**, 811–9 (2011).
53. Renshaw, S. *et al.* A transgenic zebrafish model of neutrophilic inflammation. *Blood* **108**, 3976–8 (2006).
54. Dahm, R. & Nusslein-Volhard, C. *Zebrafish: a Practical Approach*. (Oxford University Press, 2002).
55. Kwan, K. M. *et al.* The Tol2kit: a multisite gateway-based construction kit for Tol2 transposon transgenesis constructs. *Dev. Dyn.* **236**, 3088–99 (2007).
56. Ellett, F., Pase, L., Hayman, J. W., Andrianopoulos, A. & Lieschke, G. J. Mpeg1 Promoter Transgenes Direct Macrophage-Lineage Expression in Zebrafish. *Blood* **117**, e49–56 (2011).

57. Voelz, K., Johnston, S. A., Rutherford, J. C. & May, R. C. Automated analysis of cryptococcal macrophage parasitism using GFP-tagged cryptococci. *PLoS One* **5**, e15968 (2010).
58. Spaink, H. P. *et al.* Robotic injection of zebrafish embryos for high-throughput screening in disease models. *Methods* **62**, 246–54 (2013).
59. Zebedee, S. L. *et al.* Mouse-human immunoglobulin G1 chimeric antibodies with activities against *Cryptococcus neoformans*. *Antimicrob. Agents Chemother.* **38**, 1507–14 (1994).

Acknowledgements

We thank Arturo Casadevall for the gift of 18B7 antibody, Lisanne van Leeuwen and Astrid van der Sar for their assistance with the clodronate method, David Strutt for the use of his Leica HC microscope for India ink measurements, the Bateson Centre aquaria staff for their assistance with zebrafish husbandry and Phil Elks and Iwan Evans for critical reading of the manuscript. SAJ, AB, AL and ES were supported by Medical Research Council and Department for International Development Career Development Award Fellowship MR/J009156/1. SAJ was additionally supported by a Krebs Institute Fellowship, Medical Research Foundation grant R/140419 and Medical Research Council Center grant (G0700091). KAM and RHG were supported by a Bateson Centre Biomedical Science scholarship. RH was supported by a Colin Beattie Biomedical Science scholarship. SAJ and AAK were supported by a Wellcome Trust Strategic Award 097377/Z/11/Z. NO and SAR were supported by Biotechnology and Biological Sciences Research Council grant BB/L000830/1. SAR was supported additionally by Medical Research Council Senior Clinical Fellowship (G0701932) and Medical Research Council Programme Grant (MR/M004864/1). RCM was supported by a Lister Fellowship, Wellcome Trust project grant RCHX14191 and the European Research Council Consolidator Award “MitoFun”.

Author Contributions


A.B., K.A.M., R.H., A.L., A.A.K., H.F., E.S., S.A.R., R.C.M. and S.A.J. conceived the experiments, A.B., K.A.M., R.H., A.L., A.A.K., H.F. and S.A.J. performed experiments, A.B., K.A.M., R.O., A.L., A.A.K., H.F., R.A.G., E.S. and S.A.J. analysed the data, N.O., S.A.R., R.C.M. and S.A.J. provided reagents and A.B., K.A.M., R.O., A.L., H.F., N.O., E.S., S.A.R., R.C.M. and S.A.J. wrote the manuscript.

Additional Information

Supplementary information accompanies this paper at <http://www.nature.com/srep>

Competing financial interests: The authors declare no competing financial interests.

How to cite this article: Bojarczuk, A. *et al.* *Cryptococcus neoformans* Intracellular Proliferation and Capsule Size Determines Early Macrophage Control of Infection. *Sci. Rep.* **6**, 21489; doi: 10.1038/srep21489 (2016).

 This work is licensed under a Creative Commons Attribution 4.0 International License. The images or other third party material in this article are included in the article's Creative Commons license, unless indicated otherwise in the credit line; if the material is not included under the Creative Commons license, users will need to obtain permission from the license holder to reproduce the material. To view a copy of this license, visit <http://creativecommons.org/licenses/by/4.0/>

3.2.1 Supplementary data

1

Supplementary Information

2

3 *Cryptococcus neoformans* Intracellular Proliferation and Capsule

4 Size Determines Early Macrophage Control of Infection

5

6 Aleksandra Bojarczuk^{a,b}, Katie A. Miller^{a,b}, Richard Hotham^{a,b}, Amy Lewis^{a,b},

7 Nikolay V. Ogryzko^{a,b}, Alfred A. Kamuyango^{a,b}, Helen Frost^{c#}, Rory H.

8 Gibson^{a,b}, Eleanor Stillman^d, Robin C. May^{c,e}, Stephen A. Renshaw^{a,b} and

9 Simon A. Johnston^{a,b*}

10

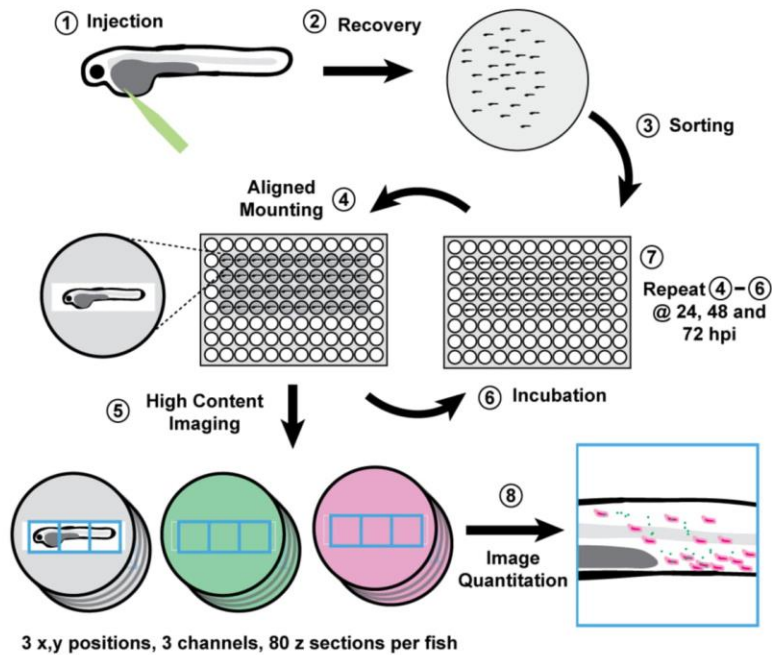
11

12

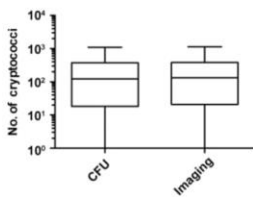
13

14 **Supplementary Figure S1**

a



b



15

16 **Method pipeline for high content imaging of zebrafish *Cryptococcus***

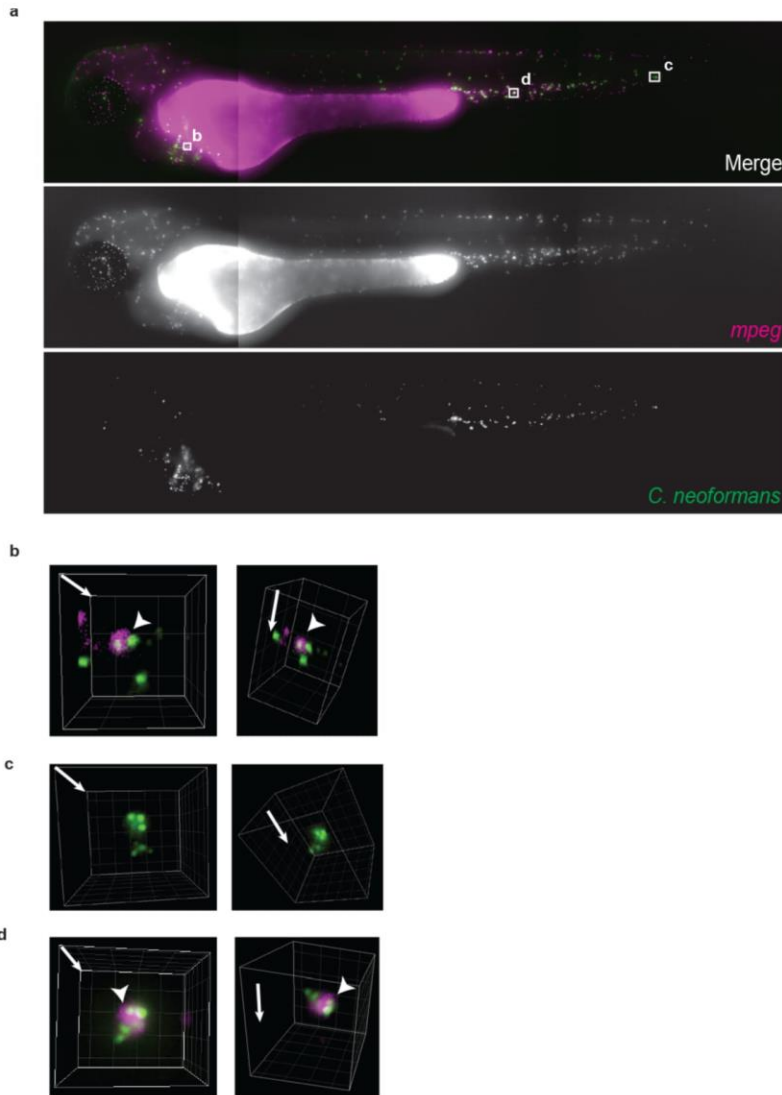
17 **infection model. (a) 1.** Anesthetized zebrafish were injected a 2 dpf with
 18 H99GFP *C. neoformans*. **2.** Zebrafish were recovered from anesthetic and
 19 any injured individuals removed. **3.** Forty zebrafish were randomly selected
 20 and sorted into 96-well plates per repeat. **4.** For imaging, zebrafish were

2

21 anesthetized and aligned in agar channels in a second 96-well plate. **5.** Three
22 dimensional image data sets were captured and the zebrafish were recovered
23 from the anesthetic and returned, to the same plate for incubation. **6.** Infected
24 zebrafish were incubated at 28°C **7.** Steps 4-6 were repeated at 24, 48 and
25 72 hpi. **8.** Each data set was manually counted to generate the values in
26 Table S1. **(b)** Comparison of the values obtained from image counts and CFU
27 plating. The number of H99GFP were counted from images described above,
28 followed by tissue dissociation and plating to establish CFU counts. Pooled
29 counts of 120 infections from n=3 repeats.
30
31

32 **Supplementary Figure S2**

33



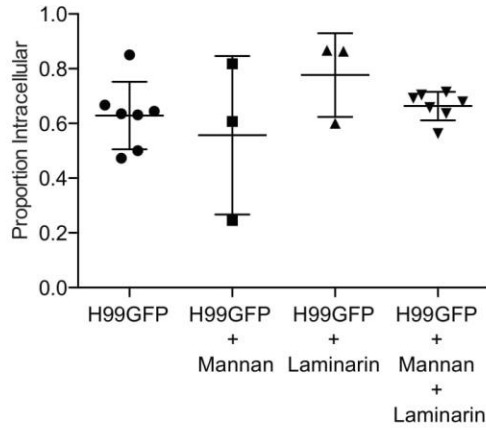
34

35

36 **Quantification of macrophage behavior in response to *Cryptococcus***
37 **during infection using *mpeg* macrophage marker. (a)** Maximum intensity
38 z-projection of example image data from high content imaging of
39 *Tg(mpeg1:mCherryCAAX)sh378* zebrafish, with mCherry labeled
40 macrophages (magenta), infected with 208 cells of *C. neoformans* strain
41 H99GFP (green), at 2 hours post infection. **(b,c,d)**. Areas boxed in (a)

42 enlarged and reconstructed in three-dimensions. Arrowheads indicate
43 intracellular cryptococci. Image pairs represent different views of same
44 volume with arrows indicating z-axis direction. Image grid is 20 μ m.

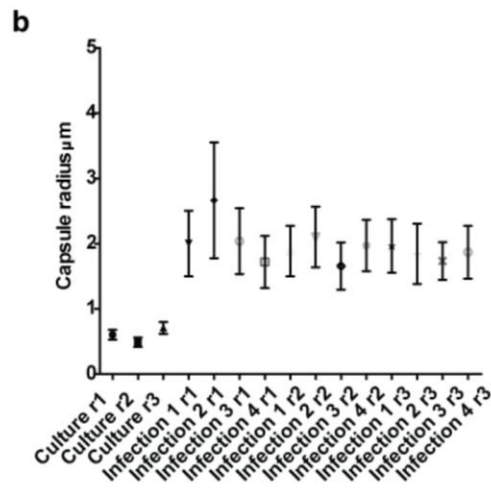
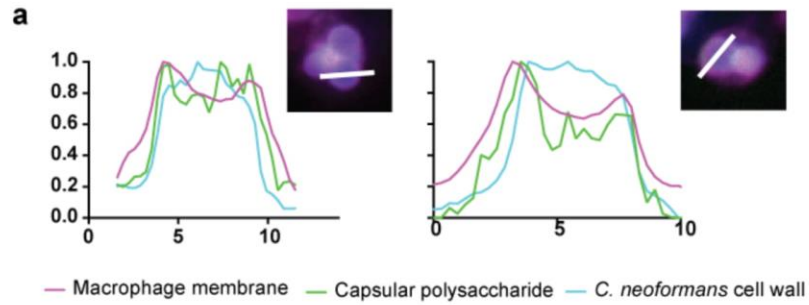
45 **Supplementary Figure S3**
46



47
48

49 **Co-injection of 100 µg/ml mannan and/or laminarin did not inhibit uptake**
50 **of cryptococci by macrophages in zebrafish.** Proportion of intracellular
51 cryptococci 2 hours post infection of *Tg(mpeg1:mCherryCAAX)sh378* with
52 $>10^1$ - 10^2 *C. neoformans* strain H99GFP alone or co-injected with 100 µg/ml
53 mannan and/or laminarin. Each point represents a separate infection plotted
54 with median and standard deviation.

55 **Supplementary Figure S4**



56

57 **Polysaccharide capsule is smaller on intracellular cryptococci and is**

58 **greatly enlarged after infection. A.** Macrophage membrane, capsule and

59 cell wall relative positions can be accurately measured from intensity profiles.

60 Normalised pixel intensity (to the brightest pixel on each path) for the three

61 channels was measured along the lines drawn and plotted. **B.** Mean and

62 standard deviation of capsule radius measurements of each control and

63 infection presented in Fig. 5i,j.

64

65 **Supplementary Table S1.**

	Median	Mean	P-value 2 hpi vs. 24 hpi
Number of Cryptococci at 2 hpi	93	168	0.037
Number of Cryptococci at 24 hpi	135	505	
Number of Intracellular Cryptococci at 2 hpi	16	34	<0.0001
Number of Intracellular Cryptococci at 24 hpi	61	154	
Number of Extracellular Cryptococci at 2 hpi	56	134	0.427
Number of Extracellular Cryptococci at 24 hpi	46	354	
Increase in Total Numbers of Cryptococci	0.89	1.42	N/A
Increase in Intracellular Numbers of Cryptococci	3.05	5.34	N/A
Increase in Extracellular Numbers of Cryptococci	-0.012	0.61	N/A

66

67 **Descriptive statistics and significance tests for the number of**

68 **cryptococci at 2 and 24 hpi.** Values derived from Data S1. Mann-Whitney

69 test used for significance comparison.

70

71

72 **Additional Legends**

73

74 **Supplementary Data S1 (see separate file).**

75 **Macrophage response data set.** Comma separated values. 'NA' represents
76 missing data values either because of direct censoring (see Materials and
77 Methods) or because missing or zero counted values prevented the
78 calculation of derived values. For the calculation of other values see Materials
79 and Methods.

80 .

81

82 **Supplementary Movie S1.**

83 **Movie of cell presented in Figure 4a.** Images are at 5 frames per second.

84

85

86

Table 3.1 Supplementary Data Set 1-macrophage response data set

Inoculum	Number of Infected Macrophages at 2 hpi	Number of Infected Macrophages at 24 hpi	Number of Cryptococci at 2 hpi	Number of Cryptococci at 24 hpi	Number of Intracellular Cryptococci at 2 hpi	Number of Intracellular Cryptococci at 24 hpi	Survival at 72 hpi	Time of Death (days)	Number of Extracellular Cryptococci at 2 hpi	Number of Extracellular Cryptococci at 24 hpi	Proportion of Cryptococci Intracellular at 2 hpi	Proportion of Cryptococci Intracellular at 24 hpi	Phagocytic Index at 2hpi	Phagocytic Index at 24 hpi	Increase in Total Numbers of Cryptococci	Increase in Intracellular Numbers of Cryptococci	Increase in Extracellular Numbers of Cryptococci
1	0	0	1	0	0	0	1	0	1	0	0	0	NA	NA	-1	NA	-1
1	0	2	1	9	0	6	1	0	1	3	0	0.67	NA	3	8	NA	2
2	0	2	4	0	0	4	1	0	2	0	0	1	NA	2	1	NA	-1
3	0	2	3	6	0	5	0	2	3	1	0	0.83	NA	2.5	1	NA	-0.67
3	0	0	3	0	0	0	1	0	3	0	0	NA	NA		-1	NA	-1
3	0	6	3	50	0	29	1	0	3	21	0	0.58	4.83	15.67	NA	NA	6
3	2	1	3	5	2	5	1	0	1	0	0.67	1	1	5	0.67	1.5	-1
4	0	1	4	12	0	8	1	0	4	4	0	0.67	8	2	NA	0	0
4	1	1	4	3	1	1	1	0	3	2	0.25	0.33	1	1	-0.25	0	-0.33
5	0	0	5	1	0	0	0	3	5	1	0	0	NA	NA	-0.8	NA	-0.8
5	0	2	5	8	0	6	1	0	5	2	0	0.75	3	0.6	NA	0	-0.6
5	2	1	5	4	2	2	1	0	3	2	0.4	0.5	1	2	-0.2	0	-0.33
5	1	1	5	5	2	5	1	0	3	0	0.4	1	2	5	0	1.5	-1
6	0	5	6	16	0	6	1	0	6	10	0	0.38	NA	1.2	1.67	NA	0.67
6	0	5	6	36	0	31	1	0	6	5	0	0.86	NA	6.2	5	NA	-0.17
6	1	1	6	11	3	7	1	0	3	4	0.5	0.64	3	7	0.83	1.33	0.33
6	3	0	6	0	4	0	1	0	2	0	0.67	NA	1.33	NA	-1	-1	-1
7	0	2	7	9	0	6	1	0	7	3	0	0.67	NA	3	0.29	NA	-0.57
7	1	2	7	4	2	4	1	0	5	0	0.29	1	2	2	-0.43	1	-1
7	5	1	7	5	6	5	1	0	1	0	0.86	NA	1.2	5	-0.29	-0.17	-1
8	5	0	8	0	8	0	0	2	0	0	1	NA	1.6	NA	-1	-1	NA
8	3	2	8	2	5	2	1	0	3	0	0.63	1	1.67	1	-0.75	-0.6	-1
9	1	3	9	22	2	11	0	3	7	11	0.22	0.5	2	3.67	1.44	4.5	0.57
10	1	0	10	3	2	0	1	0	8	3	0.2	0	2	NA	-0.7	-1	-0.63
11	2	3	11	9	3	9	1	0	8	0	0.27	1	1.5	3	-0.18	2	-1
14	3	0	14	5	4	0	0	2	10	5	0.29	0	1.33	NA	-0.64	-1	-0.5
18	5	11	18	46	8	45	0	3	10	1	0.44	0.98	1.6	4.09	1.56	4.63	-0.9
20	1	23	20	184	1	108	0	3	19	76	0.05	0.59	1	4.7	8.2	107	3
20	1	5	20	42	2	21	0	3	18	21	0.1	0.5	2	4.2	1.1	9.5	0.17
20	0	10	20	68	0	49	1	0	20	19	0	0.72	NA	4.9	2.4	NA	-0.05
22	6	4	22	13	8	11	0	3	14	2	0.36	0.85	1.33	2.75	-0.41	0.38	-0.86
22	4	3	22	44	9	39	1	0	13	5	0.41	0.89	2.25	13	1	3.33	-0.62
23	5	6	23	56	13	29	0	3	10	27	0.57	0.52	2.6	4.83	1.43	1.23	1.7
25	6	14	25	87	11	72	1	0	14	15	0.44	0.83	1.83	5.14	2.48	5.55	0.07
25	7	10	25	42	14	37	1	0	11	5	0.56	0.88	2	3.7	0.68	1.64	-0.55
26	2	4	26	17	4	9	0	3	22	8	0.15	0.53	2	2.25	-0.35	1.25	-0.64
26	6	2	26	4	12	4	0	3	14	0	0.46	1	2	2	-0.85	-0.67	-1
27	6	6	27	39	9	22	1	0	18	17	0.33	0.56	1.5	3.67	0.44	1.44	-0.06
28	1	1	28	34	2	5	1	0	26	29	0.07	0.15	2	5	0.21	1.5	0.12
28	3	2	28	35	5	7	1	0	23	28	0.18	0.2	1.67	3.5	0.25	0.4	0.22
29	9	5	29	38	18	30	0	3	11	8	0.62	0.79	2	6	0.31	0.67	-0.27
31	2	10	31	61	5	31	1	0	26	30	0.16	0.51	2.5	3.1	0.97	5.2	0.15
32	0	0	32	102	0	0	1	0	32	102	0	0	NA	NA	2.19	NA	2.19
33	4	12	33	70	6	23	1	0	27	47	0.18	0.33	1.5	1.92	1.12	2.83	0.74
37	20	11	37	72	34	45	0	3	3	27	0.92	0.63	1.7	4.09	0.95	0.32	8
38	7	9	38	60	9	44	0	3	29	16	0.24	0.73	1.29	4.89	0.58	3.89	-0.45
43	4	16	43	82	5	59	1	0	38	23	0.12	0.72	1.25	3.69	0.91	10.8	-0.39
51	7	13	51	84	12	83	0	3	39	1	0.24	0.99	1.71	6.38	0.65	5.92	-0.97
53	2	16	53	101	3	49	1	0	50	52	0.06	0.49	1.5	3.06	0.91	15.33	0.04
53	11	8	53	99	31	45	1	0	22	54	0.58	0.45	2.82	5.63	0.87	0.45	1.45
58	11	33	58	169	16	136	0	3	42	33	0.28	0.8	1.45	4.12	1.91	7.5	-0.21
60	7	28	60	168	22	117	1	0	38	51	0.37	0.7	3.14	4.18	1.8	4.32	0.34
64	6	12	64	150	14	54	1	0	50	96	0.22	0.36	2.33	4.5	1.34	2.86	0.92
65	4	7	65	56	15	15	0	3	50	41	0.23	0.27	3.75	2.14	-0.14	0	-0.18
74	9	13	74	60	22	49	0	2	52	11	0.3	0.82	2.44	3.77	-0.19	1.23	-0.79
93	11	18	93	120	20	74	1	0	73	46	0.22	0.62	1.82	4.11	0.29	2.7	-0.37
93	19	NA	93	NA	34		1	0	59	NA	0.37	NA	1.79	NA	NA	NA	NA
99	18	19	99	124	47	91	0	3	52	33	0.47	0.73	2.61	4.79	0.25	0.94	-0.37
99	11	14	99	175	23	76	1	0	76	99	0.23	0.43	2.09	5.43	0.77	2.3	0.3

Table 3.1 (continued)

Inoculum	Number of Infected Macrophages at 2 hpi	Number of Infected Macrophages at 24 hpi	Number of Cryptococci at 2 hpi	Number of Cryptococci at 24 hpi	Number of Intracellular Cryptococci at 2 hpi	Number of Intracellular Cryptococci at 24 hpi	Survival at 72 hpi	Time of Death (days)	Number of Extracellular Cryptococci at 2 hpi	Number of Extracellular Cryptococci at 24 hpi	Proportion of Cryptococci Intracellular at 2 hpi	Proportion of Cryptococci Intracellular at 24 hpi	Phagocytic Index at 2hpi	Phagocytic Index at 24 hpi	Increase in Total Numbers of Cryptococci	Increase in Intracellular Numbers of Cryptococci	Increase in Extracellular Numbers of Cryptococci
100	13	54	100	336	36	325	0	3	64	11	0.36	0.97	2.77	6.02	2.36	8.03	-0.83
105	8	18	105	109	19	98	1	0	86	11	0.18	0.9	2.38	5.44	0.04	4.16	-0.87
110	9	23	110	279	19	90	1	0	91	189	0.17	0.32	2.11	3.91	1.54	3.74	1.08
126	10	14	126	178	16	62	0	3	110	116	0.13	0.35	1.6	4.43	0.41	2.88	0.05
129	1	1	129	164	1	5	1	0	128	159	0.01	0.03	1	5	0.27	4	0.24
132	19	25	132	327	26	196	0	3	106	131	0.2	0.6	1.37	7.84	1.48	6.54	0.24
133	9	20	133	180	25	100	0	3	108	80	0.19	0.56	2.78	5	0.35	3	-0.26
148	16	31	148	292	55	239	0	2	93	53	0.37	0.82	3.44	7.71	0.97	3.35	-0.43
149	11	38	149	331	31	158	1	0	118	173	0.21	0.48	2.82	4.16	1.22	4.1	0.47
154	15	31	154	226	24	219	1	0	130	7	0.16	0.97	1.6	7.06	0.47	8.13	-0.95
166	26	73	166	607	79	523	0	3	87	84	0.48	0.86	3.04	7.16	2.66	5.62	-0.03
173	13	58	173	402	29	348	1	0	144	54	0.17	0.87	2.23	6	1.32	11	-0.63
173	13	37	173	176	38	176	1	0	135	NA		NA	2.92	4.76	0.02	3.63	NA
180	29	6	180	860	62	28	0	1	118	832	0.34	0.03	2.14	4.67	3.78	-0.55	6.05
181	13	53	181	416	35	327	0	3	146	89	0.19	0.79	2.69	6.17	1.3	8.34	-0.39
191	21	65	191	439	44	376	0	2	147	63	0.23	0.86	2.1	5.78	1.3	7.55	-0.57
202	18	63	202	463	73	443	0	3	129	20	0.36	0.96	4.06	7.03	1.29	5.07	-0.84
211	21	19	211	146	97	110	0	3	114	36	0.46	0.75	4.62	5.79	-0.31	0.13	-0.68
216	27	38	216	508	74	201	0	3	142	307	0.34	0.4	2.74	5.29	1.35	1.72	1.16
217	48	57	217	481	133	360	0	3	84	121	0.61	0.75	2.77	6.32	1.22	1.71	0.44
229	23	31	229	365	89	207	1	0	140	158	0.39	0.57	3.87	6.68	0.59	1.33	0.13
235	14	53	235	320	47	253	0	3	188	67	0.2	0.79	3.36	4.77	0.36	4.38	-0.64
245	12	24	245	326	38	159	0	2	207	167	0.16	0.49	3.17	6.63	0.33	3.18	-0.19
256	31	49	256	582	105	367	0	3	151	215	0.41	0.63	3.39	7.49	1.27	2.5	0.42
263	9	25	263	376	27	192	0	3	236	184	0.1	0.51	3	7.68	0.43	6.11	-0.22
269	22	41	269	517	83	239	0	3	186	278	0.31	0.46	3.77	5.83	0.92	1.88	0.49
273	2	3	273	2497	2	24	0	3	271	2473	0.01	0.01	1	8	8.15	11	8.13
273	44	58	273	371	135	313	0	3	138	58	0.49	0.84	3.07	5.4	0.36	1.32	-0.58
282	11	43	282	442	35	299	1	0	247	143	0.12	0.68	3.18	6.95	0.57	7.54	-0.42
290	20	20	290	413	74	113	1	0	216	300	0.26	0.27	3.7	5.65	0.42	3.03	0.39
298	24	67	298	634	76	308	0	3	222	326	0.26	0.49	3.17	4.6	1.13	0.55	0.47
300	1	24	300	1234	3	133	0	3	297	1101	0.01	0.11	3	5.54	3.11	43.33	2.71
312	34	36	312	434	134	237	0	3	178	197	0.43	0.55	3.94	6.58	0.39	0.77	0.11
317	16	41	317	457	59	258	0	3	258	199	0.19	0.56	3.69	6.29	0.44	3.37	-0.23
320	2	8	320	325	12	66	0	3	308	259	0.04	0.2	6	8.25	0.02	4.5	-0.16
323	0	4	323	73	0	5	0	3	323	68	0	0.07	NA	1.25	-0.77	NA	-0.79
323	32	90	323	773	38	447	1	0	285	326	0.12	0.58	1.19	4.97	1.39	10.76	0.14
375	3	7	375	2240	5	36	0	3	370	2204	0.01	0.02	1.67	5.14	4.97	6.2	4.96
418	6	23	418	2480	17	137	0	3	401	2343	0.04	0.06	2.83	5.96	4.93	7.06	4.84
470	42	16	470	5623	136	87	0	3	334	5536	0.29	0.02	3.24	5.44	10.96	-0.36	15.57
489	13	37	489	2398	56	266	0	3	433	2132	0.11	0.11	4.31	7.19	3.9	3.75	3.92
492	27	87	492	988	78	630	0	3	414	358	0.16	0.64	2.89	7.24	1.01	7.08	-0.14
499	8	65	499	960	28	532	0	2	471	428	0.06	0.55	3.5	8.18	0.92	18	-0.09
499	11	101	499	2594	55	863	0	3	444	1731	0.11	0.33	5	8.54	4.2	14.69	2.9
525	22	61	525	4057	62	361	0	2	463	3696	0.12	0.09	2.82	5.92	6.73	4.82	6.98
535	50	133	535	1471	211	1092	0	3	324	379	0.39	0.74	4.22	8.21	1.75	4.18	0.17
592	21	107	592	1642	56	893	0	3	536	749	0.09	0.54	2.67	8.35	1.77	14.95	0.4
618	35	56	618	981	163	481	0	3	455	500	0.26	0.49	4.66	8.59	0.59	1.95	0.1
633	23	66	633	1121	74	563	0	3	559	558	0.12	0.5	3.22	8.53	0.77	6.61	0
645	23	54	645	878	92	571	0	3	553	307	0.14	0.65	4	10.57	0.36	5.21	-0.44
750	24	NA	750	NA	101	NA	0	3	649	NA	0.13	NA	4.21	NA	NA	NA	NA
842	35	35	842	4405	190	283	0	3	652	4122	0.23	0.06	5.43	8.09	4.23	0.49	5.32
885	47	86	885	3908	151	523	0	3	734	3385	0.17	0.13	3.21	6.08	3.42	2.46	3.61

3.3 Discussion

In 2015 and 2016, three independent studies established the zebrafish embryo as a model for cryptococcal infection (Tenor *et al.*, 2015; Bojarczuk *et al.*, 2016; Davis *et al.*, 2016).

I provided a zebrafish model of *C. neoformans* infection using larvae mounted in a 96-well format for repeat imaging at day 0, 1, 2 and 3 post infection taking advantage of the zebrafish embryo's potential for high-throughput imaging and analysis. However, there are two other peer-reviewed publications reporting zebrafish-*Cryptococcus* infection models (Tenor *et al.*, 2015; Davis *et al.*, 2016). As mentioned in this thesis, the work of Tenor *et al.* was cited in my publication. The work of Davis *et al.* was not because their publication was published later than mine. It is surprising that the authors of (Davis *et al.*, 2016) did not cite my work.

One could ask how my model is better or different than of the others. Firstly, I established a model by microinjecting the pathogen at 48 hpf into the yolk sac circulation valley to produce a systemic infection. Tenor *et al.* injected at 48 hpf and into the caudal vein (Tenor *et al.*, 2015), which also produces the same effect. However my experience shows it is not possible to inject the dose they used, i.e. 10 to 20 nl (Tenor *et al.*, 2015) because the standard dose is never greater than 1 nl. Moreover, the caudal vein is too hard to inject into at 48 hpf, perhaps narrower and deeper and would require a wider needle than the ones used for bacteria. I believe this would disrupt the caudal vein. In addition, at 1 dpi many fish die from the infection (Bojarczuk, unpublished). Thus, I specifically used the circulation valley as the entry point for *Cryptococcus* and a wide needle due to cryptococcal cells being bigger in size than bacteria.

In contrast, microinjections described in (Davis *et al.*, 2016) do not provide any information about their volumes but only mention the dose of 150 and 250 cryptococcal cells per larva. Intravenous or hindbrain inoculations were performed at 28 hpf (Davis *et al.*, 2016).

However, the work of the three publications (Tenor *et al.*, 2015; Bojarczuk *et al.*, 2016; Davis *et al.*, 2016) establishes a connection among zebrafish becoming a tool to explore cryptococcosis. Studies in zebrafish have shown that ablation of

macrophages leads to high fungal burden and reduced survival (Bojarczuk et al, 2016; Tenor et al, 2015) underlining the fact that macrophages are essential for protecting zebrafish from cryptococcal disease progression. I showed it in clodronate liposomes experiment, whereas Tenor et al. by morpholino knockdown. These results corroborate the findings of others in mice (Monga, 1981; Osterholzer, Milam, et al., 2009). My work and of Tenor et al. provided validation for multiple aspects of macrophage parasitism by *C. neoformans* that have previously been characterised *in vitro*. For example, *C. neoformans* replicates intracellularly (Figure 2C in (Tenor et al., 2015) and Figure 4 in (Bojarczuk et al., 2016)) in zebrafish macrophages *in vivo* (Tenor et al., 2015; Bojarczuk et al., 2016), which is in line with previous findings *in vitro* (Ma et al., 2006; Voelz et al., 2009). I also agree with the dose-dependent mortality shown by Tenor et al. as I reported the same response with stratifications of my injections (Figure 2A in (Tenor et al., 2015) and Figure 2A in (Bojarczuk et al., 2016)). Also, Tenor et al. (2015) and I have shown that the *C. neoformans* polysaccharide capsule enlarges during infection by macrophages *in vivo* (Figures 2E-G in (Tenor et al., 2015)) and Figures 5H-J in (Bojarczuk et al., 2016)). Therefore both publications concluded that the increased capsule was sufficient to induce uncontrolled fungal growth leading to the host death. However, since I showed that intracellular proliferation is the principal factor driving the shift in the proportion of cryptococci that were intracellular at 24 hpi (Bojarczuk et al., 2016), I cannot agree with the findings that phagocytic fate of *C. neoformans* yeast cells at 13 hpi was due to phagocytosis (Tenor et al., 2015). Instead, I believe it was due to the intracellular proliferation (Bojarczuk et al., 2016).

To test the robustness of the zebrafish model for mammalian virulence determinants-infections of a number of *Cryptococcus* mutants were performed (Tenor et al., 2015). My work (Bojarczuk et al., 2016) demonstrated that infection with the *cap59* mutant resulted in zero mortality over 72 hours of infection despite using a dose that caused greater than 50% mortality in the parental H99 strain (Figure 5B). Instead, the infection with an acapsular mutant of *Cryptococcus* in (Tenor et al., 2015) resulted in 80% survival (Figure 3A) and similar fungal burden to a wild-type cryptococcal strain (Figure 3B). This highlights the role of the

capsule. It seems convincing that compromised capsule results in a similar fungal load and a high survival of the host. In this aspect, these two publications supplement each other.

The publication of Davis et al. (2016) should also be discussed. It validates previous findings that vomocytosis occurs *in vivo* (Figure 4A in (Bojarczuk *et al.*, 2016), Figure 5A in (Davis *et al.*, 2016)) and that *C. neoformans* establishes an infection in zebrafish that eventually disseminates to the brain (Figure 1I in (Davis *et al.*, 2016) and Figure 5A in (Tenor *et al.*, 2015)). This is in line what I could see in my experimental zebrafish. I never quantified this response. However, based on my observations and the findings of (Tenor *et al.*, 2015; Davis *et al.*, 2016), I believe that zebrafish can also be used to study brain invasion. The publication of Davis et al. (2016) deserves a special appreciation due to the fact of working with spores. Namely, since desiccated yeast or spores are believed to be infectious propagules (Mitchell and Perfect, 1995; Velagapudi *et al.*, 2009; Walsh *et al.*, 2019), it is dangerous to work with spores. In addition, yeast were also used as infectious particles and recognised models (Tenor *et al.*, 2015; Bojarczuk *et al.*, 2016) are most practical at using yeast cells. However, I would challenge the publication of Davis et al. (2016) in one aspect, namely it is not assuring that the findings regarding spores are truly representative of H99 virulence (serotype A) as generated spores were from serotype D strains, which are less virulent than serotype A, which was used by (Bojarczuk *et al.*, 2016) and (Tenor *et al.*, 2015). Thus, the previously described low mortality of wild-type larvae from either spores or yeast of this background, even at the highest inoculum (Figure 1B) (Davis *et al.*, 2016) is likely to result from the use of the less virulent serotype D. In contrast, yeast cells of the hyper virulent H99 (serotype A) strain killed the larvae at moderate inoculum as reported previously (Tenor *et al.*, 2015; Bojarczuk *et al.*, 2016). The publication of Davis et al. (2016) is otherwise novel, i.e. employs endothelial cells showing the lodging of *Cryptococcus* inside the brain vasculature (Figure 1I) and these cells are a temporary niche for survival (Figure 4B). It is also interesting that similarly to Tenor and colleagues, this group also investigated neutrophils role in cryptococcosis. It is surprising, given macrophages are the dominant cells engaged in the response to cryptococci (reviewed by (Mansour et al., 2014; Rudman et al., 2019)). In 2000, Marta

Feldmesser and colleagues wrote that the macrophage was the primary phagocytic cell at all times of infection in mice, but neutrophils also ingested yeast (Feldmesser *et al.*, 2000). I also showed macrophages were essential for control, as their depletion had a catastrophic effect on any restriction of fungal burden, even when neutrophil numbers were unaffected (Bojarczuk *et al.*, 2016). In fact, (Tenor *et al.*, 2015) confirmed it in zebrafish using a transient knockdown of the Spi-1 transcription factor. However, David and colleagues using IFR-8 knockout zebrafish, showed at the initial infection of the mutant that neutrophils were better killers of the pathogen at the initial infection than macrophages were (Figure 2D) (Davis *et al.*, 2016). Thus, perhaps the role of neutrophils might be undermined in the *Cryptococcus* field.

With acknowledging the work of (Tenor *et al.*, 2015; Davis *et al.*, 2016), it is my zebrafish model of cryptococcosis (Bojarczuk *et al.*, 2016) that is cited the most in comparison to the other two. Up to August 2020 it was cited 95 times, whereas (Tenor *et al.*, 2015) was cited 48 and (Davis *et al.*, 2016) 16 times. In addition, an elegant review exists, which compares all three established models and which highlights the novelty of my publication (Rosowski *et al.*, 2018).

In terms of how my work uniquely contributed to the field, the answer lies in many facts. I pioneered novel approaches to studying cryptococcosis using an experimental zebrafish model, which demonstrated for the first time how the early interactions with macrophages determined the outcome of infection. I established the model by injections facilitated by the use of Polyvinylpyrrolidone (PVP), 0.5% Phenol Red in PBS (PVP is a polymer that increases the viscosity of the injection fluid and prevents settling of microbes in the injection needle (Spaink *et al.*, 2013). This is really useful and time-saving in order to obtain very high accuracy injections with a speed of up to 300 embryos per hour in my case and the use of PVP was not described by other two groups (Tenor *et al.*, 2015; Davis *et al.*, 2016). In addition, only my method of high content imaging of the whole zebrafish allows data collection for day 0 and three consecutive days. Thus the same infections across an extended time period days can be quantified in the context of the whole organismal response. This was not described by others (Tenor *et al.*, 2015; Davis *et al.*, 2016). Next, although Tenor's group showed

intracellular proliferation *in vivo* (Figure 2C), they did not consider this event when stating that macrophages rapidly phagocytosed the majority of *C. neoformans* cells following injection (Figure 1B) (Tenor *et al.*, 2015). Cryptococcal intracellular proliferation should always be taken in consideration in the field as there is a distinct difference between completed phagocytosis and intracellular proliferation. Next, I was the first to demonstrate vomocytosis *in vivo*. Previously, this was shown indirectly in mice via flow cytometry (Nicola and Robertson, 2011). This work gave rise to a follow-up publication wherein I am the fourth author. Using my model of cryptococcosis the authors show that reducing ERK5 activity *in vivo* stimulates vomocytosis and results in reduced dissemination of infection thereby introducing ERK5 as a potential target for the future development of vomocytosis-modulating therapies (Gilbert *et al.*, 2017). In addition, my model has benefitted other projects in the Johnston lab. For example, it was used by three BMedSci students whose theses are not published and hence not cited in this paragraph. However, I can state the model was used by e.g. Richard Hotham, a co-author of (Bojarczuk *et al.*, 2016) and (Gibson *et al.*, 2018) to show dissemination of cryptococci to the swim bladder, somites and brain. It also formed a basis for work on mycophenolate mofetil (MMF). This work was further carried on by another BMedSci student, Rory Gibson and resulted in a pre-printed publication (Gibson *et al.*, 2018). The model was also used by another BmedSci student, Katherine Miller, who hypothesised that increased capsule size *in vitro* will result in an increased susceptibility to infection in zebrafish due to a decrease in rate of phagocytosis. This is published in (Bojarczuk *et al.*, 2016). The model was used by a few Johnston's PhD students, too. For instance, in her thesis, Dr Josie Gibson used it to investigate autophagy (Gibson, 2017) and in a pre-printed publication to get insight into blood vessel occlusion by *C. neoformans* (Gibson *et al.*, 2020). I am a second author of this work. Another PhD student, now Dr Hamid Fehri used my initial imaging data sets to develop automatic algorithms that can analyse different types of cells and their relations in the image to increase analysis efficiency (Fehri, 2018). External collaborations also based on my model and this resulted in publications. For instance the aforementioned publication (Gilbert *et al.*, 2017). Another example of exploiting the model is a publication on eicosanoids produced by *C.*

neoformans to support intracellular proliferation within macrophages and subsequent promotion of pathogenesis (Evans *et al.*, 2019). The model has also been optimised for high-throughput drug screening (unpublished, Christopher Donaldson, PhD student) or to mimic the mechanisms that cause this increase in intracranial pressure (unpublished, Jacqui Chalakova, PhD student).

As the research carries on not only in the Johnston lab, but worldwide it is clear the model will be used to enable new ways to diagnose, prevent or cure human disease caused by *Cryptococcus*.

Chapter 4: Characterisation of a virulence and growth defect in *Cryptococcus gattii* strain R265 with a genomic defect following GFP transformation

4.1 Introduction

Until 1949 *C. neoformans* had been considered as homogeneous species. This view changed after revealing four serotypes on the base of the antigenic properties of its polysaccharide capsule (reviewed by (Kwon-Chung and Varma, 2006)). There is an ongoing debate regarding the lineages and nomenclature of *C. neoformans*/*C. gattii* species complex mainly between the two-species concept (Kwon-Chung and Varma, 2006; Bovers *et al.*, 2008; Ngamskulrungraj, Gilgado, *et al.*, 2009; Hagen *et al.*, 2015). The genomes of *C. neoformans* and *C. gattii* are similar in 85–90% (Kavanaugh *et al.*, 2006). However, these two species are distinguishable in many ways. For instance, a morphological difference exists in basidiospores. *C. neoformans* forms rough-walled oblong to elliptical, whereas *C. gattii* produces rod shaped basidiospores with smooth walls (reviewed by (Kwon-Chung *et al.*, 2014)). In terms of metabolics, *C. neoformans* is not as efficient as *C. gattii* in the utilisation of D-amino acids ((Chang *et al.*, 2015), reviewed by (Watkins *et al.*, 2017)). However, both species have one common feature. They are both the etiologic agents of cryptococcosis. The disease results apparently from the accident inhalation of fungal cells.

4.1.1 Comparison of *C. neoformans* and *C. gattii* geographical distribution

C. neoformans and *C. gattii* present numerous differences in geographical distribution. *C. neoformans* has been mainly isolated from avian droppings, e.g. pigeons, canaries (Swinne-Desgain, 1975; Criseo *et al.*, 1995) or eagles (Caicedo *et al.*, 1999). *C. neoformans* var. *grubii* (serotype A) has a global distribution, occurring in avian excreta and some tree hollows, whereas *C. neoformans* var. *neoformans* (serotype D), also found in avian guano, prevails mainly in Europe ((Dromer, Mathoulin, Dupont and Laporte, 1996; Dromer, Mathoulin, Dupont, Letenneur, *et al.*, 1996); reviewed by (Mitchell and Perfect, 1995; Maziarz and Perfect, 2016)).

C. gattii (serotypes B and C), is endemic in tropical and subtropical regions and associated with many tree species, especially Eucalyptus trees (reviewed by (Ellis and Pfeiffer, 1990; Hagen and Boekhout, 2010; Hagen *et al.*, 2015)). However, this view has changed due to the outbreak on Vancouver Island in 1999 that represents moderate climate.

4.1.2 Comparison of *C. neoformans* and *C. gattii* infection

Comparison of *C. neoformans* and *C. gattii* infections was widely reviewed in Chapter 1. To summarise, the immune competence is a factor in cryptococcosis. *C. neoformans* mainly causes infections in profoundly immunosuppressed patients whereas *C. gattii* received attention because of devastating illness in immunocompetent individuals (reviewed by (Chen *et al.*, 2014)). A survey of (Chen *et al.*, 2000) conducted on Australians and New Zealanders during 1994–1997 identified that out of 312 episodes of cryptococcosis, *C. neoformans* caused 265 and *C. gattii* 47. *C. neoformans* was identified in 209 immunocompromised of which 133 were AIDS positive. *C. gattii* was found in 41 immunocompetent hosts. This supports the trend of *C. neoformans* being a major pathogen of the immunocompromised, especially AIDS patients and *C. gattii* of immunocompetent.

Cryptococcus is thought to enter the body through the lungs. Pulmonary disease is a primary manifestation of both species in apparently immunocompetent patients (Kerkering *et al.*, 1981; Lui *et al.*, 2006; Yang *et al.*, 2006). In the study of Australian patients between 1993 and 2000 (Jenney *et al.*, 2004) the *C. gattii* infections mostly occurred in immunocompetent patients presenting with pulmonary lesions. Another retrospective study of *C. gattii* infected patients hospitalised between 1999–2007 in British Columbia also demonstrated lung cryptococcomas in patients without HIV/AIDS (Galanis and MacDougall, 2010).

Central nervous system manifestations result from the dissemination from the lung. *C. neoformans* shows neurotropism and its major target is the central nervous system. A recent *in vitro* model of the human blood-brain barrier (BBB) of (Vu *et al.*, 2014) revealed that invasion of the CNS by *C. neoformans* requires

a secreted fungal metalloprotease. However, the trend is that *C. neoformans* targets CNS whereas *C. gattii*, the lungs. This was also confirmed in a mouse aspiration inhalation model (inhalation method). *C. neoformans*, H99 killed by brain infection while *C. gattii* by lung infection, in both BALB/C and C57BL/6 strains (Ngamskulrunroj, Chang, Sionov, *et al.*, 2012). In the study R265 wt was more virulent than H99 wt in C57BL/6 but the virulence of the strains was similar in BALB/C survival assay. Both strains manifested in high pulmonary fungal burdens. However, the lungs fungal burden was significantly higher in mice challenged with R265 wt as compared to H99 wt. Leukocyte infiltrations in the R265 wt lungs infected mice were significantly lower than in H99 wt infected lungs in both early and late time-points (Ngamskulrunroj, Chang, Sionov, *et al.*, 2012). Previous study demonstrated that *C. neoformans* did not but *C. gattii* inhibited neutrophil migration *in vitro* (Zhao Ming Dong and Murphy, 1995). Thus, it is likely that R265 wt induces a pulmonary immunosuppression. Indeed, all of the *C. gattii* strains including R265 wt triggered a less protective inflammatory response in C57BL/6 mice by suppressing neutrophil migration to the infection sites. The immune response of C57BL/6 mice to R265 wt was weak, as pro-inflammatory and protective Th1 cytokines were not produced in the lungs whereas H99 wt elicited their production. A strong inflammatory immune response might contribute to the host protection (Cheng *et al.*, 2009). However, since Th1 cytokines were measured at day 7 and 14 during infection with the prevalence of them being produced at day 7 this suggests that early Th1-type immune response might be required for protection against cryptococcosis. This data is congruent with findings of (Angkasekwina *et al.*, 2014), who also observed the same pattern of Th1 cytokines in the lungs of C57BL/6 mice measured on day 7 only. H99 wt induced a greater Th1 response than R265 wt (Angkasekwina *et al.*, 2014). This suggests that Th1-type response is needed for the clearance of the pathogen and that *C. gattii* infection dampens Th1 response, which results in the impaired ability of the host to mount protective immunity against R265 wt. Studies in mice, zebrafish and humans demonstrated some efficacy to induce anti-cryptococcal host response by administration of Th1-type cytokines (Joly *et al.*, 1994; Graybill *et al.*, 1997; Kamuyango, 2017). Treatment of both *C. neoformans* H99 wt and *C. gattii* R265 wt with Th1 cytokines activates anti-cryptococcal functions of

macrophages (Voelz *et al.*, 2009). On the other hand, Th1 response is pro-inflammatory and when exaggerated, it might be disadvantageous to the host.

Interestingly, other groups show that *C. neoformans* triggers Th2 response in mice, which is not protective (Hoag *et al.*, 1997; Chen *et al.*, 2008; Osterholzer, Surana, *et al.*, 2009; Wiesner *et al.*, 2015). Treatment with Th2 cytokines inhibits anti-cryptococcal functions of macrophages (Voelz *et al.*, 2009). Th2 response can also be detrimental to the host. For instance, IL-13, the Th2 cytokine produced during *C. neoformans* infection causes an allergic reaction presenting with lung eosinophilia, goblet cell metaplasia and elevated mucus production (Müller *et al.*, 2007). Thus, Th1/Th2 balance is essential for both cryptococci and host survival.

C. gattii recently emerged as the causative agent of cryptococcosis in otherwise healthy individuals. R265 represents the highly virulent VGIIa Vancouver Island outbreak genotype. H99 was the most intensively studied strain of *C. neoformans* worldwide. R265 and H99 strains have similar virulence in A/J mice whereas in C57BL/6 R265 is less virulent than H99 in an intranasal inoculation model (Cheng *et al.*, 2009). This is not in line with the study of (Ngamskulrungrroj, Chang, Sionov, *et al.*, 2012) in spite of the same dose used. Nevertheless, the recent research has employed KN99 (*C. neoformans*). This is due to H99 having acquired mutations of two genes that made it more virulent owing to being extensively cultured in the lab (Morrow *et al.*, 2012; Janbon *et al.*, 2014), thus not being representative of wild-type *C. neoformans*. KN99 is a mating type α , congeneric strain in the H99 genetic background (Nielsen *et al.*, 2003). KN99 behaves a lot more like the original H99. KN99 is the strain used in this present chapter.

The literature lacks R265 and KN99 alongside survival studies. Only one publication has shown prolonged survival of mice challenged with R265. However, there was 100% mortality for both strains 4 days apart (Specht *et al.*, 2017).

4.1.3 *C. gattii* R265 and hypothesis

Recently, increased attention has been drawn to *C. neoformans* sibling species, *C. gattii*. This is due to an outbreak of a fatal fungal disease caused by a highly

virulent lineage of *C. gattii*. Before 1999 *C. gattii* was never reported to cause a disease in Vancouver (Fyfe *et al.*, 2008) and was also rarely reported previously from Canada (Kwon-Chung and Bennett, 1984). In 1999 an outbreak occurred on Vancouver Island and since then has spread the Canadian mainland and into the USA causing outbreaks in otherwise healthy people. According to Centres for Disease Control and Prevention, 218 cases were reported during 1999 – 2007 in British Columbia, Canada (Galanis and MacDougall, 2010) and 96 cases between 2004–2011 in the USA Pacific Northwest (Harris *et al.*, 2011). The majority of cases in the USA come from Oregon, Washington, and California (Harris *et al.*, 2013). This means *C. gattii* has spread and expanded to temperate zones. The Vancouver Island major outbreak strain is VGIIa, and this molecular type is significantly more virulent in mice than other molecular types of *C. gattii* (Kidd *et al.*, 2004; Fraser *et al.*, 2005; Byrnes *et al.*, 2010). The *C. gattii* R265 VGIIa strain is a hyper virulent clinical isolate from the Vancouver outbreak. The outbreak has almost exclusively affected immunocompetent patients. The underlying mechanism of R265 virulence in immunocompetent individuals remains unexplained, and little is known regarding *C. gattii* growth and mechanism of infection.

I hypothesised that *C. gattii* growth assessment in the zebrafish model of cryptococcosis will reveal the cause of its virulence.

This chapter reports a systemic investigation of the virulence R265, KN99 in the zebrafish model of infection (Bojarczuk *et al.*, 2016). It is acknowledged that the model does not involve lungs but it fits with the aim of studying virulence and the early events following dissemination of cryptococci. I found that R265 was more virulent and this was confirmed in a mammalian model. To find a possible explanation of its virulence, genome sequencing and metabolic profiling were used. *C. neoformans* and *C. gattii*, aside from the differences mentioned at the beginning of this introduction, are also significantly different in their ability to utilise carbon (Bennett *et al.*, 1978) or nitrogen sources (Lee *et al.*, 2011; Ngamskulrungrroj, Chang, Roh, *et al.*, 2012). Thus, I hypothesised R265 might present with a unique metabolic profile.

4.2 Results

4.2.1 *Cryptococcus gattii* R265 infection results in decreased host survival than *C. neoformans* strain KN99 in a zebrafish model

To identify the utility of zebrafish to study *C. gattii* virulence, *C. gattii* R265 and *C. neoformans* KN99 were compared side by side. Following injection of 48 hpf zebrafish larvae with 1000 cfu of R265 wt or KN99 wt strains, R265 wt infection resulted in 11.1 % survival (Figure 4.1). In contrast, the survival was >6 fold higher for larvae injected with KN99 wt (66.7%; Figure 4.1). This delivered significantly different results as compared to studies in mice, wherein the survival curves for KN99 wt and R265 wt were nearly identical (Specht *et al.*, 2017).

Phagocyte-*Cryptococcus* interactions are important to investigate disease progression. To facilitate methods for assaying virulence, a GFP version of R265 was needed and has been previously described. *In vitro*, R265 GFP14 showed no difference in growth in rich media, under stress conditions and in macrophages compared to the parental strain (Voelz *et al.*, 2010). However, there are no reports of using it *in vivo*. To determine whether the GFP insertion had an effect on virulence, *nacre* zebrafish larvae were injected in the same manner as in the survival assay between KN99 wt and R65 wt. The injection of *C. gattii* R265 wt resulted in 23.3% survival. In contrast, the survival was >3 fold higher for larvae injected with GFP-tagged *C. gattii* R265 GFP14 and was 76.7% (Figure 4.2).

The unexpected finding signalled the need for additional studies regarding KN99 wt and KN99 GFP in order to find out whether GFP insertion influenced its virulence. No previous research has investigated KN99 GFP and KN99 wt alongside in survival assays *in vivo*. Therefore, several studies have almost exclusively focused on either KN99 wt (Nielsen *et al.*, 2003) or KN99 GFP (Gibson *et al.*, 2018). The direct comparison revealed there was no significant difference between KN99 wt and KN99 GFP (Figure 4.3). Both strains resulted in the same survival rate of 66.7%.

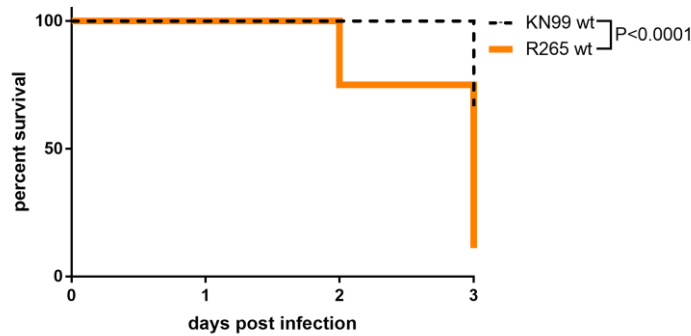


Figure 4.1 Survival of *nacre* zebrafish larvae at 3 dpi is increased with *C. neoformans* KN99 wt as compared to *C. gattii* R265 wt. injected. Zebrafish injected with with 1000 cfu of R265 wt or KN99 wt in 10% PVP, 0.5% phenol red in PBS. R265 wt is more virulent than KN99 wt. P value calculated using Log-Rank Mantel-Cox test; n=12 larvae per group in 3 independent experiments.

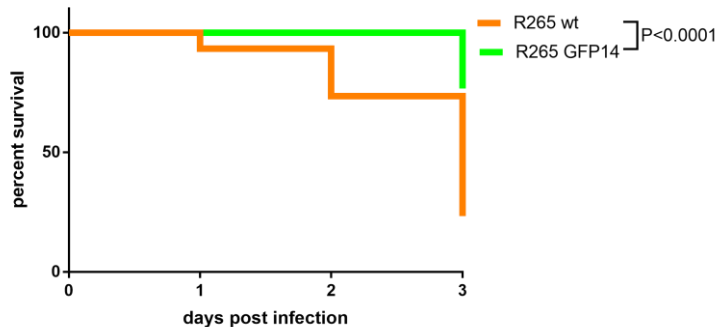


Figure 4.2 Survival of *nacre* zebrafish larvae at 3 dpi is increased with *C. gattii* R265 GFP14 strain as compared to *C. gattii* R265 wt. Zebrafish injected with 1000 cfu of R265 GFP14 or R265 wt in 10% PVP, 0.5% phenol red in PBS. P value calculated using Log-Rank Mantel-Cox test; n=10 larvae per group in 3 independent experiments

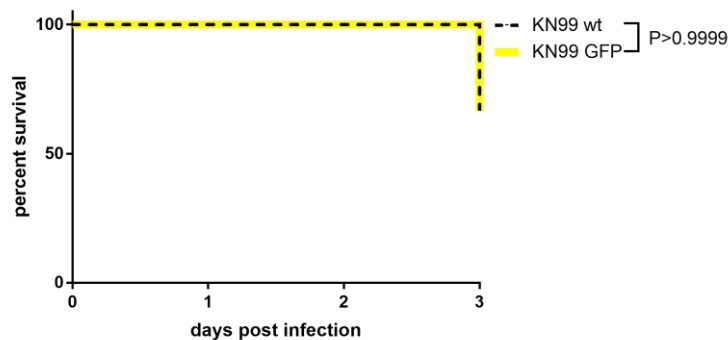


Figure 4.3 Survival of *nacre* zebrafish larvae at 3 dpi injected with *C. neoformans* KN99 wt or KN99 GFP strains is identical. Zebrafish injected with 1000 cfu of KN99 wt or KN99 GFP in 10% PVP, 0.5% phenol red in PBS. KN99 wt and KN99 GFP are equally virulent. P values were calculated using Log-Rank Mantel-Cox test; n=12 larvae per group in 3 independent experiments

The analysis of zebrafish survival led to the following conclusions: 1) R265 wt was more virulent than KN99 wt; 2) GFP insertion to KN99 did not have an effect on virulence when compared to KN99 wt 3) GFP insertion to R265 had an effect on virulence as R265 GFP was attenuated when compared to its isogenic strain R265 wt.

4.2.2 R265 GFP14 is avirulent in C57BL/6 mice

Next, to determine whether R265 GFP14 was attenuated in a mammalian host, C57BL/6 mice were utilised in the intranasal model of infection. Mice survival assay revealed that animals infected with R265 GFP14 had 100% survival (Figure 4.4). In contrast, all mice challenged with R265 wt succumbed by 20 dpf. The survival of mice infected with R265 wt was in line with previous studies (Upadhyya *et al.*, 2016).

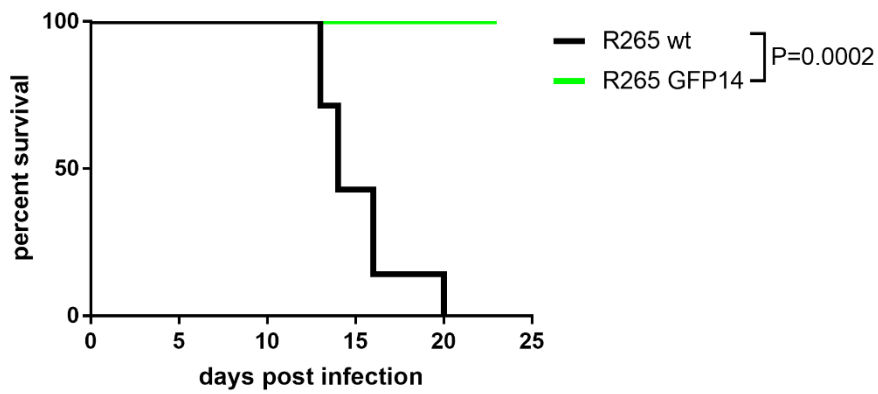


Figure 4.4 Survival of C57BL/6 mice infected with R265 GFP14 is 100%. 6-8 weeks old female mice infected intranasally with R265 wt or R265 GFP14. Inoculum 5×10^4 in $50 \mu\text{l}$ PBS; $P=0.0002$; Log-Rank Mantel-Cox; 7 female mice were used per group.

1

¹ The work was done with the help of Carl Wright and Jessica Willis, research technicians at BSU and Jacob Rudman, a PhD student in the Johnston lab, The University of Sheffield

4.2.3 R265 GFP14 has lost six genes deleted during generation of the GFP-tagged derivative of R265

From the results obtained in both larval zebrafish and murine models, it was clear that fluorescent *C. gattii* strain had impaired pathogenesis. It was therefore hypothesised that GFP randomly inserted into R265 strain (Voelz *et al.*, 2010) caused changes in the R265 parental strain genome which would be indicative to some degree as to why R265 GFP14-infected mice and zebrafish larvae showed a high survival rate. R265 wt and R265 GFP14 were whole genome sequenced (Farrer *et al.*, 2016) but their sequences were not compared in this study. Therefore, R265 wt and R265 GFP14 were compared for differences that might explain altered virulence seen for R265 GFP14. The sequencing revealed that R265 GFP14 appeared to have a region deleted in chromosome 1 before WM276 genome position (22116-30690) and R265 wt (32307-42262). This is equivalent to 32 kb deletion when R265 GFP14 and R265 wt reads were mapped to the R265 wt assembly. This resulted in the loss of six genes: CGB_A0010C, CGB_A0020C, CGB_A0030W, CGB_A0040C, CGB_A0050W and CGB_A0060W (Figure 4.5). All of them have been found in *C. gattii* reference strain WM276 (D'Souza *et al.*, 2011). Following sequencing, the next step must be to assign functions to the identified genes.

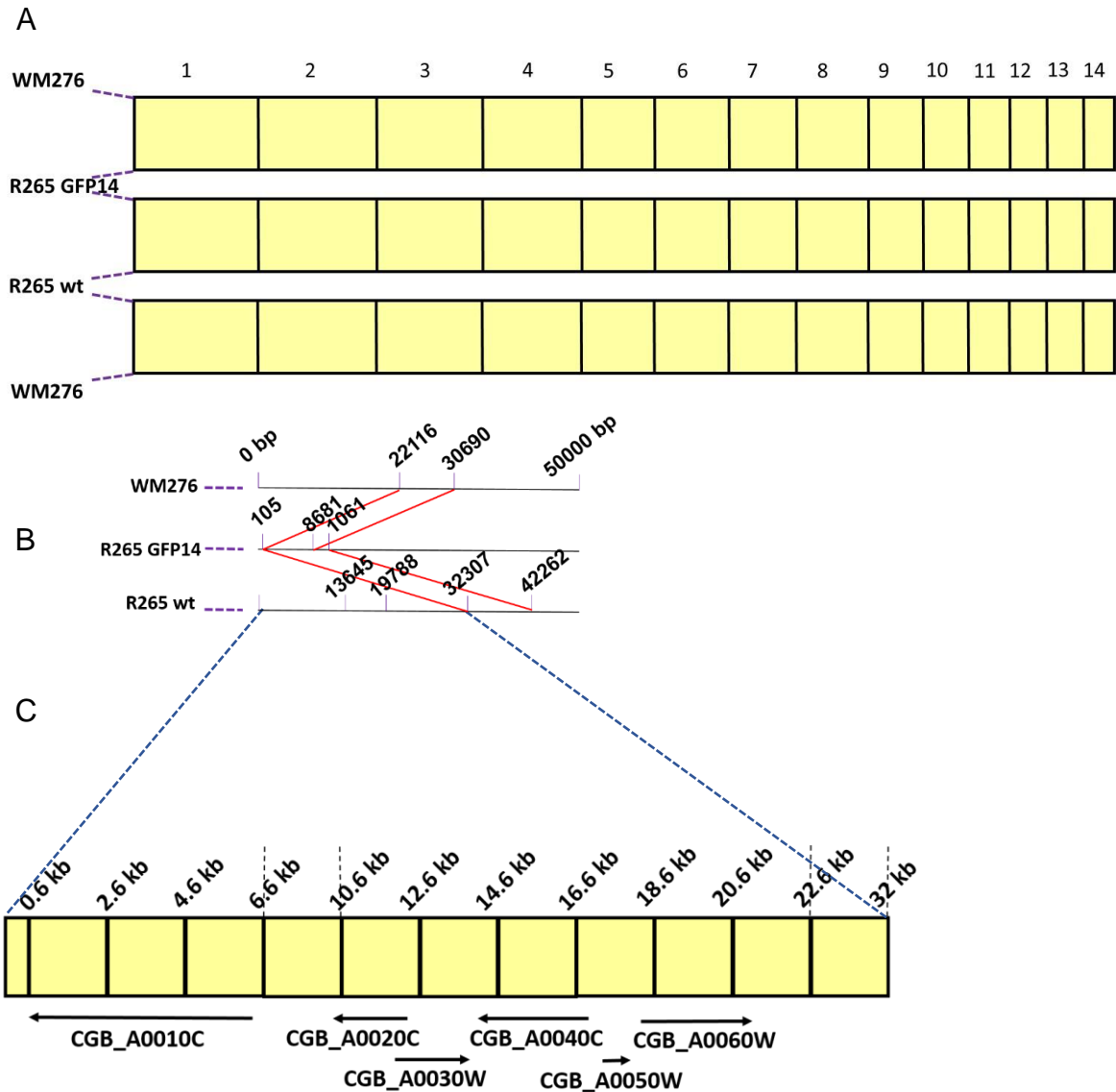


Figure 4.5 Diagrammatic representation of genome sequencing differences between *C. gattii* strains R265 wt and R265 GFP14. (A) The R265 wt and R265 GFP14 assemblies comparison to a reference genome *C. gattii* WM276 with the chromosomes concatenated together. **(B)** Alignment of contig 1 from *C. gattii* strains, WM276, R265 wt and R265 GFP14. **(C)** The missing region of R265 GFP14 but present in R265 wt is equivalent to ~32 kb. The black dashed lines indicate a different kb scale of 4 kb or 10 kb.

2

² Analysed with Dr Roy Chaudhuri in the Department of Molecular Biology and Biotechnology, The University of Sheffield

4.2.4 *In silico* analysis of function of six genes deleted during generation of the GFP-tagged derivative of R265

An obvious question arose: What are the functions of the deleted genes? Below the genes are characterised according to the available literature and Kyoto Encyclopedia of Genes and Genomes (KEGG) and a brief description of genes deleted in R265 GFP14 is shown in Table 4.1.

CGB_A0010C xenobiotic-transporting ATPase, putative

KEGG; (Kanehisaa and Goto, 2000; Kanehisa, 2019; Kanehisa *et al.*, 2019)) describes xenobiotic-transporting ATPase protein as an enzyme that catalyses the translocation of other compounds according to the following scheme: $\text{ATP} + \text{H}_2\text{O} + \text{xenobiotic}[\text{side 1}] = \text{ADP} + \text{phosphate} + \text{xenobiotic}[\text{side 2}]$. It is an ABC-type (ATP-binding cassette) xenobiotic transporter (KEGG). ABC transporters have ATP-binding cassettes which power the transporter by binding and hydrolysing ATP (reviewed by (Davidson and Chen, 2004)). The ATP-binding cassette (ABC) transporters are a family of transporter proteins that are responsible for drug resistance by pumping a variety of drugs out of the cytoplasm at the expense of ATP hydrolysis (reviewed by (Choi, 2005)). Since exporter-type ABC transporters are expressed in all species and importer-like are found in prokaryotes only (reviewed by (Locher, 2009)) it is plausible that *C. gattii* converts the energy gained from ATP hydrolysis into trans-bilayer movement of substrates out of the cytoplasm.

CGB_A0020C glucose 1-dehydrogenase, putative

Glucose 1-dehydrogenase performs reaction: $\text{D-glucose} + \text{NAD(P)}^+ = \text{D-glucono-1,5-lactone} + \text{NAD(P)H} + \text{H}^+$. This enzyme has similar activity with either NAD^+ or NADP^+ . It participates in the pentose pathway (KEGG).

CGB_A0030W racemase, putative

Racemase changes the L into D or S into R conformation of amino acids (KEGG) thus enabling their use in different metabolic pathways.

CGB_A0040C rhamnosidase B, putative

Rhamnosidase B performs hydrolysis of terminal, non-reducing beta-L-rhamnose residues in beta-L-rhamnosides. Since *C. neoformans* grows on L-rhamnose (Schmeding *et al.*, 1984), it is suggested that this enzyme is involved in rhamnose utilisation.

CGB_A0050W hypothetical protein CNB05730 is not characterised.

CGB_A0060W hypothetical protein CNB05720-only information about predicted domains exist.

Virulence is of the greatest importance for the survival of the pathogen within a host. The term “hyper virulent” often describes a strain that exhibits a significant increase in virulence compared to either the parental wild-type strain or related strains within the same species (reviewed by (Bliven and Maurelli, 2012)). R265 wt is such a strain. While investigating a strain virulence, gene loss and resulting phenotypes related to the virulence are very often studied. A question arises-how the gene/genes loss could impact R265 GFP14 virulence *in vivo*? Thus, the critical issue really is to pay attention to *Cryptococcus* expression profiles under various conditions. For instance, Fan *et al.* observed that genes encoding membrane transporters for nutrients, general metabolism, and oxidative stress response were upregulated in the presence of macrophages (Fan *et al.*, 2005). A recent publication of Farrer and colleagues also paid attention to expression profiles of *C. gattii* *in vitro* without macrophages and *ex vivo* post co-incubation with BMDMs. Transcriptome sequencing revealed that lineage VGII, to which R265 wt belongs, is transcriptionally divergent from non-VGII lineage. Moreover, the total number of differentially expressed gene changed (either up- or downregulation) for isolates *ex vivo* but not *in vitro*. One of the genes upregulated *ex vivo* was ABC transporter gene CNBG_4708, an ortholog in *C. gattii* R265 to a gene of known function in *C. neoformans* H99 (Farrer *et al.*, 2018). Interestingly, one of the genes deleted in R265 GFP14 is CGB_A0010C with conserved ABC domain. This suggests that although the exact function of this deleted gene remains unknown, it is possible that it has a role in cryptococcal virulence. However, in comparison to the parental strain R265 wt, it is known that

R265 GFP14 does not have a different ability to grow in macrophages even though it has lost its genes (Voelz *et al.*, 2010). Only, when *in vivo* the virulence of R265 GFP14 changed and in the current study this strain is attenuated in zebrafish and mice when compared to R265 wt.

It is also interesting to note that phenome-based functional analysis of the *C. neoformans* transcription factor (TF) mutant library showed differences in virulence *in vitro* versus *in vivo*. Specifically, there are genes whose deletions cause, for example, reduced virulence in mice and at the same time enhanced virulence *in vitro* in YPD at 30°C or 37°C in the means of growth, differentiation, stress responses, antifungal resistance and virulence-factor production (Jung *et al.*, 2015). This may explain some genes loss could impact virulence *in vivo*. However, this might also relate to thermotolerance, which is discussed in section 4.3.1 Temperature and thermotolerance. The same suggestion appeared in (Yang *et al.*, 2017), which referred to the study of (Jung *et al.*, 2015). Indeed, CNB05770 encoding xenobiotic-transporting ATPase in *C. neoformans* var. *neoformans* JEC21 (Loftus *et al.*, 2005), an ortholog of CGB_A0010C deleted in R265 GFP14, is induced at 37°C *in vitro* in YPD suggesting that a conserved transcriptional program is used by the fungus to alter gene expression during stressful conditions (Kraus *et al.*, 2004). By contrast, CNAG_04096 encoding racemase in *C. neoformans* var. *grubii* H99, a gene deleted in R265 GFP14, is repressed *in vitro* after internalisation by phagocytic cells (Derengowski *et al.*, 2013). CNAG_02587 encoding rhamnosidase in *C. neoformans* var. *grubii* H99 (NCBI server), which is deleted in R265 GFP14, is also downregulated *in vitro* at 37 °C in YPD (Kmetzsch *et al.*, 2011).

These findings further support the idea of changing gene expression levels under various conditions. This phenomenon is seen in other pathogenic fungi, e.g. *Aspergillus fumigatus* or *C. albicans*. Virulence associated genes are expressed at significantly higher levels during invasive infection than *in vitro* for *A. fumigatus* (Gravelat *et al.*, 2008). As for *C. albicans*, differences between *in vivo* biofilm expression data and previously reported from *in vitro* models, including alterations in metabolism and carbohydrate processing, could be due to the continuous availability of nutrients from host serum and the incorporation of the host-pathogen interaction (Nett *et al.*, 2011).

This cast a new light on the fluorescent *C. gattii* strain. R265 GFP14 was attenuated *in vivo*, in both zebrafish and mice, possibly due to the loss of six genes deleted during generation of the GFP-bearing transgenic *C. gattii*. This mutation in the R265 GFP14 caused by GFP insertion was not only specific to fish pathogenesis, but also to mice. This suggested that these six genes were important for *in vivo* virulence in both animal models, independent of the growth conditions previously tested (Voelz *et al.*, 2010). Therefore, the GFP strain was currently further analysed in order to determine how it was attenuated.

Table 4.1 List of genes deleted in R265 GFP14

gene ID	description	conserved domains
CGB_A0010C	xenobiotic-transporting ATPase, putative	1. ABCG_PDR_domain2; Second domain of the pleiotropic drug resistance-like (PDR) subfamily G of ATP-binding cassette transporters 2. ABCG_PDR_domain1; First domain of the pleiotropic drug resistance-like subfamily G of ATP-binding cassette transporters 3. 3a01205; Pleiotropic Drug Resistance (PDR) Family protein 4. ABC2_membrane; ABC-2 type transporter 5. PDR_CDR; CDR ABC transporter 6. ABC_trans_N; ABC-transporter extracellular N-terminal
CGB_A0020C	glucose 1-dehydrogenase, putative	1. abG; 3-ketoacyl-(acyl-carrier-protein) reductase; Validated 2. NADB_Rossmann; Rossmann-fold NAD(P)(+)-binding proteins
CGB_A0030W	racemase, putative	1. RK15440; L-rhamnonate dehydratase; provisional 2. MR_like_2; Mandelate racemase (MR)-like subfamily of the enolase superfamily, subgroup 2.
CGB_A0040C	rhamnosidase B, putative	1. Bac_rhamnosid; Bacterial alpha-L-rhamnosidase 2. Bac_rhamnosid_N; Alpha-L-rhamnosidase N-terminal domain
CGB_A0050W	hypothetical protein CNB05730 uncharacterised protein	not indicated on NCBI
CGB_A0060W	hypothetical protein CNB05720 uncharacterised protein	1. Zn_clus; Fungal Zn(2)-Cys(6) binuclear cluster domain 2. fungal_TF_MHR; fungal transcription factor regulatory middle homology region

Information from National Centre for Biotechnology Information (NCBI server).

4.2.5 *C. gattii* R265 GFP14 does not grow in the zebrafish

A previously developed zebrafish model of cryptococcosis (Bojarczuk *et al.*, 2016) was used to determine how the transgenic R265 GFP14 cryptococcal cells were attenuated in zebrafish, as suggested in survival assays. My zebrafish model of cryptococcosis (Bojarczuk *et al.*, 2016) provided a highly tractable system to study cryptococcal interactions with the innate immune cells such as macrophages.

Tg(mpeg1:mCherryCAAX)^{sh378} (Bojarczuk *et al.*, 2016) (expressing fluorescent marker mCherry under the control of the macrophage-specific *mpeg1* promoter) zebrafish larvae were injected at 48 hpf with 100 cfu of R265 GFP14 strain into the yolk sac circulation valley (Figure 2.5).

It was hypothesised that the observed extended survival in zebrafish challenged with R265 GFP14 was due to macrophages efficiently phagocytosing the pathogen followed by intramacrophage killing of cryptococci (and further possibilities discussed below).

R265 GFP14 did not grow in any of the analysed infected zebrafish (Figure 4.6).

In order to gain an insight into a complex process of phagocytosis, the intracellular and extracellular numbers were measured (Figure 4.7).

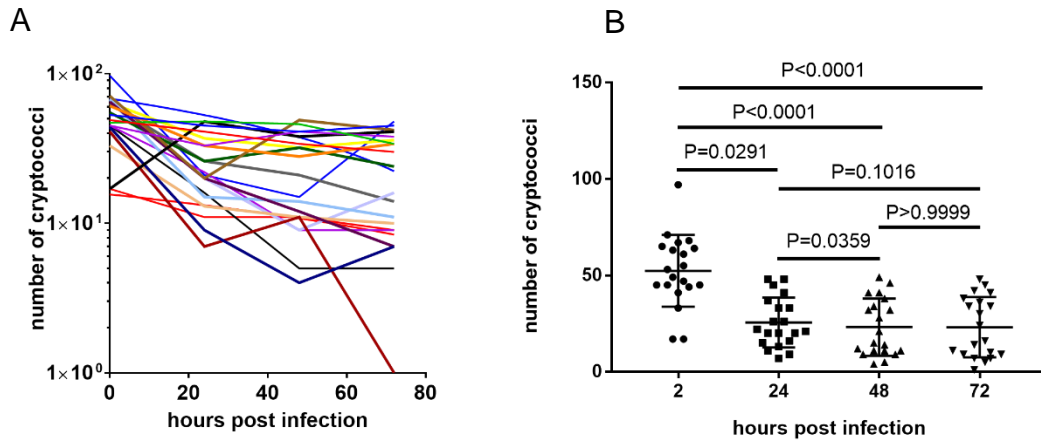


Figure 4.6 R265 GFP14 does not grow in any of the analysed infected zebrafish. (A) Progression of infection within individual zebrafish infected with 100 cfu of R265 GFP14. Cryptococci injected in 10% PVP, 0.5% phenol red in PBS into 48 hpf *Tg(mpeg1:mCherryCAAX)^{sh378}* zebrafish larvae.; n=20 per group in 3 independent experiments; in each repeat 7, 6 and 7 larvae were used. Data presented as connecting lines only. (B) The number of R265 GFP14 cryptococci decreases over time. R265 GFP14 injected in 10% PVP, 0.5% phenol red in PBS into 2 dpf (48 hpf) *Tg(mpeg1:mCherryCAAX)^{sh378}* zebrafish larvae. P values presented as One-way ANOVA (and nonparametric) in Friedman test with Dunn's multiple comparisons; data presented as connecting lines (A) and dot plot with mean \pm standard deviation (B).

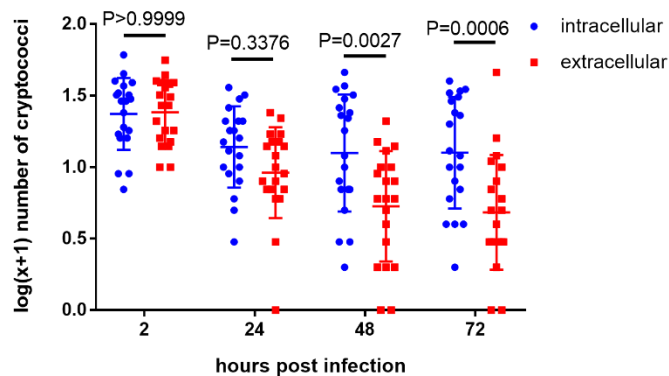


Figure 4.7 The number of extracellular cryptococci is lower than the number of intracellular cryptococci at 48 and 72 hpi. Due to nonparametric distribution of intra- and extracellular numbers of cryptococci, the data was $\log_{10}(x+1)$ transformed. This allowed for two-way ANOVA analysis. The number of extracellular cryptococci is lower than the number of intracellular cryptococci at 48 and 72 hpi. R265 GFP14 injected in 10% PVP, 0.5% phenol red in PBS into 2 dpf (48 hpf) *Tg(mpeg1:mCherryCAAX)^{sh378}* zebrafish larvae; n=20 per group in 3 independent experiments; in each repeat 7, 6 and 7 larvae were used. P values presented as RM two-way ANOVA with Sidak's post-test; data presented as interleaved scatter plot with mean \pm standard deviation.

The results led to the conclusion that the number of extracellular cryptococci at 48 and 72 hpi was lower than the number of intracellular cryptococci at these time-points. The applicability of these new results were then tested separately to investigate the changes in each portion of cryptococci between the experimental time-points.

First, the number of intracellular cryptococci was plotted (Figure 4.8). There were no significant differences between the experimental time-points.

The number of extracellular cryptococci declined over time with significant differences at 48 and 72 hpi as compared to 2 hpi ($P < 0.0001$ at both time-points) (perhaps phagocytosed and killed) (Figure 4.9).

Next, the effectiveness of macrophages during phagocytosis was investigated. This was achieved by calculating the percentage of phagocytosed cryptococci, the number of infected macrophages and phagocytic index.

The percentage of phagocytosed cryptococci was obtained as the number of intracellular (engulfed) cryptococci divided by the total number of cryptococci at a given time-point (Figure 4.10). It should be noted, that the phagocytosis percentage can apply only to the first time-point. After this time-point, phagocytosis might represent different cryptococcal fates, e.g. vomocytosis, growth within macrophages. Thus, phagocytosis at time-points other than the first one is described as the percentage proportion of intracellular cryptococci. The highest proportion of intracellular cryptococci engulfed by macrophages occurred at 72 hpi (Figure 4.10, $P=0.0045$). The last time-point was surprisingly significant considering only 50% of internalised cryptococci at 2 hpi. This suggested a small increase in the proportion of intracellular cryptococci over time. It also highlighted that little is known about the R265 GFP14 capsule. The capsule is the most important virulence factor of *C. neoformans* and it prevents phagocytosis (see Discussion section 4.3.3.3 *C. gattii* R265 GFP14 does not grow in the zebrafish).

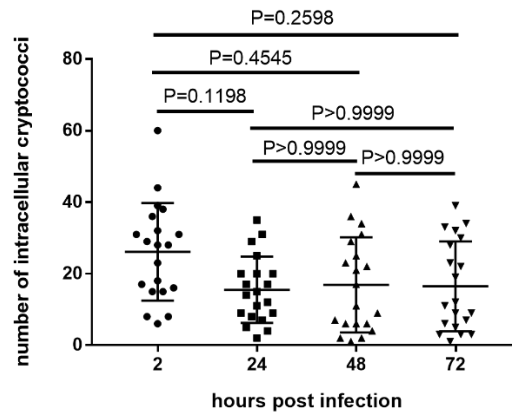


Figure 4.8 The number of intracellular cryptococci does not change throughout the course of infection. R265 GFP14 injected in 10% PVP, 0.5% phenol red in PBS into 2 dpf (48 hpf) *Tg(mpeg1:mCherryCAAX)^{sh378}* zebrafish larvae; n=20 per group in 3 independent experiments; in each repeat 7, 6 and 7 larvae were used. P values presented as One-way ANOVA (and nonparametric) in Friedman test with Dunn's multiple comparisons; data presented as scatter plot with mean \pm standard deviation.

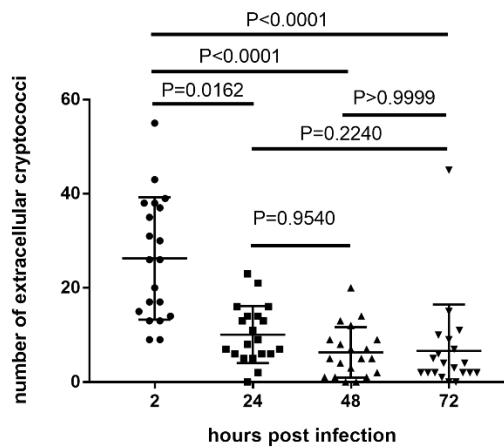


Figure 4.9 The number of extracellular cryptococci declines over the time of infection. R265 GFP14 injected in 10% PVP, 0.5% phenol red in PBS into 2 dpf (48 hpf) *Tg(mpeg1:mCherryCAAX)^{sh378}* zebrafish larvae. n=20 per group in 3 independent experiments; in each repeat 7, 6 and 7 larvae were used. P values presented as One-way ANOVA (and nonparametric) in Friedman test with Dunn's multiple comparisons; data presented as scatter plot with mean \pm standard deviation.

To investigate whether the percentage proportion of intracellular cryptococci is due to a greater number of macrophages phagocytosing R265 GFP14, the number of infected macrophages was calculated (Figure 4.11). No significant differences were found throughout the experiment. This suggests that the rate of cryptococci engulfment by macrophages is steady over the course of infection.

To investigate how many cryptococci there were per macrophage, the phagocytic index (PI) was calculated. The rate of phagocytosis defined as the ingestion of particular number of cryptococci by one macrophage (but not phagocytosis expressed as the percentage proportion of intracellular cryptococci) was similar between time-points with the exception of 48 hpi. At 2 hpi, PI appears to be non-significantly higher than all other time-points, but it is significantly higher than 48 hpi ($P=0.0036$) (Figure 4.12). There is not much difference overall and this small trend might be expected as more free cryptococcal cells would be present in the zebrafish at earlier time-points. Over time more was phagocytosed (Figure 4.10), and since some will survive within the macrophages and some will be killed the PI appears relatively constant.

Collectively, the results appeared to suggest a distinctive course of infection. To present this interesting case, a model of R265 GFP14 infection progression was proposed (Figure 4.38, see Discussion section 4.3.3.3 C. *gattii* R265 GFP14 does not grow in the zebrafish).

So far, the above results revealed that a transgenic insertion mutant of the VIO type strain R265 GFP14 was attenuated both in zebrafish and in mice. A deletion equivalent to 32 kb was identified in the GFP genome, which might be associated with better fish and mice survival as compared with its isogenic R265 wt. Given the involvement of the six genes deleted in the GFP strain, in metabolite related processes, it was hypothesised that R265 GFP14 had an altered ability to adapt to the host environment.

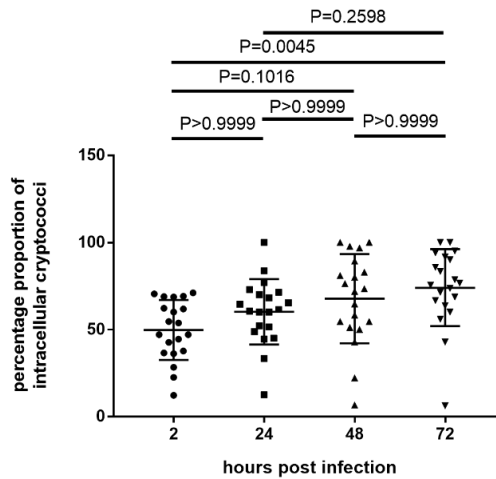


Figure 4.10 The percentage proportion of intracellular R265 GFP14 cryptococci is the greatest at 72 hpi. R265 GFP14 injected in 10% PVP, 0.5% phenol red in PBS into 2 dpf (48 hpf) *Tg(mpeg1:mCherryCAAX)^{sh378}* zebrafish larvae n=20 per group in 3 independent experiments; in each repeat 7, 6 and 7 larvae were used. P values presented as One-way ANOVA (and nonparametric) in Friedman test with Dunn's multiple comparisons; data presented as scatter plot with mean \pm standard deviation.

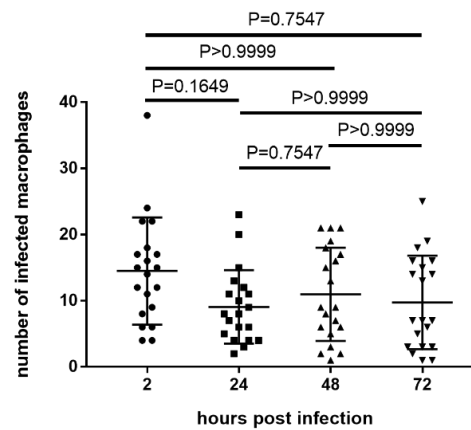


Figure 4.11 The number of infected macrophages does not change over the course of infection. R265 GFP14 injected in 10% PVP, 0.5% phenol red in PBS into 2 dpf (48 hpf) *Tg(mpeg1:mCherryCAAX)^{sh378}* zebrafish larvae n=20 per group in 3 independent experiments; in each repeat 7, 6 and 7 larvae were used. P values presented as One-way ANOVA (and nonparametric) in Friedman test with Dunn's multiple comparisons; data presented as scatter plot with mean \pm standard deviation.

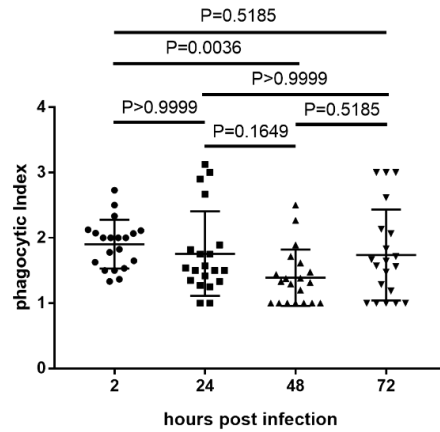


Figure 4.12 Phagocytic index (PI) is relatively constant throughout the course of infection. R265 GFP14 injected in 10% PVP, 0.5% phenol red in PBS into 2 dpf (48 hpf) *Tg(mpeg1:mCherryCAAX)^{sh378}* zebrafish larvae; n=20 fish in total from 3 repeats. P values presented as One-way ANOVA (and nonparametric) in Friedman test with Dunn's multiple comparisons; data presented as scatter plot with mean \pm standard deviation.

4.2.6 R265 GFP14 shows a growth deficit in the minimal medium

Based on the hypothesis that R265 GFP14 had a decreased ability to adapt to the host environment, it was predicted that the fungus would show a growth deficit. Therefore, its growth in rich and minimal media was measured. The rich medium was YPD, commonly used in laboratories for *Cryptococcus* cultivation. This rich medium contains 1% yeast extract, 2% peptone and 2% glucose (Ngamskulrungrroj, Himmelreich, *et al.*, 2009) in distilled water. The minimal medium is also made up in distilled water and contains potassium phosphate monobasic, magnesium sulphate, glycine, thymine and glucose with the sugar contribution at 0.27% (Zaragoza *et al.*, 2010). The minimal medium does not inhibit *C. neoformans* growth *in vitro* (Araujo *et al.*, 2012). Assuming an altered ability to the environment, it was hypothesised that these two *C. gattii* strains would grow at different rates. It was predicted that R265 GFP14 would exhibit lower growth rate in the minimal medium, which supplies less nutrients than the rich one, although still containing glucose as the sole source of carbon. The experiment was initially designed to grow cryptococci for 24 hours following the common procedure. However, due to not observing any changes after this time period, it was decided to grow the cultures for 48 hours. The R265 GFP14 strain had a deficit in growth in the minimal media in comparison to R265 wt (Figure 4.13). The result suggested the possibility of similar conditions *in vivo* in zebrafish larvae. Therefore, a growth deficit in the minimal media potentially represented attenuation *in vivo*. The implication of this finding was that R265 GFP14 might have metabolic defects resulting from the loss of the aforementioned six genes deleted during random genomic integration of GFP construct. However, it should be mentioned, that the findings from Figure 4.13 are subject to at least two limitations. First, due to growing the strains as separate cultures and not knowing their initial concentrations, it was not possible to plot the data on the same graph: day 0- two cultures of R265 wt and two of R265 GFP14 were set up, day 1- two R265 wt samples were mixed with each other and the same applied to two R265 GFP14 mixed with each other to obtain the required concentration of cells, day 2- the samples were counted in 1ml of PBS but no difference was observed. Therefore, the cells were grown for one more day and on day 3, counts were

plotted on two separate graphs, representing either R265 wt R265 GFP14 counts in rich and minimal media. In retrospect, a protocol refinement would be that on day 1, the three samples should be made at the same concentration. The growth data could then be plotted on the same graph and this would answer whether the isogenic strain grows equally well in YPD/ minimal media.

It seems the second limitation might be the use of haemocytometer, where there is the possibility that dead cells are counted. Some researchers use OD instead when counting *Cryptococcus* (Bielska *et al.*, 2018; Maurya *et al.*, 2018). However, this technique also has limitations, e.g. spectrophotometers with different optical configurations give different OD values for the same culture.

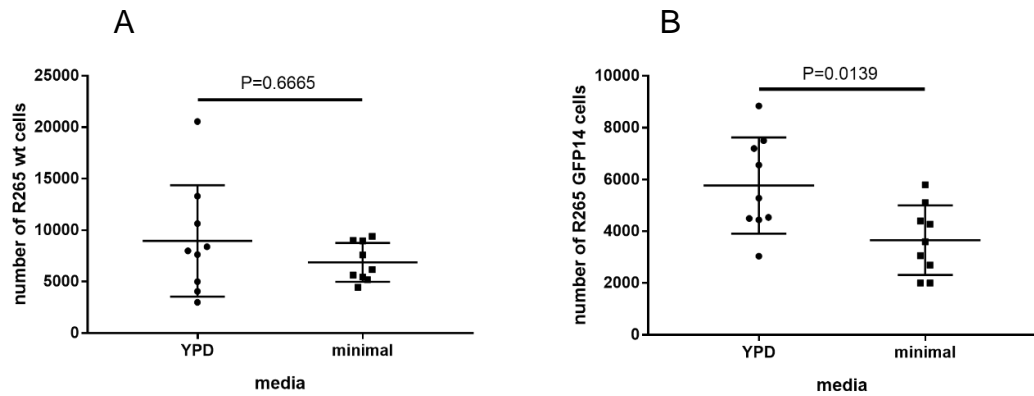


Figure 4.13 The R265 GFP14 strain had a deficit in growth in the minimal media in comparison to R265 wt. Neither YPD nor minimal medium has an effect on R265 wt (**A**) while R265 GFP14 has a significant deficit in growth in minimal media *in vitro* (**B**). The number of cells counted at 48 hours post inoculation; n=9 per group in 3 independent experiments. P values presented are Mann-Whitney test; data presented as scatter plot with mean \pm standard deviation.

4.2.7 *C. gattii* R265 GFP14 exhibits different use of carbon sources

R265 GFP14 showed a difference when cultured in YPD and minimal media. To investigate differences in the cellular metabolic pathway(s) and identify differences between the R265 GFP14 and R265 wt, a phenotypic metabolic profiling approach (Bochner *et al.*, 2011) was adapted. It is important to understand which metabolic pathways are activated or deficient and could potentially be manipulated to achieve anti-cryptococcal protection. For characterisation of potential carbon substrates utilisation and identification of the specific differences in substrates metabolism, cryptococcal cells were tested in an OmniLog™ Phenotype Microarray system. 96-well phenotype microarray plates (PM1, Technopath) were used. This technology enables the unveiling of new functions of genes by concurrently testing mutants for a large number of phenotypes (Bochner *et al.*, 2001; Bochner, 2003). The protocol was done as described previously (Zhou *et al.*, 2003; Nielsen *et al.*, 2005). This was the first time PM1 metabolic panel was performed in *C. gattii*. Due to protocol optimisation, a large number of experiments were excluded from the analysis. Thus, only two were selected and considered preliminary.

PM1 array is a novel screening approach to identify substrates that had significantly different NADH production in the R265 GFP14 compared to R265 wt. PM1 set is a 96 well plate assay with each well containing either R265 wt or R265 GFP14 and a different metabolite serving as a source of carbon. This experimental design allows for testing a unique phenotype or cell function. The analysis allows strain phenotypes to be quantitatively measured over a 36 hour time period based on colour change in each well. Cryptococcal cells are combined with a tetrazolium dye that absorbs electrons produced by yeast cell respiration. Reduction of the tetrazolium dye D yields a purple colour. The colour reaction indicates that the inoculated cells are actively metabolising a substrate in the well, producing NADH, while the lack of colour change implies that the cells are not able to utilise the substrate. Representative images of dye D colour changes with R265 wt and R265 GFP14 after 36 hours of incubation for two repeats are presented in Figure 4.14. Representative images of kinetic traces

with R265 wt and R265 GFP14 after 36 hours of incubation are presented in Figure 4.15.

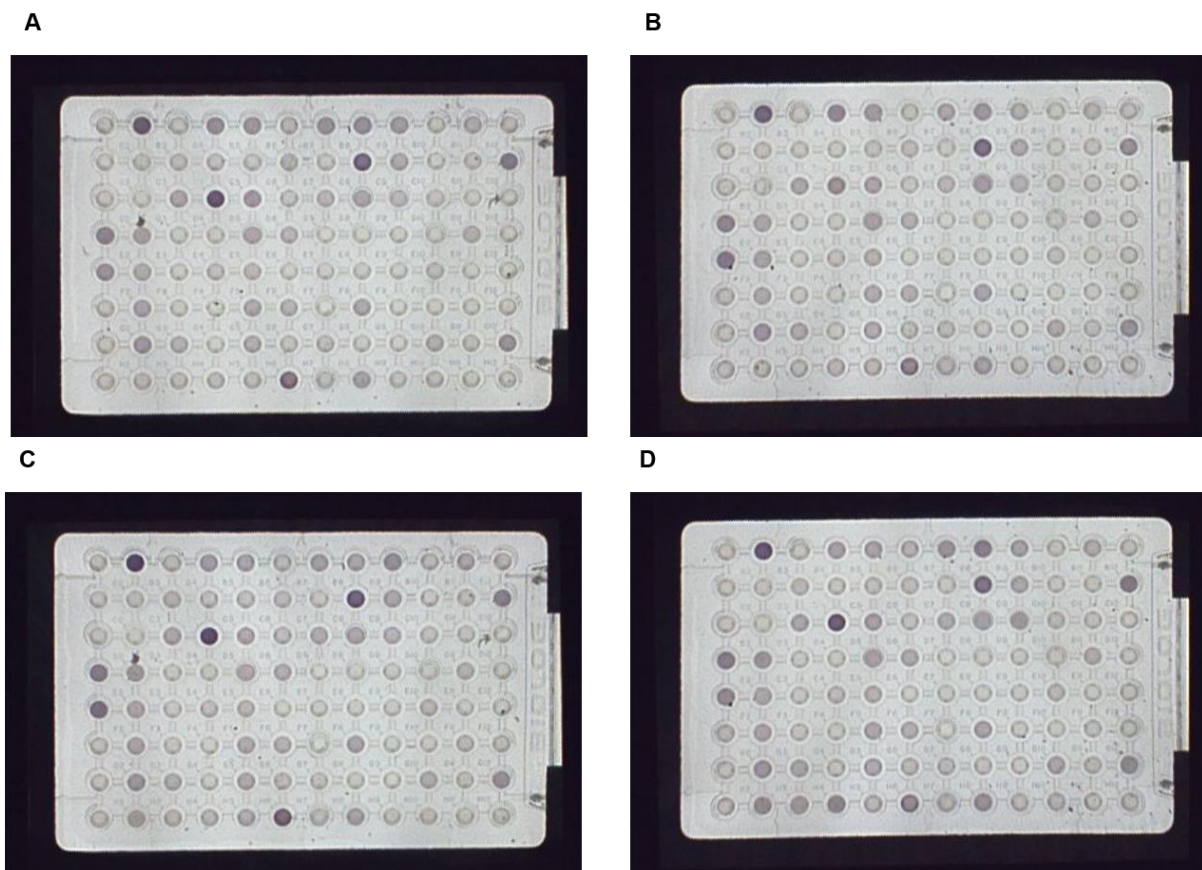


Figure 4.14 Representative images of the redox dye D colour changes. (A) R265 wt and (B) R265 GFP14 in the first run and (C) R265 wt and (D) R265 GFP14 in the second run after 36 hours of incubation.

3

³ The data was obtained with the help of Dr Scott Allen, Senior Non-Clinical Fellow in SITraN, The University of Sheffield

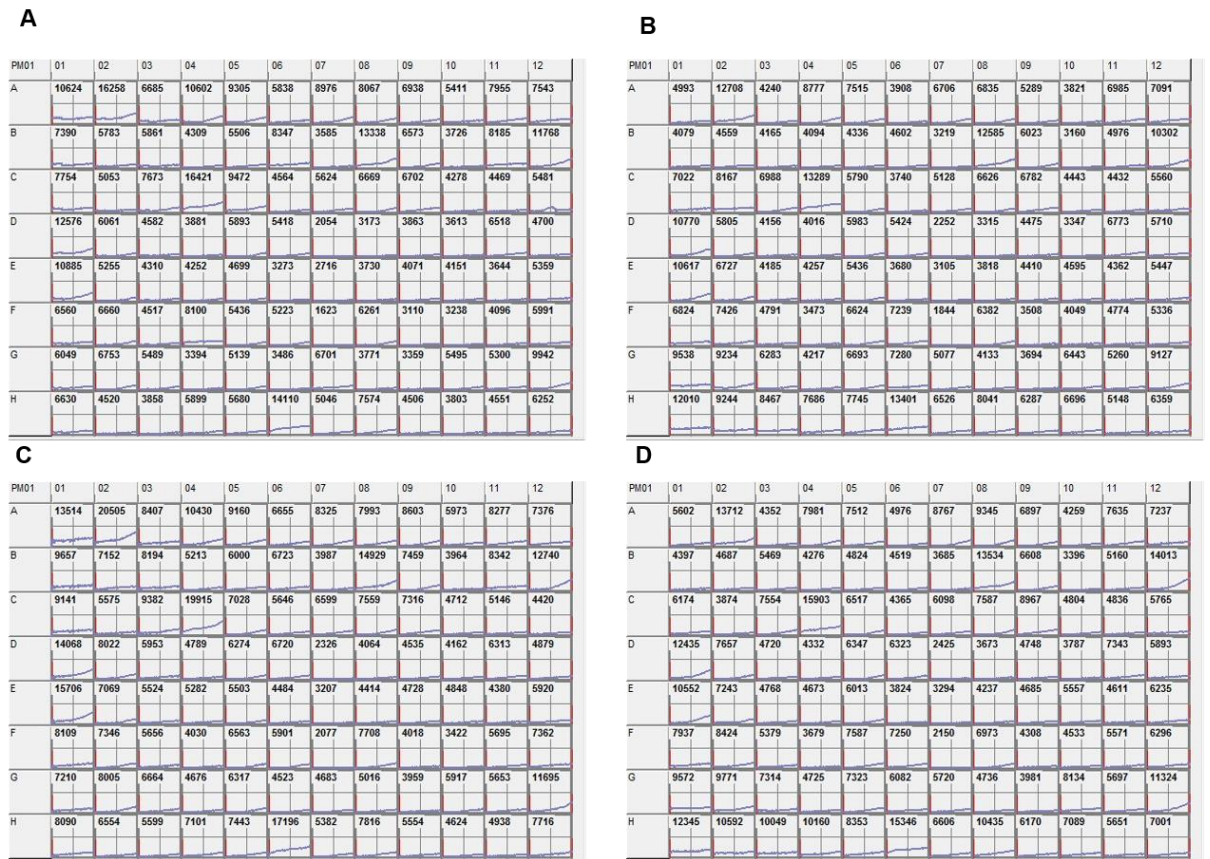


Figure 4.15 Representative images of kinetic traces. (A) R265 wt and (B) R265 GFP14 in the first run and (C) R265 wt and (D) R265 GFP14 in the second run after 36 hours of incubation.

4

⁴ The data was obtained with the help of Dr Scott Allen, Senior Non-Clinical Fellow in SITraN.

To identify the substrates in question for further kinetic analysis data from the two screens were firstly analysed by focusing on the last time-point of each experiment, this was the 36th hour. Thus, the starting point for the analysis was the creation of end-point metabolic profile at 36 hours (Figure 4.16) for all of metabolites. This did not give a true reflection of the kinetics. However, it provided an idea as to which metabolites to analyse in terms of kinetics. For all metabolites, the background (negative control) was removed in order to normalise data. The end-point profile identified a number of potential substrates candidates. The graph provided information only about data distribution but not statistical significance. In order to justify statistical differences, kinetic response curves were generated for each metabolite and two-way ANOVA was performed.

In the majority of cases, the lag phase was observed, which lasted around 1005 minutes, with a range of 810 minutes and 1065 minutes. While it was tempting to remove the lag phase data, on a final note it was decided to keep it for completeness of the assay.

It is not understood why R265 GFP14 showed higher metabolic activity than the wild-type during the lag phase. The inoculum concentration was determined by transmittance, i.e. conveniently measured from inoculum fluid tubes with the original Biolog turbidimeter. The meter was adjusted to 100% on each inoculated tube just prior to cell addition. Cells were then added mixed uniformly from top to bottom of the tube. On occasions, where the transmittance was too high, dilutions were made. The highest dilution was proximately 1:3. However, the most frequent dilutions were at proximately 1:2. This might mean that the different cultures might have been at different stages of growth phase. Taking into account the time spent on the carriage of samples from The University of Sheffield building to SiTRAN and plates preparation in the latter building, this time might have resulted in the average time from one second to one third of the experimental time in the Biolog plate reader to be spent on the adjusting to adapting to growth conditions (lag phase).

Converting the negative values was applied both to the wild-type and the GFP strains. The negative well value (A01) was removed from all the other values on the plate to normalise for background and then any negative values were converted to zero. This was done because the negative values are a measure of

the background metabolism in the cells on any given day. This will be different on different days and different runs. If normalisation is not done by removing the negative values, then there is no certainty that any increases or decreases in metabolism seen on a run to run basis are not just down to the cells being more or less active on that day. Many assays use this approach as this is a way to remove background variation seen in cells, buffers etc. (Bochner *et al.*, 2011; Allen *et al.*, 2019). Therefore, it is unlikely to lose any increase in NADH measurement. Another issue which remains is reproducibility. This issue is solved through a replication study, which must be completely independent and generate identical findings. To ensure reproducibility, the same protocol and software were used. In both runs data obtained looked similar.

In the initial screen, sixty-six compounds were identified as positive hits, reflecting P values <0.05 for genotype and time factors as well as genotype-time interaction. All the substrates showed a significant difference overall between R265 wt and R265 GFP14 (using two-way ANOVA) and a significant difference at one time-point or more (Sidak's post-test analysis). However, only twenty-one kinetic graphs (graphing reaction of NADH production as a function of substrate metabolism) showed real kinetic traces. These were identified as hits (Figure 4.17-37).

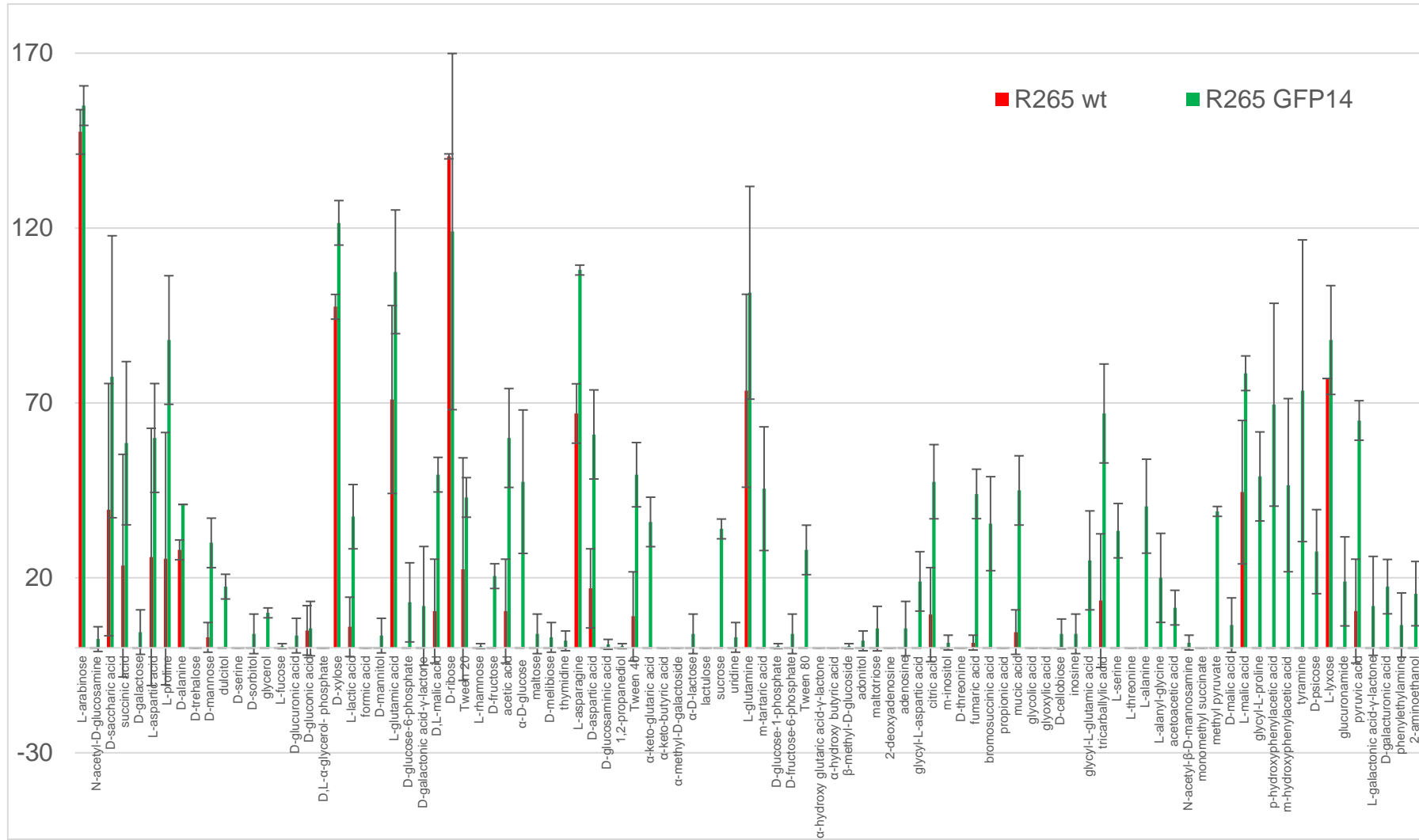


Figure 4.16 The end-point metabolic profile at 36 hours for all of metabolites. Data presented as column bars with mean \pm standard deviation.

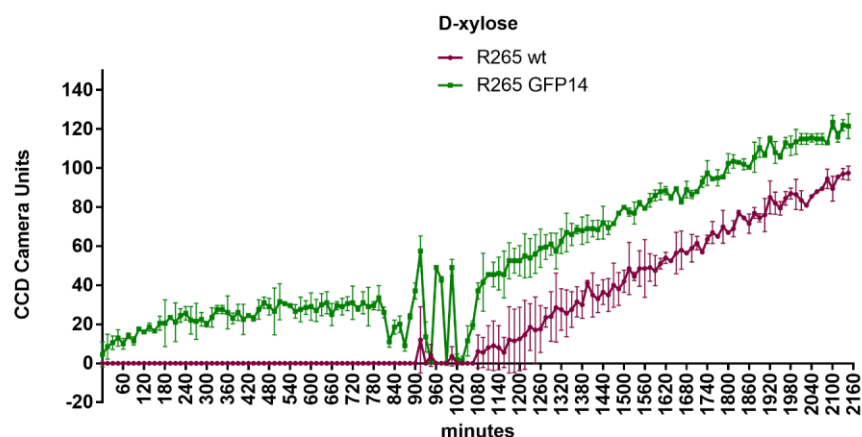


Figure 4.17 NADH production kinetics in R265 wt and R265 GFP14 with D-xylose. R265 wt (magenta) and R265 GFP14 (green). NADH production was measured using an OmniLog™ Phenotype Microarray plate reader taking CCD Camera Units readings every 15 minutes over a 36 hours period. Data presented as mean with standard error, for R265 wt and R265 GFP14 in duplicate. Background values (from a negative control) were subtracted from raw data values and any negative values were converted to zero for normalisation. To detect differences in NADH production between R265 wt and R265 GFP14, RM two-way ANOVA, with Sidak's post-test was performed. Interaction P value <0.0001, time P value<0.0001, genotype P value=0.0071. For all multiple comparisons, see Table 4.2 (Appendix 1).

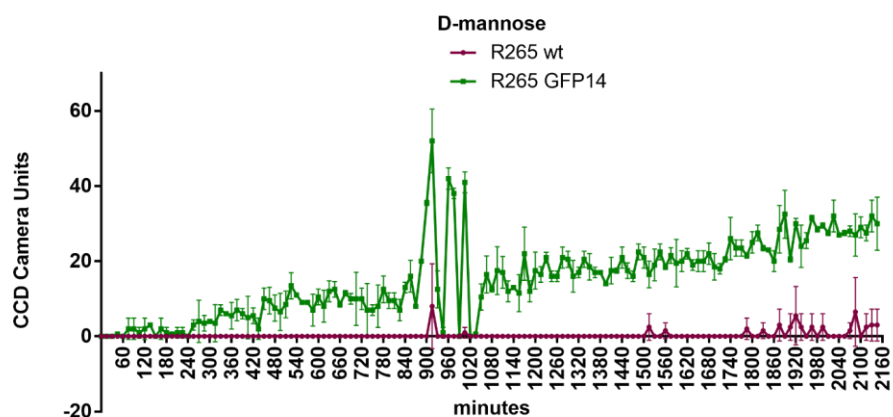


Figure 4.18 NADH production kinetics in R265 wt and R265 GFP14 with D-mannose. R265 wt (magenta) and R265 GFP14 (green). NADH production was measured using a OmniLog™ Phenotype Microarray plate reader taking CCD Camera Units readings every 15 min over a 36 hours period. Data presented as mean with standard error, for R265 wt and R265 GFP14 in duplicate. Background values (from a negative control) were subtracted from raw data values and any negative values were converted to zero for normalisation. To detect differences in NADH production between R265 wt and R265 GFP14, RM two-way ANOVA, with Sidak's post-test was performed. Interaction P value <0.0001, time P value<0.0001, genotype P value=0.0006. For all multiple comparisons, see Table 4.3 (Appendix 1).

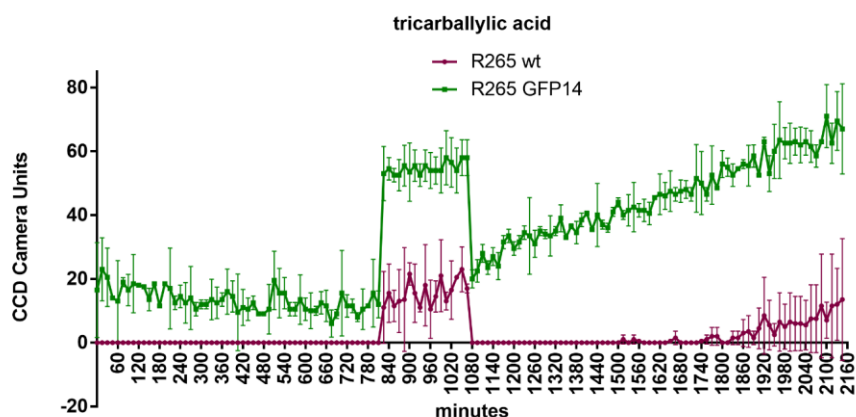


Figure 4.19 NADH production kinetics in R265 wt and R265 GFP14 with tricarballylic acid. R265 wt (magenta) and R265 GFP14 (green). NADH production was measured using a OmniLog™ Phenotype Microarray plate reader taking CCD Camera Units readings every 15 minutes over a 36 hours period. Data presented as mean with standard error, for R265 wt and R265 GFP14 in duplicate. Background values (from a negative control) were subtracted from raw data values and any negative values were converted to zero for normalisation. To detect differences in NADH production between R265 wt and R265 GFP14, RM two-way ANOVA, with Sidak's post-test was performed. Interaction P value <0.0001, time P value<0.0001, genotype P value=0.0044. For all multiple comparisons, see Table 4.4 (Appendix 1).

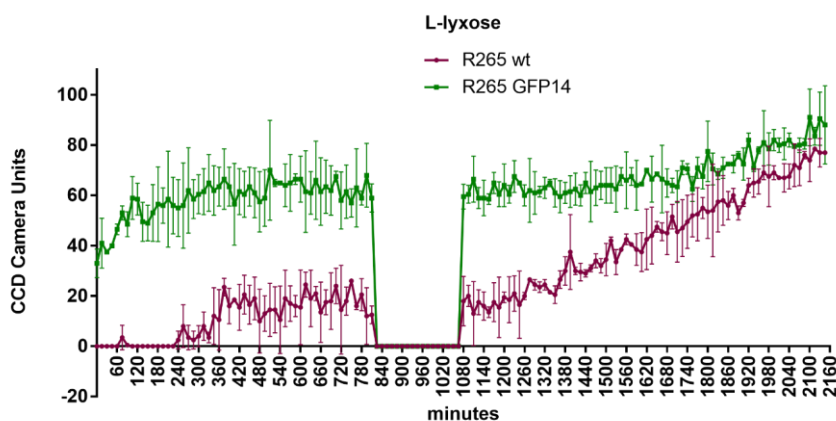


Figure 4.20 NADH production kinetics in R265 wt and R265 GFP14 with L-lyxose. R265 wt (magenta) and R265 GFP14 (green). NADH production was measured using a OmniLog™ Phenotype Microarray plate reader taking CCD Camera Units readings every 15 minutes over a 36 hours period. Data presented as mean with standard error, for R265 wt and R265 GFP14 in duplicate. Background values (from a negative control) were subtracted from raw data values and any negative values were converted to zero for normalisation. To detect differences in NADH production between R265 wt and R265 GFP14, RM two-way ANOVA, with Sidak's post-test was performed. Interaction P value <0.0001, time P value<0.0001, genotype P value=0.0098. For all multiple comparisons, see Table 4.5 (Appendix 1).

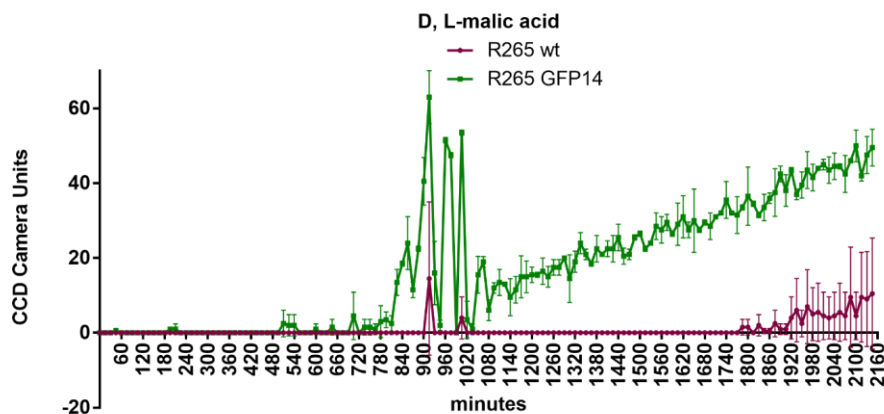


Figure 4.21 NADH production kinetics in R265 wt and R265 GFP14 with D, L-malic acid. R265 wt (magenta) and R265 GFP14 (green). NADH production was measured using a OmniLog™ Phenotype Microarray plate reader taking CCD Camera Units readings every 15 minutes over a 36 hours period. Data presented as mean with standard error, for R265 wt and R265 GFP14 in duplicate. Background values (from a negative control) were subtracted from raw data values and any negative values were converted to zero for normalisation. To detect differences in NADH production between R265 wt and R265 GFP14, RM two-way ANOVA, with Sidak's post-test was performed. Interaction P value <0.0001, time P value<0.0001, genotype P value= 0.0033. For all multiple comparisons, see Table 4.6 (Appendix 1).

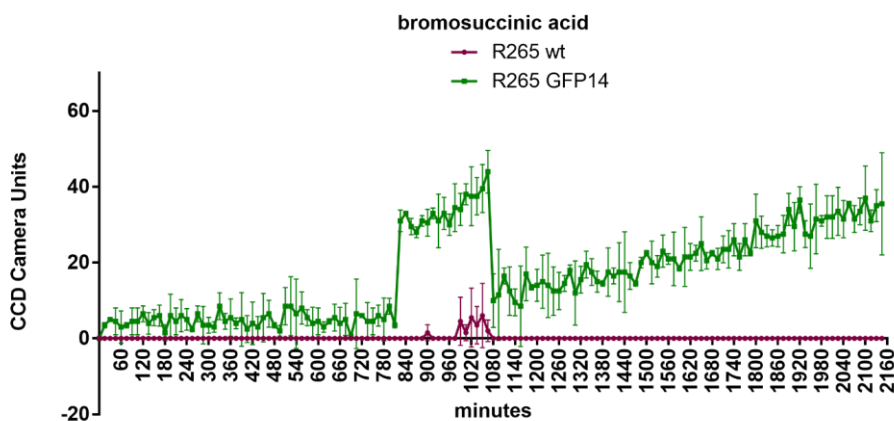


Figure 4.22 NADH production kinetics in R265 wt and R265 GFP14 with bromosuccinic acid. R265 wt (magenta) and R265 GFP14 (green). NADH production was measured using a OmniLog™ Phenotype Microarray plate reader taking CCD Camera Units readings every 15 minutes over a 36 hours period. Data presented as mean with standard error, for R265 wt and R265 GFP14 in duplicate. Background values (from a negative control) were subtracted from raw data values and any negative values were converted to zero for normalisation. To detect differences in NADH production between R265 wt and R265 GFP14, RM two-way ANOVA, with Sidak's post-test was performed. Interaction P value <0.0001, time P value<0.0001, genotype P value= 0.0168. For all multiple comparisons, see Table 4.7 (Appendix 1).

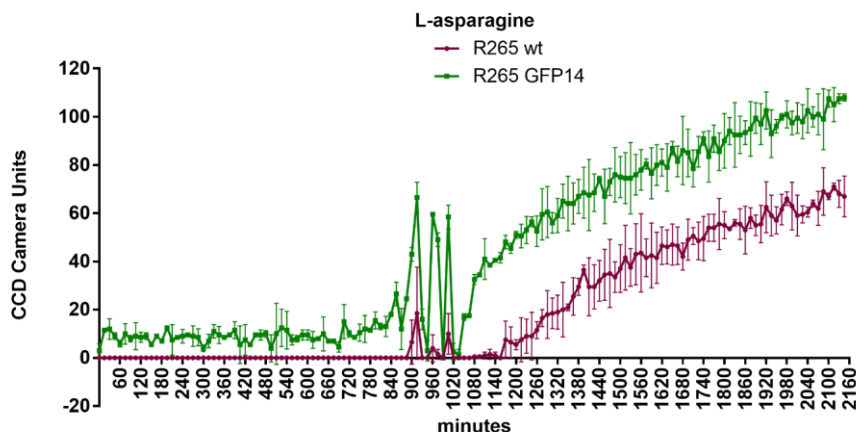


Figure 4.23 NADH production kinetics in R265 wt and R265 GFP14 with L-asparagine. R265 wt (magenta) and R265 GFP14 (green). NADH production was measured using a OmniLog™ Phenotype Microarray plate reader taking CCD Camera Units readings every 15 minutes over a 36 hours period. Data presented as mean with standard error, for R265 wt and R265 GFP14 in duplicate. Background values (from a negative control) were subtracted from raw data values and any negative values were converted to zero for normalisation. To detect differences in NADH production between R265 wt and R265 GFP14, RM two-way ANOVA, with Sidak's post-test was performed. Interaction P value <0.0001, time P value<0.0001, genotype P value= 0.0185. For all multiple comparisons, see Table 4.8 (Appendix 1).

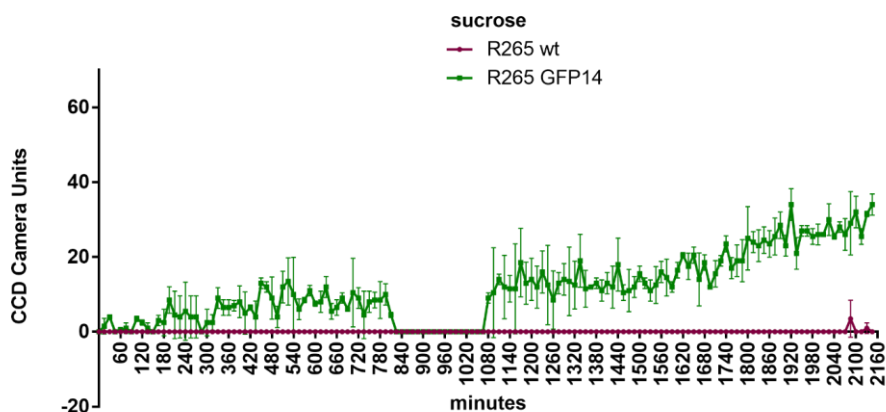


Figure 4.24 NADH production kinetics in R265 wt and R265 GFP14 with sucrose. R265 wt (magenta) and R265 GFP14 (green). NADH production was measured using a OmniLog™ Phenotype Microarray plate reader taking CCD Camera Units readings every 15 minutes over a 36 hours period. Data presented as mean with standard error, for R265 wt and R265 GFP14 in duplicate. Background values (from a negative control) were subtracted from raw data values and any negative values were converted to zero for normalisation. To detect differences in NADH production between R265 wt and R265 GFP14, RM two-way ANOVA, with Sidak's post-test was performed. Interaction P value <0.0001, time P value<0.0001, genotype P value= 0.0003. For all multiple comparisons, see Table 4.9 (Appendix 1).

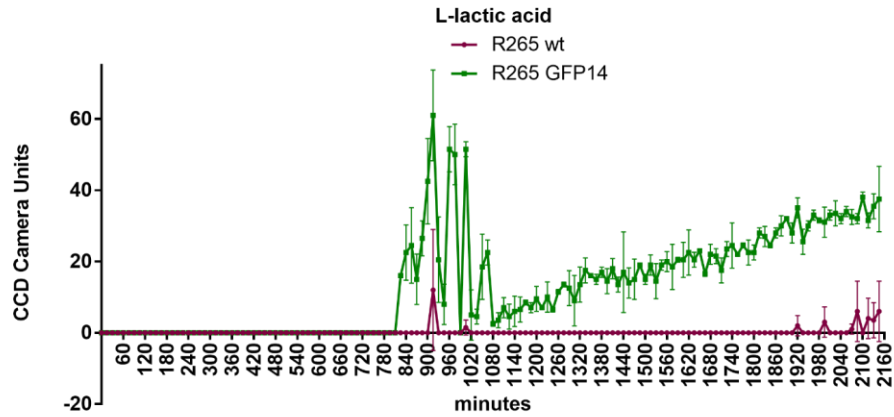


Figure 4.25 NADH production kinetics in R265 wt and R265 GFP14 with L-lactic acid. R265 wt (magenta) and R265 GFP14 (green). NADH production was measured using a OmniLog™ Phenotype Microarray plate reader taking CCD Camera Units readings every 15 minutes over a 36 hours period. Data presented as mean with standard error, for R265 wt and R265 GFP14 in duplicate. Background values (from a negative control) were subtracted from raw data values and any negative values were converted to zero for normalisation. To detect differences in NADH production between R265 wt and R265 GFP14, RM two-way ANOVA, with Sidak's post-test was performed. Interaction P value <0.0001, time P value<0.0001, genotype P value= 0.0005. For all multiple comparisons, see Table 4.10 (Appendix 1)

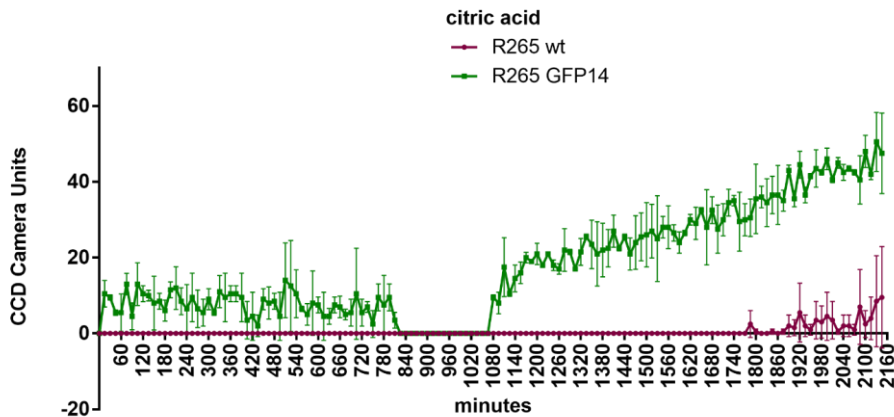


Figure 4.26 NADH production kinetics in R265 wt and R265 GFP14 with citric acid. R265 wt (magenta) and R265 GFP14 (green). NADH production was measured using a OmniLog™ Phenotype Microarray plate reader taking CCD Camera Units readings every 15 minutes over a 36 hours period. Data presented as mean with standard error, for R265 wt and R265 GFP14 in duplicate. Background values (from a negative control) were subtracted from raw data values and any negative values were converted to zero for normalisation. To detect differences in NADH production between R265 wt and R265 GFP14, RM two-way ANOVA, with Sidak's post-test was performed. Interaction P value <0.0001, time P value<0.0001, genotype P value= 0.0027. For all multiple comparisons, see Table 4.11(Appendix 1).

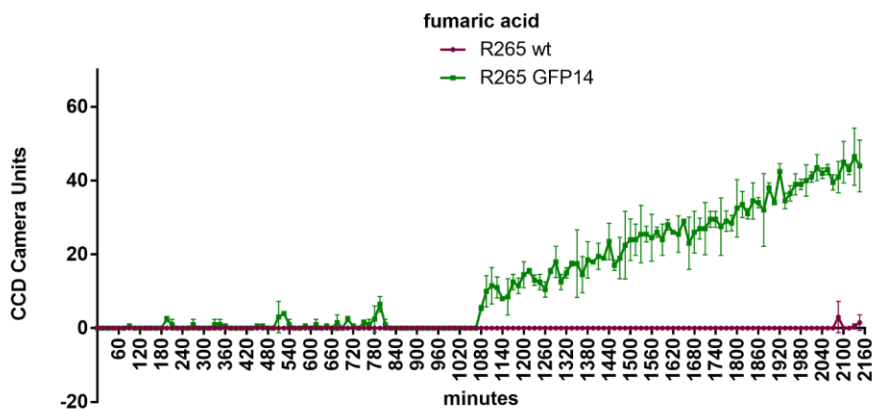


Figure 4.27 NADH production kinetics in R265 wt and R265 GFP14 with fumaric acid. R265 wt (magenta) and R265 GFP14 (green). NADH production was measured using a OmniLog™ Phenotype Microarray plate reader taking CCD Camera Units readings every 15 minutes over a 36 hours period. Data presented as mean with standard error, for R265 wt and R265 GFP14 in duplicate. Background values (from a negative control) were subtracted from raw data values and any negative values were converted to zero for normalisation. To detect differences in NADH production between R265 wt and R265 GFP14, RM two-way ANOVA, with Sidak's post-test was performed. Interaction P value <0.0001, time P value<0.0001, genotype P value= 0.0018. For all multiple comparisons, see Table 4.12 (Appendix 1).

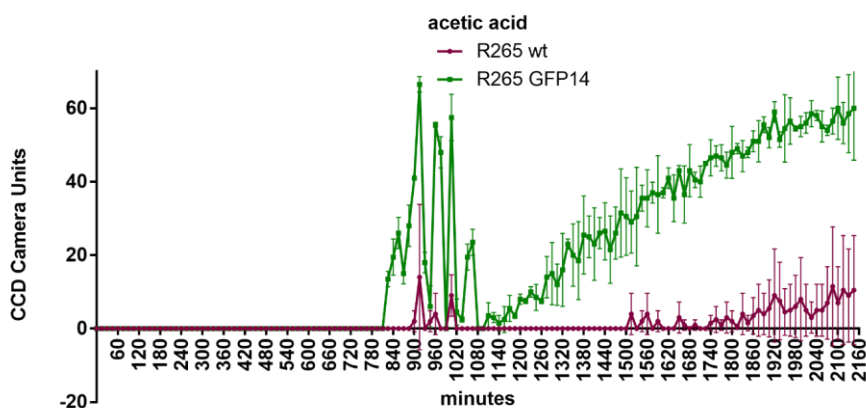


Figure 4.28 NADH production kinetics in R265 wt and R265 GFP14 with acetic acid. R265 wt and R265 GFP14. NADH production was measured using a OmniLog™ Phenotype Microarray plate reader taking CCD Camera Units readings every 15 minutes over a 36 hours period. Data presented as mean with standard error, for R265 wt and R265 GFP14 in duplicate. Background values (from a negative control) were subtracted from raw data values and any negative values were converted to zero for normalisation. To detect differences in NADH production between R265 wt and R265 GFP14, RM two-way ANOVA, with Sidak's post-test was performed. Interaction P value <0.0001, time P value<0.0001, genotype P value= 0.0059. For all multiple comparisons, see Table 4.13 (Appendix 1).

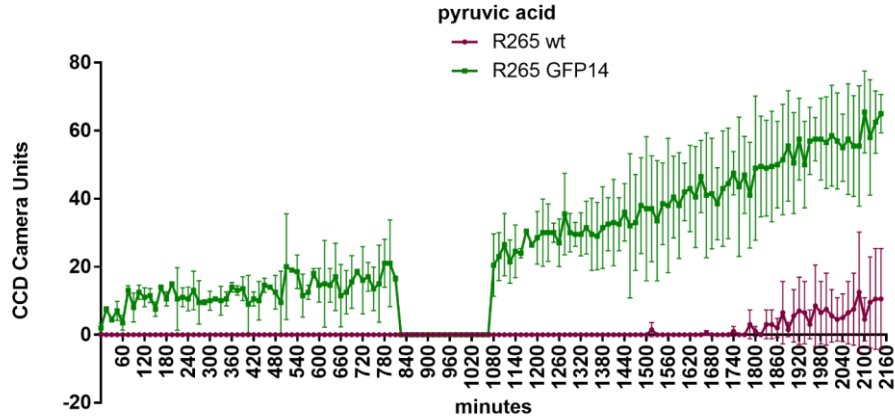


Figure 4.29 NADH production kinetics in R265 wt and R265 GFP14 with pyruvic acid. R265 wt (magenta) and R265 GFP14 (green). NADH production was measured using a OmniLog™ Phenotype Microarray plate reader taking CCD Camera Units readings every 15 minutes over a 36 hours period. Data presented as mean with standard error, for R265 wt and R265 GFP14 in duplicate. Background values (from a negative control) were subtracted from raw data values and any negative values were converted to zero for normalisation. To detect differences in NADH production between R265 wt and R265 GFP14, RM two-way ANOVA, with Sidak's post-test was performed. Interaction P value <0.0001, time P value<0.0001, genotype P value= 0.0429. For all multiple comparisons, see Table 4.14 (Appendix 1).

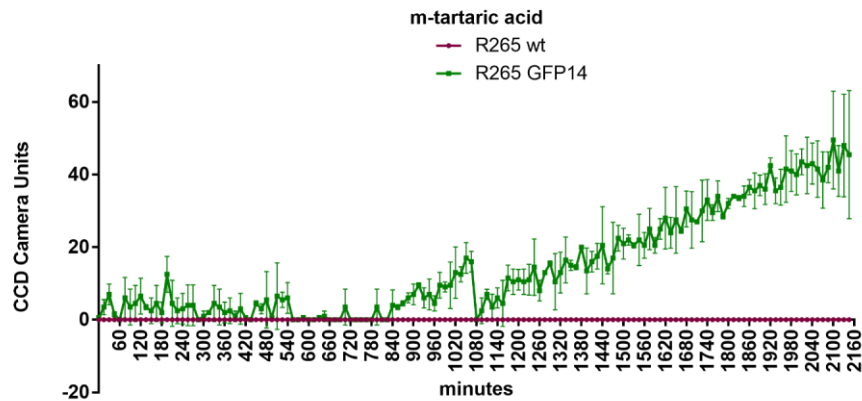


Figure 4.30 NADH production kinetics in R265 wt and R265 GFP14 with m-tartaric acid. R265 wt (magenta) and R265 GFP14 (green). NADH production was measured using a OmniLog™ Phenotype Microarray plate reader taking CCD Camera Units readings every 15 minutes over a 36 hours period. Data presented as mean with standard error, for R265 wt and R265 GFP14 in duplicate. Background values (from a negative control) were subtracted from raw data values and any negative values were converted to zero for normalisation. To detect differences in NADH production between R265 wt and R265 GFP14, RM two-way ANOVA, with Sidak's post-test was performed. Interaction P value <0.0001, time P value<0.0001, genotype P value= 0.0072. For all multiple comparisons, see Table 4.15 (Appendix 1).

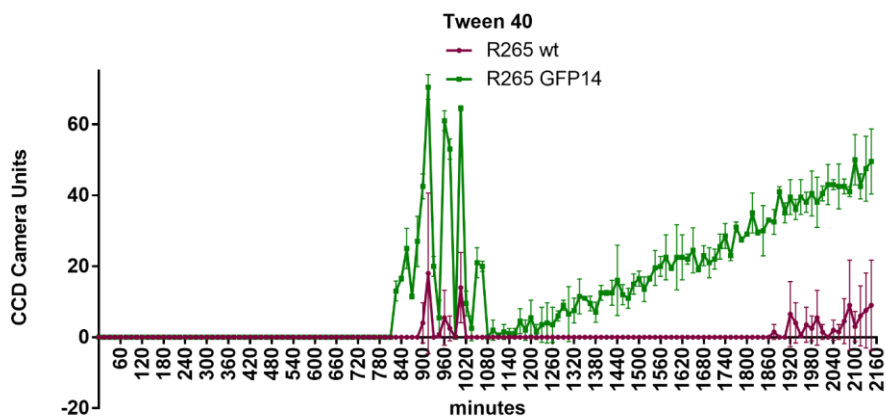


Figure 4.31 NADH production kinetics in R265 wt and R265 GFP14 with Tween 40. R265 wt (magenta) and R265 GFP14 (green). NADH production was measured using a OmniLog™ Phenotype Microarray plate reader taking CCD Camera Units readings every 15 minutes over a 36 hours period. Data presented as mean with standard error, for R265 wt and R265 GFP14 in duplicate. Background values (from a negative control) were subtracted from raw data values and any negative values were converted to zero for normalisation. To detect differences in NADH production between R265 wt and R265 GFP14, RM two-way ANOVA, with Sidak's post-test was performed. Interaction P value <0.0001, time P value<0.0001, genotype P value= 0.0088. For all multiple comparisons, see Table 4.16 (Appendix 1).

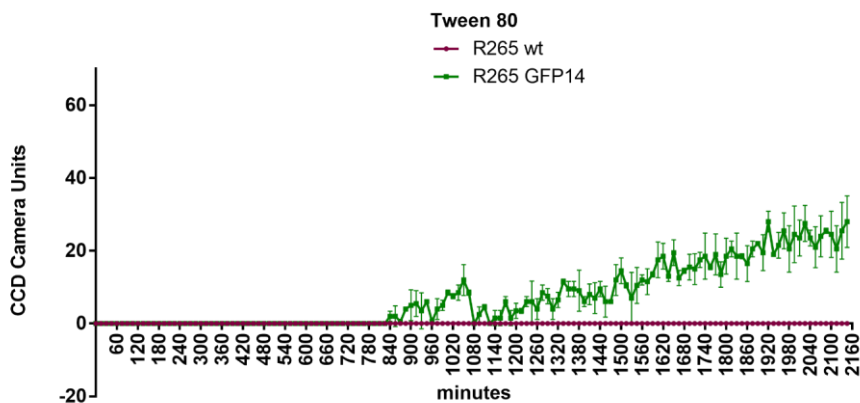


Figure 4.32 NADH production kinetics in R265 wt and R265 GFP14 with Tween 80. R265 wt (magenta) and R265 GFP14 (green). NADH production was measured using a OmniLog™ Phenotype Microarray plate reader taking CCD Camera Units readings every 15 minutes over a 36 hours period. Data presented as mean with standard error, for R265 wt and R265 GFP14 in duplicate. Background values (from a negative control) were subtracted from raw data values and any negative values were converted to zero for normalisation. To detect differences in NADH production between R265 wt and R265 GFP14, RM two-way ANOVA, with Sidak's post-test was performed. Interaction P value <0.0001, time P value<0.0001, genotype P value= 0.0059. For all multiple comparisons, see Table 4.17 (Appendix 1).

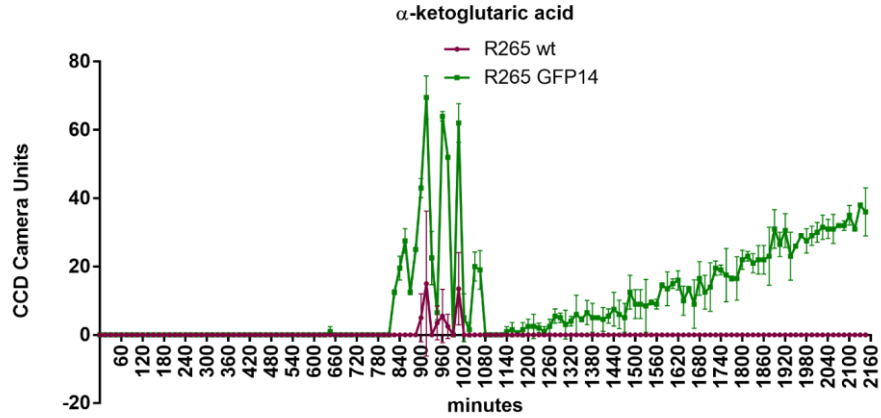


Figure 4.33 NADH production kinetics in R265 wt and R265 GFP14 with α -ketoglutaric acid. R265 wt (magenta) and R265 GFP14 (green). NADH production was measured using a OmniLog™ Phenotype Microarray plate reader taking CCD Camera Units readings every 15 minutes over a 36 hours period. Data presented as mean with standard error, for R265 wt and R265 GFP14 in duplicate. Background values (from a negative control) were subtracted from raw data values and any negative values were converted to zero for normalisation. To detect differences in NADH production between R265 wt and R265 GFP14, RM two-way ANOVA, with Sidak's post-test was performed. Interaction P value <0.0001, time P value<0.0001, genotype P value= 0.0061. For all multiple comparisons, see Table 4.18 (Appendix 1).

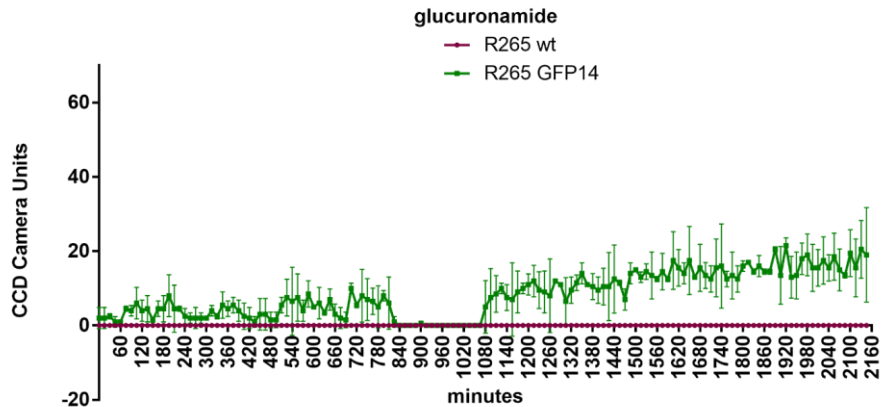


Figure 4.34 NADH production kinetics in R265 wt and R265 GFP14 with glucuronamide. R265 wt (magenta) and R265 GFP14 (green). NADH production was measured using a OmniLog™ Phenotype Microarray plate reader taking CCD Camera Units readings every 15 minutes over a 36 hours period. Data presented as mean with standard error, for R265 wt and R265 GFP14 in duplicate. Background values (from a negative control) were subtracted from raw data values and any negative values were converted to zero for normalisation. To detect differences in NADH production between R265 wt and R265 GFP14, RM two-way ANOVA, with Sidak's post-test was performed. Interaction P value <0.0001, time P value<0.0001, genotype P value= 0.0451. For all multiple comparisons, see Table 4.19 (Appendix 1).

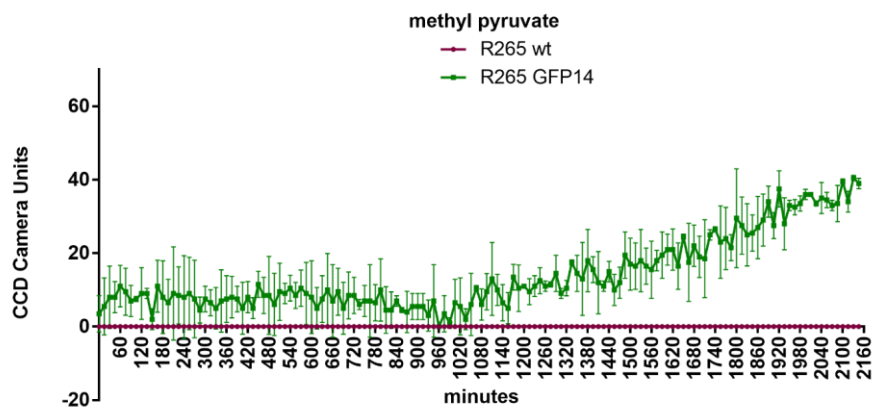


Figure 4.35 NADH production kinetics in R265 wt and R265 GFP14 with methyl pyruvate. R265 wt (magenta) and R265 GFP14 (green). NADH production was measured using a OmniLog™ Phenotype Microarray plate reader taking CCD Camera Units readings every 15 minutes over a 36 hours period. Data presented as mean with standard error, for R265 wt and R265 GFP14 in duplicate. Background values (from a negative control) were subtracted from raw data values and any negative values were converted to zero for normalisation. To detect differences in NADH production between R265 wt and R265 GFP14, RM two-way ANOVA, with Sidak's post-test was performed. Interaction P value <0.0001, time P value<0.0001, genotype P value= 0.0387. For all multiple comparisons, see Table 4.20 (Appendix 1).

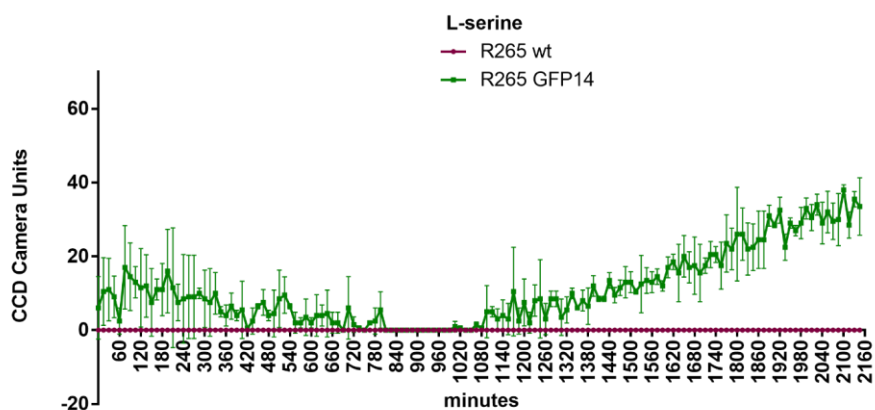


Figure 4.36 NADH production kinetics in R265 wt and R265 GFP14 with L-serine. R265 wt (magenta) and R265 GFP14 (green). NADH production was measured using a OmniLog™ Phenotype Microarray plate reader taking CCD Camera Units readings every 15 minutes over a 36 hours period. Data presented as mean with standard error, for R265 wt and R265 GFP14 in duplicate. Background values (from a negative control) were subtracted from raw data values and any negative values were converted to zero for normalisation. To detect differences in NADH production between R265 wt and R265 GFP14, RM two-way ANOVA, with Sidak's post-test was performed. Interaction P value <0.0001, time P value<0.0001, genotype P value= 0.0149. For all multiple comparisons, see Table 4.21 (Appendix 1).

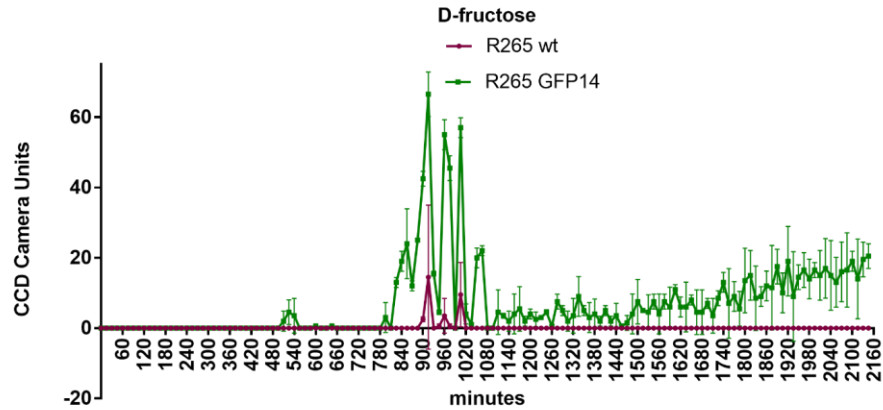


Figure 4.37 NADH production kinetics in R265 wt and R265 GFP14 with D-fructose. R265 wt (magenta) and R265 GFP14 (green). NADH production was measured using a OmniLog™ Phenotype Microarray plate reader taking CCD Camera Units readings every 15 minutes over a 36 hours period. Data presented as mean with standard error, for R265 wt and R265 GFP14 in duplicate. Background values (from a negative control) were subtracted from raw data values and any negative values were converted to zero for normalisation. To detect differences in NADH production between R265 wt and R265 GFP14, RM two-way ANOVA, with Sidak's post-test was performed. Interaction P value <0.0001, time P value<0.0001, genotype P value= 0.0333. For all multiple comparisons, see Table 4.22 (Appendix 1).

R265 GFP14 showed increased NADH production in all twenty-one substrates. Table 4.23 (see Appendix 2) shows the hits organised by the highest number of significant comparisons. It is noteworthy, that PM microplates were originally designed mostly for *E. coli*, but also included carbon sources for other microorganisms. The substrates include many categories of carbon sources. They can be categorised both structurally and functionally. For PM1 used in this study the hits can be organised as follows: amino acids (L-asparagine, L-serine), monosaccharides aldoses (D-xylose, D-mannose, L-lyxose), disaccharides (sucrose), diacid sugars (m-tartate), substituted monosaccharides (glucuronamide), fructose/mannose metabolism (D-fructose), Krebs cycle metabolites (succinate, acetate, α -ketoglutarate, citrate, fumarate), glycolysis metabolites (pyruvate) and miscellaneous (bromosuccinic acid, Tween 40, Tween 80, methyl pyruvate, tricarballylate). D, L malate remained unclassified. D-malate is involved in butanoate metabolism whereas L-malate in Krebs cycle (personal communication, Biolog technical support). L-form is naturally occurring, whereas a mixture of L- and D-malic acid is produced synthetically (Brittain, 2001). L-lactic acid falls in propanoate metabolism, according to Biolog.

4.2.8 Conclusions

In this chapter, larval zebrafish and mice survival provided a firm conclusion about R265 GFP14 virulence attenuation. It was proposed that the attenuation was associated with the loss of six genes deleted during generation of the fluorescent derivative of R265 wt. Analysis of macrophage-cryptococcal cell interactions suggested a distinctive course of infection with many alternative fates of cryptococci. To present this interesting case, a model of R265 GFP14 infection progression was proposed (see Discussion). R265 GFP14 had a growth deficit when cultured in the minimum media as compared with the rich one. This suggested the possibility of similar conditions *in vivo* in zebrafish larvae and possibly metabolic defects likely resulting from the loss of the aforementioned six genes deleted during random genomic integration of GFP construct. Therefore, a metabolic screening was approached to identify differences in the metabolic pathway(s) differences between the R265 GFP14 and R265 wt. This aspect of

the research suggested that R265 GFP14 exhibited different use of carbon sources and confirmed the R265 GFP14 was more efficient at substrate assimilation. The main conclusion that can be drawn is that there is a metabolic difference between R265 wt and R265 GFP14.

4.3 Discussion

VGII molecular type of *C. gattii* has drawn more attention than any other molecular type because it was the cause of the Canadian outbreak (Kidd *et al.*, 2004). Here I have shown that *C. gattii* R265 wt molecular type VGII is more virulent in a zebrafish model of infection than KN99 wt, which is of genotype VNI background (Nielsen *et al.*, 2003). However, insertion of GFP reduced virulence of R265 in zebrafish and mice. The GFP14 mutant was unable to increase in number in zebrafish and I concluded that it had an *in vivo* growth defect. Using an *in vitro* minimal media growth assay, I found that GFP14 was less able to grow supporting my conclusion from the zebrafish studies. To understand this growth defect I tested the metabolic activity of R265 GFP14 compared to R265 wt. I found that there was evidence of increased oxidative phosphorylation activity in the GFP14 mutant but could not conclude how this resulted in decreased growth during infection of zebrafish (discussed below). Concurrently, I found that there was a 6 gene deletion in the GFP14 R265 mutant and attempted to understand how this deletion resulted in decreased virulence. My experiments have not answered this question yet and at this stage I cannot conclude how the genotype of the GFP14 mutant results in reduced virulence.

R265 infection resulted in decreased host survival than KN99 in a zebrafish model. This is an important finding as there has been little interest in such comparisons *in vivo*. In addition, my finding corroborates the findings of the small amount of previous work investigating this question (Thompson *et al.*, 2012). While GFP insertion to KN99 did not influence the virulence of KN99 GFP, the insertion of GFP into R265 resulted in severe attenuation in zebrafish and mice. R265 strains genome sequencing revealed that R265 GFP14 lost six genes deleted during generation of the GFP-tagged derivative of R265. It was

hypothesised that the loss of these six genes accounted for the loss of virulence and that the genes are important in R265 wt pathogenesis.

To investigate how the virulence was attenuated in the host, R265 GFP14 was analysed in a zebrafish model of macrophage and cryptococcal cell interactions that permits analysis at a cellular level *in vivo*, non-invasively and over the course of infection (Bojarczuk *et al.*, 2016). It appeared that the infection with R265 GFP14 is the process of simultaneous killing of previously phagocytosed cryptococci with the internalisation of new cryptococci, which were previously extracellular. However, R265 GFP14 did not grow in any of the analysed infected zebrafish and the overall number of cryptococci was significantly reduced at the end of infection. Considering the involvement of the six genes deleted in the GFP strain, in metabolite related processes, it was hypothesised that R265 GFP14 had reduced ability to adapt to the host environment. Thus, it was predicted that the fungus would show a growth deficit. Therefore, both R265 wt and R265 GFP14 were tested for growth in rich and minimal media. R265 GFP14 failed to grow in minimal media suggesting the presence of an unrecognised auxotrophic phenotype (Dymond, 2013). This has been observed several times for *Cryptococcus* previously: *C. neoformans* mutant for *LYS9* gene (encoding saccharopine dehydrogenase) that failed to grow in YNB lysine-deficient medium and was avirulent in mice (Kingsbury *et al.*, 2004), *C. neoformans* mutant for methionine synthase gene (*MET6*) that lost viability when starved of methionine plus avirulent in mice (Pascon *et al.*, 2004). However, without being able to confirm the supplemental nutrient required, and given the lack of a causative gene, confirming autotrophy is not possible. While an uncharacterised autotrophy is a possible explanation for the growth defect, the lack of specific nutrient is not the only explanation. Other possible phenotypes would be an inability to utilise the nutrients present (lack of transporter or enzyme), failure to remove waste products from the cell, misregulation of cell growth/division signalling and machinery or non-growth response to the environment (e.g. energy used for capsule production instead of replication). To investigate some of these possibilities metabolic profiling of both strains using a phenotype microarray (PM) technology was performed. This demonstrated that the strains differed in terms

of carbon utilisation, which might shape the host-pathogen interface. Most publications make an impression that carbon must be obtained in large quantities from the environment and in the context of infection in order to sustain biosynthetic processes (reviewed by (Ene *et al.*, 2014; Ries *et al.*, 2018)). Interestingly, the loss of both hexokinases in *C. neoformans* results in the inability to utilise glucose. The loss of both hexokinases together, but not single deletions, results in reduced virulence in mice (Price *et al.*, 2011). This means that virulence and metabolism of microorganisms are uniquely interlinked. Phenotypic and virulence changes that result from changes in the genome are discussed below (see The mechanism of R265 GFP14 attenuation *in vivo*).

4.3.1 Temperature and thermotolerance

Broad thermotolerance is a widely studied aspect of cryptococci that is recognised as being an important part of their ability to cause infection in mammals and an important factor in the use of different experimental models. The ability to withstand relatively hot or cold conditions might be important for the outcome of R265 infection. There is no hard evidence in this present study that temperature is a factor. This is because the R265 GFP14 virulence phenotypes are similar in zebrafish maintained at 28°C (UK Home Office regulations) with the temperature of water controlling the zebrafish body and in mice that have the body temperature of about 37°C (Refinetti and Menaker, 1992). However, it might be that R265 GFP14 has reduced temperature stress tolerance.

Interestingly, *in vitro*, R265 GFP14 showed no difference in growth in rich (YPD) media, under stress conditions, proliferation in macrophages or in vomocytosis rates compared to the parental strain (Voelz *et al.*, 2010). However, in the publication of (Voelz *et al.*, 2010) all stress conditions as well as proliferation and vomocytosis were investigated at 37°C only whereas growth rates at both 25°C and 37°C. My thorough analysis of the figure representing growth at 25°C and 37°C in YPD in (Voelz *et al.*, 2010), leads to an interesting observation. I agree that there were no differences in the growth between R265 wt and R265 GFP14 strains at neither 25°C nor 37°C. However, a considerable difference in the growth rate can be seen between both the temperatures, which was not

addressed in the paper. R265 wt and R265 GFP14 grew worse at 25°C in contrast to 37°C. It is interesting that in the growth experiments, the variation expressed as standard error of the mean, was quite significant between the temperatures. At 37°C, the variation was much more pronounced than at 25°C for both strains. R265 GFP14 appeared with very small error bars at both temperatures when compared to other strains tested. Therefore, it would be of significant interest to test growth of R265 and R265 GFP14 under stress at different temperatures. This could be a temperature difference affect or it may be a combinatorial stress effect and therefore it would also be of interest to combine different stresses as would be present in the animal models used.

4.3.2 GFP insertion

4.3.2.1 GFP insertion effect on the course of infection

During infection, the interplay between host and pathogen are investigated to assess how host-pathogen interactions at a cellular level take place and to understand how the outcome of infection is determined (e.g. Bojarczuk *et al.*, 2016). To facilitate faster analysis of cryptococcal intracellular parasitism and aid assaying virulence, a fluorescent version of a pathogen was needed. In addition, a match between non-fluorescent and fluorescent strain in terms of virulence has to be demonstrated before its use in infection experiments. Therefore, zebrafish larvae were tested in a survival assay to evaluate whether the GFP insertion had an effect on virulence. The findings of extended survival of zebrafish challenged with R265 GFP14 were unexpected and suggested there might have been a difference between R265 wt and R265 GFP14, speculated to be associated with the GFP insertion. Therefore, I aimed to establish whether GFP insertion influenced the virulence of KN99 wt. No study to date has examined KN99 wt and KN99 GFP wt alongside *in vivo* in a survival assay. Thus, only KN99 wt can be discussed in this aspect. In my study, both strains resulted in the same rate of survival. This was broadly in line with findings of (Gibson, 2017) wherein the KN99 wt injection into zebrafish resulted in 90% survival. The slight difference in the survival curves for KN99 wt infected zebrafish might have resulted from the zebrafish strain used. In my study *nacre* was used, whereas AB was used in

(Gibson, 2017). The zebrafish data also revealed a difference in response to the R265 wt and R265 GFP14, which was surprising for isogenic strains.

Many bacterial and fungal strains have GFP markers, which does not affect their virulence. The following are examples of comparisons of virulence between GFP strains and their non-GFP isogenic strains: bacteria *in planta* *Xantomonas* PXO99GFP (Han *et al.*, 2008); *in vivo* *C. neoformans* H99 from the May lab (Voelz *et al.*, 2010) versus H99 GFP generated by (Voelz *et al.*, 2010) (Bojarczuk, unpublished), KN99 GFP (Gibson *et al.*, 2018) versus KN99 (Nielsen *et al.*, 2003) (this present study Chapter 4 in section 4.2.1). Other examples include *in vivo* bacteria *Staphylococcus aureus* SH1000 pMV158-GFP versus SH1000 (Dr Tomasz Prajsnar, the University of Sheffield, unpublished) as well as *in planta* comparison of GFP-labelled fungi *Aspergillus* to its parental strain (Rajasekaran *et al.*, 2008). Actually, the literature is not evident in side-by-side comparisons of fluorescently tagged microorganisms to their isogenic non-fluorescent strains in terms of virulence. Instead, many concentrate rather on growth comparisons *in vitro*, e.g. growth of GFP-labelled *E. coli* O157:H7, *Salmonella enteritidis*, *Listeria innocua*, *Listeria monocytogenes* versus the growth of parental strains (Ma *et al.*, 2011) or R265 GFP strains versus R265 wt (Voelz *et al.*, 2010).

Until recently, there were only two cases of published evidence that addition of a fluorescent protein to a genome of a microorganism produced a different phenotype (D'Souza *et al.*, 2011; Upadhyia *et al.*, 2017). The authors of (Upadhyia *et al.*, 2017) found no differences in growth of *Cryptococcus* KN99 mCherry in rich or nutrient deprived media, capsule inducing medium, stress conditions such as cell wall stressors, oxidative or nitrosative stress. However, there was a small increase in survival time of 19 days post infection (dpi) with KN99 mCherry expressing construct (KN99mCH) as compared to 16 dpi with KN99 wt suggesting that GFP insertion could have an impact on the outcome of survival assays and virulence. Nonetheless, the authors of (Upadhyia *et al.*, 2017) argued that the extended survival of mice with KN99mCH attributed to its slower growth *in vivo*, when mice were co-infected with KN99 wt, likely due to high expression of mCherry or due to genomic changes. However, it remains unknown whether the KN99mCH genome was sequenced for other mutations, which may be an alternative reason. The study of (D'Souza *et al.*, 2011) also produced results

which corroborated the findings of my experiments. A number of WM276 GFP *C. gattii* strains were tested in virulence assays and only WM276 GFP2 conferred avirulence in infected C57BL/6 mice via intratracheal route with 1×10^5 cfu. This was explained for changes in chromosome 11 of the transformant. This region contained 24 genes, including a putative invertase gene (CGB_K4300C), mutation of which conferred a raffinose auxotrophy. However, mutations elsewhere in the WM276gfp2 genome might account for the virulence defect. This suggests that the GFP in *C. gattii* in itself is not an issue, and instead, that the avirulent phenotype seen with zebrafish and mice is related to changes to the genome associated with the GFP insertion, i.e. six genes deletion, instead of GFP itself.

4.3.2.2 GFP insertion site

The transformation of *C. gattii* resulted in homologous integration of plasmid DNA asserting mitotically stable integration (Varma *et al.*, 1992). The homologous recombination was achieved by using *Saccharomyces cerevisiae* machinery, which assures nearly 100% homologue (Orr-Weaver *et al.*, 1981). The GFP expression was stable *in vitro* after re-streaking and growing at 25°C and 37°C as well as under stress conditions at 37°C. This implied stable ectopic integration within the genome (Voelz *et al.*, 2010). The creators of R265 GFP14 were unable to identify the GFP integration site following PCR and sequencing (Voelz, 2010). However, my analysis specified the integration site being on chromosome 1 replacing the first six genes. While there are now some ways in which to target insertion of GFP markers in the cryptococcal genomes these are still uncommon and were not performed in this case. Random integration carries the risk of the formation of inserted and deleted regions around the site of integration. It is very rare that insertion causes a significant change. However, in R265 GFP14, GFP insertion removed ~32 kb from early in chromosome 1. From this deletion there was no clear candidate for the cause of avirulence (discussed below). Given the previous study that demonstrated chromosomal changes following GFP insertion into *C. gattii* strain WM272 (D'Souza *et al.*, 2011) and that chromosomal changes have been shown in *C. neoformans* during the response to fluconazole

(Altamirano *et al.*, 2017), I would suggest that genome sequencing of cryptococcal strains with insertions is to be recommended as there may be changes more frequently than is currently recognised.

4.3.3 Virulence

4.3.3.1 Virulence of R265 wt and KN99 wt in a zebrafish model of infection

The study set out with the aim of assessing the virulence of *C. gattii* strain R265 (an isolate from the ongoing Vancouver Island Outbreak, VIO) (Kidd *et al.*, 2004) in the zebrafish. The first question in this study sought to determine the difference in the virulence between *C. gattii* R265 wt and *C. neoformans* KN99 wt (Nielsen *et al.*, 2003) (according to the old nomenclature serotype B, genotype VGIIa and serotype A background, genotype VNI background respectively). This is important to consider, as previous comparisons of systemic infection with these strains *in vivo* were not evident in the literature. Furthermore, understanding if virulence of an outbreak strain is increased in comparison to other lab strains would be beneficial to ensure research and treatment are developed to the correct efficacy.

Subcutaneous infection in C57BL/6 mice gave almost identical lethal infections caused by 1×10^4 cfu of R265 wt or KN99 wt (33 and 29 days post infection (dpi), respectively) (Specht *et al.*, 2017). However, systemic infection in zebrafish demonstrated a large difference in survival between R265 wt and KN99 wt suggesting *C. gattii* was more virulent. The zebrafish data with inoculation of 1×10^3 CFU agrees with data of (Thompson *et al.*, 2012) obtained from a mouse (ICR) brain infection model with 2×10^3 CFU inoculation. *C. gattii* strain used was 06-3908, serotype C, genotype VGIIa. This *C. gattii* strain, 06-3908 similarly to R265, is likely to be more virulent in mice than other molecular types of *C. gattii* because it represents VGIIa. VGIIa is described as the most virulent in mice (Kidd *et al.*, 2004; Fraser *et al.*, 2005; Byrnes *et al.*, 2010). *C. neoformans* used by Thompson *et al.* was USC1597 of serotype A, genotype VNI, thus it is similar to the background of KN99 wt used in my study. Others have shown that survival significantly deteriorates with VGIIa compared to VNI in *Drosophila*

melanogaster study with 5×10^3 cells inoculated through the thorax (Thompson *et al.*, 2014). However, it is not clear which VGIIa and VNI strains were used in the publication. Overall, it is clear that different cryptococcal strains exhibit altered virulence, which depends on the specific strains and infection models used. Nonetheless, the zebrafish data shows that *C. gattii* R265 wt infection results in decreased host survival than *C. neoformans* strain KN99 wt, which is broadly in line with the small amount of literature in this area (Thompson *et al.*, 2012).

4.3.3.2 Avirulence of R265 GFP14 in a mouse model of infection

The zebrafish study completed in this study on R265 GFP14 and its isogenic strain R265 wt highlighted differences in virulence. Thus, to investigate whether these results were applicable in a mammalian system a mouse model using the C57BL/6 strain was the most commonly used for studying cryptococcosis (Ngamskulrunroj, Chang, Sionov, *et al.*, 2012; Sionov *et al.*, 2015; Wiesner *et al.*, 2015). There was a large difference in survival of mice between the R265 wt and R256 GFP14 with infection with the mutant strain resulting in no mortality. The virulence of the R265 wt here was similar to published studies. For example, (Specht *et al.*, 2015) also showed deadly infection in C57BL/6 strain succumbing at 29 dpi, 28dpi (Ngamskulrunroj, Chang, Sionov, *et al.*, 2012) and 20 dpi (Upadhyia *et al.*, 2016) with the CBA/J strain.

4.3.3.3 *C. gattii* R265 GFP14 does not grow in the zebrafish

A high mortality rate with R265 wt in my zebrafish study, led to further interaction with macrophage investigations *in vivo* to assess disease progression. For this purpose, a fluorescent version was needed along with an assessment of both strains virulence. A fluorescent strain highlights its utility for elucidation of host-pathogen interactions. Due to the availability of R265 GFP14, being the best amongst other GFP mutants generated by (Voelz *et al.*, 2010), this particular strain was chosen for planned experiments. Surprisingly, the zebrafish infection with R265 GFP14 did not cause the same high level of mortality as R265 wt, suggesting that the GFP insertion was reducing virulence of the strain.

The extended survival in zebrafish challenged with R265 GFP14 raised a hypothesis of macrophages more efficiently phagocytosing the pathogen and macrophage killing of cryptococci (than wt). Therefore, the first question in the following zebrafish experiments series sought to determine whether R265 GFP14 survives in the host. The number of cryptococci was significantly lower at each time-point when compared to 2 hpi. This suggested efficient killing by macrophages. However, the number of cryptococci was not significantly different between 24, 48 and 72 hpi and appeared to be maintained at the same level. No one has examined intramacrophage killing for R265 GFP14. While intracellular proliferation rate and phagocytosis were assayed in macrophages (Voelz *et al.*, 2010), they do not directly represent the rate of death. Moreover, it was difficult to interpret such results without the context of intracellular and extracellular numbers, which are indicative of phagocytosis process. The analysis revealed that the number of extracellular cryptococci was lower than the number of intracellular cryptococci only at 48 and 72 hpi suggesting phagocytosis and possibly extracellular portion becoming a pool of intracellular cryptococci. Changes within an individual portion of cryptococci unveiled that the number of intracellular cryptococci was rather static. Interestingly, between 2 and 24 hpi intracellular proliferation is eminent in zebrafish infection with *C. neoformans* and this restrains phagocytosis (Bojarczuk *et al.*, 2016). By contrast, extracellular cryptococci dropped rapidly at 24, 48 and 72 hp when compared to 2 hpi. However, the comparison between 24, 48 and 72 hpi showed no difference somewhat suggesting stabilisation and plateau. Hence, it could be hypothesised that the infection included continuous uptake of extracellular portion and killing of internalised cryptococci. This explains the maintenance of intracellular portion. It is possible that this continuation of somewhat stabilised intracellular cryptococci is an effect of replication inside macrophages. The dominance of killing by macrophages seems more realistic since the total number of cryptococci is reduced at the end of the experiment. However, this study cannot discern intracellular proliferation, and use of time-lapse microscopy may help.

The mechanism of macrophage killing is not known for the R265 GFP14. It could be through the host reactive oxygen species (ROS) generated by macrophages.

It might be that host ROS do not facilitate intracellular survival. The opposite was seen for R265 wt (Voelz *et al.*, 2014). However, since the killing undoubtedly facilitates phagocytosis and this process is an essential function of the immune system, the latter became the primary matter of interest.

Interestingly, *in vitro*, percent phagocytosis by J774 macrophages (Voelz *et al.*, 2009) of the GFP mutant (33%) showed no difference when compared to its parental strain (38%) (Voelz *et al.*, 2010). *In vitro* J774 study of (Hansakon *et al.*, 2019) showed a significantly decreased phagocytic uptake of R265 wt at 2 hpi analysed by the (Sabiiti *et al.*, 2014) method when compared to *C. neoformans*. This publication focused attention on the cumulative comparison of 18 *C. gattii* and 23 *C. neoformans* strains but it drew up the possibility of R265 wt being not readily phagocytosed by macrophages. Perhaps the R265 GFP14 is favoured in terms of the phagocytic uptake. Unfortunately, due to practical reasons, this study was limited to the GFP strain only. It would be preferable to perform all of the host-pathogen interactions experiments in the zebrafish model with the use of the reference strain R265 wt. An apparent limitation of using R265 wt is the lack of fluorescent tag. Thus, the visualisation is limited and recognition of intracellular cryptococci straitened.

It became apparent that after infection of cryptococci, wherein the numbers of intracellular and extracellular cryptococci were similar, an immune response was initiated. To present this interesting case, a model of R265 GFP14 infection progression was proposed (Figure 4.38). Considering the fundamental assumptions of the model, all effects observed during the course of infection, were assigned to macrophages. Nonetheless, it was acknowledged that extracellular numbers could be phagocytosed by different cells of innate immunity in zebrafish.

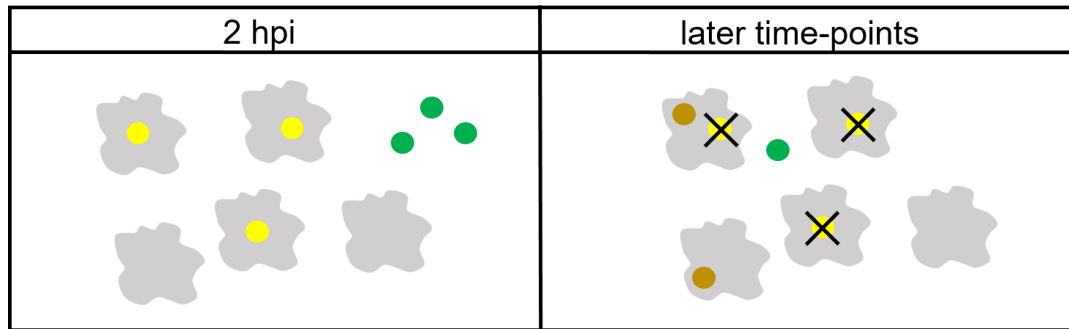


Figure 4.38 Diagrammatic representation of proposed model of R265 GFP14 infection progression in zebrafish larvae. R265 GFP14 cells (yellow) within macrophages (purple) are intracellular. R265 GFP14 cells (green) outside macrophages are extracellular. Newly internalised cryptococci are brown. One cryptococcal cell represents 10 cfu.

Based on the results it is likely, that the infection with R265 GFP14 is the process of simultaneous killing of previously phagocytosed cryptococci with the internalisation of new cryptococci, which were previously extracellular. The number of extracellular cryptococci significantly decreased over time likely due to the uptake by macrophages and subsequent phagocytosis. Although there were no significant differences between the numbers of infected macrophages, the possibility of unviable cryptococci containment cannot be excluded. Concomitantly, those cells that had been phagocytosed, might have been killed as suggested by the reduced numbers of total cryptococci injected. Again, there is no proof confirming R265 GFP14 cell death but the killing seems to be the best explanation considering the dropping numbers of injected cryptococci and the number of intracellular cryptococci remaining similar at all stages of infection. Therefore, my results indicate that *C. gattii* R265 GFP14 is attenuated in zebrafish because it is efficiently phagocytosed and killed by macrophages.

4.3.4 Analysis of phenotypes produced by R265 wt and R265 GFP14

The phenotypic analysis in this study revealed 21 potential substrate differences. The most surprising aspect of the analysis lies in the fact that the wild-type strain did not appear to use these compounds to generate NADH. R265 GFP14 appeared to use Krebs substrate (acetate, α -ketoglutarate, citrate, fumarate, malate), but R265 wt did not. Tags for functions in the tricarboxylic acid cycle

(TCA) known as the Krebs cycle, have been found for *C. neoformans* (Hu *et al.*, 2008). These included aconitase, malate dehydrogenase, isocitrate dehydrogenase, malic enzyme or fumarase (all putative) (Hu *et al.*, 2008). A comparison of the genome sequences of *C. gattii* WM276 and *C. neoformans* JEC21 shows that the WM276 has these genes (all putative) (D'Souza *et al.*, 2011). Although there are some minor chromosomal rearrangements, the majority of chromosomes are collinear between WM276 and R265 wt (D'Souza *et al.*, 2011). Aforementioned TCA related genes found in WM276 are present in R265 wt (D'Souza *et al.*, 2011). Thus it is assumed they are also present in R265 GFP14 because they are located on chromosomes other than chromosome 1 in R265 wt (D'Souza *et al.*, 2011) and some other genes important in the Krebs cycle locate on region of chromosome 1 that is assumed to be unaltered in R265 GFP14. This introduces a question: Why did R265 not seem to use Krebs substrates? What came to mind first was the fact that the plates were sealed. This is the only difference in comparison to other growth experiments in this thesis. Biolog plates were sealed to prevent a false positive reaction where dye is reduced by gas exchange with the air. Therefore, the plates were sealed for the 36 hours of the phenotypic experiments. Theoretically, the use of a sealing film can affect availability of oxygen. Since gases are constantly consumed and produced by cellular and metabolic reactions, a functional gas exchange mechanism exists to keep oxygen and carbon dioxide at a healthy level. In aerobic organisms, gas exchange is essential for respiration, which involves the uptake of oxygen and release of carbon dioxide. In the case of sealing therefore the possibility of impaired gas exchange exists, which might lead to carbon dioxide accumulation if cells use up oxygen. In other words the sealing might impair the results. Any sealed system may be prone to carbon dioxide cell injury but this would then be detected in a positive control (in my study glucose, data not shown as glucose was not a hit compound) and death resulting in no colour change would be seen. Both R265 and R265 GFP14 had colour changes for glucose. Therefore, it is rejected that the sealing impaired the results. However, this well had less colour change for R265 wt than for R265 GFP14, which was suspicious and might suggest altered physiological conditions (discussed later).

In contrast, there is no evidence of anaerobic degradation by yeast of α -ketoglutarate, citrate, acetate or fumarate in yeast. In this light, it is now reasonable to think that R265 wt simply did not perform Krebs cycle from acetate, α -ketoglutarate, citrate or fumarate. This can be supported by no growth on citrate for *C. gattii* serotype B (Chaskes *et al.*, 2008). However, a contradictory finding of the growth of *C. neoformans* var. *gatti* serotype B on this substrate was reported by (Lazéra *et al.*, 1998). Isocitrate lyase is required for growth on acetate plates (Rude *et al.*, 2002). The gene encoding isocitrate lyase is present in the R265 wt on chromosome 9 (D'Souza *et al.*, 2011) and it would be tempting to suggest that acetate could be used for energy. There is also evidence for acetic acid assimilation by *C. albidus* (Li *et al.*, 2015) and growth of *C. neoformans* H99 on acetate (Hu *et al.*, 2008). Moreover, generally *C. neoformans* serotypes B and C assimilate fumaric acid (Bennett *et al.*, 1978). Interestingly, there were two serotype B isolates which failed to assimilate L-malic acid and they also failed to assimilate fumaric acid in the study of (Bennett *et al.*, 1978). However, it is not known which of B serotype were the ones that did not utilise the compound in the publication of (Bennett *et al.*, 1978). In addition, assimilation tests are not informative of the pathway by which carbon source is used and perhaps they mean assimilatory mechanisms and not catabolic pathways. For instance, citrate can be metabolised via the glyoxylate cycle reactions, which then suggests anabolism. Perhaps this is a case for the R265 wt.

In regards to malate, the literature proposes, e.g. malate anaerobic fermentation by *Saccharomyces bailli* through the malic enzyme (Kuczynski and Radler, 1982). R265 wt has a gene encoding this enzyme and is located on chromosome 8 (putative) (D'Souza *et al.*, 2011). Therefore, there is a possibility for malate to be fermented by R265 wt. The issue in this present assay is that D, L malate was tested. As described in the result section, L-form is naturally occurring, whereas a mixture of L- and D-malic acid is produced synthetically (Brittain, 2001). Thus, it is unknown, whether the mixture would have been taken up, even to proceed with fermentation. Although fermentation cannot be excluded as the means of energy source, it has to be rejected in this present assay because it occurs in the complete absence of oxygen.

More recently, some preliminary respirometry has suggested that R265 wt respiration is abnormal. Oxygen consumption rate was measured, i.e. routine oxygen consumption, oxygen consumption not linked to ATPase function, maximum respiration and non-mitochondrial oxygen consumption. Routine oxygen consumption is measured in an oxygen-saturated solution in the respirometry chamber before any drugs are added and after cell suspension when stable oxygen flux reading appears. When this is achieved, respiration-modulating drugs are added. To measure oxygen consumption not linked to ATPase function (leak respiration), triethyltin bromide (TET) is added (Duvenage *et al.*, 2019). In the leak respiration state, proton translocation through the ATP synthase is thus inhibited by TET, which blocks protons moving through the ATP synthase (complex V) and this causes protons to accumulate in the intermembrane space. This increase inhibits electrons moving along the chain. So the change in oxygen consumption observed after TET addition tells how much electron transport is coupled to the movement of protons through the ATP synthase, which in turn tells how much it is coupled to ATP production (as movement of protons through the ATP synthase is what drives ATP production). In other words, following TET addition protons may enter the mitochondrial matrix only by diffusion, therefore termed leak respiration giving an assessment of how well electron transport is coupled to ATP production (personal communication with Dr Campbell Gourlay, University of Kent and Dr Lucian Duvenage, University of Cape Town). The maximum respiration is also called maximal electron transport chain capacity (uncoupled respiration) and measured when carbonylcyanide p-trifluoromethoxyphenylhydrazone (FCCP) is added (Duvenage *et al.*, 2019). This means electron flow through the complex I-IV is not limited by the bottleneck of oxidative phosphorylation (i.e. the action of ATP synthase). The maximum respiration is usually higher than the routine (personal communication with Dr Lucian Duvenage, University of Cape Town). Non-mitochondrial respiration is measured by addition of classical respiration inhibitors, i. e. antimycin A (complex III) and/or potassium cyanide (complex IV) (Duvenage *et al.*, 2019). The leftover oxygen consumption after antimycin/cyanide addition is the non-mitochondrial respiration as no electron transport is taking place. However, it is still possible for an organism to contain an oxidase

that is fully resistant to the inhibitor used. R265 wt possess an alternative oxidase gene (*AOX1*) (D'Souza *et al.*, 2011) and the oxidase has to be inhibited, too. *Aox1* can be inhibited with salicylhydroxamic acid SHAM (Duvenage *et al.*, 2019). The respiratory work of Dr Gourlay (unpublished) suggested that R265 respire at mitochondria but little of this respiration is coupled to ATP production. This was based on the observation that the leak respiration and routine were similar suggesting that the ETC and the oxygen consumption are not linked to ATP production at the ATP synthase. Normally oxygen consumption decreases after TET addition (personal communication with Dr Lucian Duvenage). Since the ratio between routine and leak respiration levels (respiratory control ratio) indicates how much the ETC is linked to ATP production, or how coupled respiration is (Duvenage *et al.*, 2019), it might be that respiration is not well coupled to ATP production in R265 wt strain. In addition, the leak control ratio described as the ratio of leak and the maximum capacity of ETC was very high for R265 wt as compared to other isolates tested. This suggests R265 wt is less efficient at obtaining ATP from oxidative phosphorylation. The maximal of ETC capacity (uncoupled respiration) was the highest as compared to routine, leak and non-mitochondrial respiration. However, it cannot be concluded at this stage that R265 wt might not be performing the Krebs cycle at all. This is because the measurement with FCCP (an uncoupler) disrupts the mitochondrial membrane potential and results in uninhibited electron flow through the ETC. Thus, it only shows how close to maximum capacity the organism is respiring. However, the non-mitochondrial respiration value for R265 wt was about 50% of the routine respiration (the total respiration under normal conditions). Together with the conclusion of R65 wt respiration at mitochondria not coupled to energy production, it seems plausible to think that the strain will need to rely on fermentation to produce the energy it needs for growth. Alternatively, it might be that R265 wt are dysfunctional in terms of ATP production and a good proportion of respiration occurs at alternative oxidase (*Aox1*). *Aox1* allows respiration and functioning of the TCA cycle when the ETC is disturbed (Lambers, 1982; Huh and Kang, 1999). *AOX1* is important for *C. neoformans* virulence as mice infected with *aox1* mutant had increased survival as compared to those infected with H99 (Akhter *et al.*, 2003). Alternative

oxidase is not coupled to the proton gradient generation across the mitochondrial membrane and thus is not very well coupled to ATP production. This means that alternative oxidase produces less ATP than classical oxidative phosphorylation (Helmerhorst *et al.*, 2002). Interestingly, R265 wt preliminary data with alternative oxidase inhibitor, (SHAM) suggests that it is resistant to alternative oxidase inhibition. This suggests R265 does not need the classical respiration and alternative respiration is a still functional pathway enabling the TCA cycle. Although there is no hard evidence in the respirometry that R265 wt does not perform Krebs cycle, this possibility cannot be rejected in my phenotypic array. Given that respiration behaviour could change depending on experimental condition, it is possible that in the PM1 assay, the non-mitochondrial respiration is much higher than the total respiration, which would suggest the fungus does not use the oxygen and the oxidative phosphorylation does not occur. Experiments investigating fermentation should be performed. This would give a clue about its capacity to upregulate the TCA cycle/oxidative phosphorylation if the respirometry profile changes (further discussed in section 6.2 Assessment of *C. gattii* virulence in zebrafish and mice). To conclude, all the three options are possible: fermentation, alternative respiration and the impeded TCA cycle in R265 wt. Experiments proposed to investigate these events are proposed in this chapter in section 4.3.7.3 Future work in respect to metabolic profiling of R265 and R265 GFP14.

In contrast, I believe my data suggests that R265 GFP14 utilised acetate, α -ketoglutarate, citrate, fumarate and D, L malate in the Krebs cycle. Acetate can enter the TCA cycle in the form of acetyl-CoA. A direct conversion of acetate to acetylo-CoA does not produce NADH (KEGG). This occurs via Acetate-CoA ligase (KEGG), present in R265 wt on chromosome 1 (D'Souza *et al.*, 2011). It is likely that R265 GFP14 strain possesses this enzyme as the region of Acetate-CoA ligase gene location is not affected in this strain. Further reactions of the Krebs cycle then yield NADH in R265 GFP14 but not for the wild-type. Direct α -ketoglutarate utilisation is not evident in the cryptococcal literature. α -ketoglutarate enters the TCA and yields NADH via α -ketoglutarate dehydrogenase action converting α -ketoglutarate into succinyl-CoA. R265 wt encodes the α -ketoglutarate dehydrogenase gene (putative) that is located on

chromosome 2 (D'Souza *et al.*, 2011) and therefore predicted to be unaltered in R265 GFP14. Thus, it is reasonable to think that R265 GFP14 can incorporate α -ketoglutarate into the TCA given that this region of the chromosome 2 was not disrupted by the GFP insertion. Citrate must be converted by aconitase that performs two reactions. First, a conversion of citrate to cis-aconitate and second, cis-aconitate to isocitrate. The analysis of (D'Souza *et al.*, 2011) confirms aconitase gene on chromosome 4 (putative). Thus, it is predicted this gene remains present in the GFP strain given that this region of the chromosome was not disrupted by the GFP insertion. Further reactions of the TCA yield NADH, e.g. conversion of D-isocitrate to α -ketoglutarate by the action of isocitrate dehydrogenase, predicted to be encoded on chromosome 9 (D'Souza *et al.*, 2011), which is unaltered in R265 GFP14. Fumarate can be converted in the TCA to malate via fumarase hydratase. The encoding gene is located on chromosome 3 (D'Souza *et al.*, 2011), thus this gene should be present in R265 GFP14. Although this reaction is reversible, once yielding NADH and in the reverse order NAD⁺, once fumarate is incorporated to the Krebs, it will lead to another NADH producing reactions, e.g. conversion of malate to oxaloacetate. This occurs through malate dehydrogenase. R265 wt encodes the malate dehydrogenase gene. It is located on chromosome 6 (D'Souza *et al.*, 2011), which is not affected in this study. Thus, it is assumed that R265 GFP14 also encodes this gene. Therefore, it is assumed that R265 GFP14 used both fumarate and malate in the TCA. In the case of R265 wt, as mentioned, there is no alternative degradation of fumarate. Malate could be fermented via the malic enzyme in R265 wt but fermentative conditions are ruled out in this present study because fermentation requires the absence of oxygen and this condition is rejected.

Pyruvate enters the cycle after conversion into acetyl-CoA by the pyruvate dehydrogenase, which is an oxidative process wherein NADH is produced. The pyruvate dehydrogenase gene is present in R265 wt on chromosome 1 (D'Souza *et al.*, 2011). Although this chromosome is altered in R265 GFP14, this gene occupies position on an intact remaining region. Therefore, it is plausible to think that R265 GFP14 incorporated this substrate via pyruvate dehydrogenase. Suggested fermentative mode of energy acquisition for the wild-type could convert pyruvate anaerobically to lactate by the action of lactate dehydrogenase,

which oxidises NAD⁺ to NADH (KEGG database). Indeed, R265 wt possess gene encoding this enzyme and it is located on chromosome 11 (D'Souza *et al.*, 2011). If fermentation were taking place, this is difficult to assess in this assay, as fermentation would replenish NAD⁺ from the NADH produced in glycolysis.

Pyruvate discussion raises an opportunity to discuss methyl pyruvate, which was one of the hits in the Biolog assay. Methyl pyruvate is a novel metabolic activating agent for mitochondria that seems to provoke a slight or transient increase in ROS production in tumour cells (Nishida *et al.*, 2014). It should be a substrate for the TCA cycle since it is pyruvic acid derivative. In pancreatic β cells represented as mitochondria it did not relate to mitochondrial ATP production (Lembert *et al.*, 2001; Duffer *et al.*, 2002) although produced more NAD(P)H than pyruvate (Duffer *et al.*, 2002). The NAD(P)H cannot be separated spectrally from NADH autofluorescence and the measured autofluorescence is always a mixture of both NADPH and NADH when measured as NAD(P)H (Blacker and Duchon, 2016). Therefore, the publication was not conclusive in terms of NADH levels.

Methyl pyruvate initiates depolarisation of β cells (Lembert *et al.*, 2001) and this results in the opening of voltage-dependent Ca₂⁺ channels, and influx of Ca₂⁺ is the main trigger for insulin secretion (MacDonald and Wheeler, 2003). The increase in the protonic potential is accompanied by a rise in ROS production (Korshunov *et al.*, 1997). In order to keep ROS at harmless, levels cofactors such as NADH and NADPH play essential roles. NADH generates ATP via catabolism, during which ROS are generated, whereas NADPH is needed for anabolism and protects the cell from the oxidative stress. In the aspect of the relationship between the oxidative stress regulation and the central carbon metabolism under oxidative stress condition, NADH concentration must be reduced, while NADPH level must be increased (reviewed by (Shimizu and Matsuoka, 2019)).

It might be that methyl pyruvate exerts or exacerbates harmful oxidative stress. ROS are produced mainly by mitochondria (reviewed by (Turrens, 2003; Kowaltowski *et al.*, 2009; Murphy, 2009). To keep a steady-state control over ROS production, aerobic organisms have evolved a complex array of defensive systems to eradicate ROS and return to physiological conditions (reviewed by (Birben *et al.*, 2012; Panieri and Santoro, 2016)). It is known that to help protect against the destructive effects of ROS, *Cryptococcus* produces, e.g. superoxide

dismutase (SOD) enzyme production (Cox *et al.*, 2003) that converts superoxide into sodium peroxide, which is further converted to water by glutathione peroxidase or catalase. The last two enzymes are also produced by the fungus ((Missall *et al.*, 2005) and (Giles *et al.*, 2006), respectively). Paradoxically, *C. gattii* R265 wt uses host ROS to induce an intracellular survival and proliferation within macrophages. The use of apocynin, which blocks host ROS, reduces growth of R265 wt. The R265 GFP14 was not assessed for apocynin effect (Voelz *et al.*, 2014). Generally, under stress, mitochondrial tubular morphology results from mitochondrial fusion (reviewed by (Youle and van der Bliek, 2012)). This has been observed both in *C. neoformans* under hydrogen peroxide treatment (Chang and Doering, 2018) and in *C. gattii* R265 wt (Voelz *et al.*, 2014). The fusion has been found to protect from cell death (Sugioka *et al.*, 2004; Chaudhari and Kipreos, 2017). The tubular morphology was observed for both R265 wt and R265 GFP14 after engulfment by macrophages (Voelz *et al.*, 2014). Various ROS are produced within the phagosome and cause oxidative damage. Therefore, engulfment by macrophages mimics the oxidative stress within a phagosome.

Although the reaction to host ROS is peculiar, one aspect of own ROS generation in terms of central metabolism has not been considered. As mentioned, ROS are mainly produced by mitochondria, specifically at electron transport chain (ETC) ((reviewed by (Murphy, 2009; Brand, 2010)). In order to minimise the oxidative stress and ROS production, the amount of electron flux through ETC gets decreased by repressing the respiratory chain enzymes and reducing NADH production at the TCA cycle (or e.g. by activating the glyoxylate pathway). This means that TCA cycle activity is repressed (reviewed by (Shimizu and Matsuoka, 2019)). Considering that R265 wt did not appear to perform Krebs cycle, I believe, that if methyl pyruvate induces ROS, TCA would be suppressed anyway and NADH would be minimised. Perhaps this is a case for R255 wt. Moreover, methyl pyruvate might induce strong oxidative stress in the R265 wt leading to intracellular ROS accumulation. It might be that ROS build up compromises membrane integrity. This was shown *in vitro* in R265 wt by fluconazole treatment. It led to accumulation of ROS, which correlated with compromised cryptococcal membrane integrity (Peng *et al.*, 2018). In addition, it might be that under methyl

pyruvate a tubular mitochondrial morphology is induced as demonstrated by hydrogen peroxide treatment in R265 wt (Voelz *et al.*, 2014). Given that tubular yeast are non-proliferative (Voelz *et al.*, 2014), the effect observed in my present study might be combined and R265 wt is in a somewhat metabolic latent phase. If methyl pyruvate action is through ROS, it is not understood why R265 GFP14 utilised this substrate.

Alternatively, methyl pyruvate might not be linked with detrimental ROS generation but with TCA cycle. As mentioned, pyruvate enters the cycle after conversion into acetyl-CoA by the pyruvate dehydrogenase complex (KEGG). Perhaps methyl pyruvate does not enter the TCA in R265 wt and a fermentive mode of energy acquisition would be suggested if not for the fact that the assay rejects anaerobic conditions required for fermentation. It could be argued that it is not possible by *Cryptococcus* to ferment pyruvate as the process is associated with alcohol production and there is no evidence for alcohol production in the cryptococcal field. However, an attention to pyruvate metabolism by *C. neoformans* has been drawn recently. The analysis of biofilms formed by *C. neoformans* showed that lactoylglutathione lyase is up-regulated suggesting pyruvate is likely to be used in energy metabolism via lactate metabolism (Santi *et al.*, 2014).

A suggested non-mitochondrial respiration for R265 wt, shown by the abolished TCA cycle, can also be supported by the fact that Tween 40 and Tween 80 were not metabolised. The mechanism of Tween 80 utilisation was suggested for *Pseudomonas aeruginosa* (Ohkawa *et al.*, 1979). It involves its outer membrane esterase, which has a preference for long-chain fatty acids. Mutants that do not have esterase activity do not grow on Tween 80 as a sole carbon source. Microorganisms that express esterase activity produce a halo zone around colonies due to crystals of the calcium salt of the fatty acid released by lipolysis (Sierra, 1957). This suggests a possible role of the esterase in the utilisation of fatty acids from Tween. Lipase (a subclass of esterase) activity was assessed for both *C. neoformans* and *C. gattii* (Hagen *et al.*, 2015). Interestingly, lipase activities, tested using Tweens 40 and 80, showed variable reactions among the various species in the study of (Hagen *et al.*, 2015). Furthermore, temperature

appeared to be a factor. Importantly, the activity for R265 was higher at 25°C than at 37°C. My assay was established at 30°C (Nielsen *et al.*, 2005) and the response to Tweens was lost for the wild-type R265. It would be of interest to test Tweens in an overnight growth assay using the Kurtzman method (Kurtzman *et al.*, 2011). This method tests the ability of yeast to grow on a particular carbon source. The test can be done on either solid or liquid media. The liquid media is considered more reliable due to better substrates availability. Therefore, yeast nitrogen broth (YNB) (Kurtzman *et al.*, 2011) is recommended for growth in Tweens. Nonetheless, the data for R265 GFP14 strain in Tweens suggests a fatty acids metabolism pathway. Presumably, their degradation, suggested by lipolysis in (Hagen *et al.*, 2015) and NADH formation in my study. Fatty acid degradation leads to the formation of acetyl-CoA in the final step termed β -oxidation, the entry molecule for the Krebs cycle. β -oxidation yields NADH and is well known to perform in aerobic conditions. It remains obscure, why R265 wt utilised Tweens at 25°C and at 37°C in (Hagen *et al.*, 2015). The publication of (Hagen *et al.*, 2015) regarding *C. neoformans* and *C. gattii* used a method of (Sierra, 1957) using peptone agar plates with each of the Tweens. It is harder to grow on plates in comparison to liquid media. It is concluded that incubation time for Tweens was 3-4 weeks because grow patterns on different carbon sources in (Hagen *et al.*, 2015) was investigated using the method of (Kurtzman *et al.*, 2011), which typically applies up to 4 weeks incubation. This yields a conclusion of a possible adaptation of R265 wt to utilise compounds by long incubations in the study of (Hagen *et al.*, 2015). Therefore, as mentioned, it would be recommended to repeat the growth in YNB. Although R265 wt respiration is suggested non-mitochondrial, perhaps the fungus can still use other enzymatic pathways in the mitochondria. This might be the case, as at the end of phenotypic experiment in this present study, some readings appear, e.g. for Tween 40.

In addition, the assay revealed that lactate was used by R265 GFP14. It is possible to gain NADH from this compound by the action of L-lactate dehydrogenase (KEGG). As for R265 wt, it might be that acetate was utilised in the propanoate metabolism.

All the reviewed phenotypic data so far indicates significant differences in metabolic requirements. There is one more aspect to discuss related to use of sugars. Most fungi favour assimilation of sugars because their catabolism via glycolysis and respiration is energetically favourable (reviewed by (Ene *et al.*, 2014)). In addition, it is known that *C. neoformans* requires a glycolytic pathway for disease but not for persistence (Price *et al.*, 2011). Blocking glycolysis at the entry point by deleting two hexose kinases resulted in decreased fungal persistence in the rabbit CSF model and attenuated the virulence in the murine inhalation model of cryptococcosis. Blocking the carbon exit by the deletion of pyruvate kinase enhanced the persistence in the lungs in the inhalation model without causing the disease. The removal of pyruvate kinase led to severely decreased persistence in the rabbit CSF (Price *et al.*, 2011). Therefore, glycolysis seems to be important in cryptococcal pathogenesis. Thus, one could argue that R265 wt should perform glycolysis. It is tempting to conclude that R265 wt did not perform glycolysis in the Biolog assay. The data for glucose for R265 wt is negative (not shown). Considering that *C. neoformans* grows at 2% and 0.06% of glucose in YPD *in vitro* (Williams and del Poeta, 2011), it is expected for R265 wt to grow in the Biolog assay because the concentration of glucose in this present study was 0.4% equating to 22 mM. The cells were added to the well in YNB supplemented with histidine, uracil and leucine to satisfy auxotrophic requirements for growth. After supplementing YNB medium with amino acids, which are supplements for corresponding auxotrophic markers commonly present in *Saccharomyces* laboratory, the pH of the medium was adjusted to 5.4, in agreement with the manufacturer's instructions. IFY-0 was the inoculating fluid, which is non-nutritive and is supplemented with ammonium sulphate, potassium phosphate dibasic, potassium phosphate dibasic and magnesium sulphate. Since, the YNB with acidic pH was the medium, wherein cryptococci were suspended, and the cells were added to the microplates as the last, it might be they had been acidified. It is acknowledged that cryptococci grow in culture medium at acidic pH (Levitz *et al.*, 1997). This gives it a survival advantage in the phagolysosome. It is also acknowledged that fungi have mechanisms to regulate intracellular pH and to maintain this pH homeostasis in response to environmental changes. For instance, fungal vacuolar proton-translocating ATPase (V-

ATPases) couple hydrolysis of ATP to proton transport and therefore are important in establishing pH gradients (reviewed by (Orij *et al.*, 2011)) by pumping protons out of the cytosol (Martínez-Muñoz and Kane, 2008). R265 wt possess a Vacuolar (H⁺)-ATPase subunit (putative) on chromosome 4 (D'Souza *et al.*, 2011) with V-type ATPase domain (NCBI). Still, the incubation in acidic medium can have an effect on the intracellular pH of a cell.

It is possible that YNB medium affected the intracellular pH of R265 wt. Some media contain unwanted weak acids or weak-acid buffers are added. Lowering the pH in these media results in these compounds protonation and therefore induces a weak-acid stress that lowers the intracellular pH of the cell (Orij *et al.*, 2009). The YNB contains folic acid, which in the review of (Gazzali *et al.*, 2016) is described as a weak acid. At acidic pH, a substantial fraction of weak acid gets protonated. This form easily passes the plasma membrane because it dissolves in the membrane. In the neutral cytosol, most of the weak acid dissociates. This leads to intracellular proton and anion release. Both the proton and the anion can exit the cell at the cost of ATP. The low pH of the medium causes the anions to re-associate with protons outside the cell and they diffuse back through the membrane. This might cause a constant drain on the cells energy reserves (reviewed by (Orij *et al.*, 2011)). The ability of weak acids to acidify the cytosol was considered as the main contributor to growth inhibition (Krebs *et al.*, 1983). In addition, the rate limiting enzyme of glycolysis, phosphofructokinase, is sensitive to small changes in pH in the physiological range, a high pH increasing its activity (Trivedi and Danforth, 1966). Perhaps in the Biolog assay R265 wt does not grow well, phosphofructokinase is impeded and therefore glycolysis is hampered. It would be useful in the future to run an overnight growth experiment in the Biolog media (IFY-0, YNB and a combination of both) as well as an overnight growth experiment in the concentration of glucose from the Biolog assay but in trying a different medium. This would answer whether the Biolog assay allows cryptococci growing in glucose.

In addition, R265 wt did not use fructose, sucrose or mannose, although catabolic pathways for these do not involve NADH production but eventually lead to glycolysis. If glycolysis did not occur for the wild-type when incubated in glucose,

this would explain the lack of other sugars utilisation for energy. To check if glycolysis is performed, pyruvate, the product of glycolysis, could be measured using, e.g. a fluorometric assay described by (Zhu *et al.*, 2010) or available commercially pyruvate assay.

The sugars, fructose, glucose, sucrose, mannose, are also fermentable to alcohol. This process is anaerobic and thus should not occur in my experiments. However, in some yeasts the Crabtree effect can occur repressing respiration by the fermentation pathway in aerobic conditions (De Deken, 1966) but *Cryptococcus* is Crabtree-negative. In contrast to related sugars, xylose is not fermentable. For instance, *S. cerevisiae* is considered unable to efficiently metabolise xylose to alcohol, and thus, a lot of research has engineered this yeast to allow xylose consumption and alcoholic fermentation (reviewed by (Patiño *et al.*, 2019)). Some of the suggested reasons for the impaired ability to alcohol fermentation are low xylose reductase and xylose dehydrogenase activities (Batt *et al.*, 1986) and cofactor imbalance in the xylose reductase/xylitol dehydrogenase pathway (reviewed by (Hou *et al.*, 2017)). However, even without proceeding to fermentation, both pathways (the xylose reductase and xylitol dehydrogenase) produce D-xylulose (KEGG). My study shows increased NADH production for both R265 wt and R265 GFP14 strain with D-xylulose. However, a larger increase was seen for the GFP stain. This suggested the reduction of D-xylose to xylulose. This occurs in two steps. Xylose is converted to xylitol via xylose reductase and xylitol converts into xylulose via xylitol dehydrogenase. The second reaction yields NADH. Interestingly, the analysis of (D'Souza *et al.*, 2011) indicated the absence of xylose reductase gene. However, aldo-keto reductase was assessed in the R265 wt on chromosome 11 (D'Souza *et al.*, 2011). Since aldo-keto reductases are a family of proteins that include xylose reductase, it might be that assessed by (D'Souza *et al.*, 2011) aldo-keto reductase fulfils a function of xylose reductase. Moreover, xylitol dehydrogenase gene was also assessed in R265 wt on chromosome 3 (D'Souza *et al.*, 2011). The locations of these enzymes are intact in the R265 GFP14. Therefore, it seems plausible to propose that both strains can degrade D-xylose. It is, however unexplained, why R265 GFP14 was more efficient. On a final note on sugars: glucose, fructose, sucrose and xylose supported growth of *C. gattii* NIH isolates 198 and 444 which

are of B serotype (Chaskes *et al.*, 2008). A publication of (Hagen *et al.*, 2015) describes specifically xylose utilisation by R265 wt. Xylose is proved to be assimilated by *C. neoformans* from the pentose pathway (Cherniak, O'Neill, *et al.*, 1998). This pathway is anabolic so cannot be indicated by the Biolog assay. This encourages reflection that assimilation or utilisation of a substrate does not necessarily have to support NADH production. Another example of the confusing utilisation/assimilation term is the utilisation of sucrose. There is evidence the sugar is utilised by *Cryptococcus*. In the study of (Vimercati *et al.*, 2016) a Biolog assay was used at 10°C after 4 days in the dark, but it is not known which strain was used. In (Benham, 1956) sucrose utilisation in *C. neoformans* was assessed by Wickerham's method (Wickerham, 1951) for carbon assimilation by *C. neoformans* was used, which employs 25°C and up to 24 days incubation. The publication of (Hagen *et al.*, 2015) regarding *C. neoformans* and *C. gattii* used a method of (Kurtzman *et al.*, 2011) at 25°C after 3-4 weeks of incubation. All of the methods were growth based. Thus, they rather indicate growth than NADH production. It also suggests a possible adaption to utilise substrates by long incubations. For example, malic acid is generally utilised by *C. gattii* serotype B in the mean of growth in media at 2 or 5 days (Bennett *et al.*, 1978). In my assay, the wild-type R265, serotype B did not use the substrate as a source of energy. This raises many questions, e.g. would it be used if the experiment was longer? It could be as some increasing readings appeared at about 32 hours. As mentioned long incubation times may lead to an adaption to utilise compounds.

4.3.5 The mechanism of R265 GFP14 attenuation *in vivo*

From the results obtained in both larval zebrafish and murine models, the most striking observation was that fluorescent *C. gattii* strain R265 GFP14 had impaired pathogenesis. It was therefore possible to hypothesise that the random GFP insertion into R265 wt strain (Voelz *et al.*, 2010) changed to some degree the R265 parental strain genome which resulted in a high survival of the animals. Genome sequencing revealed that region missing in R265 GFP14 was equivalent to 32 kb on R265 wt on chromosome 1, resulting in the loss of six genes (see results chapter). All of them have been found in *C. gattii* reference strain WM276 (D'Souza *et al.*, 2011). Subsequent experiments compared R265 wt with R265

GFP14 showed that these two strains exhibited different use of carbon sources and R265 GFP14 was more efficient at the substrates assimilation suggesting a metabolic difference between R265 wt and R265 GFP14.

Gene loss and virulence

The hypothesis of attenuated virulence linked to genes deletion is strongly supported by the evidence from the study of (D'Souza *et al.*, 2011). Genome hybridisation studies revealed that *C. gattii* fluorescent strain WM276 GFP2 had a missing region of ~75 kb. The deletion knocked out 24 genes in chromosome 11 and caused a virulence defect in C57BL/6 mice. The genes included a number of putative sugar transporters and glycosyl hydrolases, which are of paramount importance and *Cryptococcus* lacking these genes cannot utilise, for example, raffinose sugar. This was explained by the deletion of the invertase gene (D'Souza *et al.*, 2011) since invertase hydrolyses raffinose to melibiose and fructose (Doudoroff, 1945). Therefore, it was speculated that the deletion of six genes in my study might have detrimental consequences in the fungal growth. The growth, metabolism and virulence are interlinked. Although the literature regarding these six genes is not evident, it is possible that they have a function in R265 wt metabolism and therefore in virulence. For instance, R265 GFP14 does not have a gene encoding racemase (analysed with the help of Dr Choudhury). According to (D'Souza *et al.*, 2011), this gene is termed alanine racemase. Interestingly, alanine racemase gene knock-out attenuates the pathogenicity of bacterium *Aeromonas hydrophila* in BALB/c mice and carp fish (Liu *et al.*, 2019).

It is difficult to explain R265 GFP14 gene/genes loss in the context of virulence loss, but it might be related to the concept of antivirulence. Sporadically, certain genes must be inactivated or deleted for full expression of the pathogen phenotype to occur. These genes are described as antivirulence genes (reviewed by (Bliven and Maurelli, 2012)). This is supported by the fact that R265 GFP14 does not have a different ability to grow in macrophages in comparison to the parental strain R265 wt, even though it has lost its genes (Voelz *et al.*, 2010). In addition or alternatively, it seems important that *Cryptococcus* expression profiles

under various conditions play a role in its virulence. This clue was provided in the Results section. Moreover, gene deletion in a pathogen might improve host immune response. For instance, one of the genes deleted in R265 GFP14 is rhamnosidase (CGB_A0040C), described as putative. In many teleost fish, rhamnose-binding lectins are involved in immune responses (via complement) (Gao *et al.*, 2018). It could be that rhamnosidase in the wt strain hydrolyses rhamnose-binding lectins and thereby attenuates the host innate immune response while the opposite occurs in the GFP mutant.

Gene loss, virulence and metabolism

Gene deletion can be also linked with metabolism. For instance, the loss of both hexokinases in *C. neoformans* results in the inability to utilise glucose. The loss of both hexokinases together, but not single deletions, results in reduced virulence in mice (Price *et al.*, 2011). In reviewing the literature, carbon utilisation was found to be associated with the continued survival of host-restricted pathogens. Carbon is crucial for pathogenic fungi to grow and persist within a host (reviewed by (Ene *et al.*, 2014)). Both the pathogen and infected host compete for the same nutrients trying to influence the behaviour of the other (reviewed by (Passalacqua *et al.*, 2016)). I concentrated on carbon sources to investigate the differences between R265 wt and R265 GFP14 since pathogenic fungi have evolved different carbon assimilation profiles that presumably reflect their different niches (reviewed by (Ene *et al.*, 2014)).

This work found evidence of increased oxidative phosphorylation activity in the GFP14 mutant. It is not understood how gene deletion results, virulence results *in vivo* translate to phenotypic results. However, it is likely that R265 wt might not perform the TCA cycle because the inoculation fluid was not rich in iron and TCA and oxidative phosphorylation *C. gattii* genes are abundantly expressed when iron is available in the culture medium but not in iron replete medium (Crestani *et al.*, 2012). This means that iron reduction affects the mitochondrial function in *C. gattii*. This is interesting as iron limitation increases the capsule size (Vartivarian *et al.*, 1993). Given both CO₂ and low iron influence capsule size, this

is even more interesting because these conditions mimic some situations that *Cryptococcus* encounters during lung infection (Zaragoza, Rodrigues, *et al.*, 2010). R265 wt grew worse than R265 GFP14 in the mice lungs (personal communication, Jacob Rudman, a PhD student in the Johnston lab), which suggests that R265 wt might not perform TCA cycle either *in vivo* nor in PM1 arrays probably due to iron limitation. However, with the knowledge that R265 wt has an impaired oxidative phosphorylation, it is even harder to interpret the phenotypic data. It might be that the difference with GFP mutant might be that it is more stressed in PM1 assay and so it tries to activate mitochondria. This might result in greater metabolic flexibility with respect to carbon utilisation and metabolic adaptation but this prevents its flourish, likely due to the inability to activate the right pathway. It is not clear what the possible functions for these genes are and my PM1 array did not answer this question due to the fact of dealing with multiple knock-out mutation in the R265 GFP14. This also demonstrates that the proposed differences in the TCA cycle utilisation between R265 and R265-GFP cannot be brought to the level of six genes in total or a single gene. An apparent limitation of the phenotypic assay turned out to be its designed strength, i.e. the idea of testing a single gene under a number of nutritive conditions. The array can be used to directly assay the effects of genetic changes on cells, especially gene knock-outs, but not in the situation of testing the genes function while not knowing at all what the genes are involved in (the six genes are not fully characterised and 5 of them have domains predicted). Thus, while getting evidence of impaired oxidative phosphorylation, it is difficult to draw clear conclusions, which of the genes is involved in this process. Single knock-outs in the wt followed by PM1 arrays would help to find gene function as phenotypes are the expression of genotypes and reveal gene function when a single gene is investigated under several conditions (Bochner, 2003). Additionally, sequence similarity search should be performed with basic local alignment search tool (BLAST). This will answer if gene/genes are found in other organisms and will facilitate protein function prediction. No study to date has examined R265 metabolism *per se*. I believe that cryptococci can only establish an infection when able to acquire usable food sources. However, the literature regarding the preferences to fuel itself is not evident *in vitro* or *in vivo* for

Cryptococcus. R265 wt is VGIIa type strain from the Vancouver Island outbreak. Cryptococcosis caused by this molecular type presents with pulmonary disease in humans (Galanis *et al.*, 2009; Harris *et al.*, 2011) and mice infected with R265 wt die from extensive pulmonary infection (Ngamskulrungrroj, Chang, Sionov, *et al.*, 2012). R265 wt grew better in the lungs of mice infected in this present study whereas R265 GFP14 had impaired growth in the lungs and resulted in 100% animal survival (personal communication, Jacob Rudman, a PhD student in the Johnston lab). A comparison of previously described serial analysis of gene expression (SAGE) libraries from *C. neoformans* cells grown in YNB and low ion media with SAGE on cells recovered by bronchoalveolar lavage (BAL) from mice lungs at 8 and 24 hours after infection revealed significant differences in gene expression. For example, tags for genes encoding the TCA cycle enzymes aconitase and succinate dehydrogenase were elevated in the lung libraries. However, tags representing three other TCA cycle enzymes, namely isocitrate dehydrogenase, malic dehydrogenase and fumarase were lower in the lung libraries than in one or both of the *in vitro* libraries. Importantly, a tag for the gene encoding phosphoenolpyruvate carboxykinase (*PCK1*), which controls the only irreversible step in gluconeogenesis, was higher in both *in vivo* libraries at 8 and 24 hours post infection. *PCK1* elevation implies glucose limitation during early infection (Hu *et al.*, 2008). The authors suggested that murine pulmonary infection represents a nutrient-limiting environment for invading *C. neoformans* (Hu *et al.*, 2008). This is supported by the fact that the secretions from respiratory airways have a very low glucose concentration in healthy individuals (<0.05 mM) (Philips *et al.*, 2003). In addition, the tags for genes encoding glycolytic functions including glucose-6-phosphate isomerase and phosphoglycerate mutase were relatively low in the lung libraries. Moreover, *in vitro* analysis indicated that the expression of hexose transporter (*HXT1*) was dramatically higher at 0.2% glucose compared to 2% glucose. This suggests that *HXT1* has a role in glucose sensing in low glucose availability (Hu *et al.*, 2008). However, the tag for *PCK1* was increased in the SAGE analysis of pulmonary infection (Hu *et al.*, 2008), but not *in vitro* in macrophage internalised cryptococcal cells (Fan *et al.*, 2005). This suggests that in the publication of (Hu *et al.*, 2008) cryptococci might not have been internalised and a difference between the pulmonary infection and the intracellular

environment might exist which leads to a different metabolism mode. Phagocytosis induces genes involved in lipid degradation and fatty acid catabolism but does not induce gluconeogenesis genes (Fan *et al.*, 2005). The SAGE analysis and phagocytosis data of (Fan *et al.*, 2005) suggest that *Cryptococcus* displays different metabolic profiles depending on the *in vivo* or *in vitro* infection whether it is internalised or not. It means that *in vitro* and *in vivo* conditions might exert different energy acquisition modes. Thus, in my present *in vitro* study, R265 wt might not be performing TCA cycle. Instead, fermentation is suggested. Equally, it might be performing gluconeogenesis, which is the reverse of glycolysis and it is an anabolic process, thus NADH cannot be elevated. A switch from glycolysis to gluconeogenesis occurs in yeast. For example, in response to nutrient starvation, *Candida albicans* shifts from glycolysis to gluconeogenesis. This is seen as an adaptation to enable the host invasion and pathogenesis by *C. albicans* (Mayer *et al.*, 2013). Thus it is possible that R265 GFP14 could not adapt to *in vivo* conditions and that a potential for differential metabolic requirements across fungal pathogens exist. This might depend on the host niche occupied by each species and the models used to test each mutant (reviewed by (Ries *et al.*, 2018)). Although fungi experience a variety of micro-environmental conditions *in vivo* and the ability to adapt to and thrive under several carbon conditions is critical for virulence (Barelle *et al.*, 2006), far too little attention has been paid to *in vivo* versus *in vitro* experiments such as to genes expression of fungi that are metabolically active during host infection or *in vitro* conditions that simulate mammalian environments. Therefore, I cannot understand why *in vitro/in vivo* phenotypes are different. I was hoping to obtain some clearer conclusions from PM1 phenotypic array that would point out to a single gene, but was unfortunate and the experiment has its limitation. It became apparent that a significant inconvenience was multiple knock-out mutation of the R265 GFP14. I do not think there is a simple answer to a question how gene deletion translates into virulence or how could the R265-GFP strain exhibit greater metabolic flexibility with respect to carbon utilisation or how could this in turn result in impaired virulence. Currently it is not known if the TCA cycle utilisation always determines the cryptococcal triumph and which carbon sources have to be obtained in which quantities from the environment and in the context

of infection. Tags for functions in the tricarboxylic acid cycle (TCA) known as the Krebs cycle, have been found for *C. neoformans* (Hu et al., 2008). These included, e.g. aconitase, malate dehydrogenase, isocitrate dehydrogenase, malic enzyme or fumarase (all putative) (Hu et al., 2008). A comparison of the genome sequences of *C. gattii* WM276 and *C. neoformans* JEC21 shows that the WM276 has these genes (all putative) (D'Souza et al., 2011). Aforementioned TCA related genes found in WM276 are present in R265 wt (D'Souza et al., 2011). Thus it is assumed they are also present in R265 GFP14 because they are located on chromosomes other than chromosome 1 in R265 wt (D'Souza et al., 2011) and some other genes important in the Krebs cycle locate on region of chromosome 1 that is assumed to be unaltered in R265 GFP14. It is not understood if it will be the genes listed by (Hu et al., 2008) or by (Crestani *et al.*, 2012) that guarantee the TCA performance or if the six genes deletion incites the cycle, with a concomitant phenotype suppression. I do not know how gene deletion resolves virulence but there is an opportunity to understand it in the future (see Future work and Major experiments to bring Chapter 4 towards a publication).

4.3.6 Future work

4.3.7.1 Genetic work in R265 wt and animal survival assay

It is acknowledged that the hypothesis of deleted genes being important for virulence in animal models may raise further questions about the actual number of genes having an impact on the outcome of infection with R265 GFP14. For example, this phenotype may be caused by a single gene deletion. Thus, a further study with more focus on the genes is suggested. Particularly, single gene knock-outs in the R265 wt independently to identify whether the same phenotype seen with the GFP strain in zebrafish/mice would be reproduced. This should be confirmed by survival assays. Ideally, the goal would be to identify just one gene responsible for the high zebrafish/mice survival as seen with the GFP strain. It would appear that it would be the one of those six that had an effect. Of course, if that was unsuccessful, combinations of genes should also be tried.

However, it should be noted that in eukaryotic organisms gene positioning on a chromosome is known to affect its expression (Wilson *et al.*, 1990). This phenomenon is also seen in prokaryotes. Expression of a reporter gene cassette, comprised of *E. coli lac* promoter driving expression of GFP, varies by ~300-fold depending on its precise location on the chromosome (Bryant *et al.*, 2014). Genomes are not organised randomly. Gene positioning has remained unchanged throughout evolution, which points to a functional role for positioning in genome activity and homeostasis (reviewed by (Takizawa *et al.*, 2008)). Thus, gene positioning will be important for fungi, too. Therefore, the rescue of the phenotype seen with the R265 GFP14 might not be obtained, unless the gene/s are located in positions indicated in the R265 parental strain. An important question is also whether the downstream genes might be altered, not just the missing ones. In addition, if one of the missing genes is a regulatory, it might alter the function of others. Alternatively, another interesting experiment for the future would be with R265 GFP14 and rescuing the phenotype by reintroducing gene/few genes or all of those six genes (depending on the outcome of the above-mentioned study) with keeping the GFP in. If the virulence defect persists, this might be rather related to alternative gene/genes positioning than GFP having an effect on virulence.

4.3.7.2 Genes function

Revealing functions of genes and proteins encoded is one of the major challenges of molecular biology. Amino acid sequence determines protein structure and the structure shapes the protein function. Proteins sharing a similar sequence often have similar functions, even in distantly related organisms (reviewed by (Pearson and Sierk, 2005)). This means that orthologues proteins (the same protein in a different species) will perform similar functions. Therefore, sequence similarity search should be performed with basic local alignment search tool (BLAST). This will answer if gene/genes are found in other organisms and will facilitate protein function prediction. However, they might not be found by BLAST in other organisms as only sequenced strains show up in BLAST. This might be the case for hypothetical proteins CNB05730 and CNB05720 as they

are uncharacterised. These two genes characterisation might be a challenge since no information about them is available.

The genes might appear fungi specific. Therefore, they could be drug targeted. The genes, however, should be investigated in detail. For example, protein domains function should be characterised because their annotation is an alternative approach to sequence similarity searches. By convention, domains are defined as conserved, functionally independent protein sequences. They have specific functions, e.g. binding to a specific molecule or catalysing a reaction. Therefore, they are used for predicting the functions of whole proteins. Because the event of speciation occurred so long ago, it is accepted that a domain from different species will have similar function in *Cryptococcus*. Domain characterisation is also important in another aspect. Protein domains serve as drug targets (Wang *et al.*, 2012) and so possibly R265 wt could be drug targeted. It would be interesting to know if the genes deleted whilst GFP-tagged R265 generation have a defect in virulence. The identified genes should be searched for their role in *Cryptococcus*. For example, the study of (Martinez and Casadevall, 2007) suggested that polysaccharide matrix includes rhamnose. According to KEGG database, α -L rhamnosidase utilises an inverting mechanism of hydrolysis, releasing β -L-rhamnose. Thus, it is possible that rhamnosidase deleted in R265 GFP14, is involved in the formation of the capsule (a key virulence factor).

The proteins encoded by the genes deleted in R265 GFP14 might also be important in a wide range of metabolic processes. Thus, the genes/proteins should be searched in metabolic and cellular/molecular processes, e.g. with the KEGG database or (Hoffman-La Roche Ltd, 2014).

It would also be interesting to screen patients' samples and strains to find out if gene/genes correlate with patients' outcome/disease severity. As for the Vancouver Island outbreak strain, the gene/s could be compared to both non-outbreak *C. gattii* and *C. neoformans*. It could be that non-outbreak strains do not have the gene/genes and therefore are less virulent than the outbreak ones.

As discussed, the defect in virulence with R265 GFP14 is linked to transformation event. Interestingly, *in vitro* transformation can change chromosome sizes in *C. neoformans* (Toffaletti and Perfect, 1997). In JEC21 the karyotype variations are due to the presence of transposons (5% of its genome) (Loftus *et al.*, 2005). Karyotype differences were found under infection in mice (Fries *et al.*, 1996) and associated with phenotypic switching in rats (Fries *et al.*, 1999). Moreover, the genome plasticity was suggested to be a risk of reinfection (Brandt *et al.*, 1996). Variations were also demonstrated in *C. gattii* genome sequences of the VGI and VGIIa genotypes of *C. gattii*. The changes also applied to chromosome copy numbers and ploidy in *C. gattii* isolates displaying fluconazole heteroresistance (D'Souza *et al.*, 2011). To conclude, my study also shows karyotype change and therefore a change in the R265 GFP14 virulence resulting in impaired ability to overcome the natural defences of a host in zebrafish/ mice models. It was therefore assumed that those six genes were important for virulence. The genes were *accordingly* considered as targets in R265 infection. They can be potentially involved in human infection. For this reason, the R265 GFP14 was pursued.

4.3.7.3 Future work in respect to metabolic profiling of R265 wt and R265 GFP14

R265 wt and R265 GFP14 present with a metabolic difference in the Biolog assay. It is not understood whether R265 GFP14 presents with metabolic adaptation in this present study. At the same time, it cannot be concluded the R265 GFP14 does not have a metabolic defect. It does as indicated by impaired growth in the minimal medium in my study. It could also be that the R265 wt displays a metabolic defect in this present assay. As described, the sealing of plates preventing gas exchange might be an unexplained factor. It is also possible that in the Biolog assay the R265 wt did not grow and thus presented with interesting phenotypes. Further work is required to investigate whether the strain grows in the assay. As mentioned, the strains should be tested in an overnight growth assay in the substrates pulled out in the screen. Another concentration of glucose should be tested, too. The growths should be done in the Biolog media and different media should be tried. In addition, dye D and other dyes should be tested alongside. Apparently, dyes are all reduced to form a purple colour, but

the redox threshold at which they are reduced is different. The order of reduction power is: A>B>F>D>H>G, where A is most difficult to reduce and G most easily reduced. Recent communication with the company revealed that in the presence of a few positives, dye G should be tried (personal communication with Biolog). At the same time, it is not known what the dye D does to *C. gattii* cells and information about this dye is considered proprietary. It is possible that for R265 wt dye D is hard to reduce or dye D introduces latency in the R265 wt. Previous studies reported that some tetrazolium based dyes caused toxicity to microbes (Ullrich *et al.*, 1996). The only reason for dye D selection in my study, was a strong recommendation from Dr Barry Bochner, CEO of Biolog and the author of, e.g. (Bochner *et al.*, 2001; Bochner, 2003; Bochner *et al.*, 2011).

The Biolog assay should be repeated after checking all aforementioned parameters and reassuring the cells grow in the assay. If the same effect is seen, i.e. that a virulent R265 wt strain appears not to be performing Krebs, this should be supported by testing for the TCA occurrence *in vitro*. This can be done with, for example, TCA cycle metabolism assay kits by Merck. Additionally, respirometry work including the R265 GFP14, should be undertaken. Respirometry should include such parameters as routine mitochondrial respiration, leak respiration, non-mitochondrial oxygen consumption, maximum mitochondrial respiration rate and leak control ratio. Dr Gourlay has done this in R265 wt but the data is preliminary. Thus, more repeats are needed. Interestingly, the non-mitochondrial respiration value was about 50% of the total respiration, so R265 wt mitochondria are consuming oxygen. However, this is not coupled to energy production and so it seems R265 wt might rely on fermentation to produce energy. This implies that R265 wt might not need to perform Krebs cycle. Moreover, it may be that a good proportion of respiration is occurring at Aox1. R265 wt has Aox1 encoding gene on chromosome 2 (D'Souza *et al.*, 2011). It may be that Aox1 is consuming the oxygen and this should be further tested in future. The preliminary data suggest that R265 wt respire through Aox1 because it consumes oxygen when Aox1 is inhibited with SHAM. To check if fungi respire through Aox1, AOX1 gene knock-out should be done in R265 wt and R265 GFP14.

Alternative respiration and fermentation yield less energy than a classical respiration. Thus, R265 wt might be less efficient in energy production. Interestingly, depending on carbon sources availability, some bacteria that encode all of the enzymes for respiration, with its high energy yield, switch to less energy but faster fermentation (reviewed by (Passalacqua *et al.*, 2016)). It is acknowledged that yeast is eukaryote whereas bacteria are prokaryotes. However, it is possible that *Cryptococcus* might ferment. Although the literature characterises *Cryptococcus* as an aerobe (Odds *et al.*, 1995), fermentation has been suggested as this mode of energy acquisition for H99 *C. neoformans* (Santi *et al.*, 2014). Thus, it would be useful to feed R265 *in vitro* with glucose and measure fermentation products, e.g. lactic acid in a fluorometric lactate assay.

4.3.7.4 Linking data to assess why deleted genes are important for R265 wt virulence

The PM technology utilised in my study anticipated the effects of loss of gene function to provide a linkage between genotype and phenotype. The idea was to compare isogenic pairs of R265 wt and R265 GFP14 strains to directly assay for the cellular effects of loss of gene function (Bochner *et al.*, 2001). It became apparent that a significant inconvenience was multiple knock-out mutation of the R265 GFP14. The array is designed to investigate a single gene under several growth conditions and this study deals with six genes. Therefore, single gene knock-outs in R265 wt should be performed (described in 1.7.1) and followed by the PM1 screen. It has to be highlighted that the data from phenotypic screen can be mostly accurate for *in vitro* conditions as other microbial phenotypes might be expressed when the microbe interacts with an animal (Bochner, 2003).

Characterisation of deleted proteins is recommended. It would involve purification from *in vitro*. I would propose investigation of proteins structure. Protein structure is evolutionarily more conserved than sequence. It is believed that structural information provides a solution for many of the remaining proteins (reviewed by (Skolnick and Fetrow, 2000; Kinoshita and Nakamura, 2003)). This would require nuclear magnetic resonance (NMR) spectroscopy or x-ray crystallography for determination of the three-dimensional structures. Since the function of proteins

are not defined in this study and protein function is directly dependent on its three dimensional structure, it would be beneficial to determine their structure. Another approach would be to find binding partners to each of the six proteins of interest. This would require making six different His-tagged R265 recombinants in order to perform a silver stain, which followed by mass spectrophotometry would reveal binding partners. In addition, if a protein is predicted to have an enzymatic activity (three of the deleted proteins are enzymes, namely glucose 1-dehydrogenase, racemase and rhamnosidase), enzymatic assays could be performed to identify they substrates and pathways, which they might be involved in. Because the phenotypes in this study might change, when cryptococci interact with an animal, protein purification could be also be done *in vivo*. However, this would be very difficult. Alternatively, quantitative polymerase chain reaction (qPCR) could be performed, e.g. on cryptococci grown in different metabolic substrates and cells extracted from *in vivo* infection. This would show a particular gene expression and identify if a gene is important *in vitro* or *in vivo*. At the same time working back from phenotypic data should be done. From the array, enzymes should be searched that use the 21 substrates. This is how the data from the sequencing element of R265 wt versus R265 GFP14, knock-out genes in zebrafish, protein characterisation and proteins revealed from PM arrays could be linked to assess why the six (or one or a few) are important in R265 pathogenesis.

4.3.7 Major experiments to bring Chapter 4 towards publication

To bring this chapter towards publication I believe additional work has to be performed. In this chapter I focused on *C. gattii* that is the cause of an ongoing outbreak on Vancouver Island, which has subsequently spread to mainland Canada and the USA. This was linked to the general question I asked when appointed to the Johnston lab- how *Cryptococcus* causes a disease. This question was really important as the literature is not evident as to how it causes a disease and what is the difference between *C. neoformans* and *C. gattii* in this aspect? The literature is not evident in terms of how *C. gattii* causes a disease and what the difference between them two species in this aspect is.

I characterised a virulence and growth defect in R265 GFP14 with a genomic defect following GFP transformation hoping to reveal why the wild-type is virulent. Unfortunately, I did not fully answer the question, how *C. gattii* causes a disease. What can be concluded is that the lost six genes are important for virulence in fish and mice. These results warrant additional experiments or analyses that could help answer the research question more fully. In the discussion I described potential experiments that can be carried out in future. Here I provide the sum of crucial work before seeking publication. The main objective to answer the main question, i.e. how R265 wt causes a disease, would be to create a derivative fluorescent strain that is equally virulent as R265 wt in used animals, e.g. an mCherry version of R265. Since the R265 GFP14 has an altered genome (32 kb deletion) as compared to the parental strain, other transformants created at the time of R265 GFP14 generation (Voelz *et al.*, 2010) should be genome sequenced. If there is one that does not have an altered genome, it should be used in macrophages-cryptococci interactions assay. However, the work dedicated R265 GFP14 is meaningful and highlights the deleted six genes' importance in cryptococcal virulence. Thus, the work should be focused on those genes. The identified genes should be searched for their role in *Cryptococcus*. For instance, a publication of (Martinez and Casadevall, 2007) proposed that polysaccharide matrix includes rhamnose. According to KEGG database, α -L rhamnosidase utilises an inverting mechanism of hydrolysis, releasing β -L-rhamnose. Thus, it is possible that rhamnosidase deleted in R265 GFP14, is involved in the formation of the key virulence factor-the capsule. On that note, one of the genes upregulated *ex vivo* in lineage VGII, to which R265 wt belongs, was ABC transporter gene CNBG_4708, an ortholog to a gene of known function in *C. neoformans* H99 (Farrer *et al.*, 2018). Since one of the genes deleted in R265 GFP14 is CGB_A0010C with conserved ABC domain, it might be that the gene is upregulated *in vivo* in zebrafish and mice in my current study in R265 wt and contributes to virulence. In addition, BLAST similarity search should be done to answer if those genes are found in other organisms and this will facilitate protein function prediction. Protein domains function should be characterised because their annotation is an alternative approach to sequence similarity searches. This will all lead to a new knowledge about R265 wt candidate

virulence genes, which have been listed by me and thereby about its virulence in general.

With regard to intermediate goals referring to work on the GFP strain and trying to explain why the genes loss could impact virulence *in vivo*, they can be divided into a few themed experiments: GFP insertion, virulence in the zebrafish, and metabolic profiling of R265 wt and R265 GFP14.

With regard to GFP insertion, I do not have evidence that it is not the GFP that causes avirulence in zebrafish or mice. Only an experiment with the same knock-outs in the wild-type would inform if the GFP in itself is defective. Future investigations should also focus on other R265 GFP strains generated by (Voelz *et al.*, 2010) to determine if GFP insertion has changed their virulence. Since a GFP construct was made with the use of actin promoter, making another *C. gattii* GFP strain attached to alternative promoters and comparing the virulence of the existing strain would answer if the promoter can cause virulence defect.

With regard to the virulence in zebrafish, the dominance of killing by macrophages over the intracellular proliferation is supported by significant decrease in the number of total cryptococci and in the dropping extracellular numbers in the latest stages of infection. However, this study cannot discern intracellular proliferation, and use of time-lapse microscopy may help as it was done in (Bojarczuk *et al.*, 2016). Alternatively, removing extracellular portions of the pathogen and counting the number cryptococci at all time-points would prove the event of intracellular proliferation. It is not feasible to do so *in vivo* in comparison to *in vitro*, e.g. with gentamycin but fluconazole could be a good choice. What cannot be left unattended is the role of macrophages in R265 wt/R265 GFP14. It might be that *in vivo* macrophages are not the dominant cells combating the infection. Therefore, an experiment with clodronate should be done as in (Bojarczuk *et al.*, 2016).

Deciphering the principles as to how pathogenic yeast adapt their metabolism to a specific host microenvironment is critical for understanding cryptococcal pathogenesis. *Cryptococcus* senses the nutritional composition during the course of an infection. Therefore, metabolomic microarrays were exploited. It became apparent that this experiment had limitations. A significant inconvenience was

multiple knock-out mutation of the R265 GFP14. Thus, single knock-outs in the wild-type should be done and then phenotypic arrays performed. For example, deleting the first gene only that amongst six is already removed, would allow clear conclusion of this gene function because the array would preferably point towards specific cellular pathway and biological function. Meanwhile, without single knock-outs, growth experiments for the wild-type R265 and R265 GFP14 in hit substrates would be extremely useful in determining if they are needed for replication. This is because metabolic assays might not accurately represent changes in cell growth as they do not quantify cell proliferation. From this it would be easier to draw clear conclusions whether or not R265 wt performs Krebs cycle *in vitro* in phenotypic array settings. This was the main issue in the phenotypic work. R265 GFP14 appeared to use Krebs substrate, but R265 wt did not. I even suggested fermentation. Most definitely Krebs functions during fermentation, e.g. in *S. cerevisiae* grown in glucose there is a reduced growth rate and biomass when the gene PDA1, which is part of the pyruvate-dehydrogenase (PDH) complex that yields acetyl-CoA in the mitochondrial matrix, is disrupted (pyruvate + NAD⁺ + CoA → acetyl-CoA_{mit} + NADH + H⁺ + CO₂). This tells us that even a crabtree positive yeast will use the cycle when it is fermenting in aerobic conditions. A problem is that even in *S. cerevisiae* the interface between glycolysis and TCA is not fully defined (van Rossum *et al.*, 2016). It is not known what R265 wt does and how this relates to virulence. Thus, TCA cycle metabolism assay kits should be tried *in vitro*. Unfortunately there is no method to measure TCA cycle of microbial cells *in vivo*. SAGE on cryptococci recovered from the lungs of infected mice with a special attention to SAGE tags for genes encoding predicted functions in the TCA could be done. Transcriptome sequencing (RNA-seq) comparisons of *in vitro* results from kits to *ex vivo* (zebrafish) TCA associated genes expression levels should give a clue as to whether the wild-type is likely to perform fermentation. However, nutrient availability has an impact on expression of virulence genes. Hence, transcriptome sequencing (RNA-seq) comparisons of cells grown *in vitro* in Krebs related substrates to *ex vivo* (zebrafish) Krebs associated genes expression levels should give a clue as to whether the wild-type is likely to perform the cycle. In turn, nutrient availability has an impact on expression of virulence genes. This is important knowledge as the

TCA cycle has a central role in the regulation of energy regulation and metabolism. It is essential yeast cells have to have Krebs (or some partial Krebs cycle) activity. Yeast cells that are just fermenting or have no mitochondrial DNA are still running the Krebs cycle to support production of metabolites and certain amino acids. The data obtained from respirometry suggests that R265 must get ATP from another mechanism and so it is likely to be fermenting, too. If the final product from glucose utilisation kit is pyruvate, then glycolysis is successful. If the final product is ethanol, then this indicates fermentation. In addition, testing the growth on non-fermentable media (yeast pepton glycerol) should be done. If a strain relies mostly on fermentation and does not use oxidative phosphorylation much then it would grow poorly on such media. Again, there is no technique to measure fermentation of microbes *in vivo*. SAGE on cryptococci recovered from the lungs of infected mice with special attention to SAGE tags for genes encoding predicted functions in fermentation could be done. Transcriptome sequencing (RNA-seq) comparisons of *in vitro* results from kit to *ex vivo* fermentation associated genes expression levels should also give a clue whether the wild-type is likely to perform fermentation. Additionally, transcriptome sequencing (RNA-seq) comparisons of cells grown *in vitro* in fermentation related substrates to *ex vivo* (zebrafish) fermentation associated genes expression levels. It has to be acknowledged that R265 wt might behave differently *in vitro* and *in vivo*. This might be due to the continuous availability of nutrients from host serum and the incorporation of the host-pathogen interaction (Nett *et al.*, 2011). The underlying mechanism of *C. gattii* virulence is still unclear. However, I believe that not only known virulence factors determine cryptococcal virulence, but also variations in metabolic functions. It is very likely that differences in metabolic adaptation contribute to observed differences in pathogenicity and clinical outcome regarding *Cryptococcus* complex. Table 4.24 lists the most crucial experiments required for this chapter to be submitted for publication.

Table 4.24 The summary of core experiments to bring Chapter 4 towards manuscript publication

research question	core experiments for Chapter 4 to be submitted for publication
How does R265 wt cause a disease?	generation of a derivative fluorescent strain that is equally virulent as R265 wt in animals used (zebrafish, mice) or genome sequencing of other transformants created by (Voelz <i>et al.</i> , 2010) to find the one that does not have an altered genome; to be used in macrophages-cryptococci interactions assay in zebrafish and time-lapse microscopy as in (Bojarczuk <i>et al.</i> , 2016) using an unaltered genome fluorescence R265 derivative
Are macrophages important during cryptococcal infection in zebrafish?	zebrafish infection assay without macrophages using an unaltered genome fluorescence R265 derivative
Do cryptococci proliferate intracellularly in macrophages in zebrafish?	time-lapse microscopy as in (Bojarczuk <i>et al.</i> , 2016) using an unaltered genome fluorescence R265 derivative
Are macrophages important during cryptococcal infection in zebrafish?	zebrafish infection assay without macrophages using R265 GFP14
Do cryptococci proliferate intracellularly in macrophages in zebrafish? Does the six genes loss impact cryptococcal behaviour when in macrophages?	time-lapse microscopy as in (Bojarczuk <i>et al.</i> , 2016) using R265 GFP14
Is GFP defective itself to cause avirulence in mice and virulence attenuation in zebrafish?	six gene knock-outs in the wild-type R265 and survival assays in mice/zebrafish
What are the functions of genes deleted in R265 GFP14=what are the functions of genes present in R265 wt?	BLAST similarity search, protein domains characterisation
What is each gene function?	single knock-outs in the wild-type followed by phenotypic array
Does R265 wt rely on Krebs cycle? Does it perform Krebs cycle mostly <i>in vitro</i> or <i>in vivo</i> ?	<i>in vitro</i> TCA cycle metabolism assay kit followed by SAGE on cryptococci recovered from the lungs of infected mice with a special attention to SAGE tags for genes encoding predicted functions in the TCA and followed by transcriptome sequencing (RNA-seq) comparisons of cells grown <i>in vitro</i> in Krebs related substrates to <i>ex vivo</i> (zebrafish

Chapter: 5 Mycophenolate mofetil increases inflammation resolution in zebrafish via neutrophil apoptosis

5.1 Introduction

My zebrafish model of cryptococcosis (Bojarczuk *et al.*, 2016) has been exploited in a number of studies (Gibson, 2017; Gibson *et al.*, 2017, 2018; Gilbert *et al.*, 2017; Kamuyango, 2017; Fehri, 2018; Evans *et al.*, 2019). One of these studies was to investigate the role of mycophenolate mofetil (MMF) during *C. neoformans* infection *in vivo* in my zebrafish model (Gibson *et al.*, 2018). This study focused on macrophages, the key cells required for clearing cryptococcal infection (Feldmesser *et al.*, 2000; Tenor *et al.*, 2015; Bojarczuk *et al.*, 2016). MMF had a distinct and specific effect on macrophages, in the absence of lymphoid cells and this resulted in an increased macrophage cell death (Gibson *et al.*, 2018). This is in line with the hypothesis of MMF capable of the direct modulation of innate immune system as MMF was shown to decrease circulating neutrophil counts (Von Vietinghoff *et al.*, 2010) or infiltration of macrophages (Jiang *et al.*, 2012). In contrast there was no difference in neutrophil numbers (Gibson *et al.*, 2018). However, this was in the absence of a neutrophil insult (as neutrophils do not appear to respond to cryptococci, as discussed above) and I wanted to ask if the same effect occurred in neutrophils in the situation of neutrophilic responses. To test whether the induction of neutrophil cell death occurs under MMF treatment, I used a well described zebrafish inflammation model (Renshaw *et al.*, 2006). I hypothesised MMF would cause enhanced apoptosis in neutrophils during the resolution of inflammation following tissue injury.

5.1.1 Mechanism of MMF on lymphocytes and other effects on other cells

Mycophenolate mofetil (MMF) is an immunosuppressant and potent anti-proliferative agent against lymphocytes commonly used following organ transplant. Lymphocytes proliferation has to be suppressed as graft rejection is primarily mediated by these cells. MMF is a morpholinoethyl ester prodrug of mycophenolic acid (MPA) (Lee *et al.*, 1990) and non-competitive reversible inhibitor of inosine-5'-monophosphate dehydrogenase (IMPDH) (Smak Gregoor

et al., 2000). In humans there are two isoforms, IMPDHI and IMPDHII (Collart and Huberman, 1988; Natsumeda *et al.*, 1990). While the former is widely expressed in resting lymphocytes (Natsumeda *et al.*, 1990), the latter is abundantly produced in activated lymphocytes, shown by Epstein Barr Virus transformation (Nagai *et al.*, 1992; Alfieri *et al.*, 1994). IMPDHII is also fivefold more susceptible to inhibition by MMF than IMPDHI (Syntex laboratories in collaboration with (Allison and Eugui, 2005)). It is believed the inhibition of IMPDH occurs after inosine monophosphate (IMP) and NAD⁺ binding, after hydride transfer, and after NADH release (Fleming *et al.*, 1996).

The IMPDH enzyme is essential for *de novo* purine synthesis pathway that generates a nucleotide precursor-deoxyguanosine triphosphate (dGTP) and purine nucleoside-guanosine triphosphate (GTP) for DNA synthesis (Allison and Eugui, 1996) (Figure 5.1). However, despite decades of research, it is not known which isoform of IMPDH is crucial for *de novo* purine pathway. Previous studies have rather focused on demonstrating the inhibitory effect of the IMPDH enzyme. Treatment of phytohaemagglutinin (PHA) mitogen activated human leukemic T-lymphocytic cells and mononuclear cells with MPA resulted in significant GTP and dGTP depletion (Allison and Eugui, 1993). The effect was reversed by adding guanine or guanosine or deoxyguanosine (Allison *et al.*, 1991; Allison and Eugui, 1993). The first two efficiently restored GTP levels with lesser effect on dGTP restoration; deoxyguanosine however, efficiently recovered dGTP (Allison *et al.*, 1991). Addition of adenosine or deoxyadenosine did not restore DNA synthesis (Allison *et al.*, 1991; Allison and Eugui, 1993). Inhibition of DNA synthesis in lymphocytes was shown by the incorporation of thymidine ³H-[dThd] (Allison and Eugui, 1993), to arrest cells throughout S phase (Cohn *et al.*, 1999), thus inhibiting DNA replication. This was predominantly due to the depletion of dGTP. Lymphocytes exclusively rely on *de novo* pathway (Allison *et al.*, 1977) while other cells use additional salvage pathways. Therefore it is believed the principal effect of MMF suppression is on lymphocytes (Allison and Eugui, 2000) by blocking the source of dGTP and GTP from *de novo* guanosine nucleotide synthesis (Allison and Eugui, 1993) (Figure 5.1). However inhibition of promonocytic cell lines proliferation was also demonstrated (Eugui *et al.*, 1991).

Notably, amongst PHA stimulated primary lymphocytes and monocytes, only neutrophils did not have depleted GTP (Allison and Eugui, 1993). GTP is also required for neopterin synthesis by monocytes activated with IFN γ (Wachter *et al.*, 1989), produced by activated T-cells. Since neopterin is indicative of a pro-inflammatory immune status, it could be that MMF might suppress macrophage mediated cell damage (Allison and Eugui, 1993).

MMF also leads to apoptosis in monocytic U937 (Cohn *et al.*, 1999; Allison and Eugui, 2000; Andrikos *et al.*, 2005) and THP-1 cell lines (Cohn *et al.*, 1999). A recent study using K562 leukemic cells on how MMF induces apoptosis, found it was due to GTP drop. This augmented accumulation of pro-apoptotic factor p21 in the cell nuclei and led to cell death (Meshkini *et al.*, 2011).

It has been previously demonstrated with another IMPDH drug mizoribine, that GTP depletion in human peripheral blood T cells arrested the movement of cells from G1 to S phase of the cell cycle. The conclusion arose from unaffected initial steps of T cell activation measured by G1 phase genes expression and cell cycle analysis revealing decreased numbers of cells in S, G2, and M phases, measured by DNA content in flow cytometry (Turka *et al.*, 1991). The similar arrest is also seen in MPA treated lymphocytic (MOLT-4) and monocytic cell lines (THP-1 and U937) where cells progressed through G1 but accumulated in S phase (Cohn *et al.*, 1999). MMF treatment also promotes monocyte differentiation (Waters *et al.*, 1993). *In vitro* studies indicate MPA reduces the proliferative capacity of cell lines (promyelocytes HL60 and promonocytes U937), but also promotes differentiation of monocytes to macrophages (Waters *et al.*, 1993). The latter effect was shown with the restricted production of pro-inflammatory cytokine IL- β , which is associated with monocytes and augmented production of IL-1 receptor antagonist (IL-1RA), which is associated with macrophages (Waters *et al.*, 1993). In contrast, the differentiation of monocytes to dendritic cells is impaired with MMF, also affecting the maturation of immature monocyte-derived dendritic primary cells (Colic *et al.*, 2003). Proliferation of IC-21 macrophages has also been suppressed by MPA. The effect was reversed by the addition of guanosine, suggesting this mechanism is GTP-dependent (Jonsson and Carlsten, 2002).

5.1.2 MMF effects on glycosylation and adhesion

Adhesion of lymphocytes is required for mounting an immune response including migration to the sites of infection or inflammation (reviewed by (Dustin *et al.*, 2004)). The same applies to leukocytes (reviewed by (Ley *et al.*, 2007)). In the context of transplanted grafts, lymphocytes and leukocytes can discourage organ rejection. MMF inhibits IMPDH, which prevents DNA synthesis in T and B cells because they lack the ability to generate purines through the alternative salvage pathway. It is speculated that MMF suppresses the expression of adhesion molecules thereby decreasing the recruitment of lymphocytes and monocytes into sites of inflammation and graft rejection (Allison and Eugui, 2000)). However, an adhesion phenotype was only shown *in vitro*, wherein the number of adhering T cells was lower and the expression of some adhesion endothelial receptors was reduced (Blaheta *et al.*, 1998). Rats biopsies after induced renal failure and MMF treatment show lower numbers of lymphocytes and macrophages as well as reduced expression of some lymphocyte/monocyte adhesion molecules (Romero *et al.*, 1999). Thus, one possible explanation for reduced macrophages/lymphocytes might be inhibited adhesion. However, these publications did not account for, e.g. apoptosis of cells once they arrive for example.

MMF also has important roles in glycosylation. GTP is needed to transfer carbohydrates to glycoproteins during glycosylation. Due to guanosine depletion through MMF action the transfer of fucose- and mannose to glycoproteins serving as adhesion receptors- is impeded. This was demonstrated by measuring the expression of mannose on the surface of human peripheral blood lymphocytes, using a specific lectin for terminal mannose. MMF significantly reduced available mannose for lectin binding (Allison and Eugui, 1993). This also implies the depleted GTP source affects the glycosylation process by which glycoproteins are formed. Since some glycoproteins, such as selectins, are adhesion molecules involved in rolling steps of leukocytes to sites of inflammation (Ley, 2002), it is hypothesised that loss of adhesion might be the mechanism by which MMF decreases the recruitment of those cells to inflammation sites (Allison and Eugui,

2000). In contrast, there is some evidence MMF does not hinder glycosylation of T cells, as there is no effect on the binding of either fucose or mannose-specific lectins (Jepson *et al.*, 2000). There have been conflicting reports concerning the ability of MMF to affect either endothelial or lymphoid cell adhesion molecules. *In vivo*, the expression of lymphocyte function-associated antigen adhesion molecule (LFA-1) was reduced whereas no effect was seen with endothelium associated molecules Intercellular Adhesion Molecule 1 (ICAM-1) and VCAM-1 (Heemann *et al.*, 1996). Contrary to this, *in vitro* endothelial adhesion molecules VCAM-1, E-selectin and P-selectin were downregulated (Blaheta *et al.*, 1998). Moreover, protein glycosylation occurs in the lumen of the endoplasmic reticulum (ER) and the Golgi, and requires GTP for the movement from the first organelle to the other. This trafficking, therefore, might be impaired (Allison and Eugui, 2000).

MMF reduces the adhesion of human monocytes to human umbilical vein endothelial cells (HUVECs) shown in immunocytochemistry assay. It also inhibits the expression of intercellular adhesion molecule (ICAM-1) and Major Histocompatibility Complex (MHC-II) in primary monocytes stimulated with LPS, measured through mean fluorescence intensity. Moreover, MMF treated primary monocytes do not adhere to E-selectin. It was suggested these effects could be beneficial in acute spinal cord injury. In these conditions migration of macrophages might be deleterious promoting pro-inflammatory action (Glomsda *et al.*, 2003).

It has been suggested that MMF downregulates expression of adhesion molecules involved in leukocytes recruitment through IL-1RA production and pro-inflammatory cytokines. The IL-1RA antagonist inhibits IL-1 that induces the expression of adhesion factors (Waters *et al.*, 1993). In the blood of stable renal transplant patients treated with MMF and LPS, the production of pro-inflammatory IL-1 β , TNF α , IL-6 and IL-10 cytokines was suppressed. In addition, MMF alone significantly reduced TNF α (Weimer *et al.*, 1999). Thus MMF might be beneficial in inhibiting chronic graft rejection, where immunological destruction described by gradual and progressive deterioration of the graft is often linked to persistent inflammation and occurs after the first few months of transplantation.

Taken together, by suppressing glycosylation and antagonising the expression of adhesion molecules MMF decreases the recruitment of lymphocytes and monocytes into sites of inflammation and graft rejection. It might also contribute to reduced pro-inflammatory cytokines production and increased IL-RA, which again might be a factor in the suppressed production of adhesion molecules, seen in patients (Allison and Eugui, 2000).

Pathways of Purine Biosynthesis

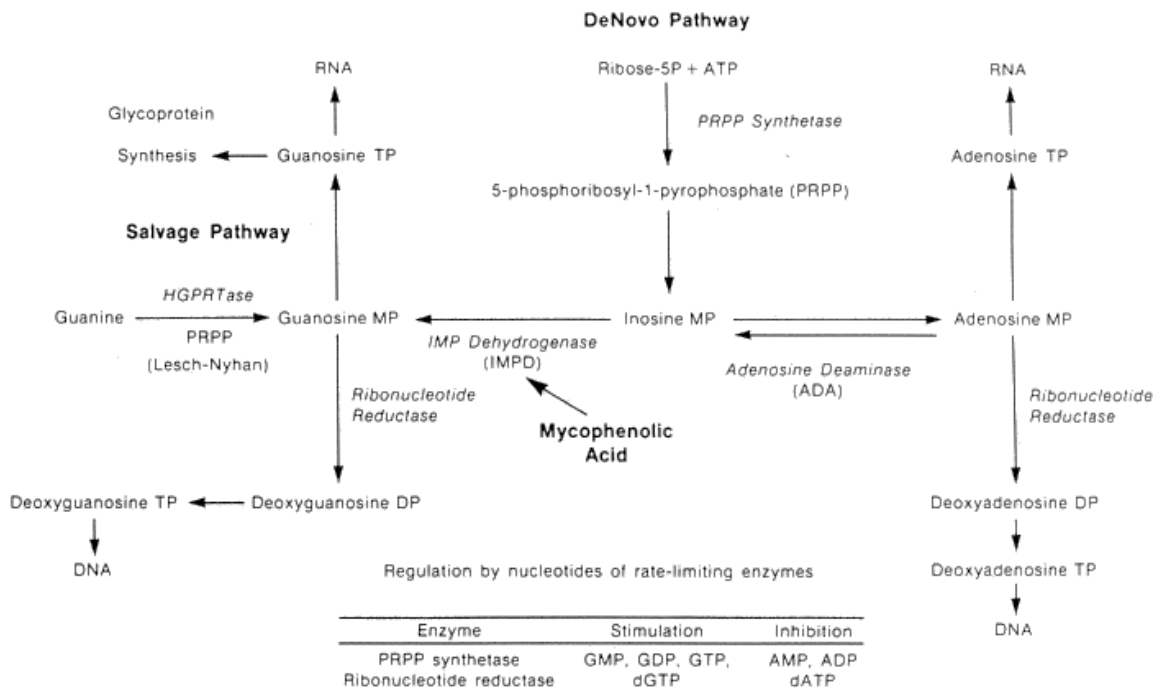


Figure 5.1 Purine biosynthesis pathways including the *de novo* pathway and salvage pathway, showing the central position of inosine monophosphate (IMP) and point of action for MPA (mycophenolic acid). Taken from (Allison, 2005).

5.1.3 Side effects of MMF described in clinical studies

MMF has known side effects. For instance, a case study reported MMF might cause neutrophil dysplasia described as nuclear hypolobulation and abnormal clumping of nuclear chromatin. In this case, the neutrophil abnormality preceded the development of neutropenia (Banerjee *et al.*, 2000). There are also reports of acute inflammatory syndrome in a kidney transplant patient with characteristics such as fever and oligoarthritis appearing within one week of increasing the MMF dosage. After MMF withdrawal, all complaints disappeared within 48 hours (Hochegger *et al.*, 2006). The syndrome was also reported after introduction of MMF in patients with Wegener's granulomatosis and resolved after MMF withdrawal (Maes, 2002). In both reports it was hypothesised that this syndrome might be due to a paradox, pro-inflammatory reaction of PMNs.

MMF in combination with cyclosporine prevents graft versus host disease (GVHD) in bone marrow transplantation due to diminishing the risk of mucositis, and causes faster neutrophil engraftment (Bolwell *et al.*, 2004). However, the latter effect has been recently contradicted in cord blood transplantation (Okamura *et al.*, 2011). This study, however, reported on MMF in combination with tacrolimus. Thus, it could be that the effect depends on calcineurin inhibitor or graft type.

Common side effects of MMF include gastrointestinal and bone marrow suppression (leukopenia and thrombocytopenia) (reviewed by (Sollinger, 2004)) and viral infections (Filler *et al.*, 2003).

5.1.4 MMF in autoimmunity

Autoimmunity is described as an immune response leading to reaction with self antigen. MMF is used in autoimmunity: vasculitis, systemic lupus erythematosus, Wegener's granulomatosis (Filler *et al.*, 2003), bowel disease (Tan and Lawrance, 2009), immune-related pulmonary fibrotic conditions: interstitial lung disease in systemic sclerosis (Ueda *et al.*, 2018), sarcoidosis (Hamzeh *et al.*, 2014) and other inflammatory conditions; e.g. myasthenia gravis (Heatwole and Ciafaloni, 2008), dermatomyositis (Orvis *et al.*, 2009). Autoimmunity results from

abnormal lymphocyte recognition of self-antigens. In many cases, this results in autoantibody production. Abnormal monocyte count is also a hallmark of autoimmunity and unresolved inflammation. MMF causes apoptosis in monocytic lineages and inhibits the differentiation of monocytes to DCs (references in Mechanism of MMF on lymphocytes and other effects on other cells). In this context, it is believed that MMF has an anti-inflammatory effect because it affects both the adaptive and innate immune systems. Indeed, the literature suggests that MMF is an anti-inflammatory drug. For instance, in a mouse model of acute lung injury induced by lipopolysaccharide (LPS), MMF impedes the influx of neutrophils and reduces pro-inflammatory TNF α and IL-1 β levels (Beduschi *et al.*, 2013). On another note, those cytokines were measured in the pleural cavity by enzyme-linked immunosorbent assay (ELISA) with monoclonal- specific antibodies for each cytokine. Therefore, it is not known which cells produced them.

In lung ischemia–reperfusion injury, when oxygen supply to the lung is limited and followed by a period of reperfusion (reviewed by (Weyker *et al.*, 2013)), MMF sequestered neutrophils, where accumulation was assessed by reduced MPO content in lung parenchyma (Farivar *et al.*, 2005). This was further explained by attenuated levels of activator protein 1 (AP-1) and early growth response 1 (EGR-1)- factors that transcriptionally regulate ICAM-1 (van de Stolpe and van der Saag, 1996; Yan *et al.*, 2000), critical to leukocytes recruitment . Moreover, it has been suggested that the attenuation of AP-1 and EGR-1 could partially mediate reduced cytokine-induced neutrophil chemoattractant (CINC) and chemokine-monocyte chemoattractant 1 (MCP-1) (Farivar *et al.*, 2005). However, the role of MCP-1 in neutrophil recruitment is debatable and the generalised anti-inflammatory effect of MMF could be due to MCP-1 not affecting neutrophils (Balamayooran *et al.*, 2011).

5.1.5 MMF's pharmacokinetics

MPA has been isolated from several species of *Penicillium* moulds (Clutterbruck *et al.*, 1932) and firstly tested against IMPDH II activity *in vitro* in a LS culture line derived from mouse L fibroblasts (Franklin and Cook, 1969). In humans,

recommended therapeutic range of MMF falls between 1.0–3.5 µg/ml through serum or plasma levels (equivalent of 3.125 µM -10.9 µM, respectively) (Tredger *et al.*, 2004). Orally dosed MMF is promptly absorbed from the gastrointestinal tract, followed by a presystemic deesterification to become MPA, the active portion. Administered intravenously, MMF's plasma concentration, both in healthy and renal insufficiency patients, decreases significantly whereas MPA concentration rises reaching its maximum peak within 1 hour (Bullingham *et al.*, 1998). MPA is glucuronidated to the inactive 7-O-mycophenolic acid glucuronide (MPAG) and the active acyl glucuronide (AcMPAG) (Ting *et al.*, 2008). Over 90% of MMF is excreted in the urine, mainly as MPAG. In healthy patients 97% of MPA and 82% of MPAG bind to serum albumins (Bullingham *et al.*, 1996, 1998). In renal insufficiency unbound MPA might be increased while the total circulating drug level is in the therapeutic range (Smak Gregoor *et al.*, 1998). Since only unbound MPA dictates the drug's immunosuppressive action on IMPDH (Nowak and Shaw, 1995), factors influencing albumins binding can alter the effect of MPA (Jeong and Kaplan, 2006). In stable renal graft recipients, the unbound MMF fraction is consistent (Kaplan *et al.*, 1999), doubled in delayed graft situations (Shaw *et al.*, 1998) and significantly increased in renal insufficiency (Kaplan *et al.*, 1998). In the first situation albumin concentration was not altered, in the second and third, decreased. It has been suggested the declined albumin could be due to renal dysfunction per se or by counteraction for albumin binding by MPAG (Kaplan *et al.*, 1999).

In addition, MPA encounters enterohepatic circulation (Figure 5.2) and reaches its secondary peak in plasma between 6-12 hours post intravenous or oral dosing (Bullingham *et al.*, 1998; Jeong and Kaplan, 2006). This is concluded from MPAG excretion in bile as the recirculated metabolite and recirculation maximum in plasma being MPA (Bullingham *et al.*, 1998). However, renal conditions do not mirror free MPA levels. Thus MMF dosage has to be thoroughly monitored (Kaplan *et al.*, 1999). Nevertheless, MMF is widely used in renal diseases and many other post transplant treatments.

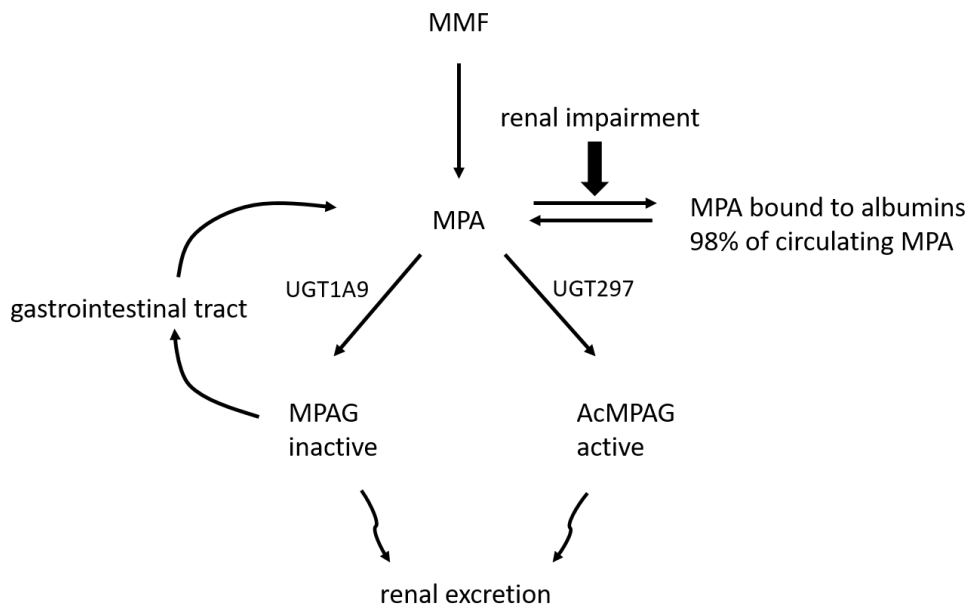


Figure 5.2 Pharmacokinetics of MMF after oral administration. MMF undergoes pre-systemic deesterification into MPA, then gets metabolised to its glucuronide forms, MPAG and AcMPAG, by different isoforms of glucuronosyltransferases (UGT) in the liver. Adapted from (Jeong and Kaplan, 2006).

5.1.6 Azathioprine (AZA)

AZA is an alternative to MMF anti-proliferative agent acting on lymphocytes inhibiting *de novo* purine and DNA synthesis. *In vivo* AZA is converted non-enzymatically to 6-mercaptopurine (6MP) (Chan *et al.*, 1990) or purine base hypoxanthine (Wright *et al.*, 2004) (Figure 5.3). Three enzymes compete to metabolise 6MP: thiopurine S-methyltransferase (TPMT), xanthine oxidase (XO) and hypoxanthine guanine phosphoribosyltransferase (HPRT) (Yatscoff *et al.*, 1998; Warner *et al.*, 2018) (Figure 5.3). 6MP metabolism involves three competing pathways. The first one is the breakdown to inactive 6-thiouric acid (6TU) excreted in the urine, the second is through methylation into methylmercaptopurine (MeMP), which inhibits *de novo* purines pathway, and the last one is degradation of 6MP into thioinosine monophosphate (TIMP), also known as 6-thioinosic acid (6TA). The last is catalysed by monophosphate dehydrogenase (IMPDH) into 6-thioguanine monophosphate (TGMP), which, via kinases, is converted into 6-thioguanine nucleotides (6TGN) via purine salvage pathway (Simsek *et al.*, 2017; Warner *et al.*, 2018).

The 6-TGTP nucleotides suppress Rac1 GTPase and finally induce T-cell apoptosis. This occurs when lymphocytes are co-stimulated with CD28 (Tiede *et al.*, 2003) known to enhance T cell proliferation, which is associated with the stimulation of T cell receptor (TCR) via activation of *Bcl-x_L* (cell survival gene) (Noel *et al.*, 1996). The blockade of Rac1 activation is mediated via binding of azathioprine-generated 6-TGTP nucleotides instead of GTP. The blockade of Rac1 target genes such as *MEK*, *NF- κ B*, and *Bcl-x_L* leading to a mitochondrial pathway of T cell apoptosis (Tiede *et al.*, 2003). The inhibition of Rac1 also encourages apoptosis of monocyte derived osteoclasts (Fukuda *et al.*, 2005). The mechanism of this event is unknown. However, it is suggested that it might be due to compromised binding of the $\alpha_v\beta_3$ osteoclast integrin to its immobilised ligand, which promotes a programmed death (Fukuda *et al.*, 2005; Zhao *et al.*, 2005; Croke *et al.*, 2011). TGN become incorporated into DNA and inhibit its synthesis (Allison, 2005), whereas MeMP nucleotides inhibit *de novo* purine synthesis by blocking the first enzyme of *de novo* purine biosynthesis; amidophosphoribosyltransferase (PRPP) (Wright *et al.*, 2004; Bowne *et al.*,

2009). In addition, TIMP is not a substrate for adenylosuccinate synthetase, the first enzyme of adenine nucleotides formation from IMP (Parker, 2009) and 6MP depletes adenine nucleotides, even to a greater extent than TGN (Dayton *et al.*, 1992). Thus, AZA inhibits adenosine nucleotide more than guanosine nucleotide formation. The opposite is true of MMF (Allison and Eugui, 2005). AZA also inhibits to some extent ATP and GTP *de novo* biosynthesis through methyl thioinosine monophosphate (MeTIMP) generation (Cara *et al.*, 2004; Petit *et al.*, 2008). MMF primarily inhibits GTP in *de novo* purine synthesis. However, it also affects ATP levels since in the purine synthesis the first fully formed purine nucleotide IMP can be converted either to adenosine monophosphate (AMP) or guanosine monophosphate (GMP) nucleotides. It was demonstrated in human peripheral blood lectin-stimulated primary lymphocytes that ATP levels were diminished as compared to monocytes and neutrophils (Allison and Eugui, 1993). The direction of the pathway is controlled by the level of the respective nucleotide. An excess of GTP will lead to the synthesis of AMP with the opposite being the case when ATP levels are higher (King, 2017). Reduced levels of ATP was found in human T cells (Qiu *et al.*, 2000).

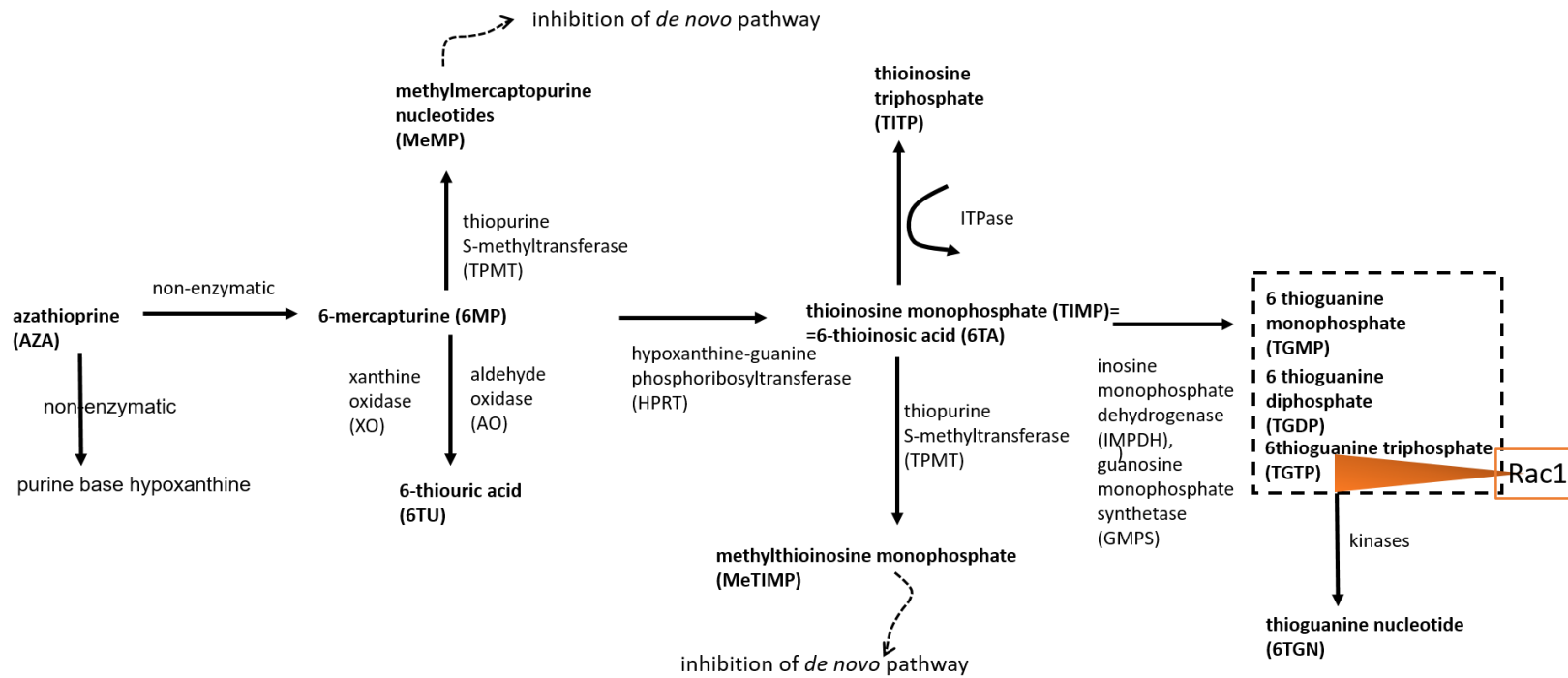


Figure 5.3 AZA metabolic pathway. Orange depicts Rac1 binding of 6-TGTP to finally induce T-cell apoptosis. Adapted from (Chan *et al.*, 1990; Wright *et al.*, 2004; Simsek *et al.*, 2017; Warner *et al.*, 2018).

5.1.7 MMF versus AZA

MMF inhibits DNA synthesis through interfering with GTP synthesis (Figure 5.1). AZA and its metabolite 6-thioguanine are two compounds that block DNA synthesis by incorporating thioguanine nucleotides into DNA (Figure 5.3). MMF results in a cellular depletion of GTP (Jagodzinski *et al.*, 2004) by directly blocking the synthesis of GMP (Allison and Eugui, 1993) achieved by inhibiting IMPDH needed for *de novo* IMP pathway.

Thus, with MMF treatment GMP can only be generated via the salvage pathway increasing the competition for GMP (mainly from nucleotide synthesis) and resulting in overall GTP depletion. By contrast, in lymphocytes, AZA allows GMP generation and therefore GTP restoration and its downstream products. This is achieved by depletion of cellular ATP through *de novo* IMP pathway. 6-thioguanine however, will predominantly block DNA synthesis (Gibson *et al.*, 2018).

How these two agents interfere with DNA and their points of action is depicted in Figure 5.4.

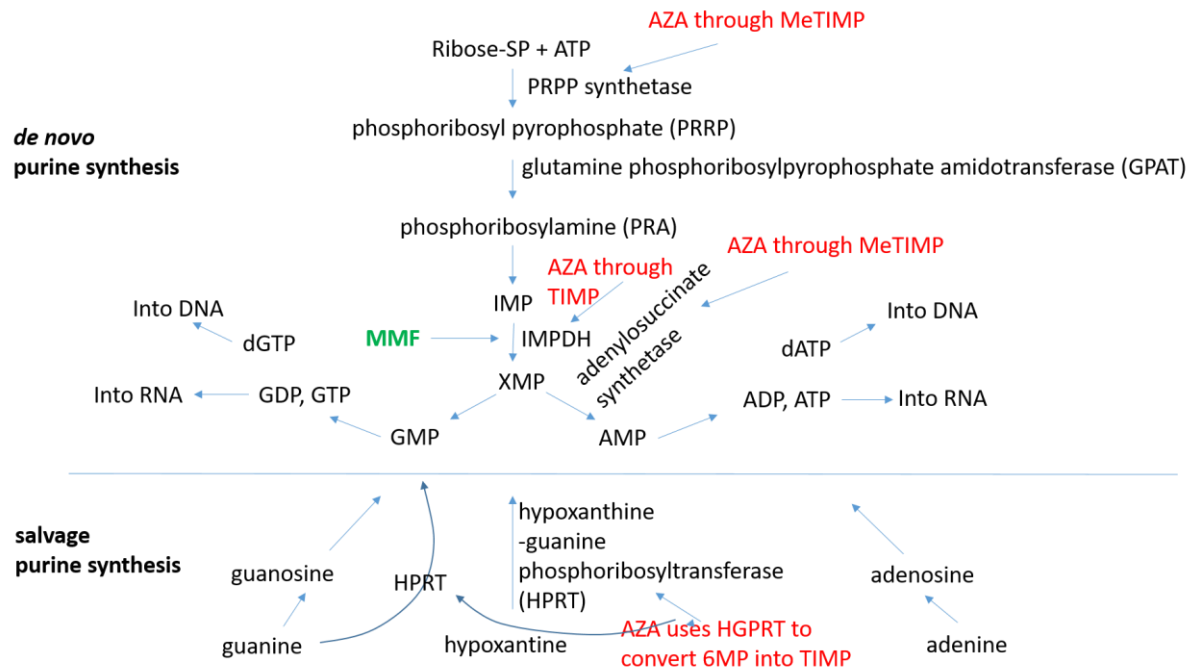


Figure 5.4 Biochemical pathways of AZA and MMF. Adapted from (Chan *et al.*, 1990; Allison and Eugui, 1993; Wright *et al.*, 2004; Simsek *et al.*, 2017; Warner *et al.*, 2018).

5.1.8 Conclusions, hypothesis and the research model

As described, a great deal of research on MMF has been conducted on lymphocytes, thus in the presence of the adaptive immunity. Therefore, it is not informative of direct effects of neutrophils. A large body of work also included monocytes and macrophages, but MMF's direct effects on neutrophils are less clear.

Considering the effectiveness of MMF, which is given for inflammatory conditions, the question has arisen if MMF might have a direct effect on neutrophils independent of lymphoid factors as neutrophils are critical in inflammatory disease. They are the most numerous type of white blood cell in human peripheral blood. Under normal conditions, leukocytes travel in the centre of blood vessels. Within the sites of inflammation, the vessels are dilated and the consequent faster blood flow enables neutrophils to interact with vascular endothelium. During an inflammatory response the induction of adhesion molecules on the endothelium within the infected/inflamed tissue along with induced changes on adhesion molecules expressed by leukocytes, recruits circulating leukocytes (recruitment of inflammatory cells was described in section 1.6.1.1.2).

Neutrophils recruited at the infection/inflammation site are considered to be a hallmark of inflammation (Donnelly and Haslett, 1992). As opposed to other cells of innate immunity, neutrophils undergo a complex migration from the vascular lumen to the tissues and in this context, they are the first cells to arrive to the infection/wound site (Voisin and Nourshargh, 2013). Under normal circumstances, neutrophils are not recruited to the inflamed site until approximately 6 hours after initiation of the inflammatory response (Serhan and Savill, 2005). In this respect, neutrophils are essential to exert host-defence actions in tissues.

Work from the Johnston group demonstrated that the total number of neutrophils is not reduced after treatment with MMF in unmanipulated or *Cryptococcus* infected *Tg(mpx:GFP)ⁱ¹¹⁴* zebrafish larvae (which lack adaptive immunity) (Gibson *et al.*, 2018). This is in line with *ex-vivo*, -rodent work which also indicates neutrophil production was not altered (Allison and Eugui, 2000).

However, in the clinic MMF is given in the context of existing inflammation. Therefore, I hypothesised that MMF would have a direct effect on neutrophil function during neutrophil inflammation. To address this hypothesis, I proposed to test MMF in the zebrafish model of neutrophilic inflammation where innate immunity operates without functional adaptive immunity (Renshaw *et al.*, 2006). In this model, neutrophilic inflammation is induced by injury to the zebrafish tail. The model enables assessment of the ability of compounds to modulate neutrophilic inflammation *in vivo* (Loynes *et al.*, 2010). Using this model, I have demonstrated that MMF treatment results in reduced neutrophil numbers and induces neutrophil apoptosis during the resolution of a neutrophilic inflammatory response, which is beneficial. I also tested if AZA can reduce the number of neutrophils following inflammatory insult. AZA does not replicate the effect observed with MMF.

5.2 Results

5.2.1 Neutrophilic inflammation is reduced with MMF treatment

To test the hypothesis that MMF has a direct effect on neutrophil function, the zebrafish tail transection assay of neutrophilic inflammation was used (Figure 2.2). In this model, an injury to the tailfin (Figure 2.2) induces a robust inflammatory response, with distinct phases of neutrophil recruitment peaking at approximately 6 hpi (Renshaw *et al.*, 2006; Gray *et al.*, 2011). At 12 hpi inflammation resolution is not entirely complete (Renshaw *et al.*, 2006), but by 24 hpi it largely is (Renshaw *et al.*, 2006); by 48 hpi recruited neutrophil numbers return to baseline (Gray *et al.*, 2011). Each phase can be easily monitored by imaging GFP-expressing neutrophils.

To observe the effect of MMF on the recruitment of neutrophils to the site of injury, zebrafish larvae were exposed to pharmacological agents immediately post-wounding. MMF demonstrated a small reduction in the number of neutrophils at 6 hpi, indicating that MMF inhibits the recruitment of neutrophils in this early phase of inflammation (Figure 5.5A), which is characterised by the rapid accumulation of immune cells. Inhibition of neutrophils recruitment with

SP600125 (c-Jun N-terminal kinase inhibitor, positive control) had a larger effect on recruitment compared to MMF ($P < 0.0001$, $P = 0.0495$, respectively).

To test the effect of MMF on resolution, MMF was applied at 4 hpi when recruitment of neutrophils was maximal. By 4 hpi, the number of neutrophils at the wound site approaches the expected peak value (Renshaw *et al.*, 2006) and the effect of drugs on the resolution phase of neutrophilic inflammation can be studied. Thus, at 4 hpi, larvae that had recruited comparable numbers of neutrophils (30-40) were subsequently treated and neutrophil counts undertaken at 6 hpi and 24 hpi. Interestingly, at 2 hpt (6 hpi) there was no effect on further neutrophil recruitment (Figure 5.5B). MMF neither augmented neutrophil numbers at 6 hpi, nor prevented the further recruitment. While there was no significant difference between controls and the MMF treated group at 6 hpi (Figure 5.5B), MMF reduced the number of neutrophils remaining at the wound site during the resolution phase of inflammation at 24 hpi (Figure 5.5C). Increased resolution was indistinguishable from treatment with the positive control.

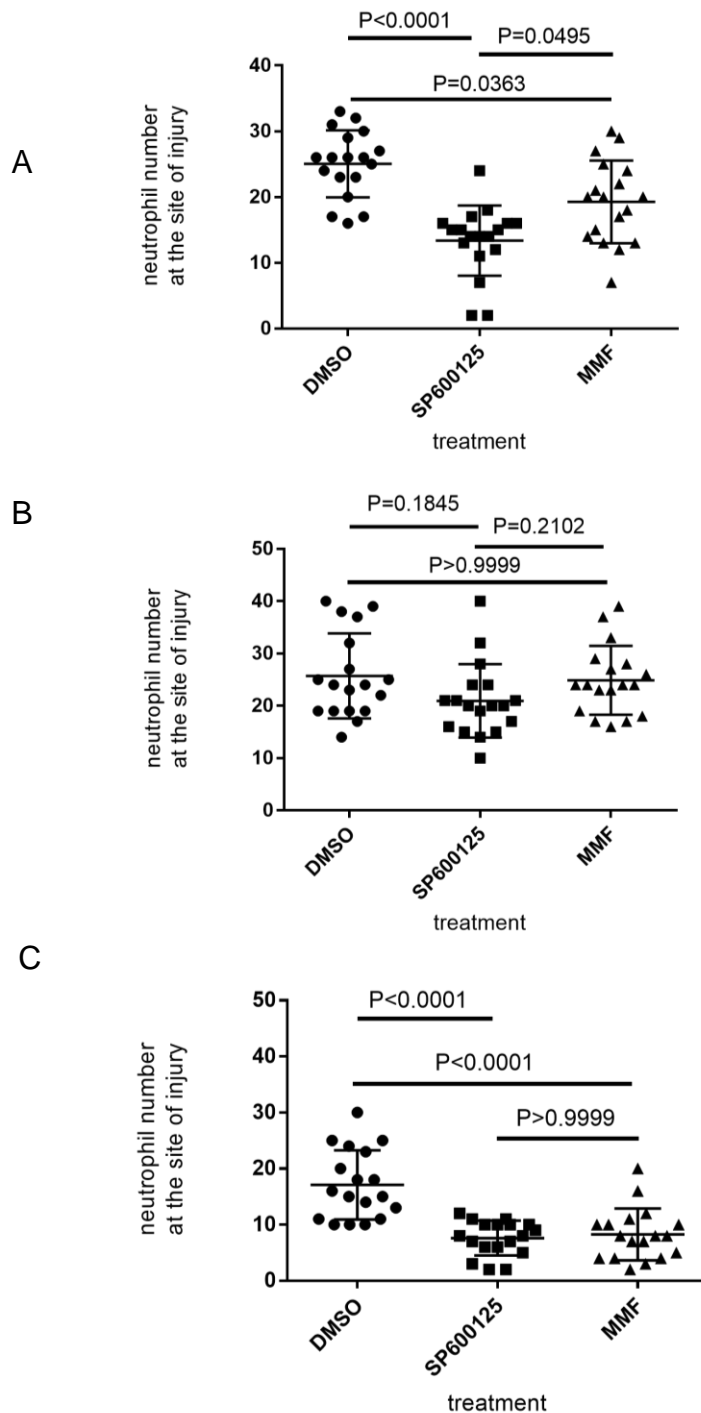


Figure 5.5 MMF accelerates resolution of neutrophilic inflammation *in vivo*.

(A) Number of neutrophils at the site of injury at 6 hpi is reduced with MMF treatment. Compounds added at the time of injury (B) MMF does not alter neutrophil recruitment at 6 hpi (2 hours after compounds addition). (C) By 24 hpi (20 hours after compounds addition) number of neutrophils at the site of injury is reduced in MMF treated group; n=18 per group in 3 independent experiments; in each repeat 6 larvae were used per treatment per time-point. P values presented as One-way ANOVA (and nonparametric) in Kruskal-Wallis test with Dunn's multiple comparisons; data presented as dot plot with mean \pm standard deviation; DMSO (vehicle control), MMF (compound of interest) and the c-Jun N-terminal kinase inhibitor, SP600125 (positive control (A. L. Robertson *et al.*, 2014)).

To find the relative contribution of recruitment and resolution in the decrease in neutrophilic inflammation with MMF treatment, the percentage change in the number of neutrophils at the site of injury in the same zebrafish between 6 and 24 hours was calculated (Figure 5.6). MMF treatment resulted in a more than 2-fold reduction in the proportion of neutrophils at the site of injury between 6 and 24 hours ($P=0.0003$). These results confirm that reduced inflammation with MMF treatment was due to increased resolution. However, it became apparent that MMF might be influencing early, but not later stages of neutrophil recruitment during the course of inflammatory response, where the neutrophil numbers usually peak at 6 hpi. However, during the resolution phase of inflammation, the 6 hpi time-point remains unaffected and a significant reduction is seen by 24 hpi.

To test whether the reduction in neutrophil recruitment on treatment with MMF may have been due to a decrease in the total number of neutrophils, the total number of neutrophils was compared. Representative images of larvae treated with DMSO and MMF after 6 and 24 hours of incubation are presented in Figure 5.7. No difference in the total number of neutrophils between treatments was found either at 6 (Figure 5.8A) or 24 hpt (Figure 5.8B) as described previously (Gibson *et al.*, 2018). Since the whole-body total neutrophil count was assessed in the absence of any inflammatory stimulus, this supported the hypothesis that MMF acts specifically on activated neutrophils participating in the inflammatory response as shown in the recruitment and resolution experiments.

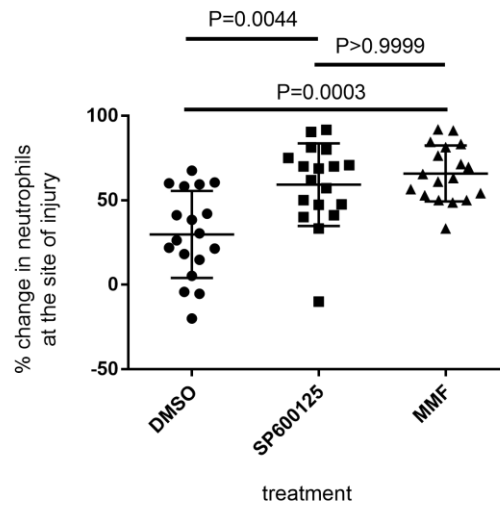


Figure 5.6 MMF results in a more than 2-fold reduction in the proportion of neutrophils at the wound site between 6-24 hpi (2 and 20 hours after compounds administration, respectively). Percentage change in number of neutrophils at the site of injury calculated by extracting the number of neutrophils at 24 hpi from the number at 6 hpi and dividing by number at the first time-point, 6 hpi; n=18 per group in 3 independent experiments; in each repeat 6 larvae were used per treatment per time-point. P values presented as One-way ANOVA (and nonparametric) in Kruskal-Wallis test with Dunn's multiple comparisons; data presented as dot plot with mean \pm standard deviation.

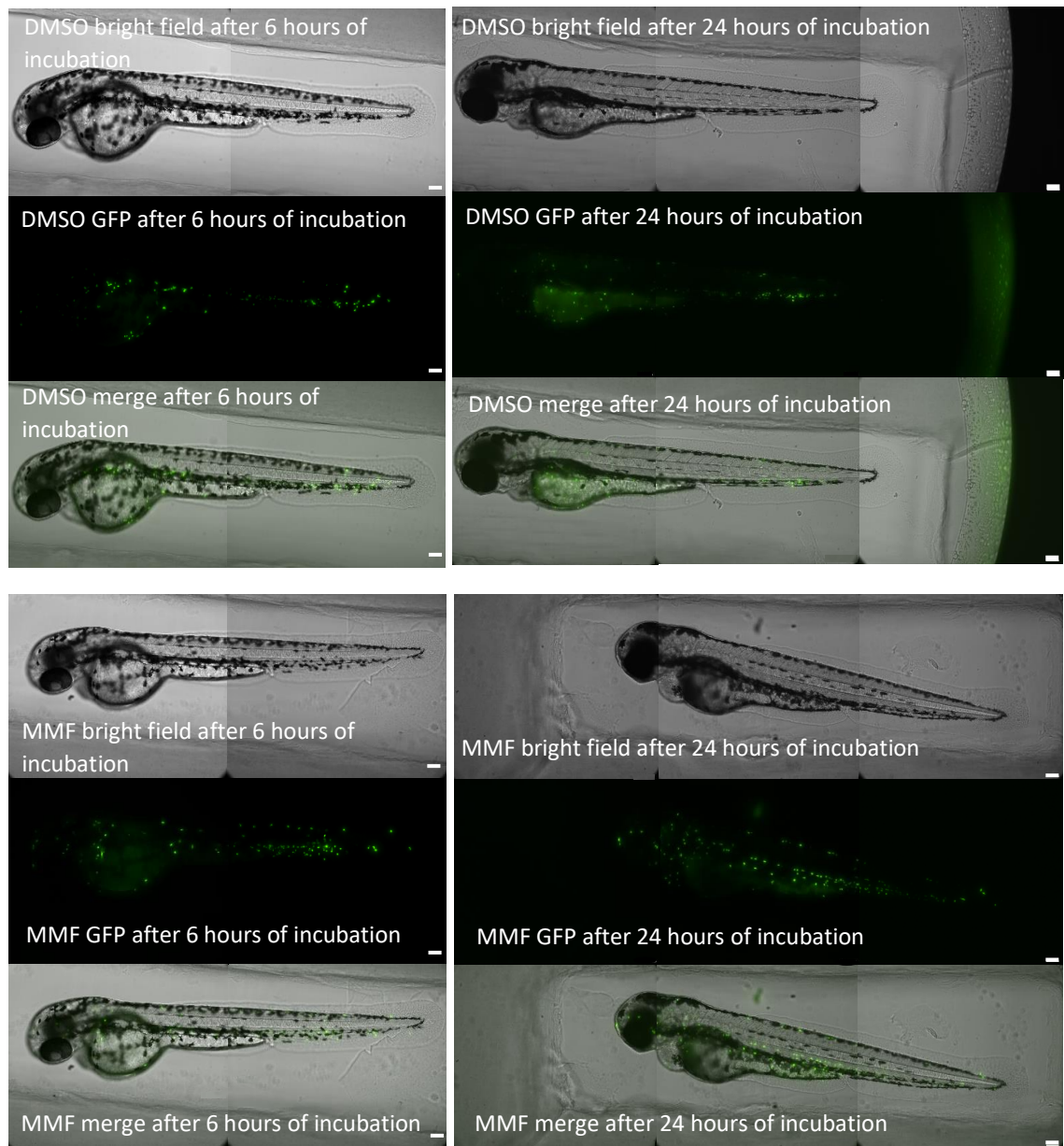


Figure 5.7 Representative images of larvae treated with DMSO and MMF after 6 and 24 hours of incubation. Scale bars are 100 μ m.

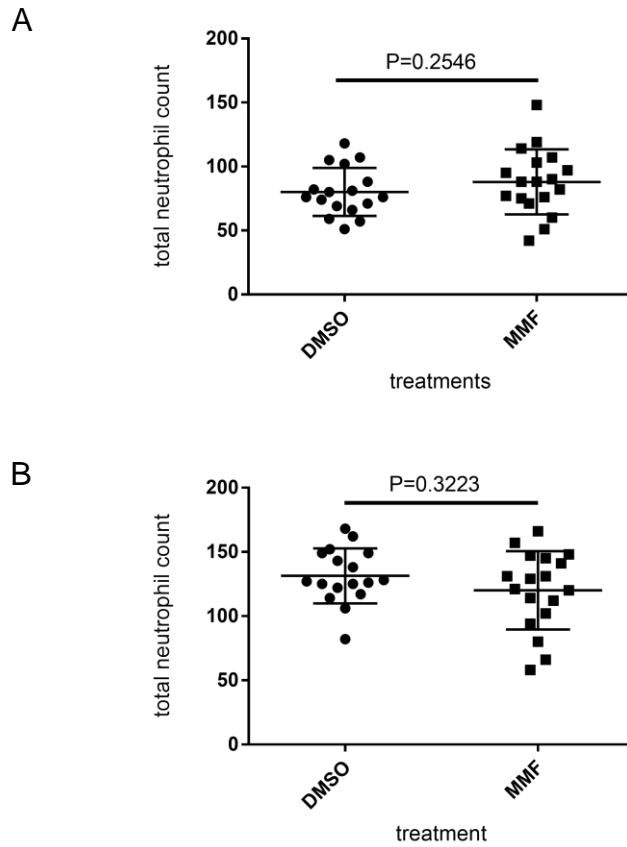


Figure 5.8 MMF has no effect on the total number of neutrophils. MMF does not alter the total number of neutrophils after (A) 6 hours incubation or (B) after 24 hours incubation; n=17-18 per group in 3 independent experiments; in each repeat 6, 6, 5 larvae were used in DMSO group at 6hpi whereas 6, 6, 6 larvae were used in MMF group at 24 hpi. P values presented are Mann-Whitney test; data presented as dot plot with mean \pm standard deviation.

Neutrophil recruitment, although necessary in the first stage of inflammation, might be a direct cause of chronic conditions. Known anti-inflammatory drugs inhibit neutrophil recruitment (Hasçelik *et al.*, 1994), consistent with results seen in both the recruitment and resolution assays (Figure 5.5). In the recruitment experiment, MMF blocked neutrophil recruitment with a small, but significant effect. In the resolution assay, MMF failed to alter numbers of neutrophils at sites of injuries at 6 hpi. In contrast, a significant drop in neutrophil numbers is seen by 24 hpi. The percentage resolution of the neutrophilic component of the inflammatory response shows a significant increase in the resolution. In this light, these findings provide a basis to believe MMF has anti-inflammatory and pro-resolution properties, which is accentuated by the fact that there is no effect on the whole body count in the absence of any inflammatory factor (Figure 5.8).

5.2.2 AZA does not replicate the effect of MMF treatment on neutrophilic inflammation

As previously described, AZA is also a lymphoid cell anti-proliferative agent. AZA was tested due to its application in a number of inflammatory conditions, e.g. Crohn's disease or ulcerative colitis (Fraser, 2002), which are also managed with MMF (Appel *et al.*, 2005). Both MMF and AZA interfere with DNA synthesis, but via distinct mechanisms act at distinct points (Figure 5.4). Here, AZA was used to distinguish whether the results seen following MMF treatment are specific to its mechanism, as AZA is one of few drugs also involved in the inhibition of *de novo* purine synthesis.

In contrast to MMF, AZA did not affect recruitment or resolution of neutrophils from wound sites (Figure 5.9A-C). Similar to MMF, no change in total neutrophil numbers in AZA-treated larvae was observed (Figure 5.10A-B).

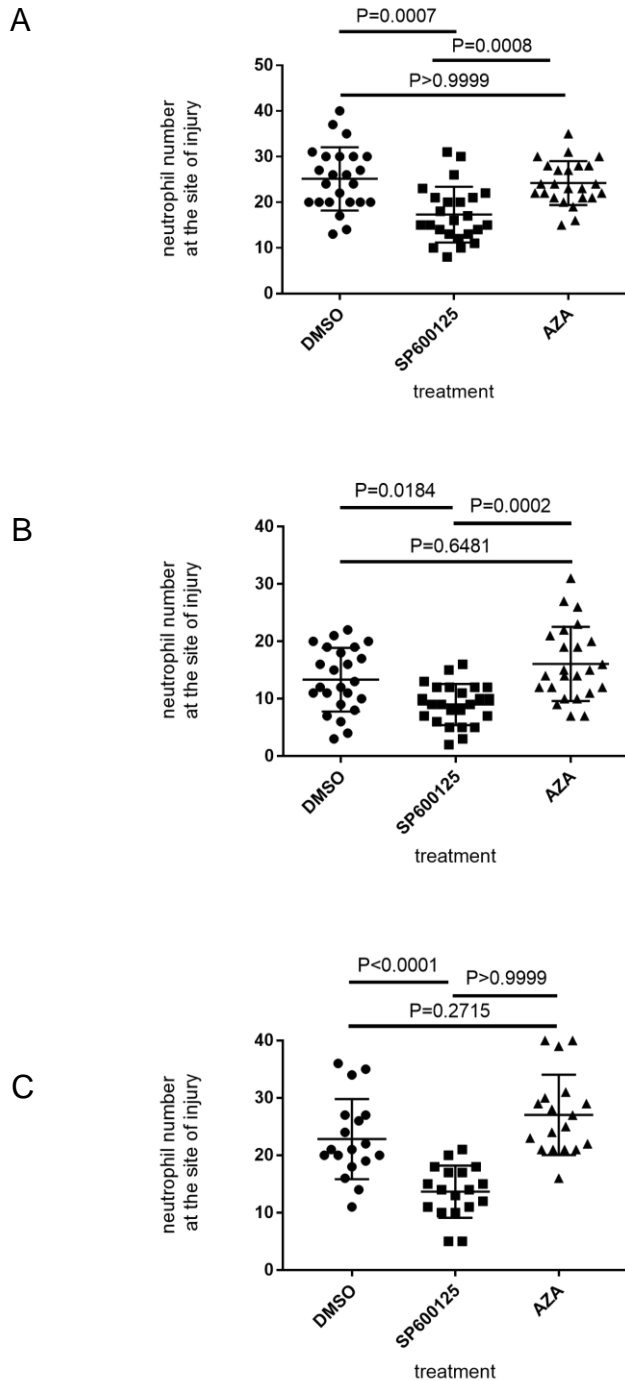


Figure 5.9 AZA does not accelerate the resolution of neutrophilic inflammation. (A) AZA has no effect on neutrophil recruitment at 6 hpi (2 hours after compounds addition); $n=24$ per group in 4 independent experiments; in each repeat 6 larvae were used per treatment (B) AZA has no effect on neutrophil recruitment at 24 hpi (20 hours after compounds addition); $n=24$ per group in 4 independent experiments; in each repeat 6 larvae were used per treatment (C) AZA has no effect on the recruitment of neutrophils at 6 hpi (compounds addition immediately after injury); $n=24$ in 4 independent experiments; in each repeat 6 larvae were used per treatment. P values presented as One-way ANOVA (and nonparametric) in Kruskal-Wallis test with Dunn's multiple comparisons; data presented as dot plot with mean \pm standard deviation.

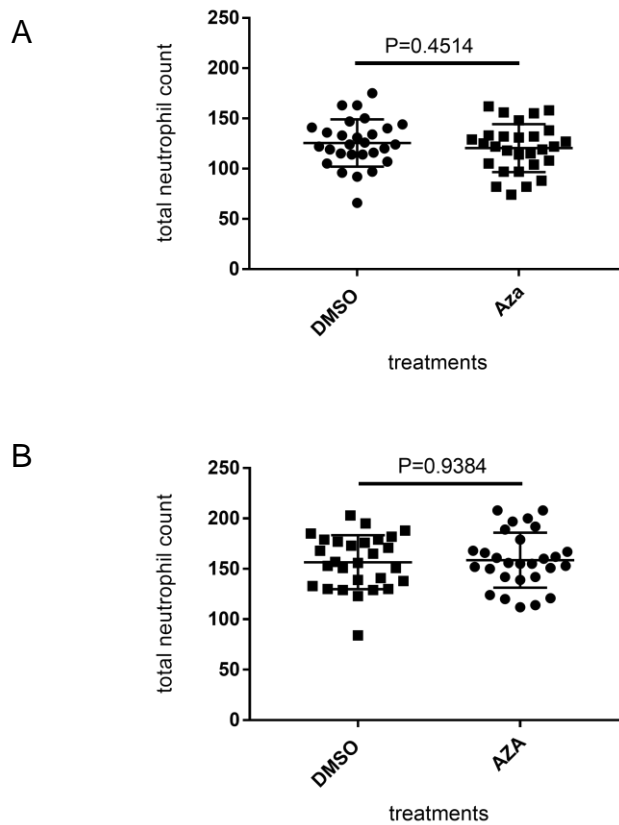


Figure 5.10 AZA has no effect on the total number of neutrophils. AZA does not affect the total number of neutrophils after **(A)** 6 hours incubation or **(B)** after 24 hours incubation; n=28 per group in 3 independent experiments; in each repeat 10,10, 8 in DMSO treatment whereas 10, 9, 9 larvae were used in AZA group at both 6 hpi and 24 hpi. P values presented are Mann-Whitney test; data presented as dot plot with mean \pm standard deviation.

5.2.3 Reverse migration is not the mechanism by which MMF accelerates inflammation resolution *in vivo*

It was first reported that neutrophils can exit inflammatory sites via a phenomenon of reverse migration over a decade ago (Tharp, 2005; Buckley *et al.*, 2006; Mathias *et al.*, 2006). There are many modes to this migration, including reverse luminal crawling, reverse abluminal-to-luminal transendothelial migration, reverse abluminal crawling, and reverse interstitial migration. In general, the term describes the general concept of retrograde neutrophil migration (Nourshargh *et al.*, 2016). The event has become accepted as a mechanism of neutrophil removal from the site of inflammation and of inflammation resolution. Neutrophils migrating away from the site of inflammation have been reported both in mammalian systems (Buckley *et al.*, 2006) and zebrafish (Mathias *et al.*, 2006; Elks *et al.*, 2011; A. L. Robertson *et al.*, 2014). The study of reverse migration could therefore identify novel means of modulating inflammation and thereby make an important contribution to counteracting negative effects of chronic inflammatory diseases.

As previously stated, the number of neutrophils at 6 hpi was not altered following MMF treatment for 2 hours. However, their number was attenuated after 20 hours of treatment indicating reduced neutrophilic inflammation. To assess neutrophil behaviour after 6 hpi, a well-established assay of neutrophil reverse migration (Elks *et al.*, 2011; A. L. Robertson *et al.*, 2014), which uses optimised photoconversion (Dixon *et al.*, 2012), was performed on *mpx:Kaede* larvae (Figure 2.4, Figure 5.11). Fluorescence time-lapse imaging of photo-converted neutrophils at the site of injury was performed. Results indicated larvae challenged with MMF had unaltered reverse migration of neutrophils from the wounded site (Figure 5.12). This suggests the retrograde migration is not the mechanism by which neutrophils are cleared from the wound site. Moreover, while there were different numbers of neutrophils at the site of injury with MMF, there was no difference in the number or rate of neutrophils leaving the site of injury (Figure 5.12). Given there was no difference in reverse migration, another mechanism of neutrophils clearance was considered, apoptosis.

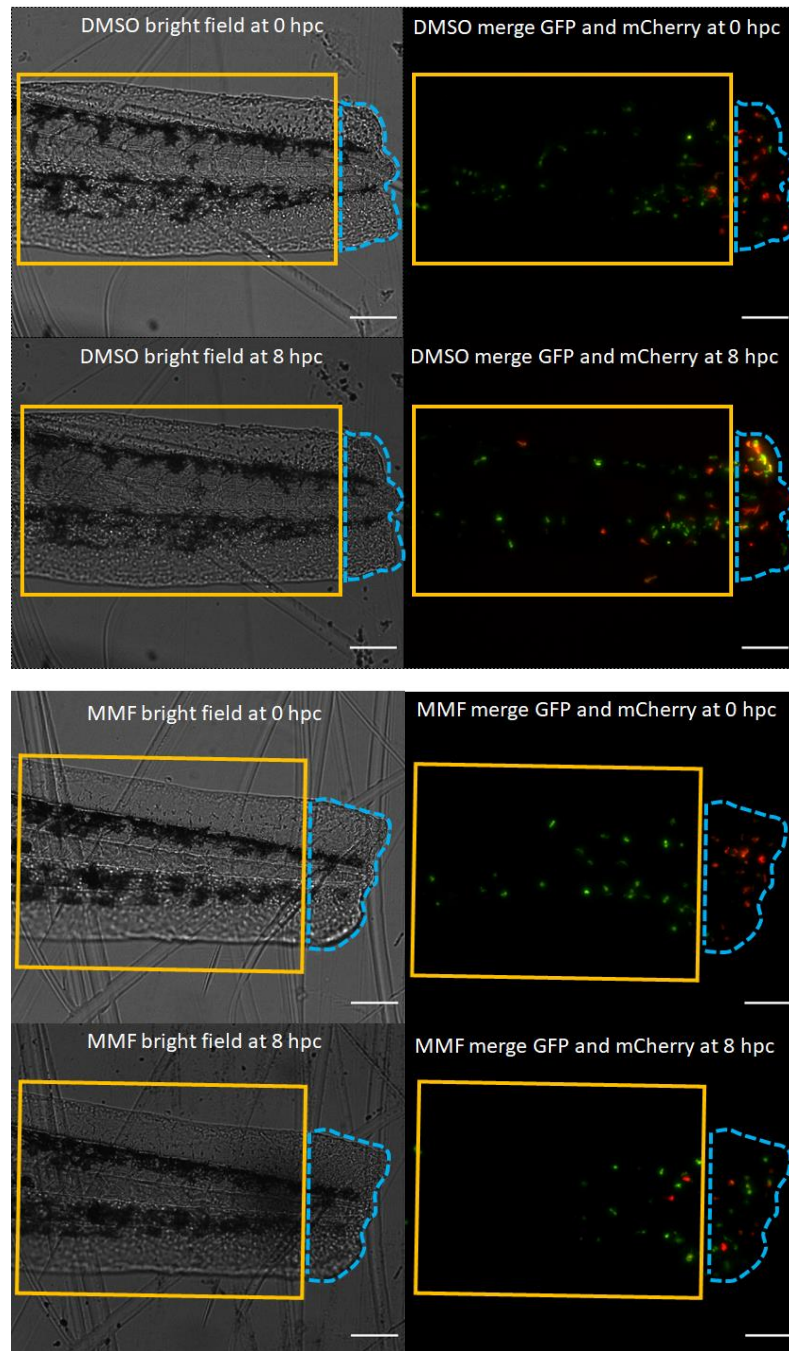


Figure 5.11 Representative images of *mpx:Kaede* larvae DMSO and MMF treated larvae at 0 and 8 hours post photoconversion (hpc). At 4 hpi the larvae with recruited neutrophils were treated with MMF or the DMSO control. At 6 hpi larvae were mounted and neutrophils at the site of injury were photo-converted from green to red. Larvae were imaged for 8 hours. The number of red neutrophils that migrated away from the site of injury into the anterior and posterior region to the circulatory loop was measured. Blue dashed line indicates the posterior region of the tail in which neutrophil recruited to the site of injury were photo-converted. Yellow box indicates the anterior region of the tail where reverse migration was assessed. Scale bars represent 100 μ m. Blue dashed line indicates the posterior region of the tail in which neutrophil recruited to the site of injury were photo-converted. Yellow box indicates the anterior region of the tail where reverse migration was assessed. Scale bars represent 100 μ m.

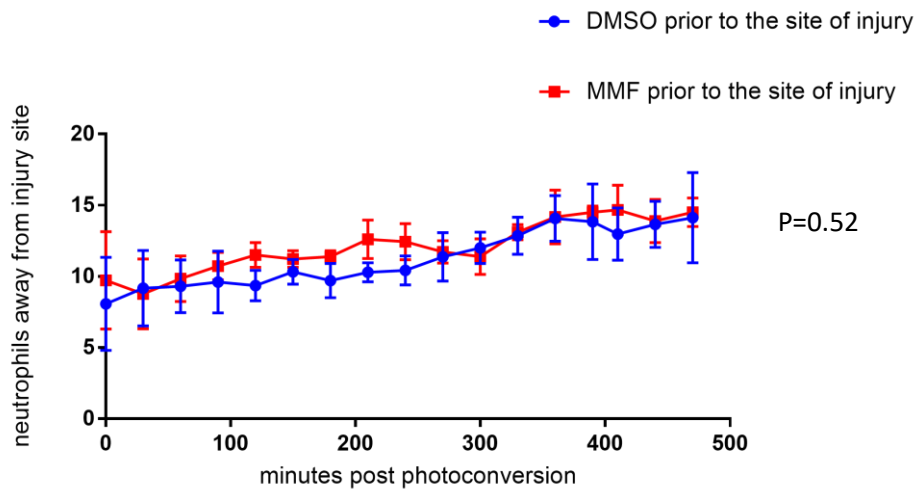


Figure 5.12 MMF does not promote reverse migration *in vivo*. Reverse migration was assessed by counting neutrophils in the posterior and anterior region to the circulatory loop. The region of interest was at the anterior of the tail and this data set was extracted to plot the number of photoconverted neutrophils leaving the area of transection. Data presented as points with connecting line with error bars. Points are the mean and the standard deviation of $n=17$ (DMSO) or $n=18$ (MMF) animals from 3 biological repeats; in each repeat 6, 6, 5 in DMSO group and 6, 6, 6 larvae were used in MMF group. Difference in slope assessed by linear regression analysis with $P=0.52$ chance of the lines being different by chance.

5.2.4 MMF induces neutrophil apoptosis in the tail injury model

Apoptosis is crucial for neutrophil functional shutdown, their clearance and timely resolution of inflammation (Haslett, 1992; Kebir and Filep, 2013). Apoptosis has been well documented as a clearance mechanism (Savill *et al.*, 1989; Grigg *et al.*, 1991; Cox *et al.*, 1995). Given there was no difference in reverse migration, apoptosis as another possible mechanism of neutrophil removal was tested. To assess for apoptosis-inducing properties of MMF, TUNEL staining *in vivo* at 12 hpi (an intermediate stage of inflammation resolution) was performed on injured 2 dpf *mpx:GFP* larvae (Figure 2.3, Figure 5.13). The number of apoptotic neutrophils (double *mpx:GFP* and TUNEL positive cells) in MMF treated larvae revealed a >2-fold increase in neutrophil apoptosis (Figure 5.14).

These findings suggest MMF promotes resolution of inflammation in the tail injury model through apoptosis. The difference in the percentage of apoptotic neutrophils between control (>1%) and MMF-treated (>2%) groups although being small, is comparable to rates of detectable apoptosis in patients with inflammatory conditions (Matute-Bello *et al.*, 1997) and agrees with differences in neutrophil numbers measured at 24 hpi.

Furthermore, at 12 hpi, the ideal time-point for assessing the resolution stage of inflammation (an intermediate stage of inflammation resolution (Loynes *et al.*, 2010)), there was a significant difference in the number of neutrophils at the site of injury with MMF (Figure 5.15), accentuating apoptosis contribution to reduced neutrophils numbers. To test for a difference between DMSO and MMF, the neutrophil number was calculated in the same fish, used in apoptosis assay. As expected, the number of neutrophils at 12 hpi was significantly different between treated groups (Figure 5.15) ($P=0.0103$). This result suggests the reduction in neutrophils numbers seen by 24 hpi in the resolution assay begins much earlier within the reduction being already statistically significant at 12 hours.

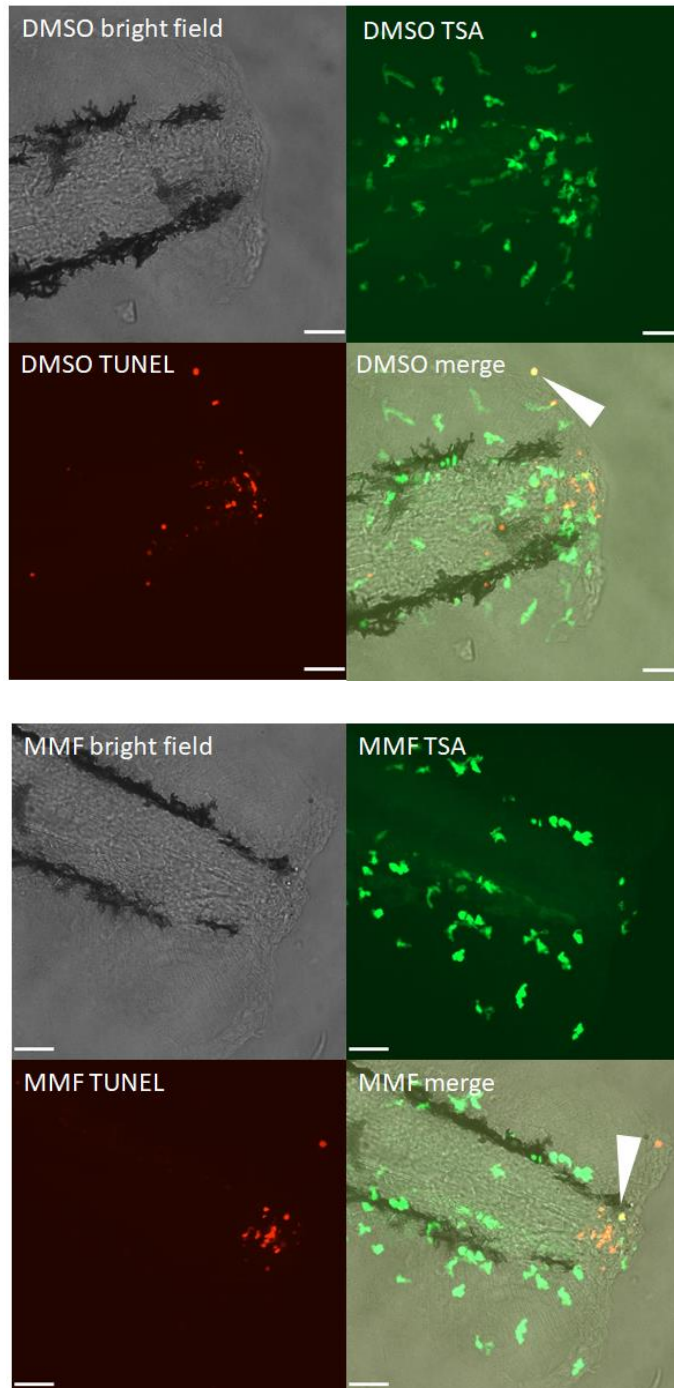


Figure 5.13 Representative images of *mpx*:GFP zebrafish fixed and stained 12 hpi for colocalisation of neutrophil (FITC-TSA) and apoptotic (TUNEL) markers. Dual staining for neutrophil and apoptosis markers provides biochemical confirmation of neutrophil apoptosis during resolution of neutrophilic inflammation in *mpx*:GFP zebrafish at 12 hpi. Yellow are apoptotic neutrophils (white arrowheads) that are double-positive (positive for green neutrophil- FITC-TSA specifically labels the Mpx protein green and positive for red apoptotic markers- TUNEL labels the Nick-ended DNA fragments red (rhodamine) when a cell undergoes apoptosis). Images are extended focus of 15 sections in the Z dimension with 5.37 μm z step. Scale bars represents 100 μm .

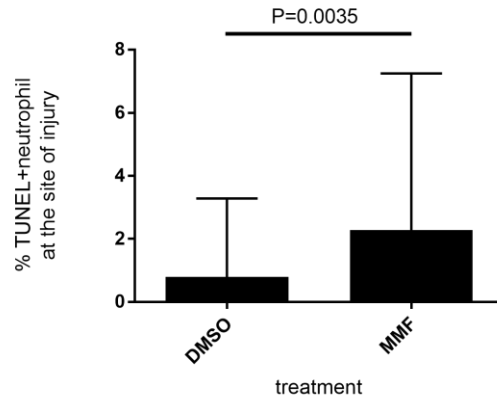


Figure 5.14 MMF increases neutrophil apoptosis at the site of inflammation. MMF treatment results in a >2-fold increase in neutrophil apoptosis at the site of injury at 12 hpi. 139 vehicle treated and 161 MMF treated *mpx:GFP* larvae from 3 independent experiments; in each repeat 27, 70, 42 in DMSO group and 48, 73, 40 larvae were used. P value presented is Mann-Whitney test; data presented as column graph bars with mean \pm standard deviation.

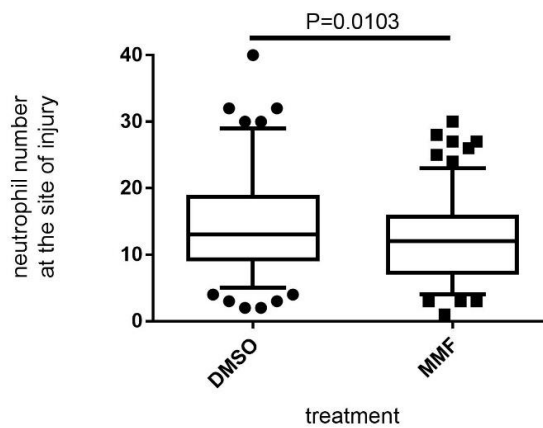


Figure 5.15 MMF reduces the number of neutrophils at the site of injury at 12 hpi. 139 vehicle treated and 161 MMF treated animals from three biological repeats; in each repeat 27, 70, 42 in DMSO group and 48, 73, 40 larvae were used. The number of *mpx:GFP* zebrafish larvae is high as this data is obtained from larvae assayed with apoptosis staining. P value presented is Mann-Whitney test; data presented as box and whiskers with 5-95 percentile.

Finally, to investigate whether inhibition of neutrophil cell death was sufficient to reverse the increased inflammation resolution identified with MMF, a pan-caspase inhibitor Z-VAD was used. The effect of MMF on neutrophil numbers was reversed by the addition of Z-VAD, confirming MMF induces caspase-dependent cell death, and the effect of MMF was reversed at both 6 and 24 hours (Figure 5.16A-B). This indicates that preventing neutrophil cell death was sufficient to reverse increased neutrophilic inflammation resolution due to MMF.

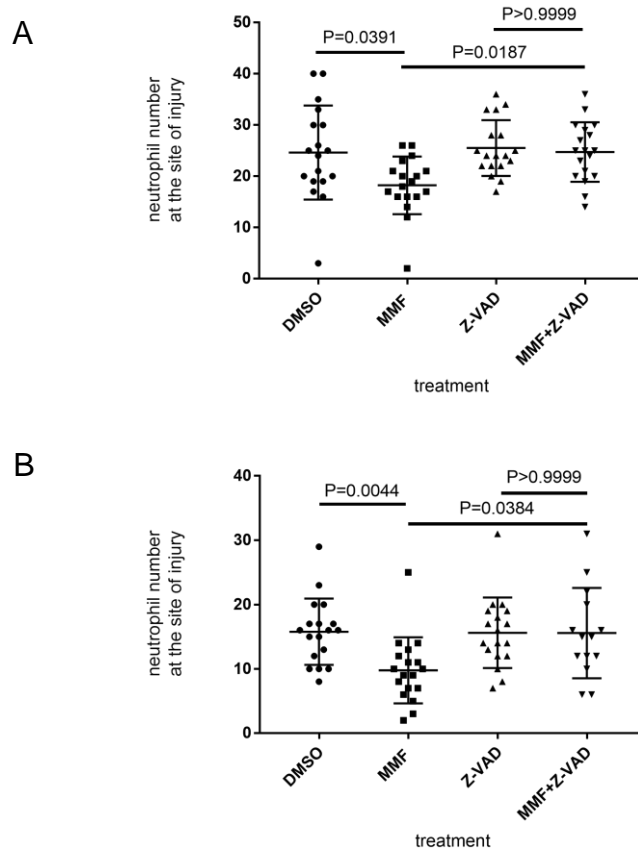


Figure 5.16 The effect of MMF is reversed with Z-VAD at both 6 and 24 hpi. Z-(**A**) Z-VAD blocks the effect of MMF at 6 hpi (2 hours after compounds administration); n=18 per group in 3 independent experiments; in each repeat 6 larvae per treatment were used (**B**) Z-VAD blocks the effect of MMF at 24 hpi (20 hours after compounds addition); n=14-18 per group in 3 independent experiment; in each repeat 6 larvae in all groups were used; at 24 hpi in DMSO, MMF, Z-VAD 6 larvae were used in each repeat whereas 5, 5, 4 in MMF+Z-VAD group. P values presented as One-way ANOVA (and nonparametric) in Kruskal-Wallis test with Dunn's multiple comparisons; data presented as dot plot with mean \pm standard deviation.

5.3 Discussion

5.3.1 The dose of MMF used in the study

The experiments in my study aimed to determine that MMF would have a direct effect on neutrophil function during neutrophil inflammation. To test this hypothesis, I used the well-described zebrafish model of neutrophilic inflammation (Renshaw *et al.*, 2006).

The dose used in the study was 0.5 μM . One could ask how the dose was chosen. As described in Chapter 2 regarding the dose chosen for the zebrafish study, when zebrafish embryos are given 1.5 μM mycophenolic acid from fertilisation, intersegmental blood vessel formation is revoked. The dose of 0.9 μM significantly reduces blood vessel formation (Wu *et al.*, 2006). A study looking at liver transplant patients treated with MMF, demonstrated mycophenolic acid concentrations in the body ranges from 1.5 μM up to 22 μM (Dasgupta *et al.*, 2013). Target therapeutic range for liver recipients is between 1.0–3.5 $\mu\text{g/ml}$ (equivalent of 3.125 μM -10.9 μM , respectively) (Tredger *et al.*, 2004). In liver transplantation 1 or 1.5 g twice daily of MMF is the standard protocol. Target dose, when combined with cyclosporine, falls between 3 μM to 11 μM (Shaw *et al.*, 2007). Recommendations obtained online from drugs.com confirm the dose for hepatic transplantations and describe the dose for renal and cardiac of 1.5 g daily (<https://www.drugs.com/dosage/mycophenolate-mofetil.html>).

It was not possible to use therapeutic doses of MMF considering angiogenic inhibition in zebrafish. Therefore, to minimise these effects it was decided to treat zebrafish with 0.5 μM . Richard Hotham, a former BMedSci student in the Johnston lab, did the establishment of this dose. Other doses were also tested in zebrafish survival assays. This level of drug was thought to still be likely to cause effects in macrophages because concentrations between 0.1 μM and 1 μM of mycophenolic acid caused apoptosis in monocytes *in vitro* (Cohn *et al.*, 1999). The dose selected was representative of therapeutic blood stream concentrations of MMF in humans.

At the same time it is acknowledged the dose response could have been done in the zebrafish tail transection assay to find the lowest dose that gives the required

effect. However, this would mean that the zebrafish would be tested under conditions where the inflammation is reduced but the immunosuppressive effect might also be reduced. This was not the aim of the experiment. I wanted the zebrafish to be immunosuppressed. Only such conditions would be informative of the real effects and the mechanism MMF exerts when the zebrafish is immunosuppressed. Thus, the safe dose of 0.5 μ M was used. This also suggests that finding the lowest dose that reduces neutrophilic inflammation in patients could be beneficial for them when the immunosuppression is not required.

5.3.2 Neutrophilic inflammation is reduced with MMF treatment

Here I have shown MMF treatment results in neutrophil cell death by apoptosis *in vivo*, thereby reducing neutrophilic inflammation. Neutrophil apoptosis, not reverse migration, is the mechanism by which MMF promotes neutrophilic inflammation resolution. Reduced neutrophil numbers are beneficial in terms of the generalised anti-inflammatory effect of MMF.

MMF is widely used and is the mainstay of post-transplant management triple immunosuppression (Vincenti, 2003). Introduced first in 1995, MMF is preferred over AZA due to a lesser risk of acute graft rejection when used in a combined therapy (Knight *et al.*, 2009; Muntean and Lucan, 2013). It is also commonly used prior to transplantations in combination with other immunosuppressants (Maamoun *et al.*, 2010), replacement regimen (Banerjee *et al.*, 2000), in chronic diseases, e.g. Crohn's (Neurath *et al.*, 1998), chronic hepatitis (Nogueras *et al.*, 2005), in renal complications and autoimmune conditions (Appel *et al.*, 2005); or as a primary treatment in interstitial lung disease (Volkman *et al.*, 2017). All of these patients are characterised by one common factor being an inflammatory insult. However, research on the specific effects of MMF on neutrophils have been scarce and thus this study was proposed to test possible mechanisms of MMF engagement in neutrophil function.

Immune-modifying agents were identified previously using the zebrafish *in vivo* model of neutrophilic inflammation (Loynes *et al.*, 2010). Roscovitine and pyocyanin (inducers of human neutrophil apoptosis (Usher *et al.*, 2002; Rossi *et*

al., 2006)) led to reduced neutrophil numbers at the wound (Loynes *et al.*, 2010). The model also identified a number of compounds that accelerated inflammation resolution in a preliminary screen, of which half had known anti-inflammatory properties (Loynes *et al.*, 2010). Another zebrafish compound screen revealed the mechanism of action of tanshinone IIA (A. L. Robertson *et al.*, 2014), known to have anti-inflammatory activity (Fan *et al.*, 2009, 2016). This model of spontaneously resolving neutrophilia enables the identification of compounds that alter recruitment of neutrophils or escalate inflammation resolution. Therefore, the use of this zebrafish model in these studies allows one to reveal an off-target effect of MMF on neutrophil function as MMF specifically targets lymphocytes. This is particularly informative in elucidating the role of neutrophils during the inflammatory response during MMF treatment.

As described previously in the *Tg(mpx:GFP)ⁱ¹¹⁴* zebrafish model, neutrophils are recruited to the injury site and their numbers approach peak levels at approximately 6 hpi (Renshaw *et al.*, 2006). At this time-point, MMF was found to reduce neutrophil numbers. There were three plausible explanations for this decrease. 1) Given the finding that MMF increased neutrophil apoptosis, it is possible that with MMF treatment apoptosis occurs earlier than at 12 hpi and therefore a reduction in neutrophils is already seen at 6 hpi; 2) MMF has been reported to reduce levels of CINC, a neutrophil pro-inflammatory chemotactic mediator in a rodent model of lung perfusion injury, therefore MMF may directly reduce neutrophil numbers at the site of injury (Farivar *et al.*, 2005); 3) Myelosuppression, which is known to be a major complication, despite MMF's greatly favourable side-effect profile (Keown *et al.*, 1996), could play a role.

Granulopoiesis in adult vertebrates or humans occurs in the bone marrow (Perry, 1971); in adult zebrafish this process occurs in the kidney, a site considered equivalent to haematopoietic human bone marrow (Lieschke *et al.*, 2001; Crowhurst *et al.*, 2002). However, in zebrafish larvae, neutrophils develop at 18-24 hpf in the yolk sac mesoderm (Bennett *et al.*, 2001), between 24-30 hpf in intermediate cell mass (Crowhurst *et al.*, 2002) and possibly in ventral venous plexus >30 hpf (Willett *et al.*, 1999). Zebrafish larvae used in the experiment were always aged 48 hpf and their neutrophils are human homologues. Therefore, it

could be that MMF suppresses granulopoiesis in zebrafish. Potentially production of granulocytes is linked with neutropenia caused by MMF (Shapiro *et al.*, 1999; Nogueras *et al.*, 2005), possibly by inhibiting IL-17 as shown in mice treated with MMF (Von Vietinghoff *et al.*, 2010). This defect could also explain the finding. However, MMF-induced neutropenia in patients occurs typically after two to three months of treatment (Banerjee *et al.*, 2000; Budde *et al.*, 2004) and perhaps longer treatment and multiple zebrafish recruitment experimental time-points would reveal the neutropenic impact of MMF on neutrophil recruitment. However, inhibited myelopoiesis would not be in agreement with the whole body findings, which will be discussed later. Also, another aspect of the recruitment result cannot be ignored. My finding suggests MMF might exert neutrophil-targeted anti-inflammatory activity, which would be in line with broadly defined anti-inflammatory properties in mice (Durez *et al.*, 1999; Monguilhott Dalmarco *et al.*, 2011; Beduschi *et al.*, 2013) and would explain why MMF is clinically widely used in inflammatory conditions.

MMF treatment also showed a pro-resolution activity by accelerating inflammation resolution through reducing the numbers of neutrophils at the site of injury in the resolution phase. While neutrophil counts at the injury site could be taken at various experimental time-points, the key concept of the experimental design of the resolution assay is to select those injured larvae that have recruited comparable numbers of neutrophils to the wound by 4 hpi without any treatment. By 4 hpi, the number of neutrophils at the wound site approaches the expected peak value (Renshaw *et al.*, 2006) and the effect of drugs on the resolution phase of neutrophilic inflammation can be studied. The first time-point being 6 hpi that is equal to 2 hpt indicated no changes between MMF and the control. This suggests that either two hours treatment is not enough time for the drug to enter the zebrafish system and no change in neutrophils accumulation was observed, or this simply is the pharmacological pattern in zebrafish. At 12 hpi the number of neutrophils at the wound site is significantly reduced, although data was gained from a different set of fish (from the apoptosis assay). The number of neutrophils by 24 hpi was strikingly lowered, indicating MMF promotes inflammation resolution. Moreover, the relative contribution of recruitment and resolution in the

decrease in neutrophilic inflammation with MMF treatment expressed as the percentage change in the number of neutrophils at the site of injury confirmed that reduced inflammation with MMF treatment was due to increased resolution. In addition, MMF did not cause any changes in neutrophil numbers when uninjured fish were tested, suggesting MMF acts on neutrophils engaged in the inflammatory response. As already stated, the total number of neutrophils assay is informative of haematopoiesis. Many drugs may have a negative effect on the haematopoietic system and peripheral blood cells (Lubran, 1989). Therefore total body counts determine if drugs alter haematopoiesis in the absence of any inflammatory stimulus. Thus, if a drug increases or decreases neutrophil recruitment/persistence at the wound site, following injury or infection, it can be ruled out that the fish have more or less neutrophils due to a change in their production. In this context, MMF did not affect that process. However, MMF might have influenced the global fish development during which at a certain point haematopoiesis begins. Due to the timing of the whole body neutrophil count experiment, which lasted 24 hours, it was not possible to detect obvious changes in development often leading to distinguishable phenotypes such as oedema and curled tails (Kok *et al.*, 2015). It is possible that after 5 dpf, larvae can show developmental abnormalities, thereby supporting the hypothesis of MMF affecting global development and thus haematopoiesis. There are reasons to doubt this explanation of inhibited haematopoiesis as the number of neutrophils in the whole body count assay was not altered. It is also possible that haematopoiesis might have been accelerated but global development hampered. However, this is not shown due to the experiment limitation.

Clinical data shows the administration of MMF in combination with tacrolimus can result in thrombocytopenia (Mourad *et al.*, 2001) and leukopenia (Hao *et al.*, 2008). The incidence of leukopenic adverse effects caused by MMF is lower as compared to AZA when these immunosuppressants are given in combination with cyclosporine and corticosteroids (Eisen *et al.*, 2005). Thus, it becomes difficult to assess whether the adverse effects result only from MMF treatment. The differences in the incidence of haematological toxicity might arise from the additionally applied immunosuppressives and other factors such as the possibility of genetic predisposition (Jacobson, 2011; Sobiak *et al.*, 2013). In contrast, the

findings demonstrated MMF in conjunction with calcineurin inhibitors did not cause leukopenia or thrombocytopenia (Sobiak *et al.*, 2013). Therefore, it is difficult to draw a clear conclusion of MMF's effect on haematopoiesis. The apparent discrepancy seems not to influence MMF use after haematopoietic cell transplantation (Giaccone *et al.*, 2005).

5.3.3 AZA does not replicate the effect of MMF treatment on neutrophilic inflammation

Thiopurines (generated by AZA) were tested in my study for their ability to influence neutrophil inflammation following inflammatory insult. No effect on total neutrophil numbers or resolution of neutrophils at the site of injury was found. However, some patients cannot take AZA due to a genetic predisposition. The mechanism of AZA induced leukopenia is not clear, but there is a recognised host genetic component with several polymorphisms identified (Weinshilboum and Sladek, 1980). AZA is a prodrug that is metabolised both enzymatically and non-enzymatically to form thioguanine nucleotides. The polymorphisms associated with AZA neutropenia are in genes that regulate thiopurine deactivation, metabolism and repair of thiopurine mediated DNA damage (Weinshilboum and Sladek, 1980; Colombel *et al.*, 2000; H. S. Kim *et al.*, 2016; Yang *et al.*, 2016). For instance, mutations of thiopurine S-methyltransferase (TPMT) result in increased 6-thioguanine nucleotides (6TGNs) concentrations, putting patients at risk of developing bone marrow suppression (Ansari *et al.*, 2002; Lennard, 2002). Thus, mutations in TPMT is a factor for casual AZA-induced leukopenia (S.-K. Yang *et al.*, 2014). High RBC TGNs have been also linked to severe leukopenia (Lennard *et al.*, 1984). More than 20% of patients have AZA discontinued because of adverse events, most commonly due to bone marrow suppression induced leukopenia (H. S. Kim *et al.*, 2016). In this present study, AZA was tested independently of the genetic predisposition to severe myelosuppression resulting in leukopenia. Perhaps this is the reason for not observing reduced neutrophils numbers in zebrafish.

It is interesting that one nucleotide antagonist (MMF) alters neutrophil numbers, while another not (AZA). AZA requires conversion to its active metabolite (6MP)

in order to function in the inhibition of purine synthesis (Berenbaum, 1971). AZA releases 6MP *in vivo* and the metabolic products derived from the 6MP are the same as those formed from 6MP, when only 6MP is tested (Elion *et al.*, 1961, 1963). It seems that conversion of AZA to 6MP differs from species to species (e.g. in rhesus monkeys to the extent of 15% (Ding and Benet, 1979), 88% in humans (Nielsen *et al.*, 2001)). Therefore, 6MP levels should be checked in zebrafish to evaluate AZA efficacy. This may provide an insight into the absence of systemic neutropenia in my studies.

5.3.4 MMF induces neutrophil apoptosis in the tail injury model

MMF significantly reduced numbers of neutrophils in the resolution stage of inflammation and TSA/TUNEL staining *in vivo* identified an increase in the percentage of apoptotic neutrophils at the site injury at the intermediate time of inflammation resolution. Using the pan-caspase inhibitor Z-VAD to inhibit apoptosis, the effect of MMF was reversed, demonstrating that preventing neutrophil cell death was sufficient to reverse neutrophilic inflammation resolution due to MMF.

Circulating neutrophils are short-lived with the half-life of 8 hours (Dancey *et al.*, 1976), which increases several fold upon entry into infected or inflamed tissues (Edwards *et al.*, 2004). At sites of inflammation they first generate signals to amplify inflammatory recruitment, and at the late stages of healing they secrete signals to dampen inflammation (Nathan, 2006). Successful resolution of inflammation depends on timely removal of neutrophils to prevent further spillage of their cytotoxic content and thus limit neutrophil pro-inflammatory potential. Aged neutrophils commit suicide in the absence of pro-inflammatory mediators ahead of their removal by macrophages, while those not involved in inflammation undergo spontaneous apoptosis. Neutrophils also undergo apoptosis during tissue healing. Programmed cell death of neutrophils and their histotoxic contents is therefore a prerequisite of resolution of inflammation (Savill *et al.*, 1989)

Using TSA/TUNEL staining in fixed larvae it was demonstrated that there was a significant increase in the percentage of apoptotic neutrophils at the wound site

at 12 hpi with MMF treatment. Moreover, at 12 hpi, there was a significant difference in the number of neutrophils at the site of injury with MMF, likely due to occurrence of apoptosis. The magnitude of the difference between the two groups is small, likely due to measuring early in the assay. Combined with the previous results of reduced numbers of neutrophils during the resolution phase of inflammation, at 24 hpi and the experiment with Z-VAD where inhibition of apoptosis is sufficient to remove the effect of MMF, it was concluded that the effect at a single 12 hpi time-point is biologically meaningful. This conclusion is also supported by the previously published work of others using this and related models: e.g. in larvae treated with compounds once inflammation was already established, at 6 hours hpi and their effects on neutrophil number assessed at 12 hpi, 4-chromanone at 1 μ M showed a reduction described as 1.5-fold (Robertson *et al.*, 2016). In another zebrafish study, pyocynin, a profound inducer of neutrophil apoptosis in human and mouse models (Usher *et al.*, 2002; Allen *et al.*, 2005) showed a >1-fold reduction in neutrophils numbers at 12 hpi (Loynes *et al.*, 2010). Considering, the total number of neutrophils following 24 hours treatment revealed no difference and MMF increased the percentage of apoptosis, it is believed apoptosis was specific to activated neutrophils participating in the inflammatory response. This general idea could be tested by activation of neutrophils via different means (e.g. pro-inflammatory cytokines) in the presence and absence of MMF.

As described, apoptosis was assessed by TSA/TUNEL. Cells undergoing apoptosis are typically characterised by rapid and dynamic alterations of the cytoskeleton, leading to membrane protrusions and altered motility patterns typical of apoptosis (Elliott and Ravichandran, 2016). Although in my study the blebbing was not investigated, the typical shrunken and rounded morphology of an apoptotic neutrophil was observed, which corroborated studies of others (Majewska *et al.*, 2000; Nagaoka *et al.*, 2008) and neutrophils *in vivo* (Loynes *et al.*, 2010).

The event of apoptosis, biochemically confirmed with TSA/TUNEL, demonstrated that >2% of detectable neutrophils were apoptotic. The 2-fold increase in neutrophil apoptosis with MMF treatment suggests the pro-resolution properties

of the drug. Perhaps this visible neutrophil effect was scored less than 3%, but it is still consistent with numbers from mammalian models and disease states (Howie *et al.*, 1994; Matute-Bello *et al.*, 1997) and seen in zebrafish (Elks *et al.*, 2011). The percentage of detectable apoptotic reported in zebrafish is always small, e.g. DMSO 1.6% vs isopimpinellin 3.3% (Robertson, 2013) or DMSO 0.7% vs tanshinone IIA 1.5% (A. L. Robertson *et al.*, 2014) or DMSO 1% vs 3.5% nedocromil (Robertson *et al.*, 2016). Thus, from other work, the >2-fold increase in neutrophil apoptosis with MMF treatment can be still considered to be biologically significant. It should be noted that detecting apoptosis reflects the equilibrium between the development of apoptosis and phagocytosis of apoptotic neutrophils, e.g. by macrophages (Matute-Bello *et al.*, 1997). Thus it is possible that low numbers of apoptotic neutrophils could be associated with a shorter life-span due to patrolling macrophages rapidly phagocytosing apoptotic cells (Savill *et al.*, 1989). Furthermore, it is technically challenging to quantify total neutrophil apoptosis with the TSA/TUNEL assay as larvae are fixed at specific time-points; more detailed analysis using live reporters/dyes would provide a clearer answer on this point. Capturing efferocytosis would doubly confirm apoptosis.

It would also be interesting to show that MMF alone or in combination with inflammatory cytokines induces neutrophil apoptosis *in vitro* to confirm the direct action of MMF. Neutrophil trafficking is regulated by cell adhesion molecules. The movement of leukocytes is facilitated by adhesive pairing between, for example, β integrin on neutrophils with its endothelial ligand ICAM-1 (Lomakina and Waugh, 2009). Apoptotic neutrophils show reduced expression of L-selectin ligand. However CD11b/ CD18 and CD11c/CD18 integrins are expressed at increased levels (Dransfield *et al.*, 1995). MMF may suppress adhesion of neutrophils to epithelium, since the study of Laurent *et al.* found that MMF impeded attachment of human monocytes to endothelial cells and laminin (Laurent *et al.*, 1996). This is consistent with what has been found in the previous study of (Huang *et al.*, 2005). They showed that MMF suppressed both mRNA and surface levels of the TNF α -induced neutrophil adhesion molecule ICAM-1 and decreased TNF α -mediated adhesion of neutrophils to endothelial cells (it is known that TNF α induces the increased expression of leukocytes integrin ligands

for ICAM-1 (reviewed in (Nourshargh *et al.*, 2010)). Future studies could fruitfully explore potential loss of adhesive properties of neutrophils *in vivo* under MMF treatment.

Another promising finding was that the number of neutrophils at the site of inflammation was reduced by MMF treatment alone, reflecting a blockade of recruitment or an induction of neutrophil apoptosis. The effect of MMF on neutrophil number was reversed by the addition of an irreversible dipeptide caspase inhibitor, Z-VAD, confirming MMF induces caspase-dependent cell death.

In vivo studies show that Z-VAD is effective in inhibiting apoptosis and death in a rodent model of TNF α induced apoptosis in liver parenchymal cells during endotoxemia (Jaeschke *et al.*, 2000). Its efficacy is confirmed in intravenous (i. v.) administration in three rodent models of apoptosis: anti-Fas-induced liver failure, transient focal brain ischemia/reperfusion, and myocardial ischemia (MCI)/reperfusion (Yang *et al.*, 2003). The Yang's findings also corroborated anti-apoptotic properties of Z-VAD *in vitro* in HeLa S3 (the third clone isolated and propagated from an immortal cell line HeLa and the letter S in honour of physician and scientist Dr. Florence Rena Sabin) and Jurkat (immortal T lymphocytes) cell lines.

Human polymorphonuclear neutrophils (PMNs) undergo a spontaneous apoptosis associated with translocation of the BCL-2-like protein BAX (internal regulator of cells-fate) to the mitochondria and subsequent caspase-3 activation. However, PMNs treated with Z-VAD show inhibited caspase-3 activation and apoptosis, but not BAX movement (Maianski, 2002). Another study showed a relationship between induced pulmonary apoptosis of PMNs by inhalation of *Escherichia coli* (*E. coli*) and attenuated lung injury with tetrapeptide Z-VAD (Sookhai *et al.*, 2002). In ischemia–reperfusion (I/R) treated with aerosolised opsonised dead bacteria and Z-VAD intratracheally five minutes prior to reperfusion, the rate of pulmonary PMN apoptosis was similar to that of the I/R normal saline control group (Sookhai *et al.*, 2002).

The findings of Yang, Maianski and Sookhai formed the basis for the hypothesis of Z-VAD delayed neutrophils apoptosis thus delaying normal resolution of

inflammation. This was tested by the Renshaw lab using *in vivo* zebrafish model of neutrophilic inflammation (Renshaw *et al.*, 2006). Z-VAD delayed the resolution of inflammation in that model. This was shown by neutrophils numbers not being reduced at the wound site at 24 hpi when Z-VAD was added post recruitment (at 4 hpi) leading to the question of caspase-dependent apoptosis determining the neutrophil lifespan during inflammation. In the total number of neutrophil assay without inflammatory stimulus-an increase in total neutrophil count suggested a role for caspase activity in the neutrophil lifespan regulation. The direct link to neutrophil apoptosis was however shown in another study of theirs (Loynes *et al.*, 2010). Z-VAD delayed the resolution of inflammation when added after recruitment, and inhibited apoptosis shown by a reduced count of apoptotic neutrophils stained with FITC-TSA and TUNEL at 12 hpi.

Therefore, Z-VAD was selected in MMF study as an agent delaying inflammation of resolution as proven to be the most potent one as compared to bacterial lipopolysaccharides endotoxin (LPS), a stable synthetic cyclic adenosine monophosphate analog (dbcAMP) or several caspase inhibitors (Loynes *et al.*, 2010).

As Z-VAD prevents neutrophil cell death, the compound was also used to test if MMF's action can be reversed. According to the zebrafish literature, the dose of 100 μ M was used.

As described, Z-VAD inhibits caspases through irreversibly binding to the catalytic site of caspase proteases (Slee *et al.*, 1996) and therefore inhibits apoptosis in many cell types. Thus, it was suspected that Z-VAD would have a greater effect in elevating neutrophil numbers present at the injury site at the later time-point. This would have been in line with zebrafish findings, as when Z-VAD was added post recruitment, less apoptotic neutrophils were observed at the wound site (Loynes *et al.*, 2010). As stated, Z-VAD is a pan-caspase inhibitor and caspases are implied in both extrinsic and intrinsic pathways of apoptosis. Extrinsic signalling is mediated by the activation of death receptors by extracellular ligands. Intrinsic, or mitochondrial, apoptosis is mediated by noxious stimuli including UV, chemotherapeutic drugs or lack of the growth factor signalling pathways. There are two classes of caspases – initiators, which promote apoptosis by cleaving and activating other caspases, and effectors, that

begin the cellular changes apoptosis associated. The intrinsic pathway is associated with initiator caspase -9; extrinsic with initiator caspases -8 and -10; both use executioner caspase -3, -6, -7 (Janeway *et al.*, 2012a). Another classification provides caspases apoptosis (caspase-3, -6, -7, -8, and -9 in mammals) and inflammation (caspase-1, -4, -5, -12 in humans and caspase-1, -11, and -12 in mice)- associated (McIlwain *et al.*, 2015). As Z-VAD inhibits caspase-1, it is therefore thought not to be a trigger of apoptosis but more an enzyme that cleaves IL-1 β to stimulate pro-inflammatory cytokines (Sun and Scott, 2016). In addition, caspases -3, -6, -7, -8, and -9 are also inhibited (Yang *et al.*, 2003). On the grounds of the above, it is speculated in my study, MMF causes apoptosis by activation of those five aforementioned caspases. This is partially in agreement with delaying resolution of inflammation by caspases-3, and -9, and to a lesser extent with -8, tested in zebrafish model of inflammation (Loynes *et al.*, 2010). This might support a role for intrinsic apoptosis in inflammation resolution in this model, and would be in accordance with data from human neutrophils data (Murphy *et al.*, 2003; Maiani *et al.*, 2004).

In summary, my data indicate that MMF induces apoptosis *in vivo* and the result casts a new light on MMF mechanism of action in the absence of adaptive immunity.

Finally, my data, and the clinical evidence for use of MMF in inflammatory disease, suggest that neutrophils may be a *de facto* target for MMF. Recently, methotrexate, another chemotherapy drug used as an anti-inflammatory agent, has been identified as new inhibitor of the JAK/STAT pathway (Thomas *et al.*, 2015). Methotrexate is classically an inhibitor of the folate pathway, via dihydrofolate reductase inhibition, but its novel JAK/STAT activity may represent a significant proportion of its anti-inflammatory effect. Recently JAK/STAT has been demonstrated to be important in the development and resolution of inflammation (Shea and Murray, 2008). *In vivo* in the mouse model of experimental lupus nephritis, MMF reduced the level of pro-inflammatory cytokines with almost the same efficacy as CP-690,550, a JAK3 inhibitor (Ripoll *et al.*, 2016) which inhibits pro-inflammatory cytokines. Thus, my study demonstrates a specific effect of MMF on neutrophil apoptosis and highlights the

need for better mechanistic understanding of MMF action specifically and immunosuppressive treatment in general (Bojarczuk and Johnston, 2017).

5.3.5. Summary and future

The aim of this project was to investigate whether MMF frequently used in the treatment of autoimmune, inflammatory conditions and following organ transplant has a direct effect on neutrophil function. To address this hypothesis, the zebrafish model of neutrophilic inflammation was employed, where innate immunity operates without functional adaptive immunity. This study arose from the work of former BMedSci students (Richard Hotham, Rory Gibson), who investigated the modulation of innate immunity focusing on macrophages by MMF in the zebrafish model of cryptococcosis. As it has been suggested that some of MMF's clinical effect might be via modulation of innate immune cell function, e.g. macrophages (Shah *et al.*, 2010; von Vietinghoff *et al.*, 2011), I concentrated on another innate immune cell type, the neutrophil, during an inflammatory insult which fits with the idea of prescribing MMF in neutrophilic autoimmunity or inflammatory conditions.

Neutrophils were initially investigated *in vivo*. However, it is interesting to discover whether the effect of MMF is confirmed *in vitro* using human neutrophils. My intention was to collaborate with Dr Lynne Prince (Department of Infection, Immunity & Cardiovascular Disease) to detail the immunology of MMF in PMN isolated from human peripheral blood. For example, an interesting way to investigate MMF effects *in vitro* is to determine the percentage of apoptosis with increasing doses of MMF alongside AZA (e.g. at concentrations of 2.5, 5, 10, 25, 50 μM) to see if MMF and AZA have any effect on neutrophil apoptosis in a 'resting state' i.e. without stimulating the cells. It is also a subject of interest to determine the percentage apoptosis with stimuli such as GM-CSF and TNF α , which are present in a site inflammation. GM-CSF and TNF α prolong neutrophil lifespan (Cowburn *et al.*, 2002). Their addition to MMF is indicative of neutrophils still undergoing apoptosis and thereby the question of MMF overcoming the effects of these two stimuli could be answered. Roscovitine in contrast has the opposite effect on neutrophils (Rossi *et al.*, 2006) so the following research

question could be answered: does MMF in conjunction with roscovitine accelerate the apoptosis further? *In vitro* experiments on human neutrophils have been completed and the data should be integrated with zebrafish data in the new version of mycophenolate manuscript submitted for publication.

The following is the summary of the *in vitro* work on MMF and human neutrophils and its relevance to the *in vivo* work.

A question arose whether *in vivo* apoptosis data was biologically meaningful given the difference in the percentage of apoptotic neutrophils between control and MMF-treated groups being small (2-fold change). Also, a putative role of MMF in neutrophil cell death seemed interesting as it might be highly beneficial in some diseases with dysregulated neutrophil cell death, e.g. lupus nephritis (Wu *et al.*, 2017). The present *in vitro* study was designed to determine the effect of MMF on human neutrophils to find support for *in vivo* work in the zebrafish model of inflammation to claim it has a direct effect on neutrophil apoptosis.

We could show that MMF showed a 3-fold increase in the number of apoptotic human neutrophils, equating to nearly 20% apoptosis. In contrast, AZA did not have any effect on apoptosis enhancement. Both MMF and AZA interfere with DNA synthesis, but via distinct mechanisms act at distinct points (Figure 5.4). Experiments performed on human neutrophils, similarly to *in vivo* work used AZA to distinguish whether the results seen following MMF treatment were specific to its mechanism. AZA did not have any effect on neutrophil apoptosis *in vitro* in the 'resting' state, i. e. without stimuli. This is an important finding in the understanding of the difference in the mechanism of action between MMF and AZA. This aspect of results of the *in vitro* study indicates that MMF can induce apoptosis without inflammatory insult highlighting it is an inducer of neutrophil apoptosis. In addition, is able to induce inflammation resolution in my zebrafish study that includes inflammatory insult. AZA does not replicate MMF treatment neither *in vitro*, nor *in vivo* suggesting that the differences in the mechanism of action between MMF and AZA are responsible for neutrophil apoptosis *in vitro* and *in vivo*. This finding is the most critical piece of information answering my research question that was made into a hypothesis in the thesis aims: immunosuppression with MMF does have an effect on neutrophils.

Some earlier *in vitro* studies indicated that mycophenolate decreases GTP levels in human lymphocytes and monocytes with an anti-proliferative result. MMF significantly depleted GTP in human lymphocytes and monocytes but not in neutrophils shown by restoration of GTP in the first two cell types after guanosine addition (Allison and Eugui, 1993). However, the authors did not account for the fact that GTP can also be replenished from ATP, which is produced from inosinate as it is GTP. This is the branch point in the synthesis of AMP and GMP. Prior research also showed that mycophenolate increases apoptosis in monocytic (THP-1 and U937) cell lines (Cohn *et al.*, 1999). A question arose if human neutrophils undergo apoptosis as a result of GTP depletion. When guanosine was added to the cultures, the MMF's effect on apoptosis was abrogated, showing that the effect was due to guanosine depletion, i.e. MMF induces guanosine-dependent cell death.

The interaction with known apoptotic signalling pathways was also investigated in human neutrophils. TNF α or GM-CSF were used to inhibit apoptosis and then MMF was added to pre-treated cells. By contrast, roscovitine was used to induce apoptosis followed by MMF addition. MMF did not reverse the effect of GM-CSF or TNF α at any concentration used, but the stimuli reversed the pro-apoptotic effect of MMF. However, with roscovitine, which is pro-apoptotic, the effect was greatly enhanced at the highest concentration of MMF used, equating to a 3.5-fold change. *In vivo* I identified a small but significant >2-fold effect on increase in neutrophil apoptosis with MMF treatment. This was without inducing apoptosis. *In vitro*, after apoptosis induction, this effect was greater and can be described as synergistic. At this stage it is not understood which signalling pathways or mechanisms are involved in the control and coordination of neutrophil apoptosis under MMF and stimuli treatments (the mechanism of roscovitine is not known). Several questions remain unanswered at present. In the zebrafish model of inflammation MMF had a protective role, i.e. increased the resolution of inflammation. Thereby, to support a proposal that MMF has anti-inflammatory and pro-resolution properties as speculated in the zebrafish work, it would be ideal to repeat one of the key experiments in human neutrophils, namely the resolution assay. It is not possible to do so *in vitro* but LPS could be used to induce inflammation and then apoptosis enhancement with MMF measured. It is worth

noting that anti-inflammatory effects and pro-resolving effects do not totally overlap. Anti-inflammation mainly describes an inhibitory action while pro-resolving functions specify certain processes, e.g. apoptosis or efferocytosis. In either case, the end point is inflammation inhibition, but only pro-resolving mediators truly enable resolution. The mechanism of action of anti-inflammatory drugs inhibiting some specific pathways and pro-resolving drugs anticipated to start off a plethora of actions might be completely different. Therefore, there is a mechanistic difference between inhibiting specific mediators, which can be detrimental for tissue, and activating cellular processes preventing tissue damage. This vision has fostered the concept that pro-resolving-based therapies will promote both anti-inflammatory and pro-resolution actions, differing from traditional anti-inflammatory agents that solely inhibit key pro-inflammatory mediators (reviewed by (Sugimoto, Sousa, *et al.*, 2016)). Moreover, pro-resolving molecules have been recently described as exerting “mild-to-moderate actions” (reviewed by (Perretti *et al.*, 2015; Sugimoto, Sousa, *et al.*, 2016)). Perhaps MMF is a potential resolution agent since it might have not blocked the anti-apoptotic actions of TNF α or GM-CSF and it caused apoptosis both *in vitro* in this current study and *in vivo* in my zebrafish work. Aforementioned experiment with LPS would confirm MMF’s pro-resolving effects in the means of enhancing apoptosis of inflamed neutrophils and their phagocytosis by macrophages. The measurement of neutrophil apoptosis should be done as before by cytospin analysis and efferocytosis could be quantified by the recently established anxA5-pHrodo tool (Stöhr *et al.*, 2018).

In summary, our study has shown that MMF both accelerates apoptosis of human neutrophils *in vitro* by depleting GTP and facilitates resolution of neutrophil-dependent inflammation *in vivo*. The data supports the investigation of MMF as a potential therapeutic agent for the treatment of neutrophil mediated inflammatory diseases. This is import due to the fact that apoptotic neutrophil itself is an important anti-inflammatory stimulus to other cells involved in the inflammation resolution (reviewed by (Fox *et al.*, 2010)). The *in vitro* data supports the idea that my *in vivo* MMF data is biologically significant and we would not have found this if we did not use the zebrafish model to begin with (personal communication with Dr Lynn Prince and Bethany Hughes).

The MMF manuscript was uploaded to bioRxiv preprint server three years ago. Here I have updated the results with *in vitro* data that is yet to be included in a new manuscript.

Chapter 6: Overall discussion and future work

6.1 The zebrafish model of *C. neoformans* infection

There are many systems in which to study cryptococcosis. However, the main question or issue to be addressed when developing a model of a disease, is to be able to emulate the biological phenomenon of interest for a disease occurring in humans (reviewed by (Swearengen, 2018)). From this point of view, models of non-biological origin, such as computer or mathematical models, will always be less attractive. *In vitro* systems, although meaningful, will not reproduce *in vivo* conditions. Thus, for infectious diseases, animal models are generally required. This is due to the fact that in many cases the disease might be lethal and therefore human subjects cannot be used in research. In addition, a model has to be well characterised and understood, i.e. similarities and differences in the physiology between animals and humans have to be incorporated into the goals of the study (reviewed by (Swearengen, 2018)). Nonetheless, over the years, the zebrafish has come to the forefront of biomedical research including human infectious diseases (reviewed by (Van Der Sar *et al.*, 2004; Sullivan and Kim, 2008; Tobin *et al.*, 2012; Varela *et al.*, 2017; Torraca and Mostowy, 2018)).

There is good conservation of the immune system between humans and zebrafish. The zebrafish immune system contains macrophages, neutrophils, lymphocytes, eosinophils, dendritic cells and NK cells (Renshaw and Trede, 2012) and all of these are found within vertebrate immune systems. Pathogen sensing occurs through PRRs as in vertebrates (Jault *et al.*, 2004). *C. neoformans* is primarily attacked through innate immune cells, especially by macrophages (Feldmesser *et al.*, 2000). The study of the innate immune response to *C. neoformans* is not confounded by adaptive arm because innate and adaptive immune systems develop at different rates. The innate cells develop at day one and during the initial 4 days, the zebrafish exhibit no adaptive markers and does not fully develop until 3 weeks ((Herbomel *et al.*, 1999), reviewed by (Sullivan and Kim, 2008)). Genome analysis shows that zebrafish share many orthologous genes, and even conserved synteny, with mammals. Zebrafish are vertebrates and thus evolutionarily closer to humans than are, for example, the fruit fly and the nematode, and they are easier to work with and to study than

mice (reviewed by (Van Der Sar *et al.*, 2004)). The use of any model host requires a trade-off towards asking new experimental questions. For example, the zebrafish immune system is highly similar to humans (reviewed by (Lieschke and Trede, 2009)). However, there are differences in the adaptive immune response where sites of maturation differ (reviewed by (Tobin *et al.*, 2012)) and there is also some evolutionary divergence in TLR signalling. In zebrafish, as opposed to mammals, LPS is not sensed by zebrafish TLR4 (Sepulcre *et al.*, 2009). However, this does not seem an issue in the context of *Cryptococcus* that lacks LPS. Another pitfall and problem of zebrafish infection models is, for example, a lack of cell markers. In zebrafish there is almost a complete lack of monoclonal antibodies against surface markers of cells of the immune system (reviewed by (Van Der Sar *et al.*, 2004)). There are distinct anatomical differences between zebrafish and mammals (using gills instead of lungs for gas exchange, haematopoiesis in the anterior kidney instead of bone marrow, lack of discernible lymph nodes, and a different reproductive system) (reviewed by (Tobin *et al.*, 2012)). Of note, I did not intend to model the likely route of human infection of a very low inoculum into the alveolar space but the route of infection directly related to the aim of studying the early events following dissemination of *C. neoformans* (Bojarczuk *et al.*, 2016). Another drawback is that due to differential immunity development rates and the fact that most zebrafish work is done under the age of 5.2 days, there are no adaptive markers in such an infection model. Therefore translating data from zebrafish studies to humans is difficult, despite providing the opportunity and basis for a human study starting point. For instance, human macrophages also operate in a context with the adaptive immunity, which might affect my findings from my model of zebrafish cryptococcosis, i.e. it is known *Cryptococcus* is readily taken when opsonised, for example, with complement or antibodies (Levitz *et al.*, 1991; Shapiro *et al.*, 2002). In adult zebrafish, the infection would have been cleared due to the action of lymphocytes and antibodies. In fact, when I was doing preliminary grant experiments in the Johnston lab, I injected *Cryptococcus* intramuscularly into 4 week old fish (about 200 cfu). Within 8 days there was no single fluorescent cryptococcal cell (Bojarczuk, unpublished). This means that in the immunocompetent, an efficient immune response will eliminate most of the inhaled cryptococci. Nonetheless, the

model is one of innate immunity to *Cryptococcus* and the most practical at that because the innate seems the most rapid and efficient response to microbial exposure (reviewed by (Trede *et al.*, 2004)). The other issue is that due to the lack of the adaptive arm, zebrafish are exposed to environmental pathogens and care must be taken during husbandry. Temperature of zebrafish incubation might be a factor. Zebrafish and their natural pathogens exist at 28°C, whereas many pathogens of humans are only infectious at 37°C (reviewed by (Meeker and Trede, 2008)). However, since *C. neoformans* appears to infect such a wide range of animal species, with very different thermoregulation, it is likely that pathogenesis is not dependent of host body temperature (Malik *et al.*, 2011). As reviewed here, some zebrafish limits can be turned into advantages. What has not been mentioned in the cryptococcal-zebrafish field is that although hundreds of embryos in a single day can be subjected to experiments, it is challenging to deal with such fragile animals. For example, on the day of *Cryptococcus* injection into embryos, hundreds of them have to be dechorionated beforehand. This is time-consuming. The injections into yolk sac do not produce systemic infections and therefore more challenging protocol had to be implemented. There is indeed tremendous concern about the route of infection. Local injections include the yolk sac, or body cavities, such as the hindbrain ventricle and otic vesicle. Other compartments include subcutaneous, intramuscular, or the notochord. Intravenous injections for establishing a rapid systemic infection are performed into the *caudal vein* blood island or duct of Cuvier (reviewed by (Torraca and Mostowy, 2018)). My model relies on injections into the yolk sac circulation valley, which also produces a systemic infection (Bojarczuk *et al.*, 2016). This was to study the early events following dissemination. The pathogen administration route depends highly on the infection type to be achieved and the goal of a study. For example, hindbrain, otic vesicle or intramuscular injections allow investigating immune cell recruitment, whereas the notochord is inaccessible to immune cells (reviewed by (Torraca and Mostowy, 2018)). My analysis of host pathogen interactions was only possible due to zebrafish embryo transparency. This allows for high resolution imaging. The imaging, in turn can be done non-invasively in real-time enabling data collection in a fairly short time. This is the biggest advantage of this system as a model of experimental cryptococcosis. The whole

fish can be imaged and this cannot be obtained in the case of other animals. Of note, when possible, it is recommended to use *nacre* background zebrafish to avoid pigment interference during real-time imaging. The visual data collected from imaging can be translated into quantitative data. Using infected embryos mounted in a 96-well format for repeat imaging at various stages of infection, I developed a high content imaging methodology that permits a full analysis of cryptococcal and macrophage cell interactions during infection (Bojarczuk *et al.*, 2016). There were additional challenges regarding imaging and image analysis: mounting embryos in agar for imaging required optimising a tool for carefully manipulating larvae using an eyelash glued to a pipette tip (undescribed in (Bojarczuk *et al.*, 2016)). Calculating and implementing the number and thickness of z sections, as well as how many fields of view, to capture the whole larvae took much optimisation to be able to collect reliable and complete data. Image analysis was completed manually and included a number of checks for double counting if cryptococci were intracellular in macrophages.

Animal models became tools for research in human infectious diseases and they contributed substantially to unravelling the physiopathology of infection and host-pathogen interactions. Guidance for 'humane experimental technique' is described by the UK's National Centre for the Replacement, Refinement and Reduction of Animals in Research (NC3Rs), which is responsible for supporting animal experimentation in the UK through the application of the core principles termed 3Rs (reviewed by (Singh, 2012)). The NC3Rs' strategy is to advance the 3Rs by focusing on their scientific impacts and benefits. The NC3Rs' objectives are advantages of my model. Replacement refers to methods which avoid or replace the use of animals. In terms of replacement alternatives it is not possible to replace the zebrafish with inanimate systems, such as computer simulations. Zebrafish already serve as relative replacements because they replace more sentient animals, such as higher vertebrates, and they are accepted to have a lower potential for pain perception.

In regards to reduction, namely methods which minimise the number of animals used per experiment, the number of animals previously calculated from published studies (Loynes *et al.*, 2010; Elks *et al.*, 2011; A. L. Robertson *et al.*, 2014) to

obtain sufficient data to answer the research questions. There is also a practice to maximise the information obtained per fish and thus a potential limit or avoidance of the subsequent use of additional animals. In addition, I also used an imaging method enabling longitudinal studies in the same animals.

In terms of refinement, which refers to methods minimising animal suffering and improving welfare, I used an appropriate anaesthetic regime for pain relief. Tricaine was used for infection or imaging purposes. In addition, I did not cause much pain and suffering, which would have been caused using other models, e.g. mice. At the same time I could identify within-host processes that would have been identified in other animals with an emphasis on the identification of host-pathogens interactions in real time, which is not possible in other models.

The welfare of zebrafish used was assured from the time the fish were born until their death. Any potential adverse effects and the times of pain or distress were monitored by Named Animal Care and Welfare Officers (NACWOs) and aquarium staff. In addition, The University of Sheffield acts under the Scientific Procedures Act 1986.

The role for modelling in supporting public health has progressively expanded since the first *Cryptococcus* isolation from a sarcoma-like lesion of a female patient's tibia (Busse, 1894). Animal models have been used in experimental research to increase human knowledge about this pathogen. My zebrafish model has contributed substantially to unravelling the physiopathology of cryptococcosis. In regards to the publication (Bojarczuk *et al.*, 2016), I demonstrated for the first time how the early interactions with macrophages determined the outcome of infection. I confirmed that in the zebrafish a phenomenon observed in mammalian infection, i.e. the polysaccharide capsule's growth, is recapitulated. This change was observable between 2 and 24 hours post infection (hpi). Early in infection, at 2 hpi, the intracellular cryptococci had significantly smaller capsule radius as compared to the extracellular portion. The measurement was done by immunofluorescence labelling of the capsule and staining of the cell wall immediately prior to infection and followed by live imaging of injected zebrafish with labelled capsule/cell wall (Bojarczuk *et al.*, 2016). At 24 hpi, fixed tissue was immunolabelled. The comparison between 2 and 24 hpi

revealed that by 24 hpi, the cryptococcal capsule was significantly enlarged (Bojarczuk *et al.*, 2016). At 24 hpi a different technique was used as changes in the capsule could not be observed live in the same way, i.e. upon replication the staining would have been lost. However, what could be done is perform the same experiment and perform *in vivo* immunolabelling, which permits observation under truly physiological conditions (reviewed by (Progatzky *et al.*, 2013)). Alternatively, at 24 hpi the zebrafish could be fixed and the capsule labelled. This would allow for measuring the size of the capsule for both intra- and extracellular portions in order to investigate the dynamics between those two cryptococcal fractions. The next step could be also testing whether the capsule thickness changes once inside a macrophage *in vivo*. This has never been investigated *in vivo*. It is acknowledged that there are different fates following the uptake by macrophages (e.g. phagocytosis, lateral transfer, death), but it would be interesting to measure the capsule radius before a particular event occurs. *In vivo* immunolabeling and live imaging/electron microscopy could be utilised.

C. neoformans is a clinically important opportunistic pathogen of humans. Here, I exploited a transparent zebrafish model of cryptococcosis to address mechanistic questions relevant to human primary immune response dynamics. My high-content imaging method in a zebrafish model of cryptococcosis (Bojarczuk *et al.*, 2016) might have many applications to impact human health. For instance, it can be used in chemical screening for novel biological and therapeutic discovery related to cryptococcosis. Zebrafish are used for this purpose (A. L. Robertson *et al.*, 2014; Wiley *et al.*, 2017); reviewed by (Bowman and Zon, 2010; Rennekamp and Peterson, 2015)). A multi-well plate screen could point to anti-cryptococcal molecules. The whole libraries could be tested as well. The exemplary libraries to be tested could be Tocris Bioscience, Sigma Lopac and John Hopkins. They are collections of biologically active compounds that have proven pharmacological activity against certain targets. Thus after investigating fungal burdens and finding hits, the pathways involved could be investigated. Drug targets between zebrafish and humans are conserved (reviewed by (Wiley *et al.*, 2017)). Thus, compounds screening can lead to the identification of candidate substances that can be further examined in pre- and

clinical trials to target cryptococcal infection. This could lead to therapeutics development. The recent work of (Kamuyango, 2017) supports this. IFN γ injection promoted the clearance of cryptococcal infection in a modified version of my model, i.e. in an intramuscular zebrafish infection model in the absence of T cells (Kamuyango, 2017). This suggests that IFN γ treatment could be beneficial in the immunocompromised. This antifungal effect was also observed in a mouse model of pulmonary infection with *C. neoformans* engineered to produce IFN γ . This *C. neoformans* strain was avirulent in mice and the Th1-type anti-cryptococcal response was stimulated (Wormley *et al.*, 2007). Th1 response induction extends mice survival (Decken *et al.*, 1998). This is important because *C. neoformans* stimulates Th2 response, which is not protective in mice (Wiesner *et al.*, 2015). In contrast, *in vitro*, treatment with IFN γ results in no change in fungistatic capacity (Voelz *et al.*, 2009). This clearly emphasizes that the use of the animal model is better suited for observing the overall effects. However, despite a wide range of advantages in using mice, the zebrafish offers significant advantages over higher vertebrates such as rapid development, ease of imaging in real time, fast procreation and cost benefits. This enables a significant progress in a project. This means that zebrafish provides a variety of advantages including the identification of disease-modifying molecules (reviewed by (Gehrig *et al.*, 2018)).

Testing a range of compounds could be done using the yolk sack infection model to represent a disseminated infection. For example, TLR agonists could be tested. This would be seen as a drug treatment (by injection or dissolve in E3 water). Some were tested by (Kamuyango, 2017) and yielded good results. The idea would be to initiate the immune response and enhance phagocytosis. It is known that an opsonic phagocytosis in the presence of an antibody is the most effective in the clearance of the pathogen (Levitz *et al.*, 1991; Shapiro *et al.*, 2002). Complement works well as an opsonin when there is no antibody (Levitz and Tabuni, 1991) but phagocytosis could be enhanced by the presence of TLR agonists when antibodies are not included. I would use the zebrafish model without the adaptive immunity and thus no antibodies involvement. If we could enhance the innate response to confine *Cryptococcus*, the chances for quicker clearance would increase. The innate responses are recognised to occur first as

there will be, for example, circulating neutrophils and tissue macrophages that would have the first interactions. Adaptive responses will take more time, but if *Cryptococcus* is the pathogen, for which there is immune memory, the reaction will be quick as it will match to a circulating antibody and trigger a large response. If the immune system is naïve to *Cryptococcus*, it will take longer as, for example, antigen presentation in lymph nodes has to take place. In both cases, naïve and experienced immunity, the enhancement of innate responses is beneficial. This means that details of appropriate immunostimulation can be identified that could be advantageous in improving the outcome of cryptococcosis and will lead to cryptococcal clearance.

The model can be pushed forward and modified. An adult model of cryptococcal infection can be developed. Due to a wide range of zebrafish transgenic lines availability, it would be possible to investigate adaptive responses and innate-adaptive crosstalk against the pathogen. Many projects could arise from the adult system. Although mice data relate to the adaptive immunity, mice cannot be imaged *in vivo* in real time to show host–pathogen interactions. The new adult zebrafish model could utilise localised injections in the swim bladder. The swim bladder is highly similar in structure and the precursor to the mammalian lung (Robertson *et al.*, 2007; Winata *et al.*, 2009). The bronchial epithelial cells of the upper airway and the alveolar epithelial cells of the lower airway are likely to be the first host cells that *Cryptococcus* engage with (reviewed by (Taylor-Smith, 2017)). Given that this pathogen involves the lungs and clinical manifestations range from asymptomatic pneumonia to severe acute respiratory distress syndrome (ARDS) (Pappas, 2001; Orsini *et al.*, 2016), it would be worth establishing an adult model of this organ infection to show similarities between swim bladder cryptococcosis in the transparent zebrafish and cryptococcal infection at the mammalian epithelium. This work could involve NF- κ B activation, induction of NF- κ B-dependent pro-inflammatory genes and an investigation into whether neutrophils or macrophages protect against death in the adult zebrafish swim bladder infection. This would examine the roles of particular cell types and molecular pathways involved in protection against *Cryptococcus*. Pulmonary involvement is not only one of the characteristics of cryptococcosis. There is also

CNS involvement, which is the cause of the greatest mortality among patients. Raised intracranial pressure in cryptococcal meningitis seen in patients is thought to be responsible for the high mortality of this group. Moreover, the disruption of blood brain barrier (BBB) and choroid plexus (CP) has been proposed as a mechanism for the raised intracranial pressure (Loyse, Wainwright, *et al.*, 2013). Thus, it would be of interest to establish a model of cryptococcal meningitis (CM). This would have to be done in unprotected zebrafish as the hindbrain is more accessible for injections. In fact, I was involved in the creation of a transgenic zebrafish model for the *in vivo* study of the blood and choroid plexus brain barriers using *claudin 5*. The gene *claudin 5a* is the zebrafish orthologue highly expressed in the BBB and CP barriers and demonstrates the conservation of the BBB and CP between humans and zebrafish (Van Leeuwen *et al.*, 2017). Thus, there is a tool to investigate CM at many angles, e.g. to answer the question whether cryptococcal cell and capsule interactions with blood brain barrier and choroid plexus correlate with the pathology of CM. This would be to identify potential new therapies for cryptococcal meningitis that will reduce intracranial pressure. Another idea as to how my model can be used to impact human health is to show a protective activation of T cells including CNS. I proved in the zebrafish model that macrophages alone cannot clear cryptococcal infection *in vivo* (Bojarczuk *et al.*, 2016). This was shown in mice (Wozniak *et al.*, 2011), which supports the zebrafish utility. At the same time no research to date has investigated how cryptococci are cleared in a healthy immune system, when lymphocytes are involved. Therefore, I would propose an adult model of infection. For instance, by using *Tg(cfms:GFP)^{sh377}* (Dee *et al.*, 2016) (labelling macrophages with GFP) and injecting *C. neoformans* strain, KN99 mCherry, could demonstrate how cryptococci are cleared. Indeed, my unpublished, preliminary data demonstrated that AB adult zebrafish, from 4 weeks post fertilisation, efficiently clear a somite infection with *C. neoformans* using a relatively small dose of 150 cells. This would be exactly the same experiment I performed in (Bojarczuk *et al.*, 2016) or in this thesis with R265 GFP14. To investigate the cross-talk between lymphocytes and macrophages as well as cryptococci, a cross between *Tg(cd4-1:mCherry)* (Dee *et al.*, 2016) and *Tg(cfms:GFP)^{sh377}* (Dee *et al.*, 2016) could be done. I would be interested in tracking T helper cells during cryptococcal infection, as they are

important in immunity. When their pool becomes depleted, e.g. due to HIV infection or in a result of immunosuppression, the host is susceptible to infections. I would be also interested in tracing macrophages as their role is significant, which was highlighted in this thesis many times. CD4 mcherry labels both T-cells and CD4⁺ expressing macrophages but in the case of the resulting line, macrophages will be labelled by *cfms*⁺CD4⁺ and *cfms*⁺CD4⁻. There will be also CD4⁺*cfms*⁻ that correspond to T helper cells, *cfms*⁺ (macrophages/monocyte/DCs) and a proportion of the CD4⁻ *cfms*⁻. The issue might be the choice of cryptococcal strain to be used as so far in the planned experiment would involve GFP or mCherry cell population. Since the available cryptococcal strains are also labelled with GFP or mCherry, the work would involve, for example, turquoise strain generation using the Tol2 Kit Gateway system (Kwan *et al.*, 2007). To conclude, zebrafish offer a unique opportunity to study the mechanisms of immunity to infection using non-invasive *in vivo* imaging of fluorescent immune system markers/reporters. To date, this has been performed almost exclusively in larval models of innate immunity. However, my preliminary data on adult zebrafish demonstrate that imaging host and pathogen interactions in adult zebrafish during cryptococcal infection is highly tractable.

To summarise, I provided an animal model creating an indispensable tool for basic and applied research to enable study of disease development *in vivo*. My model has benefitted other projects in the Johnston lab. For example, it was used by three BMedSci students; i. e. Richard Hotham, Rory Gibson and Katherine Miller. Their theses are not published and hence not cited in this section. The model was used by Richard Hotham, a co-author of (Bojarczuk *et al.*, 2016) and (Gibson *et al.*, 2018) to show dissemination of cryptococci to the swim bladder, somites and brain. It also formed a basis for work on mycophenolate mofetil (MMF). This work was further carried on by another BMedSci student, Rory Gibson and resulted in a pre-printed publication (Gibson *et al.*, 2018). The model was also used by Katherine Miller, who worked on the capsule with the hypothesis that its increased size *in vitro* will result in an increased susceptibility to infection in zebrafish due to a decrease in rate of phagocytosis. This is published in (Bojarczuk *et al.*, 2016). The model was used by a number of former PhD students in the Johnston lab, too. For example, Dr Josie Gibson used my

model to investigate autophagy (Gibson, 2017). She also used it in a pre-printed publication, wherein I am a second author. This was to investigate blood vessel occlusion by *C. neoformans* (Gibson *et al.*, 2020). Next, Dr Hamid Fehri used my initial imaging data sets to develop automatic algorithms that can analyse different types of cells and their relations in the image to increase analysis efficiency (Fehri, 2018). My model was also exploited in collaborative projects to address perplexing questions relating to this pathogen. For instance, we found that reducing the extracellular receptor kinase ERK5 activity *in vivo* stimulates vomocytosis and results in reduced dissemination of infection (Gilbert *et al.*, 2017). Next, Dr Robert Evans found that prostaglandin E₂ was sufficient to promote growth of $\Delta plb1$ and $\Delta lac1$ independent of host PGE₂ production, *in vitro* and *in vivo* in zebrafish (Evans *et al.*, 2019). The model has also been optimised for high-throughput drug screening (unpublished, Christopher Donaldson, PhD student) or to mimic the mechanisms that cause this increase in intracranial pressure (unpublished, Jacqui Chalakova, PhD student).

A fungal infection *in vivo* model and above all, the high-resolution imaging of the whole animal in understanding immune cell behaviour during animal infection, is the novelty that can provide an excellent contribution in helping to prevent and treat cryptococcal disease. Hopefully, these findings will go towards widening our understanding of this pathogen and how it causes disease to ultimately improve therapy in humans. These data would not have been found in higher vertebrates, e.g. mice due to real-time imaging limitations. Some of these data could have been found in cell lines. For instance, vomocytosis of *C. neoformans* and *C. gattii* expulsion was reported in macrophages cell lines (Alvarez and Casadevall, 2006; Ma *et al.*, 2006; Alvarez *et al.*, 2008), primary murine macrophages (Alvarez and Casadevall, 2006), primary birds macrophages (Johnston *et al.*, 2016) and primary human macrophages (Alvarez and Casadevall, 2006; Alvarez, *et al.*, 2009). However, given that pathogen's behaviour *in vitro* and *in vivo* might be different due to incorporation of the host-pathogen interaction, *in vivo* work is required. This is to show recapitulation of *in vitro* established physiopathological events or to find new behavioural differences. Having the zebrafish model, which interlocks vertebrate immunity, ease of imaging and genetic tractability, makes the research on cryptococcosis possible to expand. *C. neoformans* work

including the model (Bojarczuk *et al.*, 2016) was published in Scientific Reports and describes the complex interplay between the host and pathogen. A critical challenge will be to develop novel treatments. This requires a better understanding of both host-pathogen interplay and a relationship of the model to the human disease termed cryptococcosis. Thus, the future work was proposed.

6.2 Assessment of *Cryptococcus gattii* virulence in zebrafish and mice

The experiments in my study aimed to determine the virulence of *C. gattii* R265 wt, which has recently emerged as a pathogen of immunocompetent individuals. This strain is a clinical isolate from an ongoing outbreak on Vancouver Island (VIO) (Kidd *et al.*, 2004). Previous work has shown VIO *C. gatti* strains survive and replicate *in vitro* in macrophages at a greater rate than non-outbreak strains and their ability to replicate in macrophages is associated with virulence in a mouse model of infection (Voelz *et al.*, 2014). Previous studies have also demonstrated that VIO type strain R265 wt and its transgenic insertion mutant R265 GFP14 show normal growth in macrophages *in vitro* (Voelz *et al.*, 2010). However, despite a large body of work conducted *in vitro* and in mice on R265, the mechanism underlying its pathogenicity, growth requirements and mechanism of infection remained unknown. To identify the utility of zebrafish to study *C. gattii* virulence, first *C. gattii* R265 wt and *C. neoformans* KN99 wt were compared side by side. A series of survival experiments gave interesting findings including that GFP insertion to R265 had an effect on virulence as R265 GFP14 was attenuated when compared to its isogenic strain R265 wt. This was also confirmed in mice. Interestingly, R265 GFP14 grew worse than R265 wt in the mammalian lungs. It is generally accepted that the primary target organ for *C. gattii* is the lungs (Ngamskulrunroj, Chang, Sionov, *et al.*, 2012). As mentioned in Chapter 4 Discussion, the serial analysis of gene expression (SAGE) analysis and phagocytosis data of (Fan *et al.*, 2005) suggest that *Cryptococcus* displays different metabolic profiles depending on the experimental settings. Different profiles are obtained during *in vivo* or *in vitro* infections. This means that *in vivo* and *in vitro* conditions might exert different energy acquisition modes. Here I hypothesise that during cryptococcosis in mice used in this thesis, R265 wt

might have performed the TCA whereas R265 GFP14 might have not. Although the secretions from respiratory airways have a very low glucose concentration in healthy individuals (<0.05 mM) (<0.00009 %) (Philips *et al.*, 2003), the presence of glucose causes in Crabtree-negative fungi to up-regulate the pyruvate dehydrogenase complex, i.e. most of the carbon flows into the Krebs cycle (reviewed by (Ene *et al.*, 2014)). Some tags for function in the TCA cycle are elevated in the SAGE analysis on *C. neoformans* cells recovered from lungs of infected mice (Hu *et al.*, 2008). Therefore, to prove the TCA functioning during R265 wt infection in mice used in my study, I would infect the animals with R265 wt and R265 GFP14, isolate RNA and perform SAGE on cells recovered from the lungs. I would specifically look at the following SAGE tags for genes encoding predicted functions in the TCA (aconitase, succinate dehydrogenase, malate dehydrogenase, isocitrate dehydrogenase, malic enzyme, fumarase) (Hu *et al.*, 2008). I propose to investigate these genes described for *C. neoformans* by (Hu *et al.*, 2008) because *C. gattii* would have these genes (D'Souza *et al.*, 2011). Alternatively, qPCR could be done to check the expression of those genes. I would do the same experiment for cells recovered from the PM1 microarray assay run in the settings described using methodology described Chapter 2. This would confirm if R265 wt in the phenotypic array performed the TCA cycle. Another experiment with the same objective would be to employ a TCA cycle metabolism assay.

In the phenotypic array, it became apparent that there was less signal for the glucose well. The well had less colour change for R265 wt than for R265 GFP14. Therefore, one could ask if R265 wt performed glycolysis. Apart from the experiments proposed in Chapter 4 discussion regarding that issue, I would suggest SAGE on cells recovered from PM1 assay. I would specifically focus on the following SAGE tags for genes encoding predicted functions in glycolysis: fructose 1,6-biphosphate aldolase, phosphofructokinase, hexokinase, enolase, glucose-6-phosphate isomerase, phosphoglycerate mutase (Hu *et al.*, 2008). Alternatively, qPCR could be done.

However, it is possible that in my PM1 assay, the cells were nutrient-starved. In response to nutrient starvation, *Candida albicans* shifts from glycolysis to gluconeogenesis (Mayer *et al.*, 2013). Perhaps R265 wt shifts too and NADH

elevation cannot be observed since gluconeogenesis is anabolic. Thus I would also apply the SAGE with an attention to phosphoenolpyruvate carboxykinase (*PCK1*) (Hu *et al.*, 2008) or qPCR.

The respirometry work performed by Dr Gourlay (unpublished) suggested that R265 wt is less efficient at obtaining ATP from oxidative phosphorylation. It is not known whether R265 wt in my metabolic array performed oxidative phosphorylation or the strain relies on fermentation. To answer these questions, the following test could be run. The strains (R265 wt and R265 GFP14) should be grown on non-fermentable media, e.g. yeast extract peptone glycerol (Turcotte *et al.*, 2010) agar (YPGA) versus yeast extract peptone dextrose agar (YPDA) as a control. Potassium cyanide and SHAM should be added to the plates. The former blocks the classical respiration but might induce alternative oxidase. Thus SHAM should be added (Duvenage *et al.*, 2019). If a strain relies mostly on fermentation and does not use oxidative phosphorylation much, then it would grow poorly on YPGA in the presence of ETC drugs.

The alternative oxidase function in both strains (R265 wt and R265 GFP14) and how it contributes to the overall respiration still remains unresolved. The respirometry conducted by Dr Gourlay showed resistance to Aox inhibition by SHAM which might suggest that Aox levels are very high in R265 wt. In discussion in Chapter 4, I proposed *AOX1* gene knock-out to confirm this. However, this could also be done with knock-down of *AOX1*. Respirometry should then be done including both knock-out/knock-down and R265 wt, other VIO strains (Voelz *et al.*, 2014), R265 GFP14 and other GFP strains generated by (Voelz *et al.*, 2010). This could be also done by immunoblotting (Western blot) with the strains listed above. To find out whether the same alternative oxidase phenotype occurs in the PM1 assay, R265 wt and R265 GFP14 as well as *aox1* mutants, other VIO strains (Voelz *et al.*, 2014) and other GFP strains in R265 background (Voelz *et al.*, 2010) should be run in the metabolic assay. Then cells recovered from the hit wells described in Chapter 4's Result section should be tested by immunoblotting and these results compared to Western blot respirometry results. As suggested, R265 metabolic profile might be flexible depending on the *in vivo* or *in vitro* conditions and nutrients provided. However, I

hypothesise that even *in vitro* results might vary depending on nutrients provided. The respirometry includes YPD with 2% glucose (111 mM) (Duvenage *et al.*, 2019) whereas glucose in PM1 procedure is at 0.4% (22 mM) (personal communication with Biolog). Thus, this well should be included in the experiment for alternative oxidase profiling. The concentration of substrates as the sole source of carbon remains unknown, although within the range of 2-20 mM (personal communication with Biolog). It might be that the respirometry profile changes depending on the nutrient and its concentration.

The fact that SHAM effectively inhibits the Aox1 in R265 wt suggests the alternative respiration pathway is still functional. However, it is not known whether alternative respiration is prevalent in the respirometry or in my PM1 assay. It is not known whether the fungus switches to alternative respiration or fermentation. It is not clear whether *C. gattii* favours alternative respiration over fermentation and vice versa. Indeed, I speculated in the results in Chapter 4 that R265 wt might ferment and as mentioned above it is resistant to alternative oxidase inhibition. A lot of questions could be raised, e.g. if fermentation takes place, can alternative respiration and the Krebs cycle co-exist? A problem is that even in *S. cerevisiae* the interface between glycolysis and the TCA is not fully defined (van Rossum *et al.*, 2016). The following diagram represents cellular respiration (Figure 6.1).

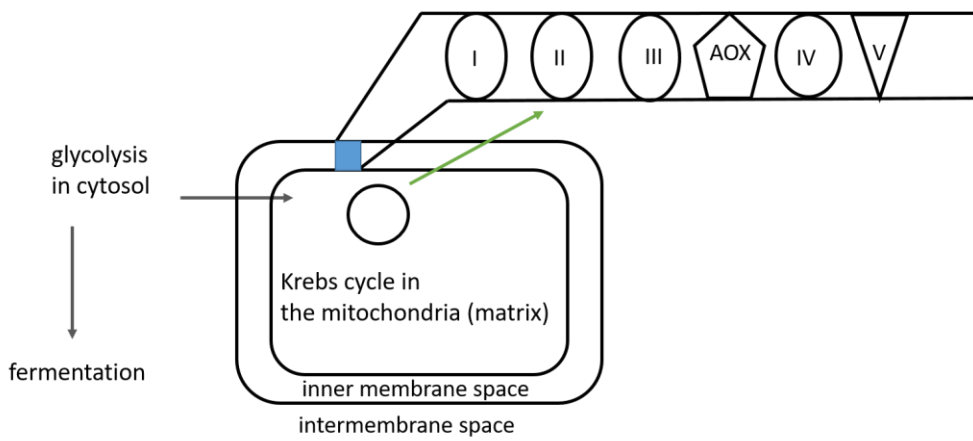


Figure 6.1 A simplified diagram of cellular respiration. I, II, III, IV and V represent ETC complexes. I-V are ETC complexes, wherein AOX is alternative oxidase.

The case is complicated as yeast cells have to have Krebs (or some partial Krebs cycle) activity. Yeast cells that are just fermenting or have no mitochondrial DNA should still run the Krebs cycle to support production of, for example, metabolites and certain amino acids. At the same time, the respirometry suggests that R265 wt must get ATP from another mechanism and so it is likely to be fermenting (communication with Dr Gourlay). Therefore, experiments to investigate fermentation phenotype would confirm whether R265 wt is able to ferment. Actually, this could also be confirmed by measuring pyruvate and ethanol. If the final product from glucose is pyruvate, then glycolysis is successful. If the final product is ethanol, then this indicates fermentation. Concomitantly, investigation of the genes that should be upregulated if Krebs cycle occurs would indicate if R265 wt or R265 GFP14 runs the cycle. In addition, *AOX1* expression would also inform if the yeast switches to the alternative respiration mode and thereby produces less energy. All options are possible because *Cryptococcus* has broken out of the opportunistic box and has become a primary pathogen of humans.

The analysis of macrophages-cryptococci interactions assayed in the zebrafish model of cryptococcosis (Bojarczuk *et al.*, 2016) was performed using R265 GFP14. This was done to evaluate how the strain was attenuated. It is clear that R265 wt should be investigated above all. This is the VIO outbreak strain and therefore one could argue this should be done primarily. Unfortunately, this strain is not fluorescent and all analysis from macrophage data set would be very difficult. In contrast, in (Bojarczuk *et al.*, 2016), the data was obtained using H99 GFP strain. This was possible because I ensured there was a match in the zebrafish survival between non-fluorescent and fluorescent strain in terms of virulence before proceeding with fluorescent strain experiments (unpublished). Since the R265 GFP14 has an altered genome (32 kb deletion) as compared to the parental strain, other transformants created at the time of R265 GFP14 generation (Voelz *et al.*, 2010) should be genome sequenced. If there is one that does not have an altered genome, it should be used in macrophages-cryptococci interactions assay.

To summarise, I discovered there are six genes related to R265 wt virulence, which could be exploited to target infection. Of note, if R265 GFP14 will ever be studied in the mammalian host, the researchers should be aware that the conclusions drawn from their studies will not be representative for its isogenic strain, R265 wt. My *C. gattii* work will be publishable upon completion of proposed experiments in the discussion section relating to Chapter 4 of my thesis.

6.3 Mycophenolate mofetil (MMF) increases inflammation resolution in zebrafish via neutrophil apoptosis

I demonstrated that MMF reduces the number of neutrophils in zebrafish during an inflammatory insult. Despite previously unexplained mechanism of action in the means of neutrophils, MMF has been prescribed in inflammatory conditions. The examples include: sarcoidosis (Kouba *et al.*, 2003), inflammatory eye disease (Thorne *et al.*, 2005; Hornbeak and Thorne, 2015), pulmonary fibrosis (Tzouveleakis *et al.*, 2011) or systemic lupus erythematosus (Pisoni *et al.*, 2005). MMF is also promising in the interstitial lung disease (Fischer *et al.*, 2013). Neutrophils are implicated in the pathology of many diseases, e.g. chronic obstructive pulmonary disease (reviewed by (Hoenderdos and Condliffe, 2013)), rheumatoid arthritis (reviewed by (Cecchi *et al.*, 2018)) or Behçet's disease (Rifaioglu *et al.*, 2014). Given, that neutrophil products are involved in the tissue damage seen in a range of inflammatory diseases, in a range of organs, including the lung (Haslett, 1999), MMF could be beneficial in neutrophil-related inflammatory diseases, e.g. in chronic obstructive pulmonary disease(COPD). Clinical trials comparing azathioprine (AZA) and MMF have been conducted on patients with lung allograft (Palmer *et al.*, 2001) and estimated MMF efficacy was similar to AZA. However, those trials have never been performed in patients without grafting factor. Only such trials would estimate MMF efficacy in COPD and other related neutrophilic diseases.

What emerges from this project is that the zebrafish model of inflammation (Renshaw *et al.*, 2006) enables not only the study of pharmaceutical agents modulating inflammation (Loynes *et al.*, 2010) but testing immunosuppressants on their role on neutrophils. It would be interesting to test other

immunosuppressive drugs used in inflammation, e.g. cyclophosphamide. This immunosuppressant is used in scleroderma lung disease (Kowal-Bielecka *et al.*, 2005). For instance cyclophosphamide reduces the neutrophilic component in idiopathic pulmonary fibrosis (O'Donnell *et al.*, 1987). Cyclophosphamide is used post transplantation and is able to induce apoptosis in T cells (Al-Homsi *et al.*, 2015) but its mechanism is not well described in the literature, especially in the context of modulating neutrophils it is not clear.

To summarise, MMF is used for a wide range of autoimmune and inflammatory conditions, but little was known about its direct effects on neutrophils. This could broaden the drug's use influencing public health.

MMF manuscript (Bojarczuk and Johnston, 2017) was revised in The Journal of Immunology in 2017 and reviewers gave favourable reports, but raised some critical points that will require amendments to the manuscript. We are now in the process of making amendments.

6.4 Thesis summary

I developed a model of zebrafish model of cryptococcosis (Bojarczuk *et al.*, 2016). I have shown that both host and pathogen factors, important in immunity and virulence can be identified using this model. The model was also well suited to expand on the virulence of VIO strain, R265. I have identified that a transgenic insertion mutant of the VIO type strain R265 (R265GFP14) cannot be a representative of R265 wt as it has 32 kb deletion resulting in the loss of six genes important in zebrafish and mice virulence. R265 wt and R265 GFP14 differ significantly in terms of pathogenesis and metabolism. This suggests the virulence of R265 wt lies in the genes deleted in R265 GFP14 and they could be exploited to target infection.

The study on susceptibility to cryptococcal infection in my model of cryptococcosis (Bojarczuk *et al.*, 2016) with an immunosuppressant mycophenolate mofetil (MMF) (Gibson *et al.*, 2018) led to MMF testing in inflammation set up (Renshaw *et al.*, 2006). This confirmed that MMF is a potent anti-inflammatory agent and I revealed its mechanism of action on neutrophils

through apoptosis. I proved that zebrafish are an effective system to study *Cryptococcus* invasiveness and a great tool to immunosuppressant testing.

Appendix 1

Table 4.2 Sidak's multiple comparisons test with D-xylose

time (minutes)	adjusted P value	time (minutes)	adjusted P value
0	>0.9999	570	0.0004
15	>0.9999	585	0.0002
30	>0.9999	600	0.0001
45	0.9748	615	0.0007
60	>0.9999	630	<0.0001
75	0.9025	645	<0.0001
90	0.9991	660	0.003
105	0.321	675	<0.0001
120	0.5795	690	0.0001
135	0.1971	705	<0.0001
150	0.4865	720	<0.0001
165	0.0634	735	0.0003
180	0.0634	750	<0.0001
195	0.0089	765	0.0001
210	0.0465	780	<0.0001
225	0.0043	795	<0.0001
240	0.0021	810	0.0014
255	0.0245	825	0.9998
270	0.0339	840	0.1971
285	0.0176	855	0.0855
300	0.0855	870	>0.9999
315	0.0089	885	0.0062
330	0.0004	900	<0.0001
345	0.0004	915	<0.0001
360	0.0014	930	0.947
375	0.0125	945	>0.9999
390	0.0014	960	<0.0001
405	0.0176	975	<0.0001
420	0.0043	990	>0.9999
435	0.0125	1005	<0.0001
450	0.0004	1020	>0.9999
465	<0.0001	1035	>0.9999
480	0.0001	1050	0.9991
495	0.001	1065	0.1143
510	<0.0001	1080	<0.0001
525	<0.0001	1095	<0.0001
540	<0.0001	1110	<0.0001
555	0.001	1125	<0.0001

Table 4.2 (continued)

1140	<0.0001	1710	0.001
1155	<0.0001	1725	<0.0001
1170	<0.0001	1740	<0.0001
1185	<0.0001	1755	0.0004
1200	<0.0001	1770	<0.0001
1215	<0.0001	1785	0.0021
1230	<0.0001	1800	<0.0001
1245	<0.0001	1815	<0.0001
1260	<0.0001	1830	0.0014
1275	<0.0001	1845	0.0004
1290	<0.0001	1860	0.0001
1305	0.0001	1875	0.0002
1320	<0.0001	1890	<0.0001
1335	<0.0001	1905	<0.0001
1350	<0.0001	1920	<0.0001
1365	<0.0001	1935	0.0014
1380	<0.0001	1950	0.001
1395	0.0003	1965	0.0002
1410	<0.0001	1980	0.0043
1425	<0.0001	1995	0.0007
1440	<0.0001	2010	<0.0001
1455	<0.0001	2025	<0.0001
1470	<0.0001	2040	<0.0001
1485	<0.0001	2055	0.0007
1500	<0.0001	2070	0.0021
1515	0.0001	2085	0.1971
1530	<0.0001	2100	<0.0001
1545	<0.0001	2115	0.0634
1560	<0.0001	2130	0.003
1575	<0.0001	2145	0.0062
1590	<0.0001		
1605	<0.0001		
1620	<0.0001		
1635	<0.0001		
1650	<0.0001		
1665	0.003		
1680	<0.0001		
1695	0.0004		

Table 4.3 Sidak's multiple comparisons test with D-mannose

time (minutes)	adjusted P value	time (minutes)	adjusted P value
0	>0.9999	570	0.054
15	>0.9999	585	0.5519
30	>0.9999	600	0.0053
45	>0.9999	615	0.2019
60	>0.9999	630	0.0004
75	>0.9999	645	0.0002
90	>0.9999	660	0.1075
105	>0.9999	675	0.001
120	>0.9999	690	0.012
135	>0.9999	705	0.012
150	>0.9999	720	0.012
165	>0.9999	735	0.5519
180	>0.9999	750	0.5519
195	>0.9999	765	0.2019
210	>0.9999	780	0.0002
225	>0.9999	795	0.0259
240	>0.9999	810	0.0259
255	>0.9999	825	0.5519
270	>0.9999	840	<0.0001
285	>0.9999	855	<0.0001
300	>0.9999	870	0.2019
315	>0.9999	885	<0.0001
330	0.5519	900	<0.0001
345	0.9187	915	<0.0001
360	0.9855	930	0.0002
375	0.5519	945	>0.9999
390	0.9187	960	<0.0001
405	0.999	975	<0.0001
420	0.9855	990	>0.9999
435	>0.9999	1005	<0.0001
450	0.012	1020	>0.9999
465	0.0259	1035	>0.9999
480	0.3511	1050	0.0053
495	0.7636	1065	<0.0001
510	0.1075	1080	0.0002
525	<0.0001	1095	<0.0001
540	0.0023	1110	<0.0001
555	0.054	1125	0.0004

Table 4.3 (continued)

1140	<0.0001	1710	<0.0001
1155	0.001	1725	<0.0001
1170	<0.0001	1740	<0.0001
1185	0.0004	1755	<0.0001
1200	<0.0001	1770	<0.0001
1215	<0.0001	1785	<0.0001
1230	<0.0001	1800	<0.0001
1245	<0.0001	1815	<0.0001
1260	<0.0001	1830	<0.0001
1275	<0.0001	1845	<0.0001
1290	<0.0001	1860	<0.0001
1305	<0.0001	1875	<0.0001
1320	<0.0001	1890	<0.0001
1335	<0.0001	1905	<0.0001
1350	<0.0001	1920	<0.0001
1365	<0.0001	1935	<0.0001
1380	<0.0001	1950	<0.0001
1395	<0.0001	1965	<0.0001
1410	<0.0001	1980	<0.0001
1425	<0.0001	1995	<0.0001
1440	<0.0001	2010	<0.0001
1455	<0.0001	2025	<0.0001
1470	<0.0001	2040	<0.0001
1485	<0.0001	2055	<0.0001
1500	<0.0001	2070	<0.0001
1515	<0.0001	2085	<0.0001
1530	<0.0001	2100	<0.0001
1545	<0.0001	2115	<0.0001
1560	<0.0001	2130	<0.0001
1575	<0.0001	2145	<0.0001
1590	<0.0001		
1605	<0.0001		
1620	<0.0001		
1635	<0.0001		
1650	<0.0001		
1665	<0.0001		
1680	<0.0001		
1695	<0.0001		

Table 4.4 Sidak's multiple comparisons test with tricarballic acid

time (minutes)	adjusted P value	time (minutes)	adjusted P value
0	0.2391	570	0.999
15	0.0025	585	0.7913
30	0.0174	600	0.999
45	0.6967	615	0.9998
60	0.8704	630	0.9998
75	0.0507	645	0.929
90	0.2391	660	0.987
105	0.0709	675	>0.9999
120	0.0981	690	>0.9999
135	0.134	705	0.3958
150	0.7913	720	0.987
165	0.0709	735	0.987
180	0.987	750	>0.9999
195	0.0709	765	0.999
210	0.1804	780	0.987
225	0.929	795	0.3958
240	0.5941	810	0.9666
255	0.929	825	<0.0001
270	0.6967	840	<0.0001
285	0.999	855	<0.0001
300	0.9666	870	<0.0001
315	0.9666	885	<0.0001
330	0.7913	900	<0.0001
345	0.929	915	<0.0001
360	0.7913	930	<0.0001
375	0.3109	945	<0.0001
390	0.5941	960	<0.0001
405	>0.9999	975	<0.0001
420	0.9959	990	<0.0001
435	0.999	1005	<0.0001
450	0.929	1020	<0.0001
465	>0.9999	1035	<0.0001
480	>0.9999	1050	<0.0001
495	0.999	1065	<0.0001
510	0.0358	1080	0.0251
525	0.3958	1095	0.0037
540	0.3958	1110	<0.0001
555	0.999	1125	0.0017

Table 4.4 (continued)

1140	<0.0001	1710	<0.0001
1155	0.0011	1725	<0.0001
1170	<0.0001	1740	<0.0001
1185	<0.0001	1755	<0.0001
1200	<0.0001	1770	<0.0001
1215	<0.0001	1785	<0.0001
1230	<0.0001	1800	<0.0001
1245	<0.0001	1815	<0.0001
1260	<0.0001	1830	<0.0001
1275	<0.0001	1845	<0.0001
1290	<0.0001	1860	<0.0001
1305	<0.0001	1875	<0.0001
1320	<0.0001	1890	<0.0001
1335	<0.0001	1905	<0.0001
1350	<0.0001	1920	<0.0001
1365	<0.0001	1935	<0.0001
1380	<0.0001	1950	<0.0001
1395	<0.0001	1965	<0.0001
1410	<0.0001	1980	<0.0001
1425	<0.0001	1995	<0.0001
1440	<0.0001	2010	<0.0001
1455	<0.0001	2025	<0.0001
1470	<0.0001	2040	<0.0001
1485	<0.0001	2055	<0.0001
1500	<0.0001	2070	<0.0001
1515	<0.0001	2085	<0.0001
1530	<0.0001	2100	<0.0001
1545	<0.0001	2115	<0.0001
1560	<0.0001	2130	<0.0001
1575	<0.0001	2145	<0.0001
1590	<0.0001		
1605	<0.0001		
1620	<0.0001		
1635	<0.0001		
1650	<0.0001		
1665	<0.0001		
1680	<0.0001		
1695	<0.0001		

Table 4.5 Sidak's multiple comparisons test with L-lyxose

time (minutes)	adjusted P value	time (minutes)	adjusted P value
0	0.0013	570	<0.0001
15	<0.0001	585	<0.0001
30	<0.0001	600	<0.0001
45	<0.0001	615	0.0001
60	<0.0001	630	<0.0001
75	<0.0001	645	<0.0001
90	<0.0001	660	<0.0001
105	<0.0001	675	<0.0001
120	<0.0001	690	<0.0001
135	<0.0001	705	<0.0001
150	<0.0001	720	<0.0001
165	<0.0001	735	<0.0001
180	<0.0001	750	0.0042
195	<0.0001	765	<0.0001
210	<0.0001	780	<0.0001
225	<0.0001	795	<0.0001
240	<0.0001	810	<0.0001
255	<0.0001	825	>0.9999
270	<0.0001	840	>0.9999
285	<0.0001	855	>0.9999
300	<0.0001	870	>0.9999
315	<0.0001	885	>0.9999
330	<0.0001	900	>0.9999
345	<0.0001	915	>0.9999
360	<0.0001	930	>0.9999
375	<0.0001	945	>0.9999
390	<0.0001	960	>0.9999
405	<0.0001	975	>0.9999
420	<0.0001	990	>0.9999
435	<0.0001	1005	>0.9999
450	<0.0001	1020	>0.9999
465	<0.0001	1035	>0.9999
480	<0.0001	1050	>0.9999
495	<0.0001	1065	>0.9999
510	<0.0001	1080	<0.0001
525	<0.0001	1095	<0.0001
540	<0.0001	1110	<0.0001
555	<0.0001	1125	<0.0001

Table 4.5 (continued)

1140	<0.0001	1710	0.8743
1155	<0.0001	1725	0.1516
1170	<0.0001	1740	0.4651
1185	<0.0001	1755	>0.9999
1200	<0.0001	1770	0.8199
1215	<0.0001	1785	>0.9999
1230	<0.0001	1800	0.1516
1245	<0.0001	1815	0.9724
1260	<0.0001	1830	>0.9999
1275	0.0003	1845	>0.9999
1290	0.0001	1860	0.9724
1305	<0.0001	1875	>0.9999
1320	<0.0001	1890	0.2295
1335	<0.0001	1905	0.9938
1350	<0.0001	1920	0.8743
1365	0.0013	1935	>0.9999
1380	0.0042	1950	>0.9999
1395	0.1516	1965	>0.9999
1410	0.0018	1980	>0.9999
1425	0.0056	1995	>0.9999
1440	0.0002	2010	>0.9999
1455	0.0056	2025	>0.9999
1470	0.013	2040	0.9992
1485	0.0024	2055	>0.9999
1500	0.0099	2070	>0.9999
1515	0.3343	2085	>0.9999
1530	0.013	2100	0.9502
1545	0.013	2115	>0.9999
1560	0.1873	2130	>0.9999
1575	0.0369	2145	>0.9999
1590	0.0769		
1605	0.0369		
1620	0.0286		
1635	0.2784		
1650	0.4651		
1665	0.4651		
1680	0.6122		
1695	>0.9999		

Table 4.6 Sidak's multiple comparisons test with D, L-malic acid

time (minutes)	adjusted P value	time (minutes)	adjusted P value
0	>0.9999	570	>0.9999
15	>0.9999	585	>0.9999
30	>0.9999	600	>0.9999
45	>0.9999	615	>0.9999
60	>0.9999	630	>0.9999
75	>0.9999	645	>0.9999
90	>0.9999	660	>0.9999
105	>0.9999	675	>0.9999
120	>0.9999	690	>0.9999
135	>0.9999	705	>0.9999
150	>0.9999	720	>0.9999
165	>0.9999	735	>0.9999
180	>0.9999	750	>0.9999
195	>0.9999	765	>0.9999
210	>0.9999	780	>0.9999
225	>0.9999	795	>0.9999
240	>0.9999	810	>0.9999
255	>0.9999	825	0.0051
270	>0.9999	840	<0.0001
285	>0.9999	855	<0.0001
300	>0.9999	870	0.0569
315	>0.9999	885	<0.0001
330	>0.9999	900	<0.0001
345	>0.9999	915	<0.0001
360	>0.9999	930	0.0002
375	>0.9999	945	>0.9999
390	>0.9999	960	<0.0001
405	>0.9999	975	<0.0001
420	>0.9999	990	>0.9999
435	>0.9999	1005	<0.0001
450	>0.9999	1020	>0.9999
465	>0.9999	1035	>0.9999
480	>0.9999	1050	0.0003
495	>0.9999	1065	<0.0001
510	>0.9999	1080	>0.9999
525	>0.9999	1095	0.0323
540	>0.9999	1110	0.0051
555	>0.9999	1125	0.0097

Table 4.6 (continued)

1140	0.3858	1710	<0.0001
1155	0.0569	1725	<0.0001
1170	0.0007	1740	<0.0001
1185	0.0007	1755	<0.0001
1200	0.0003	1770	<0.0001
1215	0.0003	1785	<0.0001
1230	<0.0001	1800	<0.0001
1245	0.0007	1815	<0.0001
1260	<0.0001	1830	<0.0001
1275	<0.0001	1845	<0.0001
1290	<0.0001	1860	<0.0001
1305	0.0014	1875	<0.0001
1320	<0.0001	1890	<0.0001
1335	<0.0001	1905	<0.0001
1350	<0.0001	1920	<0.0001
1365	<0.0001	1935	<0.0001
1380	<0.0001	1950	<0.0001
1395	<0.0001	1965	<0.0001
1410	<0.0001	1980	<0.0001
1425	<0.0001	1995	<0.0001
1440	<0.0001	2010	<0.0001
1455	<0.0001	2025	<0.0001
1470	<0.0001	2040	<0.0001
1485	<0.0001	2055	<0.0001
1500	<0.0001	2070	<0.0001
1515	<0.0001	2085	<0.0001
1530	<0.0001	2100	<0.0001
1545	<0.0001	2115	<0.0001
1560	<0.0001	2130	<0.0001
1575	<0.0001	2145	<0.0001
1590	<0.0001		
1605	<0.0001		
1620	<0.0001		
1635	<0.0001		
1650	<0.0001		
1665	<0.0001		
1680	<0.0001		
1695	<0.0001		

Table 4.7 Sidak's multiple comparisons test with bromosuccinic acid

time (minutes)	adjusted P value	time (minutes)	adjusted P value
0	>0.9999	570	>0.9999
15	>0.9999	585	>0.9999
30	>0.9999	600	>0.9999
45	>0.9999	615	>0.9999
60	>0.9999	630	>0.9999
75	>0.9999	645	>0.9999
90	>0.9999	660	>0.9999
105	>0.9999	675	>0.9999
120	>0.9999	690	>0.9999
135	>0.9999	705	>0.9999
150	>0.9999	720	>0.9999
165	>0.9999	735	>0.9999
180	>0.9999	750	>0.9999
195	>0.9999	765	>0.9999
210	>0.9999	780	>0.9999
225	>0.9999	795	0.8885
240	>0.9999	810	>0.9999
255	>0.9999	825	<0.0001
270	>0.9999	840	<0.0001
285	>0.9999	855	<0.0001
300	>0.9999	870	<0.0001
315	>0.9999	885	<0.0001
330	0.8885	900	<0.0001
345	>0.9999	915	<0.0001
360	>0.9999	930	<0.0001
375	>0.9999	945	<0.0001
390	>0.9999	960	<0.0001
405	>0.9999	975	<0.0001
420	>0.9999	990	<0.0001
435	>0.9999	1005	<0.0001
450	>0.9999	1020	<0.0001
465	>0.9999	1035	<0.0001
480	>0.9999	1050	<0.0001
495	>0.9999	1065	<0.0001
510	0.8885	1080	0.465
525	0.8885	1095	0.142
540	>0.9999	1110	0.0005
555	0.9602	1125	0.0536

Table 4.7 (continued)

1140	0.6195	1710	<0.0001
1155	0.8885	1725	<0.0001
1170	0.0002	1740	<0.0001
1185	0.0183	1755	<0.0001
1200	0.0104	1770	<0.0001
1215	0.0032	1785	<0.0001
1230	0.0104	1800	<0.0001
1245	0.0536	1815	<0.0001
1260	0.0536	1830	<0.0001
1275	0.0058	1845	<0.0001
1290	<0.0001	1860	<0.0001
1305	0.0885	1875	<0.0001
1320	0.0017	1890	<0.0001
1335	<0.0001	1905	<0.0001
1350	0.0001	1920	<0.0001
1365	0.0032	1935	<0.0001
1380	0.0058	1950	<0.0001
1395	0.0001	1965	<0.0001
1410	0.0005	1980	<0.0001
1425	0.0001	1995	<0.0001
1440	0.0001	2010	<0.0001
1455	0.0005	2025	<0.0001
1470	0.0058	2040	<0.0001
1485	<0.0001	2055	<0.0001
1500	<0.0001	2070	<0.0001
1515	<0.0001	2085	<0.0001
1530	<0.0001	2100	<0.0001
1545	<0.0001	2115	<0.0001
1560	<0.0001	2130	<0.0001
1575	<0.0001	2145	<0.0001
1590	<0.0001		
1605	<0.0001		
1620	<0.0001		
1635	<0.0001		
1650	<0.0001		
1665	<0.0001		
1680	<0.0001		
1695	<0.0001		

Table 4.8 Sidak's multiple comparisons test with L-asparagine

time (minutes)	adjusted P value	time (minutes)	adjusted P value
0	>0.9999	570	>0.9999
15	0.9997	585	>0.9999
30	0.9987	600	>0.9999
45	>0.9999	615	>0.9999
60	>0.9999	630	>0.9999
75	>0.9999	645	>0.9999
90	>0.9999	660	>0.9999
105	>0.9999	675	>0.9999
120	>0.9999	690	>0.9999
135	>0.9999	705	0.8342
150	>0.9999	720	>0.9999
165	>0.9999	735	>0.9999
180	>0.9999	750	>0.9999
195	0.9955	765	0.9987
210	>0.9999	780	0.9997
225	>0.9999	795	0.7578
240	>0.9999	810	0.9876
255	>0.9999	825	0.9876
270	>0.9999	840	0.3281
285	>0.9999	855	0.0018
300	>0.9999	870	0.9987
315	>0.9999	885	0.0074
330	>0.9999	900	<0.0001
345	>0.9999	915	<0.0001
360	>0.9999	930	0.6712
375	>0.9999	945	>0.9999
390	0.9997	960	<0.0001
405	>0.9999	975	<0.0001
420	>0.9999	990	>0.9999
435	>0.9999	1005	<0.0001
450	>0.9999	1020	>0.9999
465	>0.9999	1035	>0.9999
480	>0.9999	1050	0.4897
495	>0.9999	1065	0.4048
510	>0.9999	1080	<0.0001
525	0.9955	1095	<0.0001
540	0.9997	1110	<0.0001
555	>0.9999	1125	<0.0001

Table 4.8 (continued)

1140	<0.0001	1710	0.0006
1155	<0.0001	1725	<0.0001
1170	<0.0001	1740	<0.0001
1185	<0.0001	1755	0.0002
1200	<0.0001	1770	<0.0001
1215	<0.0001	1785	0.0001
1230	<0.0001	1800	<0.0001
1245	<0.0001	1815	<0.0001
1260	<0.0001	1830	<0.0001
1275	<0.0001	1845	<0.0001
1290	<0.0001	1860	<0.0001
1305	<0.0001	1875	<0.0001
1320	<0.0001	1890	<0.0001
1335	<0.0001	1905	<0.0001
1350	<0.0001	1920	<0.0001
1365	<0.0001	1935	<0.0001
1380	<0.0001	1950	<0.0001
1395	<0.0001	1965	<0.0001
1410	<0.0001	1980	<0.0001
1425	<0.0001	1995	<0.0001
1440	<0.0001	2010	<0.0001
1455	<0.0001	2025	<0.0001
1470	<0.0001	2040	<0.0001
1485	<0.0001	2055	<0.0001
1500	<0.0001	2070	<0.0001
1515	<0.0001	2085	0.0001
1530	<0.0001	2100	<0.0001
1545	<0.0001	2115	<0.0001
1560	<0.0001	2130	<0.0001
1575	<0.0001	2145	<0.0001
1590	<0.0001		
1605	<0.0001		
1620	<0.0001		
1635	<0.0001		
1650	<0.0001		
1665	<0.0001		
1680	<0.0001		
1695	<0.0001		

Table 4.9 Sidak's multiple comparisons test with sucrose

time (minutes)	adjusted P value	time (minutes)	adjusted P value
0	>0.9999	570	0.4577
15	>0.9999	585	0.0326
30	>0.9999	600	0.8108
45	>0.9999	615	0.6398
60	>0.9999	630	0.0087
75	>0.9999	645	>0.9999
90	>0.9999	660	0.9839
105	>0.9999	675	0.3009
120	>0.9999	690	0.9982
135	>0.9999	705	0.0603
150	>0.9999	720	0.3009
165	>0.9999	735	>0.9999
180	>0.9999	750	0.6398
195	0.4577	765	0.4577
210	>0.9999	780	0.4577
225	>0.9999	795	0.1079
240	>0.9999	810	>0.9999
255	>0.9999	825	>0.9999
270	>0.9999	840	>0.9999
285	>0.9999	855	>0.9999
300	>0.9999	870	>0.9999
315	>0.9999	885	>0.9999
330	0.3009	900	>0.9999
345	0.9839	915	>0.9999
360	0.9839	930	>0.9999
375	0.9295	945	>0.9999
390	0.6398	960	>0.9999
405	>0.9999	975	>0.9999
420	0.9839	990	>0.9999
435	>0.9999	1005	>0.9999
450	0.0021	1020	>0.9999
465	0.0087	1035	>0.9999
480	0.3009	1050	>0.9999
495	>0.9999	1065	>0.9999
510	0.0087	1080	0.3009
525	0.001	1095	0.0603
540	0.1079	1110	0.0005
555	0.9982	1125	0.0087

Table 4.9 (continued)

1140	0.0171	1710	<0.0001
1155	0.0171	1725	<0.0001
1170	<0.0001	1740	<0.0001
1185	0.0021	1755	<0.0001
1200	0.0005	1770	<0.0001
1215	0.0087	1785	<0.0001
1230	<0.0001	1800	<0.0001
1245	0.0043	1815	<0.0001
1260	0.4577	1830	<0.0001
1275	0.0021	1845	<0.0001
1290	0.0005	1860	<0.0001
1305	0.001	1875	<0.0001
1320	0.0043	1890	<0.0001
1335	<0.0001	1905	<0.0001
1350	0.0171	1920	<0.0001
1365	0.0087	1935	<0.0001
1380	0.0021	1950	<0.0001
1395	0.0326	1965	<0.0001
1410	0.0021	1980	<0.0001
1425	0.0087	1995	<0.0001
1440	<0.0001	2010	<0.0001
1455	0.0603	2025	<0.0001
1470	0.0326	2040	<0.0001
1485	0.0087	2055	<0.0001
1500	<0.0001	2070	<0.0001
1515	0.0021	2085	<0.0001
1530	0.0326	2100	<0.0001
1545	0.0043	2115	<0.0001
1560	<0.0001	2130	<0.0001
1575	0.0002	2145	<0.0001
1590	0.0087		
1605	<0.0001		
1620	<0.0001		
1635	<0.0001		
1650	<0.0001		
1665	0.0005		
1680	<0.0001		
1695	0.0087		

Table 4.10 Sidak's multiple comparisons test with L-lactic acid

time (minutes)	adjusted P value	time (minutes)	adjusted P value
0	>0.9999	570	>0.9999
15	>0.9999	585	>0.9999
30	>0.9999	600	>0.9999
45	>0.9999	615	>0.9999
60	>0.9999	630	>0.9999
75	>0.9999	645	>0.9999
90	>0.9999	660	>0.9999
105	>0.9999	675	>0.9999
120	>0.9999	690	>0.9999
135	>0.9999	705	>0.9999
150	>0.9999	720	>0.9999
165	>0.9999	735	>0.9999
180	>0.9999	750	>0.9999
195	>0.9999	765	>0.9999
210	>0.9999	780	>0.9999
225	>0.9999	795	>0.9999
240	>0.9999	810	>0.9999
255	>0.9999	825	<0.0001
270	>0.9999	840	<0.0001
285	>0.9999	855	<0.0001
300	>0.9999	870	<0.0001
315	>0.9999	885	<0.0001
330	>0.9999	900	<0.0001
345	>0.9999	915	<0.0001
360	>0.9999	930	<0.0001
375	>0.9999	945	0.5586
390	>0.9999	960	<0.0001
405	>0.9999	975	<0.0001
420	>0.9999	990	>0.9999
435	>0.9999	1005	<0.0001
450	>0.9999	1020	>0.9999
465	>0.9999	1035	>0.9999
480	>0.9999	1050	<0.0001
495	>0.9999	1065	<0.0001
510	>0.9999	1080	>0.9999
525	>0.9999	1095	>0.9999
540	>0.9999	1110	0.8918
555	>0.9999	1125	>0.9999

Table 4.10 (continued)

1140	0.9959	1710	<0.0001
1155	0.9709	1725	<0.0001
1170	0.3799	1740	<0.0001
1185	0.8918	1755	<0.0001
1200	0.1405	1770	<0.0001
1215	0.8918	1785	<0.0001
1230	0.0788	1800	<0.0001
1245	0.9709	1815	<0.0001
1260	0.0112	1830	<0.0001
1275	0.0006	1845	<0.0001
1290	0.0027	1860	<0.0001
1305	0.2384	1875	<0.0001
1320	0.0006	1890	<0.0001
1335	<0.0001	1905	<0.0001
1350	<0.0001	1920	<0.0001
1365	<0.0001	1935	<0.0001
1380	<0.0001	1950	<0.0001
1395	0.0001	1965	<0.0001
1410	<0.0001	1980	<0.0001
1425	0.0006	1995	<0.0001
1440	<0.0001	2010	<0.0001
1455	0.0003	2025	<0.0001
1470	<0.0001	2040	<0.0001
1485	<0.0001	2055	<0.0001
1500	<0.0001	2070	<0.0001
1515	<0.0001	2085	<0.0001
1530	0.0001	2100	<0.0001
1545	<0.0001	2115	<0.0001
1560	<0.0001	2130	<0.0001
1575	<0.0001	2145	<0.0001
1590	<0.0001		
1605	<0.0001		
1620	<0.0001		
1635	<0.0001		
1650	<0.0001		
1665	<0.0001		
1680	<0.0001		
1695	<0.0001		

Table 4.11 Sidak's multiple comparisons test with citric acid

time (minutes)	adjusted P value	time (minutes)	adjusted P value
0	>0.9999	570	>0.9999
15	0.3639	585	0.9695
30	0.659	600	0.9933
45	>0.9999	615	>0.9999
60	>0.9999	630	>0.9999
75	0.0381	645	0.9933
90	>0.9999	660	0.9992
105	0.0381	675	>0.9999
120	0.3639	690	>0.9999
135	0.5051	705	0.3639
150	0.9695	720	>0.9999
165	0.9089	735	0.9992
180	>0.9999	750	>0.9999
195	0.1631	765	0.659
210	0.1032	780	0.9933
225	0.9089	795	0.659
240	>0.9999	810	>0.9999
255	0.659	825	>0.9999
270	>0.9999	840	>0.9999
285	>0.9999	855	>0.9999
300	0.8018	870	>0.9999
315	>0.9999	885	>0.9999
330	0.2488	900	>0.9999
345	0.659	915	>0.9999
360	0.3639	930	>0.9999
375	0.3639	945	>0.9999
390	0.659	960	>0.9999
405	>0.9999	975	>0.9999
420	>0.9999	990	>0.9999
435	>0.9999	1005	>0.9999
450	0.8018	1020	>0.9999
465	0.9695	1035	>0.9999
480	0.9089	1050	>0.9999
495	>0.9999	1065	>0.9999
510	0.0129	1080	0.659
525	0.0635	1095	0.9695
540	0.3639	1110	0.0002
555	>0.9999	1125	0.3639

Table 4.11 (continued)

1140	0.0073	1710	<0.0001
1155	0.0012	1725	<0.0001
1170	<0.0001	1740	<0.0001
1185	<0.0001	1755	<0.0001
1200	<0.0001	1770	<0.0001
1215	<0.0001	1785	<0.0001
1230	<0.0001	1800	<0.0001
1245	<0.0001	1815	<0.0001
1260	0.0003	1830	<0.0001
1275	<0.0001	1845	<0.0001
1290	<0.0001	1860	<0.0001
1305	0.0003	1875	<0.0001
1320	<0.0001	1890	<0.0001
1335	<0.0001	1905	<0.0001
1350	<0.0001	1920	<0.0001
1365	<0.0001	1935	<0.0001
1380	<0.0001	1950	<0.0001
1395	<0.0001	1965	<0.0001
1410	<0.0001	1980	<0.0001
1425	<0.0001	1995	<0.0001
1440	<0.0001	2010	<0.0001
1455	<0.0001	2025	<0.0001
1470	<0.0001	2040	<0.0001
1485	<0.0001	2055	<0.0001
1500	<0.0001	2070	<0.0001
1515	<0.0001	2085	<0.0001
1530	<0.0001	2100	<0.0001
1545	<0.0001	2115	<0.0001
1560	<0.0001	2130	<0.0001
1575	<0.0001	2145	<0.0001
1590	<0.0001		
1605	<0.0001		
1620	<0.0001		
1635	<0.0001		
1650	<0.0001		
1665	<0.0001		
1680	<0.0001		
1695	<0.0001		

Table 4.12 Sidak's multiple comparisons test with fumaric acid

time (minutes)	adjusted P value	time (minutes)	adjusted P value
0	>0.9999	570	>0.9999
15	>0.9999	585	>0.9999
30	>0.9999	600	>0.9999
45	>0.9999	615	>0.9999
60	>0.9999	630	>0.9999
75	>0.9999	645	>0.9999
90	>0.9999	660	>0.9999
105	>0.9999	675	>0.9999
120	>0.9999	690	>0.9999
135	>0.9999	705	>0.9999
150	>0.9999	720	>0.9999
165	>0.9999	735	>0.9999
180	>0.9999	750	>0.9999
195	>0.9999	765	>0.9999
210	>0.9999	780	>0.9999
225	>0.9999	795	0.3521
240	>0.9999	810	>0.9999
255	>0.9999	825	>0.9999
270	>0.9999	840	>0.9999
285	>0.9999	855	>0.9999
300	>0.9999	870	>0.9999
315	>0.9999	885	>0.9999
330	>0.9999	900	>0.9999
345	>0.9999	915	>0.9999
360	>0.9999	930	>0.9999
375	>0.9999	945	>0.9999
390	>0.9999	960	>0.9999
405	>0.9999	975	>0.9999
420	>0.9999	990	>0.9999
435	>0.9999	1005	>0.9999
450	>0.9999	1020	>0.9999
465	>0.9999	1035	>0.9999
480	>0.9999	1050	>0.9999
495	>0.9999	1065	>0.9999
510	>0.9999	1080	0.821
525	>0.9999	1095	0.0009
540	>0.9999	1110	<0.0001
555	>0.9999	1125	0.0001

Table 4.12 (continued)

1140	0.0389	1710	<0.0001
1155	0.0163	1725	<0.0001
1170	<0.0001	1740	<0.0001
1185	<0.0001	1755	<0.0001
1200	<0.0001	1770	<0.0001
1215	<0.0001	1785	<0.0001
1230	<0.0001	1800	<0.0001
1245	<0.0001	1815	<0.0001
1260	0.0003	1830	<0.0001
1275	<0.0001	1845	<0.0001
1290	<0.0001	1860	<0.0001
1305	<0.0001	1875	<0.0001
1320	<0.0001	1890	<0.0001
1335	<0.0001	1905	<0.0001
1350	<0.0001	1920	<0.0001
1365	<0.0001	1935	<0.0001
1380	<0.0001	1950	<0.0001
1395	<0.0001	1965	<0.0001
1410	<0.0001	1980	<0.0001
1425	<0.0001	1995	<0.0001
1440	<0.0001	2010	<0.0001
1455	<0.0001	2025	<0.0001
1470	<0.0001	2040	<0.0001
1485	<0.0001	2055	<0.0001
1500	<0.0001	2070	<0.0001
1515	<0.0001	2085	<0.0001
1530	<0.0001	2100	<0.0001
1545	<0.0001	2115	<0.0001
1560	<0.0001	2130	<0.0001
1575	<0.0001	2145	<0.0001
1590	<0.0001		
1605	<0.0001		
1620	<0.0001		
1635	<0.0001		
1650	<0.0001		
1665	<0.0001		
1680	<0.0001		
1695	<0.0001		

Table 4.13 Sidak's multiple comparisons test with acetic acid

time (minutes)	adjusted P value	time (minutes)	adjusted P value
0	>0.9999	570	>0.9999
15	>0.9999	585	>0.9999
30	>0.9999	600	>0.9999
45	>0.9999	615	>0.9999
60	>0.9999	630	>0.9999
75	>0.9999	645	>0.9999
90	>0.9999	660	>0.9999
105	>0.9999	675	>0.9999
120	>0.9999	690	>0.9999
135	>0.9999	705	>0.9999
150	>0.9999	720	>0.9999
165	>0.9999	735	>0.9999
180	>0.9999	750	>0.9999
195	>0.9999	765	>0.9999
210	>0.9999	780	>0.9999
225	>0.9999	795	>0.9999
240	>0.9999	810	>0.9999
255	>0.9999	825	0.2666
270	>0.9999	840	0.0016
285	>0.9999	855	<0.0001
300	>0.9999	870	0.0915
315	>0.9999	885	<0.0001
330	>0.9999	900	<0.0001
345	>0.9999	915	<0.0001
360	>0.9999	930	0.0069
375	>0.9999	945	>0.9999
390	>0.9999	960	<0.0001
405	>0.9999	975	<0.0001
420	>0.9999	990	>0.9999
435	>0.9999	1005	<0.0001
450	>0.9999	1020	>0.9999
465	>0.9999	1035	>0.9999
480	>0.9999	1050	0.0016
495	>0.9999	1065	<0.0001
510	>0.9999	1080	>0.9999
525	>0.9999	1095	>0.9999
540	>0.9999	1110	>0.9999
555	>0.9999	1125	>0.9999

Table 4.13 (continued)

1140	>0.9999	1710	<0.0001
1155	>0.9999	1725	<0.0001
1170	>0.9999	1740	<0.0001
1185	>0.9999	1755	<0.0001
1200	>0.9999	1770	<0.0001
1215	>0.9999	1785	<0.0001
1230	0.9624	1800	<0.0001
1245	0.9996	1815	<0.0001
1260	>0.9999	1830	<0.0001
1275	0.1911	1845	<0.0001
1290	0.0915	1860	<0.0001
1305	0.5969	1875	<0.0001
1320	0.0408	1890	<0.0001
1335	<0.0001	1905	<0.0001
1350	0.001	1920	<0.0001
1365	0.0043	1935	<0.0001
1380	<0.0001	1950	<0.0001
1395	<0.0001	1965	<0.0001
1410	<0.0001	1980	<0.0001
1425	<0.0001	1995	<0.0001
1440	<0.0001	2010	<0.0001
1455	0.0002	2025	<0.0001
1470	<0.0001	2040	<0.0001
1485	<0.0001	2055	<0.0001
1500	<0.0001	2070	<0.0001
1515	<0.0001	2085	<0.0001
1530	<0.0001	2100	<0.0001
1545	<0.0001	2115	<0.0001
1560	<0.0001	2130	<0.0001
1575	<0.0001	2145	<0.0001
1590	<0.0001		
1605	<0.0001		
1620	<0.0001		
1635	<0.0001		
1650	<0.0001		
1665	<0.0001		
1680	<0.0001		
1695	<0.0001		

Table 4.14 Sidak's multiple comparisons test with pyruvic acid

time (minutes)	adjusted P value	time (minutes)	adjusted P value
0	>0.9999	570	>0.9999
15	>0.9999	585	0.8893
30	>0.9999	600	0.9994
45	>0.9999	615	0.9981
60	>0.9999	630	0.9994
75	>0.9999	645	0.9579
90	>0.9999	660	>0.9999
105	>0.9999	675	>0.9999
120	>0.9999	690	0.9951
135	>0.9999	705	0.8388
150	>0.9999	720	0.9888
165	0.9998	735	0.9579
180	>0.9999	750	>0.9999
195	0.9981	765	0.9981
210	>0.9999	780	0.4916
225	>0.9999	795	0.4916
240	>0.9999	810	0.9771
255	>0.9999	825	>0.9999
270	>0.9999	840	>0.9999
285	>0.9999	855	>0.9999
300	>0.9999	870	>0.9999
315	>0.9999	885	>0.9999
330	>0.9999	900	>0.9999
345	>0.9999	915	>0.9999
360	0.9998	930	>0.9999
375	>0.9999	945	>0.9999
390	>0.9999	960	>0.9999
405	>0.9999	975	>0.9999
420	>0.9999	990	>0.9999
435	>0.9999	1005	>0.9999
450	0.9994	1020	>0.9999
465	0.9998	1035	>0.9999
480	>0.9999	1050	>0.9999
495	>0.9999	1065	>0.9999
510	0.6385	1080	0.5644
525	0.7786	1095	0.2485
540	0.8388	1110	0.0532
555	>0.9999	1125	0.4221

Table 4.14 (continued)

1140	0.134	1710	<0.0001
1155	0.166	1725	<0.0001
1170	0.0066	1740	<0.0001
1185	0.0532	1755	<0.0001
1200	0.0194	1770	<0.0001
1215	0.0087	1785	<0.0001
1230	0.0087	1800	<0.0001
1245	0.0087	1815	<0.0001
1260	0.0416	1830	<0.0001
1275	0.0003	1845	<0.0001
1290	0.0087	1860	<0.0001
1305	0.0114	1875	<0.0001
1320	0.0114	1890	<0.0001
1335	0.0037	1905	<0.0001
1350	0.0114	1920	<0.0001
1365	0.0149	1935	<0.0001
1380	0.0037	1950	<0.0001
1395	0.0021	1965	<0.0001
1410	0.0016	1980	<0.0001
1425	0.0021	1995	<0.0001
1440	0.0002	2010	<0.0001
1455	0.0028	2025	<0.0001
1470	0.0016	2040	<0.0001
1485	<0.0001	2055	<0.0001
1500	0.0001	2070	<0.0001
1515	0.0003	2085	<0.0001
1530	0.0012	2100	<0.0001
1545	<0.0001	2115	<0.0001
1560	<0.0001	2130	<0.0001
1575	<0.0001	2145	<0.0001
1590	<0.0001		
1605	<0.0001		
1620	<0.0001		
1635	<0.0001		
1650	<0.0001		
1665	<0.0001		
1680	<0.0001		
1695	<0.0001		

Table 4.15 Sidak's multiple comparisons test with m-tartaric acid

time (minutes)	adjusted P value	time (minutes)	adjusted P value
0	>0.9999	570	>0.9999
15	>0.9999	585	>0.9999
30	0.9957	600	>0.9999
45	>0.9999	615	>0.9999
60	>0.9999	630	>0.9999
75	>0.9999	645	>0.9999
90	>0.9999	660	>0.9999
105	>0.9999	675	>0.9999
120	0.9996	690	>0.9999
135	>0.9999	705	>0.9999
150	>0.9999	720	>0.9999
165	>0.9999	735	>0.9999
180	>0.9999	750	>0.9999
195	0.0317	765	>0.9999
210	>0.9999	780	>0.9999
225	>0.9999	795	>0.9999
240	>0.9999	810	>0.9999
255	>0.9999	825	>0.9999
270	>0.9999	840	>0.9999
285	>0.9999	855	>0.9999
300	>0.9999	870	>0.9999
315	>0.9999	885	>0.9999
330	>0.9999	900	0.9957
345	>0.9999	915	0.5013
360	>0.9999	930	>0.9999
375	>0.9999	945	0.9957
390	>0.9999	960	>0.9999
405	>0.9999	975	0.5013
420	>0.9999	990	0.6633
435	>0.9999	1005	0.5013
450	>0.9999	1020	0.0179
465	>0.9999	1035	0.0317
480	>0.9999	1050	<0.0001
495	>0.9999	1065	0.0004
510	0.9996	1080	>0.9999
525	>0.9999	1095	>0.9999
540	>0.9999	1110	0.9957
555	>0.9999	1125	>0.9999

Table 4.15 (continued)

1140	>0.9999	1710	<0.0001
1155	>0.9999	1725	<0.0001
1170	0.092	1740	<0.0001
1185	0.2357	1755	<0.0001
1200	0.1501	1770	<0.0001
1215	0.2357	1785	<0.0001
1230	0.1501	1800	<0.0001
1245	0.0029	1815	<0.0001
1260	0.9199	1830	<0.0001
1275	0.0179	1845	<0.0001
1290	0.0008	1860	<0.0001
1305	0.2357	1875	<0.0001
1320	0.0179	1890	<0.0001
1335	0.0002	1905	<0.0001
1350	0.0015	1920	<0.0001
1365	0.0029	1935	<0.0001
1380	<0.0001	1950	<0.0001
1395	0.0099	1965	<0.0001
1410	0.0004	1980	<0.0001
1425	<0.0001	1995	<0.0001
1440	<0.0001	2010	<0.0001
1455	0.0054	2025	<0.0001
1470	<0.0001	2040	<0.0001
1485	<0.0001	2055	<0.0001
1500	<0.0001	2070	<0.0001
1515	<0.0001	2085	<0.0001
1530	<0.0001	2100	<0.0001
1545	<0.0001	2115	<0.0001
1560	<0.0001	2130	<0.0001
1575	<0.0001	2145	<0.0001
1590	<0.0001		
1605	<0.0001		
1620	<0.0001		
1635	<0.0001		
1650	<0.0001		
1665	<0.0001		
1680	<0.0001		
1695	<0.0001		

Table 4.16 Sidak's multiple comparisons test with Tween 40

time (minutes)	adjusted P value	time (minutes)	adjusted P value
0	>0.9999	570	>0.9999
15	>0.9999	585	>0.9999
30	>0.9999	600	>0.9999
45	>0.9999	615	>0.9999
60	>0.9999	630	>0.9999
75	>0.9999	645	>0.9999
90	>0.9999	660	>0.9999
105	>0.9999	675	>0.9999
120	>0.9999	690	>0.9999
135	>0.9999	705	>0.9999
150	>0.9999	720	>0.9999
165	>0.9999	735	>0.9999
180	>0.9999	750	>0.9999
195	>0.9999	765	>0.9999
210	>0.9999	780	>0.9999
225	>0.9999	795	>0.9999
240	>0.9999	810	>0.9999
255	>0.9999	825	0.0112
270	>0.9999	840	<0.0001
285	>0.9999	855	<0.0001
300	>0.9999	870	0.0636
315	>0.9999	885	<0.0001
330	>0.9999	900	<0.0001
345	>0.9999	915	<0.0001
360	>0.9999	930	<0.0001
375	>0.9999	945	>0.9999
390	>0.9999	960	<0.0001
405	>0.9999	975	<0.0001
420	>0.9999	990	>0.9999
435	>0.9999	1005	<0.0001
450	>0.9999	1020	0.4109
465	>0.9999	1035	>0.9999
480	>0.9999	1050	<0.0001
495	>0.9999	1065	<0.0001
510	>0.9999	1080	>0.9999
525	>0.9999	1095	>0.9999
540	>0.9999	1110	>0.9999
555	>0.9999	1125	>0.9999

Table 4.16 (continued)

1140	>0.9999	1710	<0.0001
1155	>0.9999	1725	<0.0001
1170	>0.9999	1740	<0.0001
1185	>0.9999	1755	<0.0001
1200	>0.9999	1770	<0.0001
1215	>0.9999	1785	<0.0001
1230	>0.9999	1800	<0.0001
1245	>0.9999	1815	<0.0001
1260	>0.9999	1830	<0.0001
1275	>0.9999	1845	<0.0001
1290	0.5721	1860	<0.0001
1305	0.9989	1875	<0.0001
1320	0.9559	1890	<0.0001
1335	0.0636	1905	<0.0001
1350	0.1077	1920	<0.0001
1365	0.4109	1935	<0.0001
1380	0.9904	1950	<0.0001
1395	0.0204	1965	<0.0001
1410	0.0204	1980	<0.0001
1425	0.0204	1995	<0.0001
1440	0.0002	2010	<0.0001
1455	0.0365	2025	<0.0001
1470	0.1077	2040	<0.0001
1485	0.0008	2055	<0.0001
1500	<0.0001	2070	<0.0001
1515	0.006	2085	<0.0001
1530	<0.0001	2100	<0.0001
1545	<0.0001	2115	<0.0001
1560	<0.0001	2130	<0.0001
1575	<0.0001	2145	<0.0001
1590	<0.0001		
1605	<0.0001		
1620	<0.0001		
1635	<0.0001		
1650	<0.0001		
1665	<0.0001		
1680	<0.0001		
1695	<0.0001		

Table 4.17 Sidak's multiple comparisons test with Tween 80

time (minutes)	adjusted P value	time (minutes)	adjusted P value
0	>0.9999	570	>0.9999
15	>0.9999	585	>0.9999
30	>0.9999	600	>0.9999
45	>0.9999	615	>0.9999
60	>0.9999	630	>0.9999
75	>0.9999	645	>0.9999
90	>0.9999	660	>0.9999
105	>0.9999	675	>0.9999
120	>0.9999	690	>0.9999
135	>0.9999	705	>0.9999
150	>0.9999	720	>0.9999
165	>0.9999	735	>0.9999
180	>0.9999	750	>0.9999
195	>0.9999	765	>0.9999
210	>0.9999	780	>0.9999
225	>0.9999	795	>0.9999
240	>0.9999	810	>0.9999
255	>0.9999	825	>0.9999
270	>0.9999	840	>0.9999
285	>0.9999	855	>0.9999
300	>0.9999	870	>0.9999
315	>0.9999	885	0.999
330	>0.9999	900	0.8522
345	>0.9999	915	0.6068
360	>0.9999	930	>0.9999
375	>0.9999	945	0.3515
390	>0.9999	960	>0.9999
405	>0.9999	975	0.999
420	>0.9999	990	0.8522
435	>0.9999	1005	0.0043
450	>0.9999	1020	0.0313
465	>0.9999	1035	0.0043
480	>0.9999	1050	<0.0001
495	>0.9999	1065	0.0043
510	>0.9999	1080	>0.9999
525	>0.9999	1095	>0.9999
540	>0.9999	1110	0.9759
555	>0.9999	1125	>0.9999

Table 4.17 (continued)

1140	>0.9999	1710	<0.0001
1155	>0.9999	1725	<0.0001
1170	0.3515	1740	<0.0001
1185	>0.9999	1755	<0.0001
1200	>0.9999	1770	<0.0001
1215	>0.9999	1785	<0.0001
1230	0.3515	1800	<0.0001
1245	0.3515	1815	<0.0001
1260	0.999	1830	<0.0001
1275	0.0043	1845	<0.0001
1290	0.0313	1860	<0.0001
1305	0.999	1875	<0.0001
1320	0.1738	1890	<0.0001
1335	<0.0001	1905	<0.0001
1350	0.0005	1920	<0.0001
1365	0.0005	1935	<0.0001
1380	0.0015	1950	<0.0001
1395	0.3515	1965	<0.0001
1410	0.012	1980	<0.0001
1425	0.0769	1995	<0.0001
1440	0.0005	2010	<0.0001
1455	0.3515	2025	<0.0001
1470	0.3515	2040	<0.0001
1485	<0.0001	2055	<0.0001
1500	<0.0001	2070	<0.0001
1515	<0.0001	2085	<0.0001
1530	0.0769	2100	<0.0001
1545	<0.0001	2115	<0.0001
1560	<0.0001	2130	<0.0001
1575	<0.0001	2145	<0.0001
1590	<0.0001		
1605	<0.0001		
1620	<0.0001		
1635	<0.0001		
1650	<0.0001		
1665	<0.0001		
1680	<0.0001		
1695	<0.0001		

Table 4.18 Sidak's multiple comparisons test with α -ketoglutaric acid

time (minutes)	adjusted P value	time (minutes)	adjusted P value
0	>0.9999	570	>0.9999
15	>0.9999	585	>0.9999
30	>0.9999	600	>0.9999
45	>0.9999	615	>0.9999
60	>0.9999	630	>0.9999
75	>0.9999	645	>0.9999
90	>0.9999	660	>0.9999
105	>0.9999	675	>0.9999
120	>0.9999	690	>0.9999
135	>0.9999	705	>0.9999
150	>0.9999	720	>0.9999
165	>0.9999	735	>0.9999
180	>0.9999	750	>0.9999
195	>0.9999	765	>0.9999
210	>0.9999	780	>0.9999
225	>0.9999	795	>0.9999
240	>0.9999	810	>0.9999
255	>0.9999	825	0.0005
270	>0.9999	840	<0.0001
285	>0.9999	855	<0.0001
300	>0.9999	870	0.0005
315	>0.9999	885	<0.0001
330	>0.9999	900	<0.0001
345	>0.9999	915	<0.0001
360	>0.9999	930	<0.0001
375	>0.9999	945	>0.9999
390	>0.9999	960	<0.0001
405	>0.9999	975	<0.0001
420	>0.9999	990	>0.9999
435	>0.9999	1005	<0.0001
450	>0.9999	1020	0.9998
465	>0.9999	1035	>0.9999
480	>0.9999	1050	<0.0001
495	>0.9999	1065	<0.0001
510	>0.9999	1080	>0.9999
525	>0.9999	1095	>0.9999
540	>0.9999	1110	>0.9999
555	>0.9999	1125	>0.9999

Table 4.18 (continued)

1140	>0.9999	1710	<0.0001
1155	>0.9999	1725	<0.0001
1170	>0.9999	1740	<0.0001
1185	>0.9999	1755	<0.0001
1200	>0.9999	1770	<0.0001
1215	>0.9999	1785	<0.0001
1230	>0.9999	1800	<0.0001
1245	>0.9999	1815	<0.0001
1260	>0.9999	1830	<0.0001
1275	0.9961	1845	<0.0001
1290	0.9998	1860	<0.0001
1305	>0.9999	1875	<0.0001
1320	>0.9999	1890	<0.0001
1335	0.9676	1905	<0.0001
1350	>0.9999	1920	<0.0001
1365	0.8729	1935	<0.0001
1380	0.9998	1950	<0.0001
1395	0.9998	1965	<0.0001
1410	>0.9999	1980	<0.0001
1425	0.9961	1995	<0.0001
1440	0.4958	2010	<0.0001
1455	0.9676	2025	<0.0001
1470	0.9998	2040	<0.0001
1485	0.0005	2055	<0.0001
1500	0.0997	2070	<0.0001
1515	0.0997	2085	<0.0001
1530	0.183	2100	<0.0001
1545	0.0516	2115	<0.0001
1560	0.0997	2130	<0.0001
1575	<0.0001	2145	<0.0001
1590	<0.0001		
1605	<0.0001		
1620	<0.0001		
1635	0.0256		
1650	<0.0001		
1665	0.0997		
1680	<0.0001		
1695	0.0005		

Table 4.19 Sidak's multiple comparisons test with glucuronamide

time (minutes)	adjusted P value	time (minutes)	adjusted P value
0	>0.9999	570	>0.9999
15	>0.9999	585	0.5762
30	>0.9999	600	>0.9999
45	>0.9999	615	0.9995
60	>0.9999	630	>0.9999
75	>0.9999	645	0.9659
90	>0.9999	660	>0.9999
105	0.9995	675	>0.9999
120	>0.9999	690	>0.9999
135	>0.9999	705	0.1643
150	>0.9999	720	>0.9999
165	>0.9999	735	0.7496
180	>0.9999	750	0.9659
195	0.7496	765	0.994
210	>0.9999	780	>0.9999
225	>0.9999	795	0.7496
240	>0.9999	810	0.9995
255	>0.9999	825	>0.9999
270	>0.9999	840	>0.9999
285	>0.9999	855	>0.9999
300	>0.9999	870	>0.9999
315	>0.9999	885	>0.9999
330	>0.9999	900	>0.9999
345	>0.9999	915	>0.9999
360	>0.9999	930	>0.9999
375	>0.9999	945	>0.9999
390	>0.9999	960	>0.9999
405	>0.9999	975	>0.9999
420	>0.9999	990	>0.9999
435	>0.9999	1005	>0.9999
450	>0.9999	1020	>0.9999
465	>0.9999	1035	>0.9999
480	>0.9999	1050	>0.9999
495	>0.9999	1065	>0.9999
510	>0.9999	1080	>0.9999
525	0.8877	1095	0.8877
540	0.994	1110	0.5762
555	0.8877	1125	0.1643

Table 4.19 (continued)

1140	0.8877	1710	0.0085
1155	0.9659	1725	0.0001
1170	0.4059	1740	<0.0001
1185	0.1643	1755	0.0085
1200	0.0551	1770	0.0022
1215	0.0163	1785	0.0085
1230	0.2659	1800	<0.0001
1245	0.4059	1815	<0.0001
1260	0.7496	1830	0.0005
1275	0.0163	1845	<0.0001
1290	0.0551	1860	0.0005
1305	0.994	1875	0.0005
1320	0.2659	1890	<0.0001
1335	0.0304	1905	0.0022
1350	0.0011	1920	<0.0001
1365	0.0551	1935	0.0044
1380	0.0969	1950	0.0022
1395	0.2659	1965	<0.0001
1410	0.0969	1980	<0.0001
1425	0.0969	1995	0.0001
1440	0.0085	2010	0.0001
1455	0.0304	2025	<0.0001
1470	0.9659	2040	0.0001
1485	0.0011	2055	<0.0001
1500	0.0002	2070	0.0002
1515	0.0044	2085	0.0022
1530	0.0005	2100	<0.0001
1545	0.0022	2115	0.0001
1560	0.0085	2130	<0.0001
1575	0.0005	2145	<0.0001
1590	0.0085		
1605	<0.0001		
1620	0.0001		
1635	0.0011		
1650	<0.0001		
1665	0.0044		
1680	0.0001		
1695	0.0022		

Table 4.20 Sidak's multiple comparisons test with methyl pyruvate

time (minutes)	adjusted P value	time (minutes)	adjusted P value
0	>0.9999	570	0.8648
15	>0.9999	585	0.9937
30	0.9999	600	0.9999
45	0.9999	615	>0.9999
60	0.7623	630	>0.9999
75	0.9766	645	0.9365
90	>0.9999	660	>0.9999
105	>0.9999	675	0.9766
120	0.9937	690	>0.9999
135	0.9937	705	0.9988
150	>0.9999	720	0.9988
165	0.7623	735	>0.9999
180	0.9999	750	>0.9999
195	>0.9999	765	>0.9999
210	0.9937	780	>0.9999
225	0.9988	795	0.9365
240	0.9999	810	>0.9999
255	0.9937	825	>0.9999
270	>0.9999	840	>0.9999
285	>0.9999	855	>0.9999
300	>0.9999	870	>0.9999
315	>0.9999	885	>0.9999
330	>0.9999	900	>0.9999
345	>0.9999	915	>0.9999
360	>0.9999	930	>0.9999
375	0.9999	945	>0.9999
390	>0.9999	960	>0.9999
405	>0.9999	975	>0.9999
420	0.9999	990	>0.9999
435	>0.9999	1005	>0.9999
450	0.6393	1020	>0.9999
465	0.9988	1035	>0.9999
480	0.9988	1050	>0.9999
495	>0.9999	1065	0.8648
510	0.9766	1080	>0.9999
525	0.9937	1095	0.9766
540	0.8648	1110	0.2888
555	0.9988	1125	0.9365

Table 4.20 (continued)

1140	>0.9999	1710	0.0025
1155	>0.9999	1725	<0.0001
1170	0.2063	1740	<0.0001
1185	0.8648	1755	<0.0001
1200	0.7623	1770	<0.0001
1215	0.9766	1785	0.0001
1230	0.7623	1800	<0.0001
1245	0.3915	1815	<0.0001
1260	0.7623	1830	<0.0001
1275	0.6393	1845	<0.0001
1290	0.0976	1860	<0.0001
1305	0.9937	1875	<0.0001
1320	0.8648	1890	<0.0001
1335	0.0068	1905	<0.0001
1350	0.0976	1920	<0.0001
1365	0.2888	1935	<0.0001
1380	0.0042	1950	<0.0001
1395	0.0427	1965	<0.0001
1410	0.5112	1980	<0.0001
1425	0.7623	1995	<0.0001
1440	0.0651	2010	<0.0001
1455	0.9365	2025	<0.0001
1470	0.5112	2040	<0.0001
1485	0.0009	2055	<0.0001
1500	0.011	2070	<0.0001
1515	0.0175	2085	<0.0001
1530	0.0042	2100	<0.0001
1545	0.0175	2115	<0.0001
1560	0.0427	2130	<0.0001
1575	0.0042	2145	<0.0001
1590	0.0009		
1605	0.0002		
1620	0.0002		
1635	0.0175		
1650	<0.0001		
1665	0.0068		
1680	<0.0001		
1695	0.0015		

Table 4.21 Sidak's multiple comparisons test with L-serine

time (minutes)	adjusted P value	time (minutes)	adjusted P value
0	>0.9999	570	>0.9999
15	0.5665	585	>0.9999
30	0.4273	600	>0.9999
45	0.9249	615	>0.9999
60	>0.9999	630	>0.9999
75	0.0014	645	>0.9999
90	0.0216	660	>0.9999
105	0.091	675	>0.9999
120	0.3068	690	>0.9999
135	0.2113	705	>0.9999
150	0.9992	720	>0.9999
165	0.4273	735	>0.9999
180	0.4273	750	>0.9999
195	0.0044	765	>0.9999
210	0.3068	780	>0.9999
225	0.9992	795	>0.9999
240	0.9745	810	>0.9999
255	0.9249	825	>0.9999
270	0.9249	840	>0.9999
285	0.7094	855	>0.9999
300	0.9745	870	>0.9999
315	0.9992	885	>0.9999
330	0.7094	900	>0.9999
345	>0.9999	915	>0.9999
360	>0.9999	930	>0.9999
375	>0.9999	945	>0.9999
390	>0.9999	960	>0.9999
405	>0.9999	975	>0.9999
420	>0.9999	990	>0.9999
435	>0.9999	1005	>0.9999
450	>0.9999	1020	>0.9999
465	0.9992	1035	>0.9999
480	>0.9999	1050	>0.9999
495	>0.9999	1065	>0.9999
510	0.9745	1080	>0.9999
525	0.8349	1095	>0.9999
540	>0.9999	1110	>0.9999
555	>0.9999	1125	>0.9999

Table 4.21 (continued)

1140	>0.9999	1710	0.0008
1155	>0.9999	1725	<0.0001
1170	0.5665	1740	<0.0001
1185	>0.9999	1755	0.0008
1200	0.9992	1770	<0.0001
1215	>0.9999	1785	<0.0001
1230	0.9941	1800	<0.0001
1245	0.9745	1815	<0.0001
1260	>0.9999	1830	<0.0001
1275	0.9745	1845	<0.0001
1290	0.9745	1860	<0.0001
1305	>0.9999	1875	<0.0001
1320	>0.9999	1890	<0.0001
1335	0.7094	1905	<0.0001
1350	>0.9999	1920	<0.0001
1365	0.9941	1935	<0.0001
1380	>0.9999	1950	<0.0001
1395	0.2113	1965	<0.0001
1410	0.9745	1980	<0.0001
1425	0.9745	1995	<0.0001
1440	0.0575	2010	<0.0001
1455	0.8349	2025	<0.0001
1470	0.3068	2040	<0.0001
1485	0.091	2055	<0.0001
1500	0.091	2070	<0.0001
1515	0.5665	2085	<0.0001
1530	0.1406	2100	<0.0001
1545	0.0575	2115	<0.0001
1560	0.091	2130	<0.0001
1575	0.0216	2145	<0.0001
1590	0.2113		
1605	0.0014		
1620	0.0002		
1635	0.0076		
1650	<0.0001		
1665	0.0014		
1680	0.0008		
1695	0.0076		

Table 4.22 Sidak's multiple comparisons test with D-fructose

time (minutes)	adjusted P value	time (minutes)	adjusted P value
0	>0.9999	570	>0.9999
15	>0.9999	585	>0.9999
30	>0.9999	600	>0.9999
45	>0.9999	615	>0.9999
60	>0.9999	630	>0.9999
75	>0.9999	645	>0.9999
90	>0.9999	660	>0.9999
105	>0.9999	675	>0.9999
120	>0.9999	690	>0.9999
135	>0.9999	705	>0.9999
150	>0.9999	720	>0.9999
165	>0.9999	735	>0.9999
180	>0.9999	750	>0.9999
195	>0.9999	765	>0.9999
210	>0.9999	780	>0.9999
225	>0.9999	795	>0.9999
240	>0.9999	810	>0.9999
255	>0.9999	825	0.0095
270	>0.9999	840	<0.0001
285	>0.9999	855	<0.0001
300	>0.9999	870	0.0319
315	>0.9999	885	<0.0001
330	>0.9999	900	<0.0001
345	>0.9999	915	<0.0001
360	>0.9999	930	0.0003
375	>0.9999	945	>0.9999
390	>0.9999	960	<0.0001
405	>0.9999	975	<0.0001
420	>0.9999	990	>0.9999
435	>0.9999	1005	<0.0001
450	>0.9999	1020	>0.9999
465	>0.9999	1035	>0.9999
480	>0.9999	1050	<0.0001
495	>0.9999	1065	<0.0001
510	>0.9999	1080	>0.9999
525	>0.9999	1095	>0.9999
540	>0.9999	1110	>0.9999
555	>0.9999	1125	>0.9999

Table 4.22 (continued)

1140	>0.9999	1710	>0.9999
1155	>0.9999	1725	0.7107
1170	>0.9999	1740	0.0095
1185	>0.9999	1755	0.9877
1200	>0.9999	1770	0.5426
1215	>0.9999	1785	>0.9999
1230	>0.9999	1800	0.005
1245	>0.9999	1815	0.0007
1260	>0.9999	1830	0.7107
1275	0.9472	1845	0.5426
1290	>0.9999	1860	0.0319
1305	>0.9999	1875	0.0562
1320	>0.9999	1890	<0.0001
1335	0.5426	1905	0.254
1350	>0.9999	1920	<0.0001
1365	>0.9999	1935	0.5426
1380	>0.9999	1950	0.0013
1395	>0.9999	1965	<0.0001
1410	>0.9999	1980	0.0026
1425	>0.9999	1995	<0.0001
1440	>0.9999	2010	0.0007
1455	>0.9999	2025	<0.0001
1470	>0.9999	2040	0.0007
1485	>0.9999	2055	0.0095
1500	0.9472	2070	0.0002
1515	>0.9999	2085	<0.0001
1530	>0.9999	2100	<0.0001
1545	0.9472	2115	0.0026
1560	>0.9999	2130	<0.0001
1575	0.9472	2145	<0.0001
1590	>0.9999		
1605	0.0964		
1620	>0.9999		
1635	>0.9999		
1650	0.8546		
1665	>0.9999		
1680	>0.9999		
1695	0.9877		

Appendix 2

Table 4.23 Hits from the phenotypic metabolic screen

substrate	metabolic information	information regarding <i>Cryptococcus</i>
D-xylose	<p>pentose monosaccharide sugar;</p> <p>*involved in fungal metabolism: carbohydrate metabolism (pentoses and pentose cycle); as uridine diphosphate (UDP), UDP-α-xylose next to carbohydrate metabolism (pentoses and pentose cycle);</p> <p>*not generally involved in fungal metabolism: as UDP- α-xylose in carbohydrate metabolism (di-and poly-saccharides) (Hoffman-La Roche Ltd, 2014)</p>	<p>structural element of GXM of <i>C. neoformans</i> (Bhattacharjee <i>et al.</i>, 1979b; Cherniak <i>et al.</i>, 1980; Marrifield and Stephen, 1980; Bhattacharjee <i>et al.</i>, 1981) and <i>C. gattii</i> (Bhattacharjee <i>et al.</i>, 1978, 1979a, 1980; Bacon and Cherniak, 1995) or GalXM of <i>C. neoformans</i> (Cherniak <i>et al.</i>, 1982; Turner <i>et al.</i>, 1984) and <i>C. gattii</i> (James and Cherniak, 1992); the GXMs of <i>C. neoformans</i> and <i>C. gattii</i> differ in the amount of xylose substitutions (Young and Kozel, 1993); GalXMs are also variable amongst cryptococcal species(de Jesus <i>et al.</i>, 2010); a sole carbon source through the pentophosphate pathway (hexose monophosphate shunt) in <i>C. neoformans</i> (Cherniak, O'Neill, <i>et al.</i>, 1998); assimilated by <i>C. gattii</i> (Lazéra <i>et al.</i>, 1998) and utilised by <i>Cryptococcus</i> spp. (Vimercati <i>et al.</i>, 2016); utilised by both <i>C. neoformans</i> and <i>C. gattii</i> (Hagen <i>et al.</i>, 2015); UDP-xylose is a transporter of capsular xylose in <i>C. neoformans</i> (Li <i>et al.</i>, 2018)</p>
D-mannose	<p>hexose disaccharide sugar; C'-2 epimer of glucose;</p> <p>*involved in fungal metabolism: carbohydrates metabolism (glycolysis and gluconeogenesis) (Hoffman-La Roche Ltd, 2014)</p>	<p>structural element of GXM of <i>C. neoformans</i> (Rebers <i>et al.</i>, 1958; Bhattacharjee <i>et al.</i>, 1979b, 1981; Cherniak <i>et al.</i>, 1980; Marrifield and Stephen, 1980) and <i>C. gattii</i> (Bhattacharjee <i>et al.</i>, 1978, 1979a, 1980; Bacon and Cherniak, 1995) or GalXM of <i>C. neoformans</i> (Cherniak <i>et al.</i>, 1982; Turner <i>et al.</i>, 1984) and <i>C. gattii</i> (James and Cherniak, 1992); assimilated directly into GXM of <i>C. neoformans</i> (Cherniak, O'Neill, <i>et al.</i>, 1998; Zaragoza <i>et al.</i>, 2006); GDP-mannose is a transporter of capsular mannose in <i>C. neoformans</i> (Cottrell <i>et al.</i>, 2007; Wang <i>et al.</i>, 2014)</p>

Table 4.2 (continued)

tricarballic acid	an inhibitor of the enzyme aconitase and therefore interferes with the Krebs cycle (Russell and Forsberg, 1986)	no research on <i>Cryptococcus</i> ;
L-lyxose	pentose monosaccharide sugar; C'-2 carbon epimer of xylose sugar	used as a substrate for xylose reductase by <i>C. flavus</i> (Mayr <i>et al.</i> , 2003);
D, L-malic acid	*involved in fungal metabolism: L-malate is an intermediate in Krebs cycle and therefore involved in citrate and glyoxalate cycle *not generally involved in fungal metabolism: carbon fixation (Hoffman-La Roche Ltd, 2014)	L-malic is assimilated by <i>Cryptococcus</i> spp. (Vimercati <i>et al.</i> , 2016) and by serotypes B and C of <i>C. neoformans</i> but not by serotypes A and D but (Bennett <i>et al.</i> , 1978)
bromosuccinic acid	both D- and L-bromosuccinate cause the loss of activity in the catalytic subunit of aspartate transcarbamylase (Lauritzen and Lipscomb, 1982), an enzyme that catalyses the first step in the pyrimidine biosynthetic pathway (Simmer <i>et al.</i> , 1990)	utilised by <i>C. neoformans</i> (Vimercati <i>et al.</i> , 2016)

Table 4.2 (continued)

L-asparagine	<p>α-amino acid;</p> <p>*not generally involved in fungal metabolism: amino acid metabolism (serine, threonine, cysteine, methionine) (Hoffman-La Roche Ltd, 2014)</p>	<p>induces melanin production in <i>C. neoformans</i> (Chaskes and Tyndall, 1975); <i>Cryptococcus</i> shows asparaginase activity (Imada <i>et al.</i>, 1972)</p>
sucrose	<p>monosaccharide sugar;</p> <p>*involved in fungal metabolism: carbohydrate metabolism (di- and polysaccharides);</p> <p>*not generally involved in fungal metabolism: carbon fixation (not included in fungal cellular and molecular processes) (Hoffman-La Roche Ltd, 2014)</p>	<p>utilised by <i>Cryptococcus</i> spp. (Vimercati <i>et al.</i>, 2016); utilised by both <i>C. neoformans</i> (Benham, 1956; Hagen <i>et al.</i>, 2015) and <i>C. gattii</i> (Hagen <i>et al.</i>, 2015)</p>
L-lactic acid	<p>L-lactate is involved in</p> <p>*involved in fungal metabolism: carbohydrate metabolism (pyruvate turnover); alternative respiration;</p>	<p>not assimilated by <i>C. gattii</i> (Lazéra <i>et al.</i>, 1998); lactose not utilised by either <i>C. neoformans</i> or <i>C. gattii</i> (Hagen <i>et al.</i>, 2015)</p>
citric acid	<p>as citrate:</p> <p>*involved in fungal metabolism: citrate and glyoxalate cycle (Hoffman-La Roche Ltd, 2014)</p>	<p>assimilated by <i>C. gattii</i> serotype B after recovery from an infected hamster (Lazéra <i>et al.</i>, 1998)</p>

Table 4.2 (continued)

fumaric acid	as fumarate: *involved in fungal metabolism: citrate and glyoxalate cycle; nucleotide metabolism (NAD, NADP); photo phosphorylation; oxidative phosphorylation; alternative respiration *not generally involved in fungal metabolism: amino acid metabolism (urea); amino acid metabolism (histidine); nucleotide metabolism (purines); citrate and glyoxalate cycle; purine metabolism; amino acid metabolism (histidine; amino acid metabolism (urea cycle); oxidative phosphorylation	assimilated by <i>C. neoformans</i> serotypes B and C but poorly by A and D (Bennett <i>et al.</i> , 1978)
--------------	--	--

Table 4.2 (continued)

<p>acetic acid</p>	<p>as acetate:</p> <p>*involved in fungal metabolism: bacterial metabolism (butanol/butyrate, fermentation); amino acid metabolism (lysine); amino acid metabolism (glutamate, proline, hydroxyproline); amino acid metabolism (urea); carbohydrate metabolism (pyruvate turnover); carbohydrate metabolism (pentoses and pentose cycle); carbohydrate metabolism (amino sugar derivatives); tetrapyrrole metabolism (porphyrins, cobalamin)</p> <p>*not generally involved in fungal metabolism: amino acid metabolism (serine, proline, hydroxyproline); amino acid metabolism (serine, threonine, cysteine, methionine); C1 metabolism; steroid metabolism (androgens and estrogens); lipid metabolism (fatty acids); lipid metabolism (glyco- and phospholipids)</p> <p>as active acetate, acetyl-coenzyme A (acetyl-CoA):</p> <p>*involved in fungal metabolism: bacterial metabolism (butanol/butyrate, fermentation); amino acid metabolism (serine, proline, hydroxyproline); amino acid metabolism (histidine); amino acid metabolism (lysine); amino acid metabolism (leucine, isoleucine, valine); C1 metabolism; carbohydrate metabolism (pyruvate turnover); carbohydrate metabolism (pentoses and pentose cycle); carbohydrate metabolism (amino sugar derivatives); carbohydrate metabolism (pyruvate turnover)</p> <p>*not generally involved in fungal metabolism: citrate and glyoxalate cycle; amino acid metabolism (serine, proline, hydroxyproline); amino acid metabolism (leucine, isoleucine, valine); carbohydrate metabolism (amino sugar derivatives); lipid metabolism (fatty acids); lipid metabolism (fatty acids)</p>	<p><i>C. neoformans</i> H99 strain grows on acetate (Hu <i>et al.</i>, 2008); indole-3-acetic acid stimulates mating in <i>C. gattii</i> (Xue <i>et al.</i>, 2007)</p>
--------------------	---	--

Table 4.2 (continued)

pyruvic acid	<p>as pyruvate:</p> <p>*involved in fungal metabolism: amino acid metabolism (leucine, isoleucine, valine); amino acid metabolism (serine, threonine, cysteine, methionine); amino acid metabolism (glutamate, proline, hydroxyproline); amino acid metabolism (histidine); carbohydrate metabolism (pyruvate turnover); carbohydrate metabolism (amino sugar derivatives); carbohydrate metabolism (glycolysis and glyconeogenesis); carbohydrate metabolism (acidic carbohydrate derivatives); lipid metabolism (glyco- and phospholipids); prokaryotic membranes; alternative respiration</p> <p>*not generally involved in fungal metabolism: amino acid metabolism (glutamate, proline, hydroxyproline); citrate and glyoxalate cycle; carbon fixation</p>	pyruvic acid analogue: 3-bromopyruvate (3-BP) is an antifungal against <i>C. neoformans</i> (Lis <i>et al.</i> , 2013)
m-tartaric acid	D-tartrate involved in the Krebs cycle (van Vugt-Lussenburg <i>et al.</i> , 2013);	<i>C. neoformans</i> is thought to have CNI02800 tartrate transporter, putative (NCBI); tartrate is very rare to utilise in microorganisms (Kado, 1985)
Tween 40	emulsifier; not involved in metabolic pathways	used to assess lipase activity of <i>C. neoformans</i> or <i>C. gattii</i> (Hagen <i>et al.</i> , 2015)
Tween 80	emulsifier; not involved in metabolic pathways	used to assess lipase activity of <i>C. neoformans</i> or <i>C. gattii</i> (Hagen <i>et al.</i> , 2015); utilised by <i>C. sp</i> (Vimercati <i>et al.</i> , 2016)

Table 4.2 (continued)

<p>α-ketoglutaric acid; also known as 2-oxoglutaric acid</p>	<p>*involved in fungal metabolism: amino acid metabolism (glutamate, proline, hydroxyproline); amino acid metabolism (serine, threonine, cysteine, methionine); amino acid metabolism (leucine, isoleucine, valine); amino acid metabolism (lysine); citrate and glyoxalate cycle;</p> <p>*not generally involved in fungal metabolism: amino acid metabolism (lysine) (not included in fungal metabolism); amino acid metabolism (histidine) (not included in fungal metabolism); amino acid metabolism (glutamate, proline, hydroxyproline) (not included in fungal metabolism); amino acid metabolism (leucine, isoleucine, valine) (not included in fungal metabolism); nucleotide metabolism (NAD, NADP) (not included in fungal metabolism); carbohydrate metabolism (glycolysis and gluconeogenesis) (not included in fungal metabolism)</p>	<p>α-ketoglutarate is associated with resistance to nitrosative stress (reviewed by (Zaragoza, 2019)); α-ketoglutarate secreted by <i>C. neoformans</i> (Jacobson and Petro, 1987); <i>C. neoformans</i> hypervirulence-associated protein (HVA1) shows blocked α-ketoglutarate production; in L-lysine biosynthesis <i>C. neoformans</i> (Garrad and Bhattacharjee, 1992) uses α-ketoglutarate (Xu <i>et al.</i>, 2006)</p>
<p>glucuronamide</p>	<p>hexose monosaccharide derivative related to glucuronic acid</p>	<p>utilised by <i>C. flavescens</i> (McSpadden Gardener <i>et al.</i>, 2014)</p>
<p>methyl pyruvate</p>	<p>more favourable substrate for the tricarboxylic acid (TCA) cycle than pyruvic acid (Lembert <i>et al.</i>, 2001; Duffer <i>et al.</i>, 2002)</p>	<p>no research on <i>Cryptococcus</i>; utilised by <i>Mucorales</i> spp. (Pawłowska <i>et al.</i>, 2016)</p>
<p>L-serine</p>	<p>α-amino acid</p> <p>*involved in fungal metabolism: amino acid metabolism (serine, threonine, cysteine, methionine); lipid metabolism (glyco- and phospholipids);</p> <p>*not generally involved in fungal metabolism: lipid metabolism (sphingolipids); carbohydrate metabolism (glycolysis and gluconeogenesis)</p>	<p>serine proteases are produced by <i>C. neoformans</i> (Xu <i>et al.</i>, 2014); utilised by <i>C. neoformans</i> and <i>C. gattii</i> (Min and Kwon-Chung, 1986)</p>

Table 4.2 (continued)

D-fructose	hexose monosaccharide sugar; *involved in fungal metabolism: β -D-fructose is involved in carbohydrate metabolism (di- and polysaccharides); D fructose in carbohydrates metabolism (glycolysis and gluconeogenesis (Hoffman-La Roche Ltd, 2014)	D-fructose utilised by <i>C. neoformans</i> (Onishi and Suzuki, 1968)
------------	---	---

Bibliography

- Abassi, M., Boulware, D. R. and Rhein, J. (2015) 'Cryptococcal Meningitis : Diagnosis and Management Update', *Curr Trop Med Rep*, 2(2), pp. 90–99.
- Adams, K. N., Takaki, K., Connolly, L. E., Wiedenhof, H., Winglee, K., Humbert, O., Edelstein, P. H. and Cosma, C. L. Ramakrishnan, L. (2011) 'Drug tolerance in replicating mycobacteria mediated by a macrophage-induced efflux mechanism', *Cell*, 145(1), pp. 39–53.
- Aderem, A. A., Wright, S. D., Silverstein, S. C. and Cohn, Z. A. (1985) 'Ligated complement receptors do not activate the arachidonic acid cascade in resident peritoneal macrophages', *J Exp Med*, 161(3), pp. 617–622.
- Aderem, A. and Underhill, D. M. (1999) 'Mechanism of phagocytosis in macrophages', *Annu Rev Immunol*, 17(1), pp. 593–623.
- Agner, K. (1958) 'Crystalline Myeloperoxidase', *Acta Chem Scandynavica*, 12, pp. 89–94.
- Agresti, A. and Bianchi, M. E. (2003) 'HMGB proteins and gene expression', *Curr Opin Genet Dev*, 13(2), pp. 170–178.
- Akhter, S., Mcdade, H. C., Gorch, J. M., Heinrich, G., Cox, G. M. and Perfect, J. R. (2003) 'Role of Alternative Oxidase Gene in Pathogenesis of *Cryptococcus neoformans*', *Infect Immun*, 71(10), pp. 5794–5802.
- Al-Homsi, A. S., Roy, T. S., Cole, K., Feng, Y. and Duffner, U. (2015) 'Post-transplant high-dose cyclophosphamide for the prevention of graft-versus-host disease', *Biol Blood Marrow Transplant*, 21(4), pp. 604–611.
- Alanio, A., Vernel-Pauillac, F. and Sturny-Leclère, A. (2015) 'Cryptococcus neoformans Host Adaptation: Toward Biological biological evidence of dormancy', *mBio*, 6(2), pp. e02580-14.
- Alfieri, C., Allison, A. C. and Kieff, E. (1994) 'Effect of mycophenolic acid on Epstein-Barr virus infection of human B lymphocytes', *Antimicrob Agents Chemother*, 38(1), pp. 126–129.
- Allen, L., Dockrell, D. H., Pattery, T., Lee, D. G., Cornelis, P., Hellewell, P. G. and Whyte, M. K. B. (2005) 'Pyocyanin production by *Pseudomonas aeruginosa* induces neutrophil apoptosis and impairs neutrophil-mediated host defenses in vivo', *J Immunol*, 174(6), pp. 3643–3649.
- Allen, S. P., Hall, B., Castelli, L. M., Francis, L., Woof, R., Siskos, A. P., Kouloura, E., Gray, E., Thompson, A. G., Talbot, K., Higginbottom, A., Myszczyńska, M., Allen, C. F., Stopford, M. J., Hemingway, J., Bauer, C. S., Webster, C. P., Vos, K. J. De, Turner, M. R., *et al.* (2019) 'Astrocyte adenosine deaminase loss increases motor neuron toxicity in amyotrophic lateral sclerosis', *Brain*, 142(3), pp. 586–605.
- Allison, A. C., Hovi, T., Watts, R. W. and Webster, A. D. (1977) 'The role of de novo purine synthesis in lymphocyte transformation', *Ciba Found Symp*, (48), pp. 207–24.
- Allison, A. C., Almquist, S. J., Muller, C. D. and Eugui, E. M. (1991) 'In vitro immunosuppressive effects of mycophenolic acid and an ester pro-drug, RS-

- 61443', *Transplant Proc*, 23(Suppl 2), pp. 10–14.
- Allison, A. C. (2005) 'Mechanisms of action of mycophenolate mofetil', *Lupus*, (14 Suppl 1), pp. s2–s8.
- Allison, A. C. and Eugui, E. M. (1993) 'The design and development of an immunosuppressive drug, mycophenolate mofetil', *Springer Semin Immunopathol*, 14, pp. 353–80.
- Allison, A. C. and Eugui, E. M. (1996) 'Purine metabolism and immunosuppressive effects of mycophenolate mofetil (MMF)', *Clin Transplant*, 10(1 Pt 2), pp. 77–84.
- Allison, A. C. and Eugui, E. M. (2000) 'Mycophenolate mofetil and its mechanisms of action', *Immunopharmacology*, 47(2–3), pp. 85–118.
- Allison, A. C. and Eugui, E. M. (2005) 'Mechanisms of action of mycophenolate mofetil in preventing acute and chronic allograft rejection', *Transplantation*, 80(2 Suppl), pp. S181–S190.
- Almeida, F. and Wolf, J. M. (2015) 'Virulence-Associated Enzymes of *Cryptococcus neoformans*', *Eukaryot Cell*, 14(12), pp. 1173–1185.
- Alspaugh, J. A., Pukkila-Worley, R., Harashima, T., Cavallo, L. M., Funnell, D., Cox, G. M., Perfect, J. R., Kronstad, J. W. and Heitman, J. (2002) 'Adenylyl cyclase functions downstream of the G α protein Gpa1 and controls mating and pathogenicity of *Cryptococcus neoformans*', *Eukaryot Cell*, 1(1), pp. 75–84.
- Altamirano, S., Fang, D., Simmons, C., Sridhar, S., Wu, P., Sanyal, K. and Kozubowski, L. (2017) 'Fluconazole-Induced Ploidy Change in *Cryptococcus neoformans* Results from the Uncoupling of Cell Growth and Nuclear Division', *mSphere*, 2(3), pp. e00205-17.
- Alvarez, M., Burns, T., Luo, Y., Pirofski, L. and Casadevall, A. (2009) 'The outcome of *Cryptococcus neoformans* intracellular pathogenesis in human monocytes', *BMC Microbiology*, 9(51).
- Alvarez, M. and Casadevall, A. (2006) 'Phagosome Extrusion and Host-Cell Survival after *Cryptococcus neoformans* Phagocytosis by Macrophages', *Curr Biol*, 16(21), pp. 2161–2165.
- Alvarez, M. and Casadevall, A. (2007) 'Cell-to-cell spread and massive vacuole formation after *Cryptococcus neoformans* infection of murine macrophages', *BMC Immunology*, 8(16).
- Alvarez, M., Saylor, C. and Casadevall, A. (2008) 'Antibody action after phagocytosis promotes *Cryptococcus neoformans* and *Cryptococcus gattii* macrophage exocytosis with biofilm-like microcolony formation', *Cell Microbiol*, 10(8), pp. 1622–1633.
- Ando, R., Hama, H., Yamamoto-Hino, M., Mizuno, H. and Miyawaki, A. (2002) 'An optical marker based on the UV-induced green-to-red photoconversion of a fluorescent protein', *Proc Natl Acad Sci USA*, 99(20), pp. 12651–12656.
- Andrikos, E., Yavuz, A., Bordoni, V., Ratanarat, R., De Cal, M., Bonello, M., Salvatori, G., Levin, N., Yakupoglu, G., Pappas, M. and Ronco, C. (2005) 'Effect of cyclosporine, mycophenolate mofetil, and their combination with steroids on apoptosis in a human cultured monocytic U937 cell line', *Transplant Proc*, 37(7), pp. 3226–3229.

- Angkasekwinai, P., Sringskarin, N., Supasorn, O., Fungkrajai, M., Wang, Y. H., Chayakulkeeree, M., Ngamskulrungrroj, P., Angkasekwinai, N. and Pattanapanyasat, K. (2014) 'Cryptococcus gattii infection dampens Th1 and Th17 responses by attenuating dendritic cell function and pulmonary chemokine expression in the immunocompetent hosts', *Infect Immun*, 82(9), pp. 3880–3890.
- Ank, N. and Paludan, S. R. (2009) 'Type III IFNs: New layers of complexity in innate antiviral immunity', *Biofactors*, 35(1), pp. 82–87.
- Ansari, A., Hassan, C., Duley, J., Marinaki, A., Shobowale-Bakre, E.-M., Seed, P., Meenan, J., Yim, A. and Sanderson, J. (2002) 'Thiopurine methyltransferase activity and the use of azathioprine in inflammatory bowel disease', *Aliment Pharmacol Ther*, 16(10), pp. 1743–50.
- Appel, G. B., Radhakrishnan, J. and Ginzler, E. M. (2005) 'Use of mycophenolate mofetil in autoimmune and renal diseases', *Transplantation*, 80(Suppl 2), pp. s265–s271.
- Araujo, G. de S., Fonseca, F. L., Pontes, B., Torres, A., Cordero, R. J. B., Zancopé-Oliveira, R. M., Casadevall, A., Viana, N. B., Nimrichter, L., Rodrigues, Marcio, L., Garcia, E. S., de Souza, W. and Frases, S. (2012) 'Capsules from pathogenic and non-pathogenic *Cryptococcus* spp. manifest significant differences in structure and ability to protect against phagocytic cells', *PLoS One*, 7(1), p. e29561.
- Arndt, P. G., Young, S. K., Lieber, J. G., Fessler, M. B., Nick, J. A. and Worthen, G. S. (2005) 'Inhibition of c-Jun N-terminal kinase limits lipopolysaccharide-induced pulmonary neutrophil influx', *Am J Resp Crit Care Med*, 171(9), pp. 978–986.
- Arora, S., Olszewski, M. A., Tsang, T. M., McDonald, R. A., Toews, G. B. and Huffnagle, G. B. (2011) 'Effect of cytokine interplay on macrophage polarization during chronic pulmonary infection with *Cryptococcus neoformans*', *Infect Immun*, 79(5), pp. 1915–1926.
- Auffray, C., Fogg, D., Garfa, M., Elain, G., Join-Lambert, O., Kayal, S., Sarnacki, S., Cumanó, A., Lauvau, G., Geissmann, F. and The (2007) 'Monitoring of blood vessels and tissues by a population of monocytes with patrolling behavior', *Science*, 317(5838), pp. 666–670.
- Avdi, N. J., Nick, J. A., Whitlock, B. B., Billstrom, M. A., Henson, P. M., Johnson, G. L. and Worthen, G. S. (2001) 'Tumor Necrosis Factor- α Activation of the c-Jun N-terminal Kinase Pathway in Human Neutrophils', *J Biol Chem*, 276(3), pp. 2189–2199.
- Babior, B. M. (2004) 'NADPH oxidase', *Curr Opin Immunol*, 16(1), pp. 42–47.
- Bacon, B. E. and Cherniak, R. (1995) 'Structure of the O-acetylated glucuronoxylomannan from *Cryptococcus neoformans* serotype C, as determined by 2D NMR spectroscopy', *Carbohydr Res*, 276(2), pp. 365–386.
- Baddley, J. W., Schain, D. C., Gupte, A. A., Lodhi, S. A., Kayler, L. K., Frade, J. P., Lockhart, S. R., Chiller, T., Bynon, J. S. and Bower, W. A. (2011) 'Transmission of *Cryptococcus neoformans* by organ transplantation', *Clin Infect Dis*, 52(4), pp. 94–98.
- Baddley, J. W. and Forrest, G. N. (2013) 'Cryptococcosis in solid organ

- transplantation', *Am J Transplant*, 13, pp. 242–249.
- Bahn, Y.-S., Kojima, K., Cox, G. M. and Heitman, J. (2005) 'Specialization of the HOG Pathway and Its Impact on Differentiation and Virulence of *Cryptococcus neoformans*', *Mol Biol Cell*, 16(5), pp. 5318–5328.
- Bain, C. C., Bravo-blas, A., Scott, C. L. and Perdiguero, E. G. (2014) 'Constant replenishment from circulating monocytes maintains the macrophage pool in adult intestine', *Nat Immunol*, 15(10), pp. 929–937.
- Balamayooran, G., Batra, S., Balamayooran, T., Cai, S. and Jeyaseelan, S. (2011) 'Monocyte Chemoattractant Protein 1 Regulates Pulmonary Host Defense via Neutrophil Recruitment during *Escherichia coli* Infection', *Infect Immun* 79(7), pp. 2567–2577.
- Banchereau, J. and Steinman, R. M. (1998) 'Dendritic cells and the control of immunity', *Nature*, 392(6673), pp. 245–252.
- Banerjee, R., Halil, O., Bain, B. J., Cummins, D. and Banner, N. R. (2000) 'Neutrophil dysplasia caused by mycophenolate mofetil', *Transplantation*, 70(11), pp. 1608–1610.
- Banjara, M. and Ghosh, C. (2017) 'Sterile Neuroinflammation and Strategies for Therapeutic Intervention', *Int J Inflamm*, 2017(8385961).
- Barelle, C. J., Priest, C. L., Maccallum, D. M., Gow, N. A. R., Odds, F. C. and Brown, A. J. P. (2006) 'Niche-specific regulation of central metabolic pathways in a fungal pathogen', *Cell Microbiol*, 8(6), pp. 961–971.
- Barton, G. M. (2008) 'A calculated response: control of inflammation by the innate immune system', *J Clin Invest*, 118(2), pp. 413–420.
- Batt, C. A., Caryallo, S., Easson, D. D., Akedo, M. and Sinskey, A. J. (1986) 'Direct evidence for a xylose metabolic pathway in *Saccharomyces cerevisiae*', *Biotechnol Bioeng*, 28(4), pp. 549–553.
- Bauman, S. K., Nichols, K. L. and Murphy, J. W. (2000) 'Dendritic cells in the induction of protective and nonprotective anticryptococcal cell-mediated immune responses', *J Immunol*, 165(1), pp. 158–167.
- Beardsley, J., Sorrell, T. C. and Chen, S. C. A. (2019) 'Central nervous system cryptococcal infections in non-HIV infected patients', *J Fungi (Basel)*, 5(3), p. 71.
- Beckman, J. S., Beckman, T. W., Chen, J., Marshall, P. A. and Freeman, B. A. (1990) 'Apparent hydroxyl radical production by peroxynitrite: Implications for endothelial injury from nitric oxide and superoxide', *Proc Natl Acad Sci U S A*, 87(4), pp. 1620–1624.
- Beduschi, M. G., Guimarães, C. L., Buss, Z. S. and Dalmarco, E. M. (2013) 'Mycophenolate mofetil has potent anti-inflammatory actions in a mouse model of acute lung injury', *Inflammation*, 36(3), pp. 729–737.
- Belaouaj, A., McCarthy, R., Baumann, M., Gao, Z., Ley, T. J., Abraham, S. N. and Shapiro, S. D. (1998) 'Mice lacking neutrophil elastase reveal impaired host defense against gram negative bacterial sepsis', *Nat Med*, 4(5), pp. 615–618.
- Bellingan, G. J., Caldwell, H., Howie, S. E., Dransfield, I. and Haslett, C. (1996) 'In vivo fate of the inflammatory macrophage during the resolution of inflammation:

inflammatory macrophages do not die locally, but emigrate to the draining lymph nodes', *J Immunol*, 157(6), pp. 2577–2585.

- Bemis, D. A., Krahwinkel, D. J., Bowman, L. A., Mondon, P. and Kwon-Chung, K. J. (2000) 'Temperature-sensitive strain of *Cryptococcus neoformans* producing hyphal elements in a feline nasal granuloma', *J Clin Microbiol*, 38(2), pp. 926–928.
- Bengtsson, T., Dahlgren, C., Stendahl, O. and Andersson, T. (1991) 'Actin assembly and regulation of neutrophil function: effects of cytochalasin B and tetracaine on chemotactic peptide-induced O₂- production and degranulation', *J Leukoc Biol*, 49(3), pp. 236–244.
- Benham, R. W. (1956) 'The genus *Cryptococcus*', *Bacteriol Rev*, 20(3), pp. 189–201.
- Bennett, C. M., Kanki, J. P., Rhodes, J., Liu, T. X., Paw, B. H., Kieran, M. W., Langenau, D. M., Delahaye-brown, A., Zon, L. I., Fleming, M. D. and Look, A. T. (2001) 'Myelopoiesis in the zebrafish, *Danio rerio*', *Blood*, 98(3), pp. 643–651.
- Bennett, J. E., Dismukes, W. E., Duma, R. J., Medoff, G., Sande, M. A., Gallis, H., Leonard, J., Fields, B. T., Bradshaw, M., Haywood, H., McGee, Z., Cate, T. R., Cobbs, C. G., Warner, J. F. and Alling, D. W. (1979) 'A comparison of amphotericin B alone and combined with flucytosine in the treatment of cryptococcal meningitis', *N Engl J Med.*, 301(3), pp. 126–31.
- Bennett, J. E., Theodore, T. S. and Biochemical, T. S. T. (1978) 'Biochemical differences between serotypes of *Cryptococcus neoformans*', *Sabouraudia*, 16(3), pp. 167–174.
- Benoist, C. and Mathis, D. (2002) 'Mast cells in autoimmune disease', *Nature*, 420(6917), pp. 875–878.
- Berenbaum, M. C. (1971) 'Is azathioprine a better immunosuppressive than 6-mercaptopurine?', *Clin Exp Immunol*, 8(1), pp. 1–8.
- Bergsbaken, T., Fink, S. L. and Cookson, B. T. (2009) 'Pyroptosis: host cell death', *Nat Rev Microbiol*, 7(2), pp. 99–109.
- Berliner, N. (2008) 'Lessons from congenital neutropenia: 50 years of progress in understanding myelopoiesis', *Blood*, 111(12), pp. 5427–5433.
- Bernhard, W., Hoffmann, S., Dombrowsky, H., Rau, G. A., Kamlage, A., Kappler, M., Haitsma, J. J., Freihorst, J., Von der Hardt, H. and Poets, C. F. (2001) 'Phosphatidylcholine molecular species in lung surfactant composition in relation to respiratory rate and lung development', *Am J Respir Cell Mol Biol*, 25(6), pp. 725–731.
- Beutler, B. (2004) 'Innate immunity: An overview', *Mol Immunol*, 40(12), pp. 845–859.
- Bhattacharjee, A. K., Kwon-Chung, K. J. and Glaudemans, C. P. J. (1978) 'On the structure of the capsular polysaccharide from *Cryptococcus neoformans* serotype C', *Immunochemistry*, 15(9), pp. 673–679.
- Bhattacharjee, A. K., Kwon-Chung, K. J. and Glaudemans, C. P. J. (1979a) 'On the structure of the capsular polysaccharide from *Cryptococcus Neoformans* serotype C-II', *Mol Immunol*, 16(7), pp. 531–532.
- Bhattacharjee, A. K., Kwon-Chung, K. J. and Glaudemans, C. P. J. (1979b) 'The structure of the capsular polysaccharide from *Cryptococcus neoformans*

- serotype D', *Carbohydr Res*, 73, pp. 183–192.
- Bhattacharjee, A. K., Kwon-Chung, K. J. and Glaudemans, C. P. J. (1980) 'Structural studies on the major, capsular polysaccharide from *Cryptococcus bacillisporus* serotype B', *Carbohydr Res*, 82(1), pp. 103–111.
- Bhattacharjee, A. K., Kwon-Chung, K. J. and Glaudemans, C. P. J. (1981) 'Capsular polysaccharides from a parent strain and from a possible, mutant strain of *Cryptococcus neoformans* serotype A', *Carbohydr Res*, 95(2), pp. 237–247.
- Bianchi, M. E. (2007) 'DAMPs, PAMPs and alarmins: all we need to know about danger', *J Leukoc Biol*, 81(1), pp. 1–5.
- Bicanic, T., Brouwer, A. E., Meintjes, G., Rebe, K., Limmathurotsakur, D., Chierakul, W., Teparrakkul, P., Loyse, A., White, N. J., Wood, R., Jaffar, S. and Harrison, T. (2009) 'Relationship of cerebrospinal fluid pressure, fungal burden and outcome in patients with cryptococcal meningitis undergoing serial lumbar punctures', *AIDS*, 23(6), pp. 701–706.
- Bielska, E., Sisquella, M. A., Aldeieg, M., Birch, C., Donoghue, E. J. O. and May, R. C. (2018) 'Pathogen-derived extracellular vesicles mediate virulence in the fatal human pathogen *Cryptococcus gattii*', *Nat Commun*, 9(1556), pp. 1–9.
- Birben, E., Sahiner, U. M., Sackesen, C., Erzurum, S. and Kalayci, O. (2012) 'Oxidative stress and antioxidant defense', *World Allergy Organ J*, 5(1), pp. 9–19.
- Blacker, T. B. and Duchon, M. R. (2016) 'Investigating mitochondrial redox state using NADH and NADPH autofluorescence', *Free Radic Biol Med*, 100, pp. 53–65.
- Blaheta, R. A., Leckel, K., Wittig, B., Zenker, D., Oppermann, E., Harder, S., Scholz, M., Weber, S., Schuldes, H., Encke, A. and Markus, B. H. (1998) 'Inhibition of endothelial receptor expression and of T-cell ligand activity by mycophenolate mofetil', *Transpl Immunol*, 6(4), pp. 251–259.
- Blankenship, J. R. and Mitchell, A. P. (2006) 'How to build a biofilm: a fungal perspective', *Curr Opin Microbiol*, 9(6), pp. 588–594.
- Bliven, K. A. and Aurelli, A. T. (2012) 'Antivirulence genes: Insights into pathogen evolution through gene loss', *Infect Immun*, 80(12), pp. 4061–4070.
- Bochner, B. R. (2003) 'New technologies to assess genotype–phenotype relationships', *Nat Rev Genet*, 4, pp. 309–314.
- Bochner, B. R., Siri, M., Huang, R. H., Noble, S., Lei, X. H., Clemons, P. A. and Wagner, B. K. (2011) 'Assay of the multiple energy-producing pathways of mammalian cells', *PLoS One*, 6(3), pp. 1–8.
- Bochner, B. R., Gadzinski, P. and Panomitros, E. (2001) 'Phenotype Microarrays for high-throughput phenotypic testing and assay of gene function', *Genome Res*, 11(7), pp. 1246–1255.
- Boeltz, S., Amini, P., Anders, H. J., Andrade, F., Bilyy, R., Chatfield, S., Cichon, I., Clancy, D. M., Desai, J., Dumych, T., Dwivedi, N., Gordon, R. A., Hahn, J., Hidalgo, A., Hoffmann, M. H., Kaplan, M. J., Knight, J. S., Kolaczowska, E., Kubes, P., *et al.* (2019) 'To NET or not to NET: current opinions and state of the science regarding the formation of neutrophil extracellular traps', *Cell Death Differ*, 26(3), pp. 395–408.

- Bojarczuk, A., Miller, K. A., Hotham, R., Lewis, A., Ogryzko, N. V., Kamuyango, A. A., Frost, H., Gibson, R. H., Stillman, E., May, R. C., Renshaw, S. A. and Johnston, S. A. (2016) 'Cryptococcus neoformans Intracellular Proliferation and Capsule Size Determines Early Macrophage Control of Infection', *Sci Rep* 6(21489).
- Bojarczuk, A. and Johnston, S. A. (2017) 'Mycophenolate Mofetil Increases Inflammation Resolution In Zebrafish Via Neutrophil Apoptosis', *bioRxiv*.
- Bolaños, B. and Mitchell, T. G. (1989) 'Phagocytosis and Killing of Cryptococcus neoformans by Rat Alveolar Macrophages in the Absence of Serum', *J Leukoc Biol*, 46(6), pp. 521–528.
- Bolwell, B., Sobecks, R., Pohlman, B., Andresen, S., Rybicki, L., Kuczkowski, E. and Kalaycio, M. (2004) 'A prospective randomized trial comparing cyclosporine and short course methotrexate with cyclosporine and mycophenolate mofetil for GVHD prophylaxis in myeloablative allogeneic bone marrow transplantation', *Bone Marrow Transplant*, 34(7), pp. 621–625
- Bonilla, F. A. and Oettgen, H. C. (2010) 'Adaptive immunity', *J Allergy Clin Immunol*, 125(2 Suppl 2), pp. S33–S40.
- Borregaard, N. (2010) 'Neutrophils, from Marrow to Microbes', *Immunity*, 33(5), pp. 657–670.
- Bos, A., Wever, R. and Roos, D. (1978) 'Characterization and quantification of the peroxidase in human monocytes', *Biochim Biophys Acta*, 525(1), pp. 37–44.
- Bose, I., Reese, A. J., Ory, J. J., Doering, T. L. and Janbon, G. (2003) 'A Yeast under Cover : the Capsule of Cryptococcus neoformans', *Eukaryot Cell*, 2(4), pp. 655–663.
- Botts, M. R., Huang, M., Borchardt, R. K., Hull, C. M. and Hull, C. M. (2014) 'Developmental cell fate and virulence are linked to trehalose homeostasis in Cryptococcus neoformans', *Eukaryot Cell*, 13(9), pp. 1158–1168.
- Bouklas, T., Diago-Navarro, E., Wang, X., Fenster, M. and Fries, B. C. (2015) 'Characterization of the virulence of Cryptococcus neoformans strains in an insect model', *Virulence*, 6(8), pp. 809–813.
- Boulware, D. R., Rolfes, M. A., Rajasingham, R., von Hohenberg, M., Qin, Z., Taseera, K., Schutz, C., Kwizera, R., Butler, E. K., Meintjes, G., Muzoora, C., Bischof, J. C. and Meya, D. B. (2014) 'Multisite validation of cryptococcal antigen lateral flow assay and quantification by laser thermal contrast', *Emerg Infect Dis*, 20(1), pp. 45–53.
- Bovers, M., Hagen, F., Kuramae, E. E. and Boekhout, T. (2008) 'Six monophyletic lineages identified within Cryptococcus neoformans and Cryptococcus gattii by multi-locus sequence typing', *Fungal Genet Biol*, 45(4), pp. 400–421.
- Bowman, T. V. and Zon, L. I. (2010) 'Swimming into the Future of Drug Discovery: In Vivo Chemical Screens in Zebrafish', *Nat Rev Drug Discov*, 5(2), pp. 159–161.
- Bowne, W. B., Michl, J., Bluth, M. H., Zenilman, M. E. and Pincus, M. R. (2009) 'Enzymology of Purine and Pyrimidine Antimetabolites Used in the Treatment of Cancer', *Chem Rev*, 109(7), pp. 2880–2893.
- Bradford, K. and Shih, D. Q. (2011) 'Optimizing 6-mercaptopurine and azathioprine therapy in the management of inflammatory bowel disease', *World J*

- Gastroenterol*, 17(37), pp. 4166–4173.
- Brand, M. D. (2010) 'The sites and topology of mitochondrial superoxide production', *Exp Gerontol*, 45(7–8), pp. 466–472.
- Brandt, M. E., Pfaller, M. A., Hajjeh, R. A., Graviss, E. A., Rees, J., Spitzer, E. D., Pinner, R. W. and Mayer, L. W. (1996) 'Molecular subtypes and antifungal susceptibilities of serial *Cryptococcus neoformans* isolates in human immunodeficiency virus-associated Cryptococcosis', *J Infect Dis*, 174(4), pp. 812–820.
- Bratton, D. L. and Henson, P. M. (2011) 'Neutrophil clearance: When the party is over, clean-up begins', *Trends Immunol*, 32(8), pp. 350–357.
- Braun, J. S., Novak, R., Herzog, K.-H., Bodner, S. M., Cleveland, J. L. and Tuomanen, E. I. (1999) 'Neuroprotection by a caspase inhibitor in acute bacterial meningitis', *Nat Med*, 5(3), pp. 298–302.
- Bray, D. H., Squire, S. B., Bagdades, E., Mulvenna, P. M., Johnson, M. A. and Poulter, L. W. (1992) 'Alveolar macrophage populations are distorted in immunocompromised patients with pneumonitis', *Eur Respir J*, 5(5), pp. 545–552.
- Brett, J., Schmidt, A. M., Yan, S. D., Zou, Y. S., Weidman, E., Pinsky, D., Nowygrod, R., Nepper, M., Przysiecki, C. and Shaw, A. (1993) 'Survey of the distribution of a newly characterized receptor for advanced glycation end products in tissues', *Am J Pathol*, 143(6), pp. 1699–1712.
- Brinkmann, V., Reichard, U., Goosmann, C., Fauler, B., Uhlemann, Y., Weiss, D. S., Weinrauch, Y. and Zychlinsky, A. (2004) 'Neutrophil extracellular traps kill bacteria', *Science*, 303(5663), pp. 1532–1535.
- Brittain, H. G. (2001) 'Malic acid', in Brittain, H. G. (ed.) *Analytical Profiles of Drug Substances and Excipients*. 1st edn. New York: Elsevier, pp. 153–195.
- Brizendine, K. D. and Pappas, P. G. (2010) 'Cryptococcal meningitis: Current approaches to management in patients with and without AIDS', *Curr Infect Dis Rep*, 12(4), pp. 299–305.
- Brothers, K. M., Gratacap, R. L., Barker, S. E., Newman, Z. R., Norum, A. and Wheeler, R. T. (2013) 'NADPH Oxidase-Driven Phagocyte Recruitment Controls *Candida albicans* Filamentous Growth and Prevents Mortality', *PLoS Pathog*, 9(10), p. e1003634.
- Brouckaert, G., Kalai, M., Krysko, D. V., Saelens, X., Vercammen, D., Ndlovu, 'Matladi, Haegeman, G., D'Herde, K. and Vandenabeele, P. (2004) 'Phagocytosis of Necrotic Cells by Macrophages Is Phosphatidylserine Dependent and Does Not Induce Inflammatory Cytokine Production', *Mol Biol Cell*, 15(3), pp. 3751–3737.
- Brown, A. J., Haynes, K. and Quinn, J. (2009) 'Nitrosative and oxidative stress responses in fungal pathogenicity', *Curr Opin Microbiol*, 12(4), pp. 384–391.
- Brown, K. E., Brunt, E. M. and Heinecke, J. W. (2001) 'Immunohistochemical detection of myeloperoxidase and its oxidation products in Kupffer cells of human liver', *Am J Pathol*. American Society for Investigative Pathology, 159(6), pp. 2081–2088.
- Brown, S. M., Campbell, L. T. and Lodge, J. K. (2007) '*Cryptococcus neoformans*, a

- fungus under stress', *Curr Opin Microbiol*, 10(4), pp. 320–325.
- Brueske, C. H. (1986) 'Proteolytic activity of a clinical isolate of *Cryptococcus neoformans*', *J Clin Microbiol*, 23(3), pp. 631–633.
- Bruner, K. T., Franco-Paredes, C., Henao-Martínez, A. F., Steele, G. M. and Chastain, D. B. (2018) 'Cryptococcus gattii Complex Infections in HIV-Infected Patients, Southeastern United States', *Emerg Infect Dis*, 24(11), pp. 1998–2002.
- Bryant, J. A., Sellars, L. E., Busby, S. J. W. and Lee, D. J. (2014) 'Chromosome position effects on gene expression in *Escherichia coli* K-12', *Nucleic Acids Res*, 42(18), pp. 11383–11392.
- Buchanan, K. L. and Doyle, H. A. (2000) 'Requirement for CD4+ T lymphocytes in host resistance against *Cryptococcus neoformans* in the central nervous system of immunized mice', *Infect Immun*, 68, pp. 456–462.
- Buckley, C. D., Ross, E. A., McGettrick, H. M., Osborne, C. E., Haworth, O., Schmutz, C., Stone, P. C. W., Salmon, M., Matharu, N. M., Vohra, R. K., Nash, G. B. and Rainger, G. E. (2006) 'Identification of a phenotypically and functionally distinct population of long-lived neutrophils in a model of reverse endothelial migration', *J Leukoc Biol*, 79(2), pp. 303–311.
- Budde, K., Curtis, J., Knoll, G., Chan, L., Neumayer, H. H., Seifue, Y. and Hall, M. (2004) 'Enteric-coated mycophenolate sodium can be safely administered in maintenance renal transplant patients: results of a 1-year study', *Am J Transplant*, 4(2), pp. 237–243.
- Bullingham, R. E., Nicholls, A. and Hale, M. (1996) 'Pharmacokinetics of mycophenolate mofetil (RS61443): a short review', *Transplant Proc*, 28(2), pp. 925–929.
- Bullingham, R. E. S., Nicholls, A. J. and Kamm, B. R. (1998) 'Clinical Pharmacokinetics of Mycophenolate Mofetil', *Clin Pharmacokinet*, 34(6), pp. 429–455.
- Burgon, J. and Renshaw, S. A. (2013) 'Serum and Glucocorticoid Regulated Kinase 1 (SGK1) Regulates Neutrophil Clearance During Inflammation Resolution', *J Immunol*, 192(4), pp. 1796–1805.
- Busse, O. (1894) 'Über parasitäre Einschlüsse und ihre Züchtung', *Zentralblatt Bakteriologie*, 16, pp. 175–180.
- Bustamante-Marin, X. M. and Ostrowski, L. E. (2018) 'Cilia and Mucociliary Clearance', *Cold Spring Harb Perspect Biol*, 9(4), p. a028241.
- Butler, M. J. and Day, A. W. (1998) 'Fungal melanins: a review', *Can J Microbiol*, 44(12), pp. 1115–1136.
- Butterfield, T. A., Best, T. M. and Merrick, M. A. (2006) 'The dual roles of neutrophils and macrophages in inflammation: a critical balance between tissue damage and repair', *J Athl Train*, 41(4), pp. 457–465.
- Byrnes, E. J., Li, W., Lewit, Y., Ma, H., Voelz, K., Ren, P., Carter, D. A., Chaturvedi, V., Bildfell, R. J., May, R. C. and Heitman, J. (2010) 'Emergence and Pathogenicity of Highly Virulent *Cryptococcus gattii* Genotypes in the Northwest United States', *PLoS Pathog*, 6(4), p. e1000850.

- Byrnes, E. J. (2011) 'The Outbreak of *Cryptococcus gattii* in Western North America: Epidemiology and Clinical Issues', *Curr Infect Dis Rep*, 13(3), pp. 256–261.
- Cafarchia, C., Romito, D., Iatta, R., Camarda, A., Montagna, M. T. and Otranto, D. (2006) 'Role of birds of prey as carriers and spreaders of *Cryptococcus neoformans* and other zoonotic yeasts', *Med Mycol*, 44(6), pp. 485–492.
- Caicedo, L. D., Alvarez, M. I., Delgado, M. and Cárdenas, A. (1999) 'Cryptococcus neoformans in bird excreta in the city zoo of Cali, Colombia', *Mycopathologia*, 147(3), pp. 121–124.
- Callewaert, L. and Michiels, C. W. (2010) 'Lysozymes in the animal kingdom', *J Biosci*, 35(1), pp. 127–160.
- Camargo, J. F., Simkins, J., Schain, D. C., Gonzalez, A. A., Alcaide, M. L., Anjan, S., Guerra, G., Roth, D., Kupin, W. L., Mattiazzi, A., Tan, Y., Milikowski, C., Morris, M. I. and Abbo, L. M. (2018) 'A cluster of donor-derived *Cryptococcus neoformans* infection affecting lung, liver, and kidney transplant recipients: Case report and review of literature', *Transpl Infect Dis*, 20(2), p. e12836.
- Campbell, J. J., Qin, S., Bacon, K. B., Mackay, C. R. and Butcher, E. C. (1996) 'Biology of chemokine and classical chemoattractant receptors: Differential requirements for adhesion-triggering versus chemotactic responses in lymphoid cells', *J Cell Biol*, 134(1), pp. 255–266.
- Campuzano, A. and Wormley, F. (2018) 'Innate Immunity against *Cryptococcus*, from Recognition to Elimination', *J Fungi (Basel)*, 4(1), p. 33.
- Capilla, J., Clemons, K. V. and Stevens, D. A. (2007) 'Animal models: An important tool in mycology', *Med Mycol*, 45(8), pp. 657–684.
- Cara, C. J., Pena, A. S., Sans, M., Rodrigo, L., Guerrero-Esteo, M., Hinojosa, J., García-Paredes, J. and Guijarro, L. G. (2004) 'Reviewing the mechanism of action of thiopurine drugs: towards a new paradigm in clinical practice', *Med Sci Monit*, 10(11), pp. RA247-254.
- Carreras, M. C., Pargament, G. A., Catz, S. D., Poderoso, J. J. and Boveris, A. (1994) 'Kinetics of nitric oxide and hydrogen peroxide production and formation of peroxynitrite during the respiratory burst of human neutrophils', *FEBS Lett*, 341(1), pp. 65–68.
- Cartwright, G. E., Athens, J. W. and Wintrobe, M. M. (1964) 'The kinetics of granulopoiesis in normal man', *Blood*, 24, pp. 780–803.
- Carvalho, R., de Sonnevile, J., Stockhammer, O. W., Savage, N. D. L., Veneman, W. J., Ottenhoff, T. H. M., Dirks, R. P., Meijer, A. H. and Spaink, H. P. (2011) 'A high-throughput screen for tuberculosis progression', *PLoS One*, 6(2), p. e16779.
- Casadevall, A., Coelho, C., Cordero, R. J. B., Dragotakes, Q., Jung, E., Vij, R. and Wear, M. P. (2019) 'The capsule of *Cryptococcus neoformans*', *Virulence*, 10(1), pp. 822–831.
- Casadevall, A., Coelho, C. and Alanio, A. (2018) 'Mechanisms of *Cryptococcus neoformans*-mediated host damage', *Front Immunol*, 9(APR), pp. 1–8.
- Casadevall, A. and Pirofski, L. A. (2007) 'Accidental virulence, cryptic pathogenesis, martians, lost hosts, and the pathogenicity of environmental microbes', *Eukaryot*

Cell, 6(12), pp. 2169–2174.

- Casadevall, A., Steenbergen, J. N. and Nosanchuk, J. D. (2003) “Ready made” virulence and “dual use” virulence factors in pathogenic environmental fungi - The *Cryptococcus neoformans* paradigm’, *Curr Opin Microbiol*, 6(4), pp. 332–337.
- Cecchi, I., Arias de la Rosa, I., Menegatti, E., Roccatello, D., Collantes-Estevez, E., Lopez-Pedreira, C. and Barbarroja, N. (2018) ‘Neutrophils: Novel key players in Rheumatoid Arthritis. Current and future therapeutic targets’, *Autoimmun Rev*, 17(11), pp. 1138–1149.
- Chan, L. C., Erdmann, H., Gruber, A., Matas, J. and Canafax, M. (1990) ‘Azathioprine Metabolism: Pharmacokinetics Acid and 6-Thioguanine Nucleotides in Renal Transplant Patients’, *J Clin Pharmacol*, 30(4), pp. 358–363.
- Chang, A. C. Y. and Cohen, Stanley, N. (1978) ‘Construction and characterization of amplifiable multicopy DNA cloning vehicles derived from the P15A cryptic miniplasmid’, *J Bacteriol*, 134(3), pp. 1141–1156.
- Chang, A. L. and Doering, T. L. (2018) ‘Maintenance of mitochondrial morphology in *Cryptococcus neoformans* is critical for stress resistance and virulence’, *mBio*, 9(6), pp. e01375-18.
- Chang, M. R., Paniago, A. M. M., Silva, M. M., Lazera, M. S. and Wanke, B. (2007) ‘Prostatic cryptococcosis- a case report’, *J Venom Anim Toxins Incl Trop Dis*, 14, pp. 378–385.
- Chang, Y. C., Wickes, B. L., Miller, G. F., Penoyer, L. A. and Kwon-Chung, K. J. (2000) ‘*Cryptococcus neoformans* STE12 α regulates virulence but is not essential for mating’, *J Exp Med*, 191(5), pp. 871–881.
- Chang, Y. C., Stins, M. F., McCaffery, M. J., Miller, G. F., Pare, D. R., Dam, T., Paul-Satyaseela, M., Kim, K. S., Kwon-Chung, K. J. and Paul-Satyasee, M. (2004) ‘Cryptococcal yeast cells invade the central nervous system via transcellular penetration of the blood-brain barrier’, *Infect Immun*, 72(9), pp. 4985–4995.
- Chang, Y. C., Bien, C. M., Lee, H., Espenshade, P. J. and Kwon-Chung, K. J. (2007) ‘Sre1p, a regulator of oxygen sensing and sterol homeostasis, is required for virulence in *Cryptococcus neoformans*’, *Mol Microbiol*, 64(3), pp. 614–629.
- Chang, Y. C., Lamichhane, A. K., Bradley, J., Rodgers, L., Ngamskulrungrroj, P. and Kwon-Chung, K. J. (2015) ‘Differences between *Cryptococcus neoformans* and *Cryptococcus gattii* in the molecular mechanisms governing utilization of D-amino acids as the sole nitrogen source’, *PLoS One*, 10(7), pp. 1–20.
- Chang, Y. C. and Kwon-Chung, K. J. (1994) ‘Complementation of a Capsule-Deficient Mutation of *Cryptococcus neoformans* Restores Its Virulence’, *Mol Cell Biol*, 14(7), pp. 4912–4919.
- Chang, Y. C. and Kwon-Chung, K. J. (1998) ‘Isolation of the third capsule-associated gene, CAP60, required for virulence in *Cryptococcus neoformans*’, *Infect Immun*, 66(5), pp. 2230–2236.
- Chang, Y. C. and Kwon-Chung, K. J. (1999) ‘Isolation, characterization, and localization of a capsule-associated gene, CAP10, of *Cryptococcus neoformans*’, *J Bacteriol*, 181(18), pp. 5636–5643.

- Chang, Y. C., Penoyer, L. A. and Kwon-Chung, K. J. (1996) 'The Second Capsule Gene of *Cryptococcus neoformans*, CAP64, Is essential for Virulence', *Infect Immun*, 64(6), pp. 1977–1983.
- Chaplin, D. D. (2010) 'Overview of immune response', *J Allergy Clin Immunol*, 125, pp. S3–S23.
- Chapman-Smith, J. S. (1977) 'Cryptococcal chorioretinitis: a case report', *Br J Ophthalmol*, 61(6), pp. 411–413.
- Chapuis, F., Rosenzweig, M., Yagello, M., Ekman, M., Biberfeld, P. and Gluckman, J. C. (1997) 'Differentiation of human dendritic cells from monocytes in vitro', *Eur J Immunol*, 27(2), pp. 431–41.
- Charlier, C., Nielsen, K., Daou, S., Brigitte, M., Chretien, F. and Dromer, F. (2009) 'Evidence of a role for monocytes in dissemination and brain invasion by *Cryptococcus neoformans*', *Infect Immun*, 77(1), pp. 120–127.
- Chaskes, S., Frases, S., Cammer, M., Gerfen, G. and Casadevall, A. (2008) 'Growth and pigment production on D-tryptophan medium by *Cryptococcus gattii*, *Cryptococcus neoformans*, and *Candida albicans*', *J Clin Microbiol*, 46(1), pp. 255–264.
- Chaskes, S. and Tyndall, R. L. (1975) 'Pigment production by *Cryptococcus neoformans* from para and ortho diphenols: effect of the nitrogen source', *J Clin Microbiol*, 1(6), pp. 509–514.
- Chatterjee, B. E., Yona, S., Rosignoli, G., Young, R. E., Nourshargh, S., Flower, R. J. and Perretti, M. (2005) 'Annexin 1-deficient neutrophils exhibit enhanced transmigration in vivo and increased responsiveness in vitro', *J Leukoc Biol*, 78(3), pp. 639–646.
- Chaturvedi, V., Wong, B. and Newman, S. L. (1996) 'Oxidative killing of *Cryptococcus neoformans* by human neutrophils. Evidence that fungal mannitol protects by scavenging reactive oxygen intermediates', *J Immunol*, 156(10), pp. 3836–3840.
- Chau, T. T., Mai, N. H., Phu, N. H., Nghia, H. D., Chuong, L. V., Sinh, D. X., Duong, V. A., Diep, P. T., Campbell, J. I., Baker, S., Hien, T. T., Laloo, D. G., Farrar, J. J. and Day, J. N. (2010) 'A prospective descriptive study of cryptococcal meningitis in HIV uninfected patients in Vietnam - high prevalence of *Cryptococcus neoformans* var *grubii* in the absence of underlying disease', *BMC Infect Dis*, 10(199).
- Chaudhari, S. N. and Kipreos, E. T. (2017) 'Increased mitochondrial fusion allows the survival of older animals in diverse *C. Elegans* longevity pathways', *Nat Commun*, 8(1), p.182.
- Chen, G.-H., Teitz-Tennenbaum, S., Neal, L. M., Murdock, B. J., Malachowski, A. N., Dils, A. J., Olszewski, M. A. and Osterholzer, J. J. (2016) 'Local GM-CSF-dependent differentiation and activation of pulmonary dendritic cells and macrophages protect against progressive cryptococcal lung infection in mice', *J Immunol*, 196(4), pp. 1810–1821.
- Chen, G. H., Olszewski, M. A., McDonald, R. A., Wells, J. C., Paine, R., Huffnagle, G. B. and Toews, G. B. (2007) 'Role of granulocyte macrophage colony-stimulating factor in host defense against pulmonary *Cryptococcus neoformans* infection

- during murine allergic bronchopulmonary mycosis', *Am J Pathol*, 170(3), pp. 1028–1040.
- Chen, G. H., McNamara, D. A., Hernandez, Y., Huffnagle, G. B., Toews, G. B. and Olszewski, M. A. (2008) 'Inheritance of immune polarization patterns is linked to resistance versus susceptibility to *Cryptococcus neoformans* in a mouse model', *Infect Immun*, 76(6), pp. 2379–2391.
- Chen, G. Y. and Nuñez, G. (2010) 'Sterile inflammation : sensing and reacting to damage', *Nat Rev Immunol*, 10(12), pp. 826–837.
- Chen, L., Deng, H., Cui, H., Fang, J., Zuo, Z., Deng, J., Li, Y., Wang, X. and Zhao, L. (2018) 'Inflammatory responses and inflammation-associated diseases in organs', *Oncotarget*, 9(6), pp. 7204–7218.
- Chen, L. C., Goldman, D. L., Doering, T. L., Pirofski, L. A. and Casadevall, A. (1999) 'Antibody response to *Cryptococcus neoformans* proteins in rodents and humans', *Infect Immun*, 67(5), pp. 2218–2224.
- Chen, S., Sorrell, T., Nimmo, G., Speed, B., Currie, B., Ellis, D., Marriott, D., Pfeiffer, T., Parr, D. and Byth, K. (2000) 'Epidemiology and Host- and Variety-Dependent Characteristics of Infection Due to *Cryptococcus neoformans* in Australia and New Zealand', *Clin Infect Dis*, 31(2), pp. 499–508.
- Chen, S. C. A., Meyer, W. and Sorrell, T. C. (2014) '*Cryptococcus gattii* infections', *Clin Microbiol Rev*, 27(4), pp. 980–1024.
- Chen, Y. L., Lehman, V. N., Lewit, Y., Averette, A. F. and Heitman, J. (2013) 'Calcineurin governs thermotolerance and virulence of *cryptococcus gattii*', *G3 (Bethesda)*, 3(3), pp. 527–539.
- Cheng, P. Y., Sham, A. and Kronstad, J. W. (2009) '*Cryptococcus gattii* isolates from the British Columbia cryptococcosis outbreak induce less protective inflammation in a murine model of infection than *Cryptococcus neoformans*', *Infect Immun*, 77(10), pp. 4284–4294.
- Cherniak, R., Reiss, E., Slodki, M. E., Plattner, R. D. and Blumer, S. O. (1980) 'Structure and antigenic activity of the capsular polysaccharide of *Cryptococcus neoformans* serotype A', *Mol Immunol*, 17(8), pp. 1025–1032.
- Cherniak, R., Valafar, H., Morris, L. C. and Valafar, F. (1998) '*Cryptococcus neoformans* chemotyping by quantitative analysis of 1H nuclear magnetic resonance spectra of glucuronoxylomannans with a computer-simulated artificial neural network', *Clin Diagn Lab Immunol*, 5(2), pp. 146–159.
- Cherniak, R., Jones, R. and Reiss (1988) 'Structure determination of *Cryptococcus neoformans* serotype A-variant glucuronoxylomannan by 13C-n.m.r. spectroscopy', *Carbohydr Res*, 172(1), pp. 113–138.
- Cherniak, R., Morris, L. C. and Turner, S. H. (1992) 'Glucuronoxylomannan of *Cryptococcus neoformans* serotype D: structural analysis by gas-liquid chromatography and 13C-nuclear magnetic resonance spectroscopy', *Carbohydr Res*, 223, pp. 263–269.
- Cherniak, R., O'Neill, E. B. and Sheng, S. (1998) 'Assimilation of xylose, mannose, and mannitol for synthesis of glucuronoxylomannan of *Cryptococcus neoformans* determined by 13C nuclear magnetic resonance spectroscopy', *Infect Immun*, 66(6), pp. 2996–2998.

- Cherniak, R., Reiss, E. and Turner, S. (1982) 'A galactoxylomannan antigen of *Cryptococcus neoformans* serotype A', *Carbohydr Res*, 103(2), pp. 239–250.
- Cherniak, R. and Sundstrom, J. B. (1994) 'Polysaccharide antigens of the capsule of *Cryptococcus neoformans*', *Infect Immun*, 62(5), pp. 1507–1512.
- Chiapello, L. S., Aoki, M. P., Rubinstein, H. R. and Masih, D. T. (2003) 'Apoptosis induction by glucuronoxylomannan of *Cryptococcus neoformans*', *Med Mycol*, 41(4), pp. 347–53.
- Chiapello, L. S., Baronetti, J. L., Aoki, M. P., Gea, S., Rubinstein, H. and Masih, D. T. (2004) 'Immunosuppression, interleukin-10 synthesis and apoptosis are induced in rats inoculated with *Cryptococcus neoformans* glucuronoxylomannan', *Immunology*, 113(3), pp. 392–400.
- Choi, C. H. (2005) 'ABC transporters as multidrug resistance mechanisms and the development of chemosensitizers for their reversal', *Cancer Cell Int*, 5, pp. 1–13.
- Chrétien, F., Lortholary, O., Kansau, I., Neuville, S., Gray, F. and Dromer, F. (2002) 'Pathogenesis of Cerebral *Cryptococcus neoformans* Infection after Fungemia', *J Infect Dis*, 186(4), pp. 522–530.
- Christianson, J. C., Engber, W. and Andes, D. (2003) 'Primary cutaneous cryptococcosis in immunocompetent and immunocompromised hosts', *Med Mycol*, 41(3), pp. 177–188.
- Chun, C. D., Liu, O. W. and Madhani, H. D. (2007) 'A link between virulence and homeostatic responses to hypoxia during infection by the human fungal pathogen *Cryptococcus neoformans*', *PLoS Pathog*, 3(2), p. e22.
- Cichetti, G., Allen, P. G. and Glogaure, M. (2002) 'Chemotactic Signaling Pathways in Neutrophils: from receptor to actin assembly', *Crit Rev Oral Biol Med*, 13(3), pp. 220–228.
- Clutterbruck, P. W., Lovell, R. and Raistrick, H. (1932) 'Studies in the biochemistry of micro-organisms: The metabolic products of the *Penicillium brevi-compactum* series', *Biochem J*, 26(5), pp. 1441–1458.
- Cobcroft, R., Kronenberg, H. and Wilkinson, T. (1978) '*Cryptococcus* in bagpipes', *The Lancet*, 1(8078), pp. 1368–1369.
- Coenjaerts, F. E. J., Hoepelman, A. I. M., Scharringa, J., Aarts, M., Ellerbroek, P. M., Bevaart, L., Van Strijp, J. A. G. and Janbon, G. (2006) 'The Skn7 response regulator of *Cryptococcus neoformans* involved in oxidative stress signalling and augments intracellular survival in endothelium', *FEMS Yeast Res*, 6(4), pp. 652–661.
- Cohn, R. G., Mirkovich, A., Dunlap, B., Burton, P., Chiu, S. H., Eugui, E. and Caulfield, J. P. (1999) 'Mycophenolic acid increases apoptosis, lysosomes and lipid droplets in human lymphoid and monocytic cell lines', *Transplantation*, 68(3), pp. 411–8.
- Colic, M., Stojic-Vukanic, Z., Pavlovic, B., Jandric, D. and Stefanoska, I. (2003) 'Mycophenolate mofetil inhibits differentiation, maturation and allostimulatory function of human monocyte-derived dendritic cells', *Clin Exp Immunol*, 134(1), pp. 63–69.

- Collart, F. R. and Huberman, E. (1988) 'Cloning and Sequence Analysis of the Human and Chinese Hamster', *J Biol Chem*, 263(30), pp. 15769–15772.
- Colombel, J. F., Ferrari, N., Debuysere, H., Marteau, P., Gendre, J. P., Bonaz, B., Soulé, J. C., Modigliani, R., Touze, Y., Catala, P., Libersa, C. and Broly, F. (2000) 'Genotypic analysis of thiopurine S-methyltransferase in patients with Crohn's disease and severe myelosuppression during azathioprine therapy', *Gastroenterology*, 118(6), pp. 1025–1030.
- Colotta, F., Re, F., Polentarutti, N., Sozzani, S. and Mantovani, A. (1992) 'Modulation of granulocyte survival and programmed cell death by cytokines and bacterial products', *Blood*, 80(8), pp. 2012–2020.
- Colucci-Guyon, E., Tinevez, J.-Y., Renshaw, S. A. and Herbomel, P. (2011) 'Strategies of professional phagocytes in vivo: unlike macrophages, neutrophils engulf only surface-associated microbes', *J Cell Sci*, 124(18), pp. 3053–3059.
- Coovadia, Y., Mahomed, S., Dorasamy, A. and Chang, C. (2015) 'A comparative evaluation of the Gram stain and India ink stain for the rapid diagnosis of cryptococcal meningitis in HIV infected patients in Durban', *S Afr J Infect Dis*, 30(2), pp. 61–63.
- Cordero, R. J. B., Pontes, B., Guimarães, A. J., Martinez, L. R., Rivera, J., Fries, B. C., Nimrichter, L., Rodrigues, M. L., Viana, N. B. and Casadevall, A. (2011) 'Chronological aging is associated with biophysical and chemical changes in the capsule of *Cryptococcus neoformans*', *Infect Immun*, 79(12), pp. 4990–5000.
- Cottrell, T. R., Griffith, C. L., Liu, H., Nenninger, A. A. and Doering, T. L. (2007) 'The pathogenic fungus *Cryptococcus neoformans* expresses two functional GDP-mannose transporters with distinct expression patterns and roles in capsule synthesis', *Eukaryot Cell*, 6(5), pp. 776–785.
- Cowburn, A. S., Cadwallader, K. A., Reed, B. J., Farahi, N. and Chilvers, E. R. (2002) 'Role of PI3-kinase-dependent Bad phosphorylation and altered transcription in cytokine-mediated neutrophil survival', *Blood*, 100(7), pp. 2607–2616.
- Cox, G., Crossley, J. and Xing, Z. (1995) 'Macrophage engulfment of apoptotic neutrophils contributes to the resolution of acute pulmonary inflammation in vivo', *Am J Respir Cell Mol Biol*, 12(2), pp. 232–237.
- Cox, G. M., Rude, T. H., Dykstra, C. C. and Perfect, J. R. (1995) 'The actin gene from *Cryptococcus neoformans*: structure and phylogenetic analysis', *J Med Vet Mycol*, 33(4), pp. 261–266.
- Cox, G. M., Harrison, T. S., Mcdade, H. C., Taborda, C. P., Heinrich, G., Casadevall, A. and Perfect, J. R. (2003) 'Superoxide dismutase influences the virulence of *Cryptococcus neoformans* by affecting growth within macrophages', *Infect Immun*, 71(1), pp. 173–180.
- Crestani, J., Carvalho, P. C., Han, X., Seixas, A., Broetto, L., da Gama Fischer, J. de S., Staats, C. C., Schrank, A., Yates III, J. R. and Vainstein, M. H. (2012) 'Proteomic profiling of the influence of iron availability on *Cryptococcus gattii*', *J Proteome Res*, 11(1), pp. 189–205.
- Criseo, G., Bolignano, M. S., De Leo, F. and Staib, F. (1995) 'Evidence of canary droppings as an important reservoir of *Cryptococcus neoformans*', *Zentralbl*

- Bakteriol*, 282(3), pp. 244–254.
- Croke, M., Ross, F. P., Korhonen, M., Williams, D. A., Zou, W. and Teitelbaum, S. L. (2011) 'Rac deletion in osteoclasts causes severe osteopetrosis', *J Cell Sci*, 124(Pt 22), pp. 3811–3821.
- Cros, J., Cagnard, N., Woollard, K., Patey, N., Zhang, S.-Y., Senechal, B., Puel, A., Biswas, S. K., Moshous, D., Picard, C., Jais, J.-P., D'Cruz, D., Casanova, J.-L., Trouillet, C. and Geissmann, F. (2010) 'Human CD14^{dim} monocytes patrol and sense nucleic acids and viruses via TLR7 and TLR8 receptors', *Immunity*, 33(3), pp. 375–386.
- Crowhurst, M. O., Layton, J. E. and Lieschke, G. J. (2002) 'Developmental biology of zebrafish', *Int J Dev Biol*, 46(4), pp. 483–492.
- Cruickshank, J. G., Cavill, R. and Jelbert, M. (1973) 'Cryptococcus neoformans of Unusual Morphology', *Appl Microbiol*, 25(2), pp. 309–312.
- Cuffari, C. (2006) 'A physician's guide to azathioprine metabolite testing', *Gastroenterol Hepatol (N Y)*, 2(1), pp. 58–63.
- Cuomo, C. A., Rhodes, J. and Desjardins, C. A. (2018) 'Advances in Cryptococcus genomics: Insights into the evolution of pathogenesis', *Mem Inst Oswaldo Cruz*, 113(7), pp. 1–7.
- Curnock, A. P., Logan, M. K. and Ward, S. G. (2002) 'Chemokine signalling: Pivoting around multiple phosphoinositide 3-kinases', *Immunology*, 105(2), pp. 125–136.
- Cyster, J. G. and Allen, C. D. C. (2019) 'B cell responses: cell interaction dynamics and decisions', *Cell*, 177(3), pp. 524–540.
- d'Alençon, C. A., Peña, O. A., Wittmann, C., Gallardo, V. E., Jones, R. A., Loosli, F., Liebel, U., Grabher, C. and Allende, M. L. (2010) 'A high-throughput chemically induced inflammation assay in zebrafish', *BMC Biol*, 8(151).
- D'Souza, C. A., Kronstad, J. W., Taylor, G., Warren, R., Yuen, M., Hu, G., Jung, W. H., Sham, A., Kidd, S. E., Tangen, K., Lee, N., Zeilmaker, T., Sawkins, J., McVicker, G., Shah, S., Gnerre, S., Griggs, A., Zeng, Q., Bartlett, K., *et al.* (2011) 'Genome variation in *Cryptococcus gattii*, an emerging pathogen of immunocompetent hosts', *mBio*, 2(1), pp. e00342-10.
- Dahlgren, C. and Karlsson, A. (1999) 'Respiratory burst in human neutrophils', *J Immunol Methods*, 232(1–2), pp. 3–14.
- Dale, D. C., Boxer, L. and Liles, W. C. (2008) 'The phagocytes: neutrophils and monocytes', *Blood*, 112(4), pp. 935–945.
- Dancey, J. T., Deubelbeiss, K. A. and Harker and Finch, L. A. C. A. (1976) 'Neutrophil kinetics in man', *J Clin Invest*, 58(3), pp. 705–715.
- Dasgupta, A., Johnson, M. and Tso, G. (2013) 'Mathematical equations to calculate true mycophenolic acid concentration in human plasma by using two immunoassays with different cross-reactivities with acyl glucuronide metabolite: Comparison of calculated values with values obtained by using an HPLC-UV', *J Clin Lab Anal*, 27(4), pp. 290–293.
- Davidson, A. L. and Chen, J. (2004) 'ATP-Binding cassette transporters in bacteria', *Annu Rev Biochem*, 73(1), pp. 241–268.

- Davies, L. C., Jenkins, S. J., Allen, J. E. and Taylor, P. R. (2013) 'Tissue-resident macrophages', *Nat Immunol*, 14(10), pp. 986–995.
- Davis, J. A., Horn, D. L. and Marr, K. A. (2009) 'Central nervous system involvement in cryptococcal infection in individuals after solid organ transplantation or with AIDS', *Transpl Infect Dis*, 11(5), pp. 432–437.
- Davis, J. Muse, Huang, M., Botts, M. R., Hull, C. M. and Huttenlocher, A. (2016) 'A zebrafish model of cryptococcal infection reveals roles for macrophages, endothelial cells, and neutrophils in the establishment and control of sustained fungemia', *Infect Immun*, 84(10), pp. 3047–3062.
- Davis, M. J., Tsang, T. M., Qiu, Y., Dayrit, J. K., Freij, J. B., Huffnagle, G. B. and Olszewski, M. A. (2013) 'Macrophage M1/M2 polarization dynamically adapts to changes in cytokine microenvironments in *Cryptococcus neoformans* infection', *mBio*, 4(3), pp. e00264-13.
- Davison, J. M., Akitake, C. M., Goll, M. G., Rhee, J. M., Gosse, N., Baier, H., Halpern, M. E., Leach, S. D. and Parsons, M. J. (2007) 'Transactivation from Gal4-VP16 transgenic insertions for tissue- specific cell labeling and ablation in zebrafish', *Dev Biol.*, 304(2), pp. 811–824.
- Dayton, J. S., Turka, L. A., Thompson, C. B. and Mitchell, B. S. (1992) 'Comparison of the effects of mizoribine with those of azathioprine, 6-mercaptopurine, and mycophenolic acid on T lymphocyte proliferation and purine ribonucleotide metabolism', *Mol Pharmacol*, 41(4), pp. 671–676.
- Decken, K., Köhler, G., Palmer-Lehmann, K., Wunderlin, A., Mattner, F., Magram, J., Gately, M. K. and Alber, G. (1998) 'Interleukin-12 is essential for a protective Th1 response in mice infected with *Cryptococcus neoformans*', *Infect Immun*, 66(10), pp. 4994–5000.
- Dee, C. T., Nagaraju, R. T., Athanasiadis, E. I., Gray, C., Fernandez del Ama, L., Johnston, S. A., Secombes, C. J., Cvejic, A. and Hurlstone, A. F. L. (2016) 'CD4-Transgenic Zebrafish Reveal Tissue-Resident Th2- and Regulatory T Cell-like Populations and Diverse Mononuclear Phagocytes', *J Immunol*, 197(9), pp. 3520–3530.
- De Deken, R. H. (1966) 'The Crabtree effect: a regulatory system in yeast', *J Gen Microbiol*, 44(2), pp. 149–156.
- DeLeon-Rodriguez, C. M. and Casadevall, A. (2016) 'Cryptococcus neoformans: Tripping on acid in the phagolysosome', *Front Microbiol*, 7(164).
- Delfino, D., Cianci, L., Migliardo, M., Mancuso, G., Cusumano, V., Corradini, C. and Teti, G. (1996) 'Tumor necrosis factor-inducing activities of *Cryptococcus neoformans* components', *Infect Immun*, 64(12), pp. 5199–5204.
- Della, B. V., Grzeskowiak, M. and Rossi, F. (1990) 'Studies on molecular regulation of phagocytosis and activation of the NADPH oxidase in neutrophils. IgG- and C3b-mediated ingestion and associated respiratory burst independent of phospholipid turnover and Ca²⁺ transients', *J Immunol*, 144(4), pp. 1411–1417.
- Demetter, P., De Vos, M., Van Huysse, J. A., Baeten, D., Ferdinande, L., Peeters, H., Mielants, H., Veys, E. M., De Keyser, F. and Cuvelier, C. A. (2005) 'Colon mucosa of patients both with spondyloarthritis and Crohn's disease is enriched with macrophages expressing the scavenger receptor CD163', *Ann Rheum Dis*,

- 64(2), pp. 321–324.
- Denning, D. W., Tucker, R. M., Hanson, L. H., Hamilton, J. R. and Stevens, D. A. (1989) 'Itraconazole therapy for cryptococcal meningitis and cryptococcosis', *Arch Intern Med*, 149(10), pp. 2301–2308.
- Denning, D. W., Armstrong, R. W., Lewis, B. H. and Stevens, D. A. (1991) 'Elevated cerebrospinal fluid pressures in patients with cryptococcal meningitis and acquired immunodeficiency syndrome', *Am J Med*, 91(3), pp. 267–272.
- Derengowski, L. da S., Paes, H. C., Albuquerque, P., Tavares, A. H. F. P., Fernandes, L., Silva-Pereira, I. and Casadevall, A. (2013) 'The transcriptional response of *Cryptococcus neoformans* to ingestion by *Acanthamoeba castellanii* and macrophages provides insights into the evolutionary adaptation to the mammalian host', *Eukaryot Cell*, 12(5), pp. 761–774.
- Dewar, G. J. and Kelly, J. K. (2008) 'Cryptococcus gattii: An emerging cause of pulmonary nodules', *Can Respir J*, 15(3), pp. 153–158.
- Diamond, R. D., May, J. E., Kane, M., Frank, M. M. and Bennett, J. E. (1973) 'The Role of Late Complement Components and the Alternate Complement Pathway in Experimental Cryptococcosis', *Proc Soc Exp Biol Med*, 144(1), pp. 312–315.
- Diamond, R. D., May, J. E., Kane, M. A., Frank, M. M. and Bennett, J. E. (1974) 'The role of the classical and alternate complement pathways in host defenses against *Cryptococcus neoformans* infection', *J Immunol*, 112(6), pp. 2260–2270.
- Diamond, R. D. and Bennett, J. E. (1973) 'Growth of *Cryptococcus neoformans* within human macrophages in vitro', *Infect Immun*, 7(2), pp. 231–236.
- Diamond, R. D., Root, R. K. and Bennett, J. E. (1972) 'Factors influencing killing of *Cryptococcus neoformans* by human leukocytes in vitro', *J Infect Dis*, 125(4), pp. 367–376.
- Ding, A. H., Nathan, C. F. and Stuehr, D. J. (1988) 'Release of reactive nitrogen intermediates and reactive oxygen intermediates from mouse peritoneal macrophages. Comparison of activating cytokines and evidence for independent production', *J Immunol*, 141(7), pp. 2407–2412.
- Ding, T. L. and Benet, L. Z. (1979) 'Comparative bioavailability and pharmacokinetic studies of azathioprine and 6-mercaptopurine in the rhesus monkey', *Drug Metab Dispos*, 7(6), pp. 373–377.
- Dismukes, W. E., Cloud, G., Gallis, H. A., Kerkering, T. M., Medoff, G., Craven, P. C., Kaplowitz, L. G., Fisher, J. F., Gregg, C. R., Bowles, C. A., Shadomy, S., Stamm, A. M., Diasio, R. B., Kaufman, L., Soong, S. and Blackwelder, W. C. (1987) 'Treatment of cryptococcal meningitis with combination amphotericin B and flucytosine for four as compared with six weeks', *N Engl J Med*, 317(6), pp. 334–341.
- Dixon, G., Elks, P. M., Loynes, C. A., Whyte, M. K. B. and Renshaw, S. A. (2012) 'A method for the in vivo measurement of zebrafish tissue neutrophil lifespan', *ISRN Hematol*, 2012, pp. 1–6.
- Djordjevic, J. T. (2010) 'Role of phospholipases in fungal fitness, pathogenicity, and drug development - lessons from *Cryptococcus neoformans*', *Front Microbiol*, 1, pp. 1–13.

- Doherty, C. M. and Forbes, R. B. (2014) 'Diagnostic lumbar puncture', *Ulster Med J*, 83(2), pp. 93–102.
- Dong, Z. M. and Murphy, J. W. (1993) 'Mobility of human neutrophils in response to *Cryptococcus neoformans* cells, culture filtrate antigen, and individual components of the antigen', *Infect Immun*, 61(12), pp. 5067–5077.
- Dong, Zhao Ming and Murphy, J. W. (1995) 'Effects of the two varieties of *Cryptococcus neoformans* cells and culture filtrate antigens on neutrophil locomotion', *Infect Immun*, 63(7), pp. 2632–2644.
- Dong, Z M and Murphy, J. W. (1995) 'Effects of the varieties of *Cryptococcus neoformans* cells and culture filtrate antigens on neutrophil locomotion', *Infect Immun*, 63(7), pp. 2544–2632.
- Dong, Z. M. and Murphy, J. W. (1997) 'Cryptococcal polysaccharides bind to CD18 on human neutrophils', *Infect Immun*, 65(2), pp. 557–563.
- Donnelly, S. C. and Haslett, C. (1992) 'Cellular mechanisms of acute lung injury: implications for future treatment in the adult respiratory distress syndrome', *Thorax*, 47(4), pp. 260–263.
- Dooley, K. and Zon, L. I. (2000) 'Zebrafish: a model system for the study of human disease', *Curr Opin Genet Dev*, 10(3), pp. 252–256.
- Doudoroff, M. (1945) 'On the utilization of raffinose by *Pseudomonas saccharophila*', *J Biol Chem*, 157(2), pp. 699–706.
- Dransfield, I., Stocks, C. S. and Haslett, C. (1995) 'Regulation of Cell-Adhesion Molecule Expression and Function-Associated With Neutrophil Apoptosis', *Blood*, 85(11), pp. 3264–3273.
- Drew, B. and Leewenburgh, C. (2002) 'Aging and the role of reactive nitrogen species', *Ann N Y Acad Sci*, 959, pp. 66–81.
- Dromer, F., Mathoulin, S., Dupont, B., Brugiére, O. and Letenneur, L. (1996) 'Comparison of the efficacy of amphotericin B and fluconazole in the treatment of cryptococcosis in human immunodeficiency virus-negative patients: retrospective analysis of 83 cases. French Cryptococcosis Study Group', *Clin Infect Dis*, 22, pp. S154–S160.
- Dromer, F., Mathoulin, S., Dupont, B. and Laporte, A. (1996) 'Epidemiology of Cryptococcosis in France: a 9-Year Survey (1985-1993)', *Clin Infect Dis*, 23(1), pp. 82–90.
- Dromer, F., Mathoulin, S., Dupont, B., Letenneur, L. and Ronin, O. (1996) 'Individual and environmental factors associated with infection due to *cryptococcus neoformans* serotype D', *Clin Infect Dis*, 23(1), pp. 91–96.
- Duffer, M., Krippeit-drews, P., Buntinas, L., Siemen, D. and Drews, G. (2002) 'Methyl pyruvate stimulates pancreatic β -cells by a direct effect on KATP channels, and not as a mitochondrial substrate', *Biochem J*, 368(Pt 3), pp. 817–825.
- Dukic-Stefanovic, S., Schinzel, R., Riederer, P. and Münch, G. (2001) 'AGES in brain ageing: AGE-inhibitors as neuroprotective and anti-dementia drugs?', *Biogerontology*, 2(1), pp. 19–34.
- Duque, G. A. and Descoteaux, A. (2014) 'Macrophage cytokines: Involvement in immunity and infectious diseases', *Front Immunol*, 5(49).

- Durez, P., Appelboom, T., Pira, C., Stordeur, P., Vray, B. and Goldman, M. (1999) 'Anti-inflammatory properties of mycophenolate mofetil in murine endotoxemia: inhibition of TNF- α and upregulation of IL-10 release', *Int J Immunopharmacol*, 21(9), pp. 581–587.
- Dustin, M. L., Bivona, T. G. and Philips, M. R. (2004) 'Membranes as messengers in T cell adhesion signalling', *Nat Immunol*, 5(4), pp. 363–372.
- Duvenage, L., Munro, C. A. and Gourlay, C. (2019) *High Resolution Spirometry in Candida albicans*. *Bio-protocol*. Available at: <https://bio-protocol.org/e3361> (Accessed: 29 September 2019).
- Dykstra, M. A., Friedman, L. and Murphy, J. W. (1977) 'Capsule size of *Cryptococcus neoformans*: control and relationship to virulence', *Infect Immun*, 16(1), pp. 129–135.
- Dymond, J. S. (2013) 'Saccharomyces Cerevisiae Growth Media', *Methods Enzymol*. 4th edn, 533, pp. 191–204.
- Edwards, S. W., Derouet, M., Howse, M. and Moots, R. J. (2004) 'Regulation of neutrophil apoptosis by Mcl-1', *Biochem Soc Trans*, 32(Pt3), pp. 489–492.
- Eisen, H. J., Kobashigawa, J., Keogh, A., Bourge, R., Renlund, D., Mentzer, R., Alderman, E., Valantine, H., Dureau, G., Mancini, D., Mamelok, R., Gordon, R., Wang, W., Mehra, M., Constanzo, M. R., Hummel, M. and Johnson, J. (2005) 'Three-year results of a randomized, double-blind, controlled trial of mycophenolate mofetil versus azathioprine in cardiac transplant recipients', *J Heart Lung Transplant*, 24(5), pp. 517–525.
- Eldik, L. J. Van and Griffin, W. S. T. (1994) 'S100 β expression in Alzheimer's disease: relation to neuropathology in brain regions', *Biochim Biophys Acta*, 1223(3), pp. 398–403.
- Elion, B., Callahan, S., Nathan, H., Bieber, S., Hitchings, G. H. and Rundle, R. W. (1963) 'Potentiation by inhibition of drug degradation: 6-substituted purines and xanthine oxidase', *Biochem Pharmacol*, 12(1), pp. 85–93.
- Elion, G., Callahan, S., Bieber, S., Hitchings, G. and Rundles RW (1961) 'A summary of investigations with 6-[(1-methyl-4-nitro-5-imidazolyl) thiolpurine]', *Cancer Chemother Rep*, 14, pp. 93–98.
- Elks, P. M., Van Eeden, F. J., Dixon, G., Wang, X., Reyes-Aldasoro, C. C., Ingham, P. W., Whyte, M. K. B., Walmsley, S. R. and Renshaw, S. A. (2011) 'Activation of hypoxia-inducible factor-1 α (hif-1 α) delays inflammation resolution by reducing neutrophil apoptosis and reverse migration in a zebrafish inflammation model', *Blood*, 118(3), pp. 712–722.
- Ellett, F., Pase, L. and Hayman, John W. Andrianopoulos, Alex Lieschke, G. J. (2011) 'mpeg1 promoter transgenes direct macrophage-lineage expression in zebrafish', *Blood*, 117(4), pp. e49–e56.
- Elliott, M. R. and Ravichandran, K. S. (2016) 'The Dynamics of Apoptotic Cell Clearance', *Dev Cell*, 38(2), pp. 147–160.
- Ellis, D. H. and Pfeiffer, T. J. (1990) 'Ecology, life cycle, and infectious propagule of *Cryptococcus neoformans*', *Lancet*, 336(8720), pp. 923–925.
- Ene, I. V., Brunke, S., Brown, A. J. P. and Hube, B. (2014) 'Metabolism in fungal

- pathogenesis', *Cold Spring Harb Perspect Med*, 4(12), pp. 1–21.
- Engqvist-Goldstein, Å. E. Y. and Drubin, D. G. (2003) 'Actin Assembly and Endocytosis: From Yeast to Mammals', *Annu Rev Cell Dev Biol*, 19(1), pp. 287–332.
- Ensan, S., Li, A., Besla, R., Degousee, N., Cosme, J., Roufaiel, M., Shikatani, E. A., El-Maklizi, M., Williams, J. W., Robins, L., Li, C., Lewis, B., Yun, T. J., Lee, J. S., Wieghofer, P., Khattar, R., Farrokhi, K., Byrne, J., Ouzounian, M., *et al.* (2016) 'Self-renewing resident arterial macrophages arise from embryonic CX3CR1(+) precursors and circulating monocytes immediately after birth', *Nat Immunol*, 17(2), pp. 159–168.
- Epelman, S., Lavine, K. J., Beaudin, A. E., Sojka, D. K., Carrero, J. A., Calderon, B., Brija, T., Gautier, E. L., Ivanov, S., Satpathy, A. T., Schilling, J. D., Schwendener, R., Sergin, I., Razani, B., Forsberg, E. C., Yokoyama, W. M., Unanue, E. R., Colonna, M., Randolph, G. J., *et al.* (2014) 'Embryonic and adult-derived resident cardiac macrophages are maintained through distinct mechanisms at steady state and during inflammation', *Immunity*, 40(1), pp. 91–104.
- Erke, K. H. (1976) 'Light microscopy of basidia, basidiospores, and nuclei in spores and hyphae of *Filobasidiella neoformans* (*Cryptococcus neoformans*)', *J Bacteriol*, 128(1), pp. 445–455.
- Eugui, E. M., Almquist, S. J., Muller, C. D. and Allison, A. C. (1991) 'Lymphocyte-selective cytostatic and immunosuppressive effects of mycophenolic acid in vitro: role of deoxyguanosine nucleotide depletion', *Scand J Immunol*, 33(2), pp. 161–73.
- Evans, R. J., Li, Z., Hughes, W. S., Djordjevic, J. T., Nielsen, K. and May, R. C. (2015) 'Cryptococcal phospholipase B1 is required for intracellular proliferation and control of titan cell morphology during macrophage infection', *Infect Immun*, 83(4), pp. 1296–1304.
- Evans, R. J., Pline, K., Loynes, C. A., Needs, S., Aldrovandi, Maceler Tiefenbach, J., Bielska, E., Rubino, R. E., Nicol, C. J., May, R. C., Krause, H. M., O'Donnell, V. B., Renshaw, S. A. and Johnston, S. A. (2019) 'Fungal derived 15-keto-prostaglandin E₂ activates host peroxisome proliferator-activated receptor gamma (PPAR-γ) to promote *C. neoformans* growth during infection', *PLoS Pathog*, 15(3), p. e1007597.
- Fadok, V. A., Bratton, D. L., Rose, D. M., Pearson, A., Ezekewitz, R. A. and Henson, P. M. (2000) 'A receptor for phosphatidylserine-specific clearance of apoptotic cells', *Nature*, 405(6782), pp. 85–90.
- Fadok, V. A., Bratton, D. L., Guthrie, L. and Henson, P. M. (2001) 'Differential effects of apoptotic versus lysed cells on macrophage production of cytokines: role of proteases', *J Immunol*, 166(11), pp. 6847–6854.
- Fadok, V. A., De Cathelineau, A., Daleke, D. L., Henson, P. M. and Bratton, D. L. (2001) 'Loss of phospholipid asymmetry and surface exposure of phosphatidylserine is required for phagocytosis of apoptotic cells by macrophages and fibroblasts', *J Biol Chem*, 276(2), pp. 1071–1077.
- Fadok, V. A., Bratton, D. L. and Henson, P. M. (2001) 'Phagocyte receptors for

- apoptotic cells: recognition, uptake, and consequences', *J Clin Invest*, 108(7), pp. 957–962.
- Fadok, V. a, Bratton, D. L., Konowal, A., Freed, P. W., Westcott, J. Y. and Henson, P. M. (1998) 'Macrophages That Have Ingested Apoptotic Cells In Vitro Inhibit Proinflammatory Cytokine Production Through Autocrine / Paracrine Mechanisms Involving TGF- β , PGE2, and PAF', *J Clin Invest*, 101(28), pp. 890–898.
- Falloon, J. and Gallin, J. I. (1986) 'Neutrophil granules in health and disease', *J Allergy Clin Immunol*, 77(5), pp. 653–662.
- Fan, G., Jiang, X., Wu, X., Fordjour, P. A., Miao, L., Zhang, H., Zhu, Y. and Gao, X. (2016) 'Anti-Inflammatory Activity of Tanshinone IIA in LPS-Stimulated RAW264.7 Macrophages via miRNAs and TLR4–NF- κ B Pathway', *Inflammation*, 39(1), pp. 375–384.
- Fan, G. W., Gao, X. M., Wang, H., Zhu, Y., Zhang, J., Hu, L. M., Su, Y. F., Kang, L. Y. and Zhang, B. L. (2009) 'The anti-inflammatory activities of Tanshinone IIA, an active component of TCM, are mediated by estrogen receptor activation and inhibition of iNOS', *J Steroid Biochem Mol Biol*, 113(3–5), pp. 275–280.
- Fan, W., Kraus, P. R., Boily, M. J. and Heitman, J. (2005) 'Cryptococcus neoformans gene expression during murine macrophage infection', *Eukaryot Cell*, 4(8), pp. 1420–1433.
- Fang, F. C. (2004) 'Antimicrobial reactive oxygen and nitrogen species: Concepts and controversies', *Nat Rev Microbiol*, 2(10), pp. 820–832.
- Fang, W., Chen, M., Liu, J., Hagen, F., Ms, A., Al-Hatmi, Zhang, P., Guo, Y., Boekhout, T., Deng, D., Xu, J., Pan, W. and Liao, W. (2016) 'Cryptococcal meningitis in systemic lupus erythematosus patients: pooled analysis and systematic review', *Emerg Microbes Infect*, 5(9), p. e95.
- Farivar, A.S., Mackinnon-Patterson, B. C., Mccourtie, A. S. and Mulligan, M. S. (2005) 'The anti-inflammatory properties of Mycophenolate Mofetil in experimental lung ischemia reperfusion injury', *J Heart Lung Transplant*, 24(2), pp. 2235-2242.
- Farmer, S. G. and Komorowski, R. A. (1973) 'Histologic response to capsule-deficient Cryptococcus neoformans', *Arch Pathol.*, 96(6), pp. 383–387.
- Farrer, R. A., Voelz, K., Henk, D. A., Johnston, S. A., Fisher, M. C., May, R. C. and Cuomo, C. A. (2016) 'Microevolutionary traits and comparative population genomics of the emerging pathogenic fungus *Cryptococcus gattii*', *Philos Trans R Soc Lond B Biol Sci*, 371(1709). p. 20160021
- Farrer, R. A., Ford, C. B., Rhodes, J., Delorey, T., May, R. C., Fisher, M. C., Cloutman-Green, E., Balloux, F. and Cuomo, C. A. (2018) 'Transcriptional Heterogeneity of *Cryptococcus gattii* VGII Compared with Non-VGII Lineages Underpins Key Pathogenicity Pathways', *mSphere*, 3(5), pp. e00445-18.
- Farrera, C. and Fadeel, B. (2013) 'Macrophage Clearance of Neutrophil Extracellular Traps Is a Silent Process', *J Immunol*, 191(5), pp. 2647–2656.
- Faurschou, M. and Borregaard, N. (2003) 'Neutrophil granules and secretory vesicles in inflammation', *Microbes Infect*, 5(14), pp. 1317–1327.
- Feehan, K. T. and Gilroy, D. W. (2019) 'Is Resolution the End of Inflammation?',

Trends Mol Med, 25(3), pp. 198–214.

- Fehri, H. (2018) *Automatic Segmentation of Cells of Different Types in Fluorescence Microscopy Images (PhD thesis)*. The University of Sheffield.
- Feldmesser, M., Kress, Y., Novikoff, P. and Casadevall, A. (2000) 'Cryptococcus neoformans is a facultative intracellular pathogen in murine pulmonary infection', *Infect Immun*, 68(7), pp. 4225–4237.
- Feldmesser, M., Kress, Y. and Casadevall, A. (2001) 'Dynamic changes in the morphology of *Cryptococcus neoformans* during murine pulmonary infection', *Microbiology (Reading)*, 147(Pt8), pp. 2355–65.
- Fels, A. O. and Cohn, Z. A. (1986) 'The alveolar macrophage', *J Appl Physiol*, 60(2), pp. 353–369.
- Fenton, M. J., Buras, J. A. and Donnelly, R. P. (1992) 'IL-4 reciprocally regulates IL-1 and IL-1 receptor antagonist expression in human monocytes', *J Immunol*, 149(4), pp. 1283–1288.
- Fernandes, K. E., Dwyer, C., Campbell, L. T. and Carter, D. A. (2016) 'Species in the *Cryptococcus gattii* Complex Differ in Capsule and Cell Size following Growth under Capsule-inducing conditions', *mSphere*, 1(6), pp. e00350-16.
- Filippi, M. D. (2016) 'Mechanism of Diapedesis: Importance of the Transcellular Route', *Adv Immunol*, 129, pp. 25–53.
- Filler, G., Hansen, M., LeBlanc, C., Lepage, N., Franke, D., Mai, I. and Feber, J. (2003) 'Pharmacokinetics of mycophenolate mofetil for autoimmune disease in children', *Pediatr Nephrol*, 18(5), pp. 445–449.
- Fink, S. L. and Cookson, B. T. (2006) 'Caspase-1-dependent pore formation during pyroptosis leads to osmotic lysis of infected host macrophages', *Cell Microbiol*, 8(11), pp. 1812–1825.
- Fischer, A., Brown, K. K., Du Bois, R. M., Frankel, S. K., Cosgrove, G. P., Fernandez-Perez, E. R., Huie, T. J., Krishnamoorthy, M., Meehan, R. T., Olson, A. L., Solomon, J. J. and Swigris, J. J. (2013) 'Mycophenolate Mofetil Improves Lung Function in Connective Tissue Disease-associated Interstitial Lung Disease', *J Rheumatol*, 40(5), pp. 640–646.
- Fisher, A. B., Dodia, C., Tan, Z., Ayene, I. and Eckenhoff, R. G. (1991) 'Oxygen-dependent lipid peroxidation during lung ischemia', *J Clin Invest*, 88(2), pp. 674–679.
- Fleming, M. A. *, Chambers, S. P., Connelly, Patrick R., ‡, Nimmegern, E., Fox, T., Bruzzese, F. J., Hoe, S. T., Fulghum, J. R., Livingston, D. J., Stuver, C. M., Sintchak, M. D., Wilson, K. P. and Thomson*, J. A. (1996) 'Inhibition of IMPDH by Mycophenolic Acid: Dissection of Forward and Reverse Pathways Using Capillary Electrophoresis', *Biochemistry*, 35(22), pp. 6990–6997.
- Fleshner, M., Frank, M. and Maier, S. F. (2017) 'Danger Signals and Inflammasomes: Stress-Evoked Sterile Inflammation in Mood Disorders', *Neuropsychopharmacology*, 42(1), pp. 36–45.
- Flieger, A., Frischknecht, F., Häcker, G., Hornef, M. W. and Pradel, G. (2018) 'Pathways of host cell exit by intracellular pathogens', *Microb Cell*, 5(12), pp. 525–544.

- Focosi, D., Maggi, F., Pistello, M., Boggi, U. and Scatena, F. (2011) 'Immunosuppressive monoclonal antibodies: Current and next generation', *Clin Microbiol Infect*, 17(12), pp. 1759–1768.
- Foell, D., Wittkowski, H., Vogl, T. and Roth, J. (2006) 'S100 proteins expressed in phagocytes: a novel group of damage-associated molecular pattern molecules', *J Leukoc Biol*, 81(1), pp. 28–37.
- Follin, P. and Dahlgren, C. (1992) 'Phagocytosis by lipopolysaccharide-primed human neutrophils is associated with increased extracellular release of reactive oxygen metabolites', *Inflammation*, 16(2), pp. 83–91.
- Forrest, G. N., Bhalla, P., Debess, E. E., Winthrop, K. L., Lockhart, S. R., Mohammadi, J. and Cieslak, P. R. (2015) 'Cryptococcus gattii infection in solid organ transplant recipients: Description of Oregon outbreak cases', *Transpl Infect Dis*, 17(3), pp. 467–476.
- Fox, S., Leitch, A. E., Duffin, R., Haslett, C. and Rossi, A. G. (2010) 'Neutrophil apoptosis: Relevance to the innate immune response and inflammatory disease', *J Innate Immun*, 2(3), pp. 216–227.
- Franchi, L., Eigenbrod, T. and Núñez, G. (2009) 'TNF- α Mediate Sensitization to ATP and Silica via the NLRP3 Inflammasome in the Absence of Microbial Stimulation', *J Immunol*, 183(2), pp. 792–796.
- Franklin, T. J. and Cook, J. M. (1969) 'The inhibition of nucleic acid synthesis by mycophenolic acid', *Biochem J*, 113(3), pp. 515–524.
- Franzot, S. P., Mukherjee, J., Cherniak, R., Chen, L. C., Hamdan, J. S. and Casadevall, A. (1998) 'Microevolution of a standard strain of *Cryptococcus neoformans* resulting in differences in virulence and other phenotypes', *Infect Immun*, 66(1), pp. 89–97.
- Franzot, S. P., Salkin, I. F. and Casadevall, A. (1999) '*Cryptococcus neoformans* var. *grubii*: separate varietal status for *Cryptococcus neoformans* serotype A isolates', *J Clin Microbiol*, 37(3), pp. 838–840.
- Frasch, S. C., Henson, P. M., Nagaosa, K., Fessler, M. B., Borregaard, N. and Bratton, D. L. (2004) 'Phospholipid Flip-Flop and Phospholipid Scramblase 1 (PLSCR1) Co-localize to Uropod Rafts in Formylated Met-Leu-Phe-stimulated Neutrophils', *J Biol Chem*, 279(17), pp. 17625–17633.
- Fraser, A. G. (2002) 'The efficacy of azathioprine for the treatment of inflammatory bowel disease: a 30 year review', *Gut*, 50(4), pp. 485–489.
- Fraser, J. A., Giles, S. S., Wenink, E. C., Geunes-Boyer, S. G., Wright, J. R., Diezmann, S., Allen, A., Stajich, J. E., Dietrich, F. S., Perfect, J. R. and Heitman, J. (2005) 'Same-sex mating and the origin of the Vancouver Island *Cryptococcus gattii* outbreak', *Nature*, 437(7063), pp. 1360–1364.
- Frases, S., Pontes, B., Nimrichter, L., Rodrigues, M. L., Viana, N. B. and Casadevall, A. (2009) 'The elastic properties of the *Cryptococcus neoformans* capsule', *Biophys J*, 97(4), pp. 937–945.
- Frevert, C. W., Felgenhauer, J., Wygrecka, M., Nastase, M. V. and Schaefer, L. (2018) 'Danger-Associated Molecular Patterns Derived From the Extracellular Matrix Provide Temporal Control of Innate Immunity', *J Histochem Cytochem*, 66(4), pp. 213–227.

- Fridovich, I. (1995) 'Superoxide Radical and Superoxide Dismutase', *Annu Rev Biochem*, 64, pp. 97–112.
- Fries, B. C., Chen, F., Currie, B. P. and Casadevall, A. (1996) 'Karyotype Instability in Cryptococcus neoformans Infection', *J Clin Microbiol*, 34(6), pp. 1531–1534.
- Fries, B. C., Goldman, D. L., Cherniak, R., Ju, R. and Casadevall, A. (1999) 'Phenotypic switching in Cryptococcus neoformans strain 24067A associated with changes in virulence, polysaccharide structure, and cellular morphology', *Infect Immun*, 67(11), pp. 6076–6083.
- Fries, B. C., Taborda, C. P., Serfass, E. and Casadevall, A. (2001) 'Phenotypic switching of Cryptococcus neoformans occurs in vivo and influences the outcome of infection', *J Clin Invest*, 108(11), pp. 1639–1648.
- Fromtling, R. A., Shadomy, H. J. and Jacobson, E. S. (1982) 'Decreased virulence in stable, acapsular mutants of Cryptococcus neoformans', *Mycopathologia*, 79(1), pp. 23–29.
- Fu, C., Sun, S., Billmyre, R. B., Roach, K. C. and Heitman, J. (2015) 'Unisexual versus bisexual mating in Cryptococcus neoformans: Consequences and biological impacts', *Fungal Genet Biol*, 78, pp. 65–75.
- Fuchs, B. B. and Mylonakis, E. (2006) 'Using non-mammalian hosts to study fungal virulence and host defense', *Curr Opin Microbiol*, 9(4), pp. 346–351.
- Fuchs, T. A., Abed, U., Goosmann, C., Hurwitz, R., Schulze, I., Wahn, V., Weinrauch, Y., Brinkmann, V. and Zychlinsky, A. (2007) 'Novel cell death program leads to neutrophil extracellular traps', *J Cell Biol*, 176(2), pp. 231–241.
- Fukuda, A., Hikita, A., Wakeyama, H., Akiyama, T., Oda, H., Nakamura, K. and Tanaka, S. (2005) 'Regulation of osteoclast apoptosis and motility by small GTPase binding protein Rac1', *J Bone Miner Res*, 20(12), pp. 2245–2253.
- van Furth, R. and Cohn, Z. A. (1968) 'The origin and kinetics of mononuclear phagocytes', *J Exp Med*, 128(3), pp. 415–435.
- Furze, R. C. and Rankin, S. M. (2008) 'Neutrophil mobilization and clearance in the bone marrow', *Immunology*, 125(3), pp. 281–288.
- Futosi, K., Fodor, S. and Mócsai, A. (2013) 'Neutrophil cell surface receptors and their intracellular signal transduction pathways', *Int Immunopharmacol*, 17(3), pp. 638–650.
- Fyfe, M., MacDougall, L., Romney, M., Starr, M., Pearce, M., Mak, S., Mithani, S. and Kibsey, P. (2008) 'Cryptococcus gattii infections on Vancouver Island, British Columbia, Canada: emergence of a tropical fungus in a temperate environment', *Can Commun Dis Rep*, 34(6), pp. 1–12.
- Gadebusch, H. H. and Johnson, A. G. (1996) 'Natural Host Resistance to Infection with Cryptococcus neoformans : IV . The Effect of Some Cationic Proteins on the Experimental Disease', *J Infect Dis*, 116, pp. 551–565.
- Gaipl, U. S., Brunner, J., Beyer, T. D., Voll, R. E., Kalden, J. R. and Herrmann, M. (2003) 'Disposal of dying cells: A balancing act between infection and autoimmunity', *Arthritis Rheum*, 48(1), pp. 6–11.
- Gaipl, U. S., Franz, S., Voll, R. E., Sheriff, A., Kalden, J. R. and Herrmann, M. (2004) 'Defects in the disposal of dying cells lead to autoimmunity', *Curr Rheumatol*

Rep, 6(6), pp. 401–407.

- Galanis, E., Hoang, L., Kibsey, P., Morshed, M. and Phillips, P. (2009) 'Clinical presentation, diagnosis and management of *Cryptococcus gattii* cases: Lessons learned from British Columbia', *Can J Infect Dis Med Microbiol*, 20(1), pp. 23–28.
- Galanis, E. and MacDougall, L. (2010) 'Epidemiology of *Cryptococcus gattii*, British Columbia, Canada, 1999-2007', *Emerg Infect Dis*, 16(2), pp. 251–257.
- Gallo, P. M. and Gallucci, S. (2013) 'The dendritic cell response to classic, emerging, and homeostatic danger signals. Implications for autoimmunity', *Front Immunol*, 4(138).
- Gao, C., Su, B., Zhang, D., Yang, N., Song, L., Fu, Q., Zhou, S., Tan, F. and Li, C. (2018) 'L-rhamnose-binding lectins (RBLs) in turbot (*Scophthalmus maximus* L.): Characterization and expression profiling in mucosal tissues', *Fish Shellfish Immunol*, 80(264–273).
- Garaude, J., Acín-Pérez, R., Martínez-Cano, S., Enamorado, M., Ugolini, M., Nistal-Villán, E., Hervás-Stubbs, S., Pelegrín, P., Sander, L. E., Enríquez, J. A. and Sancho, D. (2016) 'Mitochondrial respiratory-chain adaptations in macrophages contribute to antibacterial host defense', *Nat Immunol*, 17(9), pp. 1037–1045.
- Garcia-Hermoso, D., Dromer, F. D. and Janbon, G. (2004) '*Cryptococcus neoformans*', *Infect Immun*, 72(6), pp. 3359–3365.
- Garcia-Hermoso, D., Janbon, G. and Dromer, F. (1999) 'Epidemiological Evidence for Dormant *Cryptococcus neoformans* Infection', *J Clin Microbiol*, 37(10), pp. 3204–3209.
- García-Rivera, J., Chang, Y. C., Kwon-Chung, K. J. and Casadevall, A. (2004) '*Cryptococcus neoformans* CAP59 (or Cap59p) is involved in the extracellular trafficking of capsular glucuronoxylomannan', *Eukaryot Cell*, 3(2), pp. 385–392.
- Garelnabi, M., Taylor-Smith, L. M., Bielska, E., Hall, R. A., Stones, D. and May, R. C. (2018) 'Quantifying donor-to-donor variation in macrophage responses to the human fungal pathogen *Cryptococcus neoformans*', *PLoS One*, 13(3), pp. 1–12.
- Garrad, R. C. and Bhattacharjee, J. K. (1992) 'Lysine biosynthesis in selected pathogenic fungi: Characterization of lysine auxotrophs and the cloned LYS1 gene of *Candida albicans*', *J Bacteriol*, 174(22), pp. 7379–7384.
- Garrod, T., Lee, L. and Pitzalis, C. (2006) 'Molecular mechanisms of cell recruitment to inflammatory sites: general and tissue-specific pathways', *Rheumatology (Oxford)*, 45(3), pp. 250–260.
- Gaudino, S. J. and Kumar, P. (2019) 'Cross-talk between antigen presenting cells and T cells impacts intestinal homeostasis, bacterial infections, and tumorigenesis', *Front Immunol*, 10(360).
- Gautier, E. L., Ivanov, S., Lesnik, P. and Randolph, G. J. (2013) 'Local apoptosis mediates clearance of macrophages from resolving inflammation in mice', *Blood*, 122(15), pp. 2714–2722.
- Gazzali, A. M., Lobry, M., Colombeau, L., Acherar, S., Azaïs, H., Mordon, S., Arnoux, P., Baros, F., Vanderesse, R. and Frochot, C. (2016) 'Stability of folic acid under several parameters', *Eur J Pharm*, 93, pp. 419–430.

- Gehrig, J., Pandey, G. and Westhoff, J. H. (2018) 'Zebrafish as a model for drug screening in genetic kidney diseases', *Front Pediatr*, 6(183).
- Geiger, T. L. and Sun, J. C. (2016) 'Development and Maturation of Natural Killer Cells', *Curr Opin Immunol*, 39, pp. 82–89.
- Geissmann, F., Jung, S. and Littman, D. R. (2003) 'Blood monocytes consist of two principal subsets with distinct migratory properties', *Immunity*, 19(1), pp. 71–82.
- Gernez, Y., Tirouvanziam, R. and Chanez, P. (2010) 'Neutrophils in chronic inflammatory airway diseases: can we target them and how?', *Eur Respir J*, 35(3), pp. 467–469.
- Gerstein, A. C., Jackson, K. M., McDonald, T. R., Wang, Y., Lueck, B. D., Bohjanen, S., Smith, K. D., Akampurira, A., Meya, D. B., Xue, C., Boulware, D. R. and Nielsen, K. (2019) 'Identification of pathogen genomic differences that impact human immune response and disease during cryptococcus neoformans infection', *mBio*, 10(4), pp. 1–22.
- Gerstein, A. C. and Nielsen, K. (2017) 'It's not all about us: evolution and maintenance of Cryptococcus virulence requires selection outside the human host', *Yeast*, 34(4), pp. 143–154.
- Ghannoum, M. A. (2000) 'Potential Role of Phospholipases in Virulence and Fungal Pathogenesis', *Clin Microbiol Rev*, 13(1), pp. 122–143.
- Giaccone, L., McCune, J. S., Maris, M. B., Gooley, T. A., Sandmaier, B. M., Slattery, J. T., Cole, S., Nash, R. A., Storb, R. F. and Georges, G. E. (2005) 'Pharmacodynamics of mycophenolate mofetil after nonmyeloablative conditioning and unrelated donor hematopoietic cell transplantation', *Blood*, 106(13), pp. 4381–4388.
- Gibson, J. F., Evans, R. J., Bojarczuk, A., Hotham, R., Lagendijk, A. K., Hogan, B. M., Renshaw, S. A. and Johnston, S. A. (2017) 'Dissemination of Cryptococcus neoformans via localised proliferation and blockage of blood vessels', *bioRxiv*.
- Gibson, J. F. (2017) *In vivo imaging and analysis of host-pathogen interactions of intracellular pathogens (PhD Thesis)*. Sheffield: The University of Sheffield.
- Gibson, J. F., Bojarczuk, A., Evans, R. J. and Kamuyango, A. (2020) 'Blood vessel occlusion by Cryptococcus neoformans is a mechanism for haemorrhagic dissemination of infection', *bioRxiv*.
- Gibson, R. H., Evans, R. J., Hotham, R., Bojarczuk, A., Lewis, A., Bielska, E., May, R. C., Elks, P. M., Renshaw, S. A. and Johnston, S. A. (2018) 'Mycophenolate mofetil increases susceptibility to opportunistic fungal infection independent of lymphocytes', *bioRxiv*.
- Gilbert, A. S., Seoane, P. I., Sephton-Clark, P., Bojarczuk, A., Hotham, R., Giurisato, E., Sarhan, A. R., Hillen, A., Velde, G. Vande, Gray, N. S., Alessi, D. R., Cunningham, D. L., Tournier, C., Johnston, S. A. and May, R. C. (2017) 'Vomocytosis of live pathogens from macrophages is regulated by the atypical MAP kinase ERK5', *Sci Adv*, 3(8), p. e1700898.
- Gilbert, N. M., Lodge, J. K. and Specht, C. A. (2011) 'The cell wall of Cryptococcus', in Heitman, J. et al. (eds) *Cryptococcus From human pathogen to model yeast*. Washington, pp. 67–80.

- Giles, S. S., Stajich, J. E., Nichols, C., Gerrald, Q. D., Alspaugh, J. A., Dietrich, F. and Perfect, J. R. (2006) 'The *Cryptococcus neoformans* catalase gene family and its role in antioxidant defense', *Eukaryot Cell*, 5(9), pp. 1447–1459.
- Ginhoux, F., Greter, M., Leboeuf, M., Sayan, N., See, P., Gokhan, S., Mehler, M. F., Conway, S. J., Ng, L. G., Stanley, R. I. E., Samokhvalov, I. M. and Merad, M. (2010) 'Fate Mapping Analysis Reveals That Adult Microglia Derive from Primitive Macrophages Florent', *Science*, 5(330), pp. 841–845.
- Ginhoux, F., Schultze, J. L., Murray, P. J., Ochando, J. and Biswas, S. K. (2015) 'New insights into the multidimensional concept of macrophage ontogeny, activation and function', *Nat Immunol*, 17(1), pp. 34–40.
- Ginhoux, F. and Jung, S. (2014) 'Monocytes and macrophages: Developmental pathways and tissue homeostasis', *Nat Rev Immunol*, 14(6), pp. 392–404.
- Glomsda, B. A., Blaheta, R. A. and Hailer, N. P. (2003) 'Inhibition of monocyte/endothelial cell interactions and monocyte adhesion molecule expression by the immunosuppressant mycophenolate mofetil', *Spinal Cord*, 41(11), pp. 610–619.
- Goldman, D. L., Lee, S. C., Mednick, A. J., Montella, L. and Casadevall, A. (2000) 'Persistent *Cryptococcus neoformans* pulmonary infection in the rat is associated with intracellular parasitism, decreased inducible nitric oxide synthase expression, and altered antibody responsiveness to cryptococcal polysaccharide', *Infect Immun*, 68(2), pp. 832–838.
- Goldsmith, J. R. and Jobin, C. (2012) 'Think small: Zebrafish as a model system of human pathology', *J Biomed Biotechnol*, 2012.
- Goldstein, E., Lippert, W. and Warshauer, D. (1974) 'Pulmonary alveolar macrophage. Defender against bacterial infection of the lung', *J Clin Invest*, 54(3), pp. 519–528.
- Gomes, L. C., Benedetto, G. Di and Scorrano, L. (2011) 'During autophagy mitochondria elongate, are spared from degradation and sustain cell viability', *Nat Cell Biol*, 13(5), pp. 589–598.
- Gomes, M. C. and Mostowy, S. (2020) 'The Case for Modeling Human Infection in Zebrafish', *Trends Microbiol*, 28(1), pp. 10–18.
- Gong, T., Liu, L., Jiang, W. and Zhou, R. (2020) 'DAMP-sensing receptors in sterile inflammation and inflammatory diseases', *Nat Rev Immunol*, 20(2), pp. 95–112.
- Gordon, S. and Plüddemann, A. (2017) 'Tissue macrophages: Heterogeneity and functions', *BMC Biology*, 15(1), p. 53.
- Goren, M. B. and Warren, J. (1968) 'Immunofluorescence studies of reactions at the cryptococcal capsule', *J Infect Dis*, 118(2), pp. 215–229.
- Grabiec, A. M. and Hussell, T. (2016) 'The role of airway macrophages in apoptotic cell clearance following acute and chronic lung inflammation', *Semin Immunopathol*, 38(4), pp. 409–423.
- Granger, D. L., Perfect, J. R. and Durack, D. T. (1985) 'Virulence of *Cryptococcus neoformans*. Regulation of capsule synthesis by carbon dioxide', *J Clin Invest*, 76(2), pp. 508–516.
- Gravelat, F. N., Doedt, T., Chiang, L. Y., Liu, H., Filler, S. G., Patterson, T. F. and

- Sheppard, D. C. (2008) 'In vivo analysis of *Aspergillus fumigatus* developmental gene expression determined by real-time reverse transcription-PCR', *Infect Immun*, 76(8), pp. 3632–3639.
- Gray, C., Loynes, C. A., Whyte, M. K. B., Crossman, D. C., Renshaw, S. A. and Chico, T. J. A. (2011) 'Simultaneous intravital imaging of macrophage and neutrophil behaviour during inflammation using a novel transgenic zebrafish', *Thromb Haemost*, 105(5), pp. 811–819.
- Graybill, J. R., Bocanegra, R., Lambros, C. and Luther, M. F. (1997) 'Granulocyte colony stimulating factor therapy of experimental cryptococcal meningitis', *J Med Vet Mycol*, 35(4), pp. 243–247.
- Graybill, J. R., Sobel, J., Saag, M., van der Horst, C., Powderly, W., Cloud, G., Riser, L., Hamill, R. and Dismukes, W. (2000) 'Diagnosis and Management of Increased Intracranial Pressure in Patients with AIDS and Cryptococcal Meningitis', *Clin Infect Dis*, 30(1), pp. 47–54.
- Green, G. M. and Kass, E. H. (1964) 'The role of alveolar macrophage in the clearance of bacteria from the lung', *J Exp Med*, 119, pp. 167–176.
- Gregory, C. D. and Devitt, A. (2004) 'The macrophage and the apoptotic cell: An innate immune interaction viewed simplistically?', *Immunology*, 113(1), pp. 1–14.
- Grigg, J. M., Silverman, M., Savill, J. S., Sarraf, C. and Haslett, C. (1991) 'Neutrophil apoptosis and clearance from neonatal lungs', *The Lancet*, 338(8769), pp. 720–722.
- Guerrero, A., Jain, N., Goldman, D. L. and Fries, B. C. (2006) 'Phenotypic switching in *Cryptococcus neoformans*', *Microbiology*, 152(Pt1), pp. 3–9.
- Guillot, L., Carroll, S. F., Badawy, M. and Qureshi, S. T. (2008) '*Cryptococcus neoformans* induces IL-8 secretion and CXCL1 expression by human bronchial epithelial cells', *Respir Res*, 9(1), p. 9.
- Guillot, L., Carroll, S. F., Homer, R. and Qureshi, S. T. (2008) 'Enhanced innate immune responsiveness to pulmonary *Cryptococcus neoformans* infection is associated with resistance to progressive infection', *Infect Immun*, 76(10), pp. 4745–4756.
- Gupta, A., Majumdar, S. and Sanyal, S. (1994) 'Isolation and chemical composition of lung surfactant from human amniotic fluid.', *Indian J Med Res*, 99, pp. 77–81.
- Gupta, G. and Fries, B. C. (2010) 'Variability of phenotypic traits in *Cryptococcus* varieties and species and the resulting implications for pathogenesis', *Future Microbiol*, 5(5), pp. 775–787.
- Guttman, J. A. and Finlay, B. B. (2009) 'Tight junctions as targets of infectious agents', *Biochim Biophys Acta*. Elsevier B.V., 1788(4), pp. 832–841.
- Haas, C., Ryffel, B. and Le Hir, M. (1997) 'IFN-gamma is essential for the development of autoimmune glomerulonephritis in MRL/lpr mice', *J Immunol*, 158(11), pp. 5484–5491.
- Haddow, L. J., Colebunders, R., Meintjes, G., Lawn, S. D., Elliott, J. H., Manebe, Y. C., Bohjanen, P. R., Sungkanuparph, S., Easterbrook, P. J., French, M. A. and Boulware, D. R. (2011) 'Cryptococcal immune reconstitution inflammatory

- syndrome in HIV-1–infected individuals: literature review and proposed clinical case definitions’, *Lancet Infect Dis*, 10(11), pp. 791–802.
- Hagen, F., Khayhan, K., Theelen, B., Kolecka, A., Polacheck, I., Sionov, E., Falk, R., Parnmen, S., Lumbsch, H. T. and Boekhout, T. (2015) ‘Recognition of seven species in the *Cryptococcus gattii*/*Cryptococcus neoformans* species complex’, *Fungal Genet Biol*, 78, pp. 16–48.
- Hagen, F. and Boekhout, T. (2010) ‘The Search for the Natural Habitat of *Cryptococcus gattii*’, *Mycopathologia*, 170(4), pp. 209–211.
- Hallett, J. M., Leitch, A. E., Riley, N. A., Duffin, R., Haslett, C. and Rossi, A. G. (2008) ‘Novel pharmacological strategies for driving inflammatory cell apoptosis and enhancing the resolution of inflammation’, *Trends Pharmacol Sci*, 29(5), pp. 250–257.
- Hallett, M. B. and Lloyds, D. (1995) ‘Neutrophil priming: the cellular signals that say “amber” but not “green”’, *Immunol Today*, 16(6), pp. 264–268.
- Han, S. W., Park, C. J., Lee, S. W. and Ronald, P. C. (2008) ‘An efficient method for visualization and growth of fluorescent *Xanthomonas oryzae* pv. *oryzae* in planta’, *BMC Microbiol*, 8, pp. 1–9.
- Hansakon, A., Mutthakalin, P., Ngamskulrungrroj, P., Chayakulkeeree, M. and Angkasekwina, P. (2019) ‘*Cryptococcus neoformans* and *Cryptococcus gattii* clinical isolates from Thailand display diverse phenotypic interactions with macrophages’, *Virulence*, 10(1), pp. 26–36.
- Hao, C., Anwei, M., Bing, C., Baiyong, S., Weixia, Z., Chuan, S., Erzhen, C., Xiaying, D., Weihua, Q., Weiping, Y., Chenghong, P. and Hongwei, L. (2008) ‘Monitoring mycophenolic acid pharmacokinetic parameters in liver transplant recipients: prediction of occurrence of leukopenia’, *Liver Transpl*, 14(8), pp. 1165–1173.
- Hardison, S. E., Ravi, S., Wozniak, K. L., Young, M. L., Olszewski, M. A., Wormley, F. L., Mitchell, T. G., Perfect, J. R., Powderly, W. G., Aguirre, K., Havell, E. A., Gibson, G. W., Johnson, L. L., Arora, S., Hernandez, Y., Erb-Downward, J. R., McDonald, R. A., Toews, G. B., Huffnagle, G. B., *et al.* (2010) ‘Pulmonary infection with an interferon-gamma-producing *Cryptococcus neoformans* strain results in classical macrophage activation and protection’, *Am J Pathol*, 176(2), pp. 774–785.
- Hamzeh, N., Voelker, A., Forssén, A., Gottschall, B. E., Rose, C., Mroz, P. and Maier, L. A. (2014) ‘Efficacy of Mycophenolate Mofetil in Sarcoidosis’, *Respir Med*, 108(11), pp. 1663–1669.
- Harris, D. P., Haynes, L., Sayles, P. C., Duso, D. K., Eaton, S. M., Lepak, N. M., Johnson, L. L., Swain, S. L. and Lund, F. E. (2000) ‘Reciprocal regulation of polarized cytokine production by effector B and T cells’, *Nat Immunol*, 1(6), pp. 475–482.
- Harris, J. R., Lockhart, S. R., Debess, E., Marsden-Haug, N., Goldoft, M., Wohrle, R., Lee, S., Smelser, C., Park, B. and Chiller, T. (2011) ‘*Cryptococcus gattii* in the United States: clinical aspects of infection with an emerging pathogen’, *Clin Infectious Dis*, 53(12), pp. 1188–1195.
- Harris, J. R., Lockhart, S. R., Sondermeyer, G., Vugia, D. J., Crist, M. B., D’Angelo, M. T., Sellers, B., Franco-Paredes, C., Makvandi, M., Smelser, C., Greene, J.,

- Stanek, D., Signs, K., Nett, R. J., Chiller, T. and Park, B. J. (2013) 'Cryptococcus gattii infections in multiple states outside the US Pacific Northwest', *Emerg Infect Dis*, 19(10), pp. 1620–1626.
- Harrison, J. E. and Schultz, J. (1976) 'Studies on the chlorinating activity of myeloperoxidase', *J Biol Chem*, 251(5), pp. 1371–1374.
- Hasçelik, G., ŞLener, B. and Hasçelik, Z. (1994) 'Effect of Some Anti-Inflammatory Drugs on Human Neutrophil Chemotaxis', *J Int Med Res*, 22(2), pp. 100–106.
- Haslett, C. (1992) 'Resolution of acute inflammation and the role of apoptosis in the tissue fate of granulocytes', *Clin Sci*, 83, pp. 639–648
- Haslett, C. (1997) 'Granulocyte apoptosis and inflammatory disease', *Br Med Bull*, 53(3), pp. 669–83.
- Haslett, C. (1999) 'Granulocyte apoptosis and its role in the resolution and control of lung inflammation', *Am J Respir Crit Care Med*, 160(5 Pt2), pp. S5-S11.
- Hatch, T. F. (1961) 'Distribution and deposition of inhaled particles in respiratory tract', *Bacteriol Rev*, 25(3), pp. 237–240.
- Headland, S. E. and Norling, L. V. (2015) 'The resolution of inflammation: Principles and challenges', *Semin Immunol*, 27(3), pp. 149–160.
- Heatwole, C. and Ciafaloni, E. (2008) 'Mycophenolate mofetil for myasthenia gravis: A clear and present controversy', *Neuropsychiatr Dis Treat*, 4(6), pp. 1203–1209.
- Heemann, U., Azuma, H., Hamar, P., Schmid, C., Tilney, N. and Philipp, T. (1996) 'Mycophenolate mofetil inhibits lymphocyte binding and the upregulation of adhesion molecules in acute rejection of rat kidney allografts', *Transpl Immunol*, 4(1), pp. 64–67.
- Heit, B., Tavener, S., Raharjo, E. and Kubes, P. (2002) 'An intracellular signaling hierarchy determines direction of migration in opposing chemotactic gradients', *J Cell Biol*, 159(1), pp. 91–102.
- Helmerhorst, E. J., Murphy, M. P., Troxler, R. F. and Oppenheim, F. G. (2002) 'Characterization of the mitochondrial respiratory pathways in *Candida albicans*', *Biochim Biophys Acta*, 1556(1), pp. 73–80.
- Helming, L. (2011) 'Inflammation: cell recruitment versus local proliferation', *Curr Biol*, 21(14), pp. R548–R550.
- Henao-Martínez, A. F. and Beckham, J. D. (2015) 'Cryptococcosis in Solid Organ Transplant Recipients', *Curr Opin Infect Dis*, 28(4), pp. 300–307.
- Henneke, P. and Golenbock, D. T. (2004) 'Phagocytosis, innate immunity, and host-pathogen specificity', *J Exp Med*, 199(1), pp. 1–4.
- Henson, P. M., Bratton, D. L. and Fadok, V. A. (2001) 'Apoptotic cell removal', *Curr Biol*, 11(19), pp. R795-R805.
- Herant, M., Heinrich, V. and Dembo, M. (2006) 'Mechanics of neutrophil phagocytosis: experiments and quantitative models', *J Cell Sci*, 119(9), pp. 1903–1913.
- Herbomel, P., Thisse, B. and Thisse, C. (1999) 'Ontogeny and behaviour of early macrophages in the zebrafish embryo', *Development*, 126(17), pp. 3735–45.
- Herbst, S., Shah, A., Mazon Moya, M., Marzola, V., Jensen, B., Reed, A., Birrell, M. A., Saijo, S., Mostowy, S., Shaunak, S. and Armstrong-James, D. (2015)

- 'Phagocytosis-dependent activation of a TLR9-BTK-calcineurin-NFAT pathway co-ordinates innate immunity to *Aspergillus fumigatus*', *EMBO Mol Med*, 7(3), p. 240-258
- Hibbs, J. B. J., Tainor, R. R., Vavrin, Z. and Rachlin, E. M. (1988) 'Nitric oxide: A cytotoxic activated macrophage effector molecule', *Biochem Biophys Res Commun*, 157(1), pp. 87–94.
- Hoag, K. A., Street, N. E., Huffnagle, G. B. and Lipscomb, M. F. (1995) 'Early cytokine production in pulmonary *Cryptococcus neoformans* infections distinguishes susceptible and resistant mice', *Am J Respir Cell Mol Biol*, 13(4), pp. 487–95.
- Hoag, K. A., Lipscomb, M. F. and Izzo, A. A. (1997) 'IL-12 and IFN- γ are required for initiating the protective Th1 response to pulmonary cryptococcosis in resistant CB-17 mice', *Am J Respir Cell Mol Biol*, 17(6), pp. 733–739.
- Hoang, L. M. N., Maguire, J. A., Doyle, P., Fyfe, M. and Roscoe, D. L. (2004) 'Cryptococcus neoformans infections at Vancouver Hospital and Health Sciences Centre (1997-2002): epidemiology, microbiology and histopathology', *J Med Microbiol*, 53(Pt9), pp. 935–940.
- Hochegger, K., Gruber, J. and Lhotta, K. (2006) 'Acute inflammatory syndrome induced by mycophenolate mofetil in a patient following kidney transplantation', *Am J Transpl*, 6(4), pp. 852–854.
- Hoeffel, G. and Ginhoux, F. (2018) 'Fetal monocytes and the origins of tissue-resident macrophages', *Cell Immunol*, 330, pp. 5–15.
- Hoenderdos, K. and Condliffe, A. (2013) 'The neutrophil in chronic obstructive pulmonary disease: Too little, too late or too much, too soon?', *Am J Respir Cell Mol Biol*, 48(5), pp. 531–539.
- Hoffman-La Roche Ltd (2014) <https://www.roche.com/>. Available at: https://www.roche.com/sustainability/philanthropy/science_education/pathways.htm (Accessed: 28 July 2019).
- Hofmann, M. A., Drury, S., Fu, C., Qu, W., Taguchi, A., Lu, Y., Avila, C., Kambham, N., Bierhaus, A., Nawroth, P., Neurath, M. F., Slattery, T., Beach, D., McClary, J., Nagashima, M., Morser, J., Stern, D. and Schmidt, A. M. (1999) 'RAGE mediates a novel proinflammatory axis: a central cell surface receptor for S100/calgranulin polypeptides', *Cell*, 97(7), pp. 889–901.
- Holm, B. A., Wang, Z. and Egan, Edmund A Notter, R. H. (1996) 'Content of dipalmitoyl phosphatidylcholine in lung surfactant: ramifications for surface activity', *Pediatr Res*, 39(5), pp. 805–811.
- Hornbeak, D. M. and Thorne, J. E. (2015) 'Immunosuppressive therapy for eye diseases: Effectiveness, safety, side effects and their prevention', *Taiwan J Ophthalmol*, 5(4), pp. 156–163.
- van der Horst, C. M., Saag, M. S., Cloud, G. A., Hamill, R. J., Graybill, J. R., Sobel, J. D., Johnson, P. C., Tuazon, C. U., Kerkering, T., Moskovitz Bruce L., Powderly William G., Dismukes William E., the National Institute of Allergy and Infectious Diseases Mycoses Study Group and Group, A. C. T. (1997) 'Treatment of cryptococcal meningitis associated with the acquired immunodeficiency syndrome', *N Engl J Med*, 337(1), pp. 15–21.
- Hou, J., Qiu, C., Shen, Y., Li, H. and Bao, X. (2017) 'Engineering of *Saccharomyces*

- cerevisiae for the efficient co-utilization of glucose and xylose', *FEMS yeast research*, 17(4), pp. 1–11.
- Howe, K., Clark, M. D., Torroja, C. F., Torrance, J., Muffato, M., Collins, J. E., Humphray, S., McLaren, K., Matthews, L., McLaren, S., Sealy, I., Caccamo, M., Churcher, C., Barrett, J. C., Koch, R., Rauch, G., White, S., Kilian, B., Quintais, L. T., *et al.* (2013) 'The zebrafish reference genome sequence and its relationship to the human genome', *Nature*, 496(7446), pp. 498–503.
- Howie, S. E. M., Sommerfield, A. J., Gray, E. and Harrison, D. J. (1994) 'Peripheral T lymphocyte depletion by apoptosis after CD4 ligation in vivo: selective loss of CD44 and "activating" memory T cells', *Clin Exp Immunol*, 95(1), pp. 195–200.
- Hu, G., Cheng, P.-Y., Sham, A., Perfect, J. R. and Kronstad, J. W. (2008) 'Metabolic adaptation in *Cryptococcus neoformans* during early murine pulmonary infection', *Mol Microbiol*, 69(6), pp. 1456–1475.
- Huang, J. S., Guh, J. Y., Chen, H. C., Hung, W. C., Lai, Y. H. and Chuang, L. Y. (2001) 'Role of receptor for advanced glycation end-product (RAGE) and the JAK/STAT-signaling pathway in AGE-induced collagen production in NRK-49F cells', *J Cell Biochem*, 81(1), pp. 102–113.
- Huang, S. H., Yu, C. H. and Chien, Y. L. (2015) 'Light-addressable measurement of in vivo tissue oxygenation in an unanesthetized Zebrafish embryo via phase-based phosphorescence lifetime detection', *Sensors (Basel)*, 15(4), pp. 8146–8162.
- Huang, Y., Liu, Z., Huang, H., Liu, H. and Li, L. (2005) 'Effects of mycophenolic acid on endothelial cells', *Int Immunopharmacol*, 5(6), pp. 1029–1039.
- Huffnagle, G. B., Boyd, M. B., Street, N. E. and Lipscomb, M. F. (1998) 'IL-5 Is Required for Eosinophil Recruitment, Crystal Deposition, and Mononuclear Cell Recruitment During a Pulmonary *Cryptococcus neoformans* Infection in Genetically Susceptible as Mice (C57BL/6)', *J Immunol*, 160(5), pp. 2393–2400.
- Huffnagle, G. B. and McNeil, L. K. (1999) 'Dissemination of *C. neoformans* to the central nervous system: role of chemokines, Th1 immunity and leukocyte recruitment', *J Neurovirol*, 5(1), pp. 76–81.
- Huh, W. K. and Kang, S. O. (1999) 'Molecular cloning and functional expression of alternative oxidase from *Candida albicans*', *J Bacteriol*, 181(13), pp. 4098–4102.
- Hull, C. M. and Heitman, J. (2002) 'Genetics of *Cryptococcus neoformans*', *Ann Rev Genet*, 36(1), pp. 557–615.
- Husain, S., Wagener, M. M. and Singh, N. (2001) 'Cryptococcus neoformans infection in organ transplant recipients: variables influencing clinical characteristics and outcome', *Emerg Infect Dis*, 7(3), pp. 375–381.
- Iba, T., Hashiguchi, N., Nagaoka, I., Tabe, Y. and Murai, M. (2013) 'Neutrophil cell death in response to infection and its relation to coagulation', *J Intensive Care*, 1(1), pp. 1–10.
- Ibrahim, A. S., Filler, S. G., Alcouloumre, M. S., Kozel, T. R., Edwards, J. E. and Ghannoum, M. A. (1995) 'Adherence to and damage of endothelial cells by *Cryptococcus neoformans* in vitro: role of the capsule', *Infect Immun*, 63(11),

- pp. 4368–4374.
- Idnurm, A., Reedy, J. L., Nussbaum, J. C. and Heitman, J. (2004) 'Cryptococcus neoformans virulence gene discovery through insertional mutagenesis', *Eukaryot Cell*, 3(2), pp. 420–429.
- Idnurm, A., Bahn, Y.-S., Nielsen, K., Lin, X., Fraser, J. A. and Heitman, J. (2005) 'Deciphering the Model Pathogenic Fungus Cryptococcus Neoformans', *Nat Rev Microbiol*, 3(10), pp. 753–764.
- Idnurm, A. and Heitman, J. (2005) 'Light controls growth and development via a conserved pathway in the fungal kingdom', *PLoS Biol*, 3(4), pp. 0615–0626.
- Idnurm, A. and Lin, X. (2015) 'Rising to the challenge of multiple Cryptococcus species and the diseases they cause', *Fungal Genet Biol*, 78, pp. 1–6.
- Iles, K. E. and Forman, H. J. (2002) 'Macrophage signaling and respiratory burst', *Immunol Res*, 26(1–3), pp. 95–105.
- Imada, A., Igarasi, S., Nakahama, K. and Isono, M. (1972) 'Asparaginase and Glutaminase Activities of Micro-organisms', *J Gen Microbiol*, 76(1), pp. 85–99.
- Ishii, D., Schenk, A. D., Baba, S. and Fairchild, R. L. (2011) 'Role of TNF α in Early Chemokine Production and Leukocyte Infiltration into Heart Allografts', *Am J Transplant*, 10(1), pp. 59–68.
- Isles, H. M., Muir, C. F., Hamilton, N., Kadochnikova, A., Loynes, C. A., Kadiramanathan, V., Elks, P. M. and Renshaw, S. A. (2019) 'Non-apoptotic pioneer neutrophils initiate an endogenous swarming response in a zebrafish tissue injury model', *bioRxiv*.
- Italiani, P. and Boraschi, D. (2014) 'From monocytes to M1/M2 macrophages: Phenotypical vs. functional differentiation', *Front Immunol*, 5(514).
- Iwasaki, A. and Medzhitov, R. (2010) 'Regulation of adaptive immunity by the innate immune system', *Science*, 327(5963), pp. 291–295.
- Iwasaki, A. and Medzhitov, R. (2015) 'Control of adaptive immunity by the innate immune system', *Nat Immunol*, 16(4), pp. 343–353.
- Iyengar, R., Stuehr, D. J. and Marletta, M. A. (1987) 'Macrophage synthesis of nitrite, nitrate, and N-nitrosamines: precursors and role of the respiratory burst', *Proc Natl Acad Sci U S A*, 84(18), pp. 6369–6373.
- Iyer, S. S., Pulskens, W. P., Sadler, J. J., Butter, L. M., Teske, G. J., Ulland, T. K., Eisenbarth, S. C., Florquin, S., Flavell, R. A., Leemans, J. C. and Sutterwala, F. S. (2009) 'Necrotic cells trigger a sterile inflammatory response through the Nlrp3 inflammasome', *Proc Natl Acad Sci U S A*, 106(48), pp. 20388–20393.
- Jacobson, E. S. (2000) 'Pathogenic roles for fungal melanins', *Clin Microbiol Rev*, 13(4), pp. 708–717.
- Jacobson, E. S. and Petro, M. J. (1987) 'Extracellular iron chelation in cryptococcus neoformans', *J Med Vet Mycol*, 25(6), pp. 415–418.
- Jacobson, E. S., Tingler, M. J. and Quynn, P. L. (1989) 'Effect of hypertonic solutes upon the polysaccharide capsule in Cryptococcus neoformans', *Mycoses*, 32(1), pp. 14–23.
- Jacobson, E. S. and Tinnell, S. B. (1993) 'Antioxidant Function of Fungal Melanin', *J*

Bacteriol, 175(21), pp. 7102–7104.

- Jacobson, P. A. (2011) 'Genetic Determinants of Mycophenolate Related Anemia and Leukopenia Following Transplantation', *Transplantation*, 19(3), pp. 309–316.
- Jaeschke, H., Farhood, A., Cai, S. X., Tseng, B. Y. and Bajt, M. L. (2000) 'Protection against TNF-induced liver parenchymal cell apoptosis during endotoxemia by a novel caspase inhibitor in mice', *Toxicol Appl Pharmacol*, 169(1), pp. 77–83.
- Jagodzinski, P., Lizakowski, S., Smolenski, R. T., Slominska, E. M., Goldsmith, D., Simmonds, H. A. and Rutkowski, B. (2004) 'Mycophenolate mofetil treatment following renal transplantation decreases GTP concentrations in mononuclear leucocytes', *Clin Sci (Lond)*, 107(1), pp. 69–74.
- Jain, N., Li, L., McFadden, D. C., Banarjee, U., Wang, X., Cook, E. and Fries, B. C. (2006) 'Phenotypic switching in a *Cryptococcus neoformans* variety *gattii* strain is associated with changes in virulence and promotes dissemination to the central nervous system', *Infect Immun*, 74(2), pp. 896–903.
- Jain, N. and Fries, B. C. (2008) 'Phenotypic Switching of *Cryptococcus neoformans* and *Cryptococcus gattii*', *Mycopathologia*, 166(4), pp. 181–188.
- Jakubzick, C., Gautier, E. L., Gibbings, S. L., Sojka, D. K., Schlitzer, A., Johnson, T. E., Ivanov, S., Duan, Q., Bala, S., Condon, T., Rooijen, N. Van, Grainger, J. R., Belkaid, Y., Ma, A., Riches, D. W. H., Yokoyama, W. M., Ginhoux, F. and Henson, P. M. (2013) 'Minimal differentiation of classical monocytes as they survey steady-state tissues and transport antigen to lymph nodes', *Immunity*, 39(3), pp. 599–610.
- James, P. G. and Cherniak, R. (1992) 'Galactoxylomannans of *Cryptococcus neoformans*', *Infect Immun*, 60(3), pp. 1084–1088.
- Janbon, G., Ormerod, K. L., Paulet, D., Byrnes, E. J., Yadav, V., Chatterjee, G., Mullapudi, N., Hon, C. C., Billmyre, R. B., Brunel, F., Bahn, Y. S., Chen, W., Chen, Y., Chow, E. W. L., Coppée, J. Y., Floyd-Averette, A., Gaillardin, C., Gerik, K. J., Goldberg, J., *et al.* (2014) 'Analysis of the Genome and Transcriptome of *Cryptococcus neoformans* var. *grubii* Reveals Complex RNA Expression and Microevolution Leading to Virulence Attenuation', *PLoS Genet*, 10(4), p. e1004261.
- Janeway, C. A. J., Travers, P. and Walport, M. (2012a) 'Signalling Through Immune-System Receptors', in Lawrence, E. (ed.) *Immunobiology*. 8th edn. St. Louis: Garland Science, pp. 239–333.
- Janeway, C. A. J., Travers, P. and Walport, M. (2012b) 'The Induced Responses of Innate Immunity', in Lawrence, E. (ed.) *Immunobiology*. 8th edn. St. Louis: Garland Science, pp. 75–125.
- Janossy, G., Panayi, G., Duke, O., Bofill, M., Poulter, L. W. and Goldstein, G. (1981) 'Rheumatoid arthritis: a disease of T-lymphocyte/macrophage immunoregulation', *Lancet*, 318(8251), pp. 839–842.
- Jarašūnienė, M., Šerpytienė, E., Mackevičiūtė, J., Lauraitis, J. and Grigaitienė, J. (2020) 'Skin cryptococcosis in an immunocompromised renal-transplant recipient', *Med Mycol Case Rep*, 28, pp. 33–35.
- Jarvis, J. and Harrison, T. (2008) 'Pulmonary Cryptococcosis', *Semin Respir Crit Care*

- Med*, 29(2), pp. 141–150.
- Jasiak, N. M. and Park, J. M. (2016) 'Immunosuppression in Solid-Organ Transplantation: Essentials and Practical Tips', *Crit Care Nurs Q*, 39(3), pp. 227–240.
- Jault, C., Pichon, L. and Chluba, J. (2004) 'Toll-like receptor gene family and TIR-domain adapters in *Danio rerio*', *Mol Immunol*, 40(11), pp. 759–771.
- Jaye, D. L., Waites, K. B., Parker, B., Bragg, S. L. and Moser, S. A. (1998) 'Comparison of two rapid latex agglutination tests for detection of cryptococcal capsular polysaccharide', *Am J Clin Pathol*, 109(5), pp. 634–641.
- Jenney, A., Pandithage, K., Fisher, D. A. and Currie, B. J. (2004) 'Cryptococcus infection in tropical Australia', *J Clin Microbiol*, 42(8), pp. 3865–3868.
- Jeong, H. and Kaplan, B. (2006) 'Therapeutic monitoring of mycophenolate mofetil', *Clin J Am Soc Nephrol*, 2(1), pp. 184–191.
- Jepson, S., Brogan, I. J., Stoddart, R. W. and Hutchinson, I. V. (2000) 'Mycophenolic acid does not inhibit protein glycosylation in T lymphocytes', *Transpl Immunol*, 8(3), pp. 169–175.
- De Jesús-Berríos, M., Liu, L., Nussbaum, J. C., Cox, G. M., Stamler, J. S. and Heitman, J. (2003) 'Enzymes that counteract nitrosative stress promote fungal virulence', *Curr Biol*, 13(22), pp. 1963–1968.
- de Jesus, M., Chow, S. K., Cordero, R. J. B., Frases, S. and Casadevall, A. (2010) 'Galactoxylomannans from *Cryptococcus neoformans* varieties *neoformans* and *grubii* are structurally and antigenically variable', *Eukaryot Cell*, 9(7), pp. 1018–1028.
- Jiang, S., Tang, Q., Rong, R., Tang, L., Xu, M., Lu, J., Jia, Y., Ooi, Y., Hou, J., Guo, J., Yang, B. and Zhu, T. (2012) 'Mycophenolate mofetil inhibits macrophage in filtration and kidney fibrosis in long-term ischemia – reperfusion injury', *Eur J Pharmacol*, 688(1–3), pp. 56–61.
- Jo, E.-K., Kim, J. K., Shin, D.-M. and Sasakawa, C. (2016) 'Molecular mechanisms regulating NLRP3 inflammasome activation', *Cell Mol Immunol*, 13(2), pp. 148–159.
- Johnston, S. A. and May, R. C. (2010) 'The human fungal pathogen *Cryptococcus neoformans* escapes macrophages by a phagosome emptying mechanism that is inhibited by arp2/3 complex-mediated actin polymerisation', *PLoS Pathog*, 6(8), pp. 27–28.
- Johnston, S. A. and May, R. C. (2013) 'Cryptococcus interactions with macrophages: Evasion and manipulation of the phagosome by a fungal pathogen', *Cell Microbiol*, 15(3), pp. 403–411.
- Johnston, S. A., Voelz, K. and May, R. C. (2016) 'Cryptococcus neoformans Thermotolerance to Avian Body Temperature Is Sufficient For Extracellular Growth But Not Intracellular Survival In Macrophages', *Sci Rep*, 6(20977).
- Joly, V., Saint-julien, L. and Carbon, C. (1994) 'In Vivo Activity of Interferon- γ in Combination with Amphotericin B in the Treatment of Experimental Cryptococcosis', *J Infect Dis*, 170(5), pp. 1331–1334.
- Jonsson, C. A. and Carlsten, H. (2002) 'Mycophenolic acid inhibits inosine 5'-

- monophosphate dehydrogenase and suppresses production of pro-inflammatory cytokines, nitric oxide, and LDH in macrophages', *Cell Immunol*, 216(1–2), pp. 93–101.
- Jung, H. C., Eckmann, L., Yang, S., Panja, A., Fierer, J., Morzycka-Wroblewska, E. and Kagnoff, M. F. (1995) 'A distinct array of proinflammatory cytokines is expressed in human colon epithelial cells in response to bacterial invasion', *J Clin Invest*, 95(1), pp. 55–65.
- Jung, K. W., Yang, D. H., Maeng, S., Lee, K. T., So, Y. S., Hong, J., Choi, J., Byun, H. J., Kim, H., Bang, S., Song, M. H., Lee, J. W., Kim, M. S., Kim, S. Y., Ji, J. H., Park, G., Kwon, H., Cha, S., Meyers, G. L., *et al.* (2015) 'Systematic functional profiling of transcription factor networks in *Cryptococcus neoformans*', *Nat Commun*, 6(6757).
- Jung, W. H., Hu, G., Kuo, W. and Kronstad, J. W. (2009) 'Role of ferroxidases in iron uptake and virulence of *Cryptococcus neoformans*', *Eukaryotic Cell*, 8(10), pp. 1511–1520.
- Jurado, R. and Walker, K. H. (1990) 'Cerebrospinal Fluid', in Walker, K. H., Hall, W. D., and Hurst, J. W. (eds) *Clinical Methods: The History, Physical, and Laboratory Examinations*. 3rd edn. Boston: Butterworths, pp. 371–382.
- Kado, C. I. (1985) 'Tartrate catabolism gene (U.S. patent 4520106)', *United States Patent*. U.S. Federal Government.
- Kaiko, G. E., Horvat, J. C. and Beagley, K. W. (2008) 'Immunological decision-making : how does the immune system decide to mount a helper T-cell response ?', *Immunology*, 123(3), pp. 326–338.
- Kambayashi, T. and Laufer, T. M. (2014) 'Atypical MHC class II-expressing antigen-presenting cells: can anything replace a dendritic cell?', *Nat Rev Immunol*, 14(11), pp. 719–730.
- Kambugu, A., Meya, D. B., Rhein, J., Brien, M. O., Janoff, E. N., Ronald, A. R., Kanya, M. R., Mayanja-kizza, H., Sande, M. A., Bohjanen, P. R. and Boulware, D. R. (2008) 'Outcomes of cryptococcal meningitis in Uganda before and after the availability of HAART', *Clin Infect Dis*, 46(11), pp. 1694–1701.
- Kamo, N., Ke, B., Ghaffari, A. A., Busuttill, R. W., Cheng, G. and Kupiec-Weglinski, J. W. (2013) 'The ASC/Caspase-1/IL-1 β signaling triggers inflammatory responses by promoting HMGB1 induction in liver ischemia- reperfusion injury', *Hepatology*, 58(1), pp. 351–362.
- Kamuyango, A. A. (2017) *Stimulation of innate immune resistance leads to clearance of C. neoformans infection in zebrafish (PhD thesis)*. The University of Sheffield.
- Kanehisa, M., Sato, Y., Furumichi, M., Morishima, K. and Tanabe, M. (2019) 'New approach for understanding genome variations in KEGG', *Nucleic Acids Res*, 47(D1), pp. D590–D595.
- Kanehisa, M. (2019) 'Toward understanding the origin and evolution of cellular organisms', *Protein Sci*, 28(11), pp. 1947–1951.
- Kanehisa, M. and Goto, S. (2000) 'KEGG: Kyoto Encyclopedia of Genes and Genomes', *Nucleic Acids Res*, 28(1), pp. 27–30.
- Kanterman, J., Sade-Feldman, M. and Baniyash, M. (2012) 'New insights into chronic

- inflammation-induced immunosuppression', *Semin Cancer Biol*, 22(4), pp. 307–318.
- Kaplan, B., Gruber, S., Nallamathou, R., Katz, S. and Shaw, L. (1998) 'Decreased protein binding of mycophenolic acid associated with leukopenia in a pancreas transplant recipient with renal failure', *Transplantation*, 65(8), pp. 1127–1129.
- Kaplan, B., Meier-Kriesche, H. U., Friedman, G., Mulgaonkar, S., Gruber, S., Korecka, M., Brayman, K. L. and Shaw, L. M. (1999) 'The effect of renal insufficiency on mycophenolic acid protein binding', *J Clin Pharmacol*, 39, pp. 715–20.
- Kaplan, M. J. (2013) 'Role of neutrophils in systemic autoimmune diseases', *Arthritis Res Ther*, 15(5), p. 219.
- Karstaedt, A. S., Crewe-Brown, H. H. and Dromer, F. (2002) 'Cryptococcal meningitis caused by *Cryptococcus neoformans* var. *gattii*, serotype C, in AIDS patients in Soweto, South Africa', *Med Mycol*, 40(1), pp. 7–11.
- Kashem, A., Endoh, M., Yano, N., Yamauchi, F., Nomoto, Y. and Sakai, H. (1996) 'Expression of inducible-NOS in human glomerulonephritis: The possible source is infiltrating monocytes/macrophages', *Kidney Int*, 50(2), pp. 392–399.
- Kato, A., Favoreto Jr., S., Avila, P. C. and Schleimer, R. P. (2007) 'TLR3- and Th2 cytokine-dependent production of thymic stromal lymphopoietin in human airway epithelial cells', *J Immunol*, 179(2), pp. 1080–1087.
- Kauffman, H. F. (2006) 'Innate immune responses to environmental allergens', *Clin Rev Allergy Immunol*, 30(2), pp. 129–40.
- Kavanaugh, L. A., Fraser, J. A. and Dietrich, F. S. (2006) 'Recent evolution of the human pathogen *Cryptococcus neoformans* by intervarietal transfer of a 14-gene fragment', *Mol Biol Evol*, 23(10), pp. 1879–1890.
- Kebir, D. El and Filep, J. G. (2013) 'Modulation of neutrophil apoptosis and the resolution of inflammation through $\beta 2$ integrins', *Front Immunol*, 4(60), pp.1-15.
- Kechichian, T. B., Shea, J. and Del Poeta, M. (2007) 'Depletion of alveolar macrophages decreases the dissemination of a glucosylceramide-deficient mutant of *Cryptococcus neoformans* in immunodeficient mice', *Infect Immun*, 75(10), pp. 4792–4798.
- Kelly, R. M., Chen, J., Yauch, L. E. and Levitz, S. M. (2005) 'Opsonic requirements for dendritic cell-mediated responses to *Cryptococcus neoformans*', *Infect Immun*, 73(1), pp. 592–598.
- Keown, P., Häyry, P., Morris, P., Stiller, C., Barker, C., Carr, L., Landsberg, D., Hardie, I., Rigby, R., Isoniemi, H., Gray, D., Belitsky, P., McDonald, A., Mathew, T., Clarkson, A., Barratt, L., Buchholz, B., Walker, R., Kirste, G., Muirhead, N., Tiller, D., Duggin, G., Halloran, P., Daloz, P., St. Louis, G., Russell, D., Ludwin, D., Vialtel, P., Binswanger, U., Buckels, J. A. C., Touraine, J. L., Hickey, D., Remuzzi, G., Locatelli, G., Lam, F. T. and Tapper, E. (1996) 'A blinded, randomized clinical trial of mycophenolate mofetil for the prevention of acute rejection in cadaveric renal transplantation', *Transplantation*, 61(7), pp. 1029-1037.
- Kerkering, T. M., Duma, R. J. and Shadomy, S. (1981) 'The evolution of pulmonary cryptococcosis: clinical implications from a study of 41 patients with and without compromising host factors', *Ann Intern Med*, 94(5), pp. 611–616.

- Kettle, A. J. and Winterbourn, C. C. (1997) 'Myeloperoxidase: a key regulator of neutrophil oxidant production', *Redox Rep*, 3(1), pp. 3–15.
- Kidd, S. E., Hagen, F., Tschärke, R. L., Huynh, M., Bartlett, K. H., Fyfe, M., MacDougall, L., Boekhout, T., Kwon-Chung, K. J. and Meyer, W. (2004) 'A rare genotype of *Cryptococcus gattii* caused the cryptococcosis outbreak on Vancouver Island (British Columbia, Canada)', *Proc Natl Acad Sci U S A*, 101(49), pp. 17258–17263.
- Kiener, B. P. A., Davis, P. M., Starling, G. C., Mehlin, C., Klebanoff, S. J., Ledbetter, J. A. and Liles, W. C. (1997) 'Differential induction of apoptosis by Fas-Fas ligand interactions in human monocytes and macrophages', *J Exp Med.*, 185(8), pp. 1511–1516.
- Kiertiburanakul, S., Wirojtananugoon, S., Prachartam, R. and Sungkanuparph, S. (2006) 'Cryptococcosis in human immunodeficiency virus-negative patients', *Int J Infect Dis*, 10(1), pp. 72–78.
- Kim-Park, W. K., Moore, M. A., Hakki, Z. W. and Kowolik, M. J. (1997) 'Activation of the neutrophil respiratory burst requires both intracellular and extracellular calcium', *Ann N Y Acad Sci*, 832, pp. 394–404.
- Kim, H. S., Cheon, J. H., Jung, E. S., Park, J., Aum, S., Park, S. J., Eun, S., Lee, J., Rütther, U., Yeo, G. S. H., Ma, M., Park, K. S., Naito, T., Kakuta, Y., Lee, J. H., Kim, W. H. and Lee, M. G. (2016) 'A coding variant in FTO confers susceptibility to thiopurine-induced leukopenia in East Asian patients with IBD', *Gut*, 66(11), pp. 1926–1935.
- Kim, Y. K., Shin, J. S. and Nahm, M. H. (2016) 'NOD-Like Receptors in Infection, Immunity, and Diseases', *Yonsei Med J*, 57(1), pp. 5–14.
- Kinder, B. W., Brown, K. K., Schwarz, M. I., Ix, J. H., Kervitsky, A. and King, T. E. (2008) 'Baseline BAL neutrophilia predicts early mortality in idiopathic pulmonary fibrosis', *Chest*, 133(1), pp. 226–232.
- King, M. W. (2017) *Nucleotide Metabolism: Nucleic Acid Synthesis*. Available at: <https://themedicalbiochemistrypage.org/nucleotide-metabolism.php> (Accessed: 27 May 2018).
- Kingsbury, J. M., Yang, Z., Ganous, T. M., Cox, G. M. and McCusker, J. H. (2004) 'Novel chimeric spermidine synthase-saccharopine dehydrogenase gene (SPE3-LYS9) in the human pathogen *Cryptococcus neoformans*', *Eukaryot Cell*, 3(3), pp. 752–763.
- Kinoshita, K. and Nakamura, H. (2003) 'Protein informatics towards function identification', *Curr Opin Struct Biol*, 13(3), pp. 396–400.
- Kirkpatrick, W. R., Najvar, L. K., Bocanegra, R., Patterson, T. F. and Graybill, J. R. (2007) 'New guinea pig model of cryptococcal meningitis', *Antimicrob Agents Chemother*, 51(8), pp. 3011–3013.
- Klebanoff, S. J. (1993) 'Reactive nitrogen intermediates and antimicrobial activity: role of nitrite', *Free Radic Biol Med*, 14(4), pp. 351–360.
- Klebanoff, S. J. (2005) 'Myeloperoxidase : friend and foe', *J Leukoc Biol*, 77(5), pp. 598–625.
- Klengel, T., Liang, W., Chaloupka, J., Ruoff, C., Naglik, J. R., Eckert, S. E., Mogensen,

- E. G., Tuite, M. F., Levin, L. R., Buck, J. and Mühlischlegel, F. A. (2005) 'Fungal adenylyl cyclase integrates CO₂ sensing with cAMP signaling and virulence', *Curr Biol*, 15(22), pp. 2021–2026.
- Kmetzsch, L., Staats, C. C., Simon, E., Fonseca, F. L., Oliveira, D. L., Joffe, L. S., Rodrigues, J., Lourenço, R. F., Gomes, S. L., Nimrichter, L., Rodrigues, M. L., Schrank, A. and Vainstein, M. H. (2011) 'The GATA-type transcriptional activator Gat1 regulates nitrogen uptake and metabolism in the human pathogen *Cryptococcus neoformans*', *Fungal Genet Biol*, 48(2), pp. 192–199.
- Knight, S. R., Russell, N. K., Barcena, L. and Morris, P. J. (2009) 'Mycophenolate mofetil decreases acute rejection and may improve graft survival in renal transplant recipients when compared with azathioprine: a systematic review', *Transplantation*, 87(6), pp. 785–794.
- Knodler, L. A., Bestor, A., Hansen-Wester, I., Hensel, M., Vallance, B. A. and Steelemortimer, O. (2005) 'Cloning vectors and fluorescent proteins can significantly inhibit *Salmonella enterica* virulence in both epithelial cells and macrophages: implications for bacterial pathogenesis studies', *Infect Immun*, 73(10), pp. 7027–7031.
- Knowles, M. R. and Boucher, R. C. (2002) 'Mucus clearance as a primary innate defense mechanism for mammalian airways', *J Clin Invest*, 109(5), pp. 571–577.
- Kobayashi, K., Takahashi, K. and Nagasawa, S. (1995) 'The role of tyrosine phosphorylation and Ca²⁺ accumulation in fcy-receptor-mediated phagocytosis of human neutrophils', *J Biochem*, 117(6), pp. 1156–1161.
- Koenderman, L. (2019) 'Inside-out control of Fc-receptors', *Front Immunol*, 10(544)
- Koh, T. J. and DiPietro, L. A. (2011) 'Inflammation and wound healing: the role of the macrophage', *Expert Rev Mol Med*, 13, p. e23.
- Kok, F. O., M. Shin, M., Ni, C.-W., Gupta, A., Grosse, A. S., van Impel, A., Kirchmaier, B.C. Peterson-Maduro, J Kourkoulis, G. Male, I DeSantis, D.F. Sheppard-Tindell, S. Ebarasi, L. Betsholtz, C. Schulte-Merker, S., Wolfe, A. and Lawson, N. D. (2015) 'Reverse genetic screening reveals poor correlation between Morpholino-induced and mutant phenotypes in zebrafish', *Dev Cell*, 16(4), pp. 461–470.
- Kolaczowska, E. and Kubes, P. (2013) 'Neutrophil recruitment and function in health and inflammation', *Nat Rev Immunol*, 13(3), pp. 159–175.
- Kontoyiannis, D. P., Peitsch, W. K., Reddy, B. T., Whimbey, E. E., Han, X. Y., Bodey, G. P. and Rolston, K. V. I. (2001) 'Cryptococcosis in Patients with Cancer', *Clin Infect Dis*, 32(11), pp. e145–e150.
- Korfel, A., Menssen, H. D., Schwartz, S. and Thiel, E. (1998) 'Cryptococcosis in Hodgkin's disease: description of two cases and review of the literature', *Ann Hematol*, 76(6), pp. 283–286.
- Korkaz, B., Horwitz, M. S., Jenne, D. E. and Gauthier, F. (2010) 'Neutrophil elastase, proteinase 3, and cathepsin G as therapeutic targets in human diseases', *Pharmacol Rev*, 62(4), pp. 726–759.
- Korshunov, S. S., Skulachev, V. P. and Starkov, A. A. (1997) 'High protonic potential actuates a mechanism of production of reactive oxygen species in

- mitochondria', *FEBS Lett*, 416(1), pp. 15–18.
- Koseki, N., Deguchi, J., Yamashita, A., Miyawaki, I. and Funabashi, H. (2014) 'Establishment of a novel experimental protocol for drug-induced seizure liability screening based on a locomotor activity assay in zebrafish', *J Toxicol Sci*, 39(4), pp. 579–600.
- Kouba, D. J., Mimouni, D., Rencic, A. and Nousari, H. C. (2003) 'Mycophenolate mofetil may serve as a steroid-sparing agent for sarcoidosis', *Br J Dermatol*, 148(1), pp. 147–148.
- Kowal-Bielecka, O., Kowal, K., Rojewska, J., Bodzenta-Lukaszyk, A., Siergiejko, Z., Sierakowska, M. and Sierakowski, S. (2005) 'Cyclophosphamide reduces neutrophilic alveolitis in patients with scleroderma lung disease: A retrospective analysis of serial bronchoalveolar lavage investigations', *Ann Rheum Dis*, 64(9), pp. 1343–1346.
- Kowaltowski, A. J., de Souza-Pinto, N. C., Castilho, R. F. and Vercesi, A. E. (2009) 'Mitochondria and reactive oxygen species', *Free Radic Biol Med*, 47(4), pp. 333–343.
- Kozel, T. R. and Follette, J. L. (1981) 'Opsonization of encapsulated *Cryptococcus neoformans* by specific anticapsular antibody', *Infect Immun*, 31(3), pp. 978–984.
- Kozel, T. R., Highison, B. and Stratton, C. J. (1984) 'Localization on encapsulated *Cryptococcus neoformans* of serum components opsonic for phagocytosis by macrophages and neutrophils', *Infect Immun*, 43(2), pp. 574–579.
- Kozel, T. R. and Pfrommer, G. S. T. (1986) 'Activation of the complement system by *Cryptococcus neoformans* leads to binding of iC3b to the yeast', *Infect Immun*, 52(1), pp. 1–5.
- Kozel, T. R., Wilson, M. A. and Murphy, J. W. (1991) 'Early events in initiation of alternative complement pathway activation by the capsule of *Cryptococcus neoformans*', *Infect Immun*, 59(9), pp. 3101–3110.
- Kozubowski, L., Lee, S. C. and Heitman, J. (2008) 'Signalling pathways in the pathogenesis of *Cryptococcus*', *Cell Microbiol*, 23(1), pp. 370–380.
- Kraus, P. R., Boily, M. J., Giles, S. S., Stajich, J. E., Allen, A., Cox, G. M., Dietrich, F. S., Perfect, J. R. and Heitman, J. (2004) 'Identification of *Cryptococcus neoformans* temperature-regulated genes with a genomic-DNA microarray', *Eukaryot Cell*, 3(5), pp. 1249–1260.
- Krebs, H. A., Wiggins, D., Stubbs, M., Sols, A. and Bedoya, F. (1983) 'Studies on the mechanism of the antifungal action of benzoate', *Biochem J*, 214(3), pp. 657–663.
- Kronstad, J. W., Attarian, R., Cadieux, B., Choi, J., D'Souza, C. A., Griffiths, E. J., Geddes, J. M. H., Hu, G., Jung, W. H., Kretschmer, M., Saikia, S. and Wang, J. (2011) 'Expanding fungal pathogenesis: *Cryptococcus* species break out of the opportunistic box', *Nat Rev Microbiol*, 9(3), pp. 193–203
- Krysan, D. J. (2015) 'Toward improved anti-cryptococcal drugs: Novel molecules and repurposed drugs', *Fungal Genet Biol*, 78, pp. 93–98.
- Krysko, O., De Ridder, L. and Cornelissen, M. (2004) 'Phosphatidylserine exposure

- during early primary necrosis (oncosis) in JB6 cells as evidenced by immunogold labeling technique', *Apoptosis*, 9(4), pp. 495–500.
- Kubes, P. and Mehal, W. Z. (2012) 'Sterile inflammation in the liver', *Gastroenterology*, 143(5), pp. 1158–1172.
- Kuczynski, J. T. and Radler, F. (1982) 'The anaerobic metabolism of malate of *Saccharomyces bailii* and the partial purification and characterization of malic enzyme', *Arch Microbiol*, 131, pp. 266–270.
- Kurtzman, C. P., Fell, J. W., Boekhout, T. and Robert, V. (2011) 'Methods for isolation, phenotypic characterization and maintenance of yeasts', in Kurtzman, C. P., Fell, J. W., and Boekhout, T. (eds) *The Yeasts – A Taxonomic Study*. 5th edn. Amsterdam: Elsevier Science, pp. 87–110.
- Kwan, K. M., Fujimoto, E., Grabher, C., Mangum, B. D., Hardy, M. E., Campbell, D. S., Parant, J. M., Yost, H. J., Kanki, J. P. and Chien, C. Bin (2007) 'The Tol2kit: A multisite gateway-based construction Kit for Tol2 transposon transgenesis constructs', *Dev Dyn*, 236(11), pp. 3088–3099.
- Kwon-Chung, K. J. (1975) 'A New Genus, *Filobasidiella*, the Perfect State of *Cryptococcus neoformans*', *Mycologia*, 67(6), pp. 1197–2000.
- Kwon-Chung, K. J. (1976a) 'A new species of *Filobasidiella*, the sexual state of *Cryptococcus neoformans* B and C serotypes', *Mycologia*, 68(4), pp. 943–946.
- Kwon-Chung, K. J. (1976b) 'Morphogenesis of *Filobasidiella neoformans*, the Sexual State of *Cryptococcus neoformans*', *Mycologia*, 68(4), pp. 821–833.
- Kwon-Chung, K. J., Fraser, J. A., Doering, T. L., Wang, Z. A., Janbon, G., Idnurm, A. and Bahn, Y.-S. (2014) '*Cryptococcus neoformans* and *Cryptococcus gattii*, the Etiologic Agents of Cryptococcosis', *Cold Spring Harb Perspect Med*, 4(7), p. a019760.
- Kwon-Chung, K. J., Bennett, J. E., Wickes, B. L., Meyer, W., Cuomo, C. A., Wollenburg, K. R., Bicanic, T. A., Castañeda, E., Chang, Y. C., Chen, J., Cogliati, M., Dromer, F., Ellis, D., Filler, S. G., Fisher, M. C., Harrison, T. S., Holland, S. M., Kohno, S., Kronstad, J. W., *et al.* (2017) 'The Case for Adopting the "Species Complex" Nomenclature for the Etiologic Agents of Cryptococcosis', *mSphere*, 2(1), pp. e00357-16.
- Kwon-Chung, K. J. and Bennett, J. E. (1978) 'Distribution of α and a mating types of *Cryptococcus neoformans* among natural and clinical isolates', *Am J Epidemiol*, 108(4), pp. 337–40.
- Kwon-Chung, K. J. and Bennett, J. E. (1984) 'Epidemiologic differences between the two varieties of *Cryptococcus neoformans*', *Am J Epidemiol*, 120(1), pp. 123–130.
- Kwon-Chung, K. J., Edman, J. C. and Wickes, B. L. (1992) 'Genetic association of mating types and virulence in *Cryptococcus neoformans*', *Infect Immun*, 60(2), pp. 602–605.
- Kwon-Chung, K. J. and Varma, A. (2006) 'Do major species concepts support one, two or more species within *Cryptococcus neoformans*?', *FEMS Yeast Res*, 6(4), pp. 574–587.
- Lacy, P. (2006) 'Mechanisms of degranulation in neutrophils', *Allergy Asthma Clin*

Immunol, 2(3), pp. 98–108.

- Lambers, H. (1982) 'Cyanide-resistant respiration: A non-phosphorylating electron transport pathway acting as an energy overflow', *Physiol Plant*, 55(4), pp. 478–485.
- Lämmermann, T., Afonso, P. V., Angermann, B. R., Wang, J. M., Kastenmüller, W., Parent, C. A. and Germain, R. N. (2013) 'Neutrophil swarms require LTB4 and integrins at sites of cell death in vivo', *Nature*, 498(7454), pp. 371–375
- Larsen, R. A., Leal, M. A. E. and Chan, L. S. (1990) 'Fluconazole compared with amphotericin B plus flucytosine for CM in AIDS', *Ann Intern Med*, 113, pp. 183–187.
- Latouche, G. N., Sorrell, T. C. and Meyer, W. (2002) 'Isolation and characterisation of the phospholipase B gene of *Cryptococcus neoformans* var. *gattii*', *FEMS Yeast Res*, 2(4), pp. 551–561.
- Laurent, A. F., Dumont, S., Poindron, P. and Muller, C. D. (1996) 'Mycophenolic acid suppresses protein N-linked glycosylation in human monocytes and their adhesion to endothelial cells and to some substrates', *Exp Hematol*, 24(1), pp. 59–67.
- Lauritzen, A. M. and Lipscomb, W. N. (1982) 'Modification of three active site lysine residues in the catalytic subunit of aspartate transcarbamylase by D- and L-bromosuccinate', *J Biol Chem*, 257(3), pp. 1312–1319.
- Lavi, L. E. and Holcenberg, J. S. (1985) 'A rapid and sensitive high-performance liquid chromatographic assay for 6-mercaptopurine metabolites in red blood cells', *Anal Biochem*, 144(2), pp. 514–521.
- Lawrence, T., Willoughby, D. A. and Gilroy, D. W. (2002) 'Anti-inflammatory lipid mediators and insights into the resolution of inflammation', *Nat Rev Immunol*, 2(10), pp. 787–795.
- Laxalt, K. A. and Kozel, T. R. (1979) 'Chemotaxis and activation of the alternative complement pathway by encapsulated and non-encapsulated *Cryptococcus neoformans*', *Infect Immun*, 26(2), pp. 435–440.
- Lazarevic-Pasti, T., Leskovac, A. and Vasic, V. (2015) 'Myeloperoxidase Inhibitors as Potential Drugs', *Curr Drug Metab*, 16(3), pp. 168–190.
- Lazéra, M. S., Cavalcanti, M. A. S., Trilles, L., Nishikawa, M. M. and Wanke, B. (1998) '*Cryptococcus neoformans* var. *gattii* - Evidence for a natural habitat related to decaying wood in a pottery tree hollow', *Med Mycol*, 36(2), pp. 119–122.
- Lee, A., Toffaletti, D. L., Tenor, J., Soderblom, E. J., Thompson, J. W., Moseley, M. A., Price, M. and Perfect, J. R. (2010) 'Survival defects of *Cryptococcus neoformans* mutants exposed to human cerebrospinal fluid result in attenuated virulence in an experimental model of meningitis', *Infect Immun*, 78(10), pp. 4213–4225.
- Lee, D., Jang, E. H., Lee, M., Kim, S. W., Lee, Y., Lee, K. T. and Bahna, Y. S. (2019) 'Unraveling melanin biosynthesis and signaling networks in *Cryptococcus neoformans*', *mBio*, 10(5), pp. 1–21.
- Lee, S. C., Kress, Y., Zhao, M. L., Dickson, D. W. and Casadevall, A. (1995) '*Cryptococcus neoformans* survive and replicate in human microglia', *Lab Invest*, 73(6), pp. 871–879.

- Lee, S. C., Phadke, S., Sun, S. and Heitman, J. (2012) 'Pseudohyphal growth of *Cryptococcus neoformans* is a reversible dimorphic transition in response to ammonium that requires Amt1 and Amt2 ammonium permeases', *Eukaryot Cell*, 11(11), pp. 1391–1398.
- Lee, W. A., Gu, L., Mikszta, A. R., Chu, N., Leung, K. and Nelson, P. H. (1990) 'Bioavailability Improvement of Mycophenolic Acid Through Amino Ester Derivatization', *Pharm Res*, 7(2), pp. 161–166.
- Lee, W. L., Harrison, R. E. and Grinstein, S. (2003) 'Phagocytosis by neutrophils', *Microbes Infect*, 5(14), pp. 1299–1306.
- Van Leeuwen, L. M., Evans, R. J., Jim, K. K., Verboom, T., Bojarczuk, A., Malicki, J., Johnston, S. A. and Marijke Van Der Sar, A. (2017) 'A transgenic zebrafish model for the in vivo study of the blood and choroid plexus brain barriers using claudin 5', *Biol Open*, 17(2), pp. 1–12.
- Legate, K. R., Wickström, S. A. and Fässler, R. (2009) 'Genetic and cell biological analysis of integrin outside-in signaling', *Genes Dev*, 23(4), pp. 397–418.
- Lembert, N., Joos, H. C., Idahl, L.-A., Ammon, H. P. T. and Wahl, M. A. (2001) 'Methyl pyruvate initiates membrane depolarization and insulin release by metabolic factors other than ATP', *Biochem J*, 354, pp. 345–350.
- Lemke, H. (2018) 'Immune response regulation by antigen receptors' clone-specific nonself parts', *Front Immunol*, 9(1471).
- Lennard, L. (2002) 'TPMT in the treatment of Crohn's disease with azathioprine', *Gut*, 51(2), pp. 143–146.
- Lennard, L., Van Loon, J. A. and Weinshilboum, R. M. (1989) 'Pharmacogenetics of acute azathioprine toxicity: relationship to thiopurine methyltransferase genetic polymorphism', *Clin Pharmacol Ther*, 46(2), pp. 149–154.
- Lennard, L., Murphy, M. and Maddocks, J. (1984) 'Severe megaloblastic anaemia associated with abnormal azathioprine metabolism', *Br J Clin Pharmacol*, 17(2), pp. 171–172.
- León, B., López-Bravo, M. and Ardavin, C. (2005) 'Monocyte-derived dendritic cells', *Semin Immunol*, 17(4), pp. 313–318.
- Lesavre, P. and Halbwachs-Mecarelli, L. (2000) 'Neutrophils: molecules, functions and pathophysiological aspects', *Lab Invest*, 80(5), pp. 617–653.
- Levitz, S. and DiBenedetto, D. (1989) 'Paradoxical role of capsule in murine bronchoalveolar macrophage-mediated killing of *Cryptococcus neoformans*', *J Immunol*, 142, pp. 659–665.
- Levitz, S. M. (1991) 'The Ecology of *Cryptococcus neoformans* and the Epidemiology of Cryptococcosis', *Rev Infect Dis*, 13(6), pp. 1163–1169.
- Levitz, S. M., Harrison, T. S., Tabuni, A. and Liu, X. (1997) 'Chloroquine induces human mononuclear phagocytes to inhibit and kill *Cryptococcus neoformans* by a mechanism independent of iron deprivation', *J Clin Invest*, 100(6), pp. 1640–1646.
- Levitz, S. M., Nong, S. H., Seetoo, K. F., Harrison, T. S., Speizer, R. A. and Simons, E. R. (1999) '*Cryptococcus neoformans* resides in an acidic phagolysosome of human macrophages', *Infect Immun*, 67(2), pp. 885–890.

- Levitz, S. M., Farrell, T. P. and Maziarz, R. T. (1991) 'Killing of *Cryptococcus neoformans* by human peripheral blood mononuclear cells stimulated in culture', *J Infect Dis*, 163(5), pp. 1108–1113.
- Levitz, S. M. and Specht, C. A. (2006) 'The molecular basis for the immunogenicity of *Cryptococcus neoformans* mannoproteins', *FEMS Yeast Res*, 6(4), pp. 513–524.
- Levitz, S. M. and Tabuni, A. (1991) 'Binding of *Cryptococcus neoformans* by human cultured macrophages. Requirements for multiple complement receptors and actin', *J Clin Invest*, 87(2), pp. 528–535.
- Lew, D. P., Andersson, T., Hed, J., Di Virgilio, F., Pozzan, T. and Stendahl, O. (1985) 'Ca²⁺-dependent and Ca²⁺-independent phagocytosis in human neutrophils', *Nature*, 315(6019), pp. 509–511.
- Ley, K. (2002) 'Integration of inflammatory signals by rolling neutrophils', *Immunol Rev*, 186(7), pp. 8–18.
- Ley, K. (2003) 'The role of selectins in inflammation and disease', *Trends Mol Med*, 9(6), pp. 263–268.
- Ley, K., Laudanna, C., Cybulsky, M. I. and Nourshargh, S. (2007) 'Getting to the site of inflammation: The leukocyte adhesion cascade updated', *Nat Rev Immunol*, 7(9), pp. 678–689.
- Ley, K. (2017) 'M1 Means Kill; M2 Means Heal', *J Immunol*, 199(7), pp. 2191–2193.
- Li, L. X., Rautengarten, C., Heazlewood, J. L. and Doering, T. L. (2018) 'Xylose donor transport is critical for fungal virulence', *PLoS Pathog*, 14(1), pp. 1–20.
- Li, M., Carpio, D. F., Zheng, Y., Bruzzo, P., Singh, V., Ouaz, F., Medzhitov, R. M. and Beg, A. A. (2001) 'An essential role of the NF- κ B / Toll-like receptor pathway in induction of inflammatory and tissue-repair gene expression by necrotic cells', *J Immunol*, 166(12), pp. 7128–7135.
- Li, X., Xiong, L., Chen, Xuefang, Huang, C., Chen, Xinde and Ma, L. (2015) 'Effects of Acetic Acid on Growth and Lipid Production by *Cryptococcus albidus*', *J Am Oil Chem Soc*, 92(8), pp. 1113–1118.
- Li, Y., Fang, W., Jiang, W., Hagen, F., Liu, J., Zhang, L., Hong, N., Zhu, Y., Xu, X., Lei, X., Deng, D., Xu, J., Liao, W., Boekhout, T., Chen, M. and Pan, W. (2017) 'Cryptococcosis in patients with diabetes mellitus II in mainland China: 1993-2015', *Mycoses*, 60(11), pp. 706–713.
- Lian, T., Simmer, M. I., D'Souza, C. A., Steen, B. R., Zuyderduyn, S. D., Jones, S. J. M., Marra, M. A. and Kronstad, J. W. (2005) 'Iron-regulated transcription and capsule formation in the fungal pathogen *Cryptococcus neoformans*', *Mol Microbiol*, 55(5), pp. 1452–1472.
- Lieschke, Graham J, Oates, A. C., Crowhurst, M. O., Ward, A. C., Layton, J. E., Lieschke, G. J., Oates, A. C., Crowhurst, M. O., Ward, A. C. and Layton, J. E. (2001) 'Morphologic and functional characterization of granulocytes and macrophages in embryonic and adult zebrafish', *Blood*, 98(10), pp. 3087–3096.
- Lieschke, G. J. and Currie, P. D. (2007) 'Animal models of human disease: zebrafish swim into view', *Nat Rev Genet*, 8(5), pp. 353–367.
- Lieschke, G. J. and Trede, N. S. (2009) 'Fish immunology', *Curr Biol*, 19(16), pp.

R678-R682.

- Liew, P. X. and Kubes, P. (2019) 'The neutrophil's role during health and disease', *Physiol Rev*, 99(2), pp. 1223–1248.
- Lim, T. S., Murphy, J. W. and Cauley, L. K. (1980) 'Host-etiological agent interactions in intranasally and intraperitoneally induced cryptococcosis in mice', *Infect Immun*, 29(2), pp. 633–641.
- Lin, X. (2009) 'Cryptococcus neoformans: morphogenesis, infection, and evolution', *Infect Genet Evol*, 9(4), pp. 401–416.
- Lin, X. and Heitman, J. (2006) 'The biology of the Cryptococcus neoformans species complex', *Annu Rev Microbiol*, 60(1), pp. 69–105.
- Lin, Y. Y., Shiao, S. and Fang, C. T. (2015) 'Risk factors for invasive Cryptococcus neoformans diseases: a case-control study', *PLoS One*, 10(3), pp. e0119090.
- Lis, P., Niedźwiecka, K., Goffeau, A., Ułaszewski, S., Ko, Y. H., Dyląg, M. and Pedersen, P. L. (2013) '3-Bromopyruvate: a novel antifungal agent against the human pathogen Cryptococcus neoformans', *Biochem Biophys Res Commun*, 434(2), pp. 322–327.
- Lisowski, P., Strzałkowska, N., Józ, A., Jarczak, J., Kos, E. M., Krzy, J., Zwierzchowski, L. and Bagnicka, E. (2013) 'Defensins : natural component of human innate immunity', *Hum Immunol*, 74(9), pp. 1069–1079.
- Lissner, D., Schumann, M., Batra, A., Kredel, L. I., Köhl, A. A., Erben, U., May, C., Schulzke, J. D. and Siegmund, B. (2015) 'Monocyte and M1 macrophage-induced barrier defect contributes to chronic intestinal inflammation in IBD', *Inflamm Bowel Dis*, 21(6), pp. 1297–1305.
- Lister, J. A., Robertson, C. P., Lepage, T., Johnson, S. L. and Raible, D. W. (1999) 'nacre encodes a zebrafish microphthalmia-related protein that regulates neural-crest-derived pigment cell fate', *Development*, 126(17), pp. 3757–3767.
- Littman, M.L., and Borok, R. (1968) 'Relation of the pigeon to cryptococcosis: natural carrier state, heat resistance and survival of Cryptococcus neoformans', *Mycopathol Mycol Appl*, 14(35), pp. 329–345.
- Littman, M. L. (1958) 'Capsule sythesis by Cryptococcus Neoformans', *Trans N Y Acad Sci*, 20(7), pp. 623–648.
- Litvintseva, A. P., Thakur, R., Reller, L. B. and Mitchell, T. G. (2005) 'Prevalence of clinical isolates of Cryptococcus gattii serotype C among patients with AIDS in Sub-Saharan Africa ', *J Infect Dis*, 192(5), pp. 888–892.
- Litvintseva, A. P. and Mitchell, T. G. (2009) 'Most environmental isolates of Cryptococcus neoformans var. grubii (serotype A) are not lethal for mice', *Infect Immun*, 77(8), pp. 3188–3195.
- Liu, D., Zhang, T., Wang, Y., Muhammad, M., Xue, W., Ju, J. and Zhao, B. (2019) 'Knockout of alanine racemase gene attenuates the pathogenicity of Aeromonas hydrophila', *BMC Microbiol*, 19(1), pp. 72.
- Liu, H., Ma, Y., Pagliari, L. J., Perlman, H., Yu, C., Lin, A. and Pope, R. M. (2004) 'TNF-alpha-induced apoptosis of macrophages following inhibition of NF-kappaB: a central role for disruption of mitochondria', *J Immunol*, 172(3), pp. 1907–1915.

- Liu, J., Farmer, J., Lane, W., Friedman, J., Weissman, I. and Schreiber, S. (1991) 'Calcineurin is a common target of cyclophilin-cyclosporin A and FKBP-FK506 complexes', *Cell*, 66, pp. 807–815.
- Liu, L. and Sun, B. (2019) 'Neutrophil pyroptosis: new perspectives on sepsis', *Cell Mol Life Sci*, 76(11), pp. 2031–2042.
- Liu, X., Yin, S., Chen, Y., Wu, Y., Zheng, W., Dong, H., Bai, Y., Qin, Y., Li, J., Feng, S. and Zhao, P. (2018) 'LPS-induced proinflammatory cytokine expression in human airway epithelial cells and macrophages via NF- κ B, STAT3 or AP-1 activation', *Mol Med Rep*, 17(4), pp. 5484–5491.
- Liu, Y. J. and Banchereau, J. (1997) 'Regulation of B-cell commitment to plasma cells or to memory B cells', *Semin Immunol*, 9(4), pp. 235–240.
- Locher, K. P. (2009) 'Structure and mechanism of ATP-binding cassette transporters', *Philos Trans R Soc Lond B Biol Sci*, 364(1514), pp. 239–245.
- Lodge, K. M., Cowburn, A. S., Li, W. and Condliffe, A. M. (2020) 'The Impact of Hypoxia on Neutrophil Degranulation and Consequences for the Host', *Int J Mol Sci*, 21(4), p. 1183.
- Loftus, B. J., Fung, E., Roncaglia, P., Rowley, D., Amedeo, P., Vamathevan, J., Miranda, M., Anderson, I. J., Fraser, J. A., Allen, J. E., Bosdet, I. E., Brent, M. R., Chiu, R., Doering, T. L., Donlin, M. J., Souza, C. A. D., Fox, D. S., Grinberg, V., Fukushima, M., *et al.* (2005) 'The genome of the basidiomycetous yeast and human pathogen *Cryptococcus neoformans*', *Science*, 307(5713), pp. 1321–1324.
- Lomakina, E. B. and Waugh, R. E. (2009) 'Adhesion between human neutrophils and immobilized endothelial ligand vascular cell adhesion molecule 1: Divalent ion effects', *Biophys J*, 96(1), pp. 276–284.
- Love, G. L., Boyd, G. D. and Greer, D. L. (1985) 'Large *Cryptococcus neoformans* isolated from brain abscess', *J Clin Microbiol*, 22(6), pp. 1068–1070.
- Loynes, C. A., Martin, J. S., Robertson, A., Trushell, D. M. I., Ingham, P. W., Whyte, M. K. B. and Renshaw, S. A. (2010) 'Pivotal Advance: Pharmacological manipulation of inflammation resolution during spontaneously resolving tissue neutrophilia in the zebrafish', *J Leukoc Biol*, 87(2), pp. 203–212.
- Loyse, A., Thangaraj, H., Easterbrook, P., Ford, N., Roy, M., Chiller, T., Govender, N., Harrison, T. S. and Bicanic, T. (2013) 'Cryptococcal meningitis: Improving access to essential antifungal medicines in resource-poor countries', *Lancet Infect Dis*, 13(7), pp. 629–637.
- Loyse, A., Wainwright, H., Jarvis, J. N., Bicanic, T., Rebe, K., Meintjes, G. and Harrison, T. S. (2013) 'Histopathology of the arachnoid granulations and brain in HIV- associated cryptococcal meningitis: correlation with cerebrospinal fluid pressure', *AIDS*, 24(3), pp. 405–410.
- Lubran, M. M. (1989) 'Hematologic side effects of drugs', *Ann Clin Lab Sci*, 19(2), pp. 114–121.
- Lucas, S., da Luz Martins, M., Flores, O., Meyer, W., Spencer-Martins, I. and Inácio, J. (2010) 'Differentiation of *Cryptococcus neoformans* varieties and *Cryptococcus gattii* using CAP59-based loop-mediated isothermal DNA amplification', *Clin Microbiol Infect*, 16(6), pp. 711–714.

- Lui, G., Lee, N., Ip, M., Choi, K. W., Tso, Y. K., Lam, E., Chau, S., Lai, R. and Cockram, C. S. (2006) 'Cryptococcosis in apparently immunocompetent patients', *QJM*, 99(3), pp. 143–151.
- Luma, H. N., Temfack, E., Halle, M. P., Tchaleu, B. C. N., Mapoure, Y. N. and Koulla-Shiro, S. (2013) 'Cryptococcal meningoencephalitis in human immunodeficiency virus/acquired immunodeficiency syndrome in Douala, Cameroon: A Cross Sectional Study', *N Am J Med Sci*, 5(8), pp. 486–491.
- Lupo, P., Chang, Y. C., Kelsall, B. L., Farber, J. M., Pietrella, D., Vecchiarelli, A., Leon, F. and Kwon-Chung, K. J. (2008) 'The presence of capsule in *Cryptococcus neoformans* influences the gene expression profile in dendritic cells during interaction with the fungus', *Infect Immun*, 76(4), pp. 1581–1589.
- Ma, H., Croudace, J. E., Lammas, D. A. and May, R. C. (2006) 'Expulsion of live pathogenic yeast by macrophages', *Curr Biol*, 16(21), pp. 2156–2160.
- Ma, H., Croudace, J. E., Lammas, D. A. and May, R. C. (2007) 'Direct cell-to-cell spread of a pathogenic yeast', *BMC Immunol*, 8(15).
- Ma, H. (2009) *Intracellular parasitism of macrophages by Cryptococcus (PhD Thesis)*. Birmingham: The University of Birmingham.
- Ma, L. L., Wang, C. L. C., Neely, G. G., Epelman, S., Krensky, A. M. and Mody, C. H. (2004) 'NK cells use perforin rather than granulysin for anticryptococcal activity', *J Immunol*, 173(5), pp. 3357–3365.
- Ma, L., Zhang, G. and Doyle, M. P. (2011) 'Green fluorescent protein labeling of *Listeria*, *Salmonella*, and *Escherichia coli* O157:H7 for safety-related studies', *PLoS One*, 6(4), pp. e18083.
- Maamoun, H., Soliman, A. and Zayed, B. (2010) 'Cyclosporine and mycophenolate mofetil 48 hours before renal transplantation enables the use of low cyclosporine doses and achieves better graft function', *Transplant Proc*, 42(10), pp. 4033–4036.
- MacDonald, P. E. and Wheeler, M. B. (2003) 'Voltage-dependent K⁺ channels in pancreatic beta cells: Role, regulation and potential as therapeutic targets', *Diabetologia*, 46(8), pp. 1046–1062.
- MacDougall, L., Kidd, S. E., Galanis, E., Mak, S., Leslie, M. J., Cieslak, P. R., Kronstad, J. W., Morshed, M. G. and Barlett, K. H. (2007) 'Spread of *Cryptococcus gattii* in British Columbia, Canada, and detection in the Pacific Northwest, USA', *Emerg Infect Dis*, 13(1), pp. 42–50.
- MacRae, C. A. and Peterson, R. T. (2015) 'Zebrafish as tools for drug discovery', *Nat Rev Drug Discov*, 14(10), pp. 721–731.
- Maddox, B. J. E. and Serhan, C. N. (1996) 'Lipoxin A4 and B4 are potent stimuli for human monocyte migration and adhesion: selective inactivation by dehydrogenation and reduction', *J Exp Med*, 183(1), pp. 137–146.
- Maes, B. (2002) 'A new acute inflammatory syndrome related to the introduction of mycophenolate mofetil in patients with Wegener's granulomatosis', *Nephrol Dial Transplant*, 17(5), pp. 923–926.
- Mahmud, N., Klipa, D. and Ahsan, N. (2010) 'Antibody immunosuppressive therapy in solid organ transplant: Part I', *MAbs*, 2(2), pp. 148–156.

- Maianski, N. A. (2002) 'Granulocyte colony-stimulating factor inhibits the mitochondria-dependent activation of caspase-3 in neutrophils', *Blood*, 99(2), pp. 672–679.
- Maianski, N. A., Geissler, J., Srinivasula, S. M. and Alnemri, E. S. (2004) 'Functional characterization of mitochondria in neutrophils : a role restricted to apoptosis', *Cell Death Differ*, 11(2), pp. 143–153.
- Mailliard, R. B., Egawa, S., Cai, Q., Kalinska, A., Bykovskaya, S. N., Lotze, M. T., Kapsenberg, M. L., Storkus, W. J. and Kalinski, P. (2002) 'Complementary dendritic cell – activating function of CD8+ and CD4+ T cells: helper role of CD8+ T cells in the development of T helper type 1 responses', *J Exp Med*, 195(4), pp. 473–483.
- Majewska, E., Sulowska, Z. and Baj, Z. (2000) 'Spontaneous apoptosis of neutrophils in whole blood and its relation to apoptosis gene proteins', *Scand J Immunol*, 52(5), pp. 496–501.
- Majno, G. and Joris, I. (1995) 'Apoptosis, oncosis, and necrosis. An overview of cell death', *Am J Pathol*, 146(1), pp. 3–15.
- Malhotra, A., Rao, Q., Kelly, S., Schwartz, D. and Chow, R. (2017) 'A rare presentation of cryptococcal meningoencephalitis in an immunocompetent individual', *Clin Pract*, 7(4), pp. 121–123.
- Malik, R., Krockenberger, M. B., O'Brien, C. R., Carter, D. A., Meyer, W. and Canfield, P. J. (2011) 'Veterinary Insights into Cryptococcosis Caused by *Cryptococcus neoformans* and *Cryptococcus gattii*', in Heitman, J. et al. (eds) *Cryptococcus: From Human Pathogen to Model Yeast*. Washington: ASM Press, pp. 489–504.
- Mamuye, A. T., Bornstein, E., Temesgen, O., Blumberg, H. M. and Kempker, R. R. (2016) 'Point-of-care testing for cryptococcal disease among hospitalized human immunodeficiency virus-infected adults in Ethiopia', *Am J Trop Med Hyg*, 95(4), pp. 786–792.
- Manickasingham, S. and e Sousa, C. R. (2000) 'Microbial and T cell-derived stimuli regulate antigen presentation by dendritic cells in vivo', *J Immunol*, 165(9), pp. 5027–5034.
- Mansour, M. K., Reedy, J. L., Tam, J. M. and Vyas, J. M. (2014) 'Macrophage *Cryptococcus* interactions: an update', *Curr Fungal Infect Rep*, 8(1), pp. 109–115.
- Mansour, M. K., Latz, E. and Levitz, S. M. (2006) 'Cryptococcus neoformans glycoantigens are captured by multiple lectin receptors and presented by dendritic cells', *J Immunol*, 176(5), pp. 3053–3061.
- Manzer, R., Wang, J., Nishina, K., Mcconville, G. and Mason, R. J. (2006) 'Alveolar epithelial cells secrete chemokines in response to IL- β and lipopolysaccharide but not to ozone', *Am J Respir Cell Mol Biol*, 34(2), pp. 158–166.
- Marrifield, E. H. and Stephen, A. M. (1980) 'Structural investigations of two capsular polysaccharides from *cryptococcus neoformans*', *Carbohydr Res*, 86(1), pp. 69–79.
- Martínez-Muñoz, G. A. and Kane, P. (2008) 'Vacuolar and plasma membrane proton pumps collaborate to achieve cytosolic pH homeostasis in yeast', *J Biol Chem*, 283(29), pp. 20309–20319.

- Martinez, L. R. and Casadevall, A. (2005) 'Specific antibody can prevent fungal biofilm formation and this effect correlates with protective efficacy', *Infect Immun*, 73(10), pp. 6350–6362.
- Martinez, L. R. and Casadevall, A. (2007) 'Cryptococcus neoformans biofilm formation depends on surface support and carbon source and reduces fungal cell susceptibility to heat, cold, and UV light', *Appl Environ Microbiol*, 73(14), pp. 4592–4601.
- Martinez, L. R., Garcia-Rivera, J. and Casadevall, A. (2001) 'Cryptococcus neoformans var. neoformans (serotype D) strains are more susceptible to heat than C. neoformans var. grubii (serotype A) strains', *J Clin Microbiol*, 39(9), pp. 3365–3367.
- Martinon, F., Pétrilli, V., Mayor, A., Tardivel, A. and Tschopp, J. (2006) 'Gout-associated uric acid crystals activate the NALP3 inflammasome', *Nature*, 440(7081), pp. 237–241.
- Martinon, F., Mayor, A. and Tschopp, J. (2009) 'The inflammasomes: guardians of the body', *Annu Rev Immunol*, 27, pp. 229–265.
- Mathews, R. J., Robinson, J. I., Battellino, M., Wong, C., Taylor, J. C., Eyre, S., Churchman, S. M., Wilson, A. G., Isaacs, J. D., Hyrich, K., Barton, A., Plant, D., Savic, S., Cook, G. P., Sarzi-Puttini, P., Emery, P., Barrett, J. H., Morgan, A. W. and McDermott, M. F. (2014) 'Evidence of NLRP3-inflammasome activation in rheumatoid arthritis (RA); genetic variants within the NLRP3-inflammasome complex in relation to susceptibility to RA and response to anti-TNF treatment', *Ann Rheum Dis*, 73(6), pp. 1202–1210.
- Mathias, J. R., Perrin, B. J., Liu, T.-X., Kanki, J., Look, T. A. and Huttenlocher, A. (2006) 'Resolution of inflammation by retrograde chemotaxis of neutrophils in transgenic zebrafish', *J Leukoc Biol*, 80(6), pp. 1281–1288.
- Matsumura, M., Kawamura, R., Inoue, R., Yamada, K., Kawano, M. and Yamagishi, M. (2011) 'Concurrent presentation of cryptococcal meningoencephalitis and systemic lupus erythematosus', *Mod Rheumatol*, 21(3), pp. 305–308.
- Matute-Bello, G., Liles, W., Radella, F., Steinberg, K., Ruzinski, J., Jonas, M., Chi, E. and Martin, T. (1997) 'Neutrophil apoptosis in the acute respiratory distress syndrome', *Am J Respir Crit Care Med*, 156(6), pp. 1969–1977.
- Mauri, C. and Bosma, A. (2012) 'Immune regulatory function of B cells', *Annu Rev Immunol*, 30, pp. 221–241.
- Maurya, I. K., Singh, S., Tewari, R., Tripathi, M., Upadhyay, S. and Joshi, Y. (2018) 'Antimicrobial activity of *Bulbothrix setschwanensis* (Zahlbr.) Hale lichen by cell wall disruption of *Staphylococcus aureus* and *Cryptococcus neoformans*', *Microb Pathog*, 115, pp. 12–18.
- May, R. C., Stone, N. R. H., Wiesner, D. L., Bicanic, T. and Nielsen, K. (2016) 'Cryptococcus: From environmental saprophyte to global pathogen', *Nat Rev Microbiol*, 14(2), pp. 106–117.
- Mayer, F. L., Wilson, D. and Hube, B. (2013) 'Candida albicans pathogenicity mechanisms', *Virulence*, 4(2), pp. 119–128.
- Mayr, P., Petschacher, B. and Nidetzky, B. (2003) 'Xylose reductase from the Basidiomycete fungus *Cryptococcus flavus*: Purification, steady-state kinetic

- characterization, and detailed analysis of the substrate binding pocket using structureactivity relationships', *J Biochem*, 133(4), pp. 553–562.
- Maziarz, E. K. and Perfect, J. R. (2016) 'Cryptococcosis', *Infect Dis Clin North Am*, 30(1), pp. 179–206.
- McArthur, D. B. (2019) 'Emerging Infectious Diseases', *Nurs Clin North Am*, 54(2), pp. 297–311.
- Mcclelland, E. E., Bernhardt, P. and Casadevall, A. (2006) 'Estimating the relative contributions of virulence factors for pathogenic microbes', *Infect Immun*, 74(3), pp. 1500–1504.
- McCray, P. J. and Bentley, L. (1977) 'Human airway epithelia express a beta-defensin.', *Am J Respir Cell Mol Biol*, 16(3), pp. 343–9.
- McDade, H. C. and Cox, G. M. (2001) 'A new dominant selectable marker for use in *Cryptococcus neoformans*', *Med Mycol*, 39(1), pp. 151–154.
- McFadden, D. C., De Jesus, M. and Casadevall, A. (2006) 'The physical properties of the capsular polysaccharides from *Cryptococcus neoformans* suggest features for capsule construction', *J Biol Chem*, 281(4), pp. 1868–1875.
- McGaw, T. G. and Kozel, T. R. (1979) 'Opsonization of *Cryptococcus neoformans* by human immunoglobulin G: masking of immunoglobulin G by Cryptococcal polysaccharide', *Infect Immun*, 25(1), pp. 262–267.
- McIlwain, D. R., Berger, T. and Mak, T. W. (2015) 'Caspase functions in cell death and disease', *Cold Spring Harb Perspect Biol*, 7(4), p. a026716.
- McSpadden Gardener, B. B., Paul, P. A., Boehm, M. J., Rong, X. and Schisler, D. (2014) 'Methods for Using *Cryptococcus Flavescens* Strains for Biological Control of *Fusarium* Head Blight (U. S. patent US 2014/0271560 A1)'. *United States Patent*: U.S. Federal Government.
- Medzhitov, R. (2001) 'Toll-like receptors and innate immunity', *Nat Rev Immunol*, 1(2), pp. 135–145.
- Medzhitov, R. (2007) 'Recognition of microorganisms and activation of the immune response', *Nature*, 449(7164), pp. 819–826.
- Medzhitov, R. (2008) 'Origin and physiological roles of inflammation', *Nature*, 454(7203), pp. 428–435.
- Medzhitov, R. (2010) 'Inflammation 2010: new adventures of an old flame', *Cell*, 140(6), pp. 771–776.
- Meeker, N. D. and Trede, N. S. (2008) 'Immunology and zebrafish: Spawning new models of human disease', *Dev Comp Immunol*, 32(7), pp. 745–757.
- Mellman, I. and Steinman, R. M. (2001) 'Dendritic cells: specialized and regulated antigen processing machines', *Cell*, 106(3), pp. 255–258.
- Merad, M., Sathe, P., Helft, J., Miller, J. and Mortha, A. (2013) 'The dendritic cell lineage: ontogeny and function of dendritic cells and their subsets in the steady state and the inflamed setting', *Annu Rev Immunol*, 31, pp. 563-604.
- Merkel, G. J. and Cunningham, R. K. (1992) 'The interaction of *Cryptococcus neoformans* with primary rat lung cell cultures', *Med Vet Mycol*, 30(2), pp. 115–121.

- Mershon-Shier, K. L., Vasuthasawat, A., Takahashi, K., Morrison, S. L. and Beenhouwer, D. O. (2011) 'In vitro C3 deposition on *Cryptococcus* capsule occurs via multiple complement activation pathways', *Mol Immunol*, 48(15–16), pp. 2009–2018.
- Meshkini, A., Yazdanparast, R. and Nouri, K. (2011) 'Intracellular GTP level determines cell's fate toward differentiation and apoptosis', *Toxicol Appl Pharmacol*, 253(3), pp. 188–196.
- Meszáros, A. J., Reichner, J. S. and Albina, J. E. (2000) 'Macrophage-induced neutrophil apoptosis', *J Immunol*, 165(1), pp. 435–441.
- Meyer, W., Aanensen, D. M., Boekhout, T., Cogliati, M., Diaz, M. R., Esposto, M. C., Fisher, M., Gilgado, F., Hagen, F., Litvintseva, A. P., Mitchell, T. G., Simwami, S. P., Viviani, M. A. and Kwon-chung, J. (2009) 'Consensus multi-locus sequence typing scheme for *Cryptococcus neoformans* and *Cryptococcus gattii*', *Med Mycol*, 47(6), pp. 561–570.
- Meyo has, M.-C., Roux, P., Bollens, D., Chouasid, C., Rozenbaum, W., Meynard, J.-L., Poirot, J.-L., Frotier, J. and Mayaud, C. (1995) 'Pulmonary cryptococcosis : localized and disseminated infections in 27 patients with AIDS', *Clin Infect Dis*, 21(3), pp. 628–633.
- Miles, K., Clarke, D. J., Lu, W., Sibinska, Z., Beaumont, P. E., Davidson, D. J., Barr, T. A., Campopiano, D. J. and Gray, M. (2009) 'Dying and necrotic neutrophils are anti-inflammatory secondary to the release of alpha-defensins', *J Immunol*, 183(3), pp. 2122–2132.
- Min, K. H. and Kwon-Chung, K. J. (1986) 'The biochemical basis for the distinction between the two *Cryptococcus neoformans* varieties with CGB medium', *Zentralbl Bakteriol Mikrobiol Hyg A*, 261(4), pp. 471–480.
- Mirza, S. A., Phelan, M., Rimland, D., Graviss, E., Hamill, R., Brandt, M. E., Gardner, T., Sattah, M., Ponce de Leon, G., Baughman, W. and Hajjeh, R. A. (2003) 'The changing epidemiology of cryptococcosis: an update from population-based active surveillance in 2 large metropolitan areas, 1992–2000', *Clin Infect Dis*, 36(6), pp. 789–794.
- Missall, T. A., Cherry-Harris, J. F. and Lodge, J. K. (2005) 'Two glutathione peroxidases in the fungal pathogen *Cryptococcus neoformans* are expressed in the presence of specific substrates', *Microbiology*, 151(8), pp. 2573–2581.
- Missall, T. A., Pusateri, M. E. and Lodge, J. K. (2004) 'Thiol peroxidase is critical for virulence and resistance to nitric oxide and peroxide in the fungal pathogen, *Cryptococcus neoformans*', *Mol Microbiol*, 51(5), pp. 1447–1458.
- Mitchell, A. P. (2006) 'Cryptococcal virulence: Beyond the usual suspects', *J Clin Invest*, 116(6), pp. 1481–1483.
- Mitchell, T. and Feron, O. (1997) 'Nitric oxide synthases: which, where, how, and why?', *J Clin Invest*, 100(9), pp. 2424–2429.
- Mitchell, T. G., Castañeda, E., Nielsen, K., Wanke, B. and Lazera, M. S. (2011) 'Environmental Niches for *Cryptococcus Neoformans* and *Cryptococcus gattii*', in Heitman, J. et al. (eds) *From Human Pathogen to Model Yeast*. Washington: ASM Press, pp. 237–259.

- Mitchell, T. G. and Perfect, J. R. (1995) 'Cryptococcosis in the era of AIDS--100 years after the discovery of *Cryptococcus neoformans*', *Clin Microbiol Rev*, 8(4), pp. 515-548.
- Mittl, P. R. E., Di Marco, S., Krebs, J. F., Bai, X., Karanewsky, D. S., Priestle, J. P., Tomaselli, K. J. and Grütter, M. G. (1997) 'Structure of recombinant human CPP32 in complex with the tetrapeptide acetyl-Asp-Val-Ala-Asp fluoromethyl ketone', *J Biol Chem*, 272(10), pp. 6539-6547.
- Mocanu, M. M., Baxter, G. F. and Yellon, D. M. (2000) 'Caspase inhibition and limitation of myocardial infarct size: Protection against lethal reperfusion injury', *Br J Pharmacol*, 130(2), pp. 197-200.
- Mogensen, T. H. (2009) 'Pathogen recognition and inflammatory signaling in innate immune defenses', *Clin Microbiol Rev*, 22(2), pp. 240-273.
- Moilanen, E., Moilanen, T., Knowles, R., Charles, I., Kadoya, Y., Al-Saffar, N., Revell, P. A. and Moncada, S. (1997) 'Nitric oxide synthase is expressed in human macrophages during foreign body inflammation', *Am J Pathol*, 150(3), pp. 881-887.
- Molawi, K., Wolf, Y., Kandalla, P. K., Favret, J., Hagemeyer, N., Frenzel, K., Pinto, A. R., Klapproth, K., Henri, S., Malissen, B., Rodewald, H. R., Rosenthal, N. A., Bajenoff, M., Prinz, M., Jung, S. and Sieweke, M. H. (2014) 'Progressive replacement of embryo-derived cardiac macrophages with age', *J Exp Med*, 211(11), pp. 2151-2158.
- Mollinedo, F. (2019) 'Neutrophil Degranulation, Plasticity, and Cancer Metastasis', *Trends Immunol*, 40(3), pp. 228-242.
- Monari, C., Pericolini, E., Bistoni, G., Casadevall, A., Kozel, T. R. and Vecchiarelli, A. (2005) 'Cryptococcus neoformans capsular glucuronoxylomannan induces expression of fas ligand in macrophages', *J Immunol*, 174(6), pp. 3461-3468.
- Monari, C., Bistoni, F. and Vecchiarelli, A. (2006) 'Glucuronoxylomannan exhibits potent immunosuppressive properties', *FEMS Yeast Res*, 6(4), pp. 537-542.
- Monga, D. P. (1981) 'Role of macrophages in resistance of mice to experimental cryptococcosis', *Infect Immun*, 32(3), pp. 975-978.
- Monguilhott Dalmarco, E., Mendes de Córdova, C. M. and Fröde, T. S. (2011) 'Evidence of an anti-inflammatory effect of mycophenolate mofetil in a murine model of pleurisy', *Exp Lung Res*, 37(7), pp. 399-407.
- Monson, C. A. and Sadler, K. C. (2010) 'Inbreeding depression and outbreeding depression are evident in wild-type zebrafish lines', *Zebrafish*, 7(2), pp. 189-197.
- Morrow, C. A., Lee, R. I., Chow, E. W. L., Ormerod, K. L., Goldinger, A., Byrnes III, E. J., Nielsen, K., Heitman, J., Schirra, H. J. and Fraser, J. A. (2012) 'A unique chromosomal rearrangement in the *Cryptococcus neoformans* var. *grubii* type strain enhances key phenotypes associated with virulence', *mBio*, 3(2), pp. e00310-e00311.
- Mortaz, E., Alipoor, S. D., Adcock, I. M., Mumby, S. and Koenderman, L. (2018) 'Update on Neutrophil Function in Severe Inflammation', *Front Immunol*, 9, pp. 2171.

- Mosser, D. M. and Edwards, J. P. (2008) 'Exploring the full spectrum of macrophage activation', *Nat Rev Immunol*, 8(12), pp. 958–969.
- Mourad, M., Malaise, J., Eddour, D. C., De Meyer, M., König, J., Schepers, R., Squifflet, J. P. and Wallemacq, P. (2001) 'Pharmacokinetic basis for the efficient and safe use of low-dose mycophenolate mofetil in combination with tacrolimus in kidney transplantation', *Clin Chem*, 47(7), pp. 1241–1248.
- Mukaremera, L., McDonald, T. R., Nielsen, J. N., Molenaar, C. J., Akampurira, A., Schutz, C., Taseera, K., Muzoora, C., Meintjes, G., Meya, D. B., Boulware, D. R. and Nielsen, K. (2019) 'The mouse inhalation model of *Cryptococcus neoformans* infection recapitulates strain virulence in humans and shows that closely related strains can possess differential virulence', *Infect Immun*, 87(5), pp. 1–17.
- Mukaremera, L. and Nielsen, K. (2017) 'Adaptive Immunity to *Cryptococcus neoformans* Infections', *J Fungi (Basel)*, 3(4), p. 64.
- Mukherjee, R., Kanti Barman, P., Kumar Thatoi, P., Tripathy, R., Kumar Das, B. and Ravindran, B. (2015) 'Non-Classical monocytes display inflammatory features: Validation in Sepsis and Systemic Lupus Erythematosus', *Sci Rep*, 5, pp. 13886.
- Muller, H. E. and Sethi, K. K. (1972) 'Proteolytic activity of *Cryptococcus neoformans* against human plasma proteins', *Med Microbiol Immunol*, 158(2), pp. 129–134.
- Müller, S., Faulhaber, A., Sieber, C., Pfeifer, D., Hochberg, T., Gansz, M., Deshmukh, S. D., Dauth, S., Brix, K., Saftig, P., Peters, C., Henneke, P. and Reinheckel, T. (2014) 'The endolysosomal cysteine cathepsins L and K are involved in macrophage-mediated clearance of *Staphylococcus aureus* and the concomitant cytokine induction', *FASEB J*, 28(1), pp. 162–175.
- Müller, S., Ronfani, L. and Bianchi, M. E. (2004) 'Regulated expression and subcellular localization of HMGB1, a chromatin protein with a cytokine function', *J Intern Med*, 255(3), pp. 332–343.
- Müller, U., Stenzel, W., Köhler, G., Werner, C., Polte, T., Hansen, G., Schütze, N., Straubinger, R. K., Blessing, M., McKenzie, A. N. J., Brombacher, F. and Alber, G. (2007) 'IL-13 induces disease-promoting type 2 cytokines, alternatively activated macrophages and allergic inflammation during pulmonary infection of mice with *Cryptococcus neoformans*', *J Immunol*, 179(8), pp. 5367–5377.
- Muller, W. A. (2002) 'Leukocyte-endothelial cell interactions in the inflammatory response', *Lab Invest*, 82(5), pp. 521–533.
- Muller, W. A. (2003) 'Leukocyte-endothelial-cell interactions in leukocyte transmigration and the inflammatory response', *Trends Immunol*, 24(6), pp. 326–333.
- Muller, W. A. (2013) 'Getting leukocytes to the site of inflammation', *Vet Pathol*, 50(1), pp. 7–22.
- Muntean, A. and Lucan, M. (2013) 'Transplantation immunosuppression in kidney transplantation', *Clujul Med*, 86(3), pp. 177–180.
- Muraille, E., De Trez, C., Pajak, B., Brait, M., Urbain, J. and Oberdan, L. (2002) 'T cell-dependent maturation of dendritic cells in response to bacterial superantigens', *J Immunol*, 168(9), pp. 4352–4360.
- Murphy, B. M., O'Neill, A. J., Adrain, C., Watson, R. W. G. and Martin, S. J. (2003)

- 'The apoptosome pathway to caspase activation in primary human neutrophils exhibits dramatically reduced requirements for cytochrome *c*', *J Exp Med*, 197(5), pp. 625–632.
- Murphy, M. P. (2009) 'How mitochondria produce reactive oxygen species', *Biochem J*, 417(1), pp. 1–13.
- Murray, H. W., Spitalny, G. L. and Nathan, C. F. (1985) 'Activation of mouse peritoneal macrophages in vitro and in vivo by interferon-gamma', *J Immunol*, 134(3), pp. 1619–1622.
- Murray, P. J., Allen, J. E., Fisher, E. A. and Lawrence, T. (2014) 'Macrophage activation and polarization: nomenclature and experimental guidelines', *Immunity*, 41(1), pp. 14–20.
- Mwale, A., Hummel, A., Mvaya, L., Kamng'ona, R., Chimbayo, E., Phiri, J., Malamba, R., Kankwatira, A., Mwandumba, H. C. and Jambo, K. C. (2017) 'B cell, CD8⁺ T cell and gamma delta T cell infiltration alters alveolar immune cell homeostasis in HIV-infected Malawian', *Wellcome Open Res*, 2, pp. 105.
- Myers, J. T. and Swanson, J. A. (2002) 'Calcium spikes in activated macrophages during Fcγ receptor-mediated phagocytosis', *J Leukoc Biol*, 72(4), pp. 677–684.
- Mylonakis, E., Ausubel, F. M., Perfect, J. R., Heitman, J. and Calderwood, S. B. (2002) 'Killing of *Caenorhabditis elegans* by *Cryptococcus neoformans* as a model of yeast pathogenesis', *Proc Natl Acad Sci U S A*, 99(24), pp. 15675–15680.
- Mylonakis, E., Moreno, R., El Khoury, J. B., Idnurm, A., Heitman, J., Calderwood, S. B., Ausubel, F. M. and Diener, A. (2005) '*Galleria mellonella* as a model system to study *Cryptococcus neoformans* pathogenesis', *Infect Immun*, 73(7), pp. 384238–384250.
- Mylonakis, E., Casadevall, A. and Ausubel, F. M. (2007) 'Exploiting amoeboid and non-vertebrate animal model systems to study the virulence of human pathogenic fungi', *PLoS Pathog*, 3(7), pp. 0859–0865.
- Nagai, M., Natsumeda, Y. and Weber, G. (1992) 'Proliferation-linked regulation of type II IMP dehydrogenase gene in human normal lymphocytes and HL-60 leukemic cells', *Cancer Res*, 52(2), pp. 258–261.
- Nagaoka, I., Niyonsaba, F., Tsutsumi-Ishii, Y., Tamura, H. and Hirata, M. (2008) 'Evaluation of the effect of human beta-defensins on neutrophil apoptosis', *Int Immunol*, 20(4), pp. 543–553.
- Nakamura, K., Kinjo, T., Saijo, S., Miyazato, A., Adachi, Y., Ohno, N., Fujita, J., Kaku, M., Iwakura, Y. and Kawakami, K. (2007) 'Dectin-1 is not required for the host defense to *Cryptococcus neoformans*', *Microbiol Immunol*, 51(11), pp. 1115–1119.
- Narasipura, S. D., Ault, J. G., Behr, M. J., Chaturvedi, V. and Chaturvedi, S. (2003) 'Characterization of Cu, Zn superoxide dismutase (SOD1) gene knock-out mutant of *Cryptococcus neoformans* var. *gattii*: role in biology and virulence', *Mol Microbiol*, 47(6), pp. 1681–1694.
- Nathan, C. (2002) 'Points of control in inflammation', *Nature*, 420(6917), pp. 846–852.
- Nathan, C. (2006) 'Neutrophils and immunity: challenges and opportunities', *Nat Rev*

- Immunol*, 6(3), pp. 173–182.
- Nathan, C. and Ding, A. (2010) 'Nonresolving Inflammation', *Cell*, 140(6), pp. 871–882.
- Nathan, C. F., Murray, H. W., Wlebe, I. E. and Rubin, B. Y. (1983) 'Identification of interferon-gamma as the lymphokine that activates human macrophage oxidative metabolism and antimicrobial activity', *J Exp Med.*, 158(3), pp. 670–689.
- Natsumeda, Y., Ohno, S., Kawasaki, H., Konno, Y., Weber, G. and Suzuki, K. (1990) 'Two distinct cDNAs for human IMP dehydrogenase', *J Biol Chem*, 265(9), pp. 5292–5295.
- Ndrepepa, G. (2019) 'Myeloperoxidase – A bridge linking inflammation and oxidative stress with cardiovascular disease', *Clin Chim Acta*, 493, pp. 36–51.
- Neal, L. M., Xing, E., Xu, J., Kolbe, J. L., Osterholzer, J. J., Segal, B. M., Williamson, P. R. and Olszewski, M. A. (2017) 'CD4⁺ T Cells Orchestrate Lethal Immune Pathology despite Fungal Clearance during *Cryptococcus neoformans* Meningoencephalitis', *mBio*, 8(6), pp. e01415-e01417.
- Neilson, J. B., Fromtling, R. A. and Bulmer, G. S. (1977) 'Cryptococcus neoformans: size range of infectious particles from aerosolized soil', *Infect Immun*, 17(3), pp. 634–638.
- Neilson, J. B., Ivey, M. H. and Bulmer, G. S. (1978) 'Cryptococcus neoformans: pseudohyphal forms surviving culture with *Acanthamoeba polyphaga*', *Infect Immun*, 20(1), pp. 262–266.
- Nelson, R. T., Hua, J., Pryor, B. and Lodge, J. K. (2001) 'Identification of virulence mutants of the fungal pathogen *Cryptococcus neoformans* using signature-tagged mutagenesis', *Genetics*, 157(3), pp. 935–947.
- Nett, J. E., Lepak, A. J., Marchillo, K. and Andes, D. R. (2011) 'Time course global gene expression analysis of an in vivo *Candida* biofilm', *J Infect Dis*, 200(2), pp. 307–313.
- Neurath, M. F., Wanitschke, R., Peters, M., Krummenauer, F., Meyer zum Büschenfelde, K. H. and Schlaak, J. F. (1998) 'Randomised trial of mycophenolate mofetil versus azathioprine for treatment of chronic active Crohn's disease', *Gut*, 44(5), pp. 625–628.
- Neuville, S., Dromer, F., Morin, O., Dupont, B., Ronin, O. and Lortholary, O. (2003) 'Primary cutaneous cryptococcosis: a distinct clinical entity', *Clin Infect Dis*, 36(3), pp. 337–347.
- Newton, K. and Dixit, V. M. (2012) 'Signaling in innate immunity and inflammation', *Cold Spring Harb Perspect Biol*, 4(3), p. a006049.
- Ng, L. G., Qin, J. S., Roediger, B., Wang, Y., Jain, R., Cavanagh, L. L., Smith, A. L., Jones, C. A., De Veer, M., Grimbaldeston, M. A., Meeusen, E. N. and Weninger, W. (2011) 'Visualizing the neutrophil response to sterile tissue injury in mouse dermis reveals a three-phase cascade of events', *J Invest Dermatol*, 131(10), pp. 2058–2068.
- Ngamskulrungrroj, P., Sorrell, T., Chindamporn, A., Chaiprasert, A., Poonwan, N. and Meyer, W. (2008) 'Association between fertility and molecular sub-type of global isolates of *Cryptococcus gattii* molecular type VGII', *Med Mycol*, 46(7), pp. 665–

- Ngamskulrungrroj, P., Gilgado, F., Faganello, J., Litvintseva, A. P., Leal, A. L., Tsui, K. M., Mitchell, T. G., Vainstein, M. H. and Meyer, W. (2009) 'Genetic diversity of the *Cryptococcus* species complex suggests that *Cryptococcus gattii* deserves to have varieties', *PLoS One*, 4(6), p. e5862.
- Ngamskulrungrroj, P., Himmelreich, U., Breger, J. A., Wilson, C., Chayakulkeeree, M., Krockenberger, M. B., Malik, R., Daniel, H. M., Toffaletti, D., Djordjevic, J. T., Mylonakis, E., Meyer, W. and Perfect, J. R. (2009) 'The trehalose synthesis pathway is an integral part of the virulence composite for *Cryptococcus gattii*', *Infect Immun*, 77(10), pp. 4584–4596.
- Ngamskulrungrroj, P., Price, J., Sorrell, T., Perfect, J. R. and Meyer, W. (2011) 'Cryptococcus gattii virulence composite: candidate genes revealed by microarray analysis of high and less virulent Vancouver island outbreak strains', *PLoS One*, 6(1), pp. e16076.
- Ngamskulrungrroj, P., Chang, Y., Roh, J. and Kwon-Chung, K. J. (2012) 'Differences in nitrogen metabolism between *Cryptococcus neoformans* and *C. gattii*, the two etiologic agents of cryptococcosis', *PLoS One*, 7(3), pp. e34258.
- Ngamskulrungrroj, P., Chang, Y., Sionov, E. and Kwon-Chung, K. J. (2012) 'The primary target organ of *Cryptococcus gattii* is different from that of *Cryptococcus neoformans* in a murine model', *mBio*, 3(3), pp. e00103-e00112.
- Nguyen, G. T., Green, E. R. and Meccas, J. (2017) 'Neutrophils to the ROScUE: Mechanisms of NADPH Oxidase Activation and Bacterial Resistance', *Front Cell Infect Microbiol*, 7, p. 373.
- Nicola, A. M., Albuquerque, P., Martinez, L. R., Dal-Rosso, R. A., Saylor, C., De Jesus, M., Nosanchuk, J. D. and Casadevall, A. (2012) 'Macrophage autophagy in immunity to *Cryptococcus neoformans* and *Candida albicans*', *Infect Immun*, 80(9), pp. 3065–3076.
- Nicola, A. M. and Robertson, E. J. (2011) 'Nonlytic exocytosis of *Cryptococcus neoformans* from macrophages occurs in vivo and is influenced by phagosomal pH', *mBio*, 2(4), pp. e00167-e00211.
- Nidhi, A., Meena, A., Sreekumar, A. and Daga, M. K. (2017) 'Corticosteroid-induced cryptococcal meningitis in patient without HIV', *BMJ Case Rep*, 4(2017), p. bcr 2016216496.
- Nielsen, K., Cox, G. M., Wang, P., Toffaletti, D. L., Perfect, J. R. and Heitman, J. (2003) 'Sexual cycle of *Cryptococcus neoformans* var. *grubii* and Virulence of congenic α and α isolates', *Infect Immun*, 71(9), pp. 4831–4841.
- Nielsen, K., Cox, G. M., Litvintseva, A. P., Mylonakis, E., Malliaris, S. D., Daniel, K., Jr, B., Giles, S. S., Mitchell, T. G., Perfect, J. R., Heitman, J., Benjamin, D. K. and Casadevall, A. (2005) '*Cryptococcus neoformans* { α } strains preferentially disseminate to the central nervous system during coinfection', *Infect Immun*, 73(8), pp. 4922–4933.
- Nielsen, K., De Obaldia, A. L. and Heitman, J. (2007) '*Cryptococcus neoformans* mates on pigeon guano: Implications for the realized ecological niche and globalization', *Eukaryot Cell*, 6(6), pp. 949–959.
- Nielsen, O. H., Vainer, B. and Rask-Madsen, J. (2001) 'Review aerticle: the treatment

- of inflammatory bowel disease with 6-mercaptopurine or azathioprine', *Aliment Pharmacol Ther*, 15(11), pp. 1699–1708.
- Nishida, N., Yasui, H., Nagane, M., Yamamori, T. and Inanami, O. (2014) '3-Methyl pyruvate enhances radiosensitivity through increasing mitochondria-derived reactive oxygen species in tumor cell lines', *J Radiat Res*, 55(3), pp. 455–463.
- Noel, P. J., Boise, L. H., Green, J. M. and Thompson, C. B. (1996) 'CD28 costimulation prevents cell death during primary T cell activation', *J Immunol*, 157(2), pp. 636–642.
- Nogueras, F., Espinosa, M. D., Mansilla, A., Torres, J. T., Cabrera, M. A. and Martín-Vivaldi, R. (2005) 'Mycophenolate Mofetil-Induced Neutropenia in Liver Transplantation', *Transplant Proc*, 37(3), pp. 1509–1511.
- Noris, M. and Remuzzi, G. (2013) 'Overview of complement activation and regulation', *Semin Nephrol*, 33(6), pp. 479–492.
- Nosanchuk, J. D., Rosas, A. L. and Casadevall, A. (1998) 'The antibody response to fungal melanin in mice', *J Immunol*, 160(12), pp. 6026–6031.
- Nourshargh, S., Hordijk, P. L. and Sixt, M. (2010) 'Breaching multiple barriers: Leukocyte motility through venular walls and the interstitium', *Nat Rev Mol Cell Biol*, 11(5), pp. 366–378.
- Nourshargh, S., Renshaw, S. A. and Imhof, B. A. (2016) 'Reverse Migration of Neutrophils: Where, When, How, and Why?', *Trends Immunol*, 37(5), pp. 273–286.
- Nowak, I. and Shaw, L. M. (1995) 'Mycophenolic acid binding to human serum albumin: characterization and relation to pharmacodynamics', *Clin Chem*, 41(7), pp. 1011–1017.
- Nunes, P. and Demaurex, N. (2010) 'The role of calcium signaling in phagocytosis', *J Leukoc Biol*, 88(1), pp. 57–68.
- Nüsslein-Volhard, C. and Dahm, R. (2002) 'Zebrafish: A Practical Approach', Oxford, Oxford University Press.
- O'Donnell, K., Keogh, B., Cantin, A. and Crystal, R. G. (1987) 'Pharmacologic suppression of the neutrophil component of the alveolitis in idiopathic pulmonary fibrosis', *Am Rev Respir Dis*, 136(2), pp. 288–292.
- O'Neill, S., O'Neill, A. J., Conroy, E., Brady, H. R., Fitzpatrick, J. M. and Watson, R. W. (2000) 'Altered caspase expression results in delayed neutrophil apoptosis in acute pancreatitis', *J Leukoc Biol*, 68(1), pp. 15–20.
- Odds, F. C., De Backer, T., Dams, G., Vranckx, L. and Woestenborghs, F. (1995) 'Oxygen as limiting nutrient for growth of *Cryptococcus neoformans*', *J Clin Microbiol*, 33(4), pp. 995–997.
- Odds, F. C., Oris, M., Van Dorsselaer, P. and Van Gerven, F. (2000) 'Activities of an intravenous formulation of itraconazole in experimental disseminated *Aspergillus*, *Candida*, and *Cryptococcus* infections', *Antimicrob Agents Chemother*, 44(11), pp. 3180–3183.
- Odom, A., Muir, S., Lim, E., Toffaletti, D. L., Perfect, J. and Heitman, J. (1997) 'Calcineurin is required for virulence of *Cryptococcus neoformans*', *EMBO J*, 16(10), pp. 2576–2589.

- Ofek, I., Goldhar, J. and Keisari, Y. (1995) 'Nonopsonic phagocytosis of microorganisms', *Annu Rev Microbiol*, 49, pp. 239–276.
- Ohkawa, I., Shiga, S. and Kageyama, M. (1979) 'An Esterase on the Outer of Long Membrane Chain of Pseudomonas Acyl Esters', *J Biochem*, 86(3), pp. 643–656.
- Okagaki, L. H., Wang, Y., Ballou, E. R., O'Meara, T. R., Bahn, Y. S., Alspaugh, J. A., Xue, C. and Nielsen, K. (2011) 'Cryptococcal Titan Cell Formation Is Regulated by G-Protein Signaling in Response to Multiple Stimuli', *Eukaryot Cell*, 10(10), pp. 1306–1316.
- Okagaki, L. H. and Nielsen, K. (2012) 'Titan cells confer protection from phagocytosis in *Cryptococcus neoformans* infections', *Eukaryot Cell*, 11(6), pp. 820–826.
- Okamura, A., Shimoyama, M., Ishii, S., Wakahashi, K., Asada, N., Kawano, H., Kawamori, Y., Nishikawa, S., Minagawa, K., Katayama, Y. and Matsui, T. (2011) 'Delayed neutrophil engraftment in cord blood transplantation with intensive administration of mycophenolate mofetil for GVHD prophylaxis', *Bone Marrow Transplant*, 46(1), pp. 148–149.
- Oladele, R. O., Bongomin, F., Gago, S. and Denning, D. W. (2017) 'HIV-associated cryptococcal disease in resource-limited settings: A case for "prevention is better than cure"?'', *J Fungi (Basel)*, 3(4), pp. 1–18.
- De Oliveira, S., Rosowski, E. E. and Huttenlocher, A. (2016) 'Neutrophil migration in infection and wound repair: going forward in reverse', *Nat Rev Immunol*, 16(6), pp. 378–391.
- de Oliveira Schneider, R., de Souza Süffert Fogaça, N., Kmetzsch, L., Schrank, A., Vainstein, M. H. and Staats, C. C. (2012) 'Zap1 regulates zinc homeostasis and modulates virulence in *Cryptococcus gattii*', *PLoS One*, 7(8), p. e43773.
- Olszewski, M. A., Noverr, M. C., Chen, G. H., Toews, G. B., Cox, G. M., Perfect, J. R. and Huffnagle, G. B. (2004) 'Urease Expression by *Cryptococcus neoformans* promotes microvascular sequestration, thereby enhancing central nervous system invasion', *Am J Pathol*, 164(5), pp. 1761–1771.
- Onishi, H. and Suzuki, T. (1968) 'Production of D-mannitol and glycerol by yeasts', *Appl Microbiol*, 16(12), pp. 1847–1852.
- Onyango, A. N. (2016) 'Endogenous generation of singlet oxygen and ozone in human and animal tissues: Mechanisms, biological significance, and influence of dietary components', *Oxid Med Cell Longev*, 2016, p. 2398573.
- Orij, R., Postmus, J., Ter Beek, A., Brul, S. and Smits, G. J. (2009) 'In vivo measurement of cytosolic and mitochondrial pH using a pH-sensitive GFP derivative in *Saccharomyces cerevisiae* reveals a relation between intracellular pH and growth', *Microbiology*, 155(1), pp. 268–278.
- Orij, R., Brul, S. and Smits, G. J. (2011) 'Intracellular pH is a tightly controlled signal in yeast', *Biochim Biophys*, 1810(10), pp. 933–944.
- Orr-Weaver, T. L., Szostak, J. W. and Rothstein, R. J. (1981) 'Yeast transformation: a model system for the study of recombination', *Proc Natl Acad Sci U S A*, 78(10), pp. 6354–6358.
- Orsini, J., Blaak, C., Tam, E., Rajayer, S. and Morante, J. (2016) 'Disseminated

- cryptococcal infection resulting in acute respiratory distress syndrome (ARDS) as the initial clinical presentation of AIDS', *Intern Med*, 55(8), pp. 995–998.
- Ortega-Gómez, A., Perretti, M. and Soehnlein, O. (2013) 'Resolution of inflammation: An integrated view', *EMBO Mol Med*, 5(5), pp. 661–674.
- Orvis, A. K., Wesson, S. K., Breza, T. S., Church, A. A., Mitchell, C. L. and Watkins, S. W. (2009) 'Mycophenolate mofetil in dermatology', *J Am Acad Dermatol*, 60(2), pp. 183–199.
- Ospelt, C. and Gay, S. (2010) 'TLRs and chronic inflammation', *Int J Biochem Cell Biol*, 42(4), pp. 495–505.
- Ost, K. S., O'Meara, T. R., Huda, N., Esher, S. K. and Alspaugh, J. A. (2015) 'The *Cryptococcus neoformans* Alkaline Response Pathway: Identification of a Novel Rim Pathway Activator', *PLoS Genet*, 11(4), pp. e1005159.
- Osterholzer, J. J., Surana, R., Milam, J. E., Montano, G. T., Chen, G.-H., Sonstein, J., Curtis, J. L., Huffnagle, G. B., Toews, G. B. and Olszewski, M. A. (2009) 'Cryptococcal urease promotes the accumulation of immature dendritic cells and a non-protective T2 immune response within the lung', *Am J Pathol*, 174(3), pp. 932–943.
- Osterholzer, J. J., Milam, J. E., Chen, G. H., Toews, G. B., Huffnagle, G. B. and Olszewski, M. A. (2009) 'Role of dendritic cells and alveolar macrophages in regulating early host defense against pulmonary infection with *Cryptococcus neoformans*', *Infect Immun*, 77(9), pp. 3749–3755.
- Otteson, E. W., Welch, W. H. and Kozel, T. R. (1994) 'Protein-Polysaccharide Interactions. A monoclonal antibody specific for the capsular polysaccharide of *Cryptococcus neoformans*', *J Biol Chem*, 269(3), pp. 1858–1864.
- Ozato, K., Tsujimura, H. and Tamura, T. (2002) 'Toll-like receptor signaling and regulation of cytokine gene expression in the immune system', *Biotechniques*, 33(suppl 66-8, 70, 72 passim).
- Pabst, M. J. and Johnston, R. B. (1980) 'Increased production of superoxide anion by macrophages exposed in vitro to muramyl dipeptide or lipopolysaccharide', *J Exp Med*, 151(1), pp. 101–114.
- Paiva, C. N. and Bozza, M. T. (2014) 'Are reactive oxygen species always detrimental to pathogens?', *Antioxid Redox Signal*, 20(6), pp. 1000–1034.
- Palmer, S. M., Baz, M. A., Sanders, L., Miralles, A. P., Lawrence, C. M., Rea, J. B., Zander, D. S., Edwards, L. J., Staples, E. D., Tapson, V. F. and Davis, R. D. (2001) 'Results of a randomized, prospective, multicenter trial of mycophenolate mofetil versus azathioprine in the prevention of acute lung allograft rejection', *Transplantation*, 71(12), pp. 1772–1776.
- Panieri, E. and Santoro, M. M. (2016) 'ROS homeostasis and metabolism: A dangerous liason in cancer cells', *Cell Death Dis*, 7(6), pp. e2253.
- Pappas, P. G. (2001) 'Therapy of cryptococcal meningitis in non-HIV-infected patients', *Curr Fungal Infect Rep*, 3(4), pp. 365–370.
- Pappas, P. G., Alexander, B. D., Andes, D. R., Hadley, S., Kauffman, C. A., Freifeld, A., Anaissie, E. J., Brumble, L. M., Herwaldt, L., Ito, J., Kontoyiannis, D. P., Lyon, G. M., Marr, K. A., Morrison, V. A., Park, B. J., Patterson, T. F., Perl, T.

- M., Oster, R. A., Schuster, M. G., *et al.* (2010) 'Invasive fungal infections among organ transplant recipients: results of the Transplant-Associated Infection Surveillance Network (TRANSNET)', *Clin Infect Dis*, 50(8), pp. 1101–1111.
- Park, B. J., Wannemuehler, K. A., Marston, B. J., Govender, N., Pappas, P. G. and Chiller, T. M. (2009) 'Estimation of the current global burden of cryptococcal meningitis among persons living with HIV/AIDS', *AIDS*, 23(4), pp. 525–530.
- Parker, W. P. (2009) 'Enzymology of purine and pyrimidine antimetabolites used in the treatment of cancer', *Chem Rev*, 109(7), pp. 2880–2893.
- Parkin, J. and Cohen, B. (2001) 'An overview of the immune system', *Lancet*, 357(9270), pp. 1777–1789.
- Pascon, R. C., Ganous, T. M., Kingsbury, J. M., Cox, G. M. and McCusker, J. H. (2004) 'Cryptococcus neoformans methionine synthase: Expression analysis and requirement for virulence', *Microbiology*, 150(Pt9), pp. 3013–3023.
- Passalacqua, K. D., Charbonneau, M.-E. and O'Riordan, M. X. D. (2016) 'Bacterial Metabolism Shapes the Host–Pathogen Interface', *Microbiol Spectr*, 4(3), pp. 1–30.
- Patel, A. A., Zhang, Y., Fullerton, J. N., Boelen, L., Rongvaux, A., Maini, A. A., Bigley, V., Flavell, R. A., Gilroy, D. W., Asquith, B., Macallan, D. and Yona, S. (2017) 'The fate and lifespan of human monocyte subsets in steady state and systemic inflammation', *J Exp Med*, 214(7), pp. 1913–1923.
- Patel, S. (2018) 'Danger-Associated Molecular Patterns (DAMPs): the Derivatives and Triggers of Inflammation', *Curr Allergy Asthma Rep*, 18(11), pp. 63.
- Patiño, M. A., Ortiz, J. P., Velásquez, M. and Stambuk, B. U. (2019) 'd -Xylose consumption by nonrecombinant *Saccharomyces cerevisiae*: A review ', *Yeast*, pp. 541–556.
- Pawłowska, J., Aleksandrak-Piekarczyk, T., Banach, A., Kiersztyn, B., Muszewska, A., Serewa, L., Szatraj, K. and Wrzosek, M. (2016) 'Preliminary studies on the evolution of carbon assimilation abilities within Mucorales', *Fungal Biol*, 120(5), pp. 752–763.
- Peacock, J. L. and Peacock, P. J. (2011) *Oxford handbook of medical statistics*. Edited by C. Barnes et al. Oxford, New York: Oxford University Press.
- Pearson, W. R. and Sierk, M. L. (2005) 'The limits of protein sequence comparison?', *Curr Opin Struct Biol*, 15(3), pp. 254–260.
- Peiseler, M. and Kubes, P. (2019) 'More friend than foe: The emerging role of neutrophils in tissue repair', *J Clin Invest*, 129(7), pp. 2629–2639.
- Peng, C. A., Gaertner, A. A. E., Henriquez, S. A., Fang, D., Colon-Reyes, R. J., Brumaghim, J. L. and Kozubowski, L. (2018) 'Fluconazole induces ROS in *Cryptococcus neoformans* and contributes to DNA damage in vitro', *PLoS One*, 13(12), p. e0208471.
- Perfect, J. R., Rude, T. H., Penning, L. M. and Johnson, S. A. (1992) 'Cloning the *Cryptococcus neoformans* TRP1 gene by complementation in *Saccharomyces cerevisiae*', *Gene*, 122(1), pp. 213–217.
- Perfect, J. R. (2006) '*Cryptococcus neoformans*: the yeast that likes it hot', *FEMS Yeast Res*, 6(4), pp. 463–468.

- Perfect, J. R., Dismukes, W. E., Dromer, F., Goldman, D. L., Graybill, J. R., Hamill, R. J., Harrison, T. S., Larsen, R. A., Lortholary, O., Nguyen, M. H., Pappas, P. G., Powderly, W. G., Singh, N., Sobel, J. D. and Sorrel, T. C. (2010) 'Clinical practice guidelines for the management of cryptococcal disease: 2010 update by the infectious diseases society of america', *Clin Infect Dis.*, 50(3), pp. 291–322.
- Perfect, J. R. and Bicanic, T. (2015) 'Cryptococcosis diagnosis and treatment: what do we know now', *Fungal Genet Biol*, 78, pp. 49–54.
- Perfect, J. R., Lang, S. D. and Durack, D. T. (1980) 'Chronic cryptococcal meningitis: a new experimental model in rabbits', *Am J Pathol*, 101(1), pp. 177–194.
- Pericolini, E., Gabrielli, E., Cenci, E., De Jesus, M., Bistoni, F., Casadevall, A. and Vecchiarelli, A. (2009) 'Involvement of glyco-receptors in galactoxylomannan-induced T cell death', *J Immunol*, 182(10), pp. 6003–6010.
- Perlman, H., Pagliari, L. J., Georganas, C., Mano, T., Walsh, K. and Pope, R. M. (1999) 'FLICE-inhibitory protein expression during macrophage differentiation confers resistance to fas-mediated apoptosis', *J Exp Med*, 190(11), pp. 1679–1688.
- Perretti, M., Leroy, X., Bland, E. J. and Montero-Melendez, T. (2015) 'Resolution Pharmacology: Opportunities for Therapeutic Innovation in Inflammation', *Trends Pharmacol Sci*, 36(11), pp. 737–755.
- Perry, S. (1971) 'Proliferation of myeloid cells', *Annu Rev Med*, 22, pp. 171–184.
- Petit, E., Langouet, S., Akhdar, H., Nicolas-Nicolaz, C., Guillouzo, A. and Morel, F. (2008) 'Differential toxic effects of azathioprine, 6-mercaptopurine and 6-thioguanine on human hepatocytes', *Toxicol in Vitro*, 22(3), pp. 632–642.
- Petri, B., Phillipson, M. and Kubes, P. (2008) 'The physiology of leukocyte recruitment: an in vivo perspective', *J Immunol*, 180(10), pp. 6439–6446.
- Petri, B. and Sanz, M. J. (2018) 'Neutrophil chemotaxis', *Cell Tissue Res*, 371(3), pp. 425–436.
- Petzold, E. W., Himmelreich, U., Mylonakis, E., Rude, T., Toffaletti, D., Cox, G. M., Miller, J. L. and Perfect, J. R. (2006) 'Characterization and regulation of the trehalose synthesis pathway and its importance in the pathogenicity of *Cryptococcus neoformans*', *Infect Immun*, 74(10), pp. 5877–5887.
- Pfeilschifter, J., Eberhardt, W., Hummel, R., Kunz, D., Mühl, H., Nitsch, D., Plüss, C. and Walker, G. (1996) 'Therapeutic strategies for the inhibition of inducible nitric oxide synthase- potential for a novel class of anti-inflammatory agents', *Cell Biol Int*, 20(1), pp. 51–58.
- Phadke, S. S., Feretzaki, M., Clancey, S. A., Mueller, O. and Heitman, J. (2014) 'Unisexual reproduction of *Cryptococcus gattii*', *PLoS One*, 9(10), p. e111089.
- Philips, B. J., Meguer, J. X., Redman, J. and Baker, E. H. (2003) 'Factors determining the appearance of glucose in upper and lower respiratory tract secretions', *Intensive Care Med*, 29(12), pp. 2204–2210.
- Phillipson, M., Heit, B., Parsons, S. A., Petri, B., Mullaly, S. C., Colarusso, P., Gower, R. M., Neely, G., Simon, S. I. and Kubes, P. (2009) 'Vav1 is Essential for Mechanotactic Crawling and Migration of Neutrophils out of the Inflamed

- Microvasculature', *J Immunol*, 182(11), pp. 6870–6878.
- Pillay, J., den Braber, I., Vrisekoop, N., Kwast, L. M., de Boer, R. J., Borghans, J. A., Tesselaar, K. and Koenderman, L. (2010) 'In vivo labeling with $^2\text{H}_2\text{O}$ reveals a human neutrophil lifespan of 5.4 days', *Blood*, 116(4), pp. 625–627.
- Pisoni, C. N., Sanchez, F. J., Karim, Y., Cuadrado, M. J., D'Cruz, D. P., Abbs, I. C., Khamasta, M. A. and Hughes, G. R. (2005) 'Mycophenolate mofetil in systemic lupus erythematosus: efficacy and tolerability in 86 patients', *J Rheumatol*, 32(6), pp. 1047–1052.
- Pitzurra, L., Cherniak, R., Giammarioli, M., Perito, S., Bistoni, F. and Vecchiarelli, A. (2000) 'Early induction of interleukin-12 by human monocytes exposed to *Cryptococcus neoformans* mannoproteins', *Infect Immun*, 68(2), pp. 558–563.
- del Poeta, M., Toffaletti, D. L., Rude, T. H., Sparks, S. D., Heitman, J. and Perfect, J. R. (1999) '*Cryptococcus neoformans* differential gene expression detected in vitro and in vivo with green fluorescent protein', *Infect Immun*, 67(4), pp. 1812–1820.
- Price, M. S., Betancourt-Quiroz, M., Price, J. L., Toffaletti, D. L., Vora, H., Hu, G., Kronstad, J. W., Perfect, J. R. (2011) '*Cryptococcus neoformans* requires a functional glycolytic pathway for disease but not persistence in the host', *mBio*, 2(3), pp. e00103-e00111.
- Profaci, C. P., Munji, R. N., Pulido, R. S. and Daneman, R. (2020) 'The blood-brain barrier in health and disease: Important unanswered questions', *J Exp Med*, 217(4), pp. e20190062.
- Progatzky, F., Dallman, M. J. and Lo Celso, C. (2013) 'From seeing to believing: Labelling strategies for in vivo cell-tracking experiments', *Interface Focus*, 3(3), p. 20130001.
- Pupjalis, D., Goetsch, J., Kottas, D. J., Gerke, V. and Rescher, U. (2011) 'Annexin A1 released from apoptotic cells acts through formyl peptide receptors to dampen inflammatory monocyte activation via JAK/STAT/SOCS signalling', *EMBO Mol Med*, 3(2), pp. 102–114.
- Qin, Q.M., Luo, J., Lin, X., Pei, J., Li, L., Ficht, T. A. and de Figueiredo, P. (2011) 'Functional analysis of host factors that mediate the intracellular lifestyle of *Cryptococcus neoformans*', *PLoS Pathog*, 7(6), pp. e1002078.
- Qiu, Y., Fairbanks, L. D., Rückemann, K., Hawrylowicz, C. M., Richards, D. F., Kirschbaum, B. and Simmonds, H. A. (2000) 'Mycophenolic acid-induced GTP depletion also affects ATP and pyrimidine synthesis in mitogen-stimulated primary human T-lymphocytes.', *Transplantation*, 69(5), pp. 890–897.
- Qu, C., Brinck-Jensen, N. S., Zang, M. and Chen, K. (2014) 'Monocyte-derived dendritic cells: Targets as potent antigen-presenting cells for the design of vaccines against infectious diseases', *Int J Infect Dis*, 19(1), pp. 1–5.
- Qureshi, A., Grey, A., Rose, K. L., Schey, K. L. and Del Poeta, M. (2011) '*Cryptococcus neoformans* modulates extracellular killing by neutrophils', *Front Microbiol*, 2, p. 193.
- Rabadi, M. M., Ghaly, T., Goligorsky, M. S. and Ratliff, B. B. (2012) 'HMGB1 in renal ischemic injury', *Am J Physiol Renal Physiol*, 303(6), pp. F873–F885.
- Radil, R., Beckman, J. S., Bush, K. M. and Freeman, B. A. (1991) 'Peroxyinitrite oxidation of sulfhydryls. The cytotoxic potential of superoxide and nitric oxide', *J*

Biol Chem, 266(7), pp. 4244–4250.

- Rajasekaran, K., Cary, J. W., Cotty, P. J. and Cleveland, T. E. (2008) 'Development of a GFP-expressing *Aspergillus flavus* strain to study fungal invasion, colonization, and resistance in cottonseed', *Mycopathologia*, 165(2), pp. 89–97.
- Rajasingham, R., Smith, R. M., Park, B. J., Jarvis, J. N., Govender, N. P., Chiller, T. M., Denning, D. W., Loyse, A. and Boulware, D. R. (2017) 'Global burden of disease of HIV-associated cryptococcal meningitis: an updated analysis', *Lancet Infect Dis*, 17(8), pp. 873–881.
- Rajasingham, R., Wake, R. M., Beyene, T., Katende, A., Letang, E. and Boulware, D. R. (2019) 'Cryptococcal Meningitis Diagnostics and Screening in the Era of Point-of-Care Laboratory Testing', *J Clin Microbiol*, 57(1), pp. e01238-18.
- Rajasingham, R., Meya, D. B. and Boulware, D. R. (2012) 'Integrating cryptococcal antigen screening and pre-emptive treatment into routine HIV care', *J Acquir Immune Defic Syndr*, 59(5), pp. e85-91.
- Ramos, C. L., Pou, S., Britigan, B. E., Cohen, M. S. and Rosen, G. M. (1992) 'Spin trapping evidence for myeloperoxidase-dependent hydroxyl radical formation by human neutrophils and monocytes', *J Biol Chem*, 267(12), pp. 8307–8312.
- Rath, P. C. and Aggarwal, B. B. (1999) 'TNF-induced signaling in apoptosis', *J Clin Immunol*, 19(6), pp. 350–364.
- Reardon, S. (2016) 'A mouse's house may ruin experiments', *Nature*, 530(7590), pp. 264.
- Rebers, P. A., Barker, S. A., Heidelberger, M., Dische, Z. and Evans, E. E. (1958) 'Precipitation of the Specific Polysaccharide of *Cryptococcus neoformans* A by Types II and XIV Antipneumococcal Sera', *J Am Chem Soc*, 80(5), pp. 1135–1137.
- Reed, J. C. (2002) 'Apoptosis-based therapies', *Nat Rev Drug Discov*, 1(2), pp. 111–121.
- Refinetti, R. and Menaker, M. (1992) 'The circadian rhythm of body temperature', *Physiol Behav*, 51(3), pp. 613–637.
- Reise Sousa, C. (2004) 'Activation of dendritic cells: Translating innate into adaptive immunity', *Curr Opin Immunol*, 16(1), pp. 21–25.
- Reiss, E., Cherniak, R., Eby, R. and Kaufman, L. (1984) 'Enzyme immunoassay detection of IgM to galactoxylomannan of *Cryptococcus neoformans*', *Diagn Immunol*, 2(2), pp. 109–115.
- Reiss, F. and Szilagyi, G. (1967) 'The effect of mammalian and avian sera on the growth of *Cryptococcus neoformans*', *J Invest Dermatol*, 48(3), pp. 264–265.
- Rennekamp, A. J. and Peterson, R. T. (2015) '15 years of zebrafish chemical screening', *Curr Opin Chem Biol*, 24, pp. 58–70.
- Renshaw, S. A., Loynes, C. A., Trushell, D. M., Elworthy, S., Ingham, P. W. and Whyte, M. K. (2006) 'A transgenic zebrafish model of neutrophilic inflammation', *Blood*, 108(13), pp. 3976–3978.
- Renshaw, S. A. and Trede, N. S. (2012) 'A model 450 million years in the making: zebrafish and vertebrate immunity', *Dis Models Mech*, 5(1), pp. 38–47.

- Rhein, J. and Boulware, D. (2012) 'Prognosis and management of cryptococcal meningitis in patients with human immunodeficiency virus infection', *Neurobehav HIV Med*, 4, pp. 45–61.
- Rhodes, J. C., Polacheck, I. and Kwon-Chung, K. J. (1982) 'Phenoloxidase activity and virulence in isogenic strains of *Cryptococcus neoformans*', *Infect Immun*, 36(3), pp. 1175–1184.
- Ries, L. N. A., Beattie, S., Cramer, R. A. and Goldman, G. H. (2018) 'Overview of carbon and nitrogen catabolite metabolism in the virulence of human pathogenic fungi', *Mol Microbiol*, 107(3), pp. 277–297.
- Rifaioğlu, E. N., Bülbül Şen, B., Ekiz, Ö. and Cigdem Dogramaci, A. (2014) 'Neutrophil to lymphocyte ratio in Behçet's disease as a marker of disease activity', *Acta Dermatovenerol Alp Pannonica Adriat*, 23(4), pp. 65–67.
- Ripoll, È., de Ramon, L., Draibe Bordignon, J., Merino, A., Bolaños, N., Goma, M., Cruzado, J. M., Grinyó, J. M. and Torras, J. (2016) 'JAK3-STAT pathway blocking benefits in experimental lupus nephritis', *Arthritis Res Ther*, 18(1), p. 134.
- Rittershaus, P. C., Kechichian, T. B., Allegood, J. C., Merrill, A. H. Jr, Hennig, M., Luberto, C. and Del Poeta, M. (2006) 'Glucosylceramide synthase is an essential regulator of pathogenicity of *Cryptococcus neoformans*', *J Clin Invest*, 116(6), pp. 1651–1659.
- Rivera, J., Feldmesser, M., Cammer, M. and Casadevall, A. (1998) 'Organ-dependent variation of capsule thickness in *Cryptococcus neoformans* during experimental murine infection', *Infect Immun*, 66(10), pp. 5027–5030.
- Robertson, A. L., Ogryzko, N. V., Henry, K. M., Loynes, C. A., Foulkes, M. J., Meloni, M. M., Wang, X., Ford, C., Jackson, M., Ingham, P. W., Wilson, H. L., Farrow, S. N., Solari, R., Flower, R. J., Jones, S., Whyte, M. K. and Renshaw, S. A. (2016) 'Identification of benzopyrone as a common structural feature in compounds with anti-inflammatory activity in a zebrafish phenotypic screen', *Dis Model Mech*, 9(6), pp. 621–632.
- Robertson, A. L. (2013) *A novel anti-inflammatory mechanism identified by an in vivo chemical genetic screen (PhD thesis)*. The University of Sheffield.
- Robertson, A. L., Holmes, G. R., Bojarczuk, A. N., Burgon, J., Loynes, C. A., Chimen, M., Sawtell, A. K., Hamza, B., Willson, J., Walmsley, S. R., Anderson, S. R., Coles, M. C., Farrow, S. N., Solari, R., Jones, S., Prince, L. R., Irimia, D., Rainger, G. E., Kadiramanathan, V., *et al.* (2014) 'A zebrafish compound screen reveals modulation of neutrophil reverse migration as an anti-inflammatory mechanism', *Sci Transl Med*, 6(225), p. 225ra29.
- Robertson, E. J., Najjuka, G., Rolfes, M. A., Akampurira, A., Jain, N., Anantharanjit, J., von Hohenberg, M., Tassieri, M., Carlsson, A., Meya, D. B., Harrison, T. S., Fries, B. C., Boulware, D. R. and Bicanic, T. (2014) '*Cryptococcus neoformans* ex vivo capsule size is associated with intracranial pressure and host immune response in hiv-associated cryptococcal meningitis', *J Infect Dis*, 209(1), pp. 74–82.
- Robertson, G. N., McGee, C. A., Dumbarton, T. C., Croll, R. P. and Smith, F. M. (2007) 'Development of the swimbladder and its innervation in the zebrafish,

- Danio rerio', *J Morphol*, 268(11), pp. 967–985.
- Robinson, J. M., Ohira, T. and Badwey, J. A. (2004) 'Regulation of the NADPH-oxidase complex of phagocytic leukocytes. Recent insights from structural biology, molecular genetics, and microscopy', *Histochem Cell Biol*, 122(4), pp. 293–304.
- Robinson, N., Ganesan, R., Hegedűs, C., Kovács, K., Kufer, T. A. and Virág, L. (2019) 'Programmed necrotic cell death of macrophages: Focus on pyroptosis, necroptosis, and parthanatos', *Redox Biol*, 26, pp. 101239.
- Rocha, J. D., Nascimento, M. T., Decote-Ricardo, D., Côrte-Real, S., Morrot, A., Heise, N., Nunes, M. P., Previato, J. O., Mendonça-Previato, L., DosReis, G. A., Saraiva, E. M. and Freire-de-Lima, C. G. (2015) 'Capsular polysaccharides from *Cryptococcus neoformans* modulate production of neutrophil extracellular traps (NETs) by human neutrophils', *Sci Rep*, 5, p. 8008.
- Rodrigues, M. L., Travassos, L. R., Miranda, K. R., Franzen, A. J., Rozental, S., de Souza, W., Alviano, C. S. and Barreto-Bergter, E. (2000) 'Human antibodies against a purified glucosylceramide from *Cryptococcus neoformans* inhibit cell budding and fungal growth', *Infect Immun*, 68(12), pp. 7049–7060.
- Rodrigues, M. L., Nimrichter, L., Oliveira, D. L., Frases, S., Miranda, K., Zaragoza, O., Alvarez, M., Nakouzi, A., Feldmesser, M. and Casadevall, A. (2007) 'Vesicular polysaccharide export in *Cryptococcus neoformans* is a eukaryotic solution to the problem of fungal trans-cell wall transport', *Eukaryot Cell*, 6(1), pp. 48–59.
- Rodrigues, M. L., Nakayasu, E. S., Oliveira, D. L., Nimrichter, L., Nosanchuk, J. D., Almeida, I. C. and Casadevall, A. (2008) 'Extracellular vesicles produced by *Cryptococcus neoformans* contain protein components associated with virulence', *Eukaryot Cell*, 7(1), pp. 58–67.
- Rodrigues, M. L., Nimrichter, L., Oliveira, D. L., Nosanchuk, J. D. and Casadevall, A. (2008) 'Vesicular Trans-Cell Wall Transport in Fungi: A Mechanism for the Delivery of Virulence-Associated Macromolecules?', *Lipid Insights*, 2, pp. 27–40.
- Romero, F., Rodríguez-Iturbe, B., Parra, G., González, L., Herrera-Acosta, J. and Tapia, E. (1999) 'Mycophenolate mofetil prevents the progressive renal failure induced by 5/6 renal ablation in rats', *Kidney Int*, 55(3), pp. 945–955.
- Riera Romo, M., Perez-Martinez, D. and Castillo Ferrer, C. (2016) 'Innate immunity in vertebrates : an overview', *Immunology*, 148(2), pp. 125–139.
- Roos, D., Lutter, R. and Bolscher, B. G. J. M. (1988) 'The Respiratory Burst and the NADPH Oxidase of Phagocytic Leukocytes', in Sbarra, A. J. and Strauss, R. R. (eds) *The Respiratory Burst and Its Physiological Significance*. Boston: Springer, pp. 53–54.
- Rosales, C., Demaurex, N., Lowell, C. A. and Uribe-Querol, E. (2016) 'Neutrophils: Their Role in Innate and Adaptive Immunity', *J Immunol Res*, 2016, p. 1469780.
- Rosales, C. (2017) 'Fcy Receptor Heterogeneity in Leukocyte Functional Responses', *Front Immunol*, 8, p. 280.
- Rosen, L. B., Freeman, A. F., Yang, L. M., Jutivorakool, K., Olivier, K. N., Angkasekwinai, N., Suputtamongkol, Y., Bennett, J. E., Pyrgos, V., Williamson, P. R., Ding, L., Holland, S. M. and Browne, S. K. (2013) 'Anti-GM-CSF

- autoantibodies in patients with cryptococcal meningitis', *J Immunol*, 190(8), pp. 3959–3966.
- Rosenwasser, L. J. (1998) 'Biologic activities of IL-1 and its role in human disease', *J Allergy Clin Immunol*, 102(3), pp. 344–350.
- Rosowski, E. E., Knox, B. P., Archambault, L. S., Huttenlocher, A., Keller, N. P., Wheeler, R. T. and Davis, J. M. (2018) 'The Zebrafish as a Model Host for Invasive Fungal Infections', *J Fungi (Basel)*, 4(4), p. 136.
- Rossi, A. G., Sawatzky, D. A., Walker, A., Ward, C., Sheldrake, T. A., Riley, N. A., Caldicott, A., Martinez-Losa, M., Walker, T. R., Duffin, R., Gray, M., Crescenzi, E., Martin, M. C., Brady, H. J., Savill, J. S., Dransfield, I. and Haslett, C. (2006) 'Cyclin-dependent kinase inhibitors enhance the resolution of inflammation by promoting inflammatory cell apoptosis', *Nat Med*, 12(9), pp. 1056–1064.
- van Rossum, H. M., Kozak, B. U., Niemeijer, M. S., Duine, H. J., Luttik, M. A., Boer, V. M., Kötter, P., Daran, J. M., van Maris, A. J. and Pronk, J. T. (2016) 'Alternative reactions at the interface of glycolysis and citric acid cycle in *Saccharomyces cerevisiae*', *FEMS Yeast Res*, 16(3), p. fow017.
- Rubartelli, A., Lotze, M. T., Latz, E. and Manfredi, A. (2013) 'Mechanisms of sterile inflammation', *Front Immunol*, 4, pp. 398.
- Rubin, R. H., Wolfson, J. S., Cosimi, A. B. and Tolkoff-Rubin, N. E. (1981) 'Infection in the renal transplant recipient', *Am J Med*, 70(2), pp. 405–411.
- Rude, T. H., Toffaletti, D. L., Cox, G. M. and Perfect, J. R. (2002) 'Relationship of the glyoxylate pathway to the pathogenesis of *Cryptococcus neoformans*', *Infect Immun*, 70(10), pp. 5684–5694.
- Rudman, J., Evans, R. J. and Johnston, S. A. (2019) 'Are macrophages the heroes or villains during cryptococcosis?', *Fungal Genet Biol*, 132, pp. 103261.
- Ruedl, C., Kopf, M. and Bachmann, M. F. (1999) 'CD8(+) T cells mediate CD40-independent maturation of dendritic cells in vivo', *J Exp Med*, 189(12), pp. 1875–1884.
- Russell, J. B. and Forsberg, N. (1986) 'Production of tricarballic acid by rumen microorganisms and its potential toxicity in ruminant tissue metabolism', *Br J Nutr*, 56(1), pp. 153–162.
- Saag, M. S., Powderly, W. G., Cloud, G. A., Robinson, P., Grieco, M. H., Sharkey, P. K., Thompson, S. E., Sugar, A. M., Tuazon, C. U., Fisher, J. F., *et al.* (1992) 'Comparison of amphotericin B with fluconazole in the treatment of acute AIDS-associated cryptococcal meningitis', *N Engl J Med*, 326(2), pp. 83-89.
- Saag, M. S., Graybill, R. J., Larsen, R. A., Pappas, P. G., Perfect, J. R., Powderly, W. G., Sobel, J. D. and Dismukes, W. E. (2000) 'Practice guidelines for the management of cryptococcal disease. Infectious Diseases Society of America', *Clin Infect Dis*, 30(4), pp. 710–718.
- Sabiiti, W., Robertson, E., Beale, M., Johnston, S. A., Brouwer, A. E., Loyse, A., Jarvis, J. N., Gilbert, A. S., Fisher, M. C., Harrison, T. S., May, R. C. and Bicanic, T. (2014) 'Efficient phagocytosis and laccase activity are associated with adverse clinical outcome of HIV-associated cryptococcosis', *J Clin Invest*, 124(5), pp.2000-2008.

- Sabiiti, W., May, R. C. and Pursall, E. R. (2012) 'Experimental models of cryptococcosis', *Int J Microbiol*, 2012, pp. 626745.
- Sadik, C. D. and Luster, A. D. (2012) 'Lipid-cytokine-chemokine cascades orchestrate leukocyte recruitment in inflammation', *J Leukoc Biol*, 91(2), pp. 207–215.
- Saijo, T., Chen, J., Chen, S. C., Rosen, L. B., Yi, J., Sorrell, T. C., Bennett, J. E., Holland, S. M., Browne, S. K. and Kwon-chung, K. J. (2014) 'Autoantibodies are a risk factor for central nervous system infection by *Cryptococcus gattii* in otherwise immunocompetent patients', *mBio*, 5(2), pp. e00912-e00914.
- Sampath, P., Moideen, K., Ranganathan, U. D. and Bethunaickan, R. (2018) 'Monocyte Subsets: Phenotypes and Function in Tuberculosis Infection', *Front Immunol*, 9, pp. 1726.
- Sándor, N., Lukácsi, S., Ungai-Salánki, R., Orgován, N., Szabó, B., Horváth, R., Erdei, A. and Bajtay, Z. (2016) 'CD11c/CD18 Dominates Adhesion of Human Monocytes, Macrophages and Dendritic Cells over CD11b/CD18', *PLoS One*, 11(9), p. e0163120.
- Santi, L., Beys-da-Silva, W. O., Berger, M., Calzolari, D., Guimarães, J. A., Moresco, J. J. and Yates, J. R. 3rd. (2014) 'Proteomic profile of *Cryptococcus neoformans* biofilm reveals changes in metabolic processes', *J Proteome Res*, 13(3), pp. 1545–1559.
- van der Sar, A. M., Appelmek, B. J., Vandenbroucke-Grauls, C. M. and Bitter, W. (2004) 'A star with stripes: zebrafish as an infection model', *Trends Microbiol*, 12(10), pp. 451–457.
- Savill, J. and Haslett, C. (1995) 'Granulocyte clearance by apoptosis in the resolution of inflammation', *Semin Cell Biol*, 6(6), pp. 385–393.
- Savill, J. S., Wyllie, A. H., Henson, J. E., Walport, M. J., Henson, P. M. and Haslett, C. (1989) 'Macrophage phagocytosis of aging neutrophils in inflammation. Programmed cell death in the neutrophil leads to its recognition by macrophages', *J Clin Invest*, 83(3), pp. 865–875.
- Sawyer, D. W., Sullivan, J. A. and Mandell, G. L. (1985) 'Intracellular free calcium localization in neutrophils during phagocytosis', *Science*, 230(4726), pp. 663–666.
- Scaffidi, P., Misteli, T. and Bianchi, M. E. (2002) 'Release of chromatin protein HMGB1 by necrotic cells triggers inflammation', *Nature*, 418(6894), pp. 191–195.
- Schaefer, L. (2014) 'Complexity of danger: the diverse nature of damage-associated molecular patterns', *J Biol Chem*, 289(51), pp. 35237–35245.
- Schett, G. and Neurath, M. F. (2018) 'Resolution of chronic inflammatory disease: universal and tissue-specific concepts', *Nat Commun*, 9(1), pp. 3261.
- Schirmer, R. H., Adler, H., Pickhardt, M. and Mandelkow, E. (2011) "Lest we forget you - methylene blue...", *Neurobiol Aging*, 32(12), pp. 2325.e7-2325.e16.
- Schleimer, R. P., Kato, A., Kern, R., Kuperman, D. and Avila, P. C. (2007) 'Epithelium: at the interface of innate and adaptive immune responses', *J Allergy Clin Immunol*, 120(6), pp. 1279–1284.
- Schmeding, K. A., Jong, S. C. and Hugh, R. (1984) 'Biochemical variation of *Cryptococcus neoformans*', *Mycopathologia*, 84(2–3), pp. 121–131.

- Schmidt, A. M., Yan, S. D., Brett, J., Mora, R., Nowygrod, R. and Stern, D. (1993) 'Regulation of human mononuclear phagocyte migration by cell surface-binding proteins for advanced glycation end products', *J Clin Invest*, 91(5), pp. 2155–2168.
- Schmidt, S., Zimmermann, S. Y., Tramsen, L., Koehl, U. and Lehrnbecher, T. (2013) 'Natural killer cells and antifungal host response', *Clin Vaccine Immunol*, 20(4), pp. 452–458.
- Selders, G. S., Fetz, A. E., Radic, M. Z. and Bowlin, G. L. (2017) 'An overview of the role of neutrophils in innate immunity, inflammation and host-biomaterial integration', *Regen Biomater*, 4(1), pp. 55–68.
- Senghor, Y., Guitard, J., Angoulvant, A. and Hennequin, C. (2018) 'Cryptococcal antigen detection in broncho-alveolar lavage fluid', *Med Mycol*, 56(6), pp. 774–777.
- Seok, J., Warren, H. S., Cuenca, A. G., Mindrinos, M. N., Baker, H. V., Xu, W., Richards, D. R., McDonald-Smith, G. P., Gao, H., Hennessy, L., Finnerty, C. C., López, C. M., Honari, S., Moore, E. E., Minei, J. P., Cuschieri, J., Bankey, P. E., Johnson, J. L., Sperry, J., *et al.* (2013) 'Genomic responses in mouse models poorly mimic human inflammatory diseases', *Proc Natl Acad Sci U S A*, 110(9), pp. 3507–3512.
- Sepulcre, M. P., Alcaraz-Pérez, F., López-Muñoz, A., Roca, F. J., Meseguer, J., Cayuela, M. L. and Mulero, V. (2009) 'Evolution of lipopolysaccharide (LPS) recognition and signaling: fish TLR4 does not recognize LPS and negatively regulates NF-kappaB activation', *J Immunol*, 182(4), pp. 1836–1845.
- Serbina, N. V., Jia, T., Hohl, T. M. and Pamer, E. G. (2008) 'Monocyte-mediated defense against microbial pathogens', *Annu Rev Immunol*, 26, pp. 412–452.
- Serbina, N. V. and Pamer, E. G. (2006) 'Monocyte emigration from bone marrow during bacterial infection requires signals mediated by chemokine receptor CCR2', *Nat Immunol*, 7(3), pp. 311–317.
- Serhan, C. N. (2007) 'Resolution phase of inflammation: novel endogenous anti-inflammatory and proresolving lipid mediators and pathways', *Annu Rev Immunol*, 25(1), pp. 101–137.
- Serhan, C. N. and Levy, B. D. (2018) 'Resolvins in inflammation: emergence of the pro-resolving superfamily of mediators', *J Clin Invest*, 128(7), pp. 2657–2669.
- Serhan, C. N. and Savill, J. (2005) 'Resolution of inflammation: the beginning programs the end', *Nat Immunol*, 6(12), pp. 1191–1197.
- Shah, K. K., Pritt, B. S. and Alexander, M. P. (2017) 'Histopathologic review of granulomatous inflammation', *J Clin Tuberc Other Mycobact Dis*, 7, pp. 1–12.
- Shah, S. I., Bui, H., Velasco, N. and Rungta, S. (2017) 'Incidental Finding of Cryptococcus on Prostate Biopsy for Prostate Adenocarcinoma Following Cardiac Transplant: Case Report and Review of the Literature', *Am J Case Rep*, 18, pp. 1171–1180.
- Shah, S. K., Phan, N. B., Goyal, G. and Sharma, G. (2010) 'Pulmonary alveolar proteinosis in a 67-year-old woman with Wegener's granulomatosis', *J Gen Intern Med*, 25(10), pp. 1105–1108.

- Shang, L., Ananthakrishnan, R., Li, Q., Quadri, N., Abdillahi, M., Zhu, Z., Qu, W., Rosario, R., Touré, F., Yan, S. F., Schmidt, A. M. and Ramasamy, R. (2010) 'RAGE modulates hypoxia/reoxygenation injury in adult murine cardiomyocytes via JNK and GSK-3 β signaling pathways', *PLoS ONE* 5(4), pp. e10092.
- Shao, W. H. and Cohen, P. L. (2011) 'Disturbances of apoptotic cell clearance in systemic lupus erythematosus', *Arthritis Res Ther*, 13(1), p.202.
- Shapiro, R., Jordan, M. L., Scantlebury, V. P., Vivas, C., Marsh, J. W., McCauley, J., Johnston, J., Randhawa, P., Irish, W., Gritsch, H. A., Naraghi, R., Hakala, T. R., Fung, J. J. and Starzl, T. E. (1999) 'A prospective, randomized trial of tacrolimus/prednisone versus tacrolimus/prednisone/mycophenolate mofetil in renal transplant recipients', *Transplantation*, 67(3), pp. 411–415.
- Shapiro, S., Beenhouwer, D. O., Feldmesser, M., Taborda, C., Carroll, M. C. Casadevall, A., Scharff, M. D. (2002) 'Immunoglobulin G monoclonal antibodies to *Cryptococcus neoformans* protect mice deficient in complement component C3', *Infect Immun*, 70(5), pp. 2598–2604.
- Shaw, L. M., Mick, R., Nowak, I., Korecka, M. and Brayman, K. L. (1998) 'Pharmacokinetics of mycophenolic acid in renal transplant patients with delayed graft function', *J Clin Pharmacol*, 38(3), pp. 268–275.
- Shaw, L. M., Figurski, M., Milone, M. C., Trofe, J. and Bloom, R. D. (2007) 'Therapeutic drug monitoring of mycophenolic acid', *Clin J Am Soc Nephrol*, 2(5), pp. 1062–1072.
- Shaw, P. J., McDermott, M. F. and Kanneganti, T. D. (2011) 'Inflammasomes and autoimmunity', *Trends Mol Med*, 17(2), pp. 57–64.
- O'Shea, J. J. and Murray, P. J. (2008) 'Cytokine signaling modules in inflammatory responses', *Immunity*, 28(4), pp. 477–487.
- Shelburne, S. A. 3rd, Darcourt, J., White, A. C. Jr, Greenberg, S. B., Hamill, R. J., Atmar, R. L. and Visnegarwala, F. (2005) 'The role of immune reconstitution inflammatory syndrome in AIDS-related *Cryptococcus neoformans* disease in the era of highly active antiretroviral therapy', *Clin Infect Dis*, 40(7), pp. 1049–1052.
- Shen, H., Kreisel, D. and Goldstein, D. R. (2013) 'Processes of sterile inflammation', *J Immunol*, 191(6), pp. 2857–2863.
- Shi, C. and Pamer, E. G. (2011) 'Monocyte recruitment during infection and inflammation', *Nat Rev Immunol*, 11(11), pp. 762–774.
- Shi, Y., Evans, J. E. and Rock, K. L. (2003) 'Molecular identification of a danger signal that alerts the immune system to dying cells', *Nature*, 425(6957), pp. 516–521.
- Shibata, Y., Berclaz, P. Y., Chroneos, Z. C., Yoshida, M., Whitsett, J. A. and Trapnell, B. C. (2001) 'GM-CSF regulates alveolar macrophage differentiation and innate immunity in the lung through PU.1', *Immunity*, 15(4), pp. 557–567.
- Shimizu, K. and Matsuoka, Y. (2019) 'Redox rebalance against genetic perturbations and modulation of central carbon metabolism by the oxidative stress regulation', *Biotechnol Adv*, 37(8), p. 107441.
- Sierra, G. (1957) 'A simple method for the detection of lipolytic activity of microorganisms and some observations on the influence of the contact between cells

- and fatty substrates', *Antonie Van Leeuwenhoek*, 23(1), pp. 15–22.
- Silva, M. G., Schrank, A., Bailão, E. F., Bailão, A. M., Borges, C. L., Staats, C. C., Parente, J. A., Pereira, M., Salem-Izacc, S. M., Mendes-Giannini, M. J., Oliveira, R. M., Silva, L. K., Nosanchuk, J. D., Vainstein, M. H. and de Almeida Soares, C. M. (2011) 'The homeostasis of iron, copper, and zinc in *paracoccidioides brasiliensis*, *cryptococcus neoformans* var. *Grubii*, and *cryptococcus gattii*: a comparative analysis', *Front Microbiol*, 2, p. 49.
- Silveira, F. P., Husain, S., Kwak, E. J., Linden, P. K., Marcos, A., Shapiro, R., Fontes, P., Marsh, J. W., de Vera, M., Tom, K., Thai, N., Tan, H. P., Basu, A., Soltys, K. and Paterson, D. L. (2007) 'Cryptococcosis in liver and kidney transplant recipients receiving anti-thymocyte globulin or alemtuzumab', *Transpl Infect Dis*, 9(1), pp. 22–27.
- Simmer, J. P., Kelly, R. E., Rinker, A. G. Jr, Zimmermann, B. H., Scully, J. L., Kim, H. and Evans, D. R. (1990) 'Mammalian dihydroorotase: nucleotide sequence, peptide sequences, and evolution of the dihydroorotase domain of the multifunctional protein CAD', *Proc Natl Acad Sci U S A*, 87(1), pp. 174–178.
- Simsek, M., Meijer, B., Mulder, C. J. J., van Bodegraven, A. A. and de Boer, N. K. H. (2017) 'Analytical Pitfalls of Therapeutic Drug Monitoring of Thiopurines in Patients With Inflammatory Bowel Disease', *Ther Drug Monit*, 39(6), pp. 584–588.
- Singh, J. (2012) 'The national centre for the replacement, refinement, and reduction of animals in research', *J Pharmacol Pharmacother*, 3(1), pp. 87–89.
- Singh, N., Alexander, B. D., Lortholary, O., Dromer, F., Gupta, K. L., John, G. T., del Busto, R., Klintmalm, G. B., Somani, J., Lyon, G. M., Pursell, K., Stosor, V., Munoz, P., Limaye, A. P., Kalil, A. C., Pruett, T. L., Garcia-Diaz, J., Humar, A., Houston, S., *et al.* (2007) 'Cryptococcus neoformans in organ transplant recipients: impact of calcineurin-inhibitor agents on mortality', *J Infect Dis*, 195(5), pp. 756–764.
- Sionov, E., Mayer-Barber, K. D., Chang, Y. C., Kauffman, K. D., Eckhaus, M. A., Salazar, A. M., Barber, D. L. and Kwon-Chung, K. J. (2015) 'Type I IFN Induction via Poly-ICLC Protects Mice against Cryptococcosis', *PLoS Pathog*, 11(8), p. e1005040.
- Skolnick, J. and Fetrow, J. S. (2000) 'From genes to protein structure and function: Novel applications of computational approaches in the genomic era', *Trends Biotechnol*, 18(1), pp. 34–39.
- Slee, E. A., Zhu, H., Chow, S. C., MacFarlane, M., Nicholson, D. W. and Cohen, G. M. (1996) 'Benzyloxycarbonyl-Val-Ala-Asp (OMe) fluoromethylketone (Z-VAD.FMK) inhibits apoptosis by blocking the processing of CPP32', *Biochem J*, 315(Pt1)(Pt1), pp. 21–24.
- Smak Gregoor, P. J., Hesse, C. J., van Gelder, T., van der Mast, B. J., IJzermans, J. N., van Besouw, N. M. and Weimar, W. (1998) 'Relation of mycophenolic acid trough levels and adverse events in kidney allograft recipients', *Transplant Proc*, 30(4), pp. 1192–1193.
- Smak Gregoor, P. J., van Gelder, T. and Weimar, W. (2000) 'Mycophenolate mofetil, Cellcept, a new immunosuppressive drug with great potential in internal

- medicine', *Neth J Med*, 57(6), pp. 233–246.
- Sobiak, J., Kamińska, J., Glyda, M., Duda, G. and Chrzanowska, M. (2013) 'Effect of mycophenolate mofetil on hematological side effects incidence in renal transplant recipients', *Clin Transplant*, 27(4), pp. E407–414.
- Sollinger, H. W. (2004) 'Mycophenolates in transplantation', *Clin Transplant*, 18(5), pp. 485–492.
- Soltani, M., Bayat, M., Hashemi, S. J., Zia, M. and Pestechian, N. (2013) 'Isolation of *Cryptococcus neoformans* and other opportunistic fungi from pigeon droppings', *J Res Med Sci*, 18(1), pp. 56–60.
- Sookhai, S., Wang, J. J., McCourt, M., Kirwan, W., Bouchier-Hayes, D. and Redmond, P. (2002) 'A novel therapeutic strategy for attenuating neutrophil-mediated lung injury in vivo', *Ann Surg*, 235(2), pp. 285–291.
- Sorci, G., Riuzzi, F., Giambanco, I. and Donato, R. (2013) 'RAGE in tissue homeostasis, repair and regeneration', *Biochim Biophys Acta*, 1833(1), pp. 101–109.
- Sorrell, T. C. (2001) '*Cryptococcus neoformans* variety *gattii*', *Med Mycol*, 39(2), pp. 155–168.
- Spaink, H. P., Cui, C., Wiweger, M. I., Jansen, H. J., Veneman, W. J., Marín-Juez, R., de Sonnevile, J., Ordas, A., Torraca, V., van der Ent, W., Leenders, W. P., Meijer, A. H., Snaar-Jagalska, B. E. and Dirks, R. P. (2013) 'Robotic injection of zebrafish embryos for high-throughput screening in disease models', *Methods*, 62(3), pp. 246–254.
- Sparrer, K. M. and Gack, M. U. (2016) 'Intracellular detection of viral nucleic acids', *Curr Opin Microbiol*, 26, pp. 1–9.
- Specht, C. A., Lee, C. K., Huang, H., Tipper, D. J., Shen, Z. T., Lodge, J. K., Leszyk, J., Ostroff, G. R. and Levitz, S. M. (2015) 'Protection against Experimental Cryptococcosis following Vaccination with Glucan Particles Containing *Cryptococcus* Alkaline Extracts', *mBio*, 6(6), pp. e01905-e01915.
- Specht, C. A., Lee, C. K., Huang, H., Hester, M. M., Liu, J., Luckie, B. A., Torres Santana, M. A., Mirza, Z., Khoshkenar, P., Abraham, A., Shen, Z. T., Lodge, J. K., Akalin, A., Homan, J., Ostroff, G. R. and Levitz, S. M. (2017) 'Vaccination with Recombinant *Cryptococcus* Proteins in Glucan Particles Protects Mice against Cryptococcosis in a Manner Dependent upon Mouse Strain and *Cryptococcal* Species', *mBIO*, 8(6), pp. e01872-e01917.
- Speed, B. and Dunt, D. (1995) 'Clinical and host differences between infections with the two varieties of *Cryptococcus neoformans*', *Clin Infect Dis*, 21(1), pp. 28–34.
- Sprague, A. H. and Khalil, R. A. (2009) 'Inflammatory cytokines in vascular dysfunction and vascular disease', *Biochem Pharmacol*, 78(6), pp. 539–552.
- Springer, D. J., Phadke, S., Billmyre, B. and Heitman, J. (2012) '*Cryptococcus gattii*, no longer an accidental pathogen?', *Curr Fungal Infect Rep*, 6(4), pp. 245–256.
- Springer, D. J., Billmyre, R. B., Filler, E. E., Voelz, K., Pursall, R., Mieczkowski, P. A., Larsen, R. A., Dietrich, F. S., May, R. C., Filler, S. G. and Heitman, J. (2014) '*Cryptococcus gattii* VGIII isolates causing infections in HIV/AIDS patients in Southern California: identification of the local environmental source as arboreal',

PLoS Pathog, 10(8), p. e1004285.

- Springer, T. A. (1994) 'Traffic signals of lymphocyte recirculation and leucocyte emigration: the multistep paradigm', *Cell*, 76(2), pp. 301–314.
- Steele, K. T., Thakur, R., Nthobatsang, R., Steenhoff, A. P. and Bisson, G. P. (2010) 'In-hospital mortality of HIV-infected cryptococcal meningitis patients with *C. gattii* and *C. neoformans* infection in Gaborone, Botswana', *Med Mycol*, 48(8), pp. 1112–1115.
- Steen, B. R., Zuyderduyn, S., Toffaletti, D. L., Marra, M., Jones, S. J., Perfect, J. R. and Kronstad, J. (2003) 'Cryptococcus neoformans gene expression during experimental cryptococcal meningitis', *Eukaryot Cell*, 2(6), pp. 1336–1349.
- Steenbergen, J. N. and Casadevall, A. (2000) 'Prevalence of *Cryptococcus neoformans* var. *neoformans* (Serotype D) and *Cryptococcus neoformans* var. *grubii* (Serotype A) isolates in New York City', *J Clin Microbiol*, 38(5), pp. 1974–1976.
- Steenbergen, J. N. and Casadevall, A. (2003) 'The origin and maintenance of virulence for the human pathogenic fungus *Cryptococcus neoformans*', *Microbes Infect*, 5(7), pp. 667–675.
- Steenbergen, J. N., Shuman, H. A. and Casadevall, A. (2001) 'Cryptococcus neoformans interactions with amoebae suggest an explanation for its virulence and intracellular pathogenic strategy in macrophages', *Proc Natl Acad Sci U S A*, 98(26), pp. 15245–15250.
- Stein, M., Keshav, S., Harris, N. and Gordon, S. (1992) 'Interleukin 4 potently enhances murine macrophage mannose receptor activity: a marker of alternative immunologic macrophage activation', *J Exp Med*, 176(1), pp. 287–292.
- Stephen, C., Lester, S., Black, W., Fyfe, M. and Raverty, S. (2002) 'Multispecies outbreak of cryptococcosis on southern Vancouver Island, British Columbia', *Can Vet J*, 43(10), pp. 792–794.
- Stöhr, R., Deckers, N., Schurgers, L., Marx, N. and Reutelingsperger, C. P. (2018) 'AnnexinA5-pHrodo: a new molecular probe for measuring efferocytosis', *Sci Rep*, 8(1), p. 17731.
- van de Stolpe, A. and van der Saag, P. T. (1996) 'Intercellular adhesion molecule-1', *J Mol Med*, 74(1), pp. 13–33.
- Strober, W., Murray, P. J., Kitani, A. and Watanabe, T. (2006) 'Signalling pathways and molecular interactions of NOD1 and NOD2', *Nat Rev Immunol*, 6(1), pp. 9–20.
- Suárez-Peñaranda, J. M., Rodríguez-Calvo, M. S., Ortiz-Rey, J. A., Muñoz, J. I., Sánchez-Pintos, P., Da Silva, E. A., De la Fuente-Buceta, A. and Concheiro-Carro, L. (2002) 'Demonstration of apoptosis in human skin injuries as an indicator of vital reaction', *Int J Legal Med*, 116(2), pp. 109–112.
- Sugimoto, M. A., Vago, J. P., Teixeira, M. M. and Sousa, L. P. (2016) 'Annexin A1 and the Resolution of Inflammation: Modulation of Neutrophil Recruitment, Apoptosis, and Clearance', *J Immunol Res*, 2016, p. 8239258.
- Sugimoto, M. A., Sousa, L. P., Pinho, V., Perretti, M. and Teixeira, M. M. (2016)

- 'Resolution of Inflammation: What Controls Its Onset?', *Front Immunol*, 7, p. 160.
- Sugioka, R., Shimizu, S. and Tsujimoto, Y. (2004) 'Fzo1, a protein involved in mitochondrial fusion, inhibits apoptosis', *J Biol Chem*, 279(50), pp. 52726–52734.
- Sugita, T., Ikeda, R. and Shinoda, T. (2001) 'Diversity among strains of *Cryptococcus neoformans* var. *gattii* as revealed by a sequence analysis of multiple genes and a chemotype analysis of capsular polysaccharide', *Microbiol Immunol*, 45(11), pp. 757–768.
- Sullivan, C. and Kim, C. H. (2008) 'Zebrafish as a model for infectious disease and immune function', *Fish Shellfish Immunol*, 25(4), pp. 341–350.
- Summers, C., Rankin, S. M., Condliffe, A. M., Singh, N., Peters, A. M. and Chilvers, E. R. (2010) 'Neutrophil kinetics in health and disease', *Trends Immunol*, 31(8), pp. 318–324.
- Sun, D. and Shi, M. (2016) 'Neutrophil swarming toward *Cryptococcus neoformans* is mediated by complement and leukotriene B₄', *Biochem Biophys Res Commun*, 477(4), pp. 945–951.
- Sun, J. C. and Lanier, L. L. (2009) 'Natural killer cells remember: an evolutionary bridge between innate and adaptive immunity?', *Eur J Immunol*, 39(8), pp. 2059–2064.
- Sun, L., Zhou, H., Zhu, Z., Yan, Q., Wang, L., Liang, Q. and Ye, R. D. (2015) 'Ex vivo and in vitro effect of serum amyloid a in the induction of macrophage M2 markers and efferocytosis of apoptotic neutrophils', *J Immunol*, 194(10), pp. 4891–4900.
- Sun, Q. and Scott, M. J. (2016) 'Caspase-1 as a multifunctional inflammatory mediator: noncytokine maturation roles', *J Leukoc Biol*, 100(5), pp. 961–967.
- Sun, S., Priest, S. J. and Heitman, J. (2019) '*Cryptococcus neoformans* Mating and Genetic Crosses', *Curr Protoc Microbiol*, 53(1), pp. e75.
- Sunderkötter, C., Nikolic, T., Dillon, M. J., Van Rooijen, N., Stehling, M., Drevets, D. A. and Leenen, P. J. (2004) 'Subpopulations of mouse blood monocytes differ in maturation stage and inflammatory response', *J Immunol*, 172(7), pp. 4410–4417.
- Sutterwala, F. S., Ogura, Y., Szczepanik, M., Lara-Tejero, M., Lichtenberger, G. S., Grant, E. P., Bertin, J., Coyle, A. J., Galán, J. E., Askenase, P. W. and Flavell, R. A. (2006) 'Critical role for NALP3/CIAS1/Cryopyrin in innate and adaptive immunity through its regulation of caspase-1', *Immunity*, 24(3), pp. 317–327.
- Swearengen, J. R. (2018) 'Choosing the right animal model for infectious disease research', *Animal Model Exp Med*, 1(2), pp. 100–108.
- Swinne-Desgain, D. (1975) '*Cryptococcus neoformans* of saprophytic origin', *Sabouraudia*, 13(3), pp. 303–308.
- Swinne-Desgain, D. (1976) '*Cryptococcus neoformans* in the crops of pigeons following its experimental administration', *Sabouraudia*, 14(3), pp. 313–317.
- Syme, R. M., Bruno, T. F., Kozel, T. R. and Mody, C. H. (1999) 'The capsule of *Cryptococcus neoformans* reduces T-lymphocyte proliferation by reducing

- phagocytosis, which can be restored with anticapsular antibody', *Infect Immun*, 67(9), pp. 4620–4627.
- Syme, R. M., Spurrell, J. C., Amankwah, E. K., Green, F. H. and Mody, C. H. (2002) 'Primary dendritic cells phagocytose *Cryptococcus neoformans* via mannose receptors and Fcγ receptor II for presentation to T lymphocytes', *Infect Immun*, 70(11), pp. 5972–5981.
- Tacker, J. R., Farhi, F. and Bulmer, G. S. (1972) 'Intracellular fate of *Cryptococcus neoformans*', *Infect Immun*, 6(2), pp. 162–167.
- Taimur, S. (2018) 'Yeast Infections in Solid Organ Transplantation', *Infect Dis Clin North Am*, 32(3), pp. 651–666.
- Takeda, K. and Akira, S. (2005) 'Toll-like receptors in innate immunity', *Int Immunol*, 17(1), pp. 1–14.
- Takeuchi, O. and Akira, S. (2010) 'Pattern recognition receptors and inflammation', *Cell*, 140(6), pp. 805–820.
- Takizawa, T., Meaburn, K. J. and Misteli, T. (2008) 'The meaning of gene positioning', *Cell*, 135(1), pp. 9–13.
- Tan, T. and Lawrance, I. C. (2009) 'Use of mycophenolate mofetil in inflammatory bowel disease', *World J Gastroenterol*, 15(13), pp. 1594–1549.
- Tanaka, E., Ito-Kuwa, S., Nakamura, K., Aoki, S., Vidotto, V. and Ito, M. (2005) 'Comparisons of the laccase gene among serotypes and melanin-deficient variants of *Cryptococcus neoformans*', *Microbiol Immunol* 49(3), pp. 209–217.
- Taylor-Smith, L. M. (2017) 'Cryptococcus–epithelial interactions', *J Fungi (Basel)*, 3(4), p. 53.
- Taylor-Smith, L. M. and May, R. C. (2016) 'New weapons in the *Cryptococcus* infection toolkit', *Curr Opin Microbiol*, 34, pp. 67–74
- Taylor, P. R., Martinez-Pomares, L., Stacey, M., Lin, H.-H., Brown, G. D. and Gordon, S. (2005) 'Macrophage Receptors and Immune Recognition', *Annu Rev Immunol*, 23(1), pp. 901–944.
- Teh, Y. C., Ding, J. L., Ng, L. G. and Chong, S. Z. (2019) 'Capturing the fantastic voyage of monocytes through time and space', *Front Immunol*, 10, p. 834.
- Temfack, E., Boyer-Chammard, T., Lawrence, D., Delliere, S., Loyse, A., Lanternier, F., Alanio, A. and Lortholary, O. (2019) 'New Insights Into *Cryptococcus* Spp. Biology and Cryptococcal Meningitis', *Curr Neurol Neurosci Rep*, 19(10), p. 81.
- Tenforde, M. W., Mokomane, M., Leeme, T., Patel, R. K. K., Lekwape, N., Ramodimoosi, C., Dube, B., Williams, E. A., Mokobela, K. O., Tawanana, E., Pilatwe, T., Hurt, W. J., Mitchell, H., Banda, D. L., Stone, H., Molefi, M., Mokgacha, K., Phillips, H., Mullan, P. C., *et al.* (2017) 'Advanced human immunodeficiency virus disease in Botswana following successful antiretroviral therapy rollout: Incidence of and temporal trends in cryptococcal meningitis', *Clin Infect Dis*, 65(5), pp. 779–786.
- Tenforde, M. W., Shapiro, A. E., Benjami Rouse, Jarvis, J. N., Li, T., Eshun-Wilson, I. and Ford, N. (2018) 'Treatment for HIV-associated cryptococcal meningitis', *Cochrane Database Syst Rev*, 7(7), p. CD005647.

- Tenor, J. L., Oehlers, S. H., Yang, J. L., Tobin, D. M. and Perfect, J. R. (2015) 'Live imaging of host-parasite interactions in a zebrafish infection model reveals cryptococcal determinants of virulence and central nervous system invasion', *mBio*, 6(5), pp. 1–11.
- Tharp, W. G. (2005) 'Neutrophil chemorepulsion in defined interleukin-8 gradients in vitro and in vivo', *J Leukoc Biol*, 79(3), pp. 539–554.
- Thoma-Uszynski, S. (2001) 'Induction of Direct Antimicrobial Activity Through Mammalian Toll-Like Receptors', *Science*, 291(5508), pp. 1544–1547.
- Thomas, S., Fisher, K. H., Snowden, J. A., Danson, S. J., Brown, S. and Zeidler, M. P. (2015) 'Methotrexate is a JAK/STAT pathway inhibitor', *PLoS One*, 10(7), pp. 1–15.
- Thompson, G. R., Wiederhold, N. P., Najvar, L. K., Bocanegra, R., Kirkpatrick, W. R., Graybill, J. R. and Patterson, T. F. (2012b) 'A murine model of *Cryptococcus gattii* meningoencephalitis', *J Antimicrob Chemother*, 67(6), pp. 1432–1438.
- Thompson, G. R., Albert, N., Hodge, G., Wilson, M. D., Sykes, J. E., Bays, D. J., Firacative, C., Meyer, W. and Kontoyiannis, D. P. (2014) 'Phenotypic differences of *Cryptococcus* molecular types and their implications for virulence in a drosophila model of infection', *Infect Immun*, 82(7), pp. 3058–3065.
- Thornberry, N. A. and Lazebnik, Y. (1998) 'Caspases: enemies within', *Science*, 281(5381), pp. 1312–1316.
- Thorne, J. E., Jabs, D. A., Qazi, F. A., Quan, D. N., Kempen, J. H. and Dunn, J. P. (2005) 'Mycophenolate mofetil therapy for inflammatory eye disease', *Ophthalmology*, 112(8), pp. 1472–1477.
- Tiede, I., Fritz, G., Strand, S., Poppe, D., Dvorsky, R., Strand, D., Lehr, H. A., Wirtz, S., Becker, C., Atreya, R., Mudter, J., Hildner, K., Bartsch, B., Holtmann, M., Blumberg, R., Walczak, H., Iven, H., Galle, P. R., Ahmadian, M. R., *et al.* (2003) 'CD28-dependent Rac1 activation is the molecular target of azathioprine in primary human CD4+ T lymphocytes', *J Clin Invest*, 111(8), pp. 1133–1145.
- Ting, L. S. L., Partovi, N., Levy, R. D., Riggs, K. W. and Ensom, M. H. H. (2008) 'Pharmacokinetics of mycophenolic acid and its phenolic-glucuronide and acyl glucuronide metabolites in stable thoracic transplant recipients', *Ther Drug Monit*, 30(3), pp. 282–291.
- Tobin, D. M., Vary, J. C., Ray, J. P., Walsh, G. S., Dunstan, S. J., Bang, N. D., Hagge, D. A., Khadge, S., King, M. C., Hawn, T. R., Moens, C. B. and Ramakrishnan, L. (2010) 'The *Ita4h* locus modulates susceptibility to mycobacterial infection in zebrafish and humans', *Cell*, 140(5), pp. 717–730.
- Tobin, D. M., May, R. C. and Wheeler, R. T. (2012) 'Zebrafish: A see-through host and a fluorescent toolbox to probe host-pathogen interaction', *PLoS Pathog*, 8(1), p. e1002349.
- Toffaletti, D. L. and Perfect, J. R. (1997) 'Study of *Cryptococcus neoformans* actin gene regulation with a β -galactosidase-actin fusion', *J Med Vet Mycol*, 35(5), pp. 313–320.
- Torraca, V. and Mostowy, S. (2018) 'Zebrafish Infection: From Pathogenesis to Cell Biology', *Trends Cell Biol*, 28(2), pp. 143–156.

- Torres-Duñas, D., Celes, M. R. N., Freitas, A., Alves-Filho, J. C., Spiller, F., Dal-Secco, D., Dalto, V. F., Rossi, M. A., Ferreira, S. H. and Cunha, F. Q. (2007) 'Peroxynitrite mediates the failure of neutrophil migration in severe polymicrobial sepsis in mice', *Br J Pharmacol*, 152(3), pp. 341–352.
- Trede, N. S., Langenau, D. M., Traver, D., Look, A. T. and Zon, L. I. (2004) 'The use of zebrafish to understand immunity', *Immunity*, 20(4), pp. 367–379.
- Tredger, J. M., Brown, N. W., Adams, J., Gonde, C. E., Dhawan, A., Rela, M. and Heaton, N. (2004) 'Monitoring mycophenolate in liver transplant recipients: toward a therapeutic range', *Liver Transpl*, 10(4), pp. 492–502.
- Trevijano-Contador, N., Rueda, C. and Zaragoza, O. (2016) 'Fungal morphogenetic changes inside the mammalian host', *Semin Cell Dev Biol*, 57, pp. 100–109.
- Trivedi, B. and Danforth, W. H. (1966) 'Effect of pH on the Kinetics of Frog Muscle Phosphofructokinase', *J. Biol Chem*, 241, pp. 4110–4112.
- Troutman, T. D., Bazan, J. F. and Pasare, C. (2012) 'Toll-like receptors, signaling adapters and regulation of the pro-inflammatory response by PI3K', *Cell Cycle*, 11(19), pp. 3559–3567.
- Tsou, C.-L., Peters, W., Si, Y., Slaymaker, S., Aslanian, A. M., Weisberg, S. P., Mack, M. and Charo, I. F. (2007) 'Critical roles for CCR2 and MCP-3 in monocyte mobilization from bone marrow and recruitment to inflammatory sites', *J Clin Invest*, 117(4), pp. 902–909.
- Turcotte, B., Liang, X. B., Robert, F. and Soontorngun, N. (2010) 'Transcriptional regulation of nonfermentable carbon utilization in budding yeast', *FEMS Yeast Res*, 10(1), pp. 2–13.
- Turka, L. A., Dayton, J., Sinclair, G., Thompson, C. B. and Mitchell, B. S. (1991) 'Guanine ribonucleotide depletion inhibits T cell activation. Mechanism of action of the immunosuppressive drug mizoribine', *J Clin Invest*, 87(3), pp. 940–948.
- Turner, S. H., Cherniak, R. and Reiss, E. (1984) 'Fractionation and characterization of galactoxylomannan from *Cryptococcus neoformans*', *Carbohydr Res*, 125(2), pp. 343–349.
- Turrens, J. F. (2003) 'Mitochondrial formation of reactive oxygen species', *J Physiol*, 552(2), pp. 335–344.
- Tzouveleakis, A., Bouros, E., Oikonomou, A., Ntoliou, P., Zacharis, G., Kolios, G. and Bouros, D. (2011) 'Effect and safety of mycophenolate mofetil in idiopathic pulmonary fibrosis', *Pulm Med*, 2011, p. 849035.
- Ueda, T., Sakagami, T., Kikuchi, T. and Takada, T. (2018) 'Mycophenolate mofetil as a therapeutic agent for interstitial lung diseases in systemic sclerosis', *Respir Investig*, 56(1), pp. 14–20.
- Ueno, K., Yanagihara, N., Otani, Y., Shimizu, K., Kinjo, Y. and Miyazaki, Y. (2019) 'Neutrophil-mediated antifungal activity against highly virulent *Cryptococcus gattii* strain R265', *Med Mycol Mycology*, 57(8), pp. 1046–1054.
- Ullrich, S., Karrasch, B., Hoppe, H. G., Jeskulke, K. and Mehrens, M. (1996) 'Toxic effects on bacterial metabolism of the redox dye 5-cyano-2,3-ditolyl tetrazolium chloride', *Appl Environ Microbiol*, 62(12), pp. 4587–4593.
- Upadhyay, R., Campbell, L. T., Donlin, M. J., Aurora, R. and Lodge, J. K. (2013) 'Global

Transcriptome Profile of *Cryptococcus neoformans* during Exposure to Hydrogen Peroxide Induced Oxidative Stress', *PLoS One*, 8(1), p. e55110.

- Upadhyaya, R., Woei, L. C., Maybruck, B., Specht, C. A., Levitz, S. M. and Lodge, J. K. (2016) 'Induction of Protective Immunity to Cryptococcal Infection in Mice by a Heat-Killed, Chitosan-Deficient Strain of *Cryptococcus*', *mBio*, 7(3), pp. e00547-16.
- Upadhyaya, R., Lam, W. C., Maybruck, B., Donlin, M. J., Chang, A. L., Kayode, S., Ormerod, K. L., Fraser, J. A., Doering, T. L. and Lodge, J. K. (2017) 'A fluorogenic *C. neoformans* reporter strain with a robust expression of m-cherry expressed from a safe haven site in the genome', *Fungal Genet Biol*, 108, pp. 13–25.
- Usher, L. R., Lawson, R. A., Geary, I., Taylor, C. J., Bingle, C. D., Taylor, G. W. and Whyte, M. K. B. (2002) 'Induction of neutrophil apoptosis by the *Pseudomonas aeruginosa* exotoxin pyocyanin: a potential mechanism of persistent infection', *J Immunol*, 168(4), pp. 1861–1868.
- Valdivia, R. H. and Falkow, S. (1996) 'Bacterial genetics by flow cytometry: rapid isolation of *Salmonella typhimurium* acid-inducible promoters by differential fluorescence induction', *Mol Microbiol*, 22(2), pp. 367–78.
- Vandanmagsar, B., Youm, Y., Ravussin, A., Galgani, J. E., Stadler, K., Mynatt, R. L., Ravussin, E., Stephens, J. M. and Dixit, V. D. (2011) 'Obesity induced autoinflammation', *Nat Med*, 17(2), pp. 179–188.
- Vandenabeele, P., Galluzzi, L., Vanden Berghe, T. and Kroemer, G. (2010) 'Molecular mechanisms of necroptosis: An ordered cellular explosion', *Nat Rev Mol Cell Biol*, 11(10), pp. 700–714.
- Varela, M., Figueras, A. and Novoa, B. (2017) 'Modelling viral infections using zebrafish: Innate immune response and antiviral research', *Antiviral Res*, 139, pp. 59–68.
- Varma, A., Edman, J. C. and Kwon-Chung, K. J. (1992) 'Molecular and genetic analysis of URA5 transformants of *Cryptococcus neoformans*', *Infect Immun*, 60(3), pp. 1101–1108.
- Vartivarian, S. E., Reyes, G. H., Jacobson, E. S., James, P. G., Cherniak, R., Mumaw, V. R. and Tingler, M. J. (1989) 'Localization of mannoprotein in *Cryptococcus neoformans*', *J Bacteriol*, 171(12), pp. 6850–6852.
- Vartivarian, S. E., Anaissie, E. J., Cowart, R. E., Sprigg, H. A., Tingler, M. J., Jacobson, E. S., The, S., Diseases, I., Jan, N., Vartivarian, S. E., Anaissie, E. J., Cowart, R. E., Sprigg, H. A., Tingler, M. J. and Jacobson, E. S. (1993) 'Regulation of Cryptococcal Capsular Polysaccharide by Iron', *J Infect Dis*, 167(1), pp. 186–190.
- Vecchiarelli, A. (2000) 'Immunoregulation by capsular components of *Cryptococcus neoformans*', *Medical Mycol*, 38(6), pp. 407–17.
- Vecchiarelli, A., Pietrella, D., Lupo, P., Bistoni, F., McFadden, D. C. and Casadevall, A. (2003) 'The polysaccharide capsule of *Cryptococcus neoformans* interferes with human dendritic cell maturation and activation', *J Leukoc Biol*, 74(3), pp. 370–378.
- Van Der Veen, B. S., De Winther, M. P. J. and Heeringa, P. (2009) 'Myeloperoxidase:

- Molecular mechanisms of action and their relevance to human health and disease', *Antioxid Redox Signal*, 11(11), pp. 2899–2937.
- Velagapudi, R., Hsueh, Y.-P., Geunes-Boyer, S., Wright, J. R. and Heitman, J. (2009) 'Spores as infectious propagules of *Cryptococcus neoformans*', *Infect Immun*, 77(10), pp. 4345–4355.
- Vender, S. G., Ganpath, V., Charles, R. W. and Cooper, K. (1988) 'Localized osseous cryptococcal infection: Report of 2 cases', *Acta Orthopaedica*, 59(6), pp. 720–722.
- Vénéreau, E., Ceriotti, C. and Bianchi, M. E. (2015) 'DAMPs from cell death to new life', *Front Immunol*, 6, p.422
- Verreck, F. A. W., De Boer, T., Langenberg, D. M. L., Hoeve, M. A., Kramer, M., Vaisberg, E., Kastelein, R., Kolk, A., De Waal-Malefyt, R. and Ottenhoff, T. H. M. (2004) 'Human IL-23-producing type 1 macrophages promote but IL-10-producing type 2 macrophages subvert immunity to (myco)bacteria', *Proc Natl Acad Sci U S A*, 101(13), pp. 4560–4565.
- Vieira, O. V., Botelho, R. J. and Grinstein, S. (2002) 'Phagosome maturation: Aging gracefully', *Biochemical Journal*, 366(3), pp. 689–704.
- von Vietinghoff, S., Koltsova, E. K., Mestas, J., Diehl, C. J., Witztum, J. L. and Ley, K. (2011) 'Mycophenolate Mofetil Decreases Atherosclerotic Lesion Size by depression of aortic T lymphocyte and IL-17-mediated macrophage accumulation', *J Am Coll Cardiol*, 57(21), pp. 2194–2204.
- Von Vietinghoff, S., Ouyang, H. and Ley, K. (2010) 'Mycophenolic acid suppresses granulopoiesis by inhibition of interleukin-17 production', *Kidney Int*, 78(1), pp. 79–88.
- Vimercati, L., Hamsher, S., Schubert, Z. and Schmidt, S. K. (2016) 'Growth of high-elevation *Cryptococcus* sp. during extreme freeze–thaw cycles', *Extremophiles*, 20(5), pp. 579–588.
- Vincenti, F. (2003) 'Immunosuppression minimization: Current and future trends in transplant immunosuppression', *J Am Soc Nephrol*, 14(7), pp. 1940–1948.
- Vivier, E., Raulet, D. H., Moretta, A., Caligiuri, M. A., Zitvogel, L., Lanier, L. L., Yokoyama, W. M. and Ugolini, S. (2016) 'Innate or adaptive immunity? The example of natural killer cells', *Science*, 331(6013), pp. 44–49.
- Voelz, K., Johnston, S. A., Rutherford, J. C. and May, R. C. (2010) 'Automated analysis of cryptococcal macrophage parasitism using GFP-tagged cryptococci', *PLoS One*, 5(12), p. e15968.
- Voelz, K. (2010) *Interactions during cryptococcosis (PhD thesis)*. Birmingham: University of Birmingham.
- Voelz, K., Johnston, S. A., Smith, L. M., Hall, R. A., Idnurm, A. and May, R. C. (2014) "'Division of labour" in response to host oxidative burst drives a fatal *Cryptococcus gattii* outbreak', *Nat Commun*, 5, p. 5194.
- Voelz, K., Lammas, D. A. and May, R. C. (2009) 'Cytokine signaling regulates the outcome of intracellular macrophage parasitism by *Cryptococcus neoformans*', *Infect Immun*, 77(8), pp. 3450–3457.
- Voelz, K. and May, R. C. (2010) 'Cryptococcal interactions with the host immune

- system', *Eukaryot Cell*, 9(6), pp. 835–846.
- Vogt, K. L., Summers, C., Chilvers, E. R. and Condliffe, A. M. (2018) 'Priming and de-priming of neutrophil responses in vitro and in vivo', *Eur J Clin Invest*, 48(Suppl 2), p. e12967.
- Voisin, M. B. and Nourshargh, S. (2013) 'Neutrophil transmigration: Emergence of an adhesive cascade within venular walls', *J Innate Immun*, 5(4), pp. 336–347.
- Volkman, H. E., Pozos, T. C., Zheng, J., Davis, J. M., Rawls, J. F. and Ramakrishnan, L. (2010) 'Tuberculous Granuloma Induction via Interaction of a Bacterial Secreted Protein with Host Epithelium', *Science*, 327(5964), pp. 466–469.
- Volkman, E. R., Tashkin, D. P., Li, N., Roth, M. D., Khanna, D., Hoffmann-Vold, A. M., Kim, G., Goldin, J., Clements, P. J., Furst, D. E. and Elashoff, R. M. (2017) 'Mycophenolate Mofetil Versus Placebo for Systemic Sclerosis–Related Interstitial Lung Disease: An Analysis of Scleroderma Lung Studies I and II', *Arthritis Rheumatol*, 69(7), pp. 1451–1460.
- Vu, K., Weksler, B., Romero, I., Couraud, P. O. and Gelli, A. (2009) 'Immortalized human brain endothelial cell line HCMEC/D3 as a model of the blood-brain barrier facilitates in vitro studies of central nervous system infection by cryptococcus neoformans', *Eukaryot Cell*, 8(11), pp. 1803–1807.
- Vu, K., Tham, R., Uhrig, J. P., Thompson, G. R., Na Pombejra, S., Jamklang, M., Bautos, J. M. and Gelli, A. (2014) 'Invasion of the central nervous system by Cryptococcus neoformans requires a secreted fungal metalloprotease', *mBio*, 5(3), pp. e01101-14.
- van Vugt-Lussenburg, B. M. A., van der Weel, L., Hagen, W. R. and Hagedoorn, P. L. (2013) 'Biochemical Similarities and Differences between the Catalytic [4Fe-4S] Cluster Containing Fumarases FumA and FumB from Escherichia coli', *PLoS One*, 8(2), p. e55549
- Wachter, H., Fuchs, D., Hausen, A., Reibnegger, G. and Werner, E. R. (1989) 'Neopterin as marker for activation of cellular immunity: immunologic basis and clinical application', *Adv Clin Chem*, 27, pp. 81–141.
- Wager, C. M. L., Hole, C. R., Wozniak, K. L., Olszewski, M. A. and Wormley Jr., F. L. (2014) 'STAT1 Signaling is Essential for Protection against Cryptococcus neoformans Infection in Mice', *J Immunol*, 193(8), pp. 4060–4071.
- Wager, C. M. L. and Wormley, F. L. (2014) 'Classical versus alternative macrophage activation: The Ying and the Yang in host defense against pulmonary fungal infections', *Mucosal Immunol*, 7(5), pp. 1023–1035.
- Walenkamp, a M., Chaka, W. S., Verheul, a F., Vaishnav, V. V, Cherniak, R., Coenjaerts, F. E. and Hoepelman, I. M. (1999) 'Cryptococcus neoformans and its cell wall components induce similar cytokine profiles in human peripheral blood mononuclear cells despite differences in structure', *FEMS Immunol Med Microbiol*, 26(3–4), pp. 309–318.
- Walsh, N. M., Botts, M. R., McDermott, A. J., Ortiz, S. C., Wüthrich, M., Klein, B. and Hull, C. M. (2019) 'Infectious particle identity determines dissemination and disease outcome for the inhaled human fungal pathogen Cryptococcus', *PLoS Pathog*, 15(6), p. e1007777.
- Wang, J. (2018) 'Neutrophils in tissue injury and repair', *Cell Tissue Res*, 371(3), pp.

531–539.

- Wang, L. and Lin, X. (2011) 'Mechanisms of unisexual mating in *Cryptococcus neoformans*', *Fungal Genet Biol*, 48(7), pp. 651–660.
- Wang, W. Z., Fang, X.-H., Stephenson, L. L., Khiabani, K. T. and Zamboni, W. A. (2008) 'Ischemia/reperfusion-induced necrosis and apoptosis in the cells isolated from rat skeletal muscle', *J Orthop Res*, 26(3), pp. 351–356.
- Wang, Y. and Casadevall, A. (1994) 'Susceptibility of melanized and nonmelanized *Cryptococcus neoformans* to nitrogen- and oxygen-derived oxidants', *Infect Immun*, 62(7), pp. 3004–3007.
- Wang, Y. and Jönsson, F. (2019) 'Expression, role, and regulation of neutrophil Fcγ receptors', *Front Immunol*, 10(1958).
- Wang, Y. Y., Nacher, J. C. and Zhao, X. M. (2012) 'Predicting drug targets based on protein domains', *Mol Biosyst*, 8(5), pp. 1528–34.
- Wang, Y., Aisen, P., Casadevall, A., Wang, Yulin and Aisen, Philip (1995) 'Cryptococcus neoformans melanin and virulence: mechanism of action', *Infect Immun*, 63(8), pp. 3131–3136.
- Wang, Z. A., Griffith, C. L., Skowrya, M. L., Salinas, N., Williams, M., Maier, E. J., Gish, S. R., Liu, H., Brent, M. R. and Doering, T. L. (2014) 'Cryptococcus neoformans dual GDP-mannose transporters and their role in biology and virulence', *Eukaryot Cell*, 13(6), pp. 832–842.
- Wang, Z. A., Li, L. X. and Doering, T. L. (2018) 'Unraveling synthesis of the cryptococcal cell wall and capsule', *Glycobiology*, 28(10), pp. 719–730.
- Ward, C., Dransfield, I., Chilvers, E. R., Haslett, C. and Rossi, A. G. (1999) 'Pharmacological manipulation of granulocyte apoptosis: potential therapeutic targets', *Trends Pharmacol Sci*, 20(12), pp. 503–509.
- Warkentien, T. and Crum-Cianflone, N. F. (2010) 'An Update on Cryptococcosis Among HIV-Infected Persons', *Int J STD AIDS*, 21(10), pp. 679–684.
- Warner, B., Johnston, E., Arenas-Hernandez, M., Marinaki, A., Irving, P. and Sanderson, J. (2018) 'A practical guide to thiopurine prescribing and monitoring in IBD', *Frontline Gastroenterol*, 9(1), pp. 10–15.
- Waters, R. V., Webster, D. and Allison, A. C. (1993) 'Mycophenolic acid and some antioxidants induce differentiation of monocytic lineage cells and augment production of the IL-1 receptor antagonist', *Ann N Y Acad Sci*, 696, pp. 185–196.
- Watkins, R., King, J. and Johnston, S. (2017) 'Nutritional Requirements and Their Importance for Virulence of Pathogenic *Cryptococcus* Species', *Microorganisms*, 5(4), p. 65.
- Webster, B., Assil, S. and Dreux, M. (2016) 'Cell-Cell Sensing of Viral Infection by Plasmacytoid Dendritic Cells', *J Virol*, 90(22), pp. 10050–10053.
- Weimer, R., Melk, A., Daniel, V., Friemann, S., Padberg, W., Mandelbaum, A., Wiesel, M., Staehler, G. and Opelz, G. (1999) 'Monocyte responses in patients with chronic renal transplant rejection: beneficial effects of MMF-based immunosuppression', *Transplantation*, 67(7), p. S27.

- Weinshilboum, R. M. and Sladek, S. L. (1980) 'Mercaptopurine pharmacogenetics: monogenic inheritance of erythrocyte thiopurine methyltransferase activity', *Am J Hum Genet*, 32(5), pp. 651–662.
- Weiss, S. J. (1989) 'Tissue destruction by neutrophils', *N Engl J Med*, 320(6), pp. 365–76.
- Weyker, P. D., Webb, C. A. J., Kiamanesh, D. and Flynn, B. C. (2013) 'Lung ischemia reperfusion injury: a bench-to bedside review', *Semin Cardiothorac Vasc Anesth*, 17(1), pp. 28–43.
- Wickerham, L. J. (1951) 'Taxonomy of yeasts', *Tech Bull*, 1029
- Wickes, B. L., Mayorga, M. E., Edman, U. and Edman, J. C. (1996) 'Dimorphism and haploid fruiting in *Cryptococcus neoformans*: association with the alpha-mating type', *Proc Natl Acad Sci U S A*, 93(14), pp. 7327–7331.
- Wiesner, D. L., Specht, C. A., Lee, C. K., Smith, K. D., Mukaremera, L., Lee, S. T., Lee, C. G., Elias, J. A., Nielsen, J. N., Boulware, D. R., Bohjanen, P. R., Jenkins, M. K., Levitz, Stuart M, Nielsen, K., Brown, G. D., Denning, D. W., Gow, N. A., Levitz, S M, Netea, M. G., *et al.* (2015) 'Chitin recognition via chitotriosidase promotes pathologic type-2 helper T cell responses to cryptococcal infection', *PLoS Pathog*, 11(3), p. e1004701
- Wiley, D. S., Redfield, S. E. and Zon, L. I. (2017) 'Chemical screening in zebrafish for novel biological and therapeutic discovery', *Methods Cell Biol*, 138, pp. 651–679.
- Willett, C. E., Cortes, A., Zuasti, A. and Zapata, A. G. (1999) 'Early hematopoiesis and developing lymphoid organs in the zebrafish', *Dev Dyn*, 214(4), pp. 323–336.
- Williams, V. and del Poeta, M. (2011) 'Role of Glucose in the Expression of *Cryptococcus neoformans* Antiphagocytic Protein 1, App1', *Eukaryot Cell*, 10(3), pp. 293–301.
- Williamson, P. R. (1994) 'Biochemical and molecular characterization of diphenol oxidase of *Cryptococcus neoformans*: identification as a laccase', *J Bacteriol*, 176(3), pp. 656–664.
- Williamson, P. R., Wakamatsu, K., Ito, S., Williamson, P. R. and Wakamatsu, K. (1998) 'Melanin biosynthesis in *Cryptococcus neoformans*', *J Bacteriol*, 180(6), pp. 1–4.
- Wilson, C., Bellen, H. J. and Gehring, W. J. (1990) 'Position Effects on eucariotic gene expression', *Annu Rev Cell Biol*, (6), pp. 679–714.
- Wilson, D. E. , Bennett, J. E. and Bailey, J. W. (1968) 'Serologic grouping of *Cryptococcus neoformans*', *Proc Soc Exp Biol Med*, 127(3), pp. 820–823.
- Wilson, T. S., Fleming, W. A., Robinson, F. L. J. and Nicholl, B. (1970) 'Cryptococcal meningitis associated with steroid therapy', *J Clin Pathol*, 23(8), pp. 657–663.
- Winata, C. L., Korzh, S., Kondrychyn, I., Zheng, W., Korzh, V. and Gong, Z. (2009) 'Development of zebrafish swimbladder: The requirement of Hedgehog signaling in specification and organization of the three tissue layers', *Dev Biol*, 331(2), pp. 222–236.
- Wiseman, J. C. D., Ma, L. L., Marr, K. J., Jones, G. J. and Mody, C. H. (2007) 'Perforin-Dependent Cryptococcal Microbicidal Activity in NK Cells Requires

- PI3K-Dependent ERK1/2 Signaling', *J Immunol*, 178(10), pp. 6456–6464.
- Wofsy, D. (1990) 'Regulation of immunity by anti-T-cell antibodies', *West J Med*, 153(3), pp. 265–268.
- Wolf, A. A., Yáñez, A., Barman, P. K. and Goodridge, H. S. (2019) 'The Ontogeny of Monocyte Subsets', *Front Immunol*, 10, p. 1642
- Wong, B., Perfect, J. R., Beggs, S. and Wright, K. A. (1990) 'Production of the hexitol D-mannitol by *Cryptococcus neoformans* in vitro and in rabbits with experimental meningitis', *Infect Immun*, 58(6), pp. 1664–1670.
- Wong, K. L., Tai, J. J. Y., Wong, W. C., Han, H., Sem, X., Yeap, W. H., Kourilsky, P. and Wong, S. C. (2011) 'Gene expression profiling reveals the defining features of the classical, intermediate, and nonclassical human monocyte subsets', *Blood*, 118(5), pp. 16–31.
- Wood, L. and Miedzinski, L. (1996) 'Skeletal cryptococcosis: Case report and review of the literature', *Can J Infect Dis*, 7(2), pp. 125–132.
- Woodfin, A., Voisin, Mathieu-Benoit Imhof, B. A., Dejana, E. and Engelhardt, Britta and Nourshargh, S. (2009) 'Endothelial cell activation leads to neutrophil transmigration as supported by the sequential roles of ICAM-2, JAM-A, and PECAM-1', *Blood*, 113(24), pp. 6246–6257.
- Woodring, J. H., Ciporkin, G., Lee, C., Worm, B. and Woolley, S. (1996) 'Pulmonary cryptococcosis', *Semin Roentgenol*, 31(1), pp. 67–75.
- Wooten, D. K., Xie, X., Bartos, D., Busche, R. A., Longmore, G. D. and Watowich, S. S. (2008) 'Cytokine signaling through Stat3 activates integrins, promotes adhesion, and induces growth arrest in the myeloid cell line 32D', *J Biol Chem*, 283(1), pp. 1–7.
- Wormley, F. L., Perfect, J. R., Steele, C. and Cox, G. M. (2007) 'Protection against cryptococcosis by using a murine gamma interferon-producing *Cryptococcus neoformans* strain', *Infect Immun*, 75(3), pp. 1453–1462.
- Wozniak, K. L., Vyas, J. M. and Levitz, S. M. (2006) 'In vivo role of dendritic cells in a murine model of pulmonary cryptococcosis', *Infect Immun*, 74(7), pp. 3817–3824.
- Wozniak, K. L., Young, M. L. and Wormley, F. L. (2011) 'Protective immunity against experimental pulmonary cryptococcosis in T cell-depleted mice', *Clin Vaccine Immunol*, 18(5), pp. 717–723.
- Wright, H. L., Moots, R. J., Bucknall, R. C. and Edwards, S. W. (2010) 'Neutrophil function in inflammation and inflammatory diseases', *Rheumatology*, 49(9), pp. 1618–1631.
- Wright, L., Bubb, W., Davidson, J., Santangelo, R., Krockenberger, M., Himmelreich, U. and Sorrell, T. (2002) 'Metabolites released by *Cryptococcus neoformans* var. *neoformans* and var. *gattii* differentially affect human neutrophil function', *Microbes Infect*, 4(14), pp. 1427–1438.
- Wright, S., Sanders, D. S., Lobo, A. J. and Lennard, L. (2004) 'Clinical significance of azathioprine active metabolite concentrations in inflammatory bowel disease', *Gut*, 53(8), pp. 1123–1128.
- Wright, S. D. and Silverstein, S. C. (1983) 'Receptors for C3b and C3bi promote

- phagocytosis but not the release of toxic oxygen from human phagocytes', *J Exp Med.*, 158(6), pp. 2016–2023.
- Wu, G., Vilchez, R. ., Eidelman, B., Fung, J., Kormos, R. and Kusne, S. (2002) 'Cryptococcal meningitis: An analysis among 5521 consecutive organ transplant recipients', *Transpl Infect Dis*, 4(4), pp. 183–188.
- Wu, H., Fu, S., Zhao, M., Lu, L. and Lu, Q. (2017) 'Dysregulation of cell death and its epigenetic mechanisms in systemic lupus erythematosus', *Molecules*, 22(1), p. 30.
- Wu, X., Zhong, H., Song, J., Damoiseaux, R., Yang, Z. and Lin, S. (2006) 'Mycophenolic acid is a potent inhibitor of angiogenesis', *Arterioscler Thromb Vasc Biol*, 26(10), pp. 2414–2416.
- Wynn, T. a., Chawla, A. and Pollard, J. W. (2013) 'Origins and hallmarks of macrophages: development, homeostasis, and disease', *Nature*, 496(7446), pp. 445–455.
- Xu, C. Y., Zhu, H. M., Wu, J. H., Wen, H. and Liu, C. J. (2014) 'Increased permeability of blood-brain barrier is mediated by serine protease during *Cryptococcus meningitis*', *J Int Med Res*, 42(1), pp. 85–92.
- Xu, H., Andi, B., Qian, J., West, A. H. and Cook, P. F. (2006) 'The α -amino adipate pathway for lysine biosynthesis in fungi', *Cell Biochem Biophys*, 46(1), pp. 43–64.
- Xue, C., Tada, Y., Dong, X. and Heitman, J. (2007) 'The human fungal pathogen *Cryptococcus* can complete its sexual cycle during a pathogenic association with plants', *Cell Host Microbe*, 1(4), pp. 263–273.
- Yamada, W., Yamada, H., Murata, K., Kosugi, H., Asano, Y., Mochizuki, K. and Ishida, K. (2019) 'Case of cryptococcal choroiditis in adult with T-cell leukemia/lymphoma', *J Infect Chemother*, 25(1), pp. 59–64.
- Yamasaki, S., Ishikawa, E., Sakuma, M., Hara, H., Ogata, K. and Saito, T. (2008) 'Mincle is an ITAM-coupled activating receptor that senses damaged cells', *Nat Immunol*, 9(10), pp. 1179–1188.
- Yan, S. F., Fujita, T., Lu, J., Okada, K., Shan Zou, Y., Mackman, N., Pinsky, D. J. and Stern, D. M. (2000) 'Egr-1, a master switch coordinating upregulation of divergent gene families underlying ischemic stress', *Nat Med*, 6(12), pp. 1355–1361.
- Yancey, P. H. and Siebenaller, J. F. (1999) 'Trimethylamine oxide stabilizes teleost and mammalian lactate dehydrogenases against inactivation by hydrostatic pressure and trypsinolysis', *J Exp Biol*, 202(Pt 24), pp. 3597–3603.
- Yang, C. J., Hwang, J. J., Wang, T. H., Cheng, M. S., Kang, W. Y., Chen, T. C. and Huang, M. S. (2006) 'Clinical and radiographic presentations of pulmonary cryptococcosis in immunocompetent patients', *Scand J Infect Dis*, 38(9), pp. 788–793.
- Yang, D. H., Jung, K. W., Bang, S., Lee, J. W., Song, M. H., Floyd-Averette, A., Festa, R. A., Ianiri, G., Idnurm, A., Thiele, D. J., Heitman, J. and Bahn, Y. S. (2017) Rewiring of signaling networks modulating thermotolerance in the human pathogen *Cryptococcus neoformans*, *Genetics*, 205(1), pp. 201-219

- Yang, J., Zhang, L., Yu, C., Yang, X. F. and Wang, H. (2014) 'Monocyte and macrophage differentiation: Circulation inflammatory monocyte as biomarker for inflammatory diseases', *Biomarker Res*, 2(1), p. 1
- Yang, L., Froio, R. M., Sciuto, T. E., Dvorak, A. M., Alon, R. and W., L. (2005) 'ICAM-1 regulates neutrophil adhesion and transcellular migration of TNF- α -activated vascular endothelium under flow', *Blood*, 106(2), pp. 584–592.
- Yang, S.-K., Hong, M., Baek, J., Choi, H., Zhao, W., Jung, Y., Haritunians, T., Ye, B. D., Kim, K. J., Park, S. H., Park, S. K., Yang, D. H., Dubinsky, M., Lee, I., McGovern, D. P. B., Liu, J. and Song, K. (2014) 'A common missense variant in NUDT15 confers susceptibility to thiopurine-induced leukopenia', *Nat Genet*, 46(9), pp. 1017–1020.
- Yang, S.-K., Hong, M., Baek, J., Choi, H., Zhao, W., Jung, Y., Haritunians, T., Ye, B. D., Kim, K.-J., Park, S. H., Park, S.-K., Yang, D.-H., Dubinsky, M., Lee, I., McGovern, D. P. B., Liu, J. and Song, K. (2016) 'A common missense variant in NUDT15 confers susceptibility to thiopurine-induced leukopenia', 46(9), pp. 1017–1020.
- Yang, W., Guastella, J., Huang, J. C., Wang, Y., Zhang, L., Xue, D., Tran, M., Woodward, R., Kasibhatla, S., Tseng, B., Drewe, J. and Cai, S. X. (2003) 'MX1013, a dipeptide caspase inhibitor with potent in vivo antiapoptotic activity', *Br J Pharmacol*, 140(2), pp. 402–412.
- Yao, Z. R., Liao, W. and Chen, R. (2005) 'Management of cryptococcosis in non-HIV-related patients', *Med Mycol*, 43(3), pp. 245–251.
- Yaoita, H., Ogawa, K., Maehara, K. and Maruyama, Y. (1998) 'Attenuation of ischemia/reperfusion injury in rats by a caspase inhibitor', *Circulation*, 97(3), pp. 276–281.
- Yatscoff, R. W., Aspeslet, L. J. and Gallant, H. L. (1998) 'Pharmacodynamic monitoring of immunosuppressive drugs', *Clin Chem*, 44(2), pp. 428–432.
- Yin, C. and Heit, B. (2018) 'Armed for destruction: formation, function and trafficking of neutrophil granules', *Cell Tissue Res*, 371(3), pp. 455–471.
- Yoder, M. C. (2014) 'Inducing definitive hematopoiesis in a dish', *Nat Biotechnol*, 32(6), pp. 539–541.
- Yona, S., Buckingham, J. C., Perretti, M. and Flower, R. J. (2004) 'Stimulus-specific defect in the phagocytic pathways of annexin 1 null macrophages', *Br J Pharmacol*, 142(5), pp. 890–898.
- Yoneyama, M. and Fujita, T. (2008) 'Structural Mechanism of RNA recognition by the RIG-I-like receptors', *Immunity*, 29(2), pp. 178–181.
- You, M. and Xu, J. (2018) 'The effects of environmental and genetic factors on the germination of basidiospores in the *Cryptococcus gattii* species complex', *Sci Rep*, 8(1), p. 15260.
- Youle, R. J. and van der Bliek, A. M. (2012) 'Mitochondrial fission, fusion, and stress. Science', *Science*, 337(6098), pp. 1062–1065.
- Young, B. J. and Kozel, T. R. (1993) 'Effects of strain variation, serotype, and structural modification on kinetics for activation and binding of C3 to *Cryptococcus neoformans*', *Infect Immun*, 61(7), pp. 2966–2972.

- Young, J. D.-E., Ko, S. S. and Cohn, Z. A. (1984) 'The increase in intracellular free calcium associated with IgG gamma 2b/gamma 1 Fc receptor-ligand interactions: role in phagocytosis', *Proc Natl Acad Sci U S A*, 81(17 I), pp. 5430–5434.
- Young, S. K. and Arndt, P. G. (2009) 'c-Jun NH2-terminal kinase regulates lipopolysaccharide-induced pulmonary mononuclear cell recruitment via CCL2', *Exp Lung Res*, 35(8), pp. 682–700.
- Zaragoza, O. and Nielsen, K. (2013) 'Titan cells in *Cryptococcus neoformans*: Cells with a giant impact', *Curr Opin Microbiol*, 16(4), pp. 409–413.
- Zaragoza, O., Telzak, A., Bryan, R. A., Dadachova, E. and Casadevall, A. (2006) 'The polysaccharide capsule of the pathogenic fungus *Cryptococcus neoformans* enlarges by distal growth and is rearranged during budding', *Mol Microbiol*, 59(1), pp. 67–83.
- Zaragoza, O., Alvarez, M., Telzak, A., Rivera, J. and Casadevall, A. (2007) 'The relative susceptibility of mouse strains to pulmonary *Cryptococcus neoformans* infection is associated with pleiotropic differences in the immune response', *Infect Immun*, 75(6), pp. 2729–2739.
- Zaragoza, O., Chrisman, C. J., Castelli, M. V., Frases, S., Cuenca-Estrella, M., Rodríguez-Tudela, J. L. and Casadevall, A. (2008) 'Capsule enlargement in *Cryptococcus neoformans* confers resistance to oxidative stress suggesting a mechanism for intracellular survival', *Cell Microbiol*, 10(10), pp. 2043–2057.
- Zaragoza, O., Rodrigues, M. L., Jesus, M. De, Frases, S., Casadevall, A., Micología, S. De, Nacional, C., Instituto, D. M., Carlos, D. S. and Crta, I. I. I. (2009) 'The capsule of the fungal pathogen *Cryptococcus Neoformans*', *Adv Appl Microbiol*, 68, pp. 133–216.
- Zaragoza, O., Rocío, G. R., Nosanchuk, J. D., Cuenca-Estrella, M., Rodríguez-Tudela, J. L. and Casadevall, A. (2010) 'Fungal cell gigantism during mammalian infection', *PLoS Pathog*, 6(6), p. e1000945.
- Zaragoza, O. (2019) 'Basic principles of the virulence of *Cryptococcus*', *Virulence*, 10(1), pp. 490–501.
- Zaragoza, O. and Casadevall, A. (2006) 'Monoclonal antibodies can affect complement deposition on the capsule of the pathogenic fungus *Cryptococcus neoformans* by both classical pathway activation and steric hindrance', *Cell Microbiol*, 8(12), pp. 1862–1876.
- Zaragoza, O., Fries, B. C. and Casadevall, A. (2003) 'Induction of capsule growth in *Cryptococcus neoformans* by mammalian serum and CO (2)', *Infect Immun*, 71(11), pp. 6155–6164.
- Zarbock, A. and Ley, K. (2008) 'Mechanisms and consequences of neutrophil interaction with the endothelium', *Am J Pathol*, 172(1), pp. 1–7.
- Zhang, M., Sun, D., Liu, G., Wu, H., Zhou, H. and Shi, M. (2016) 'Real-time in vivo imaging reveals the ability of neutrophils to remove *Cryptococcus neoformans* directly from the brain vasculature', *J Leukoc Biol*, 99(3), pp. 467–473.
- Zhang, Y., Bai, X.-T., Zhu, K.-Y., Jin, Y., Deng, M., Le, H.-Y., Fu, Y.-F., Chen, Y., Zhu, J., Look, A. T., Kanki, J., Chen, Z., Chen, S.-J. and Liu, T. X. (2008) 'In Vivo

Interstitial Migration of Primitive Macrophages Mediated by JNK-Matrix Metalloproteinase 13 Signaling in Response to Acute Injury', *J Immunol*, 181(3), pp. 2155–2164.

- Zhang, Y., Wang, F., Tompkins, K. C., McNamara, A., Jain, A. V, Moore, B. B., Toews, G. B., Huffnagle, G. B. and Olszewski, M. A. (2009) 'Robust Th1 and Th17 Immunity Supports Pulmonary Clearance but Cannot Prevent Systemic Dissemination of Highly Virulent *Cryptococcus neoformans* H99', *Am J Pathol*, 175(6), pp. 2489–2500.
- Zhao, H., Ross, F. P. and Teitelbaum, S. L. (2005) 'Unoccupied $\alpha\beta 3$ integrin regulates osteoclast apoptosis by transmitting a positive death signal', *Mol Endocrinol*, 19(3), pp. 771–780.
- Zhao, R., Liang, H., Clarke, E., Jackson, C. and Xue, M. (2016) 'Inflammation in chronic wounds', *Int J Mol Sci*, 17(12), p. 2085.
- Zheng, C. F., Ling, L. M., Jones, G. J., Gill, M. J., Krensky, A. M., Kubes, P. and Mody, C. H. (2007) 'Cytotoxic CD4+ T cells use granulysin to kill *Cryptococcus neoformans*, and activation of this pathway is defective in HIV patients', *Blood*, 109(5), pp. 2049–2057.
- Zheng, X. F., Hong, Y. X., Feng, G. J., Zhang, G. F., Rogers, H., Lewis, M. A. O., Williams, D. W., Xia, Z. F., Song, B. and Wei, X. Q. (2013) 'Lipopolysaccharide-induced M2 to M1 macrophage transformation for IL-12p70 production is blocked by *Candida albicans* mediated up-regulation of EBI3 expression', *PLoS One*, 8(5), p. e63967.
- Zhou, L., Lei, X. H., Bochner, B. R. and Wanner, B. L. (2003) 'Phenotype microarray analysis of *Escherichia coli* K-12 mutants with deletions of all two-component systems', *J Bacteriol*, 185(16), pp. 4956–4972.
- Zhou, R., Tardivel, A., Thorens, B., Choi, I. and Tschopp, J. (2010) 'Thioredoxin-interacting protein links oxidative stress to inflammasome activation', *Nat Immunol*, 11(2), pp. 136–140.
- Zhu, A., Romero, R. and Petty, H. R. (2010) 'A sensitive fluorimetric assay for pyruvate', *Anal Biochem*, 391(1), pp. 146–151.
- Zhu, H., Hart, C. A., Sales, D. and Roberts, N. B. (2006) 'Bacterial killing in gastric juice- effect of pH and pepsin on *Escherichia coli* and *Helicobacter pylori*', *J Med Microbiol*, 55(Pt9), pp. 1265–1270.
- Ziegler-Heitbrock, L., Ancuta, P., Crowe, S., Dalod, M., Grau, V., Hart, D. N., Leenen, P. J. M., Liu, Y. J., MacPherson, G., Randolph, G. J., Scherberich, J., Schmitz, J., Shortman, K., Sozzani, S., Strobl, H., Zembala, M., Austyn, J. M. and Lutz, M. B. (2010) 'Nomenclature of monocytes and dendritic cells in blood', *Blood*, 116(16), pp. e74-e80.

